Charles University
Faculty of Science

Study program:
Molecular and Cellular Biology, Genetics and Virology

Mgr. Yaroslava Groza

Doctoral thesis

Non-immunoglobulin binding proteins with immunomodulatory potential in autoimmune diseases

Supervisor: RNDr. Petr Malý, CSc.

Prague, 2024

Univerzita Karlova
Přírodovědecká Fakulta

Studijní program:
Molekulární a Buněčná Biologie, Genetika a Virologie

Mgr. Yaroslava Groza

Disertační práce

Neimunoglobulinové vazebné proteiny s imunomodulačním potenciálem u autoimunitních onemocnění

Školitel: RNDr. Petr Malý, CSc.

Praha, 2024

Prohlašuji, že jsem práci napsala samostatně pod vedením RNDr. Petra Malého, CSc. Veškeré použité zdroje a literaturu jsem řádně citovala a práce ani její podstatná část nebyla použita k získání jiného nebo podobného typu univerzitní kvalifikace. Při přípravě práce jsem použila nástroje umělé inteligence k opravě jazyka a zlepšení čitelnosti.

V Praze, dne _____ _____

Yaroslava Groza

Acknowledgements

I would like to express my deepest gratitude to my supervisor, **RNDr. Petr Malý, CSc.**, for giving me the opportunity to join his team and conduct research under his leadership, and for making my adaptation in the new country easier. His guidance, encouragement, and patience have been invaluable for my professional development. I am particularly grateful for his kind support and for pushing me forward whenever I felt uncertain and hesitant.

I extend my heartfelt thanks to my colleagues from the Laboratory of Ligand Engineering, Institute of Biotechnology, for sharing their experience, assisting with my experiments, giving me good advice, soft skills to improve research productivity, and creating a healthy work environment. I am highly thankful to **Mgr. Kuchař Milan, Ph.D.**, for advising me regarding my research, while always having friendly cheerful attitude. I am grateful to **Mgr. Natalya Panova, Ph.D.**, who shared her reasearch and life experience, and told me many interesting things about her interests, such as art, ballet, and literature.

I would like to thank our collaborators, including **MUDr. Karel Smetana Jr.**, **DrSc., MUDr. Lukáš Lacina, Ph.D.**, **Prof. Mgr. MUDr. Milan Raška, Ph.D.**, and the members of his group; **Ing. Radim Osička, Ph.D.**, **Ing. Jiří Černý, Ph.D.**, and **Mgr. Olga Šebestová Janoušková, Ph.D.** Their scientific enthusiasm and expertise have led to productive collaborations and interesting results.

I am very grateful to my family, especially my mother, **Valentyna Groza**, for inspiring me with her example and providing me an unwavering support in every situation. Also, I want to thank my father **Olexandr Groza** for his advice and guidance. I also wish to acknowledge my late grandfather, **Klimyk Anatoliy**, a renowned scientist who inspired me to pursue an academic path. I also want to thank my dear friends, especially **Liliia**, **Pasha**, and **Dan**, for being there to share my joy and comfort me during challenging times.

Last but not least, I would like to quote the inspirational words of Calvin Cordozar Broadus Jr. to: "…thank me for doing all this hard work. I wanna thank me for never quitting. I wanna thank me for being me at all times…"

Abstract

Intercellular communication enables cells to interact with each other and their environment to coordinate their essential activities and functions. Immune cells, dispersed throughout the body, particularly rely on signaling mediator molecules and cognate receptors to exchange information with other immune cells and somatic cells. Accordingly, dysregulation of cell communication can disrupt normal cellular functions, leading to the development of pathological conditions. Extensive research in immunology has identified signaling mediators that are dysregulated or misused in various conditions. Therefore, the main focus of this PhD project is therapeutic targeting of the immune receptors in pathological conditions such as autoimmunity and cancer.

In this project, protein engineering approach was employed to develop small protein binders with potential applications in research, diagnostics, and therapy. These novel protein binders were developed from a highly complex combinatorial library created through mutagenesis of selected residues of albumin binding domain (ABD) or Myomedin protein scaffold. This approach expands the therapeutic protein toolkit with specific high-affinity small protein binders possessing favorable biophysical properties that can be produced in cost-effective bacterial system. The functional activity and efficacy of these binders were evaluated in both *in vitro* and *in vivo* disease models.

For the initial molecular target, interleukin-6 (IL-6) was selected due to its involvement in various autoimmune diseases such as immunoglobulin A nephropathy (IgAN) and inflammatory bowel disease (IBD), as well as significant contribution to cancer progression by affecting tumor cells or tumor microenvironment. To inhibit IL-6 signaling, thus, a collection of ABD-derived small protein binders NEF targeting IL-6 receptor alpha (IL-6Rα) was developed by directed evolution. The resulting NEF variants demonstrated specificity and high binding affinity to the IL-6Rα, as well as inhibitory potential. These ABD binders effectively suppressed B cell maturation, laying foundation for further research about their applicability in IgAN. An emerging body of evidence underscores the importance of IL-6 in IgAN, as discussed in the review article published as part of this PhD study. Also, NEF variants targeting IL-6 signaling efficiently diminished intestinal inflammation markers in chemically-induced colitis murine model. Finally, NEF blockers exhibit significant reduction of the proliferation and migration of cancer cell lines while outperforming the commercial antibody Tocilizumab in some instances. The encouraging experimental outcomes inspired a patent application, which is currently being evaluated by the Industrial Property Office of the Czech Republic.

Another part of the PhD project was focused on targeting IL-22 mediated signaling in IBD. According to the current state of knowledge, IL-22 signaling has dual role in intestinal inflammation depending on the disease context. Using protein engineering, ABR variants were developed from the ABD combinatorial library, which specifically target IL-22R1 subunit of the IL-22 receptor complex. The specificity and inhibitory potential of IL-22R1 blockers was demonstrated in *in vitro* assays. Additionally, the most promising ABR variants demonstrated anti-inflammatory potential in the DSS-induced acute colitis murine model, highlighting the significant role of IL-22-mediated signaling in intestinal inflammation. Hence, the ABR proteins can provide valuable molecular clues for future IBD drug development.

Furthermore, this PhD thesis describes research efforts on developing therapeutic tools to predict the efficiency of immune checkpoint inhibitor therapy in cancer patients. In this context, MBA ligands targeting PD-1 as molecular target were developed from the Myomedin scaffold, which recognize both the murine and human receptors with high specificity and affinity. The diagnostic potential of MBA ligands was evaluated using tissue sections of human tonsils and patients with non-small cell lung carcinoma (NSCLC) and using Positron Emission Tomography (PET) imaging in mice.

Finally, considering the emerging role of the triggering receptor expressed on myeloid cells 2 (TREM-2)—a member of immunoglobulin superfamily, in inflammatory disorders and cancer, the cellular and molecular biology of the TREM-2 was reviewed. Additionally, the clinical relevance of the TREM-2 in cancer progression and a therapeutic potential of TREM2-targeting molecules in cancer therapy alone or in combination with immune checkpoint inhibitors was emphasized.

Abstrakt

Mezibuněčná komunikace umožňuje buňkám vzájemně interagovat a komunikovat se svým okolím pro koordinaci základních činností a funkcí. Imunitní buňky, rozptýlené po celém těle, se při výměně informací s jinými imunitními a somatickými buňkami zejména spoléhají na signální molekuly a rozpoznávající receptory. Proto může dysregulace buněčné komunikace narušit normální buněčné funkce a vést k rozvoji patologických stavů. Rozsáhlý výzkum v imunologii identifikoval několik specifických signálních mediátorů, které jsou v různých podmínkách dysregulovány nebo zneužívány. Hlavním cílem tohoto doktorského projektu je proto terapeutické cílení imunitních receptorů v patologických stavech, jako je autoimunita a rakovina.

V tomto projektu byl použit přístup proteinového inženýrství k vývoji malých proteinových vazebných molekul s potenciálním využitím ve výzkumu, diagnostice a terapii. Tyto nové proteinové vazebné molekuly byly vyvinuty z vysoce komplexní kombinatorické knihovny vytvořené mutagenezí vybraných reziduí albumin-vazebné domény (ABD) nebo Myomedinového proteinového skafoldu. Tento přístup rozšiřuje sadu terapeutických proteinů o specifické vysoko-afinitní malé proteinové vazebné molekuly s příznivými biofyzikálními vlastnostmi, které lze vyrábět v nákladově efektivním bakteriálním systému. Funkční aktivita a účinnost těchto vazebných molekul byly hodnoceny jak v *in vitro, tak in vivo* modelech nemocí.

Pro počáteční molekulární cíl byl vybrán receptor interleukinu-6 (IL-6) kvůli jeho zapojení do různých autoimunitních chorob, jako je imunoglobulin A nefropatie (IgAN) a chronické střevní záněty, stejně jako významný příspěvek k progresi rakoviny působením na nádorové buňky nebo nádorové mikroprostředí. K inhibici signalizace IL-6 byla řízenou evolucí vyvinuta sbírka od ABD odvozených malých proteinových vazebných molekul NEF cílených na IL-6 receptor alfa (IL-6Rα). Výsledné ABD varianty prokázaly specifitu a vysokou afinitu vazby k IL-6Rα, stejně jako inhibiční potenciál. Tyto ABD vazebné molekuly účinně potlačily maturaci B buněk, což poskytuje základ pro další výzkum jejich aplikovatelnosti v IgAN. Rostoucí množství důkazů zdůrazňuje důležitost IL-6 v IgAN, jak je diskutováno v přehledovém článku publikovaném jako součást této doktorské studie. Také NEF varianty cílené na signalizaci IL-6 účinně snižovaly markery střevního zánětu v chemicky indukovaném modelu kolitidy u myší. Nakonec blokátory NEF vykazovaly významné snížení proliferace a migrace nádorových buněčných linií, přičemž v některých případech překonávaly komerční protilátku Tocilizumab. Povzbuzující experimentální výsledky inspirovaly podání patentové přihlášky, která je v současnosti hodnocena Úřadem průmyslového vlastnictví České Republiky.

Další část doktorského projektu byla zaměřena na cílení signalizace zprostředkované IL-22 při IBD. Podle současného stavu poznání má signalizace IL-22

dvojí roli ve střevním zánětu v závislosti na kontextu choroby. Pomocí proteinového inženýrství byly z kombinatorické knihovny ABD vyvinuty ABR varianty, které specificky cílí na podjednotku IL-22R1 komplexu receptoru pro IL-22. Specifita a inhibiční potenciál blokátorů IL-22R1 byly prokázány v *in vitro* testech. Navíc nejpřesvědčivější ABR varianta prokázala protizánětlivý potenciál v modelu akutní kolitidy vyvolané DSS u myší, což zdůrazňuje významnou roli signalizace zprostředkované IL-22 ve střevním zánětu. Proto mohou ABR proteiny poskytnout cenné molekulární stopy pro budoucí vývoj léků na IBD.

Dále tato doktorská práce zahrnuje výzkumné úsilí na vývoji terapeutických nástrojů k predikci účinnosti terapie pomocí blokace imunitních kontrolních bodů u pacientů s rakovinou. V tomto kontextu byly z myomedinového skafoldu vyvinuty MBA ligandy cílené na PD-1 jako molekulární cíl, které rozpoznávají jak lidské, tak myší receptory s vysokou specifitou a afinitou. Diagnostický potenciál MBA ligandů byl hodnocen pomocí tkáňových řezů lidské krční mandle a na řezech pacientů s nemalobuněčným plicním karcinomem (NSCLC), a také pomocí *in vivo* zobrazování pozitronovou emisní tomografií (PET) u myší.

Nakonec, s ohledem na rostoucí roli receptoru 2 myeloidních buněk (TREM-2) u zánětlivých poruch a rakoviny, byla přezkoumána buněčná a molekulární biologie TREM-2 v přehledovým článku. Navíc byla zdůrazněna klinická relevance TREM-2 v progresi rakoviny a terapeutický potenciál molekul cílených na TREM-2 v terapii rakoviny samostatně nebo v kombinaci s inhibitory imunitních kontrolnícbodů.

Table of Contents

1. Introduction

Unlike somatic cells in the other tissues of the body, immune cells are dispersed throughout the organism by the circulatory system. To mount efficient, systematic, and accurate responses locally or at long distances, cell-to-cell communication between immune cells or immune cells and tissues is mediated by a class of regulatory molecules called cytokines [1]. Over 130 cytokines are known that can mediate signaling in an autocrine, paracrine, or endocrine manner via cytokine-specific surface receptors (**Figure 1**). These signaling molecules are typically proteins (5–70 kDa) that are further classified into chemokines (CKs), colony-stimulating factors (CSFs), interleukins (ILs), interferons (IFNs), lymphokines, monokines, tumor necrosis factors (TNFs), and transforming growth factors (TGFs) [2, 3].

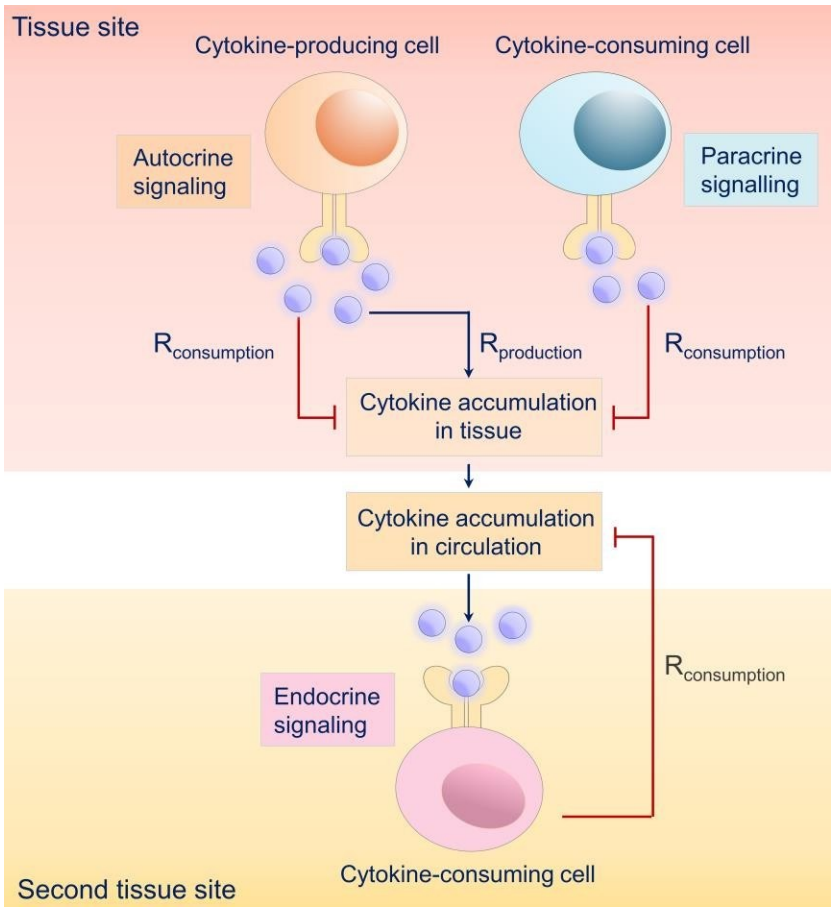

Figure 1. Modes of cell-to-cell communication mediated by cytokines. Based on the location of the cytokine-responsive cell, intercellular communication is classified into three types. Autocrine signaling happens when a cell responds to a cytokine produced by itself. Paracrine signaling takes place between two cells in proximity. In the case of endocrine signaling, cells are spatially distant, so signaling mediators travel through the circulatory system. The rate of cytokine production ($R_{production}$) and rate of cytokine consumption ($R_{consumption}$) determine the mode of intercellular signaling. The scheme is adapted and replotted from Ref [1].

In general, cytokines are primarily produced by immune cells, such as macrophages, lymphocytes, and mast cells, but a myriad of studies have also detected cytokines secretion by non-immune cells, such as endothelial cells, fibroblasts, and various stromal cells, under specific conditions. Correspondingly, cells targeted by cytokines expressed high-affinity cognate receptors that upon binding with specific cytokine initiates intercellular signaling, resulting in an alternation in specific gene transcription. Thereby, cytokines alter cell proliferation and differentiation, as well as trigger or modify particular cell functions. Usually, a single cytokine can be secreted by more than one cell type [4]. Consequently, cytokines elicit two characteristics under physiological or pathological conditions: (a) functional pleiotropy—an ability to exhibit a wide spectrum of functional responses in different types of cell subsets, and (b) functional redundancy—an exhibition of overlapping activities exhibited by the set of cytokines [5-7].

In the context of disease, cytokines are often found at the epicenter of pathological processes. Thus, dysregulation in cytokine production or cytokine-mediated signaling can often lead to an array of immune-mediated diseases such as chronic inflammation, autoimmunity, and cancer [8, 9]. Given the pivotal role of cytokines in various diseases, therapeutic strategies aimed at inhibiting their activity have gained significant attention [2, 8]. Accordingly, the development of cytokine and/or cytokine receptor neutralization therapeutics has been a breakthrough for common autoimmune diseases, such as rheumatoid arthritis (RA) and IBD [10-12]. One of the pioneering cytokine neutralization therapies involves the use of monoclonal antibodies (mAbs). These engineered mAbs are designed to specifically target cytokines or receptors, thereby neutralizing their activity [13]. In addition to mAbs, small molecule inhibitors, cytokine traps, and soluble cytokine receptors as ligands or blockers have been developed [14-16]. These ligands can specially bind to cytokines to prevent their interaction with the cell surface expressed cognate receptors and initiate downstream signaling.

Cytokine neutralization strategy has revolutionized the treatment of autoimmune diseases by specifically targeting the inflammatory cytokines that drive these conditions. For example, mAbs targeting interleukin-1 (IL-1) [17] and interleukin-6 (IL-6) [18] are widely applied for the treatment of inflammatory diseases. Besides, cytokine neutralization has also profoundly impacted cancer therapy by targeting the pro-tumorigenic cytokines that promote tumor growth and suppress anti-tumor immunity. By neutralizing these pro-tumorigenic cytokines, researchers have been able to disrupt the supportive environment required by the tumors, thereby enhancing the efficacy of conventional therapies, and improving patient outcomes. One notable example is the neutralization of tumor necrosis factor-alpha (TNFα), whose chronic

production in the tumor microenvironment (TME) can support tumor growth and metastasis [19].

1.1. Biology of Interleukin 6

1.1.1. IL-6 structure and signaling

Interleukin-6 (IL-6) is a pleiotropic cytokine with both homeostatic and proinflammatory functions [20]. Many cells, including astrocytes, endothelial cells, fibroblasts, keratinocytes, lymphocytes, monocytes, macrophages, and peripheral blood mononuclear cells (PBMCs), can secrete IL-6 under specific-stimulatory environments [21]. For instance, secretion of IL-6 can be initiated by infection, trauma, stress, metabolic abnormalities, and immune complexes (ICs). Signaling molecules, such as IL-1, TNFs, damage-associated molecular patterns (DAMPs) or pathogen-associated molecular patterns (PAMPs), trigger IL-6 secretion by multiple immune and stromal cells, including monocytes, macrophages, and endothelial cells [22]. Under normal conditions, the IL-6 level does not exceed the low pg/ml range [23], however, it becomes significantly elevated during pathological conditions such as acute inflammation [24].

In the three-dimensional (3D) structure, IL-6 cytokine comprises a four-helical bundle linked by loops and an additional mini-helix of 185 amino acids with an estimated molecular weight of 21.01 kDa [21]. It is a member of the IL-6 family of cytokines which includes IL-6, IL-11, IL-27, IL-31, IL-35, and IL-39, leukaemia inhibitory factor (LIF), ciliary neurotrophic factor (CNTF), cardiotrophin-1 (CT-1), and oncostatin-M (OSM) [25]. Although the structure is conserved between IL-6 family representatives, sequence homology is rather low [26]. The IL-6 signals via the IL-6 receptor complex (IL-6R), which is composed of subunits IL-6Rα and glycoprotein 130 (gp130), to display the biological effects [27]. The IL-6Rα is specific only for the IL-6 cytokine, whereas the gp130 is a signal-transducing subunit, which is shared among most cytokines of the IL-6 family. Typically, the assembly of the IL-6R signaling complex occurs in three steps. In the first step, the IL-6 forms a complex with the IL-6Rα subunit, which is capable of further interaction with the gp130. Neither the IL-6 nor IL-6Rα alone exhibits reasonable affinity for the gp130 [28, 29]. In the following step, the IL-6/IL-6Rα complex binds to the gp130 [28]. Finally, the IL-6/IL-6Rα/gp130 complex binds to the second gp130 or another already assembled IL-6/IL-6Rα/gp130 complex. Consequently, the IL-6/IL-6Rα/gp130 hexameric complex with 2:2:2 stoichiometry is held together by 10 protein-protein interfaces. In humans, IL-6Rα has been reported with a binding affinity of 9 nmol/l for the IL-6, and the gp130 shows a stronger binding to the IL-6/IL-6Rα dimer (KD = 0.8 nmol/l), therefore, leading to the activation of IL-6-mediated signaling at very low concentration [28].

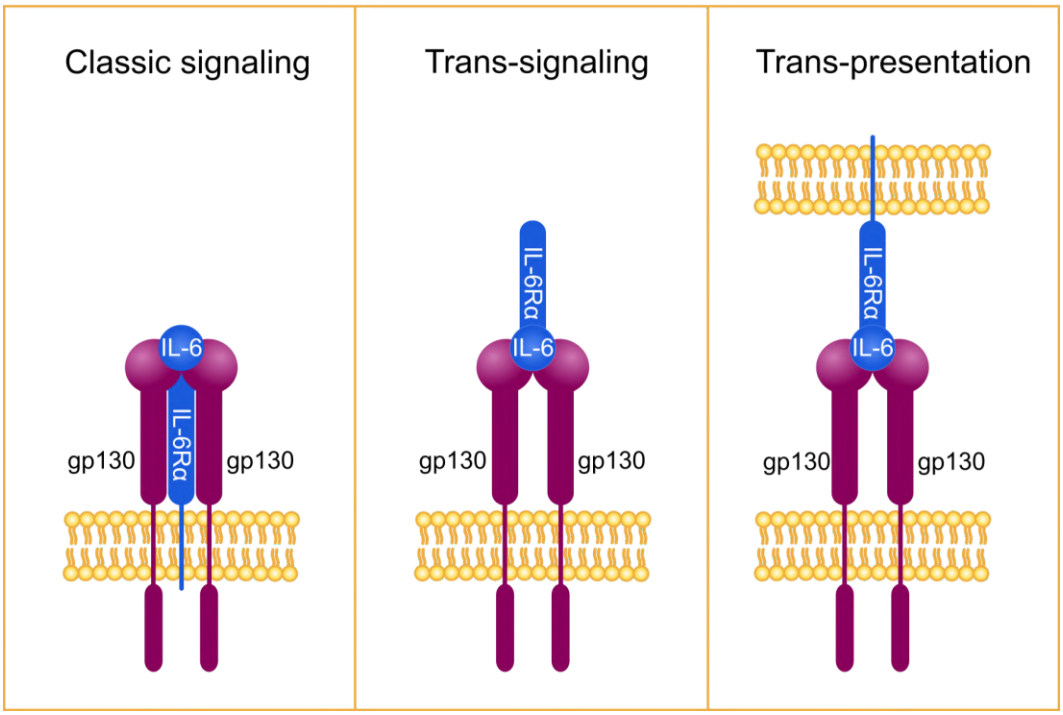

Figure 2. IL-6 signaling modes. Classic signaling (*left*) occurs when both IL-6Rα and gp130 are membrane-bound. First, IL-6 docks with membrane-bound IL-6Rα (mbIL-6Rα), resulting IL-6/mbIL-6Rα complex then associates with gp130. This leads to the gp130 dimerization and activation of downstream signaling. In another scenario (*center*), IL-6Rα can be in a soluble form. When IL-6 binds to soluble IL-6Rα (sIL-6Rα), the IL-6/sIL-6Rα complex can activate cells that express gp130 but lack membrane-bound IL-6Rα, a process known as Trans-signaling. Whereas Trans-presentation involves direct cell-to-cell interaction (*right*). Herein, the IL-6/IL-6Rα complex is formed within a cell and presented on its surface, where it interacts with the gp130 on an adjacent cell to initiate signaling.

The molecular interaction of the IL-6/IL-6Rα complex with the signal-transducing membrane protein gp130 promotes its dimerization and subsequently, initiates intracellular signaling. Although the gp130 receptor is expressed in the majority of the cells in the body, the membrane-bound IL-6Rα (mbIL-6Rα) is expressed only in some cell types, such as leukocytes (monocytes, macrophages, neutrophils, some types of T cells, and activated B cells), hepatocytes, intestinal epithelial cells, podocytes, osteocytes, and osteoclasts [21]. Therefore, the classic IL-6 signaling is limited only to these cell types [30, 31]. Also, soluble IL-6R (sIL-6R) produced via ADAMs (a disintegrin and metalloproteinases) activity or alternative mRNA splicing expands the IL-6 signaling options via the alternative signaling mode "trans-signaling" (**Figure 2**). The IL-6 forms a complex with the sIL-6Rα and then activates signaling via the gp130 on the target cell surface. As a result, it significantly expands the pool of IL-6 target cells, including embryonic stem cells, endothelial cells, hematopoietic progenitor cells, osteoclasts, and neuronal cells [32]. As only a part of the IL-6 is

trapped in the IL-6/sIL-6Rα complexes, so signaling mostly occurs via cis-signaling mode. Another role of sIL-6Rα might be the buffering of the IL-6, so that it is eliminated more slowly from the circulation. In contrast, soluble gp130 selectively inhibits the IL-6/sIL-6Rα complex-mediated [33]. Available research data suggests that classical signaling mediates anti-inflammatory, pro-resolution, and anti-bacterial activities while pro-inflammatory activities are typically regulated by trans-signaling and at times by trans-presentation [21, 34].

Additionally, the third mode of IL-6-mediated signaling has been newly discovered in mice called trans-presentation or cluster signaling, where a direct interaction between cells is required. In this case, the IL-6/IL-6Rα complex is assembled in the endosome of presenting cells and exported to its surface. Then, the surface displayed IL-6/IL-6Rα complex in the presenting cells interacts with the gp130 in the recipient cells to trigger the IL-6 signaling. It was demonstrated that dendritic cells (DCs) activate cognate pathogenic Th17 via the IL-6-mediated trans-presentation signaling in mice [35]. Of note, independent of IL-6 expression, both IL-6Rα and gp130 are constitutively internalized through a clathrin-mediated mechanism. This endocytosis is a prerequisite for IL-6-mediated signal transduction. The IL-6Rα contains a di-leucin internalization motif in the intracellular part which induces constitutive receptor internalization via endocytosis. Most of the endocytosed receptor is then delivered to lysosomes for degradation with only a minor fraction sorted for recycling. Experimental studies showed that mbIL-6Rα halves within 60 min due to constitutive internalization. IL-6 does not trigger receptor endocytosis but promotes receptor recycling [36].

Moreover, IL-6 also activates the Janus kinase 2/signal transducer and activator of the transcription 3 (JAK2/STAT3) signaling pathway via the common co-receptor gp130 (**Figure 3**) [37]. The classical JAK2/STAT3 signaling pathway involves STAT3 phosphorylation at tyrosine 705 (Tyr705). However, another phosphorylation at serine 727 (Ser727) is triggered by different kinases, such as ERK1/2, MAPK p38, and JNK [38]. Thus, the phosphorylation of S727 allows STAT3 to achieve maximal transcriptional activity [39], although the effect seems to be dependent on the promotor or cellular context [40]. Consequently, various proteins that define IL-6 biological functions are upregulated via JAK2/STAT3 signaling, including survival proteins (XIAP, Bcl-2, Bcl-xL, and Mcl-1), cell cycle progression proteins (cyclin D1-D2, cyclin B1, and c-Myc), pro-angiogenic factors (HIF-1 and VEGF-A), and extracellular matrix (ECM) remodeling proteins (MMP-2, MMP-9, uPA, and cathepsin) [41-45]. Other pathways utilized for IL-6 signaling are mitogen-activated protein kinase (MAPK), phosphoinositide 3-kinase (PI3K)/protein kinase B (Akt), and gp130/SFK/YAP [46-48]. Furthermore, it was shown

that IL-6 exposure could lead to an increase in the expression of IL-6R, potentially leading to a feedback loop that amplifies the IL-6-induced impact [49].

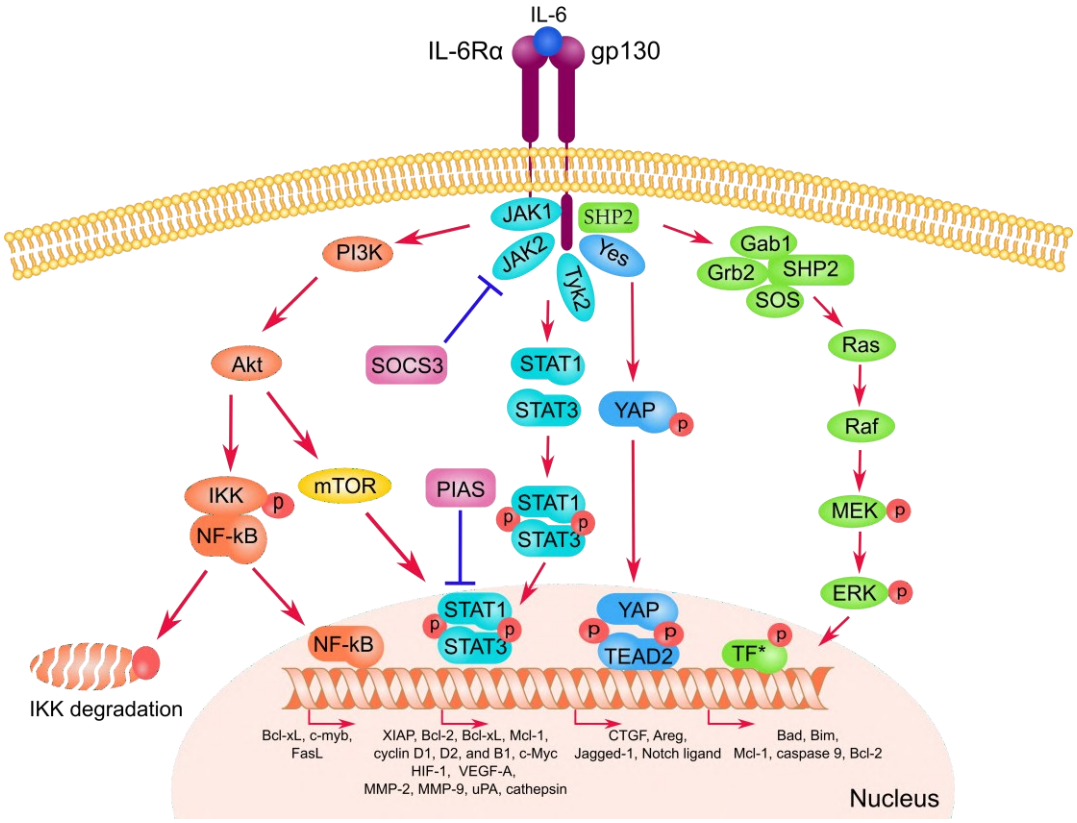

Figure 3. IL-6 signaling pathways. The JAK2/STAT3 pathway is a key signaling pathway for IL-6. The assembly of the IL-6 receptor complex triggers the recruitment of JAK kinases to the intracellular domain of gp130. These JAKs phosphorylate five tyrosine residues on the gp130. Next, the STAT3 and STAT1 proteins are recruited to these phosphorylated tyrosines on JAKs and gp130. Following their recruitment, STAT proteins are phosphorylated, dimerized, and translocated to the nucleus to activate the transcription of target genes. Alternatively, SHP2 is also recruited to the phosphorylated tyrosines on the gp130. Also, the JAK-dependent phosphorylation of SHP2 initiates activation of the MAPK pathway. While the SHP2 recruits Grb2 and SOS, and sustains the MAPK pathway activation, for which Gab1 is required. This complex assembly leads to Ras activation, which then activates Raf. In turn, Raf phosphorylates and activates MAPK kinase, which then phosphorylates JNK, p38, Erk5, and Erk1/2, stimulating their translocation into the nucleus. Another kinase, PIP3, is activated in a JAK-SHP2-Gab1-dependent manner. Additionally, the Src family kinase (SFK) member Yes associates with gp130, stabilizing YAP through tyrosine phosphorylation. YAP then translocates to the nucleus and functions as a co-activator for the transcription factor TEAD2. Proteins such as SOCS and PIAS are involved in the downregulation of IL-6 signaling.

1.1.2. IL-6-mediated innate and adaptive immunity

IL-6 controls both innate and adaptative immune responses. A detailed summary of IL-6 functions is provided in **Table 1**. Under innate immunity, IL-6 plays a central role in

the activation of different inflammatory pathways [50]. Upon pathogen detection, locally secreted IL-6 flows via the bloodstream to the liver, where it induces acute-phase protein production (APP), including C-reactive protein (CRP), serum amyloid A (SAA) protein, complement C3, haptoglobin, antitrypsin, fibrinogen, hepcidin, thrombopoietin, etc. On the contrary, IL-6 reduces the production of albumin and cytochrome P450 (CYP450) in the liver [51]. Also, IL-6 increases blood vessel permeability directly by inducing the internalization of vascular endothelial adhesion molecule (VE-cadherin or CD144) which hold together endothelial cells [51]. Additionally, IL-6 stimulates the expression of other adhesion molecules such as intercellular adhesion molecule 1 (ICAM-1), vascular cell adhesion protein 1 (VCAM-1), and E-selectins, to allow accumulation of extravascular inflammatory cells [52].

Neutrophils are the first cells that actively migrate to the site of inflammation. Activation of pattern recognition receptors, such as Toll-like receptors (TLRs), induces IL-6 secretion by neutrophils and monocytes or macrophages [53]. Also, IL-6 regulates innate immunity by controlling innate immune cell activity, as it triggers the recruitment, adhesion, activation, differentiation, and survival of neutrophils, tissue-resident and inflammatory monocytes, and innate lymphoid cell populations including natural killer cells [54, 55]. When neutrophils undergo apoptosis, ADAM17-dependent shedding of IL-6Rα is triggered from the cell membrane to the surrounding medium [56]. sIL-6Rα then interacts with IL-6 and induces endothelial cells to produce monocyte chemoattractant protein 1 (MCP1), a chemokine responsible for subsequent attraction of monocytes. Therefore, IL-6 contributes to the transition from neutrophilic to monocytic infiltration at sites of inflammation at a later stage of acute phase response (APR) [57-59], a process which besides defense against infection seems to be important in chronic inflammation development and inflammation resolution. Additionally, by inducing monocyte expression of macrophage colony-stimulating factor (M-CSF) receptors, IL-6 promotes the differentiation of monocytes to macrophages [60]. It can also activate anti-inflammatory IL-10$^+$ M2-like (M2d) macrophages [61].

In the case of adaptive immunity, IL-6 promotes B cell terminal differentiation [62] and plays a role in regulatory B cell induction [63, 64]. Besides B cells, IL-6 profoundly affects T cell-mediated immune responses [65, 66]. It influences the survival of CD4$^+$ T cells, presumably by inducing Bcl-2 expression. Moreover, IL-6 co-stimulates and protects CD4$^+$ T cells from activation-induced cell death (AICD) [67]. Also, IL-6 influences T-cell differentiation towards Th2, Th17, and T follicular helpers (Tfh) subpopulations while repressing Th1 and Treg subpopulations. IL-6 up-regulates IL-4 production and shifts the balance towards the Th2 subpopulation in an autocrine manner. On the other hand, IL-6 also suppresses Th1 lymphocyte differentiation and

relevant cytokine INF-γ production. Furthermore, in the presence of TGF-β, IL-6 induces differentiation of naïve $CD4^+$ T cells toward Th17 precursors which after stimulation with IL-23 mature to Th17 cells producing IL-17, IL-22, TNFα, GM-CSF, and also IL-6 [67, 68]. In contrast, TGF-β in the absence of IL-6, induces differentiation of naïve $CD4^+$ T cells into induced in cell culture regulatory T cell (iTreg) population characterized by the transcription factor FOXP3 production, which is suppressed by IL-6 stimulation [69]. While Th17 cells actively participate in inflammatory immune response and neutrophil activation, iTregs induce immune tolerance. Also, IL-6 contributes to the differentiation of naive Th cells toward IL-21-producing Tfh, which are involved in the germinal center formation and support B cell maturation, isotype switch, and affinity maturation. In contrast, Tfh differentiation is not discontinued in the absence of either IL-6 or IL-21 [70]. Whereas IL-6 promotes antibody production by directly acting on plasma cells and by indirectly promoting Bcl-6-dependent follicular $CD4^+$ T (Tfh) cell differentiation together with IL-21 [71-73]. It was shown that myeloid-derived sIL-6R complexed with IL-6 inhibits Th1 responses through STAT3-induced c-Maf. This is one of the mechanisms by which IL-6 has been characterized to inhibit T-cell immunity against tumors [74]. Thus, IL-6 is presented as one of the critical factors that contribute to the modulation of both, innate and adaptive immune responses.

1.1.3. IL-6 and wound healing

Wound healing is another process that requires IL-6 engagement, which occurs in three stages: (a) inflammation, when damaged cells and microorganisms are removed; (b) proliferation, when angiogenesis and ECM synthesis occur; and (c) remodeling, when ECM is processed. An up-regulation of IL-6 expression is reported during the inflammatory and proliferative phases while it ceases during remodeling [75]. The role of IL-6 in the inflammatory stage is similar to that in APR: leucocyte attraction, switch from neutrophil to monocyte attraction, and monocyte to macrophage differentiation. During the proliferative phase, IL-6 recruit's fibroblasts, whose function is collagen accumulation. IL-6 also induces upregulation of IL-4 expression by Th2 cells, which in turn induces a switch from inflammatory M1 macrophages to anti-inflammatory M2 macrophages [76].

Table 1. IL-6 functions in immune response and other physiological processes.

Cells	*Function of IL-6*	*Ref.*
	Innate immunity	
Hepatocytes	Stimulates APP production (CRP, serum amyloid protein A, complement C3, haptoglobin, antitrypsin, fibrinogen, hepcidin, thrombopoietin ↑; albumin and cytochrome p450 ↓)	[51]
Monocyte	Stimulates differentiation to macrophages (M-CSF ↑) Suppresses differentiation to DC	[65]
Endothelial cells	Monocyte attraction to the site of inflammation (MCP1↑)	[77]
	Adaptive immunity	
B cells	Promotes plasmablast survival Induces differentiation of B-cells into plasma cells Induces immunoglobulin production	[64]
CD4⁺ T cells	Supports survival (Bcl-2↑) and protects from AICD (FasL↓) Induces differentiation to Th2 (IL-4↑) and Suppresses differentiation to Th1 (INF-γ↓) In the presence of TGF-β induces differentiation toward Th17 precursors Suppresses differentiation to iTreg (FoxP3↓) Contributes to the differentiation to Tfh	[20, 78]
CD8⁺ T cells	Induces differentiation to subset of IL-21-producing B helper CD8+ T cells	[70, 79]
	Liver regeneration	
Hepatocytes	Stimulates proliferation and survival (FoxM1, Ref-1, Mcl-1↑).	[80]
Hepatic satellite cells	Supports hepatocyte proliferation (HGF↑).	[81]
Hepatic progenitor cells	Stimulates proliferation	[56, 82]
	Angiogenesis	
Endothelial cells	Induces increase in blood vessel cell permeability (VEV-cadherin internalization) Induces expression of adhesion molecules, which assist leukocyte extravasation (ICAM-1, VCAM-1, and E-selectins↑)	[51, 52]
	Wound-healing	
Fibroblasts	Induces type I collagen accumulation by fibroblasts, as well as TGF-β level increase	[83]
	Hematopoiesis	
Hepatocytes	Indirectly stimulates platelet production (TPO↑) Indirectly affects erythropoiesis (hepcidin↑)	[51]
	Nervous system	
Neural stem cells	Contributes to NSC differentiation into astrocytes and oligodendroglyocytes	[84]
Astrocytes	Changes the expression pattern (NGF neurotrophin ↑, TNFα ↓)	
Oligodendroglyocytes	Promotes survival and myelin production	
	Bone remodeling	
Osteoblasts	Induces surface expression of RANKL, which activate surrounding osteoclasts to resorb bone	[85, 86]
	Metabolism	
Hepatocytes	Reduces liver insulin sensitivity (IRS↓) Stimulates insulin secretion (GLP-1↑)	[87]
Muscle cells	IL-6 level is elevated during exercise. In this context, IL-6 has an anti-inflammatory effect (sTNFαR, IL-1Rα, and IL-10↑)	
Adipose cells	Induces leptin secretion, which influences appetite and caloric intake	
	Tumor development	
Tumor cells	Enhance survival (Bcl-2, Bcl-XL, Mcl-1, survivin, XIAP↑) Enhance proliferation (cyclin D1, D2, and B1, and c-Myc↑; Cdk inhibitor p21↓) Induces ECM remodeling (uPA, cathepsin, MMP-2, MMP-7 and MMP-9↑)	[88, 89]

1.1.4. Dysregulated IL-6 signaling associated disorders

Multistage involvement of IL-6 in complex physiological processes has a downside. Normally, IL-6 signaling should fade out after stress resolution. However, dysregulated

IL-6 signaling causes chronic inflammation and disturbs tissue homeostasis, leading to tissue damage and loss of function. SAA up-regulated by IL-6 has a protective function during inflammation. However, persistent high concentrations of SAA lead to the development of amyloid A amyloidosis, manifested by amyloid fibril deposition in organs and distortion of the affected organ function [90]. IL-6 is among the factors that activate mesangial cells for proliferation and activation. Dysregulated IL-6 signaling causes abnormal mesangial cell activation that disturbs kidney homeostasis and causes tissue injury, as in the case of IgAN [91, 92]. IL-6 takes part in bone metabolism by up-regulating receptor activator of nuclear factor kappa beta ligand (RANKL) on osteoblasts, which in turn activates osteoclasts for bone resorption. However, prolonged RANKL signaling leads to excessive bone resorption and subsequent osteoporosis development [86, 93]. Similarly, IL-6 contributes to cancer development [94]. Ironically, IL-6 effects that are beneficial during wound healing are turned against the organism during tumorigenesis, hence processes that occur during tumor development resemble those in wound healing. In both cases, cells show angiogenesis, proliferation, migration, and tissue remodeling.

1.1.5. IL-6 antagonists

Due to the multifunctional role of IL-6 in the pathogenesis of immune-associated diseases and cancers, inhibition of IL-6-mediated signaling might be beneficial. Although, it does not eliminate the cause of the disease, but decreases the severity of the disorder. Accordingly, IL-6 signaling can be affected by blocking of complex assembly via targeting IL-6 itself, IL-6Rα or gp130 or by blocking the most dominant IL-6-stimulated JAK/STAT pathway using JAK and STAT inhibitors. In **Table 2**, different IL-6 inhibitors are represented by mAbs, scaffold proteins, and small organic molecules.

Recently, mAbs for IL-6 or IL-6R were investigated in clinical trials and showed positive results, leading to their approval by the FDA [95]. For example, the anti-IL-6 antibody siltuximab has been approved by the FDA to treat multicentric Castleman disease [96, 97]. Also, the FDA approved the anti-IL-6R mAbs, Tocilizumab, for the treatment of rheumatoid arthritis [98, 99]. However, administration of anti-IL-6-specific mAb leads to the formation of circulating immune complexes (CICs) of IL-6/anti-IL-6 mAb which protect IL-6 cytokine clearance by the kidney. Therefore, the serum IL-6 concentration reaches mg/ml levels, clinically expressed by fever, fatigue, hypercalcaemia, and recurrence of bone pain [100, 101]. Hence, IL-6Rα inhibition is considered as an alternative therapeutic strategy. Nevertheless, a higher amount of receptor blockers should be applied to inhibit cell surface mbIL-6Rα as the serum sIL-6Rα must be saturated first.

Table 2. IL-6/IL-6R inhibitors.

Name	*Target*	*Completed clinical trial*	*Substance*	*Ref.*
Antibodies				
Siltuximab *(CNTO 328, Sylant)*	IL-6; Site I	FDA and EMA approved for iMCD	Chimeric mAb	[102-105]
Olokizumab	IL-6; Site III	Phase 3 for RA	Humanized mAb	
Clazakizumab *(ALD518, BMS-945429)*	IL-6; Site I	Phase 2 for RA	Humanized mAb	
PF-04236921	IL-6; Site I	Phase 2 for CD Phase 2 for SLE Phase 1 for RA	Humanized mAb	
Sirukumab *(CNTO 136)*	IL-6	Phase 2 for MDD Phase 3 for RA Phase 3 for GCA	Human mAb	
mAb 1339	IL-6	--	Human mAb	
MEDI 5117	IL-6	--	Human mAb	
Tocilizumab	IL-6R	FDA and EMA approved for RA Phase 4 for Schizophrenia Phase 4 for JIA Phase 3 for SS Phase 2 for HIV	Humanized mAb	
Sarilumab *(SAR153191, REGN88, Kevzara)*	IL-6R	FDA and EMA approved for RA Phase 3 for COVID-19 Phase 2 for Uveitis	Human mAb	
Vobarilizumab *(ALX-0061)*	IL-6R	Phase 2 for RA Phase 2 for SLE		
Recombinant protein				
C326	IL-6	--	Avimer scaffold	[26, 105-109]
Cytokine trap	IL-6	--	Gp130 and IL-6R fused to Fc protein	
NRI	IL-6R	--	Tocilizumab ScFv fused to IgG1 Fc	
Vobarilizumab *(ALX-0061)*	IL-6R	--	bivalent Nanobody	
SANT-7	IL-6R	--	Mutated IL-6	
Olamkicept *(FE 999301, FE301, TJ301)*	IL-6/sIL-6R complex	--	sgp130-Fc dimer	
Small organic molecules				
6a	IL-6	--	pyrrolidinesulphonylaryl	[104, 105]
ERBF	IL-6R	--	20S,21-epoxyresibufogenin-3-formate)	
ERBA	IL-6R	--	20S,21-epoxyresibufogenin-3-acetate	

FDA – Food and Drug Administration, EMA - European Medicines Agency; iMCD - idiopathic multicentric Castleman's disease; RA – Rheumatoid arthritis; SLE – Systemic lupus erythematosus; MDD – Major depressive disorder; GCA - Giant Cell Arteritis; JIA - Juvenile Idiopathic Arthritis; SS - Systemic Sclerosis.

1.2. Interleukin 6 role in cancer

IL-6 in concert with other cytokines orchestrates inflammation and wound healing. Cellular processes, including cell proliferation, tissue remodeling, cell migration, and angiogenesis, that occur during wound healing overlap with those in tumor development. HF Dvorak aptly pointed out that cancer is a "wound that does not heal" [110]. Thus, IL-6 is characterized to promote cancer development both directly and indirectly. Direct involvement of IL-6 in cancer progression occurs when IL-6 stimulates

survival, proliferation, and migration of cancer cells. Alternatively, IL-6 can influence the TME, specifically promoting angiogenesis and ECM remodeling [111]. As previously mentioned, IL-6 is also involved in metabolic regulation, thus, dysregulation of IL-6 signaling substantially contributes to cancer-associated cachexia [112].

1.2.1. Direct effect on cancer cells

STAT3 signaling plays an important role in cancer development by inducing pro-tumorigenic gene expression. Furthermore, it counteracts STAT1 signaling, which on the contrary has a suppressive effect on tumor. Thus, STAT1 out competition by STAT3 allows cancer to escape INFγ suppression. The fact that STAT3 is the main downstream target of IL-6 goes in line with the observation of IL-6 contribution to cancer progression [113]. IL-6 enhances cancer cell survival and proliferation by induction of pro-survival and anti-apoptotic factors (Bcl-2, Bcl-XL, Mcl-1, survivin, and X-linked inhibitor of apoptosis protein (XIAP), the apoptosis inhibitor survivin (also known as BIRC5) and cell cycle progression factors (increased cyclin D1, D2, and B1, and c-Myc expression and decreased cyclin-dependent kinase (Cdk) inhibitor p21 expression) [41, 44, 94]. Thereof, tocilizumab (TCZ), an anti-IL-6Rα antibody, was demonstrated to effectively suppress cell proliferation in several in vitro studies [114, 115]. Importantly IL-6 also promotes cancer stem cells, a process that is regulated by STAT3 in combination with other transcription factors, such as the Homeobox protein NANOG (hNanog). On the other hand, IL-6 signaling via the MAPK pathway contributes to drug resistance in cancer via MDR1 (multidrug transporter P-glycoprotein) activation [116].

Cancer cell growth requires space for newly formed tissue and up-regulation of oxygen supply. IL-6 up-regulates hypoxia-inducible factor-1 (HIF-1), which is crucial for vascularization in the context of oxygen shortage, as well as other pro-angiogenic factors (VEGF-A, EPAS1, adrenomedullin, and angiopoietin-like protein 4). IL-6 assists ECM remodeling by promoting both degradation and renewal. Up-regulation of proteases (uPA, cathepsin, matrix metalloproteinase (MMP)-2, MMP-7, and MMP-9) results in ECM degradation [42, 43, 117]. Therefore, the very same processes that are crucial to restoring organism integrity during wound healing (cell proliferation, angiogenesis, and ECM remodeling) are also utilized for cancer cell survival and at a later stage of metastasis. It has been reported that carcinoma cells undergo epithelial-mesenchymal transition (EMT) [118]. As a result, cells lose epithelial-polarized phenotype and acquire stem cell-like features that facilitate invasiveness and migration. Inflammation creates a favorable environment for tumor progression in general and EMT transition in particular. At the later stages of cancer progression, EMT promotes the spread of metastasis. IL-6 is involved in the process by the induction of transcriptional activators of EMT, such as zinc-finger protein SNAI1 and twist-related

protein (TWIST) [119]. For example, it was demonstrated that incubation of IL-6 with non-small cell lung cancer (NSCLC) cell lines causes morphological changes, as well as up-regulation of mesenchymal cell marker valentine and down-regulation of epithelial marker E-cadherin. Accordingly, the invasiveness of the cell lines treated with IL-6 improved [120].

1.2.2. Tumor microenvironment

The tumor microenvironment (TME) consists of all non-cancerous host cells within the tumor, such as fibroblasts, endothelial cells, and adipocytes, as well as both adaptive and innate immune cells. It also includes non-cellular elements like the ECM and soluble factors such as chemokines, cytokines, growth factors, and extracellular vesicles. The ongoing interactions between tumor cells and the TME are crucial in influencing tumor initiation, progression, metastasis, and therapeutic responses [121]. Among stromal cells, cancer-associated fibroblasts (CAFs) are the most abundant in TME. Therefore, CAFs serve as a main source of IL-6, which shapes the microenvironment by supporting chronic inflammation and tumor growth [122, 123]. As discussed above, IL-6 also induces tumor cell proliferation via up-regulation of pro-survival and cell cycle progression factors, as well as assists angiogenesis and ECM remodeling. On the other hand, IL-6 suppresses the accumulation of immune cells that eradicate tumor cells, such as $CD4^+$ Th1 cells, cytotoxic $CD8^+$ T cells, antigen-presenting DCs, and $CD4^+$ Treg cells. As mentioned in the previous chapter, IL-6 stimulates MCP-1 expression and monocyte attraction, IL-6 directs monocyte differentiation towards macrophages instead of DCs in the TME, which are required for efficient immune response [124]. Furthermore, the macrophage population is skewed from a tumoricidal M1-type phenotype to an immunosuppressive M2-type macrophage phenotype [125]. Also, IL-6 assists accumulation of $CD4^+$ Th17 and myeloid-derived suppressor cells (MDSCs). The $CD4^+$ Th17 cells are linked to chronic inflammation in many cancers, while MDSCs suppress anti-tumor immunity and facilitate tumor growth [126]. MDSCs also produce IL-6, and in synergy with nitric oxide signaling, contribute to sustained STAT3 activation, maintaining the cancer stem cell pool [127].

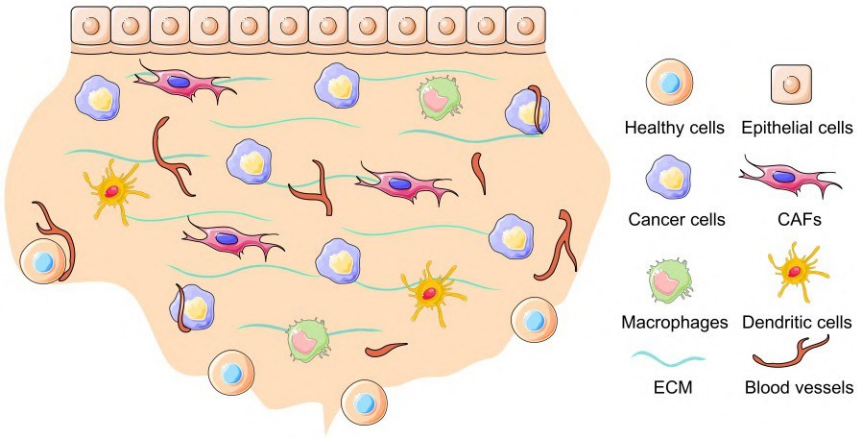

Figure 4. Tumor microenvironment. TME comprises both cellular and non-cellular components. Key cellular constituents include CAFs, endothelial cells, and various immune cells such as T-cells, B-cells, tumor-associated macrophages, DCs, neutrophils, and mast cells. These elements interact dynamically with tumor cells, promoting cancer progression through the secretion of cytokines, chemokines, and growth factors. Non-cellular components of the TME are cytokines and proteins of ECM.

1.3. Immunoglobulin A nephropathy

IgAN is the most common primary glomerulonephritis worldwide [128]. In adults' clinical presentation of the disease includes microscopic hematuria, proteinuria, and hypertension. End-stage renal disease is observed in a large cohort of patients (14-39%) within 20 years after diagnosis [129, 130]. The disease has an autoimmune origin with the kidney being a bystander in the scenario of IgAN pathogenesis. The reason for the IgAN pathology is the presence of CICs that are elevated in 50% of patients [131]. Part of the total CIC deposit in the kidney is detectable in renal biopsies with variable co-deposits, such as C3 complement, IgG, and IgM in mesangial as well as paramesangial areas [130, 132]. Generally, the CICs are formed between aberrantly glycosylated IgA1 antibodies and anti-glycan IgG or IgA autoantibodies. IgA1 has a long hinge region (HR) between C1 and C2 domains of heavy chains, which undergoes O-glycosylation at serine (Ser) and threonine (Thr) residues. Generally, glycans include GalNAc and galactose disaccharide with sialic acid attached to either or both the residues [133]. A myriad of enzymes is involved in the reaction chain, namely galNAc-, galactose-, and sialyltransferases. Thus, an aberrant glycosylation occurs as a result of galactosyltransferase and its chaperone COSMC down-regulation and sialyl-transferase up-regulation. In the case of IgAN, galactose-deficient IgA1 (Gd-IgA1) is elevated and fails to be eliminated via the liver. Gd-IgA1 are mostly found in the form of CICs that can reach 700-900 kDa size. Additionally, autoantibodies, predominantly of IgG isotype, also form complexes with IgA1 [134, 135]. Typically, IgAN is characterized as a multistep autoimmune disease, which requires several prerequisites

for pathogenesis. Four-hit hypothesis was proposed (**Figure 5**) [136]. Hit 1 is the formation of aberrantly glycosylated IgA1. Hit 2 is the development of auto-reactive IgG that targets GalNAc residues of the HR of Gd-IgA1. Hit 3 includes the formation of the IgA1-IgG and IgA1-IgA1 complexes, that can't be eliminated from the circulation via the liver. Finally, Hit 4 is the deposition of immune complexes in kidney glomeruli, which results in chronic inflammation, mesangial proliferation, and up-regulated ECM production [130].

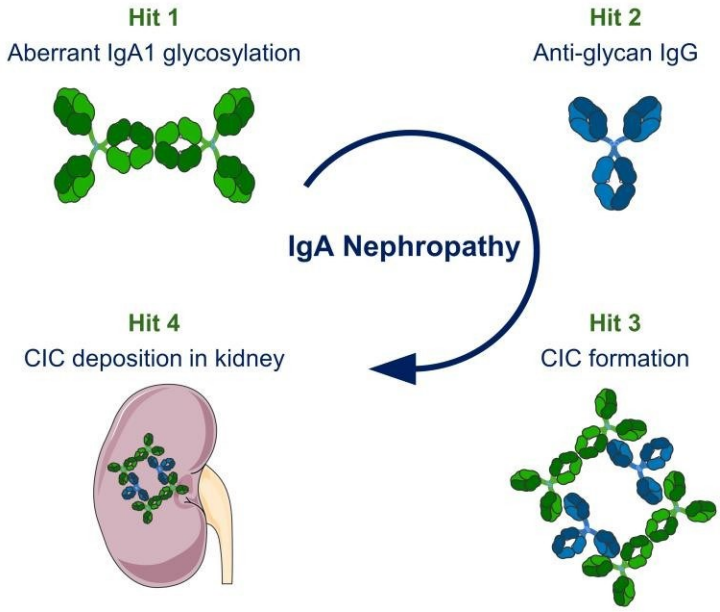

Figure 5. Four-hit hypothesis to explain IgA nephropathy pathogenesis. Hit 1 involves the formation of aberrantly glycosylated IgA1. Hit 2 is the development of auto-reactive IgG targeting GalNAc residues on the hinge region of Gd-IgA1. Hit 3 includes the formation of IgA1-IgG and IgA1-IgA1 complexes, which cannot be cleared from the circulation by the liver. Ultimately, the Hit 4 is immune complexes deposition in the kidney glomeruli, leading to chronic inflammation, mesangial proliferation, and increased ECM production.

1.3.1. Interleukin-6 role in immunoglobulin A nephropathy

Several studies have highlighted the significant role of IL-6 in IgAN progression. Investigation of biopsy samples from IgAN patients explicitly demonstrates that the urinary level of IL-6 correlates with the severity of chronic histological changes [137]. Thus, IL-6 is used as a prognostic marker [138]. Also, IL-6 contributes to kidney inflammation, which is triggered by CIC deposition. Glomerular diseases are characterized by ECM accumulation and hypercellularity, which stems from mesangial cell proliferation, monocyte/macrophage, and T lymphocyte attraction [139-143]. In the case of IgAN, mesangial cells become activated upon encounter with CICs, begin to proliferate and produce inflammatory cytokines, including IL-6 [144, 145]. Also,

trans-signaling via IL-6/ sIL-6Rα stimulates MCP-1 expression in mesangial cells further contributing to monocyte accumulation [91]. Also, in humans, IL-6 functions as a competence factor that acts together with fibroblast growth factors (FGFs) or others to stimulate mesangial cell proliferation [146]. Other glomerular cells, such as podocytes, endothelial cells, and tubular and glomerular epithelial cells, also express IL-6 [65]. It has been demonstrated that IL-6 may also contribute to endothelial cell damage by down-regulation of VE-cadherin expression and increase permeability of human renal glomerular endothelial cells [147].

Furthermore, IL-6 positively promotes immune complex deposition [148], as it contributes to abnormal IgA1 galactosylation [149, 150]. This can be explained by the observation that IL-6 modulates the activities of key glycosyltransferases. It downregulates galactosyltransferases and its chaperone COSMC and up-regulates sialyltransferases [150]. While Gd-IgA1 has also been found in healthy individuals, their secretion is highly increased in IgA1-producing cells of IgAN patients. This could be explained by abnormal signaling, as in cells from IgAN patients' amplitude and persistence of STAT3 phosphorylation is significantly increased [151]. Additionally, $CD38^{+}CD19^{+}$ plasma cells, which produce both Gd-IgA1 and anti-glycan antibodies, are found in higher numbers in patients with IgAN [152]. The origin of Gd-IgA-producing plasma cells is not precisely determined. However, there is some evidence that these cells inhabit mucosal surfaces because instances of hematuria correlate with infections in the upper respiratory tract or gastrointestinal tract infections [153]. Indeed, PAMPs-mediated TLR9 activation leads to increased IL-6 and APRIL production. IL-6 supports the proliferation of immunoglobulin-producing cells and the terminal differentiation of plasma cells.[154]. Considering that IL-6 was shown to significantly contribute to IgAN disease, progression its blockage may be a promising therapeutic strategy with higher specificity than available options up to date, aiming to reduce proteinuria, control blood pressure, and suppress the inflammatory response [153].

1.4. Inflammatory Bowel Disease

The gastrointestinal (GI) tract maintains homeostasis by balancing tolerance to non-pathogenic commensal bacteria, self-antigens, and food antigens, with an immune response against pathogenic organisms [155]. A mucus layer and single intestinal epithelial layer segregate the gut lumen from lamina propria, and is inhabited by several mucosal immune cells, such as APCs, mast cells, neutrophils, eosinophils, T and B lymphocytes, Natural killer (NK) cells and natural killer T (NKT) cells [156]. Disruption of the delicate balance within the GI immune system leads to pathologies such as IBD [155]. Despite IBD development has not been fully investigated, evidence points out

that the disease occurs because of mucosal barrier alteration and increased intestinal permeability due to environmental factors, genetic predisposition, infection, or mucosal immune dysregulation [155]. The encounter between APCs and intestinal bacterial flora triggers activation of $CD4^+$ T lymphocytes and up-regulation of inflammation mediators, namely tumor necrosis factor alpha (TNFα), interferon-gamma (IFNγ), IL-1β, IL-6, IL-8, IL-12, IL-17, IL-18, IL-23, and IL-27 [157, 158]. Although, gut antigens are continuously sensed by APCs via PRR under normal conditions, increased levels of luminal antigens lead to uncontrolled T lymphocyte activation. Also, increased expression of TLR2, TLR4, CD40, and CCR7 by the macrophages and DCs of the IBD patients promotes inflammation and pro-inflammatory cytokine up-regulation [159-162].

IBD is a chronic disease with periods of remission and relapses that lead to the damage of intestinal tissue [163-165]. It can be subdivided into Crohn's disease (CD) and ulcerative colitis (UC) [157]. Usually, IBD symptoms occur in people of young age (15 – 35 years) with equal sex distribution [164]. While UC is restricted to the mucosal layer of the colon or large intestine, CD may occur within the whole digestive tract and affects all tissue layers with granuloma formation [164-166].

As was mentioned above, macrophages and T-cells are the main contributors to IBD pathogenesis. Abnormal $CD4^+$ T cell activation is manifested as increased proliferation, enhanced migration to the intestinal mucosa, apoptosis resistance, and dysregulated cytokine production. Consequently, T lymphocytes accumulate in mucosal tissues and sustain inflammation [167-169]. However, cytokine profiles observed in UC and CD are different, thus different effector T cell subsets are involved in the pathogenesis. Th1 cells whose signature cytokines are IFNγ, and TNFα dominate in CD pathogenesis. Alternatively, in UC development, an important role belongs to Th2 cells and their respective cytokines IL-4 and IL-13. In both cases, a relatively new Th17 subset secreting IL-17A, IL-21, and IL-22 plays an important role. On the other hand, the balance between Th17 and Treg is skewed [156]. Additionally, ILC3 cells, which produce IL-17A-like Th17 cells, and ILC1 cells, which exhibit a Th1 cytokine profile, are present in increased amounts in the inflamed tissues of CD patients. [155].

The main focus of the current IBD treatment strategy is managing the inflammation and supporting the state of remission [164]. For this purpose, immunosuppressive drugs with broad effects, such as corticosteroids and aminosalicylates, are being used [170]. However, a more specific approach would be the blocking of cytokines that contribute to acute and chronic inflammation in IBD pathogenesis. Thus, inhibition of TNFα signaling with mAbs, like infliximab, adalimumab, certolizumab, and golimumab, have been proved to be a successful example for IBD treatment [155]. Also, experimental strategies targeting ILCs depletion

and lymphocytes homing inhibition are being investigated in IBD [155]. At severe stages of IBD, surgical intervention might be necessary to remove inflamed tissue. Additionally, IBD patients have a higher risk of gastrointestinal cancers, especially colorectal cancer, necessitating regular endoscopic and other screening procedures [164, 171].

1.4.1. *IL-6 role in inflammatory bowel disease*

Increased levels of IL-6 production by PBMCs and cultures have been observed from intestinal biopsy specimens of IBD patients [172, 173]. Also, the serum level of IL-6 was elevated and has predictive value for relapse risk during remission [174]. In a murine model with severe colonic inflammation induced by 2-5% Dextran Sulfate Sodium (DSS), mRNA levels of IL-6, and TNFα were elevated. DSS-induced colitis in mice mimics human UC. DSS causes epithelial damage in the colon and triggers an inflammatory response. Therefore, it is a widely used model due to its simplicity and reproducibility [175, 176].

Aberrant IL-6 production results from the intestinal barrier damage observed in IBD patients, as it has been demonstrated that LPS stimulates the up-regulation of IL-6 production [164]. Due to limited IL-6Rα expression, trans-signaling is mainly considered as the major mechanism of IL-6-mediated signaling in mucosa. Macrophages were identified as the main producers of sIL-6Rα, though T cells and epithelial cells also contribute [177]. Phosphorylation of STAT3 in response to IL-6 signaling triggers Bcl-2 and Bcl-xL expression, which in turn contributes to apoptosis resistance of lamina propria T lymphocytes [178]. Also, in IEC and Caco2 cell lines, IL-6 up-regulated ICAM-1 expression via the NF-κβ pathway, which in turn may facilitate lymphocyte recruitment [179]. Furthermore, IL-6 orchestrates T cells infiltration via chemokines (CCL4, CCL5) and chemokine receptors (CCR3, CCR4, CCR5, and CXCR3) expression [180]. Summarizing all the above, IL-6 facilitates T cell accumulation and intestinal inflammation propagation in IBD. Another role of IL-6 in the context of IBD is IL-17 up-regulation via stimulation of Th17 differentiation. It is well established that IL-23 in synergy with IL-6 promotes Th17 generation [20, 181]. Of note, Th17 cells also produce IL-6 thus contributing to the positive-feedback loop [182]. Therefore, IL-6 inhibition may be a promising therapeutic option for IBD. Interference with IL-6 signaling using mAbs successfully suppressed intestinal inflammation in IBD murine models [178, 183]. However, precautions should be taken when considering IL-6 inhibition, as this cytokine has also protective functions. For instance, it promotes the proliferation and regeneration of intestinal epithelial cells, thereby contributing to intestinal barrier integrity and mucus secretion. IL-6-deficient mice developed more

severe inflammation after DSS treatment [184-186]. Therefore, the disease stage should be considered during the IL-6-based treatment in IBD.

1.5. Biology of Interleukin-22

IL-22 is an IL-10 family cytokine [187]. It adopts a α-helical structure stabilized by two disulphide bridges with helices pre-A, and A to F connected by the loops. IL-22 can form non-covalent dimers and tetramers, although monomer is an active form of the cytokine [188, 189]. Primarily, Th17, Th22, and ILC3s are producers of IL-22. Th1 cells produce IL-22 in response to IL-12. Additionally, $CD8^+$ T cells, γδ T cells, NKT cells, and NK cells were also described to produce IL-22 [190-192].

IL-22 signals via IL-22 receptor complex, which is composed of a high-affinity subunit, IL-22R1, and a low-affinity subunit, IL-10R2. While IL-10R2 is ubiquitously expressed, IL-22R1 is more restricted; thus, it determines the cell specificity [193]. Expression of IL-22R1 is mainly restricted to the cells of non-hematopoietic origin that compose barrier tissues such as gastrointestinal and respiratory tract, and skin. Additionally, cells of the liver, kidney, and pancreas also express IL-22R1. Epithelial cells, pancreatic cells, and hepatocytes are the major targets of IL-22 signaling. IL-22R1 level in keratinocytes and dermal fibroblasts becomes upregulated in the presence of IFNγ and TNFα [194]. Therefore, IL-22 responsiveness is determined by the crosstalk between the immune system and epithelia. IL-22 is a unique interleukin as it does not regulate the immune system directly but contributes to the barrier tissue integrity and regeneration. IL-22 binds to IL-22R1 with an affinity of 1-20 nM but has no affinity for IL-10R2. However, the IL-22/IL-22R1 complex with 1:1 stoichiometry interacts with IL-10R2 with a measurable affinity of 7-45 μM [195-197]. It can be explained by the observation that structural change occurs in IL-22 upon interaction with IL-22R1 that allows cytokine interaction with IL-10R2 [195]. As a result, the assembly of IL-22R complex occurs in two steps resulting in ternary complex formation that initiates downstream signaling. Both receptor subunits are involved in the signaling of other cytokines as well. IL-10, IL-26, IL-28, and IL-29 require IL-10R2 as a part of their respective receptor complexes. IL-20 and IL-24 signal via IL-22R1 and IL-20R2 mediating very similar effects to those of IL-22. However, both IL-20 and IL-24 signal through different receptor complexes resulting in different outcomes. Therefore, IL-22R1 is a more efficient target than IL-22 because this way signalization cannot be compensated by the other cytokines [198]. Typically, IL-22R complex assembly triggers signaling via the JAK/STAT pathway, where receptor-associated JAK1 and Tyk2 become trans-phosphorylated and further phosphorylate STAT transcription factors at Tyr705. Mainly STAT3 transcription factor is responsible for the IL-22 effects, but STAT1 and

STAT5 phosphorylation is observed [199]. Other signaling pathways, namely MAPK and PI3K/mTOR also take part in IL-22 signalization [200].

IL-22 binding protein (IL-22BP) serves as an endogenous inhibitor of IL-22, playing a critical role in regulating its biological activity. IL-22BP binds IL-22 with high affinity, preventing it from interacting with IL-22R1 on epithelial cells. This inhibition is crucial for maintaining a balance between IL-22-induced protective and pathogenic effects. Under normal conditions, IL-22BP is highly expressed in the colon, providing a check on IL-22 activity. However, during acute inflammation, such as that induced by DSS, IL-22BP expression is significantly reduced [201]. It has been mentioned that multiple IL-22 effects appear in epithelial cells of the barrier surfaces, IL-22 participates in the innate immune protection of tissues (**Figure 6**). Upon signaling, antibacterial proteins (β-defensin 2 (BD2), BD3, S100A7, S100A8, S100A9, S100A12, regenerating islet-derived protein (REG) family members, and lipocalin 2), and mucus-associated proteins (mucin 1 (MUC1), MUC3, MUC10, and MUC13) expressions are upregulated [202-204]. This way IL-22 regulates natural human microflora that populates barrier surfaces in respiratory and digestive systems to ensure the defense against pathogens. For example, it was demonstrated that IL-22 is essential for host defense against *Klebsiella pneumoniae* in the lung and *Citrobacter rodentium* in the intestine [202, 204]. Also, IL-22 orchestrates chemokine production. As a result, chemokines that attract neutrophils and granulocytes (CXCL1, CXCL5, and CXCL9) become upregulated, while TH17 cell- and TH2 cell-attracting chemokine CCL22 becomes downregulated [202]. Aside from defensins and chemokines, IL-22 upregulates other cytokines that are important for immune response, such as IL-6, G-CSF, and IL-1α [204]. Therefore, IL-22 injection in mice is sufficient to trigger local or systemic inflammation. Further, IL-22 suppresses epithelial cell differentiation and enhances migration via induction of ECM-degrading enzymes MMP1 and MMP3 expression [205]. In the liver, similarly to IL-6, IL-22 induces APP production (such as serum amyloid A, α1 antichymotrypsin, haptoglobin, and lipopolysaccharide (LPS)-binding protein). Additionally, IL-22 upregulates anti-apoptotic (BCL2, BCLXL, and myeloid cell leukaemia sequence 1 (MCL1)), and cell cycle proteins (as retinoblastoma-like protein 2, cyclin D1, p21, and cyclin-dependent kinase 4 (CDK4)) expression, thus promotes cell proliferation at stressful conditions [206]. Also, IL-22 has been described to elevate antioxidant expression, such as metallothionein 1 and metallothionein 2. Importantly, IL-22 induces the proliferation and survival of progenitor stem cells, which are essential for liver regeneration in case of injury. High levels of IL-22R1 are expressed in the pancreas. However, little is known about the effects of IL-22 on pancreatic cells aside from acinar cells. In acinar cells, IL-22 induces the expression of antimicrobial, regenerative (REG3, REG3γ, and osteopontin) and anti-apoptotic proteins [207].

IL-22 can exert both protective and pathological effects. Plausibly, the outcome of the IL-22 depends on the context-dependent synergistic action with other cytokines. For instance, in case of asthma-associated lung inflammation, IL-22 was shown to reduce chemokine and Th2 cytokine production, eosinophil infiltration, and airway constriction [208]. In pancreatitis, IL-22 also had a protective effect by reducing infiltration of immune cells, serum levels of digestive enzymes, and necrosis of the pancreas in the mouse model [209]. Therefore, in such cases, supplementation of IL-22 may be a promising therapeutic intervention. On the contrary, dysregulated IL-22 signaling may invoke various pathogenic conditions such as skin diseases (psoriasis, atopic dermatitis, and acne inversa) and colorectal cancer [198]. Psoriasis was the first disease associated with abnormal IL-22 regulation, where IL-22 level in circulation is highly correlated with the disease severity. The pathology is caused by keratinocyte hyperproliferation and impaired differentiation [199, 210]. Blocking of TNFα is a promising therapeutic strategy for psoriasis treatment. Differentiation and infiltration of IL-22-producing cells (Th1, Th17, and Th22) is stimulated by TNFα. Correspondingly, application of TNFα blockers correlates with reduced expression of IL-22 and its downstream molecules, such as IL-20 and BD2 [211]. However, inhibition of IL-22 signaling may be a more specific therapeutic option with fewer side effects. In the case of cancer, IL-22 does not contribute to cancer incidence but may support tumor growth when it has already occurred [212].

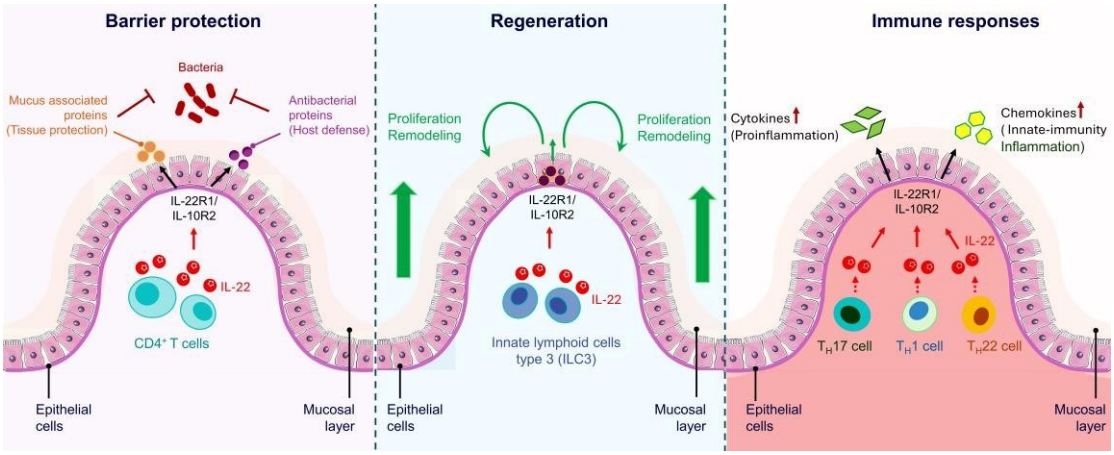

Figure 6. IL-22 functions. IL-22 acts on non-hematopoietic cells that form barrier tissues such as the gastrointestinal and respiratory tracts, and the skin. This cytokine ensures barrier protection by upregulating antibacterial proteins and mucus-associated proteins. IL-22 enhances epithelial cell proliferation and regeneration. Additionally, IL-22 orchestrates the production of cytokines and chemokines, thereby regulating the immune response and attracting neutrophils and granulocytes.

1.5.1. IL-22 in inflammatory bowel disease

Increased IL-22 levels are observed locally as well as in the blood in the case of IBD. The importance of the cytokine is underlined by the fact that IBD susceptibility genes, such as IL-23R, STAT3, and MUC1, are closely associated with IL-22 signaling [213]. In different murine models, IL-22 demonstrated a protective effect. This might be explained by the increased mucus production or enhanced epithelial cell proliferation and regeneration [214, 215]. IL-22 promotes mucosal healing by activating STAT3 and inducing the expression of anti-apoptotic and pro-proliferative genes [216, 217]. Also, IL-22 induces intestinal stem cell activation [218, 219]. On the contrary in a different context, IL-22 contributes to colitis-associated damage while cytokine neutralization ameliorates it. For instance, in some conditions, IL-22-induced epithelial proliferation may be pathogenic, resulting in epithelial hyperplasia, which causes greater intestinal pathology and weight loss [220, 221]. In DSS-treated $MSC^{-/-}$ mice increased levels of IL-6 and IL-22 were observed, accompanied by weight loss of the animals. IL-22 inhibition with IL-22BP-Ig rescued mice from the weight loss [222]. Research on IL-23R-dependent colitis in anti-CD40 models revealed that IL-22 produced by ILC3 in response to IL-23R signaling is partially responsible for the development of pathology, demonstrating the damaging effect of IL-22 overexpression. In this model, IL-22 directly or indirectly causes an increase in INFγ expression while IL-10 becomes downregulated. Additionally, a slight decrease in IL-6 level as a result of IL-22 neutralization was also observed, although the difference was not statistically significant. Furthermore, IL-22 stimulated neutrophil attraction via CXCL2 and CXCL5, thus supporting inflammation. Downregulation of (MMP)-2 and MMP-9 by IL-22 may result in decreased tissue remodeling [221, 223]. It has been reported that IL-22 is significantly elevated in Helicobacter-colonized IL-10-deficient mice and is essential for the development of spontaneous colitis. IL-22 produced by ILC3s and Th17 cells is found to be responsible for the pathological features of colitis, including epithelial hyperplasia, microbial dysbiosis, and chronic inflammation [224, 225]. Another proposed mechanism of IL-22-mediated intestinal damage is increased expression of Reg3-γ, a C-type lectin antimicrobial molecule that selectively binds and lyses Gram-positive bacteria, but not Gram-negative bacteria [226]. Disruptions in the composition of the commensal flora can potentially worsen colitis [220]. Therefore, dysregulated IL-22 expression can be harmful in the context of intestinal damage.

1.6. Checkpoint inhibition

Cancer treatment has been rejuvenated and revolutionized by the advent of immunotherapy. This therapeutic approach aims to assist the patient's immune system to recognize and attack cancer cells. There are two immunotherapeutic strategies,

involving cell therapy and immune checkpoint blockade (ICB) [227, 228]. Immune checkpoint molecules are immunosuppressive receptors on tumor-reactive T cells and their ligands on cancer cells, such as programmed cell death-1 (PD-1, CD279) and its two ligands: programmed cell death-ligand 1 (PD-L1, CD 274) and PD-L2 (CD273) [229]. PD-1 and PD-L1 balance activation signals, which are received by immune effector cells, to adjust adequate immune response. Disruption of this equilibrium due to PD-1/PD-L1 interaction blockage or constant PD-1/PD-L1 binding may lead to immune system hyperresponsiveness or suppression of immunity, respectively [227, 228, 230]. Some types of cancers abuse the PD-1/PD-L1 system to evade immune clearance due to the exhaustion of tumor infiltrating $CD8^+$ T lymphocytes [231].

PD-1 receptor is a transmembrane protein from the B7 family with co-inhibitory function. PD-1 receptor is a 288 amino acid type I transmembrane glycoprotein with size of 55 kDa [232]. Human PD-1 (hPD-1) and mice PD-1 (mPD-1) share relatively high similarity in both nucleotide and amino acid levels within the coding regions 70% and 60%, respectively [233]. Identity in 14 out of 17 residues crucial for binding is conserved between mice and human PD-1 [234]. This fact facilitates receptor investigation in murine models. PD-1 is expressed on the surface of activated, but not in resting, T lymphocytes [232, 235]. Among different T cell populations presenting PD-1, there are Treg cells, helper T cells, effector T cells, and memory T cells [227]. Other cell types, such as DC, NK cells, B lymphocytes, and some myeloid cells, can also express PD-1 [236]. On the other hand, PD-L1 is detected in cells of the immune system, pancreatic isles, placenta, epithelial cells, and some tumor cells [233, 234, 237]. At the molecular level, the PD-1/PD-L1 pathway reduces effector T cell functions by decreasing cytokine production, reducing proliferation, and inhibiting response to antigenic stimuli [232, 235].

Cancer cells can overexpress PD-L1 to deactivate tumor-infiltrated T cells [238]. In such cases, ICB therapy demonstrates high effectiveness and improves patient survival [237]. Over the last few years, ICB in combination with other therapeutic methods like radiotherapy, chemotherapy, and surgery has proven to be successful in anti-cancer treatment and has long-lasting effects. In cancers characterized with high immunogenicity, such as melanoma, non-small cell lung cancer, renal cell carcinoma, and hepatocellular carcinoma, a high response rate has been reported in up to 40% of patients [239]. Therapeutics that block the PD-1/PD-L1 pathway, including mAbs and small organic molecules, turned out to be successful in the prevention of tumor progression. Anti-PD-1 therapy characterizes a lower toxicity rate in comparison to other commonly applied standard anti-cancer treatments due to the selectivity of the immune system towards tumor antigens [237]. Currently, therapeutic approaches in

PD-1/PD-L1 axis inhibition comprise monoclonal anti-PD-1 and anti-PD-L1 antibodies (**Figure 6**).

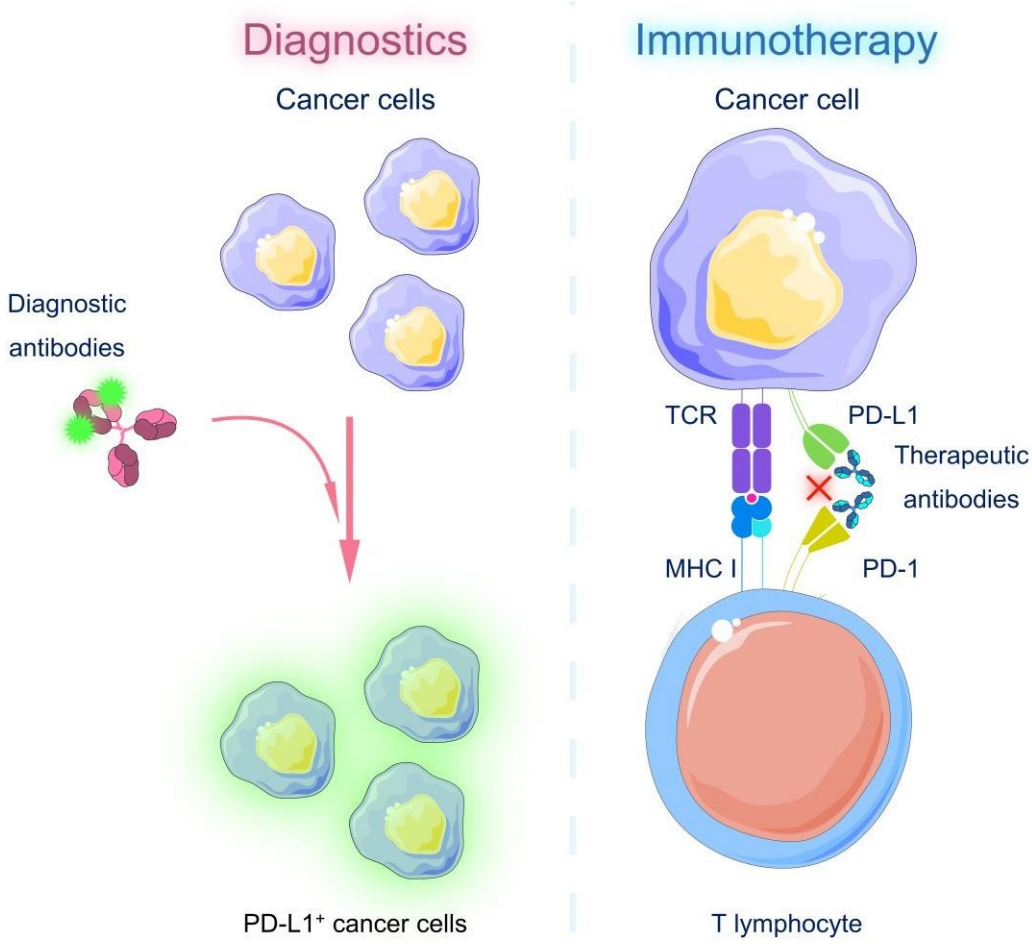

Figure 6. PD1 blockage and diagnostics. Some types of cancers abuse the PD-1/PD-L1 system to evade immune clearance. Tumor cells may overexpress PD-L1 and suppress $CD8^+$ TILs with high levels of PD-1 expression. Blocking of either PD-1 on lymphocytes or PD-L1 on cancer cells by clinically approved mAbs is a powerful therapeutic technique that allows immune cells to overcome immune checkpoint inhibition and eliminate tumor (*right*). However, prior diagnosis is required to identify patients that are the most likely to benefit from the therapy. Tumor level of PD-L1 expression is a predictive biomarker, as well as tumor-infiltrating $PD\text{-}1^+$ T lymphocytes. Diagnostic mAbs are used to assess PD-L1 or PD-1 expression (*left*).

These therapeutic antibodies have been substantially effective in the treatment of highly immunogenic cancers like NSCLC. In 2015, two mAbs targeting the PD1/PD-L1 axis were approved by the FDA for the treatment of NSCLC. Pembrolizumab was the first anti-PD-1 monoclonal antibody used in the treatment of metastatic NSCLC and another was Nivolumab [237, 238]. One of the drawbacks of mAbs is their large size causing slower clearance from the system and lower penetrance into the tumor [240, 241]. However, response to ICT is not universal, therefore robust diagnostic tools are

required to make a better treatment choice. It has been observed that depending on the level of PD-L1 in the TME, the patient's response to the ICB therapy may vary. Therefore, diagnostic antibodies are applied alongside therapeutic antibodies [242, 243]. Alternatively, adaptive immune signature in early biopsy samples, such as TILs, is a predictive biomarker for anti-PD-1 therapy efficiency [244]. Investigation of novel predictive markers and development of better diagnostic strategy would allow to help to fully realize the potential of ICB therapy.

1.7. Small protein scaffold concept

Single-domain small protein scaffold is a platform for protein binders engineering. A typical protein domain contains around 100 amino acids within the possible range of 50 to 200 [165]. The introduction of a limited number of mutations into a naturally occurring protein scaffold allows the combination of a conservative core that provides structure and randomized amino acid residues that adopt new functions. The most well-known naturally occurring protein scaffold is immunoglobulin. While most of the molecule is conserved, six CDR loops from light and heavy chains are subjected to somatic recombination and affinity maturation. Naturally occurring antibodies can recognize various antigens with high affinity and specificity. Brilliant design made immunoglobulins an invaluable tool for the vertebrate immune system, drug design, and academic research. However, immunoglobulins have a complex structure that combines multiple domains, cysteine bonds and glycosylation that makes production difficult and expensive. Also, while some antibody applications benefit from the effector function of Fc, in other cases it may be redundant.

Single-domain small protein scaffolds can improve immunoglobulin limitations while demonstrating comparable affinities and specificities. Besides, the engineering of artificial proteins offers a possibility to investigate protein design opportunities that were not selected in a course of natural evolution due to the absence of selection pressure. The main criterion for scaffold candidates is high evolutionary potential, hence the ability to adapt to new functions as a result of mutation. Favorable biophysical characteristics, such as high structural stability and water solubility, determine the evolvability of a protein scaffold [245]. Small size and an absence of disulphide bridges facilitate protein production by prokaryotic hosts or *in vitro* translation systems. New protein scaffolds may offer unique binding interfaces due to the overall fold and randomization of different structures (loops, α-helices, β-sheets, and mixed structures). Several protein-binding scaffolds have been developed and successfully tested in different applications. The most widely used scaffolds designed are Ankyrin repeats (dARPins), lipocalin domain (anticalins), and Ig-binding domain of Staphylococcal Protein A (affibodies) [246].

1.7.1. Combinatorial library

For the purpose of protein binder engineering, single-domain small protein is used as a scaffold for mutagenesis. Such a population of diversified DNA fragments is called a DNA library. A variety of methods used to generate a library of variants can be broadly divided into random and focused mutagenesis techniques. As the term implies, the former approach achieves mutagenesis in an unbiased manner across the entire gene, whereas the latter targets specific protein residues [247]. Focused randomization allows semi-rational combinatorial library design based on phylogenetic information or molecular modeling provided that the protein structure is available. A collection of synthetic DNA oligonucleotides is used to substitute wild-type residues at selected positions. Widely used methods include degenerate codons, such as the NNK (where N is any nucleotide and K is guanine or thymine) codon scheme. NNK introduces randomness at the third position of each codon, providing a controlled yet diverse representation of amino acids. This method strikes a balance between introducing diversity and maintaining a degree of specificity in the library. Disadvantages of the approach are the presence of cysteine which may lead to protein aggregation and TAG stop-codon, which may cause truncated protein production. Another notable technique is TRIM (Trinucleotide Phosphoramidite-Mediated Incorporation of Mutations), which involves the incorporation of specific trinucleotide sequences during DNA synthesis avoiding cysteine and stop codons. TRIM allows for the introduction of defined mutations at selected positions within the DNA sequence, enabling targeted diversification [248].

1.7.2. *ABD scaffold*

Albumin-binding domain (ABD) of streptococcal protein G is one of the small protein domains used for small scaffold design in our laboratory. ABD is a three-helical domain of 6 kDa size that binds human serum albumin with nanomolar affinity (PDB ID 1gjit) affinity [249, 250]. Eleven amino acids were randomized, creating a combinatorial library with a theoretical complexity of 10^{14}. Surface-exposed amino acids were selected for randomization without detrimental effects on the scaffold structure. Randomized amino acids were compactly located to create a new binding surface while holding the original 3-helical fold (**Figure 7, A**) [251]. The suitability of the ABD as a scaffold candidate and the quality of the library design were demonstrated previously by selecting high-affinity inhibitors of the IL-23 receptor [252] and IL-17 receptor A [253]. Alternatively, domain 10 of myomesin-1 protein (PDB ID 6t3o) was used to develop another scaffold, Myomedin, with a different binding geometry [254]. Two randomization concepts were applied. The Myomedin loop library contains 12

randomized residues in tree domain loops, while in the Myomedin β-sheet library, 12 randomized residues are in the β-sheet region (**Figure 7, B**).

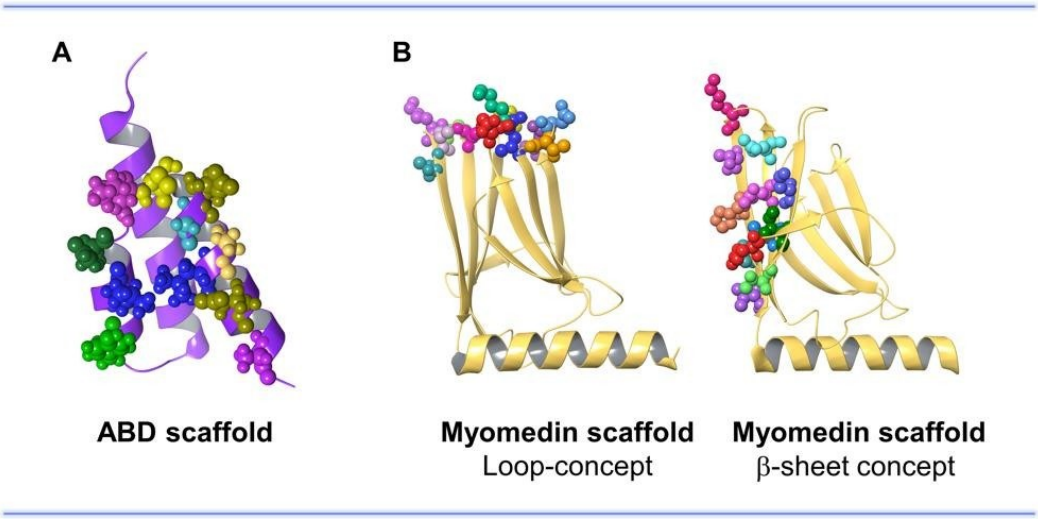

Figure 7. Small protein scaffolds. A. ABD protein structure in ribbon representation, with the 11 residues selected for randomization shown as spheres. **B.** Myomedin scaffold representation with 12 randomized residues shown as spheres. Two Myomedin randomization concepts are presented: a Myomedin loop-type library (*left*) and a Myomedin β-sheet library (*right*).

1.7.3. *In vitro display selection techniques*

A well-designed combinatorial library is likely to contain protein variants that effectively perform the required binding function. However, these few useful variants need to be filtered from a vast variety of non-binding proteins and non-folded protein sequences. Therefore, it is necessary to carry out robust selection to reduce the library to a manageable size by enriching functional protein sequences and withdrawing the majority of the rest. The selection technique broadly known as directed evolution was developed by Frances Arnold to design enzymes that function in harsh chemical conditions [255]. Directed evolution utilizes evolutionary principles to solve protein engineering problems avoiding screening of the gene variants individually. The importance of the breakthrough to academic research, chemical and pharmaceutical industries was recognized by a Nobel Prize Award in 2018. In vitro-directed evolution shares two main characteristics with Darwinian evolution. Firstly, selection is carried out within the genetically diverse population (combinatorial library). Secondly, experimental design determines selection criteria and the most "fitted" variants are positively selected from the library. Negative selection can be applied before positive selection to withdraw the least "fitted" variants. The key to implementing evolution principles *in vitro* is coupling genotype and phenotype. These can be achieved in a few ways (**Table 3**).

Table 3. Display technologies.

Method	Category	Library size	Description
Phage display	Natural particles	10^7 - 10^{11}	Uses bacteriophages to present peptides or proteins on their surfaces
Baculovirus display	Natural particles	10^6 – 10^9	Employs baculoviruses to display proteins in a eukaryotic expression system.
Yeast display	Cell-based	10^6 – 10^9	Displays peptides or proteins on the surface of yeast cells
Bacterial display	Cell-based	10^6 – 10^9	Presents proteins or peptides on the surface of bacterial cells
Mammalian display	Cell-based	10^5 – 10^8	Utilizes mammalian cells to display proteins with proper post-translational modifications.
Ribosome display	Cell-free	10^{12}	*In vitro* display technology linking proteins to their mRNA-ribosome complexes.
mRNA Display	Cell-free	10^{13}	Links peptides or proteins to their encoding mRNA for selection
Plasmid display	Cell-free	10^6 – 10^9	Uses plasmids to display peptides or proteins in various hosts
Cis display	Cell-free	10^{12}	Cell-free system where proteins are linked to their encoding mRNA.
Liposome display	Artificial vesicles	10^6 – 10^9	Incorporates peptides or proteins into liposomes for various applications

The method, known as phage display, involves the conjugation of variants from the library with a phage capsid protein so that it is expressed on the surface of a bacteriophage [256]. Analogously, cell-based methods, such as yeast display or *E. coli* display, rely on protein variant presentation on the cell surface [257, 258]. However, in both cases, cell transformation is required resulting in library size limitation [259, 260]. This obstacle can be overcome by cell-free systems such as mRNA display [261] or ribosome display [262]. Protein variants coupled with encoding DNA sequenced by one of the display technologies undergo several selection rounds to enrich the library with proteins that perform binding functions. For this purpose, protein variants are exposed to a target molecule. Variants that interact with the target molecule are collected while non-bound protein variants are withdrawn. Several iterations of a selection round iterations may be carried out with increased selection stringency conditions in each following round.

1.7.4. *Ribosome display principle*

At its core, ribosome display operates by forming stable complexes comprising mRNA, ribosome, and the nascent peptide chain (**Figure 8**). This arrangement crucially maintains the physical linkage between a protein variant and its encoding mRNA. The technique begins with the generation of a diverse library of DNA or mRNA molecules, each encoding a different protein variant. These mRNA molecules are then translated into proteins *in vitro*, but the translation process is cleverly arrested before completion by adding an antibiotic or the absence of a stop codon in a gene construct. This arrest results in the formation of the mRNA-ribosome-protein complex, effectively 'displaying' the nascent protein on the ribosome.

Subsequent steps involve the selection of protein variants that exhibit specific binding affinities. This is achieved by incubating the mRNA-ribosome-protein complexes with a target molecule, allowing binding interactions to occur. Through a series of washing steps, non-binding complexes are washed away, enriching the library with ones successfully bound to the target. The mRNA can then be isolated and amplified using reverse transcription and PCR. Then the procedure can be repeated. Ribosome display thus effectively integrates translation and selection, bypassing the need for cellular transformation and cloning, which are time-consuming and often introduce biases. The technique allows a library size of 10^{14} variants.

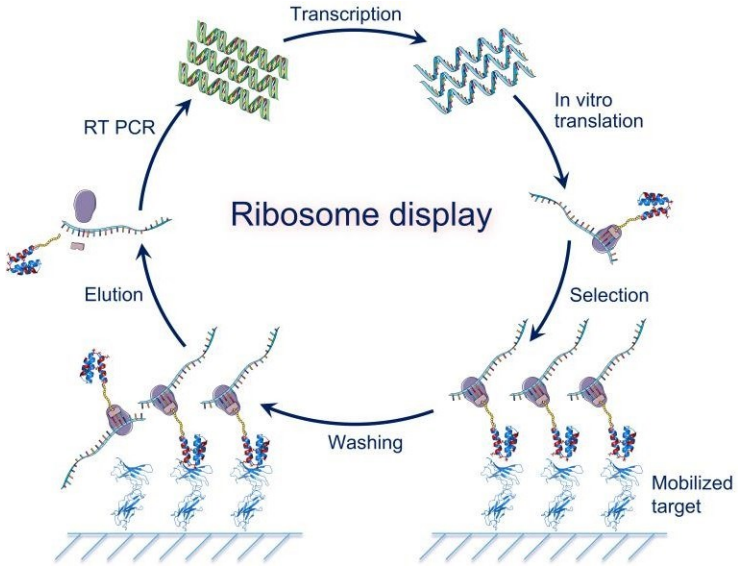

Figure 8. Ribosome display. Ribosome display is a powerful molecular biology method used in protein engineering. It allows stable complex formation between mRNA, ribosome, and nascent peptide, maintaining the link between a protein variant and its mRNA. By generating a diverse DNA/mRNA library, translating proteins *in vitro*, and arresting translation, ribosomes "display" proteins. Protein variants with desired binding affinities are selected by incubating complexes with a target, washing away non-binders, and isolating bound mRNA for amplification.

1.8. Triggering receptor expressed on myeloid cells 2

Triggering receptor expressed on myeloid cells 2 (TREM-2) is a glycosylated receptor of the immunoglobulin superfamily with anti-inflammatory function, which is predominantly expressed in myeloid cells [263]. Correspondingly, TREM-2 upregulation correlates with enhanced phagocytosis and reduced TLR-mediated inflammatory cytokine production [264-268]. On the contrary, TREM-2 downregulation reduced phagocytic activity and increased pro-inflammatory cytokine production, contributing to inflammatory injuries and disease progression [269-272]. Dysregulated TREM-2 signaling is associated with various diseases. For example, expression of mutated TREM-2 variants is associated with Alzheimer's and Parkinson's diseases [273-275]. On the other hand, dysregulated TREM-2 expression is observed in various types of cancers, such as gliomas [276, 277], triple-negative breast cancer (TNBC) [278, 279], gastric cancer (GC) [280, 281], hepatocellular carcinoma (HCC) [282], and renal cell carcinoma (RCC) [283].

TREM-2 is a 230 amino acid long protein of 26 kDa that contains V-immunoglobulin extracellular domain, trans-membrane, and intracellular regions [284]. However, a soluble form of TREM-2 that lacks a transmembrane domain also exists and transfers signals via an unknown receptor [285]. The TREM-2 receptor is associated with a signal-transducing adaptor protein DAP12 [286]. Another protein, DAP10, is also known to perform TREM-2-mediated signaling, as well as a heterodimer of both DAP10 and 12 [287]. Upon ligand binding to TREM-2, DAP12 becomes phosphorylated by Src kinase at its ITAM motifs. This phosphorylation event recruits Syk kinase, which subsequently leads to the activation of various signaling mediators [286, 288, 289]. In the TREM-2/DAP10 mediated pathway, ligand binding leads to the recruitment of PI3K and activation of grb2, leading to Akt and ERK signaling, respectively. [290]. These pathways collectively contribute to various physiological responses, including receptor-mediated phagocytosis, transcriptional regulation, metabolic homeostasis, and inflammation control [287].

According to available literature, the physiological ligands for the TREM-2 receptor are not yet known. However, numerous agents capable of binding to TREM-2 have been identified, including various anionic molecules such as phospholipids (both free and membrane-bound), deoxyribonucleic acid (DNA), low-density lipoproteins (LDL), lipopolysaccharides (LPS), bacterial products, apolipoprotein E (ApoE), and heat shock proteins (HSPs) [291-293]. Interaction with multiple ligands suggests the promiscuous nature of the TREM-2 receptor whose activation is context-dependent.

TREM-2 acts as an anti-inflammatory receptor in both adaptive and innate immunity, influencing various cell-specific functions, namely NK cell differentiation

[294], T cell regulation [268], enhanced phagocytosis [295], and anti-inflammatory responses [296]. Consequences of TREM-2 deficiency are reduced phagocytic activity and increased pro-inflammatory cytokine production, leading to inflammatory injuries and disease progression [269, 271, 297]. The scale of TREM-2 signaling is determined by its cellular expression, which is mostly restricted to myeloid cells and tissue-specific macrophages [298]. DCs [286], macrophages [299], microglia [300], mesenchymal stem cells (MSCs) [301], and NK cells [294] express TREM-2 on the membrane. For example, DCs undergo differentiation and partial maturation in response to the TREM-2 receptor activation [286]. TREM-2 signaling supports macrophage transition from pro-inflammatory to restorative states, survival in hostile environments, and phagocytic activity [302, 303]. TREM-2 influences lipid metabolism [304] and cellular energetics [305]. It enhances the clearance of apoptotic cells and debris, preventing chronic inflammation and supporting tissue repair [306].

Most of the research is concentrated on the role of TREM-2 in microglial function related to Alzheimer's disease [307, 308]. However, recent studies have expanded into the field of cancer, revealing that TREM-2 is also expressed by epithelial tumor cells, intratumoral macrophages, and myeloid regulatory cells. TREM-2 is implicated in the generation of an immunosuppressive environment to promote cancer growth [309]. It is involved in the modulation of TAMs and MDSCs, which help tumors evade the immune system [310, 311]. Targeting TREM-2 through antibody-dependent cellular cytotoxicity (ADCC) or mAbs as antagonists shows promise in reversing immunosuppression in the TME enhancing cancer immunotherapy outcomes. This discovery highlights the therapeutic potential of targeting TREM-2 in conjunction with immune checkpoint therapy [312, 313].

2. Aims of the thesis

2.1. Developing small protein inhibitors of human IL-6Rα with potential applications in cancer therapy and autoimmunity

It has been demonstrated that IL-6 signaling via its cognate IL-6R complex plays a critical role in the progression of various cancers by promoting cell proliferation, migration, and angiogenesis. Inhibition of IL-6 signaling is widely used as a therapeutic strategy for autoimmune diseases such as rheumatoid arthritis and juvenile idiopathic arthritis. This study focuses on IL-6 signal inhibition in the context of other pathologies, namely cancer and IBD. Specific blockade of the IL-6 signal can be achieved by interfering the IL-6 binding with IL-6Rα. Several molecules that block IL-6Rα have been developed, with some already approved by the FDA. Most inhibitors of the IL-6Rα are mAbs and small organic molecules. TCZ, a humanized anti-IL-6Rα mAb, is the "gold standard" for IL-6 signaling inhibition. In this project, we aimed to develop IL-6Rα-targeted small protein binders, designated NEF variants, by the selection from an ABD library capable of interfering with IL-6 binding to IL-6Rα. **More specifically aims were:**

1. To develop a collection of IL-6Rα-binding NEF variants with high affinity and specificity and investigate the binding and inhibitory properties of the best NEF variants.
2. To characterize the biophysical properties of the NEF variants including binding affinity, thermal stability, and secondary structure contents.
3. To investigate the effect of NEF binders on the proliferation and migration of melanoma, pancreatic cancer, and glioblastoma cells.
4. To compare the effects of NEF binders on cancer cell growth and migration with those of the commercial therapeutic mAb Tocilizumab, as a "gold standard".
5. To explore whether NEF binders recognize IL-6Rα on differentiated plasma cells/plasmablasts within PBMCs from human donors and verify the inhibitory potential of NEF binders for IL-6-induced plasma cell differentiation.
6. To test the most promising NEF variant for the demonstration of functional competence in the murine model of experimentally induced colitis.

2.2. Review of the recent advances in IL-6 biology and its role in IgA nephropathy development

Interleukin-6 (IL-6) is a multifunctional cytokine with both pro- and anti-inflammatory properties, playing a crucial role in immune response regulation and other physiological processes. In IgAN, IL-6 levels are elevated, leading to an increased production of galactose-deficient IgA1 (Gd-IgA1). Immunocomplex assembly between Gd-IgA1 and anti-glycan autoantibodies is the key event in disease pathogenesis,

leading to mesangial cell proliferation and glomerular injury. IL-6 inhibition has therapeutic potential for reducing these pathogenic processes. **This review aimed:**

1. To delve into the specific role of IL-6 in the development and progression of IgAN, examining the molecular mechanisms involved and the potential for IL-6-targeted therapies in managing this common form of glomerulonephritis.
2. To provide a comprehensive overview of recent advances in the understanding of IL-6 biology.
3. To review current strategies for inhibiting IL-6 signaling, with a particular focus on the therapeutic applications and limitations of these approaches.

2.3. Developing small protein inhibitors of human IL-22R1 with protective function in murine DSS-induced colitis

IL-22 is recognized as a "dual function" cytokine that serves as a master regulator in maintaining homeostasis, preserving the structural integrity of the intestinal epithelial barrier, and protecting against bacterial pathogens. However, excessive IL-22 expression is linked to hyper-proliferation and the recruitment of pathological effector cells, resulting in tissue damage and chronic inflammation in diseases such as IBD. **In this study we aimed:**

1. To develop IL-22R1 binding proteins from the ABD library by directed evolution approach, demonstrate binding specificity of the particular candidates to the cell surface IL-22R1, and characterize binding affinity and kinetics of developed small protein targeting IL-22R1.
2. To test ABD binders' ability to block IL-22/IL-22R1 interaction and inhibit IL-22 signaling *in vitro* and *in vivo*.
3. To examine the effect of IL-22R1 inhibitors in the murine model of DSS-induced colitis and investigate the potential of the IL-22 blocking strategy in reducing inflammation and epithelial damage, which may have implications in IBD treatment.

2.4. Engineering small protein binders of PD-1-targeted for diagnostic purposes

Cancers engage in immunosuppressive interactions with local immune cells via immune checkpoint molecules PD-L1/PD-1 to avoid immune surveillance and clearance, thus promoting cancer growth. Immune checkpoint inhibitors that block PD-L1 on cancer cells or PD-1 on lymphocytes demonstrated an impressive efficiency in treatment of some cancers. Among them is NSCLC, where immune checkpoint inhibitors significantly increase patient survival rate. Identification of the patients, who are likely to benefit from the checkpoint inhibition, is important for the treatment strategy selection. Currently available mAbs for prior diagnostics suffer from a variable

quality or insufficient characterization. Therefore, small protein binders with high specificity and defined quality could improve diagnostics of NSCLC patients. **In this study we aimed:**

1. To develop a collection of PD-1-targeting small protein binders (named MBA) derived from the Myomedin scaffold for *ex vivo* diagnostic and *in vivo* imaging applications.
2. To characterize affinity and specificity of the selected binders and identify the most suitable candidates for *in vivo* PET/CT imaging of PD-1^{+} cell populations.
3. To evaluate *in vivo* biodistribution and serum stability of radiolabeled MBA variants in murine models to assess their suitability for clinical diagnostic applications.
4. To explore the diagnostic potential of selected MBA variants in clinical settings, particularly for NSCLC, by comparing their binding efficacy in tissue sections with existing antibody-based diagnostics.

2.5. A review of the published data on TREM-2 molecular biology with an emphasis on its potential as a target in cancer therapy

TREM-2, a member of the immunoglobin superfamily, is frequently explained as a reminiscent receptor in different immune cells. Though TREM-2 has been widely studied in microglia, however its cellular expression and adopted signaling pathways essentially contributing the modulation of immune system under specific conditions, such as immunosuppressive environment, are not yet fully understood. **In this review we aimed:**

1. To summarize experimental evidence about TREM-2 biology, including structural biology of TREM-2 and associated ligands, downstream signaling, and TREM-2 functions in health and disease.
2. To gather information about TREM-2 cell-specific expression and its regulation, which can be of relevance for understanding how to attenuate certain diseases.
3. To discuss the potential TREM-2 inhibition as a therapeutic strategy in conditions associated with TREM-2 dysregulation, for instance cancer immunosuppressive environment.

3. Results

3.1. Small protein inhibitors of human IL-6Rα with potential applications in cancer therapy and autoimmunity

Scientific outcomes:

Publication: Groza Y, Lacina L, Kuchař M, Rašková Kafková L, Zachová K, Janoušková O, Osička R, Černý J, Petroková H, Mierzwicka JM, Panova N, Kosztyu P, Sloupenská K, Malý J, Škarda J, Raška M, Smetana K Jr, Malý P. Small protein blockers of human IL-6 receptor alpha inhibit proliferation and migration of cancer cells. Cell Commun Signal. 2024 May 7;22(1):261. DOI: 10.1186/s12964-024-01630-w. PMID: 38715108; PMCID: PMC11075285.

Patent application: Interleukin-6 receptor blocking peptides. Authors: Malý Petr, Groza Yaroslava, Smetana Karel Jr., Lacina Lukáš. PV 2024-150. Submitted on April 19, 2024.

Background: IL-6 is a multifunctional cytokine that orchestrates the immune response. Dysregulated IL-6 signaling plays a critical role in autoimmune diseases and tumor progression, making IL-6Rα a significant target for therapeutic interventions. In this research, we describe development of small protein blockers of IL-6Rα. Our focus is to investigate the impact of the developed inhibitors on cancer cell physiology. Additionally, we explore their potential applications in autoimmune diseases.

Methods: IL-6Rα-targeted small protein binders were selected from a highly complex combinatorial library using three-round ribosome display selection. Large-scale ELISA screening of individual clones in bacterial lysates was performed to recognize the best IL-6Rα binders termed NEF. Blocking efficiency and specificity of the IMAC-purified NEF binders was confirmed using binding ELISA. Blocking properties of the NEF binders were investigated using competition ELISA. Flow Cytometry and confocal microscopy were used to monitor protein binding to cell-surface IL-6Rα. Binding affinity of NEF variants to the cell-surface IL-6Rα was measured using LigandTracer. NanoDSF was used to measure the thermal stability of NEF variants. Circular dichroism (CD) spectra measurement was conducted to determine the secondary structure content of the NEF proteins. Inhibition of IL-6 signaling function of the NEF proteins was confirmed in HEK-Blue IL-6 reporter cell assay. Suppression of STAT3 phosphorylation down-stream to IL-6Rα in the presence of NEF inhibitors was demonstrated using Western blot and immunocytochemical analysis. Molecular modelling was used to predict the binding poses of NEF proteins with IL-6Rα. Effect of NEF variants on cancer cell proliferation was monitored using iCELLigence and Incucyte methods, as well as CKK-8 proliferation assay. NEF inhibitor's migrastatic potential was evaluated in scratch wound healing assay. Binding of NEF ligands to IL-6Rα on differentiated plasma cells/plasmablasts within PBMCs from human donors, as well as inhibition of IL-6-induced plasma cell

differentiation, were monitored using flow cytometry. *In vivo* studies were conducted using a mouse model of DSS-induced colitis.

Results: We developed NEF ligands, which exhibit specific binding to human IL-6Rα. After ribosome display selection from the ABD scaffold library, individual NEF variants were screened to select the best protein binders. A total of 247 NEF variants were tested in ELISA screening. We verified specific binding for 12 NEF variants to IL-6Rα. Competition ELISA experiment demonstrated that five binders (NEF054, NEF106, NEF108, NEF163, and NEF172) effectively outcompeted IL-6 for binding to IL-6Rα. Fluorescence microscopy and flow cytometry confirmed that NEF variants, except for NEF054, recognize cell-surface IL-6Rα. We then evaluated the antagonistic activity of NEF variants using the HEK-Blue IL-6 reporter cell assay, where NEF108, NEF163, and NEF172 showed significant IL-6-mediated signaling inhibition. Biophysical characterization showed that NEF variants possess nano-molar affinity for IL-6Rα, have high thermal stability and predominantly α-helical structures. Molecular modelling analysis for NEF binders revealed that the top predicted binding modes for all modelled NEF variants on the surface of IL-6Rα overlap with the natural binding site of the IL-6, supporting their experimentally observed inhibitory action. These NEF variants reduced pSTAT3 production in pancreatic adenocarcinoma cells (PaTu) and glioblastoma cells (U87MG). NEF108, NEF163, and NEF172 markedly inhibited the proliferation of malignant melanoma (G361 and A2058) and pancreatic cancer cells (PaTu and MiaPaCa), as well as significantly suppressed the migration of malignant melanoma (A2058), pancreatic adenocarcinoma (PaTu), and glioblastoma (GAMG) cells *in vitro*. We also demonstrated that NEF binders blocked IL-6-induced differentiation of primary human B cells from human PBMCs. Under *in vivo* study, NEF108 significantly reduced inflammation and tissue damage in a DSS-induced colitis mouse model.

Contribution: Within this project, I tested target protein (IL-6Rα) immobilization to immunoplate surface prior to ribosome display to determine conditions for the selection. Also, I performed large-scale ELISA screening of NEF variants in bacterial lysates and identified a collection of the IL-6Rα binding candidates. I isolated plasmids from bacterial clones carrying IL-6Rα binding candidates and analyzed sequencing data. Then, I evaluated NEF variants binding and inhibitory properties using binding and competition ELISA with IMAC-purified NEF variants. I tested NEF variants, that were selected in ELISA experiment, for their ability to recognize membrane receptor on HEK-Blue IL-6 reporter cells and transiently transfected HEK293T cells using confocal microscopy. I carried out HEK-Blue IL-6 reporter cells assay and identified NEF variants that inhibit IL-6 signaling in cells. Also, I confirmed inhibitory properties of NEF variants. Using western blot, I demonstrated that NEF variants suppress pSTAT formation in response to IL-6 signaling in U87MG cells. I performed thermal stability measurements

using NanoDSF and CD spectra measurements. I produced proteins for all collaborative experiments. During manuscript preparation, I prepared description of the experiments that I performed. Also, I assembled introduction and made research for some parts of the discussion. I illustrated my results with the graphs and prepared some graphs using raw data provided by colleagues. I actively performed the statistical analysis of the data, manuscript assembly, figure preparation, and proofread of the manuscript.

Graphical Abstract

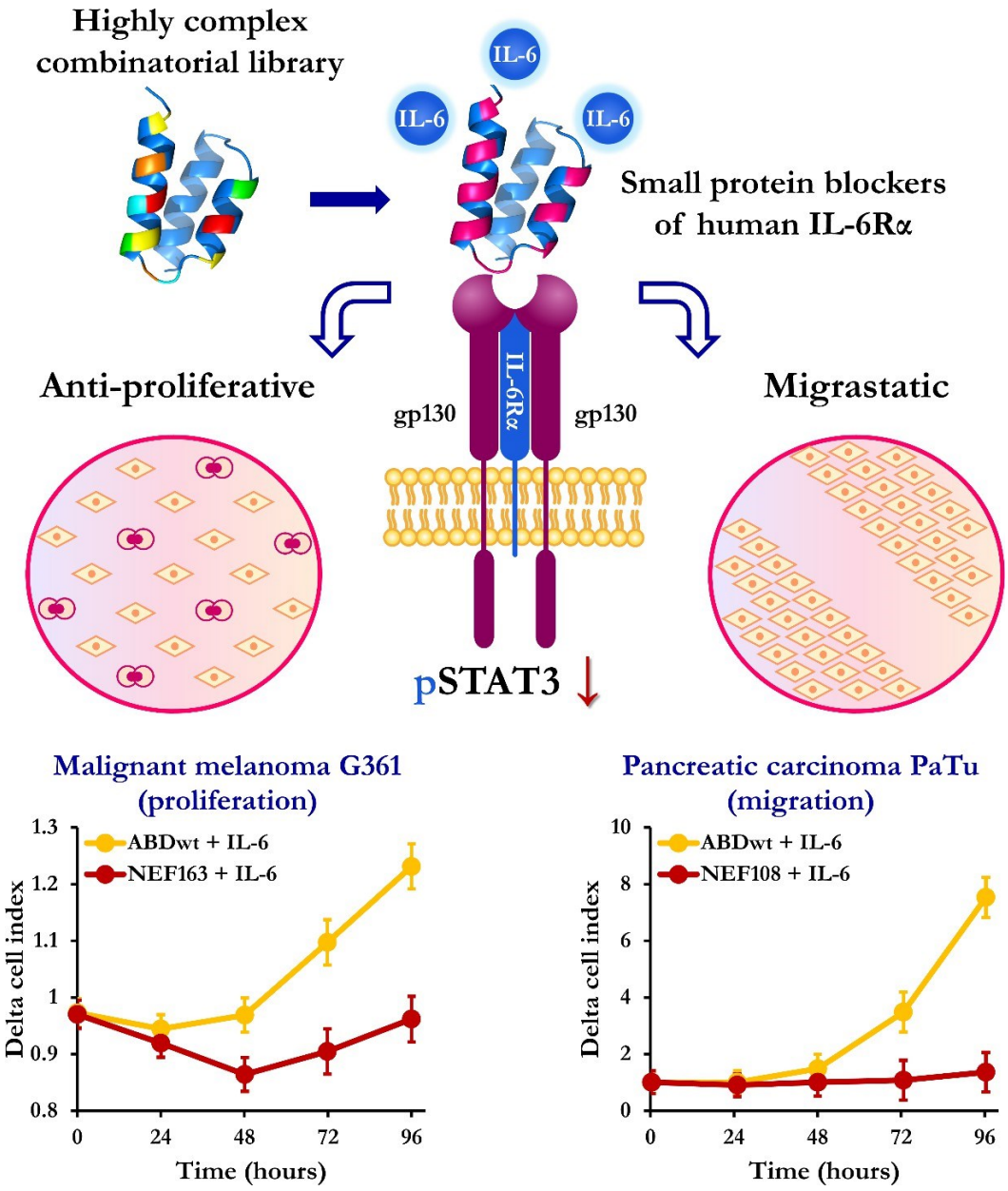

Groza *et al. Cell Communication and Signaling* (2024) 22:261
https://doi.org/10.1186/s12964-024-01630-w

Cell Communication and Signaling

RESEARCH Open Access

Small protein blockers of human IL-6 receptor alpha inhibit proliferation and migration of cancer cells

Yaroslava Groza[1], Lukáš Lacina[2,3*], Milan Kuchař[1], Leona Rašková Kafková[4], Kateřina Zachová[4], Olga Janoušková[5], Radim Osička[6], Jiří Černý[7], Hana Petroková[1], Joanna Maria Mierzwicka[1], Natalya Panova[1], Petr Kosztyu[4], Kristýna Sloupenská[4], Jan Malý[5], Jozef Škarda[8], Milan Raška[4], Karel Smetana Jr.[2] and Petr Malý[1*]

Abstract

Background Interleukin-6 (IL-6) is a multifunctional cytokine that controls the immune response, and its role has been described in the development of autoimmune diseases. Signaling via its cognate IL-6 receptor (IL-6R) complex is critical in tumor progression and, therefore, IL-6R represents an important therapeutic target.

Methods An albumin-binding domain-derived highly complex combinatorial library was used to select IL-6R alpha (IL-6Rα)-targeted small protein binders using ribosome display. Large-scale screening of bacterial lysates of individual clones was performed using ELISA, and their IL-6Rα blocking potential was verified by competition ELISA. The binding of proteins to cells was monitored by flow cytometry and confocal microscopy on HEK293T-transfected cells, and inhibition of signaling function was examined using HEK-Blue IL-6 reporter cells. Protein binding kinetics to living cells was measured by LigandTracer, cell proliferation and toxicity by iCELLigence and Incucyte, cell migration by the scratch wound healing assay, and prediction of binding poses using molecular modeling by docking.

Results We demonstrated a collection of protein variants called NEF ligands, selected from an albumin-binding domain scaffold-derived combinatorial library, and showed their binding specificity to human IL-6Rα and antagonistic effect in HEK-Blue IL-6 reporter cells. The three most promising NEF108, NEF163, and NEF172 variants inhibited cell proliferation of malignant melanoma (G361 and A2058) and pancreatic (PaTu and MiaPaCa) cancer cells, and suppressed migration of malignant melanoma (A2058), pancreatic carcinoma (PaTu), and glioblastoma (GAMG) cells in vitro. The NEF binders also recognized maturation-induced IL-6Rα expression and interfered with IL-6-induced differentiation in primary human B cells.

Conclusion We report on the generation of small protein blockers of human IL-6Rα using directed evolution. NEF proteins represent a promising class of non-toxic anti-tumor agents with migrastatic potential.

Keywords IL-6, IL-6R blockers, Cancer cell migration, Migrastatics, Malignant melanoma, Pancreatic carcinoma, GAMG glioblastoma, HEK-Blue IL-6, Protein engineering

*Correspondence:
Lukáš Lacina
lukas.lacina@lf1.cuni.cz
Petr Malý
petr.maly@ibt.cas.cz

Full list of author information is available at the end of the article

Background

Interleukin-6 (IL-6) is a pleiotropic cytokine that orchestrates multiple physiological processes. IL-6 is produced by many cells in the human body, and it is recognized by two types of cognate receptors: transmembrane and soluble [1]. IL-6 signaling is important to mediate immune responses; however, it could be misused in autoimmune diseases [2], cancer progression [3], and serious infections [4], where it can cause cytokine storm and organ failure, as observed in the COVID-19 pandemic. Thus, the IL-6 cytokine and its cognate receptor have attracted attention as important therapeutic targets [2, 4].

The IL-6 receptor complex comprises two subunits, namely interleukin-6 receptor α (IL-6Rα) and glycoprotein 130 (gp130). IL-6Rα is a non-signaling subunit that exclusively binds to IL-6. On the other hand, gp130 is a signal-transducing subunit that is shared among IL-6 family cytokines. Signaling receptor complex assembly occurs in three steps. The initial step involves the binding of IL-6 to the IL-6Rα subunit, followed by IL-6/IL-6Rα assembly with gp130. Finally, two IL-6/IL-6Rα/gp130 trimers form a hexameric complex that ensures gp130 dimerization and signal transduction [5, 6]. While gp130 is abundant in most cells of the body, membrane IL-6Rα expression is restricted to a few cell types [7]. However, IL-6 can also initiate signaling with soluble IL-6Rα, thus broadening the responsive cell type repertoire [8]. IL-6 activates several downstream pathways, but mainly Janus kinase/signal transducer and activator of transcription (JAK/STAT) [9]. Other pathways utilized for IL-6 signaling are mitogen-activated protein kinase (MAPK), phosphoinositide 3-kinase (PI3K)/Akt, and gp130/SFK/YAP [10, 11].

Multistage involvement of IL-6 in complex physiological processes has a downside. Normally, IL-6 signaling should fade out after stress resolution. However, dysregulated IL-6 signaling causes chronic inflammation and disturbs tissue homeostasis, leading to tissue damage and loss of function [12, 13]. Similarly, IL-6 also contributes to cancer development [3, 9, 14]. The IL-6 effects, which are beneficial during wound healing, are turned against the organism during tumorigenesis; hence, processes that occur during tumor development resemble those in wound healing. In both cases, IL-6 promotes cell proliferation, tissue remodeling, cell migration, and angiogenesis. Furthermore, IL-6 attracts the immunesuppressive M2 macrophages and stimulates fibroblast differentiation into cancer-associated fibroblasts (CAFs) with a myofibroblast phenotype, thus shaping tumor microenvironment (TME) [15]. The accumulation of knowledge about the role of IL-6 in normal and pathological conditions led to the hypothesis that IL-6 blocking could be a viable therapeutic strategy for some diseases. Initially, this therapeutic option was investigated in the context of autoimmunity. The first IL-6 inhibitor, Tocilizumab (TCZ; RoActemra® or Actemra®), which blocks IL-6Rα, was approved by the Food and Drug Administration (FDA) for rheumatoid arthritis treatment [16]. However, the applicability of IL-6 inhibition to other diseases, including cancer, was also investigated. The inhibition of IL-6 can affect cancer cell proliferation and metastasis by influencing cancer cells directly or via TME. Alternatively, IL-6 antagonists can be used in combination with other medicines [17].

The IL-6Rα inhibitors are mostly represented by monoclonal antibodies (mAbs) such as TCZ, Sarilumab, and Satralizumab. Several other mAbs and small molecules are in pre-clinical and clinical trials [18]. However, single-domain protein scaffolds are valuable alternatives that offer significant benefits such as fast tissue penetration and easy molecular modification. Recently, we developed a collection of small protein blockers derived from a three-helix scaffold of the albumin-binding domain (ABD) of streptococcal protein G [19] that were targeted to human IL-23 receptor and IL-17 receptor A [20, 21]. Herein, we describe the development of a set of ABD-based IL-6Rα binding proteins that exhibited a blocking effect on IL-6-mediated signaling in vitro. Our data further underscore the role of IL-6 in cancer cell proliferation and migration, and therefore can be used as a molecular clue for the development of more efficient anti-cancer therapeutics.

Materials and methods

Antibodies, recombinant proteins, and detection agents

Human (h) IL-6Rα, anti-mouse mAb-horseradish peroxidase (HRP), neutralizing anti-hIL-6R1 mAb, anti-mouse HRP-conjugated antibody, mouse IgG1κ isotype (anti-hIL-23 (p19)) were obtained from BioLegend, San Diego, CA, USA. hIL-6, anti-hIL-6R1 rabbit polyclonal antibody (pAb), and anti-Avi-Tag mouse mAb were obtained from antibodies-online, Aachen, Germany. Anti-hIL-6 rabbit pAb was obtained from AssayPro, St. Charles, AR, USA. Streptavidin-phycoerythrin (PE) was purchased from eBioscience, San Diego, CA, USA. Isotype control antibody MOPC-21 (mouse IgG1) was obtained from EXBIO Praha, a.s., Vestec, Czech Republic. Alexa Fluor 647-conjugated goat anti-mouse IgG F(ab')2 fragment (GAM-AF647) was purchased from Jackson ImmunoResearch Laboratories, West Grove, PA, USA. Pierce High Sensitivity Streptavidin-HRP and anti-CD19 mAb PE-Alexa Fluor 610 were purchased from Thermo Fisher Scientific, Waltham, MA, USA. Anti-CD38 mAb PE/Dazzle 594 was obtained from PerkinElmer, Waltham, MA, USA. PE anti-CD126 (IL-6Rα) mAb was obtained from Sony Biotechnology, San Jose, CA, USA. Anti-pStat3 (Tyr705) rabbit mAb and anti-rabbit HRP-conjugated antibody were purchased from Abcam, Cambridge, United Kingdom.

Anti-Stat3 mouse mAb was obtained from Cell Signaling Technology, Danvers, MA, USA. Anti-α-Tubulin mouse antibody was purchased from Sigma-Aldrich, St. Louis, MO, USA. Goat anti-rabbit Abberior STAR RED was purchased from Abberior, Göttingen, Germany.

HEK-Blue cell line and growth conditions

HEK-Blue IL-6 reporter cell line (InvivoGen, San Diego, CA, USA) used in the study was cultured in Dulbecco's modified Eagle's medium (DMEM) (BioSera, Cholet, France) containing 2 mM L-glutamine and 4.5 g/l glucose, supplemented with 10% heat inactivated fetal bovine serum (FBS), and antibiotics (100 U/ml penicillin, 100 µg/ml streptomycin, 100 µg/ml Normocin (InvivoGen, San Diego, CA, USA), and HEK-Blue Selection (InvivoGen, San Diego, CA, USA)) at 37 °C in 5% CO_2. For the fluorescent microscopy, medium without Normocin and HEK-Blue Selection was used. For the signaling inhibition experiments, DMEM with 100 U/ml penicillin and 100 µg/ml streptomycin was used.

Ribosome display selection

According to the ABD-derived scaffold design, 11 residues of the ABD wild type (ABDwt) domain were randomized. The combinatorial NNK library was generated by assembly PCR and purified on 1% agarose gel, as described previously [22]. The gene construct, which was used for the ribosome display selection, contained the T7p (Bacteriophage T7 RNA Polymerase Promoter), ribosome binding site (RBS), ABD variant, TolA spacer, and lacks stop codon. The ribosome display protocol was adapted from Pluckthun's laboratory protocol [22]. Ribosome display selection was carried out on the MaxiSorp immune plate (Nunc A/S, Roskilde, Sjælland, Denmark). hIL-6Rα at a concentration of 25 µg/ml was coated overnight in carbonate buffer (35 mM Na_2CO_3, 14 mM $NaHCO_3$, pH 9.6), washed with TBS buffer (50 mM Tris-HCl, 150 mM NaCl, pH 7.4), and blocked with 3% BSA in TBS for 1 h at room temperature (RT). Following assembly, the combinatorial library was transcribed and translated using the PURExpress In Vitro Protein Synthesis Kit (NEB, Ipswich, MA, USA) according to the manufacturer's instructions. 1 µg of DNA was used per 50 µl reaction. WBT buffer (50 mM Tris-acetate, 150 mM NaCl, 50 mM MgAc, pH 7.0) with 0.5% BSA and 2.5 mg/ml heparin was added to the translation mixture. Additionally, ABDwt was added to the library mixture as a blocking agent to prevent unspecific binding of the ABD variants to the highly heterogeneous MaxiSorp surface. Then, library was transferred to a well coated with 3% BSA for pre-selection at 4 °C for 1 h. For selection, the library was transferred to a well coated with hIL-6Rα for 1 h at 4 °C. Unbound variants were washed with WBT buffer containing Tween20. A varied number of wash cycles and Tween20 concentrations were used in each selection round (Table S1). mRNA of the selected variants was released from ribosomes by elution buffer (50 mM Tris-acetate, 150 mM NaCl, 50 mM EDTA, pH 7.5), containing 50 µg/ml *S. cerevisiae* RNA and 2.5 mg/ml heparin. mRNA was purified using the High Pure RNA Isolation Kit (Roche, Basel, Switzerland) and transcribed to cDNA using GoScript Reverse Transcriptase (Promega, Madison, WI, USA). The library was assembled for the next round of selection using the same PCR assembly steps as in Ref [22], and the next round of selection followed. Three rounds were carried out. Finally, the enriched ABD library was cloned into the pET28 vector using NcoI (NEB, Ipswich, MA, USA) and BamHI HF (NEB, Ipswich, MA, USA) restriction endonucleases. The obtained plasmid library was called NEF, and gene constructs included HisTag – NEF variant – FlagTag – TolA – AviTag. Finally, the plasmids were introduced into the *E. coli* BL21-Gold (DE3) strain for protein production, and individual bacterial clones were used for ELISA screening.

Protein production

The overnight cultures of individual bacterial colonies of *E. coli* BL21-Gold (DE3) transformed with a gene of interest were grown in Luria-Bertani (LB) media with 60 µg/ml of kanamycin (Km) overnight at 37 °C. Overnight culture was inoculated in LB medium with Km at 50 times dilution. After the bacterial culture had reached OD_{600} = 0.6, protein expression was induced with 1 mM isopropyl β-d-1-thiogalactopyranoside (IPTG) for 4 h at 37 °C. Bacterial cultures were centrifuged at 7000×g and 4 °C for 10 min. The cell pellets were harvested and stored at -20 °C. For the production of biotinylated protein in the *E. coli* BirA strain, a slightly modified protocol was used. Overnight cultures were grown in LB containing both Km and 30 µg/ml of chloramphenicol (Chp). Then, 50 mM d-biotin was added for 10 min. Protein production was induced with 1.5 mM IPTG for the next 4 h at 37 °C.

Bacterial lysate preparation

The harvested cell pellets were resuspended in lysis buffer (50 mM Tris-acetate, 300 mM NaCl, pH 7.4). Then, cells were disrupted on an ice bath by sonication using Misonix S3000 sonicator with the following program: total ON time 1-5 min; 5s ON/10s OFF; Power 12 W. Following, the cell lysate was centrifuged at 18,000×g and 4 °C for 20 min to remove cell debris.

Protein purification

Proteins were purified from a lysate using affinity chromatography with Ni-NTA agarose (Qiagen, Hilden, Germany) according to the manufacturer's protocol. Briefly, cell lysate supernatant collected in the previous step was

applied to 1 ml of Ni-NTA agarose, and flow-through was collected. The procedure was repeated three times, and the protein captured on Ni-NTA agarose was washed with the wash buffer (50 mM Tris-acetate, 300 mM NaCl, 20 mM imidazole, pH 8.0). Protein was eluted from Ni-NTA agarose with 1 ml of elution buffer (50 mM Tris-acetate, 150 mM NaCl, 250 mM imidazole, pH 8.0) per fraction and stored at 4 °C. To reduce endotoxin concentration, an additional purification step with isopropanol (50 mM Tris-acetate, 60% isopropanol, pH 8.0) was applied. To prepare endotoxin-free protein isolate, Polymyxin B-Agarose (Sigma-Aldrich, St. Louis, MO, USA) was used after Ni-NTA purification with isopropanol.

ELISA screening

The NEF proteins were produced in 5 ml *E. coli* BL21-Gold (DE3) bacterial culture and 1 ml cell lysates were used for the ELISA screening. Briefly, hIL-6Rα (2 µg/ml in carbonate buffer) was immobilized on the MaxiSorp plate at 4 °C overnight and blocked with Pierce Protein-Free Blocking Buffer (Thermo Fisher Scientific, Waltham, MA, USA) for 1 h at RT. Under similar conditions, lysozyme (2 µg/ml) was immobilized to test the specificity of the NEF variants. The bacterial lysate containing the NEF variant was 4,000 times diluted in PBSTB (PBS amended with 0.05% Tween20 and 1% BSA) and added in the following ELISA step. Next, after thrice washing with PBST (PBS with 0.05% Tween20), the NEF variant detection was carried out using α-Avi-Tag mouse mAb (1:5,000) and α-mouse mAb-HRP (1:5,000) in PBSTB. Following, 3,3',5,5'-Tetramethylbenzidine (TMB) (TestLine, Brno, Czech Republic) substrate was added and incubated for 30 min in the dark at RT. Then, the reaction was stopped using 2 M H_2SO_4 and absorbance at 450 nm wavelength was measured for the degraded substrate using Epoch 2 microplate spectrophotometer (BioTek, Santa Clara, CA, USA).

Sequence analysis of selected variants

Plasmids containing NEF variants were isolated using the QIAprep Spin Miniprep Kit (Qiagen, Hilden, Germany). DNA was eluted from a column using sterile water. Plasmids were sequenced using the pETup primer (5'-ATGC GTCCGGCGTAGA-3'). Sequencing data were analyzed using SnapGene software (GSL Biotech LLC, San Diego, CA, USA).

Binding ELISA

For binding ELISA, NEF variants were expressed in 100 ml culture of the *E. coli* BirA strain, and proteins were extracted and purified from lysates, as mentioned in earlier sections. Briefly, ELISA was carried out using hIL-6Rα (5 µg/ml in carbonate buffer) immobilized on the PolySorp plate overnight at 4 °C (Nunc A/S, Roskilde, Sjælland, Denmark). Also, BSA was immobilized to test the specificity of the NEF variants. Following, plates were blocked with PBSTB for 2 h at RT. Then, serially diluted, 5 times per step, NEF variants were added to hIL-6Rα and further incubated for the next 1 h RT. Neutralizing anti-hIL-6R1 mAb was used as a positive control, while mouse IgG1κ isotype (anti-hIL-23 (p19)) and ABDwt were used as negative controls. Detection was carried out using Pierce High Sensitivity Streptavidin-HRP (1:10,000) and anti-mouse mAb-HRP (1:5,000) in PBSTB. TMB was added and signal was detected as reported in previous section.

Competition ELISA

To perform competition ELISA, hIL-6Rα (1.5 µg/ml in carbonate buffer) was immobilized on the MaxiSorp plate overnight at 4 °C. Then, the plate was blocked with Pierce Protein-Free Blocking Buffer for 1 h at RT. Next, 0.25 µg/ml of hIL-6 together with an increasing concentration of the purified NEF variants in PBSTB was added and incubated for the next 1 h at RT. Anti-hIL-6R1 mAb was used as a positive control, while mouse IgG1κ isotype (anti-hIL-23 (p19)) and ABDwt were used as negative controls. Finally, hIL-6 was detected using anti-hIL-6 rabbit pAb (1:1,000) and anti-rabbit pAb-HRP conjugate (1:4,000) in PBSTB. TMB was added and signal was detected as reported in previous section.

Confocal microscopy

HEK-Blue IL-6 reporter cells were seeded on the sterile 24-well plate (TPP, Trasadingen, Switzerland) and cultured overnight. Following, hIL-6 (10 ng/ml concentration) was added to the cell culture and incubated for the next 3 h, adapted from Ref [23]. Meanwhile, in vivo biotinylated NEF variants (10 µg/ml or 250 nM concentration) were mixed with 4 µg/ml of Streptavidin-conjugated Alexa Fluor 568 (Invitrogen, Waltham, MA, USA) in DMEM, incubated for 30 min at RT, and centrifuged at 18,000×g for 10 min at RT. Afterwards, the NEF/Streptavidin complex was added to HEK-Blue IL-6 reporter cells and incubated for 5 h at 37 °C. Then, cells were washed five times with PBS and fixed with 4% paraformaldehyde (PFA) for 15 min at RT. Imaging was performed using the Zeiss LSM 780 confocal microscope. Under similar conditions, the HEK293T cell line was treated and used as a negative control to investigate the NEF specificity.

Additionally, NEF proteins detection on the hIL-6Rα-transfected HEK293T cells was also performed. Briefly, HEK293T cells were seeded on 18-mm cover glass (P-Lab, Prague, Czech Republic). After reaching 80% confluence, cells were transfected with the *hIL-6Rα* gene in the pcDNA6 vector, 1 µg DNA per transfection. Plasmid DNA was mixed with PEI at a ratio of 1:4 (w/w) and incubated for 20 min at RT. This mixture was then added

to HEK293T cells in a serum-free medium, followed by 6 h incubation at 37 °C. Afterwards, the medium was exchanged with complete DMEM medium, and cells were incubated for the next 48 h. HEK293T cells treated with PEI reagent alone (no DNA) were used as a mock control. Meanwhile, the NEF variants were labeled with fluorescein isothiocyanate (FITC) (Sigma-Aldrich, St. Louis, MO, USA), where 50 ng of FITC in dimethyl sulfoxide (DMSO) was used per 1 µg of protein, and labeling was performed in carbonate buffer (pH 9.6) for 90 min at 37 °C. HEK293T (48 h post-transfection) cells were incubated with 40 µg/ml (1 µM) FITC-labeled NEF variants in DMEM for 1 h RT. Next, cells were washed five times with PBS and fixed with 4% PFA for 15 min. Afterwards, cells were washed three times with PBS and blocked with 1.5% BSA in PBS for 30 min. Following, cells were incubated with 5 µg/ml anti-hIL-6R1 rabbit pAb and 1 µg/ml goat anti-rabbit Abberior STAR RED antibody in PBST with 1.5% BSA. Finally, cells were transferred to the glass slide (P-Lab, Prague, Czech Republic) with mounting medium Vectashield with DAPI (Vector Laboratories, Newark, CA, USA). Imaging was performed using the Carl Zeiss LSM 880 NLO confocal microscope.

HEK-Blue IL-6 reporter cell assay

For the HEK-Blue IL-6 reporter assay, 3.6×10^4 HEK-Blue IL-6 cells in 180 µl volume per well were seeded on a sterile 96-well cell culture plate (Nunc A/S, Roskilde, Sjælland, Denmark). Then, cells in each well were incubated with 2–5 ng/ml hIL-6 for 21 h in the presence of an increasing concentration (up to 10 µM) of immobilized metal affinity chromatography (IMAC)-purified NEF protein or neutralizing antibody (TCZ or anti-hIL-6R1 mAb) in 20 µl volume. After the incubation, 20 µl of cell supernatant was mixed with 180 µl of the Quanti-Blue Solution and incubated for 3 h at 37 °C in the dark. To detect the secreted SEAP, absorbance at 620 nm was measured with Epoch 2 microplate spectrophotometer.

Flow cytometry assay

Cultured HEK-Blue IL-6 and HEK293T cells were collected and washed in HEPES-buffered salt solution (HBSS buffer; 10 mM HEPES, 140 mM NaCl, 5 mM KCl, pH 7.4) supplemented with 2 mM $CaCl_2$, 2 mM $MgCl_2$, 1% (w/v) glucose, and 1% (v/v) FCS (cHBSS buffer). 2×10^5 cells/sample in HBSS-Ca/Mg buffer was incubated with 10 µg/ml of biotin-labeled ligands (NEFs and ABDwt) for 30 min at 4 °C. Following this, the cells were washed with cHBSS buffer and then incubated with PE-labeled Streptavidin (1:400) at 4 °C for 30 min. Next, cells were washed and resuspended in cHBSS buffer, and finally investigated by flow cytometry using a FACS LSR II instrument (BD Biosciences, San Jose, CA, USA) in the presence of 1 µg/ml of Hoechst 33258. Then, the collected data was processed with appropriate gatings to exclude debris, cell aggregates, and dead cells (Hoechst 33258-positive staining) using the FlowJo software (BD Biosciences, Franklin Lakes, NJ, USA). The binding data was deduced from the mean fluorescence intensities (MFI) of cell-bound ligands and expressed as relative values, with the highest MFI value of the ligand taken as 100%. For antibody binding, 2×10^5 cells/sample were incubated with anti-hIL-6R1 mAb (1:100) or IgG1κ isotype control (1:100) in HBSS-Ca/Mg buffer at 4 °C for 30 min. Next, cells were washed and incubated with the GAM-AF647 antibody (1:500) at 4 °C for 30 min. After that, cells were washed and resuspended in cHBSS buffer and then analyzed by flow cytometry as described above.

LigandTracer assay

One day before the transfection, 1×10^6 HEK293T cells were seeded on a Petri dish (Nunc A/S, Roskilde, Sjælland, Denmark) and incubated overnight in a slant position in 5% CO_2 incubator. Transfection with *hIL-6Rα* was carried out as above. Finally, after 18 h of post-transfection, binding of the NEF binders to the cell surface expressed hIL-6Rα was measured using the LigandTracer Green Line instrument (Ridgeview Instruments AB, Uppsala, Sweden) coupled with a Red (632 nm) - Near-infrared (NIR; 670 nm) detector. Herein, detection of the fluorescence signal corresponding to the in vivo biotinylated NEF binders was done as follows: (i) the baseline measurement was performed in the absence of the NEF proteins and fluorophores (only DMEM medium) for at least 15 min; (ii) during association phase, the fluorescence signal after addition of the in vivo biotinylated NEF variants preincubated with Streptavidin-APC conjugate was measured for at least 30 min (until the signal reached saturation state); and (iii) during dissociation phase, the measurement of the signal after medium exchange (DMEM only) was performed for at least 30 min (until the signal intensity was significantly reduced). Finally, the binding kinetics and 'One-to-one' or 'One-to-one depletion corrected' evaluation methods were applied for the calculation of kinetic parameters (ka, kd, and K_D) using TraceDrawer 1.7.1 software.

For competition assay, NEF variants binding to the *hIL-6Rα*-transfected HEK293T cells was detected in absence or presence of hIL6 or TCZ using above protocol with slight modifications. Briefly, upon stabilization of baseline fluorescence signal, association phase was initiated by addition of selected concentration of in vivo biotinylated NEF variant to the cells. During the association phase, an increasing concentration of hIL6 (25 and 100 nM) or TCZ (3, 50 and 300 nM) were added to the cells at a specific interval (ca. every 30 min). Finally, the dissociation was performed by exchanging the culture medium containing NEF variants, hIL6 or TCZ with the fresh

medium without additives. Under similar conditions, non-transfected HEK293T cells were treated with NEF variants and used as a negative control to investigate the NEF specificity.

Binding of NEF proteins to primary B cells

Peripheral blood mononuclear cells (PBMCs) isolation was performed in Ficoll-Paque PLUS medium (VWR, Radnor, PE, USA) using density gradient centrifugation. To get activated B cells, 2×10^6 PBMCs/ml were cultured in DMEM supplemented with 10% FBS, penicillin/streptomycin, and 5 µg PWM/ml at 37 °C for 96 h in 5% CO_2 incubator. Unstimulated PBMCs were grown in the same cultivation medium without PWM under similar culture conditions. Next, cells were divided into aliquots – 2×10^5 cells per aliquot. Each aliquot was stained with anti-CD19 mAb PE-Alexa Fluor 610, anti-CD38 mAb PE/Dazzle 594, and 1 µg of NEF binder or 5 µl of PE anti-CD126 (IL-6Rα) mAb, incubated overnight at 4 °C. For NEF binder's detection, Streptavidin-PE conjugate antibody was incubated for 30 min at RT. Samples were measured by the Sony SP6800 Spectral Cell Analyzer (Sony Biotechnology, San Jose, CA, USA) and the data was processed using FlowJo V10 software.

IL-6-mediated B cells differentiation inhibition assay

Herein, PBMCs were isolated as described in the NEF binding assay. Briefly, PBMCs were resuspended in complete RPMI 1640 medium containing 10% FBS and antibiotics (penicillin and streptomycin). Then, 1×10^6 cells per well were mounted on the 96-well panel. First, cells were incubated with 100 nM NEF binders for 2 h, and then 10 ng/ml hIL-6 was added to the cells. Following, cells were incubated for the next 7 days. On 4th day, one-half of the medium was replaced with fresh medium containing hIL-6 and NEF binders. On day 7, cells were stained for flow cytometry analysis. Herein, Fc receptors on the surface of B cells were blocked by 10% heat-inactivated human sera for 10 min at RT. After washing with PBS, anti-CD19 mAb FITC, anti-CD38 mAb PE-Texas Red, and anti-IgA mAb Pacific Blue were added to the cells, followed by 30 min incubation in the dark at RT. Finally, cells were washed with PBS and examined by the SONY flow cytometer SH800. Data was analyzed in FlowJo V10 software, and analyzed for statistical validation in GraphPad Prism software.

Cell proliferation assay

Briefly, 5×10^3 glioblastoma GAMG cells were seeded on a 96-well cultivation plate (TPP, Trasadingen, Switzerland) in 100 µl of complete DMEM. The next day, the culture medium was supplemented with a serial dilution of 1.6 µM to 0.003 µM for both the NEF binders (test) and ABDwt (negative control). Following, the cells were cultivated for the next 24 h, and the cell counting kit (CCK-8) (Sigma-Aldrich, St. Louis, MO, USA) reagent was added, followed by incubation for the next 2 h. Then, absorbance of the metabolized CCK-8 reagent was measured at 450 nm using a spectrophotometer. Finally, the proliferation rate of the cells was calculated from the calibration curve of non-treated cells, which were plated between 5×10^4 to 5×10^2 cells in 100 µl per well. The experiments for all the proteins were repeated twice in triplicates.

Scratch migration assay

The polydimethylsiloxane inserts (kindly provided by University of J. E. Purkyně in Ústí nad Labem, Ústí nad Labem, Czech Republic) were placed into wells of 6-well cultivation plates. Inserts allowed the seeding and culturing of GAMG cells into two separate chambers with a 1 mm thick partition between them. Briefly, 1×10^5 GAMG cells in 300 µl of complete DMEM (supplemented with 10% FBS and penicillin/streptomycin) were seeded in each chamber of the wells and incubated for the next 24 h. Then, the inserts were removed, which resulted in scratch (gap) formation in the wells. Following, the wells were rinsed twice with the culture medium to remove unattached cells, and the cell growth in the scratch area was checked using light microscopy. Next, the culture medium was replaced with a mixture of 2 ml of DMEM supplemented with 200 nM NEF binders (test) and ABDwt (negative control). Also, half of the samples were incubated with hIL-6 (50 ng/ml). Following, the cells were allowed to migrate in the scratch area by incubation at 37 °C for 48 h in 5% CO_2 incubator. Finally, all the wells were washed with fresh medium to remove unattached cells, and cell migration was visualized using an Olympus light microscope. All the captured images were evaluated for scratch width using the ImageJ software Fiji. The experiments for all the proteins were repeated twice in triplicates.

Cell proliferation assay by Incucyte

In this assay, 5×10^3 cells (melanoma A2058 and pancreatic PaTu cancer cell lines) per well in DMEM enriched by NEF binders or controls were seeded on the 96-well plates. The following day, the growth medium was replaced, and continuous screening was initiated using Incucyte S3 Live-Cell Analysis System (Sartorius Lab Instruments GmbH & Co. KG, Goettingen, Germany). All experiments were performed in six technical replicates (wells) using four defined points for confluence measurement every 2 h for the next four consecutive days. The resulting confluence was determined using the Incucyte Cell-by-Cell Analysis Software Module (Sartorius Lab Instruments GmbH & Co. KG, Goettingen,

Germany), and data (in%) were exported for statistical analysis.

Proliferation and cytotoxicity measurements by iCELLigence

Herein, 5 × 10^4 cells (human primary fibroblasts, melanoma (G361 and A2058) and pancreatic (PaTu and Mia-PaCa) cancer cell lines) per well in DMEM enriched by NEF binders or controls, were seeded on the E-plates L8 (8 wells). Next, the continuous cell screening was initiated using the Real-Time Cellular Analysis (RTCA) iCELLigence instrument (Agilent Technologies, Inc., Santa Clara, CA, USA) for four consecutive days in standard incubator conditions. All experiments were performed in two technical replicates (wells); visualization and analysis were performed using RTCA software, the proliferation/cytotoxicity protocol, and normalized for presentation as the Delta Cell Index according to manufacturer instructions.

Migration (wound healing) assay by Incucyte

In this assay, cells (melanoma A2058 and pancreatic PaTu cancer cell lines) were seeded at 7 × 10^4 per well in 96-well plates. The next day, the medium was replaced, and cells were preincubated with inhibitors overnight. Afterwards, standardized wounds were created using Incucyte WoundMaker - a 96-pin mechanical device, and continuous screening was initiated using the Live-Cell Analysis System Incucyte S3. All experiments were performed in six technical replicates (wells) using two defined points for wound size measurement every 2 h up to three consecutive days. The resulting wound healing data acquired using the Incucyte Scratch Wound Analysis Software Module was exported and analyzed for statistical analysis.

Analysis of pSTAT3 activity in cancer cells

Pancreatic carcinoma (PaTu) cells were seeded at a density of 2 × 10^4/cm^2 in a culture medium (DMEM supplemented with 10% FBS) and incubated for 24 h to fully attach and initiate proliferation. Consequently, the medium was replaced with a new complete medium enriched with NEF variants or ABDwt control, respectively. After overnight preincubation, cells were stimulated with hIL-6 (10 ng/ml) for 15 min and analyzed immunocytochemically. The phosphorylated STAT3 (pSTAT3) cell staining results were scored visually based on weighted intensity (assuming 0 for no staining, 1 for weak staining, 2 for moderate staining, and 3 for strong staining).. Mitotic cells are highlighted by black arrows. Examples of weakly positive nuclei (intensity = 1) are indicated by empty arrowheads, and medium-to-strongly positive nuclei (intensity = 2–3) are indicated by full black arrowheads.

Western blot

In this study, 6 × 10^5/ml U87MG cells in 2 ml were seeded on the 6-well plate overnight. Following, cell medium was exchanged with FCS-free DMEM and further incubated for 9 h at 37 °C. Then, pSTAT3 was induced by 100 ng/ml of hIL-6 in the presence of increasing concentrations of NEF variants, ABDwt, or TCZ in serum-free medium for 15 min. Next, cells were washed with ice-cold PBS and harvested with 100 µl of lysis buffer (25 mM Tris, 150 mM NaCl, 1 mM EDTA, 1% Triton, 4 mM Na_3VO_4, pH 7.4) supplemented with protease inhibitor cocktail (1:100) (Sigma-Aldrich, St. Louis, MO, USA). After that, cell lysis was carried out on ice for 30 min and samples were centrifuged using 18,000×g at 4 °C for 10 min. The supernatant was used for protein quantification with the BCA assay (Thermo Scientific, Waltham, MA, USA). Afterwards, protein (45 µg of total protein per well) was mixed with sample loading buffer (200 mM Tris-HCl, 20% Glycerol, 10% SDS, 0.05% bromophenol blue, 125 mM DTT, pH 6.8) and heated for 5 min at 95 °C. Subsequently, proteins were separated using 12% SDS-PAGE gel electrophoresis. Then, gel was transferred onto a nitrocellulose membrane (0.2 µm, Bio-Rad, Prague, Czech Republic) and blocked with 5% milk PBST (0.1% Tween20). Anti-pStat3 (Tyr705) rabbit mAb (1:2,000) and anti-rabbit HRP-conjugated antibody (1:2,000) were then used to distinguish pSTAT3. Following, the membrane was incubated with SuperSignal West Pico PLUS Chemiluminescent Substrate (Sigma-Aldrich, St. Louis, MO, USA) at RT for 1.5 min to detect the specific pSTAT3 bands. Then, imaging was made with Azure 280 (Azure Biosystems, Sierra Court Suites, AB, USA). Antibodies were stripped using stripping buffer (12 mM glycine, 50 mM NaCl, pH 2.8) for 30 min at RT. After repeated blocking with 5% milk PBST, a total STAT3 was also detected with anti-Stat3 mouse mAb (1:1,000), and Tubulin was detected with anti-α-Tubulin mouse antibody (1:100). Finally, the anti-mouse HRP-conjugated antibody (1:2,000) was used for detection as described above.

Molecular modeling

We modeled the structure of the ABD-derived NEF binders based on the structure of the wild type ABD (pdb id 1gjt [24]) as the template using the MODELLER 9v14 software suite [25]. The IL-6Rα structure was obtained from the crystal structure of the ternary IL-6/IL-6Rα/IL-6R beta (β) complex (pdb id 1p9m [5]). For protein-protein docking with flexible side chains, we utilized a local version of the ClusPro server [26, 27], using chains A and C from the 1p9m structure as the receptor (corresponding to IL-6Rα domains 1 to 3, residues 24 to 321, according to the UniProt [28] record P40189 and hIL-6Rα domains 2 and 3, residues 115 to 315, according to

the UniProt record P08887) and the modeled NEF variants as ligands. The docking results were visualized with PyMOL version 2.6.0 (The PyMOL Molecular Graphics System, Schrödinger, LLC, New York, NY, USA).

Determination of thermal stability

The fluorescence shift in tryptophan and tyrosine residues of the NEF variants in the temperature gradient was measured with the NanoDSF method using the Prometheus NT.48 instrument (NanoTemper Technologies GmbH, Munich, Germany). NEF samples were prepared in PBS (pH 7.4) at a concentration of 500 µg/ml and loaded into Prometheus Standard Capillaries (NanoTemper Technologies GmbH, Munich, Germany), followed by a rise in temperature from 20 to 80 °C at a rate of 1 °C/min. The excitation power was set at 70% while the tryptophan and tyrosine fluorescence emission intensities were measured. The resulting curves were plotted as a first derivative of the 350 nm/330 nm ratio as a function of temperature. Temperature melting points were estimated from the resulting curves.

Circular dichroism spectra measurement

Far UV circular dichroism (CD) spectra of NEF variants were measured using a Chirascan Plus spectrometer (Applied Photophysics, Surrey, UK). Samples were prepared in PBS (pH 7.4) at a concentration of 200 µg/ml. Samples were loaded into a quartz cuvette with a path length of 1 cm. The measurement was done within a range of 195–260 nm, 1 nm per step, at RT. The buffer spectra were subtracted from the resulting protein sample spectra. The analysis of CD data was done with the CDNN software (Applied Photophysics Ltd, Leatherhead, UK).

Induction and assessment of NEF108 protection in DSS-induced acute colitis

8-9 weeks old female C57Bl/6 mice (AnLab, Prague, Czech Republic) weighing between 18 and 22 g (weight before treatment) were kept under standardized conditions at a temperature of 21 -22 °C and conditions with a 12:12-h light/dark cycle and ad libitum access to food and water. We tested the effect of NEF108 protein in preventative-therapeutic regime of Dextran sulphate sodium (DSS)-induced colitis. NEF108 protein was administered by i.p. route in form of recombinant protein solution in sterile PBS once a day. Administration of NEF108 started three days before the induction of acute colitis by providing 2.5% DSS in drinking water (w/v) DSS (MW approximately 40 kDa; TdB Labs, Uppsala, Sweden) and followed for next 4 days together with DSS. At the end of experiment, the animals were euthanized by cervical dislocation in Ketamine/Xylazine anesthesia. The length of the colon was measured between the caecum and proximal rectum. The terminal third of the colon was dissected into pieces for Real Time RT-PCR (qRT-PCR) and histochemistry. Tissues for IL-1β mRNA expression was determined according to previously reported method [29]. For the elimination of DSS residues lithium chloride RNA purification was performed [30]. IL-1ß forward primer sequence was TGCCACCTTTTGAC AGTGATG and reverse primer was ATGTGCTGCTG CGAGATTTG. Tissue samples for histology were fixed in 10% neutral-buffered formalin (Merck), and paraffin-embedded. Sections were stained with hematoxylin and eosin (H&E, Merck) and classified by a pathologist without prior knowledge of treatment status of individual mouse according to the classification published by Erben et al. [31], Table S4. BX43 microscope equipped with CCD camera was employed (Olympus, Tokio, Japan). Experimental protocol was approved by Ethics Committee of the Faculty of Medicine and Dentistry (Palacky University Olomouc, Czech Republic), and the Ministry of Education, Youth and Sports, Czech Republic (MSMT-10,947/2021-3).

Statistics and reproducibility

All the experiments were performed at least two times with a minimum of technical triplicates, unless otherwise specified. GraphPad Prism version 8.0.1 (GraphPad Software Inc., San Diego, CA, USA) or OriginLab version 2023b (OriginLab Corporation, Northampton, MA, USA) was used for the statistical analysis. Error bars indicate the mean ± standard deviation (SD), unless noted otherwise. On the generated data sets, one-way ANOVA ($p < 0.05$) with Tukey's post-hoc test was marked as statistically significant. Respective significance values are also indicated in the figure legends.

Results

Identification of hIL-6Rα-binding proteins by screening of ABD combinatorial library variants

Ribosome display was used to expose the ABD library to the selection pressure. Human recombinant soluble IL-6Rα was used as a molecular target for the positive selection of protein binders in 3-round ribosome display. In each selection round, the stringency of washing conditions was increased (Table S1), and after the final selection round, an enriched cDNA library was subcloned into a pET28b vector, thus forming a plasmid library called NEF. Then, *E. coli* BL21 cells were transformed with the NEF library, and bacterial clones' lysates were tested by ELISA on a MaxiSorp plate using anti-Avitag mouse mAb and anti-mouse mAb-HRP conjugate. Lysozyme was used as a negative control for the detection of non-specific NEF variants. A total of 247 NEF protein variants were screened (Fig. S1). The NEF variants that demonstrated substantial binding to hIL-6Rα

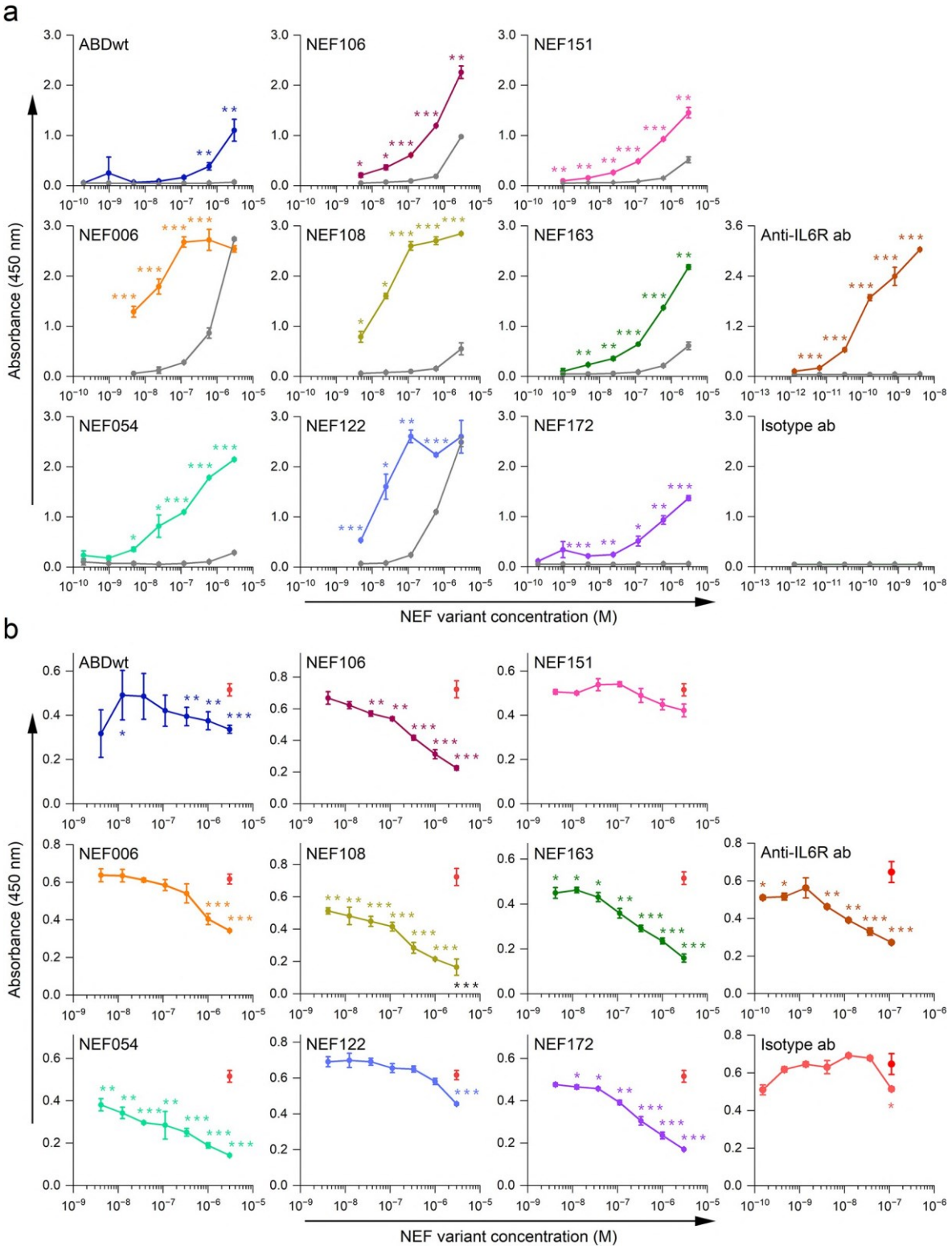

Fig. 1 (See legend on next page.)

(See figure on previous page.)

Fig. 1 Analysis of binding specificity and affinity of selected NEF variants using ELISA. (**a**) Recombinant hIL-6Rα or BSA were immobilized on the PolySorp plate. Binding of serially diluted in vivo biotinylated NEF proteins to immobilized hIL-6Rα (colored curves) or BSA (grey curve) was detected using Streptavidin-HRP conjugate and measured at 450 nm wavelength. Binding of anti-IL6R1 mAb and isotype IgG1κ to hIL-6Rα was detected with the anti-mouse-HRP conjugate. Each point depicts the average of a duplicate with SD. Statistical significance is provided for NEF proteins binding to hIL-6Rα in comparison to BSA (**b**) For competition ELISA, hIL-6Rα was immobilized on the MaxiSorp plate, and hIL-6 cytokine with different concentrations of a purified NEF variant as sample while anti-IL6R1 mAb or irrelevant IgG1κ isotype and ABDwt as controls were also added. The hIL-6 cytokine was detected by anti-IL-6 rabbit pAb, followed by anti-rabbit IgG-HRP conjugate. Red dots represent hIL-6 binding to hIL-6Rα as a control, while each colored line represents hIL-6 binding to hIL-6Rα in the presence of serially diluted NEF protein. Each point depicts the average of the triplicate readings with respective SD. Statistical significance is provided for hIL-6 binding to hIL-6Rα in the presence or absence of the NEF variants. (**a, b**) * = $p < 0.05$; ** = $p < 0.01$; *** = $p < 0.001$; ANOVA. All experiments were performed in at least two independent experiments

were selected for verification by DNA sequencing. The selection criteria for substantial binding were absorbance higher than 0.3 a.u. and a difference in measured absorbance exceeding 25% in comparison to coated lysozyme. Accordingly, plasmids carrying 40 NEF variants were isolated and sequenced. After the sequence analysis, all the mutated and redundant NEF variants were withdrawn. Consequently, a collection of 30 unique NEF variants was obtained as a result of ELISA screening.

Binding of NEF variants to hIL-6Rα tested by ELISA

The collected 30 NEF variants determined by large-scale ELISA screening were produced in *E. coli* BL21 *BirA* host cells as 38 kDa TolA fusion proteins with C-terminal biotinylation at Avi-tag. The NEF proteins were purified using IMAC chromatography and verified for specific binding to the recombinant hIL-6Rα produced in the eukaryotic expression system. The binding of serially diluted NEF variants to IL-6Rα was compared to BSA (as a negative control), which were immobilized on the PolySorp plate, and the signal was detected using Streptavidin-HRP conjugate. From the collection of 18 tested NEF variants, 12 binders exhibited a preferential binding to IL-6Rα compared to BSA (Fig. 1a). These 12 binders were selected for further analysis. The absence of ABDwt binding to hIL-6Rα indicates that binding of NEF proteins to hIL-6Rα is not an inherited property of the ABD scaffold but occurs as a result of amino acid randomization. Also, the neutralizing anti-IL6R1 mAb and mouse isotype IgG1κ binding functions were verified for the recombinant hIL-6Rα protein (Fig. 1a).

Competition of NEF proteins with IL-6 cytokine for binding to IL-6Rα by ELISA

To identify hIL-6Rα blocking variants from the collection of selected NEF binders, a competition ELISA was performed. The soluble hIL-6Rα protein was immobilized on the MaxiSorp plate, and samples of serially diluted NEF proteins with a constant concentration of hIL-6 cytokine were added. The amount of hIL-6 bound to hIL-6Rα was then detected using anti-hIL-6 rabbit pAb followed by anti-rabbit pAb-HRP conjugate. Consequently, five NEF variants (NEF054, NEF106, NEF108, NEF163, and NEF172) (Table S2) were able to outcompete hIL-6 binding to hIL-6Rα in a concentration-dependent manner. In contrast, three other variants (NEF006, NEF122, and NEF151) and ABDwt demonstrated no inhibitory potential. The neutralizing anti-IL6R1 mAb and mouse isotype IgG1κ were used as a positive and negative controls, respectively to verify ELISA experiment design (Fig. 1b).

Binding of NEF proteins to cell surface receptor tested by fluorescence microscopy

To verify whether NEF proteins recognize the cell surface hIL-6Rα, HEK-Blue IL-6 cells expressing hIL-6Rα were used. The NEF054, NEF106, NEF108, NEF163, and NEF172 were produced as in vivo biotinylated products and further labeled using Streptavidin-Alexa Fluor 568 conjugate. As shown in Fig. 2 by confocal microscopy on PFA-fixed cells, all the five NEF variants exhibited substantial binding to HEK-Blue IL-6 cells compared to non-transfected HEK293T cells without hIL-6Rα expression (Fig. 2). However, hIL-6Rα expression on HEK-Blue IL-6 is rather low for detection by confocal microscopy. Thus, NEF binding to IL-6Rα on the cell surface needs to be verified by flow cytometry.

Binding of NEF ligands to HEK-Blue IL-6 cells tested by flow cytometry

We used HEK-Blue IL-6 cells to verify the specificity of NEF binders by flow cytometry. In Fig. 3a, HEK-Blue IL-6 cells show substantial expression of IL-6Rα (IL-6R1), as confirmed by the specific binding of anti-IL6R1 mAb, in contrast to isotype antibody control or non-transfected HEK293T cells. As further shown in Fig. 3a, NEF protein variants significantly bind to HEK-Blue IL-6 cells, except for NEF054. Of interest, the strongest binding was demonstrated by NEF172 and NEF163 proteins, while ABDwt (used as a negative control) showed no binding to HEK-Blue IL-6 cells. These results further support the specificity of the tested NEF binders to the hIL-6Rα protein.

IL-6 inhibition cell assay

The HEK-Blue IL-6 reporter cell assay was used to investigate whether NEF variants inhibit the IL-6-mediated signaling in the cells. In the HEK-Blue IL-6 cells, hIL6-mediated signal transduction activates the JAK/STAT

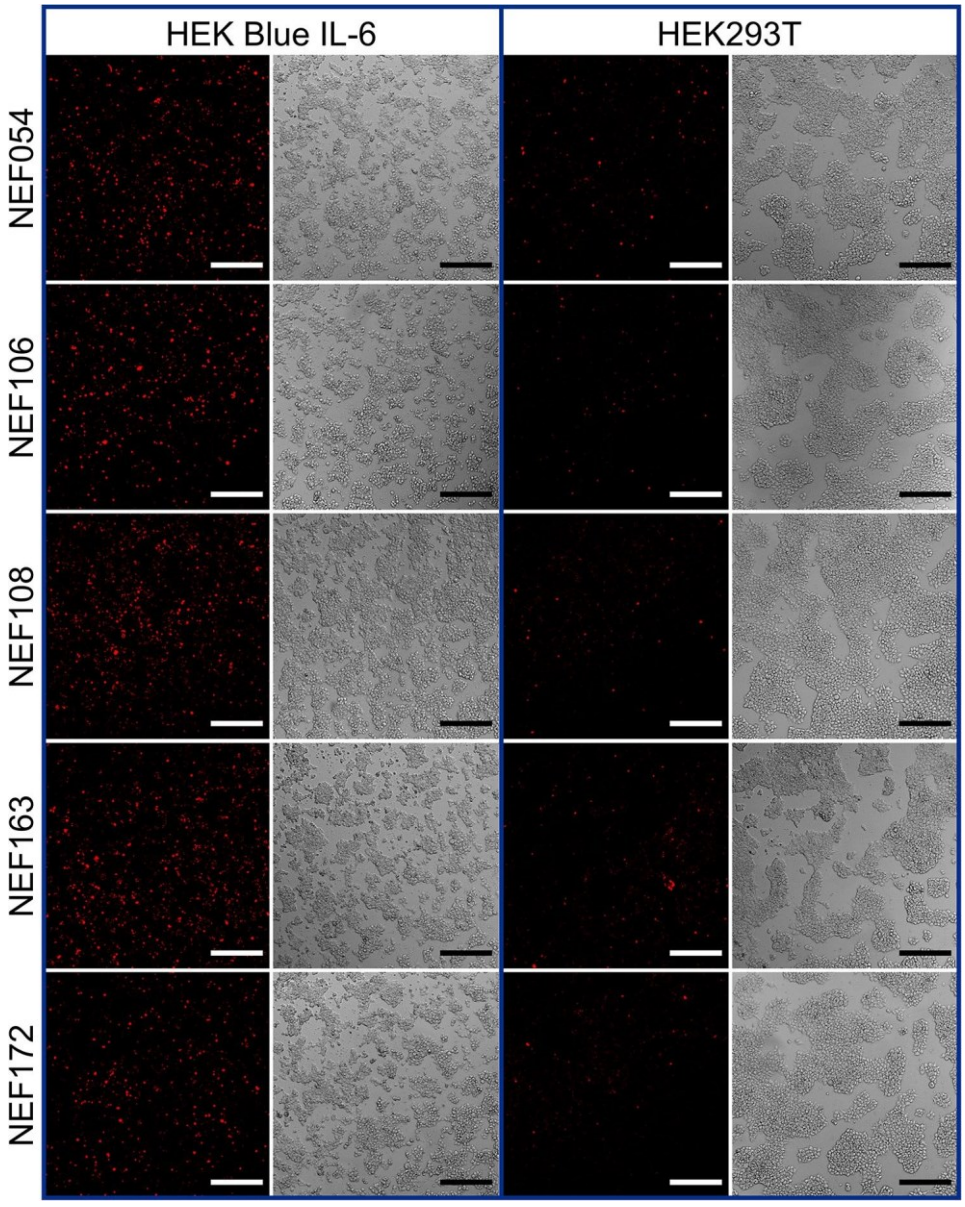

Fig. 2 Confocal microscopy with fluorescently labeled NEF variants. In vivo biotinylated NEF proteins labeled with Streptavidin-Alexa Fluor 568 conjugate (250 nM concentration) were added to hIL-6 activated HEK-Blue IL-6 and HEK293T cells. After 5 h , cells were fixed with 4% PFA, and the binding of NEF proteins was visualized using the Zeiss LSM 780 microscope. The magnification bar represents 50 µm

signaling pathway, which results in SEAP secretion in the cell culture medium that can be detected using QuantiBlue substrate. To detect inhibition of the hIL-6Rα, a constant concentration of hIL-6 was mixed with various concentrations of NEF variants and added to the reporter cells. In this assay, we investigated four NEF variants (NEF106, NEF108, NEF163, and NEF172) along with anti-hIL-6R1 mAb and TCZ (positive inhibitory controls) and ABDwt (negative control). In Fig. 3b, ABDwt did not affect hIL-6 signaling even at the highest concentration. Therefore, ABDwt does not compete with hIL-6 for hIL-6Rα binding, or induce a cytotoxic effect on HEK-Blue IL-6 cells. Likewise, no inhibitory effect was observed for NEF106. On the contrary, NEF108, NEF163, and NEF172 demonstrated a 65–70% reduction in SEAP secretion in response to hIL-6 signaling, which was relatively similar to the inhibition trend of the anti-hIL-6R1 mAb and TCZ positive controls (Fig. 3b). In particular, NEF163 showed an inhibitory effect in the concentration range of 10 nM to 10 µM, while both NEF108 and NEF172 inhibited hIL-6Rα in the range of 200 nM to 10 µM. Consequently, the competition with hIL-6 for hIL-6Rα binding observed in ELISA for NEF108, NEF163, and NEF172 was translated into functional hIL-6 signaling inhibition in the cell assay.

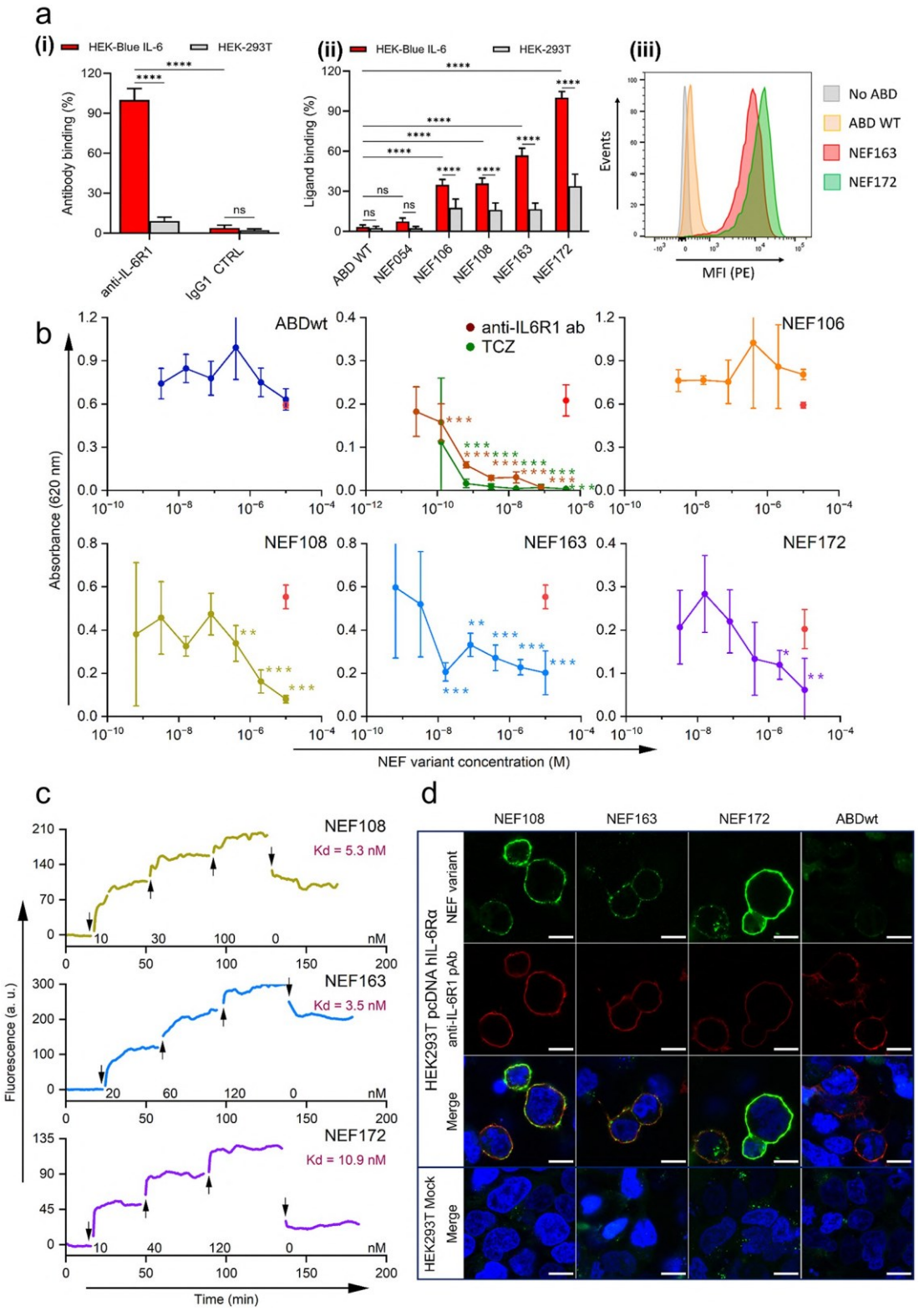

Fig. 3 (See legend on next page.)

(See figure on previous page.)

Fig. 3 (**a**) NEF ligands bind to HEK cells expressing hIL-6Rα. (**i**) Anti-IL6R1 mAb or IgG1 isotype (IgG1 CTRL) binding to HEK-Blue IL-6 and HEK-293T. MFI for anti-IL6R1 mAb measured on HEK-Blue IL-6 was taken as 100%. (**ii**) NEF variants and ABDwt binding to HEK-Blue IL-6 and HEK293T. Data were deduced from MFI and expressed as the percentage of NEF172 binding to HEK-Blue IL-6 (taken as 100%). (**i-ii**) Bars represent the average with SD of three experiments performed in duplicate (ns, $p > 0.05$; **** = $p < 0.0001$; ANOVA). (**iii**) A typical flow cytometry histogram from a representative binding experiment to HEK-Blue IL-6 is shown. (**b**) HEK-Blue IL-6 inhibition experiment. NEF variants inhibit SEAP secretion by hIL-6-induced HEK-Blue IL-6. The absorbance of the supernatant of unstimulated cells was subtracted. ABDwt was used as a negative control, neutralizing anti-hIL-6R1 mAb and TCZ – as positive controls. The red dot represents IL-6 stimulation of HEK-Blue IL-6. Each line represents IL-6 stimulation of HEK-Blue IL-6 treated with serially diluted NEF protein. Each point depicts the average of triplicate with SD. * = $p < 0.05$; ** = $p < 0.01$; *** = $p < 0.001$; ANOVA, provides the statistical significance of IL-6R-mediated SEAP secretion in the presence of NEF or ABDwt, as well as anti-hIL-6R1 mAb and TCZ in comparison to IL-6 alone. All experiments were conducted at least twice, independently. (**c**) Kinetics and binding affinity measurements of NEF variants to cell-surface IL-6Rα using the LigandTracer. The binding of NEF variants was monitored in real-time by LigandTracer method and used to calculate K_D. (**d**) Confocal microscopy with fluorescently labeled NEF variants. FITC-labeled (green) NEF variants' binding was compared to ABDwt binding to *hIL-6Rα*-transfected HEK293T and Mock-transfected HEK293T. Anti-hIL-6Rα pAb (red) was used to confirm hIL-6Rα expression. The magnification bar represents 10 μm

Kinetics and binding affinity of NEF variants to cell surface hIL-6Rα

The *hIL-6Rα*-transfected HEK293T cells were used to monitor the NEF variants' binding kinetics and affinity using the LigandTracer Green Line instrument. To measure association kinetics, the *hIL-6Rα*-transfected HEK293T cells were treated with several concentrations of the in vivo biotinylated NEF variants (NEF108, NEF163, and NEF172), labeled with Streptavidin-APC conjugate. After the signal saturation, the *hIL-6Rα*-transfected HEK293T cell medium containing NEF variants was replaced with a fresh medium to measure dissociation kinetics. Both NEF variant association and dissociation kinetics were then monitored in real-time by fluorescent signal detection via the Red-NIR detector (632–670 nm (ex/em)), and the resulting curves for each NEF variant were analyzed to calculate binding affinity (K_D) (Fig. 3c). All three variants demonstrated binding affinity in a nanomolar (nM) range, where NEF163 exhibits the highest affinity (K_D = 3.5 nM), followed by NEF108 (K_D = 5.3 nM), and NEF172 (K_D = 10.9 nM).

Further, to verify the cell surface binding of NEF variants on *hIL-6Rα*-transfected HEK293T cells, we used confocal microscopy to visualize the fluorescently labeled NEF108, NEF163, and NEF172 variants. We found that all three NEF variants bind to cell surface hIL-6Rα, as this binding co-localizes with staining of anti-hIL-6R1 rabbit pAb (Fig. 3d).

Inhibitory effect of NEF binders on hIL-6Rα-mediated pSTAT3 signaling

To further support that NEF binders inhibit pSTAT3 production, hIL-6-stimulated pancreatic carcinoma cells (PaTu cell line) were treated in the presence or absence of NEF binders and analyzed immunocytochemically (Fig. 4). We detected an increase in pSTAT3-positive cells after hIL-6 stimulation in comparison to unstimulated cells (Fig. 4a-c). Meanwhile, PaTu cells pre-incubated with NEF proteins (NEF108, NEF163, and NEF172) and stimulated with hIL-6 comparatively showed a decrease in the number of pSTA3-positive nuclei (Fig. 4d-f). Also, we observed only a small number of cells with weak nuclear positivity for pSTAT3(S727) in unstimulated cells. In mitotic cells (examples highlighted by black arrows), STAT3(S727) phosphorylation is known as a mitosis-associated event [32]. Thus, we have excluded these mitotic cells from our observations. After stimulation by hIL-6 for 15 min, we observed an increased number of pSTAT3(S727) positive nuclei in PaTu cells, including highly positive cells (highlighted by black arrowheads), and in control cells (ABDwt-treated) (Fig. 4c). In contrast, hIL-6 treatment in pretreated PaTu cells with NEF108, NEF163, and NEF172 did not show an increase in the number of positive nuclei or intensity by comparison to the control cells (Fig. 4d-f).

To further verify the role of NEF proteins on signal transduction, we detected pSTAT3(T705) in cell lysates of hIL-6-activated U87MG cells, which are reported to be hIL-6R positive [33, 34]. In Fig. 4 g, h, Western blot data confirm that NEF variants reduce pSTAT3(T705) production in U87MG cells. We also used the TCZ antibody as a positive control and ABDwt parental non-mutated scaffold protein as a negative control (Fig. 4 g, h). The NEF172 variant was found to be the strongest inhibitor, while NEF163 and NEF108 exhibited only a moderate or weak inhibitory effect on STAT3(T705) phosphorylation (Fig. 4h). Overall, this observation demonstrates the effect of NEF proteins on the inhibition of IL-6R-mediated signal transduction.

Effect of NEF binders on human primary dermal fibroblasts and malignant melanoma cells

The chimeric protein composed of hIL-6 and its receptor β-mimicking the transactivation pathways of soluble hIL-6 receptors occupied with hIL-6 influenced the normal human primary fibroblast DFO35 (Fig. 5a). The proliferation of DFO35 is not affected by a high dose of LPS, as demonstrated in Figures S2 and S3. Also, the application of hIL-6 and NEF binders to DFO35 cell culture has practically no effect on their growth characteristics (Fig. 5b). On the other hand, the application of hIL-6 to the culture of both cutaneous melanoma G361 and A2058 cells exhibited a small effect on their growth characteristics (Fig. 5c, d). The NEF binders to hIL-6Rα were

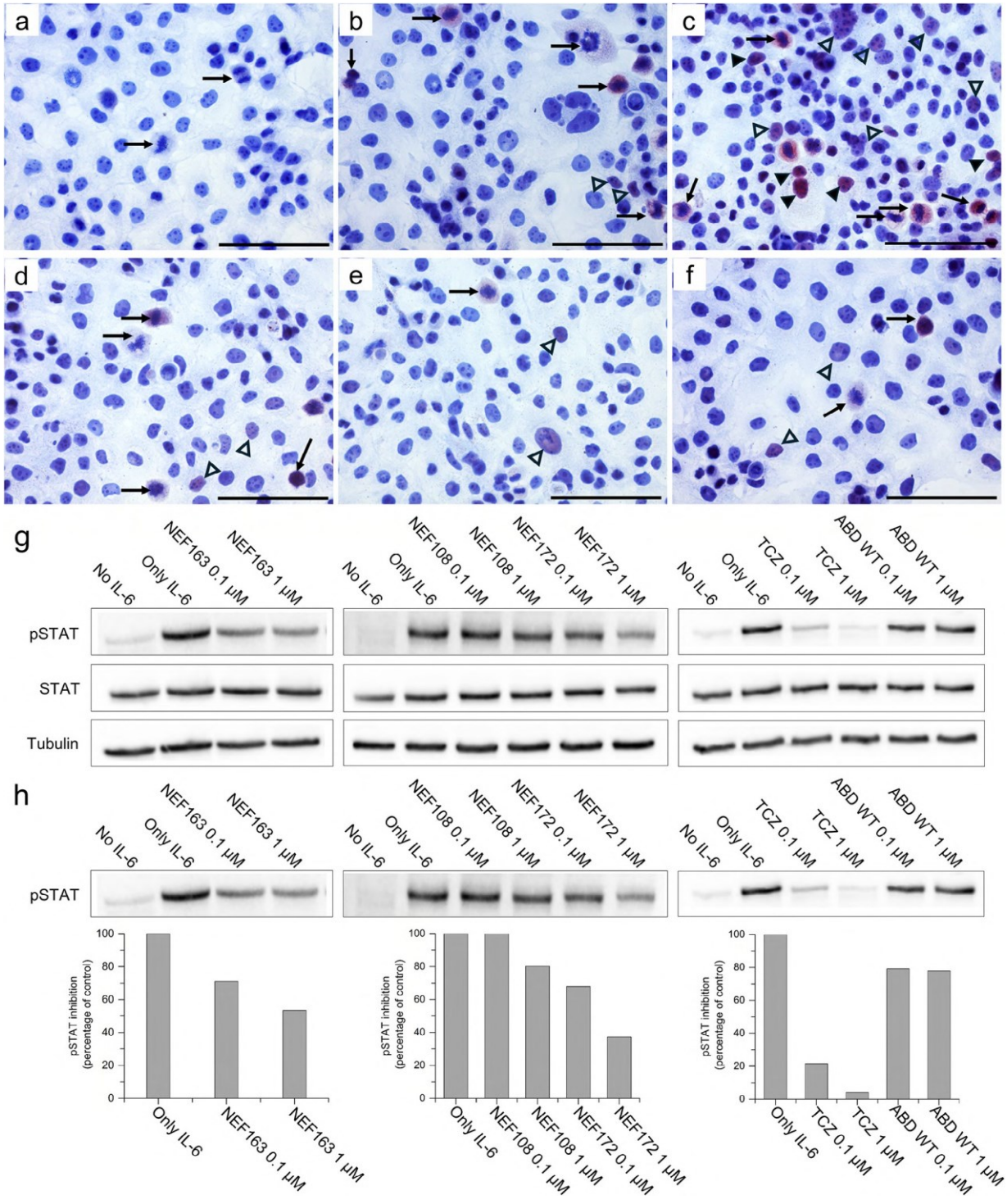

Fig. 4 Analysis of NEF binders inhibitory activity on pSTAT3 production in carcinoma cells. (**a-f**) Immunocytochemical analysis of pSTAT3(S727) staining in pancreatic carcinoma PaTu cells; (**a**) negative control, (**b**) ABDwt pretreated cells without IL-6 stimulation, (**c**) ABDwt pretreated cells after IL-6 stimulation, (**d**) NEF108 pretreated cells after IL-6 stimulation, (**e**) NEF163 pretreated cells after IL-6 stimulation, and (**f**) NEF172 pretreated cells, after IL-6 stimulation. The magnification bar represents 100 µm. (**g, h**) Analysis of the inhibitory effect of NEF proteins on STAT3(T705) phosphorylation by Western blot on U87MG glioblastoma cells. (**g**) Cells were incubated in serum-free medium for 9 h. Afterwards, activation of pSTAT3 was carried out using hIL-6 in the presence of NEF binders for 15 min. TCZ antibody and ABDwt were used as positive and negative controls. Cells were lysed and protein concentration was calculated. The total protein amount per lane was 45 µg. Detection of bands on the membrane was performed by rabbit anti-pSTAT3(T705) mAb, anti-Stat3 mouse mAb, anti-alpha Tubulin mAb, and anti-rabbit-IgG-HRP or anti-mouse IgG-HRP conjugates, respectively. (**h**) Densitogram of the signal measured for pSTAT3(T705) in U87MG cell lysates evaluated by the ImageJ software.

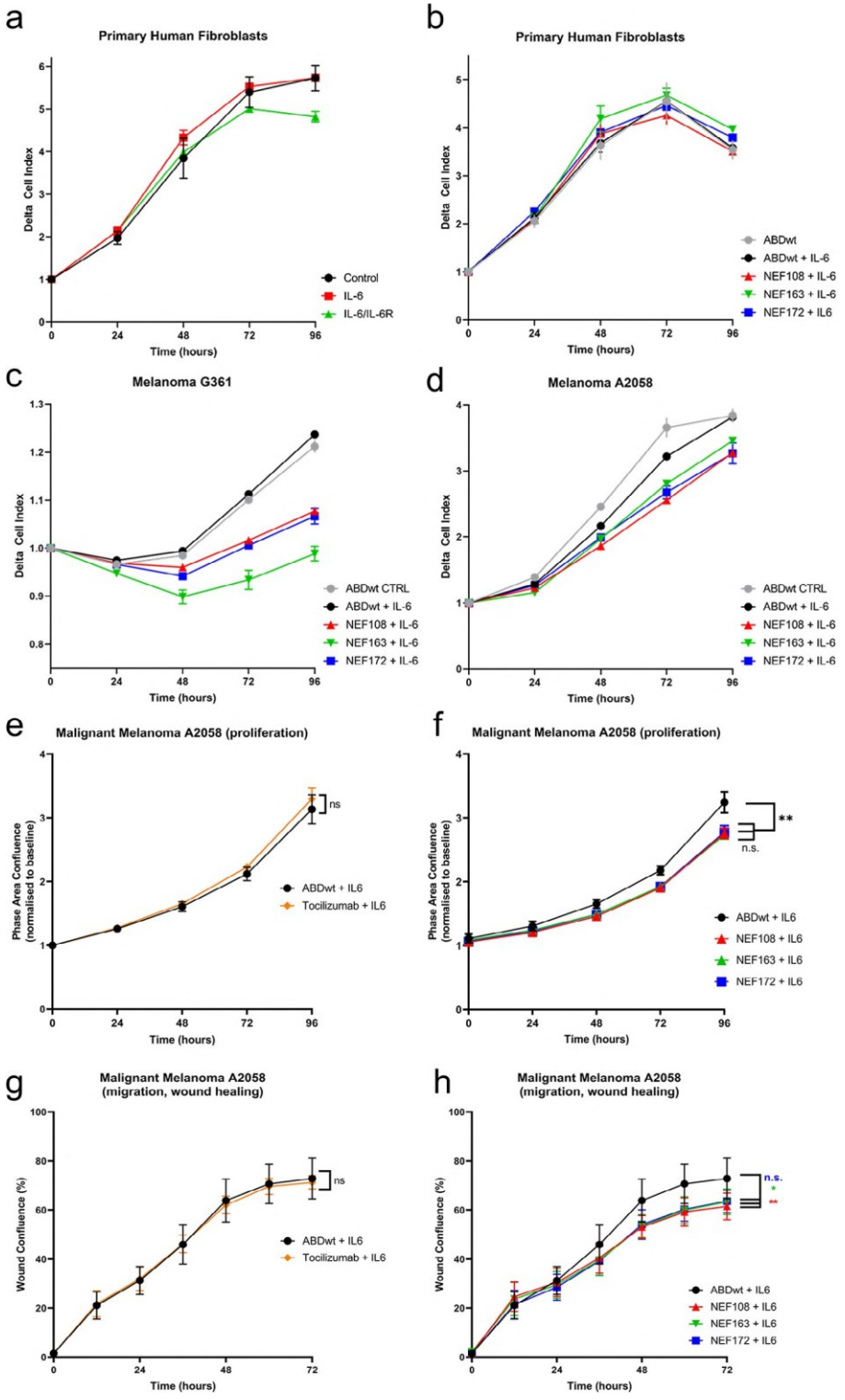

Fig. 5 Effect of NEF binders on cell proliferation and migration. (**a-d**) Cell proliferation assay (iCELLigence). (**a**) The effect of IL-6 and chimeric proteins composed of IL-6 and IL-6R (IL-6/IL-6Rα) was compared with the growth of non-influenced control fibroblasts. (**b, c, d**) Effects of the proteins ABDwt (control), (**b, c, d**) ABDwt + IL-6, (**b, c, d**) NEF108 + IL-6, (**b, c, d**) NEF163 + IL-6, and (**b, c, d**) NEF172 + IL-6, are shown on (**a-b**) human primary fibroblasts, (**c**) melanoma cells G361, and (**d**) A2058. (**e, f**) NEF inhibitors also reduce proliferation of A2058 melanoma cells measured by automatic optical instrumentation (Incucyte) in comparison to ABDwt and monoclonal humanized TCZ antibody. (**g, h**) Scratch test measurements using Incucyte instrumentation and software. Among the three tested NEF binders, NEF108 significantly reduces the migration of A2058 melanoma cells in comparison to the clinically employed TCZ antibody. Herein, * = $p < 0.05$; ** = $p < 0.01$, and n.s. = not significant provides the statistical significance of the data

not toxic for both studied cell lines. Melanoma cells were sensitive to the NEF binders, but the results were cell line specific, with a higher effect on G361 cells than on A2058 cells (Fig. 5c, d). The highest efficiency was observed for binder NEF163 in G361 cells (Fig. 5c). The inhibitory effect of NEF proteins on the proliferation of A2058 cells was also confirmed by an independent method using Incucyte (Fig. 5e, f). In addition, substantial suppression of A2058 melanoma cell migration was observed using the Scratch wound healing assay by Incucyte (Fig. 5g, h).

NEF binders suppress proliferation and migration of pancreatic cancer cells

The inhibitory effect of NEF proteins on the proliferation of MiaPaCa pancreatic cancer cells was also observed (Fig. S4). The gold standard for hIL-6Rα inhibition is the humanized monoclonal TCZ antibody, which was clinically approved. The effect of supplementation of this antibody to the culture medium on the growth characteristics of the PaTu cell line (ductal adenocarcinoma of the pancreas) was observed. However, it was negligible even after stimulation by hIL-6 (Fig. 6a). The application of NEF binders to these cells was more efficient; namely, the application of the NEF108 binder induced the highest effect (Fig. 6b). The result of the MTT test and microscopic observation demonstrated that this binder is not toxic because the MTT test showed a good metabolic condition of cells based on the NADH-dependent oxidoreductase activity of mitochondrial enzymes (Fig. 6c, d). The difference in the measurements (iCELLigence) between the application of ABDwt with hIL-6 and NEF108 with hIL-6 is, therefore, conditioned by the reduced migration activity of PaTu cells after NEF108 treatment (Fig. 6c, d). The automated scratch assay (IncuCyte) supported the observation and clearly demonstrated the statistically significant anti-migratory effect of NEF108 application to PaTu cells (Fig. 6e-g).

To verify the effect of NEF proteins on the proliferation of PaTu cells, we performed an independent cell proliferation assay using Incucyte (Fig. 7a-d). While we did not observe any substantial effect of TCZ on PaTu cell proliferation (Fig. 7a), we confirmed a prominent inhibition of the NEF108 variant (Fig. 7b). Similarly, TCZ had no effect on the migration of PaTu cells tested by Incucyte in the wound healing assay (Fig. 7c). In correlation to PaTu proliferation data, NEF108 exhibited the most prominent inhibitory effect on cell migration (Fig. 7d). Thus, the three selected NEF binders exhibit a considerable anti-proliferation and anti-migration effect on pancreatic cancer cells.

Expression of IL-6 and IL-6Rα on PaTu cells and staining with NEF variants

PaTu cells strongly expressed hIL-6 (Fig. 7e), and the receptor for this cytokine (hIL-6Rα) was also detected in vitro (Fig. 7f). STAT3 (Fig. 7g), the principal downstream effector of the hIL-6 signaling pathway, was detected in cells; it was phosphorylated (on serine 727, pSTAT3) upon hIL-6 stimulation and present in nuclei (Fig. 7h). PaTu cells bind NEF variants with high affinity (NEF108 - Fig. 7i, NEF163 - Fig. 7j, and NEF172 - Fig. 7k). This contrasted with the ABDwt control, which did not bind to the cells (Fig. 7l). Negative controls for in vivo biotinylated proteins were performed using HRP-labeled Extravidin (Fig. 7m), and negative controls for antibody-based staining used isotype immunoglobulins (Fig. 7n).

Effect of NEF binders on migration and proliferation of GAMG glioblastoma cells and binding pose prediction for NEF proteins

The migration assay using GAMG cells shows the highest anti-migration potential of NEF172 (in average 200 µm), followed by NEF163 (in average 100 µm). The NEF108 did not show any substantial anti-migration effect (Fig. 8a); similarly, the ABDwt control showed no scratch gap (Fig. 8b). The incubation with hIL-6 increases the anti-migration effect of both NEF172 and NEF163 proteins (Fig. 8a). In the case of NEF172, the scratch gap was increased to 300 µm, and in the case of NEF163, to 150 µm (Fig. 8a, c, d). The incubation with hIL-6 did not change the effect of NEF108 (Fig. 8a).

Additionally, the effect of NEF proteins on the proliferation of GAMG glioblastoma cells was tested. Cells were incubated with different concentrations of NEF ligands for 24 h, and cell numbers were estimated by the CCK-8 kit. Results are presented as a floating bar chart in Fig. 8e; only the variant NEF172 demonstrated an inhibitory effect on proliferation of GAMG cells at the highest concentration.

To explain the observed inhibitory function of the NEF variants, we performed binding mode prediction on IL-6Rα (Fig. 8k-m). The top three predicted binding modes for all modeled NEF variants share a common site on hIL-6Rα. A comparison of the NEF binding prediction to the existing crystal structure of the hIL-6/hIL-6Rα complex (Fig. 8n) reveals that the natural hIL-6/hIL-6Rα binding site overlaps with the predicted NEF binding modes, supporting the experimentally observed inhibitory action of NEF variants.

Biophysical characterization of NEF binders

To estimate the thermal stability of the NEF variants (NEF108, NEF163, and NEF172), melting temperature was measured using the NanoDSF method (Fig. S5). The melting temperature of NEF variants (NEF-TolA) was

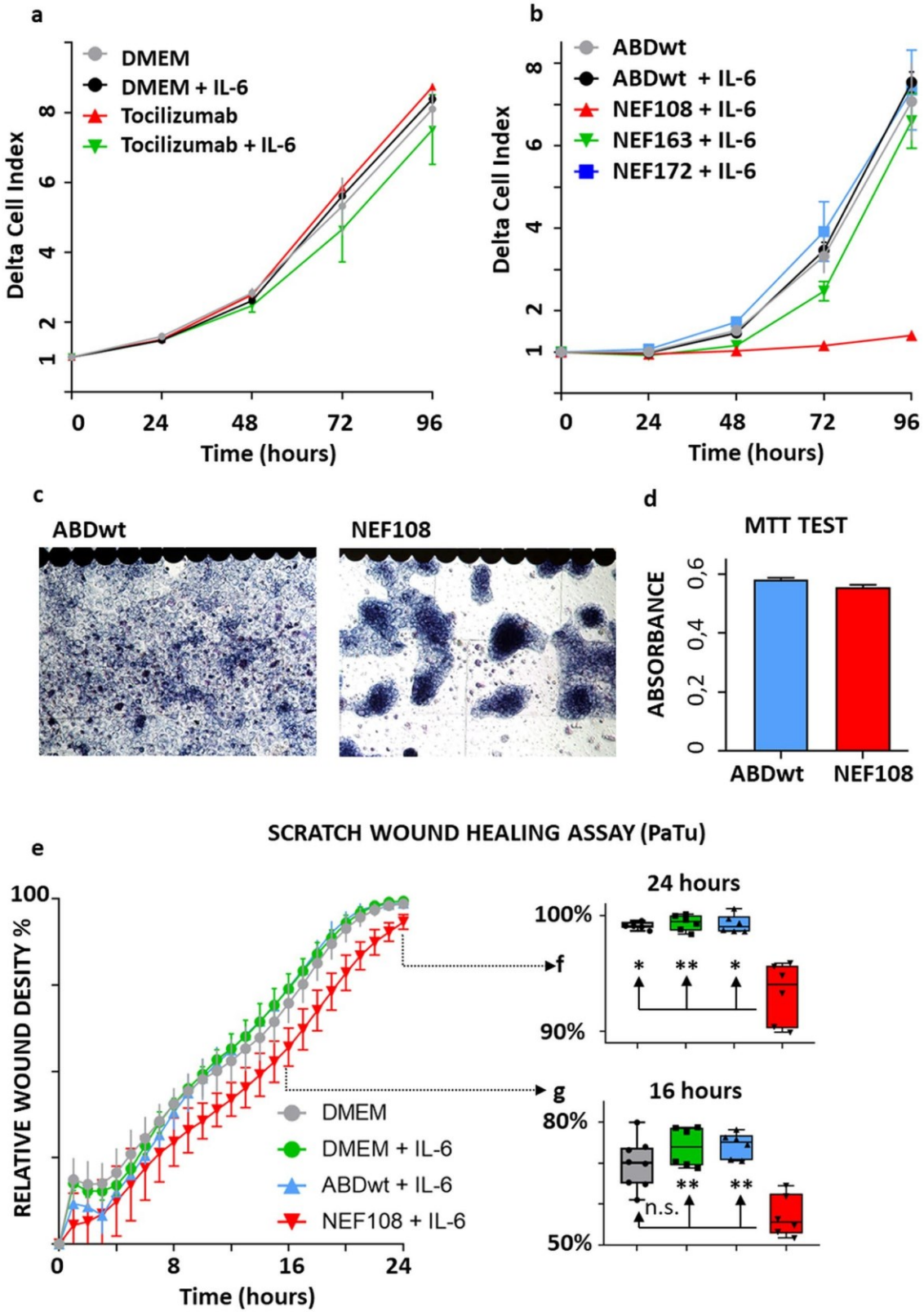

Fig. 6 Cell proliferation assay (iCELLigence real-time cell analyzer) and Scratch test (IncuCyte). Effect of clinically approved hIL-6Rα inhibitor (**a**) Tocilizumab (TCZ) on the growth of cells of the PaTu cell line from the ductal adenocarcinoma of the pancreas in comparison to (**b**) NEF binders. (**c, d**) The high effect of NEF108 was conditioned by the inhibition of cell migration as detected by microscopy (ABDwt versus NEF108) and the MTT test. (**e-g**) The Scratch test (IncuCyte) demonstrated the inhibitory effect of NEF108 on the migration of PaTu cells. Herein, * = $p < 0.05$; ** = $p < 0.01$, and n.s. = not significant provides the statistical significance of the data

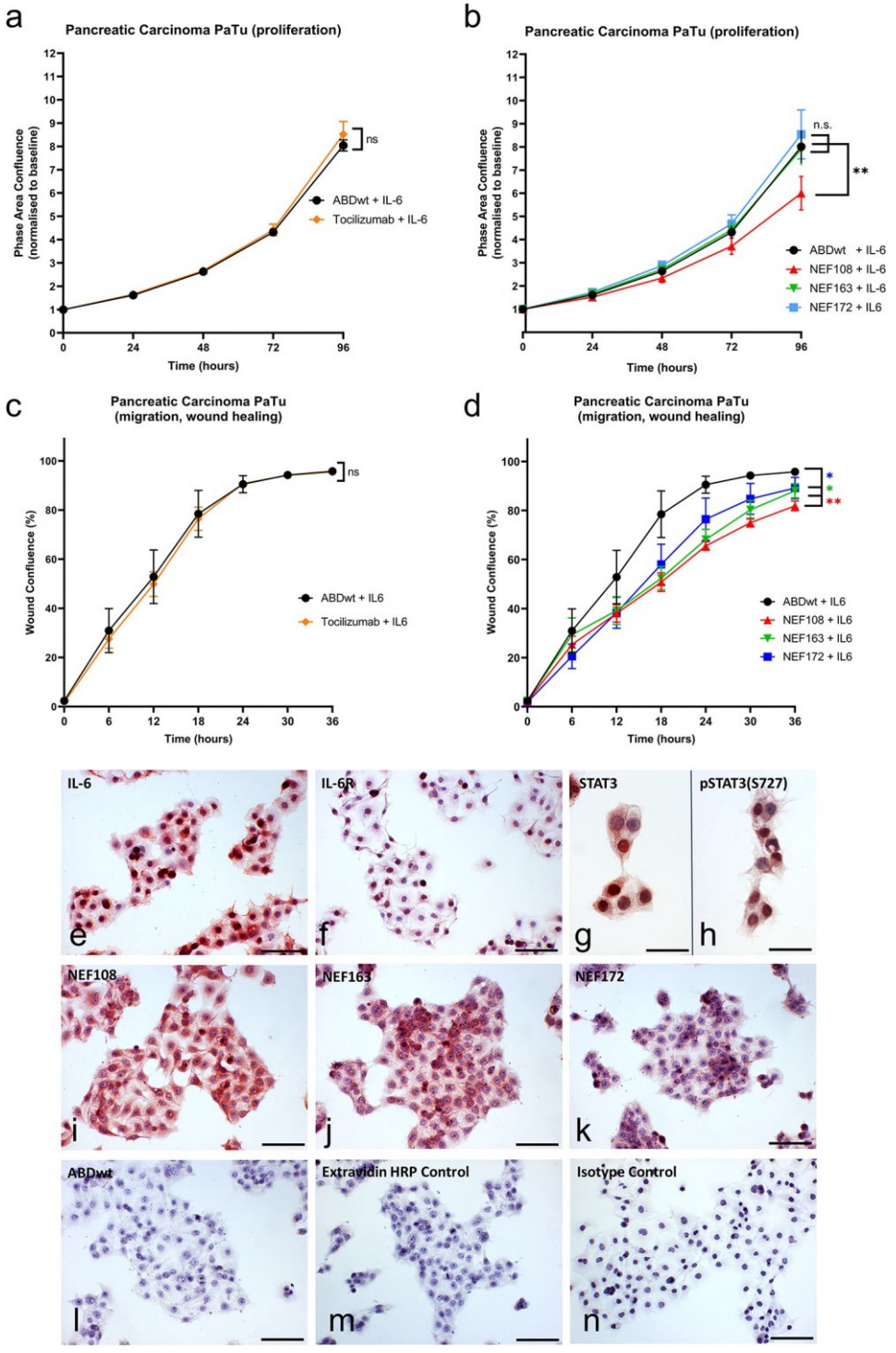

Fig. 7 (See legend on next page.)

compared to that of ABDwt-TolA. The melting temperature for ABDwt-TolA was 66.5 °C, which is similar to the previously reported value [35]. The melting temperatures for NEF108, NEF163, and NEF172 were 60.5 °C, 54.0 °C, and 59.3 °C, respectively (Table S3). Therefore, randomization of ABD scaffold wild-type residues caused different degrees of destabilization among NEF variants, which is expected considering the number of introduced mutations. However, the stability of the selected NEF variants remains high and meets the declared application requirement. In this study, thermal stability was tested in PBS but it can vary with buffer composition.

(See figure on previous page.)

Fig. 7 Effect of NEF blockers on PaTu cell proliferation, migration, IL-6, and IL-6R expression. (**a-b**) For the cell proliferation assay, PaTu cells per well were seeded on 96-well plates overnight. The next day, the medium was replenished for continuous screening in the (**a**) presence of ABDwt and tocilizumab (TCZ) or (**b**) NEF proteins using the Incucyte. All experiments were performed in six technical replicates (wells) using four defined points for confluence measurement every 2 h for four consecutive days. Resulting confluence was determined by Proliferation software and obtained data (in%) were analysed using GraphPad Prism (* = $p < 0.05$; ** = $p < 0.01$; n.s. = not significant, ANOVA). (**c-d**) For the migration (wound healing) assay, PaTu cells per well were seeded on 96-well plates. The next day, the medium replaced, and cells were preincubated with (**c**) ABDwt and tocilizumab (TCZ) or (**d**) NEF binders overnight. Afterthat, standardised wounds were created using Incucyte® WoundMaker and then continuously monitored using the Incucyte. All experiments were performed in six technical replicates (wells) using two defined points for wound size measurement every 2 h up to maximum three consecutive days. Resulting wound healing data was acquired using Incucyte® Scratch Wound analysis software and analysed using GraphPad (* = $p < 0.05$; ** = $p < 0.01$; n.s. = not significant, ANOVA). (**e**) In immunocytochemical staining, cells exhibited a high signal of IL-6 expression and (**f**) a lower but specific signal for IL-6 receptor expression. (**g, h**) The cells expressed STAT3 and were able to translocate pSTAT3 to the nucleus. (**i, j, k**) NEF binders, especially NEF108, strongly bind to PaTu cells, while (**l**) the missing ABDwt affinity to PaTu cells resulted in a negative staining. (**m**) Control reaction with isotype antibody and (**n**) Extravidin HRP conjugate confirm the specificity of immunohistochemical reactions

The far UV CD spectrum was measured to determine the secondary structure composition of NEF variants. CD spectra of NEF variants were compared with ABDwt-TolA CD spectra (Fig. S6). ABDwt-TolA is a fusion protein of three α-helical ABD domains fused with the TolA domain, which is composed of a long α-helix and α + β globule (pdb: P19934). Analysis of CD spectra for ABDwt-TolA revealed that proteins contain predominantly α-helical structures, while other secondary structure types are present in low content. In the case of the NEF variants, α-helix is still the predominant structural type in all NEF variants, but to a lesser degree compared to ABDwt, while the presence of other structural types increased. The result corresponds to the Tm values obtained. NEF108 has only slightly higher Tm according to NanoDSF and α-helical content according to CD spectra than NEF172. Similarly, NEF163 has significantly lower Tm and α-helical content compared to NEF108 and NEF172.

Binding of NEF proteins to human peripheral blood mononuclear cells

To confirm the specificity of NEF binding to hIL-6Rα present on primary blood cells, PBMCs were purified by gradient centrifugation, and differentiation of B cells was induced by pokeweed mitogen (PWM) lasting for 4 days to obtain activated plasmablasts/plasma cells ($CD19^+CD38^+$) positive for hIL-6Rα [36, 37]. The results are summarized in Fig. 9. Unstimulated and PWM-stimulated PBMCs were stained with anti-CD19 and anti-CD38 antibodies and, at the same time, with either anti-IL-6Rα antibody or with one of the NEF binders, NEF108, NEF163, and NEF172, or ABDwt protein to detect the presence of the hIL-6Rα receptor. Flow cytometry data show that all three NEF binders, NEF163, NEF172, and NEF108, are able to recognize hIL-6Rα with the same (NEF172) or better (NEF163 and NEF108) ability than anti-IL6Rα antibody (Fig. 9a).

Further, we tested the ability of NEF binders to inhibit IL-6-mediated in vitro activation and differentiation of B cells within the PBMC population toward plasmablasts/plasma cells. As shown in Fig. 9b, left panel, B cells differentiate toward a population of plasmablasts/plasma cells, reaching 60% of total $CD19^+$ cells. In contrast, hIL-6 induced PBMCs simulation in the presence of NEF binders (NEF108, NEF163, and NEF172) significantly reduced the activation toward plasmablasts/plasma cells comparable to the levels in nonstimulated controls. In addition, we tested the ability of NEF binders to inhibit IL-6-induced PBMCs differentiation toward $IgA1^+$ plasmablasts/plasma cells, as we reported earlier [38, 39]. Similarly, for the total population of plasmablasts/plasma cells, NEF binders inhibited IgA^+ subset activation toward plasmablasts/plasma cells (Fig. 9b, middle panel). We also measured the mean fluorescence intensity (MFI) of the CD38 marker, which is substantially enhanced upon activation toward plasmablasts/plasma cells. Even here, NEF binders inhibited hIL-6-mediated activation (Fig. 9b, right subpanel) of the IgA^+ subset.

NEF108 protein significantly alleviates histomorphological markers of large intestine alterations in DSS colitis model

We tested the effect of NEF108 binder in preventative-therapeutic regime of DSS colitis by assessment the colon length and histomorphological changes, namely inflammatory cell infiltration of large intestine mucosa, epithelial changes, and mucosal architecture (Fig. 10). NEF108 significantly prevented DSS-induced colon length reduction ($p < 0.05$), significantly protected colon from the mucosal architecture alterations (ulcerations, granulation tissue, irregular crypts, crypt loss, and villous blunting) ($p < 0.01$), and significantly protected from epithelial changes (Goblet cells loss, epithelial hyperplasia, cryptitis, and crypt abscesses) ($p < 0.01$), (Fig. 10b, d, e, f). Inflammatory cell infiltrate remains without significant difference between groups drinking DSS with and without NEF108 protein administration. However, we can see less significant inflammatory cell infiltrate regarding to the naïve group of mice. Furthermore, we compared the IL-1β cytokine expression as a marker of inflammatory response to DSS. NEF108 treatment significantly reduced DSS-induced IL-1β expression (Fig. 10c).

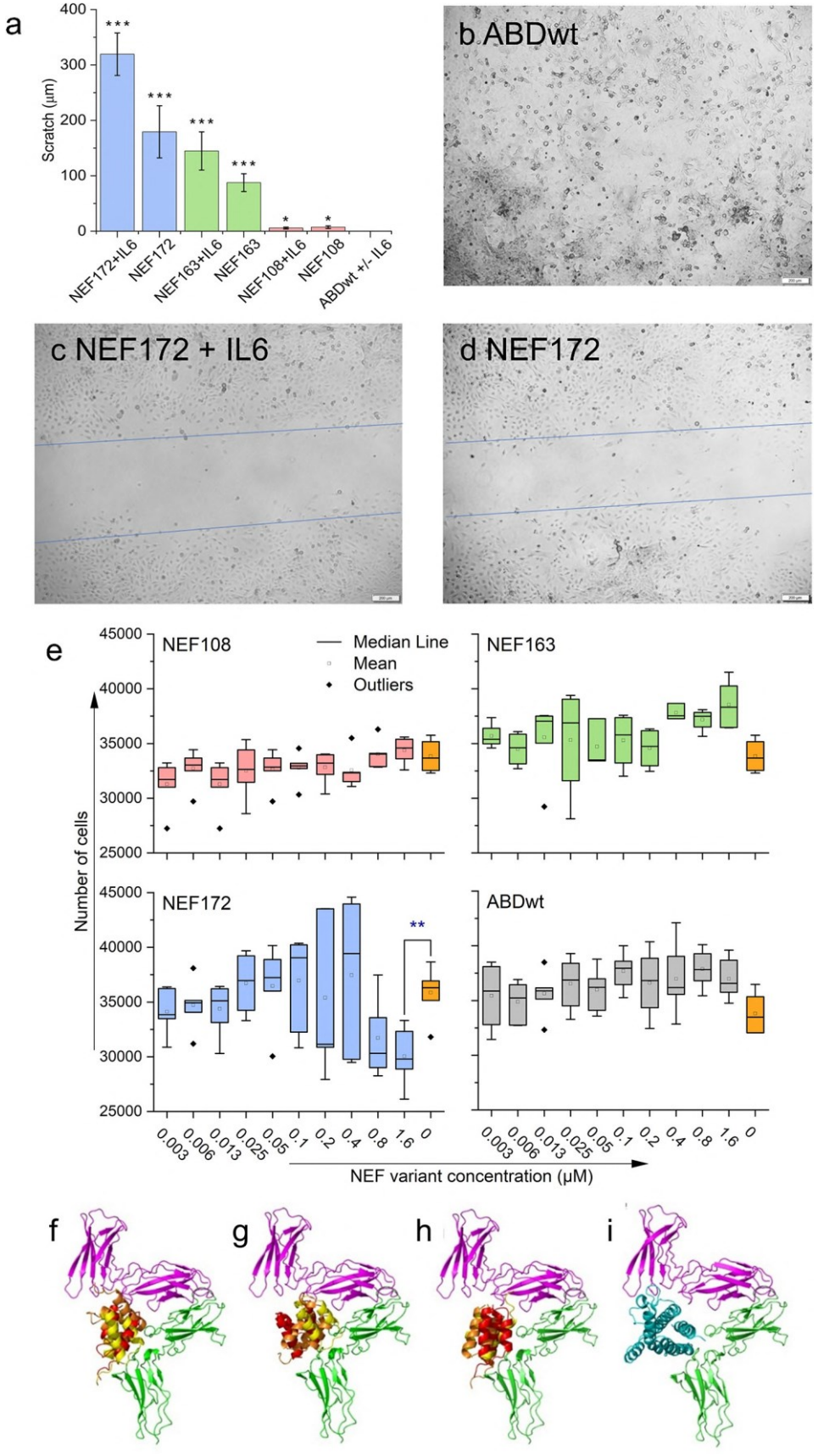

Fig. 8 (See legend on next page.)

(See figure on previous page.)

Fig. 8 Migration and proliferation of glioblastoma GAMG cells in the presence of NEF binders and prediction of binding modes of NEF proteins by docking. (**a**) Cell migration assay evaluated using the scratch gap after 48 h of incubation with 200 nM of NEF172, NEF163, and NEF108 +/- 50 ng/ml of hIL6. (**b**) Representative image for gap evaluation of ABDwt. (**c**) Width of gap evaluation for NEF172 + IL-6. (**d**) Width of gap evaluation for NEF172 without IL-6. (**e**) Cell proliferation assay for GAMG cells evaluated with the CCK-8 kit after 24 h of incubation with different concentrations of NEF proteins and ABDwt control. The results are presented as two independent experiments performed in triplicate. (**a, e**) For statistical evaluation, the one-way ANOVA was used (* = $p < 0.05$; ** = $p < 0.01$; *** = $p < 0.001$). (**f-i**) Summary of NEF variants docking to the structure of the hIL-6Rα/hIL-6Rβ complex (pdb id 1p9m). The hIL-6Rα is shown in magenta, the hIL-6Rβ in green, the hIL-6 ligand in cyan, and the NEF variants are shown in decreasing predicted order of binding as red, orange, and yellow cartoon. (**f**) Binding poses for NEF108, (**g**) for NEF163, (**h**) for NEF172, and (**i**) shows the ternary hIL-6Rα/hIL-6Rβ complex (doi https://doi.org/10.5281/zenodo.10213658)

Discussion

Cancer cells are not alone, but they represent an integral component of a highly complex ecosystem with non-cancer cells such as cancer-associated fibroblasts and immune cells [40]. The success of cancer cells depends not only on genetic alteration but it is also influenced by intercellular coordination, where cancer cells communicate with non-cancer elements through intercellular contacts or via the production of extracellular matrix or growth factors, cytokines, and/or chemokines, as well as by extracellular vesicles [41]. Interestingly, many of them have an inflammation-supporting effect. Recently, much attention has been given to the pleiotropic cytokine IL-6 because of its ability to either promote or, more rarely, inhibit tumor growth [42]. Activation of the JAK2/STAT3 signaling pathway by IL-6 has been reported to mediate tumorigenesis via regulation of key cellular processes, including apoptosis, cycle progression, proliferation, invasion, migration, metastasis, angiogenesis, and tumor cell escape from the immune system [43], as well as involvement in cancer cachexia [44], and promoting the process of epithelial-mesenchymal transition (EMT) and stem cell-like features [45]. The regulation and inhibition of the IL-6/JAK2/STAT3 pathway is conducive to cancer prevention and treatment as well as improved prognosis and, therefore, represents an important target for designing anti-cancer drugs [46, 47].

Cancer-associated fibroblasts (CAFs) are an essential component in the microenvironment of solid tumors, such as pancreatic carcinomas, and their composition changes with cancer progression [48] and metastasis [49]. A subgroup of CAFs, so-called iCAFs, are strong producers of inflammation-supporting factors, including IL-6 [50]. Blocking of the IL-6-mediated JAK2/STAT3 pathway could substantially suppress the proliferation and promote the apoptosis of glioma cells [51]. In support, in vitro blocking of IL-6R inhibits cell proliferation, invasion, and neuroglobular formation of glioma tumors [52]. Also, IL-6 trans-signaling is constitutively active in several pancreatic cancer (PC) cell lines [53]. Thus, in vitro blocking of IL-6R signaling by TCZ showed pSTAT3 downregulation and inhibition of IL-6 expression in both pancreatic cancer cells and mesenchymal stem cells (MSCs) [54]. Also, enhanced IL-6 expression was positively correlated with lymph node metastasis, tumor differentiation, and vascular invasion in PC patients [55, 56].

Based on experimental data, therapy focused on IL-6/STAT3 signaling should be a suitable target for anti-cancer therapy because it can also influence other aspects of malignant disease, such as wasting and depression. Unfortunately, as demonstrated in the therapeutic application of TCZ and other anti-IL-6 signaling drugs, their anti-cancer effect was not prominent [57]. The more perspective should be their use in combination with other anti-cancer drugs or the development of new blockers preventing interactions of IL-6 with the receptor complex. Our data demonstrate that NEF proteins (NEF108, NEF163, and NEF172) compete with IL-6 cytokine for binding to IL-6Rα in ELISA (Fig. 1b) as well as on the cell surface of *hIL-6Rα*-transfected HEK293T cells (Fig. S7). However, none of these NEF variants compete with TCZ antibody, as tested by LigandTracer method (Fig. S8, S9). Small NEF proteins, thus, should be suitable candidates for blocking IL-6 signaling because they seem to be more efficient, at least in certain cell types, than the golden standard, such as TCZ antibody, under in vitro conditions. Also, the effect of NEF proteins on normal fibroblasts is negligible, in contrast to the effect of the fusion protein IL-6/IL-6 receptor on IL-6 transactivation activity. This observation harmonizes with the data of others [58], which can be interpreted by the low expression of IL-6 receptors in fibroblasts [59] as well as documented in The Human Protein Atlas (https://www.proteinatlas.org/ENSG00000160712-IL6R).

Interestingly, the inhibitory efficiency of NEF variants varied in different cell lines. NEF163 had the most prominent effect on the proliferation of both the melanoma cell lines G361 and A2058. In the case of pancreatic cell lines, all three NEF variants had a limited effect on proliferation. However, NEF108 considerably restricted the migration of the PaTu cell line. NEF172 had the most prominent inhibitory effect on GAMG cell migration, while NEF108 and NEF163 had a weaker or no effect, respectively. These observed differences in the binding of NEF variants to cell surface hIL-6Rα could be caused by several factors. According to the NCBI and UniProt databases, there are hundreds of single nucleotide polymorphisms (SNPs) in the human *IL-6Rα* gene that are known for amino acid substitutions. However, little is known

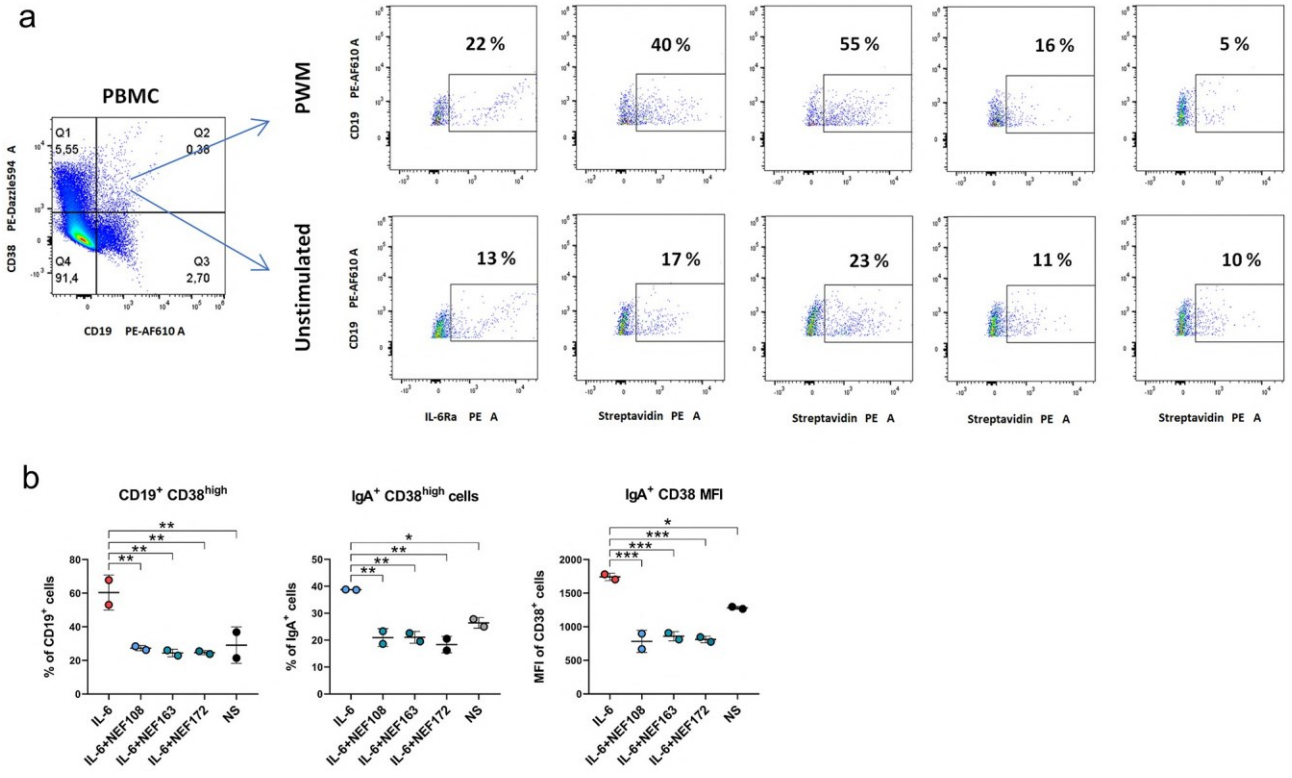

Fig. 9 Binding of NEF proteins to primary human cells. (**a**) NEF binding to IL-6Rα expressed on stimulated primary B cells. PBMCs were stimulated for 96 h with 10 µg/ml PWM. The B cell subpopulation was stained with antibodies specific to CD19 (PE-AF610), CD38 (PE-DZL594), and with either anti-IL6Rα antibody or one of the NEF binders (NEF108, NEF163, and NEF172) and detected by flow cytometry. The gating strategy for $CD19^+$ and $CD38^+$ cells is shown on the left subpanel. IL-6Rα expression was determined in the gate Q2 ($CD19^+CD38^+$), corresponding to plasmablasts/plasma cells. Plots represent populations positive for individual NEF binders or anti-IL-6Rα before and after PWM stimulation. The percentage of cells positive for IL-6Rα is shown on the plots. All tested binders show a similar (NEF172) or higher (NEF108 and NEF163) percentage of IL-6Rα-positive cells in comparison with anti-IL6Rα antibody detection. ABDwt was used as an unspecific control. (**b**) NEF inhibition of IL-6-driven stimulation of B cell differentiation toward plasmablasts/plasma cells. PBMCs were stimulated by hIL-6 for 7 days with or without NEF binders. Differentiation toward plasmablasts/plasma cells was detected as $CD19^+CD38^+$ cells and their IgA^+ subpopulation by specific fluorophore labeled mAbs by flow cytometry. *P* values were calculated using one-way ANOVA with Tukey's post-hoc test. * = $P < 0.05$, ** = $P < 0.01$, *** = $P < 0.001$. Graphs show means and SD. NS means unstimulated control in the absence of NEF binders

about their biological effect on the hIL-6Rα function. We hypothesize that these SNPs are cell line-specific, thus affecting the affinity or accessibility of the cytokine binding site for particular NEF protein variants.

To characterize NEF interaction with IL-6Rα on primary cells, we used the B cell ($CD19^+$) subpopulation of PBMCs. It was formerly reported that non-stimulated B cell populations do not express detectable levels of IL-6Rα (CD126), whereas stimulated B cell populations, including plasmablasts and early plasma cells, are IL-6Rα positive [60]. As expected, comparison of populations before and after PWM stimulation confirmed an increase in the number of NEF-stained cells analogously to anti-IL-6Rα mAb staining (Fig. 9a). This observation supports NEF binders' ability to recognize IL-6Rα in primary human cells. Furthermore, we assessed the biological function of NEF binders as potential inhibitors of IL-6 signaling on primary B cells. We followed our previous reports indicating that IL-6 could substantially contribute to B cell maturation, particularly of the IgA^+ B cell subpopulation, toward plasmablasts ($CD38^+$) [39]. Here we confirmed that all three tested NEF108, NEF163, and NEF172 binders significantly reduced the population of $CD38^+$ after IL-6 stimulation (Fig. 9b), indicating NEF proteins' ability to effectively interfere with IL-6 signaling.

Additionally, we verified the inhibitory potential of NEF108 protein on the mouse version of the IL-6 receptor using murine model of DSS-induced colitis. As shown in Fig. 10, NEF108-treated mice demonstrated a significant reduction in inflammation-induced tissue damage along with the suppression of the IL-1β cytokine expression, as a marker of inflammatory response to DSS. Although this study needs to be further extended, our preliminary results strengthen the antagonistic effectiveness of NEF proteins demonstrated in vitro.

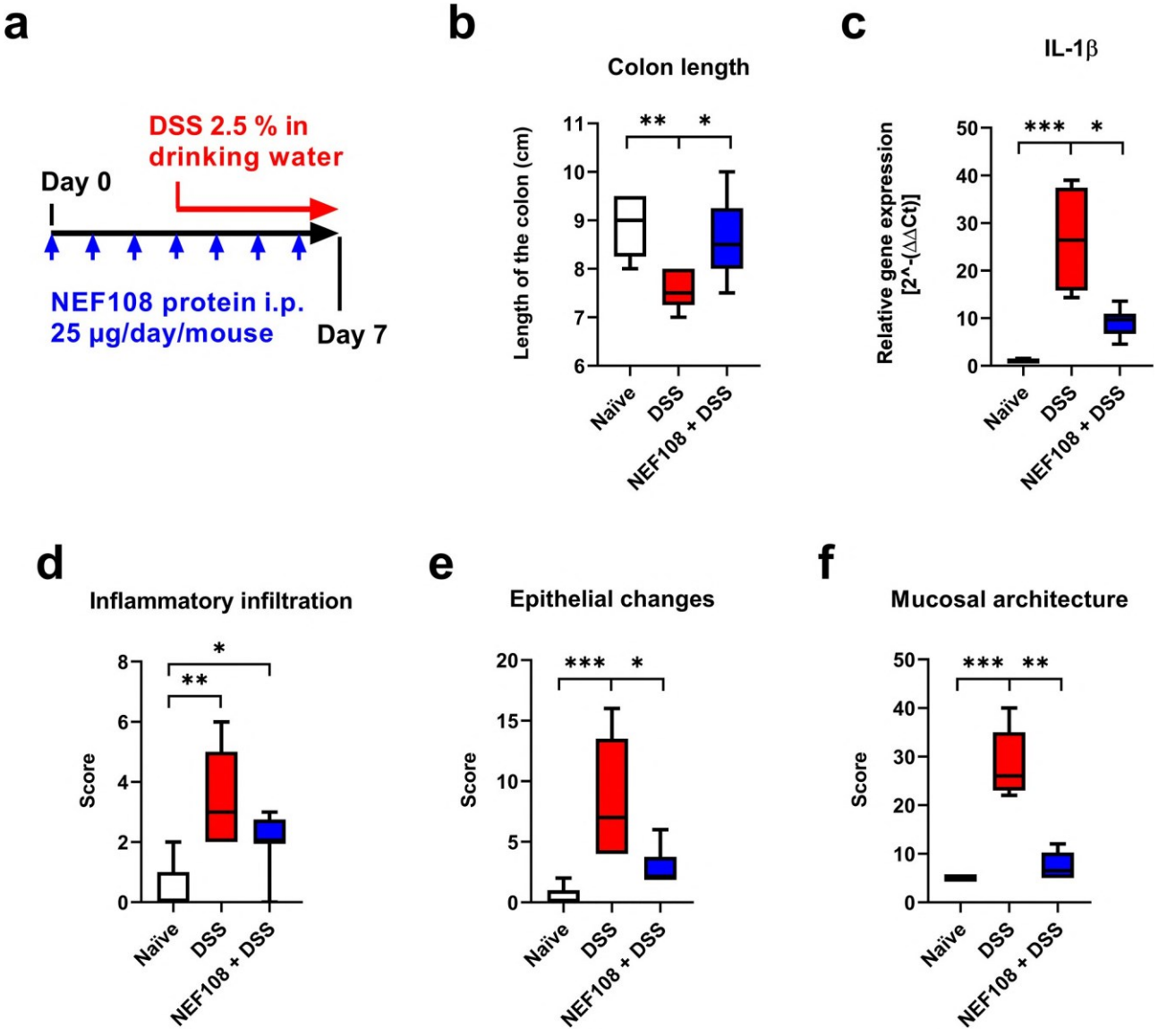

Fig. 10 Protective effect of NEF108 ligand targeting IL-6Rα in murine model of DSS-induced colitis. NEF108 ligand in preventative-therapeutic regime was tested in the model of DSS-induced colitis. (**a**) NEF108 protein was administered daily by i.p. route (blue arrow) starting three days before the administration of DSS in drinking water (red arrow). The NEF108 application continued in parallel to DSS for subsequent 4 days. After experiment termination, (**b**) the length of the colon was determined (length between caecum and rectum) – naïve group (8.9 ± 0.4 cm) and DSS group (7.4 ± 0.4 cm) in DSS mice. NEF108-treated DSS exposed mice exhibited the colon length 8.3 ± 0.7 cm. (**c**) Colon IL-1β transcript level was measured by RealTime-PCR. Histological classification was assessed for (**d**) inflammatory cell infiltrate, (**e**) epithelial changes, and (**f**) mucosal architecture. In the case of inflammatory infiltrate and epithelial changes, the effect of NEF108 was observed in approximately 50% of mice. Statistical differences were analyzed by Kruskal-Wallis one-way ANOVA followed by Dunn´s multiple comparisons test. Means with SD are shown (* = $P < 0.05$, ** = $P < 0.01$, *** = $P < 0.001$)

Conclusions

Collectively, the generated NEF binders represent a promising class of new IL-6R protein antagonists that can be instrumentalized to achieve an efficient migrastatic anti-cancer treatment. In addition, NEF binders can be further characterized for their IL-6R-blocking function in autoimmune diseases such as IgA nephropathy.

Abbreviations

ABD	Albumin-binding domain
Akt	protein kinase B
BSA	Bovine Serum Albumin
CAFs	cancer-associated fibroblasts
CCK-8	Cell counting kit-8
CD	Circular dichroism
DMEM	Dulbecco's modified Eagle's medium
DMSO	Dimethyl sulfoxide
E. coli	*Escherichia coli*
ELISA	Enzyme-linked immunosorbent assay
FBS	Fetal bovine serum
FCS	Fetal Calf Serum
FDA	Food and Drug Administration
FITC	Fluorescein isothiocyanate
gp130	glycoprotein 130

HBSS	Hank's Balanced Salt Solution
HEPES	4-(2-Hydroxyethyl)piperazine-1-ethanesulfonic acid
HRP	Horseradish peroxidase
IgG1	Immunoglobulin G1
IL-6	Interleukin-6
IL-6R	Interleukin-6 receptor
IL-6Rα	Interleukin-6 receptor alpha
IMAC	Immobilized metal affinity chromatography
IPTG	Isopropyl ß-d-1-thiogalactopyranoside
JAK	Janus kinase
mAb	Monoclonal antibody
MAPK	Mitogen-activated protein kinase
MFI	Mean fluorescence intensities
MTT	3-(4,5-Dimethylthiazol-2-yl)-2,5-Diphenyltetrazolium Bromide
NIR	Near-infrared
pAb	polyclonal antibody
PBMCs	Peripheral blood mononuclear cells
PC	*Pancreatic cancer*
PE	Phycoerythrin
PFA	Paraformaldehyde
PI3K	phosphoinositide 3-kinase
RBS	Ribosome binding site
SFK	Src Family Kinases
STAT	signal transducer and activator of transcription
T7p	Bacteriophage T7 RNA Polymerase Promoter
TCZ	Tocillizumab
TMB	3,3',5,5'-Tetramethylbenzidine
TME	Tumor microenvironment
YAP	Yes-associated protein

Supplementary Information

The online version contains supplementary material available at https://doi.org/10.1186/s12964-024-01630-w.

Supplementary Material 1

Acknowledgements

The authors are thankful to Linda Malá and Petra Kadlčáková for excellent experimental assistance. The authors also acknowledge CF CF Biophysic, CF Cryst, CF Diff of CIISB, Instruct-CZ Centre, supported by MEYS CR (LM2023042)) and European Regional Development Fund-Project, UP CIISB" (No. CZ.02.1.01/0.0/0.0/18_046/0015974).

Author contributions

Y.G. performed large scale screening and biochemical and functional analysis of protein variants. M.K. assembled ABD combinatorial library. L.L., K.S., O.J and J.M. designed and performed cancer cell proliferation and cell migration assays and analyzed data. H.P., N.P. J.M.M. performed biophysical characterization of NEF proteins. R.O. performed flow cytometry with NEF binders and analyzed data. J.Č. performed in silico analysis of NEF proteins. K.Z. and L.R.K. performed B cell binding and proliferation assays and analyzed data. P.K., K.S. and J.Š. performed experimentally induced colitis in mice and analyzed data. P.M., K.S. and M.R. conceptualized the project, directed research, designed research, analyzed data, and wrote the paper. All authors reviewed and approved the manuscript.

Funding

The authors are thankful for the received support by the Czech Science Foundation by the grant LA CEUS No. 21-16423 K, by the Ministry of Education, Youth and Sport of the Czech Republic by OP RDE project CEREBIT No. CZ.02.1.01/0.0/0.0/16_025/0007397, and for the received support from the Institute of Biotechnology of the Czech Academy of Sciences v.v.i. (Institutional Research Concept, RVO: 86652036). Authors are also grateful to Ministry of Education, Youth, and Sports of the Czech Republic for support by projects no.: LX22NPO5102 financed by the European Union – Next Generation EU as part of the Czech Recovery Plan and no.: LM2023053 – Czech National Node to the European Infrastructure for Translational Medicine, and to Charles University for support by project COOPERATIO-Onco. The project "Center for Tumor Ecology - Research of the Cancer Microenvironment Supporting Cancer Growth and Spread" (reg. No. CZ.02.1.01/0.0/0.0/16_019/0000785) supported by the Operational Programme Research, Development and Education in the regimen of the sustainability is also appreciated.

Data availability

No datasets were generated or analysed during the current study.

Declarations

Ethics approval and consent to participate

Experimental protocol for in vivo mouse experimentally induced colitis was approved by Ethics Committee of the Faculty of Medicine and Dentistry (Palacky University Olomouc, Czech Republic), and the Ministry of Education, Youth and Sports, Czech Republic (MSMT-10947/2021-3).

Consent for publication

Not applicable.

Competing interests

The authors declare no competing interests.

Author details

[1]Laboratory of Ligand Engineering, Institute of Biotechnology of the Czech Academy of Sciences, BIOCEV Research Center, Prumyslova 595, Vestec 252 50, Czech Republic
[2]Institute of Anatomy, 1st Faculty of Medicine, Charles University, U Nemocnice 3, Prague 2 12800, Czech Republic
[3]Department of Dermatovenerology, 1st Faculty of Medicine, Charles University, U Nemocnice 2, Prague 2 12000, Czech Republic
[4]Department of Immunology, Faculty of Medicine and Dentistry, Palacky University Olomouc and University Hospital Olomouc, Hněvotínská 3, Olomouc 779 00, Czech Republic
[5]Centre of Nanomaterials and Biotechnologies, University of J. E. Purkyně in Ústí nad Labem, Pasteurova 3632/15, Ústí nad Labem 400 96, Czech Republic
[6]Laboratory of Molecular Biology of Bacterial Pathogens, Institute of Microbiology of the Czech Academy of Sciences, Vídeňská 1083, Prague 14220, Czech Republic
[7]Laboratory of Structural Bioinformatics of Proteins, Institute of Biotechnology of the Czech Academy of Sciences, BIOCEV Research Center, Prumyslova 595, Vestec 252 50, Czech Republic
[8]Department of Clinical and Molecular Pathology, Faculty of Medicine and Dentistry, Palacky University Olomouc, Hněvotínská 3, Olomouc 779 00, Czech Republic

Received: 13 December 2023 / Accepted: 22 April 2024
Published online: 07 May 2024

References

1. Rose-John S, Jenkins BJ, Garbers C, Moll JM, Scheller J. Targeting IL-6 trans-signalling: past, present and future prospects. Nat Rev Immunol 2023:1–16.
2. Groza Y, Jemelkova J, Kafkova LR, Maly P, Raska M. IL-6 and its role in IgA nephropathy development. Cytokine Growth Factor Rev. 2022;66:1–14.
3. Briukhovetska D, Dorr J, Endres S, Libby P, Dinarello CA, Kobold S. Interleukins in cancer: from biology to therapy. Nat Rev Cancer. 2021;21(8):481–99.
4. Jones SA, Jenkins BJ. Recent insights into targeting the IL-6 cytokine family in inflammatory diseases and cancer. Nat Rev Immunol. 2018;18(12):773–89.
5. Boulanger MJ, Chow DC, Brevnova EE, Garcia KC. Hexameric structure and assembly of the interleukin-6/IL-6 alpha-receptor/gp130 complex. Science. 2003;300(5628):2101–4.
6. Varghese JN, Moritz RL, Lou MZ, Van Donkelaar A, Ji H, Ivancic N, Branson KM, Hall NE, Simpson RJ. Structure of the extracellular domains of the human interleukin-6 receptor alpha -chain. Proc Natl Acad Sci U S A. 2002;99(25):15959–64.
7. Scheller J, Chalaris A, Schmidt-Arras D, Rose-John S. The pro- and anti-inflammatory properties of the cytokine interleukin-6. Biochim Biophys Acta. 2011;1813(5):878–88.
8. Baran P, Hansen S, Waetzig GH, Akbarzadeh M, Lamertz L, Huber HJ, Ahmadian MR, Moll JM, Scheller J. The balance of interleukin (IL)-6, IL-6.

soluble IL-6 receptor (sIL-6R), and IL-6.sIL-6R.sgp130 complexes allows simultaneous classic and trans-signaling. J Biol Chem. 2018;293(18):6762–75.
9. Wu J, Gao FX, Wang C, Qin M, Han F, Xu T, Hu Z, Long Y, He XM, Deng X et al. IL-6 and IL-8 secreted by tumour cells impair the function of NK cells via the STAT3 pathway in oesophageal squamous cell carcinoma. J Exp Clin Canc Res 2019, 38.
10. Bongartz H, Gille K, Hessenkemper W, Mandel K, Lewitzky M, Feller SM, Schaper F. The multi-site docking protein Grb2-associated binder 1 (Gab1) enhances interleukin-6-induced MAPK-pathway activation in an SHP2-, Grb2-, and time-dependent manner. Cell Commun Signal. 2019;17(1):135.
11. Negoro S, Oh H, Tone E, Kunisada K, Fujio Y, Walsh K, Kishimoto T, Yamauchi-Takihara K. Glycoprotein 130 regulates cardiac myocyte survival in doxorubicin-induced apoptosis through phosphatidylinositol 3-kinase/Akt phosphorylation and Bcl-xL/caspase-3 interaction. Circulation. 2001;103(4):555–61.
12. Schmitt R, Stahl AL, Olin AI, Kristoffersson AC, Rebetz J, Novak J, Lindahl G, Karpman D. The combined role of galactose-deficient IgA1 and streptococcal IgA-binding M protein in inducing IL-6 and C3 secretion from human mesangial cells: implications for IgA nephropathy. J Immunol. 2014;193(1):317–26.
13. Suzuki H, Raska M, Yamada K, Moldoveanu Z, Julian BA, Wyatt RJ, Tomino Y, Gharavi AG, Novak J. Cytokines alter IgA1 O-glycosylation by dysregulating C1GalT1 and ST6GalNAc-II enzymes. J Biol Chem. 2014;289(8):5330–9.
14. Ebbing EA, van der Zalm AP, Steins A, Creemers A, Hermsen S, Rentenaar R, Klein M, Waasdorp C, Hooijer GKJ, Meijer SL, et al. Stromal-derived interleukin 6 drives epithelial-to-mesenchymal transition and therapy resistance in esophageal adenocarcinoma. Proc Natl Acad Sci U S A. 2019;116(6):2237–42.
15. Dauer DJ, Ferraro B, Song L, Yu B, Mora L, Buettner R, Enkemann S, Jove R, Haura EB. Stat3 regulates genes common to both wound healing and cancer. Oncogene. 2005;24(21):3397–408.
16. Sebba A. Tocilizumab: the first interleukin-6-receptor inhibitor. Am J Health Syst Pharm. 2008;65(15):1413–8.
17. Ghasemi K, Ghasemi K. Evaluation of the Tocilizumab therapy in human cancers: latest evidence and clinical potential. J Clin Pharm Ther. 2022;47(12):2360–8.
18. Kim GW, Lee NR, Pi RH, Lim YS, Lee YM, Lee JM, Jeong HS, Chung SH. IL-6 inhibitors for treatment of rheumatoid arthritis: past, present, and future. Arch Pharm Res. 2015;38(5):575–84.
19. Ahmad JN, Li JJ, Biedermannova L, Kuchar M, Sipova H, Semeradtova A, Cerny J, Petrokova H, Mikulecky P, Polinek J, et al. Novel high-affinity binders of human interferon gamma derived from albumin-binding domain of protein G. Proteins. 2012;80(3):774–89.
20. Kuchar M, Vankova L, Petrokova H, Cerny J, Osicka R, Pelak O, Sipova H, Schneider B, Homola J, Sebo P, et al. Human interleukin-23 receptor antagonists derived from an albumin-binding domain scaffold inhibit IL-23-dependent ex vivo expansion of IL-17-producing T-cells. Proteins. 2014;82(6):975–89.
21. Hlavnickova M, Kuchar M, Osicka R, Vankova L, Petrokova H, Maly M, Cerny J, Arenberger P, Maly P. ABD-Derived protein blockers of human IL-17 receptor A as Non-IgG Alternatives for Modulation of IL-17-Dependent Pro-inflammatory Axis. Int J Mol Sci 2018, 19(10).
22. Ahmad JN, Li J, Biedermannova L, Kuchar M, Sipova H, Semeradtova A, Cerny J, Petrokova H, Mikulecky P, Polinek J, et al. Novel high-affinity binders of human interferon gamma derived from albumin-binding domain of protein G. Proteins. 2012;80(3):774–89.
23. Flynn CM, Kespohl B, Daunke T, Garbers Y, Dusterhoft S, Rose-John S, Haybaeck J, Lokau J, Aparicio-Siegmund S, Garbers C. Interleukin-6 controls recycling and degradation, but not internalization of its receptors. J Biol Chem. 2021;296:100434.
24. Johansson MU, Frick IM, Nilsson H, Kraulis PJ, Hober S, Jonasson P, Linhult M, Nygren PA, Uhlen M, Bjorck L, et al. Structure, specificity, and mode of interaction for bacterial albumin-binding modules. J Biol Chem. 2002;277(10):8114–20.
25. Sali A, Blundell TL. Comparative protein modeling by satisfaction of spatial restraints. J Mol Biol. 1993;234(3):779–815.
26. Kozakov D, Beglov D, Bohnuud T, Mottarella SE, Xia B, Hall DR, Vajda S. How good is automated protein docking? *Proteins* 2013, 81(12):2159–66.
27. Kozakov D, Brenke R, Comeau SR, Vajda S. PIPER: an FFT-based protein docking program with pairwise potentials. Proteins. 2006;65(2):392–406.
28. UniProt C. UniProt: a worldwide hub of protein knowledge. Nucleic Acids Res. 2019;47(D1):D506–15.
29. Raskova Kafkova L, Brokesova D, Krupka M, Stehlikova Z, Dvorak J, Coufal S, Fajstova A, Srutkova D, Stepanova K, Hermanova P, et al. Secretory IgA N-glycans contribute to the protection against E. Coli O55 infection of germ-free piglets. Mucosal Immunol. 2021;14(2):511–22.
30. Juritsch AF, Moreau R. Rapid removal of dextran sulfate sodium from tissue RNA preparations for measurement of inflammation biomarkers. Anal Biochem. 2019;579:18–24.
31. Erben U, Loddenkemper C, Doerfel K, Spieckermann S, Haller D, Heimesaat MM, Zeitz M, Siegmund B, Kühl AA. A guide to histomorphological evaluation of intestinal inflammation in mouse models. Int J Clin Exp Patho. 2014;7(8):4557–U4527.
32. Shi XQ, Zhang H, Paddon H, Lee G, Cao XM, Pelech S. Phosphorylation of STAT3 Serine-727 by cyclin-dependent kinase 1 is critical for nocodazole-induced mitotic arrest. Biochemistry-Us. 2006;45(18):5857–67.
33. Kudo M, Jono H, Shinriki S, Yano S, Nakamura H, Makino K, Hide T, Muta D, Ueda M, Ota K, et al. Antitumor effect of humanized anti-interleukin-6 receptor antibody (tocilizumab) on glioma cell proliferation. Laboratory investigation. J Neurosurg. 2009;111(2):219–25.
34. Li RH, Li G, Deng L, Liu QL, Dai J, Shen J, Zhang J. IL-6 augments the invasiveness of U87MG human glioblastoma multiforme cells via up-regulation of MMP-2 and fascin-1. Oncol Rep. 2010;23(6):1553–9.
35. Alm T, Yderland L, Nilvebrant J, Halldin A, Hober S. A small bispecific protein selected for orthogonal affinity purification. Biotechnol J. 2010;5(6):605–17.
36. Hirata Y, Taga T, Hibi M, Nakano N, Hirano T, Kishimoto T. Characterization of Il-6 receptor expression by monoclonal and polyclonal antibodies. J Immunol. 1989;143(9):2900–6.
37. Zachova K, Kosztyu P, Zadrazil J, Matousovic K, Vondrak K, Hubacek P, Julian BA, Moldoveanu Z, Novak Z, Kostovcikova K et al. Role of Epstein-Barr Virus in Pathogenesis and racial distribution of IgA Nephropathy. Front Immunol 2020, 11.
38. Zachova K, Jemelkova J, Kosztyu P, Ohyama Y, Takahashi K, Zadrazil J, Orsag J, Matousovic K, Galuszkova D, Petejova N, et al. Galactose-deficient IgA1 B cells in the circulation of IgA nephropathy patients carry preferentially Lambda Light Chains and Mucosal Homing receptors. J Am Soc Nephrol. 2022;33(5):908–17.
39. Zachova K, Kosztyu P, Zadrazil J, Matousovic K, Vondrak K, Hubacek P, Kostovcikova K, Hogenova HT, Mestecky J, Raska M. Multiparametric flow cytometry analysis of peripheral blood B cell trafficking differences among Epstein-Barr virus infected and uninfected subpopulations. Biomed Pap. 2020;164(3):247–54.
40. Lacina L, Szabo P, Klepáček I, Kolář M, Smetana K. Cancer-Associated Fibroblasts and Their Role in Cancer Progression. In: *Cancer Research: An Interdisciplinary Approach* edn. Edited by Rezaei N. Cham: Springer Nature Switzerland; 2023: 103–133.
41. Nail HM, Chiu CC, Leung CH, Ahmed MMM, Wang HMD. Exosomal miRNA-mediated intercellular communications and immunomodulatory effects in tumor microenvironments. J Biomed Sci 2023, 30(1).
42. Fisher DT, Appenheimer MM, Evans SS. The two faces of IL-6 in the tumor microenvironment. Semin Immunol. 2014;26(1):38–47.
43. Fofaria NM, Srivastava SK. STAT3 induces anoikis resistance, promotes cell invasion and metastatic potential in pancreatic cancer cells. Carcinogenesis. 2015;36(1):142–50.
44. Johnson DE, O'Keefe RA, Grandis JR. Targeting the IL-6/JAK/STAT3 signalling axis in cancer. Nat Reviews Clin Oncol. 2018;15(4):234–48.
45. Xia XH, Xiao CJ, Shan H. Facilitation of liver cancer SMCC7721 cell aging by sirtuin 4 via inhibiting JAK2/STAT3 signal pathway. Eur Rev Med Pharmaco. 2017;21(6):1248–53.
46. Lee H, Jeong AJ, Ye SK. Highlighted STAT3 as a potential drug target for cancer therapy. Bmb Rep. 2019;52(7):415–23.
47. Xie Q, Yang ZJ, Huang XM, Zhang ZK, Li JB, Ju JH, Zhang H, Ma JY. Ilamycin C induces apoptosis and inhibits migration and invasion in triple-negative breast cancer by suppressing IL-6/STAT3 pathway. J Hematol Oncol 2019, 12.
48. Lavie D, Ben-Shmuel A, Erez N, Scherz-Shouval R. Cancer-associated fibroblasts in the single-cell era. Nat Cancer. 2022;3(7):793–807.
49. Friedman G, Levi-Galibov O, David E, Bornstein C, Giladi A, Dadiani M, Mayo A, Halperin C, Pevsner-Fischer M, Lavon H, et al. Cancer-associated fibroblast compositions change with breast cancer progression linking the ratio of S100A4 and PDPN CAFs to clinical outcome. Nat Cancer. 2020;1(7):692–708.
50. Vokurka M, Lacina L, Brabek J, Kolar M, Ng YZ, Smetana K. Cancer-Associated fibroblasts influence the Biological properties of Malignant Tumours via Paracrine Secretion and Exosome Production. Int J Mol Sci 2022, 23(2).
51. Zhou JP, Jiang Y, Zhao JS, Zhang HY, Fu JL, Luo P, Ma YJ, Zou D, Gao HL, Hu JF, et al. Dp44mT, an iron chelator, suppresses growth and induces apoptosis

via RORA-mediated NDRG2-IL6/JAK2/STAT3 signaling in glioma. Cell Oncol. 2020;43(3):461–75.
52. Jiang Y, Han S, Cheng W, Wang ZX, Wu AH. NFAT1-regulated IL6 signalling contributes to aggressive phenotypes of glioma. Cell Communication Signal 2017, 15.
53. Lesina M, Kurkowski MU, Ludes K, Rose-John S, Treiber M, Klöppel G, Yoshimura A, Reindl W, Sipos B, Akira S, et al. Stat3/Socs3 activation by IL-6 Transsignaling promotes progression of pancreatic intraepithelial neoplasia and development of pancreatic Cancer. Cancer Cell. 2011;19(4):456–69.
54. Antoon R, Wang XH, Saleh AH, Warrington J, Hedley DW, Keating A. Pancreatic cancer growth promoted by bone marrow mesenchymal stromal cell-derived IL-6 is reversed predominantly by IL-6 blockade. Cytotherapy. 2022;24(7):699–710.
55. Noh KW, Punispapong S, Wallace MB, Woodward TA, Raimondo M. Do cytokine concentrations in pancreatic juice predict the presence of pancreatic diseases? Clin Gastroenterol H. 2006;4(6):782–9.
56. Zhang X, Lu H, Hong WL, Liu LP, Wang SL, Zhou MT, Chen BC, Bai YH. Tyrphostin B42 attenuates trichostatin A-mediated resistance in pancreatic cancer cells by antagonizing IL-6/JAK2/STAT3 signaling. Oncol Rep. 2018;39(4):1892–900.
57. Spanko M, Strnadová K, Pavlícek AJ, Szabo P, Kodet O, Valach J, Dvoránková B, Smetana K, Lacina L. IL-6 in the ecosystem of Head and Neck Cancer: possible therapeutic perspectives. Int J Mol Sci 2021, 22(20).
58. Zongfei J, Rongyi C, Xiaomeng C, Lili M, Lingying M, Xiufang K, Xiaomin D, Zhuojun Z, Huiyong C, Ying S et al. In vitro IL-6/IL-6R trans-signaling in fibroblasts releases cytokines that May be linked to the pathogenesis of IgG4-Related disease. Front Immunol 2020, 11.
59. Rose-John S. Therapeutic targeting of IL-6 trans-signaling. Cytokine 2021, 144.
60. Jego G, Bataille R, Pellat-Deceunynck C. Interleukin-6 is a growth factor for nonmalignant human plasmablasts. Blood. 2001;97(6):1817–22.

Publisher's Note

3.2. Recent advances in IL-6 biology and its role in IgA nephropathy development

Scientific outcomes:

Publication: Groza Y, Jemelkova J, Kafkova LR, Maly P, Raska M. IL-6 and its role in IgA nephropathy development. Cytokine Growth Factor Rev. 2022 Aug; 66:1-14.
DOI: 10.1016/j.cytogfr.2022.04.001. Epub 2022 Apr 20. PMID: 35527168.

IL-6 is a multifunctional cytokine that plays a critical role in immune responses, inflammation, and various physiological processes. It is produced by a variety of cell types, including T cells, B cells, macrophages, and fibroblasts, in response to infections, tissue injuries, and other stimuli. Due to its ubiquitous nature, as well as implication in multiple diseases, IL-6 is a subject of extensive research. This review summarizes recent advances in the understanding of IL-6 biology. We recapitulate general aspects of IL-6 signaling, focusing on IL-6 receptor complex assembly, signaling modes, down-stream pathways, and target genes.

IL-6R complex is composed of unique IL-6Rα subunit and gp130 subunit that is shared among IL-6 family members. Both soluble and membrane-bound forms of IL-6Rα exist, transmitting signals to different cell types with varying outcomes. Primarily, IL-6 signals through the JAK/STAT pathway, but the MAPK, PI3K, and Src kinase pathways are also involved. Notably, the JAK/STAT and JAK/SHP2/MAPK pathways have antagonistic relationships, and maintaining a balance between these pathways is crucial for homeostasis and controlled cell responses.

Furthermore, we outline IL-6 biological functions in immune response regulation and other physiological processes. Within immune system, IL-6 induces APP production, monocyte differentiation to macrophages, and neutrophil attraction. Additionally, it promotes the differentiation of B cells into antibody-producing plasma cells and influences T cell proliferation and differentiation. Collectively, IL-6 orchestrates inflammation initiation and resolution in case of pathogen invasion and wound healing. Many of IL-6 functions lay outside of the immune system. Thus, IL-6 is also crucial for liver regeneration, promoting hepatocyte survival, proliferation, and tissue repair following injury or surgery. Moreover, IL-6 plays a role in bone remodeling by influencing osteoclast and osteoblast activity, promoting bone resorption necessary for growth and repair. Also, IL-6 serves a crucial role in metabolic regulation and neuroprotection. IL-6 signaling can be inhibited in several ways. The most specific approach involves blocking of IL-6 or IL-6Rα. Likewise, shared gp130 subunit of the receptor can be blocked, but that would affect the whole IL-6 family cytokine signaling. Alternatively, universal components of the down-stream signaling pathways may be

targeted. We made a comprehensive review on IL 6 signaling antagonists available up to date.

In IgAN, a common form of glomerulonephritis, IL-6 plays a significant role in the disease pathogenesis. Elevated IL-6 levels in IgAN increase the production of galactose-deficient IgA1 (Gd-IgA1), which is prone to forming nephritogenic immune complexes. These complexes deposit in the glomerular mesangium, causing mesangial cell proliferation and glomerular injury. The proliferation of mesangial cells is driven by IL-6-mediated signaling pathways that promote cell growth and survival. The deposition of immune complexes triggers an inflammatory response, exacerbating mesangial cell proliferation and leading to further kidney damage. This review summarizes experimental evidence about IL-6 involvement in the pathogenesis of IgAN through the production of Gd-IgA1 and regulation of mesangial cell proliferation.
Contribution: I contributed the review manuscript preparation by literature mining on IL-6 biology and writing about IL-6 structure, signaling, functions, and inhibitors. I assembled tables and figures on these topics.

Graphical Abstract

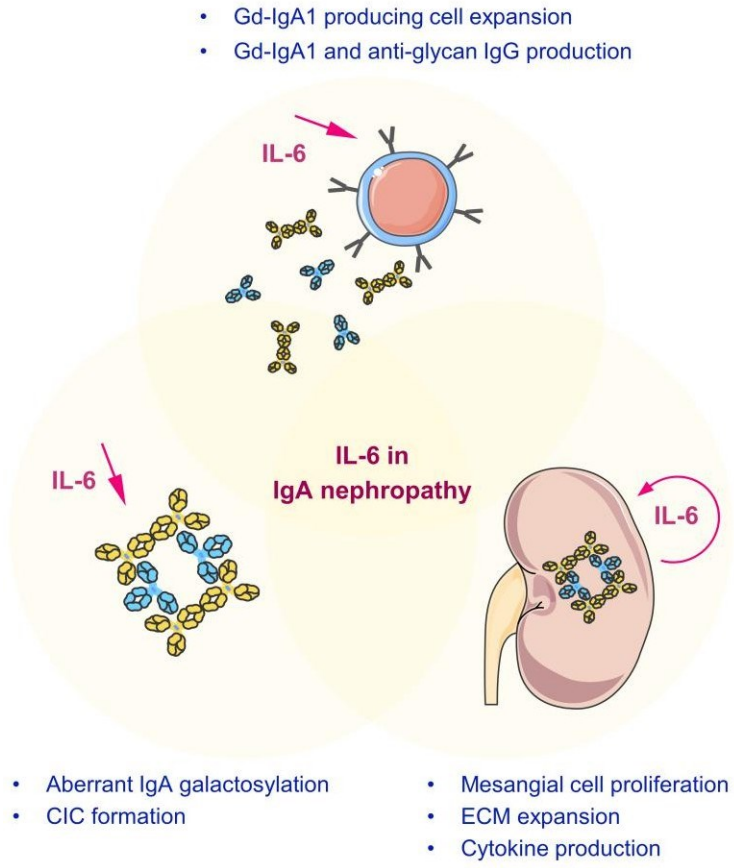

Cytokine and Growth Factor Reviews 66 (2022) 1–14

Contents lists available at ScienceDirect

Cytokine and Growth Factor Reviews

journal homepage: www.elsevier.com/locate/cytogfr

IL-6 and its role in IgA nephropathy development

Yaroslava Groza [a,1], Jana Jemelkova [b,1], Leona Raskova Kafkova [b,*], Petr Maly [a], Milan Raska [b,*]

[a] Laboratory of Ligand Engineering, Institute of Biotechnology of the Czech Academy of Sciences, BIOCEV Research Center, Prumyslova 595, Vestec 252 50, Czech Republic

[b] Department of Immunology, Faculty of Medicine and Dentistry, Palacky University Olomouc, Hnevotinska 3, Olomouc 779 00, Czech Republic

ARTICLE INFO

Key words:
IL-6
IgA nephropathy
Gp130
Galactose-deficient IgA1 (Gd-IgA1)
STAT1
STAT3

ABSTRACT

IL-6 is considered one of the well characterized cytokines exhibiting homeostatic, pro- and anti-inflammatory activities, depending on the receptor variant and the induced intracellular cis- or trans-signaling responses. IL-6-activated pathways are involved in the regulation of cell proliferation, survival, differentiation, and cell metabolism changes.

Deviations in IL-6 levels or abnormal response to IL-6 signaling are associated with several autoimmune diseases including IgA nephropathy (IgAN), one of most frequent primary glomerulonephritis worldwide. IgAN is associated with increased plasma concentration of IL-6 and increased plasma concentration of aberrantly galactosylated IgA1 immunoglobulin (Gd-IgA1). Gd-IgA1 is specifically recognized by autoantibodies, leading to the formation of circulating immune complexes (CIC) with nephritogenic potential, since CIC deposited in the glomerular mesangium induce mesangial cells proliferation and glomerular injury. Infection of the upper respiratory or digestive tract enhances IL-6 production and in IgAN patients is often followed by the macroscopic hematuria.

This review recapitulates general aspects of IL-6 signaling and summarizes experimental evidences about IL-6 involvement in the etiopathogenesis of IgA nephropathy through the production of Gd-IgA1 and regulation of mesangial cell proliferation.

1. Introduction

1.1. IL-6 – Its production and function

Interleukin-6 (IL-6) is a pleiotropic cytokine, which was originally described as an antimicrobial immune response-associated cytokine with mostly pro-inflammatory activities. Later reports identified IL-6 as the cytokine involved in the angiogenesis, bone homeostasis, glucose tolerance, hematopoiesis, and in regenerative activities in the intestine, kidney, and pancreas tissues. IL-6 importance in many processes results in its involvement in many disorders such as inflammatory and autoimmune diseases (rheumatoid arthritis, lupus erythematosus, Sjo¨gren's syndrome), neurodegenerative disorders (Alzheimer's disease, Parkinson's disease, and multiple sclerosis), kidney diseases (mesangioproliferative glomerulonephritis or lupus nephritis), metabolic disorders including type 2 diabetes, and cancers [1–9]. IL-6 is also associated with a cytokine storm in infections including COVID19 [10].

IL-6 is produced by cells of immune system and acts in paracrine and endocrine signaling [11,12]. During acute inflammation, monocytes, macrophages, and endothelial cells produce IL-6 and the IL-6 serum concentration could rise several folds in comparison to normal homeostatic values (9.2 ± 6 pg/ml)[13], reaching up to 1 μg/ml during the septic shock [14]. During the early phase of acute inflammatory response IL-6 induces hepatocytes to produce acute phase proteins (APP) e.g. C-reactive protein (CRP), serum amyloid protein A, complement components, haptoglobin, antitrypsin, fibrinogen, thrombopoietin, and reduces production of albumin, fibronectin, transferrin, and cytochrome p450 [15]. IL-6 indirectly controls erythropoiesis by stimulating the liver to release hepcidin, a master regulator of iron homeostasis, which blocks intestinal iron absorption and macrophage iron recycling, causing iron restricted erythropoiesis and anemia [16].

IL-6 promotes antibody production by up-regulation of IL-21 expression in $CD4^+$ T cells [17] followed by cooperative action of IL-6 plus IL-21 causing differentiation of B cells toward plasma cells (PC) [18,19] with sustained IL-6 supported antibody secretion [19,20]. IL-6-regulated T cell differentiation is tightly connected with

* Corresponding authors.
E-mail addresses: leona.raskova@upol.cz (L.R. Kafkova), milan.raska@upol.cz (M. Raska).
[1] These authors contributed equally to this work

https://doi.org/10.1016/j.cytogfr.2022.04.001
Received 12 March 2022; Accepted 5 April 2022
Available online 20 April 2022

upregulation of transcription factors NFAT1 (nuclear factor of activated T cells) and c-maf (v-maf avian musculoaponeurotic fibrosarcoma oncogene homologue) [21], which enhance IL-4 expression. IL-4 shifts balance towards the Th2 subpopulation. Correspondingly IL-6 suppresses Th1 lymphocytes differentiation by inducing a suppressor of cytokine signaling (SOCS)1 and inhibiting interferon (IFN)-γ expression [22]. IL-6 together with TGF-β induces differentiation of naïve $CD4^+$ T cells toward Th17 precursors, which after stimulation with IL-23, mature to Th17 cells producing IL-17, IL-21, IL-22, TNF-α, GM-CSF, and also IL-6 [23]. Additionally, IL-6 promotes the differentiation of a subset of naive $CD8^+$ T cells that express IL-6R into a unique population of effector $CD8^+$ T cells characterized by the production of high levels of IL-21 and low levels of IFN-γ. Similar to $CD4^+$ T follicular helper (Tfh) cells, IL-21–producing $CD8^+$ T cells generated in the presence of IL-6 directly provide help to B cells to induce isotype switching [24]. The IL-6 effects are summarized in Table 1.

IL-6 signals via cellular IL-6 receptor (IL-6R) which is composed of subunits IL-6Rα and gp130. IL-6Rα is nonsignaling subunit of the receptor specific only for IL-6, whereas gp130 is a signal-transducing subunit shared among cytokines of the IL-6 family (Fig. 1). IL-6 first binds to the IL-6Rα (IL-6R, CD126, gp80) forming complex, which further associates with two gp130 (Fig. 2) and initiates signal transduction called classical or "cis"-signaling (Fig. 3). Cis signaling occurs when both IL-6Rα and gp130 are membrane bound. Since IL-6Rα is expressed on surface of only some cell types (membrane bound IL-6Rα or mbIL-6Rα), such as leukocytes (monocytes, macrophages, neutrophils, some types of T cells, and activated B cells), hepatocytes, intestinal epithelial cells, podocytes, osteocytes, and osteoclasts, the cis IL-6 signaling is limited only to these cells [25,26]. B cells begin to express mbIL-6Rα when they start to differentiate toward PC [27]. MbIL-6Rα is highest on pre-plasmablasts and decreases further during maturation into plasmablasts and early PC [28] (Fig. 4**A**). Plasmablasts and PC partially secrete soluble IL-6Rα (sIL-6Rα), which contributes to the sIL-6Rα pool [19]. Resting B cells do not express mbIL-6Rα [29] with the exception of population of gut-associated lymphoid tissue (GALT) B cells [30], which express spontaneously mbIL-6Rα and respond to IL-6 by immunoglobulin production preferentially in the IgA isotype [30]. The mbIL-6Rα expression dominated on IgA^+ B cells whereas expression on IgG^+ and IgM^+ was substantially lower (Fig. 4**B**).

Alternative way of IL-6 signaling, designated as "trans" IL-6 signaling, relies on sIL-6Rα, which lacks transmembrane and cytoplasmic domains [31]. sIL-6Rα has been detected in various body fluids, and binds to IL-6 with comparable affinity as the mbIL-6Rα [32]. The sIL-6Rα together with IL-6 form soluble complex which stimulates cells, expressing on their membrane only gp130 subunit (Fig. 2).

It was experimentally determined that at physiologically relevant cytokine concentration, only a minor part of IL-6 is trapped in the IL-6/sIL-6Rα complex and thus majority of IL-6 signals in cis. IL-6 cis-signaling induces the acute-phase response and is considered to have homeostatic and anti-inflammatory effects. On the other hand, because gp130 is expressed on most cell types, trans-signaling via the sIL-6Rα can activate virtually all cells in the body. IL-6 trans-signaling mainly regulates pro-inflammatory reactions. Interestingly, a soluble form of gp130 (sgp130), produced by alternative mRNA splicing, has been shown to specifically inhibit IL-6 trans-signaling, leaving IL-6 cis-signaling largely unaffected [33] and represent thus part of inherited trans-signaling-regulating pathway.

Trans-signaling via sIL-6Rα is more pro-inflammatory then cis-signaling [34]. Pro-inflammatory activities of IL-6 include stimulation of the recruitment of inflammatory cells, inhibition of apoptosis of inflammatory cells and inhibition of regulatory T-cell differentiation. Further it influences recruitment of monocytes to the site of inflammation and macrophage differentiation from monocytes [35]. Trans-signaling works mostly in a paracrine manner. Therefore, signaling occurs predominantly in the site of local IL-6 production [36]. In analogy with other soluble cytokine receptors, association of IL-6 with

Table 1
IL-6 functions.

Target cells	*Function of IL-6*	*Reference*
Innate immunity		
Hepatocytes	Stimulates APP production (CRP, serum amyloid protein A, complement C3, haptoglobin, antitrypsin, fibrinogen, hepcidin, thrombopoietin ↑; albumin and cytochrome p450 ↓)	Narazaki and Kishimoto [15]. *The two-faced cytokine IL-6 in host defense and diseases. Int. J. Mol. Sci.* Su et al. [119]. *Interleukin-6 signaling pathway and its role in kidney disease: an update. Front. Immunol.*
Monocytes	Stimulates differentiation to macrophages (M-CSF ↑) Suppresses differentiation to dendritic cells	Kaplanski et al. 2003. *IL-6: a regulator of the transition from neutrophil to monocyte recruitment during inflammation. Trends Immunol.*
Endothelial cells	Monocyte attraction to the site of inflammation (MCP1↑)	
Adaptive immunity		
B cells	Promotes plasmablasts survival Induces differentiation of B-cells into PC Induces immunoglobulin production	Schett 2018. *Physiological effects of modulating the interleukin-6 axis. Rheumatology (Oxford)* Dienz et al. [17]. *The effects of IL-6 on CD4 T cell responses. Clinical Immunol.*
$CD4^+$ T cells	Supports survival (Bcl-2↑) Protects from AICD (FasL↓) Induces differentiation to Th2 (IL-4↑) Suppresses differentiation to Th1 (INF-γ↓) In the presence of TGF-β induces differentiation toward Th17 precursors Suppresses differentiation to iTreg (FoxP3↓) Contributes to the differentiation to Tfh	Kimura and Kishimoto 2010. *IL-6: regulator of Treg/Th17 balance. Eur. J.Immunol.* Eto et al. [18] *IL-21 and IL-6 are critical for different aspects of B cell immunity and redundantly induce optimal follicular helper CD4 T cell (Tfh) differentiation. PLoS One* Yang et al. [24]. *IL-6 promotes the differentiation of a subset of naive $CD8^+$ T cells into IL-21-producing B helper $CD8^+$ T cells. J. Exp. Med.*
$CD8^+$ T cells	Induces differentiation to subset of IL-21-producing B helper $CD8^+$ T cells	
Kidneys		
Mesangial cells	Acts as a growth factor and supports proliferation of mesangial cells Stimulates release of MCP-1	Coletta et al. [106]. *Selective induction of MCP-1 in human mesangial cells by the IL-6/sIL-6R complex. Experiment. Nephrol.* Moutabarrik et al. [123]. *Interleukin-6 and interleukin-6 receptor are expressed by cultured glomerular epithelial cells. Scand. J. Immunol.* Chan et al. 2005. *Tubular expression of angiotensin II receptors and their regulation in IgA nephropathy. J. Am. Soc. Nephrol.*
Podocytes	Stimulates IL-6 production in an autocrine manner	
Tubular epithelial cells	Regulates the expression of tubular angiotensin II receptor type 1 Upregulates the production of tubular angiotensin II	
Liver regeneration		
Hepatocytes	Stimulates proliferation and survival (FoxM1, Ref-1, Mcl-1 ↑).	Izumi et al. 2018. *Vagus-macrophage-hepatocyte link promotes post-injury liver regeneration and whole-body survival through hepatic FoxM1 activation. Nat. Commun.* Taub 2003. *Hepatoprotection via the IL-6/Stat3 pathway. J. Clin. Invest.* Fazel Modares et. al. 2019. *IL-6 trans-signaling controls liver regeneration after partial hepatectomy. Hepatology* Ji et. al. 2016. *Distinct role of interleukin-6 and tumor necrosis factor receptor-1 in oval cell- mediated liver regeneration and*
Hepatic satellite cells	Supports hepatocyte proliferation (HGF ↑).	
Hepatic progenitor cells	Stimulates proliferation	

(*continued on next page*)

Table 1 (*continued*)

Target cells	*Function of IL-6*	*Reference*
		inflammationassociated hepatocarcinogenesis. Oncotarget
Angiogenesis		
Endothelial cells	Induces increase in blood vessel cell permeability (VEV-cadherin internalization) Induces expression of adhesion molecules, that assist leukocyte extravasation (ICAM-1, VCAM-1, and E-selectins ↑)	Narazaki and Kishimoto [15]. *The two-faced cytokine IL-6 in host defense and diseases. Int. J. Mol. Sci.* Didion 2017. *Cellular and oxidative mechanisms associated with interleukin-6 signaling in the vasculature. Int. J. Mol. Sci.*
Wound healing		
Fibroblasts	Induces type I collagen accumulation by fibroblasts, as well as TGF-β level increase	Lin et al. 2003. *Essential involvement of IL-6 in the skin wound-healing process as evidenced by delayed wound healing in IL-6-deficient mice. J. Leukoc. Biol.*
Hematopoiesis		
Hepatocytes	Indirectly stimulates platelet production (TPO ↑) Indirectly affects erythropoiesis (hepcidin ↑)	Narazaki and Kishimoto [15]. *The two-faced cytokine IL-6 in host defense and diseases. Int. J. Mol. Sci.*
Nervous system		
Neural stem cells	Contributes to NSC differentiation into astrocytes and oligodendroglyocytes	Erta et al. 2012. *Interleukin-6, a major cytokine in the central nervous system. Int. J. Biol. Sci.*
Astrocytes	Changes the expression pattern (NGF neurotrophin ↑, TNF-α ↓)	
Oligodendroglyocytes	Promotes survival and myelin production	
Bone remodeling		
Osteoblasts	Induces surface expression of RANKL, which activate surrounding osteoclats to resorb bone	Gallo et al. 2014. *Innate immunity sensors participating in pathophysiology of joint diseases: a brief overview. J. Long Term Eff. Med . Implants* McGregor et al. 2019. *IL-6 exhibits both cis- and trans-signaling in osteocytes and osteoblasts, but only trans-signaling promotes bone formation and osteoclastogenesis. J. Biol. Chem.*
Metabolism		
Hepatocytes	Reduces liver insulin sensitivity (IRS↓) Stimulates insulin secretion (GLP-1↑)	Lehrskov and Christensen 2019. *The role of interleukin-6 in glucose homeostasis and lipid metabolism. Semin. Immunopathol.*
Muscle cells	IL-6 level is elevated during exercise. In this context, IL-6 has an anti-inflammatory effect (sTNFαR, IL-1Rα, and IL-10↑)	
Adipose cells	Induces leptin secretion, which influences appetite and caloric intake	
Tumor development		
Tumor cells	Enhances survival (Bcl-2, Bcl-xL, Mcl-1, survivin, XIAP ↑) Enhances proliferation (cyclin D1, D2, and B1, and c-Myc ↑; Cdk inhibitor p21 ↓) Induces ECM remodeling (uPA, cathepsin, MMP-2, MMP-7 and MMP-9↑)	Taniguchi and Karin 2014. *IL-6 and related cytokines as the critical lynchpins between inflammation and cancer. Semin. Immunol.* Malik et. al. 2020. *Cross-talk between Janus kinase signal transducer and activator of transcription pathway and transforming growth factor beta pathways and increased collagen1A1 production in uterine leiomyoma cells. F&S Science*

sIL-6Rα extends the half-life of IL-6 in the blood and reduces internalization of sIL-6Rα/IL-6 complex [31], which may (with other factors) contribute to chronic inflammatory conditions development.

The last mode of action of IL-6 has been confirmed in mice. It is called trans-presentation or cluster signaling. IL-6/IL-6Rα complex is assembled in the endosome of a presenting cell and exported to the surface. IL-6/IL-6Rα on the surface of the presenting cell interacts with gp130 on the recipient cell and induces signaling [37].

1.2. Canonical IL-6 signaling

IL-6 activates multiple signaling pathways among which the Jak/STAT pathway is the most dominant one, followed by the Ras/MAPK/Erk, the MAPK/p38, and MAPK/JNK pathways, the PI3K/Akt pathway, and the SFK-related pathways (Fig. 5).

1.2.1. Jak/STAT pathway

Dimerization of gp130 subunits, as a part of IL-6/IL-6Rα/gp130 hexamer formation, results in trans-phosphorylation of directly associated Janus kinases (Jak) prior to gp130 intracellular domain phosphorylation, where Jak1 plays a major role, followed by Jak2 [38]. The involvement of Tyk2 seems to be controversial [39,40]. Activated Jak kinases phosphorylate and activate each other which in turn leads to the tyrosine phosphorylation of the signal transducers and gp130 tyrosine residues. The phosphotyrosine residues within gp130 create docking sites for signaling molecules containing SH2 domains, such as the STAT factors. Among the gp130 tyrosine residues phosphorylated by activated Jak kinases, pY767, pY814, pY905, and pY915 interact with STAT3, and pY905 and pY915 additionally with STAT1 [41]. STATs tyrosine phosphorylation enables dimerization and STATs relocation to the nucleus, where they activate transcription of the target genes [42]. STAT3 forms homodimers and heterodimers with STAT1. Signals are typically transmitted via canonical STAT homodimers. STAT heterodimers play a role in late signaling or diminishing of signaling or transcription.

Activated STAT3 also induces expression of SOCS3. SOCS3 in tum terminates the IL-6 signaling cascades by binding to gp130-Y759 and forming a negative feedback loop that allows the cell to return to its basal (unstimulated) state [43]. SOCS3 regulates signaling via two distinct mechanisms: directly inhibiting the catalytic activity of Jak and catalyzing the ubiquitination of Jak and gp130 on Lys632 which leads to subsequent lysosomal degradation [44].

Jak/STAT pathway regulates multiple IL-6 biological effects. It induces production of survival proteins (XIAP, Bcl-2, Bcl-xL, Mcl-1), cell cycle proteins controlling proliferation (cyclin D1, D2, and B1, c-Myc), proangiogenic factors (HIF-1, VEGF-A), and ECM remodeling proteins (MMP-2, MMP-9, uPA, cathepsin) [45–49]. STAT3 signaling is involved in Th17 differentiation via regulation of RORγ transcription factor and direct activation of IL-17A and IL-17F genes transcription [50]. Specific contribution of Jak/STAT pathway in production and posttranslational modification of immunoglobulins will be discussed in later part of the manuscipt. STAT3 activation is transient under normal conditions. However, it may be activated continuously in tumors such as liver and gastric carcinomas, due to SOCS3 gene hypermethylation or SOCS3 protein degradation in proteasome leading to extended IL-6/STAT3 induced inflammation [51].

1.2.2. SHP2-dependent Ras/MAPK/Erk pathway, the MAPK/p38, and MAPK/JNK pathways

Balance between Jak/STAT and Jak/SHP2/MAPK activation is crucial for the homeostasis of the organism and for controlled cell response. The non-receptor protein tyrosine phosphatase SHP2 [(SH2)-containing protein tyrosine phosphatase 2] directly associates with gp130 and recruits adaptor protein Grb2 (growth factor receptor bound protein) to the receptor. Grb2 is constitutively associated with Sos (son of sevenless), thus the binding of Grb2 to phosphorylated SHP2 results in the recruitment of Sos to the plasma membrane. Sos is a guanine

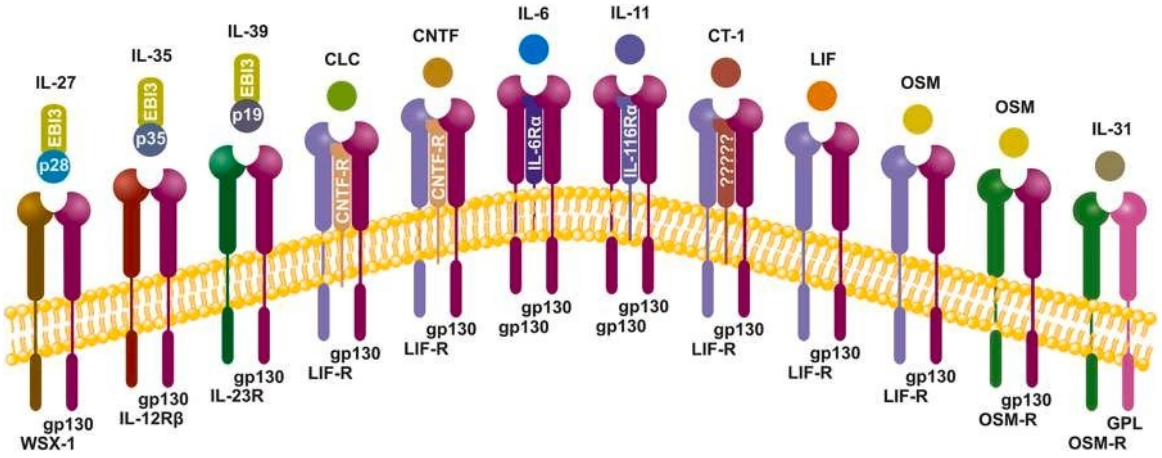

Fig. 1. Receptor complexes of IL-6 family cytokines. IL-6 family cytokines recognize gp130 homo and heterodimers. IL-6 and IL-11 signal via gp130 homodimer, while other family members require heterodimeric receptors. LIF-R/gp130 heterodimer is recognized by LIF, OSM, CT-1, CNTF, CLC. Alternatively, OSM signals via OSM-R/gp130 heterodimer. IL-31 signals via OSM-R and gp130-like protein (GPL). IL-27 and IL-29 signal via WSX1/gp130 and IL-23R/gp130 heterodimers respectively. LIF, OSM and IL-31 require only signal-transducing receptor subunits to perform signaling. CLC, CNTF, IL-6, IL-11 and CT-1 require α-subunit to initialize receptor complex assembly. IL-6 and IL-11 use IL-6Rα and IL-11Rα respectively. CNTF and CLC share CNTF-R. Presumably, CT-1 may use α-receptor as well, but it has not been confirmed yet. IL-27, IL-35, IL-39 are composed of two subunits that are co-expressed. Each of them contains identical EBI3 subunit and individual p28, p35, p19. EBI3 resembles IL6Rα and IL11Rα function.

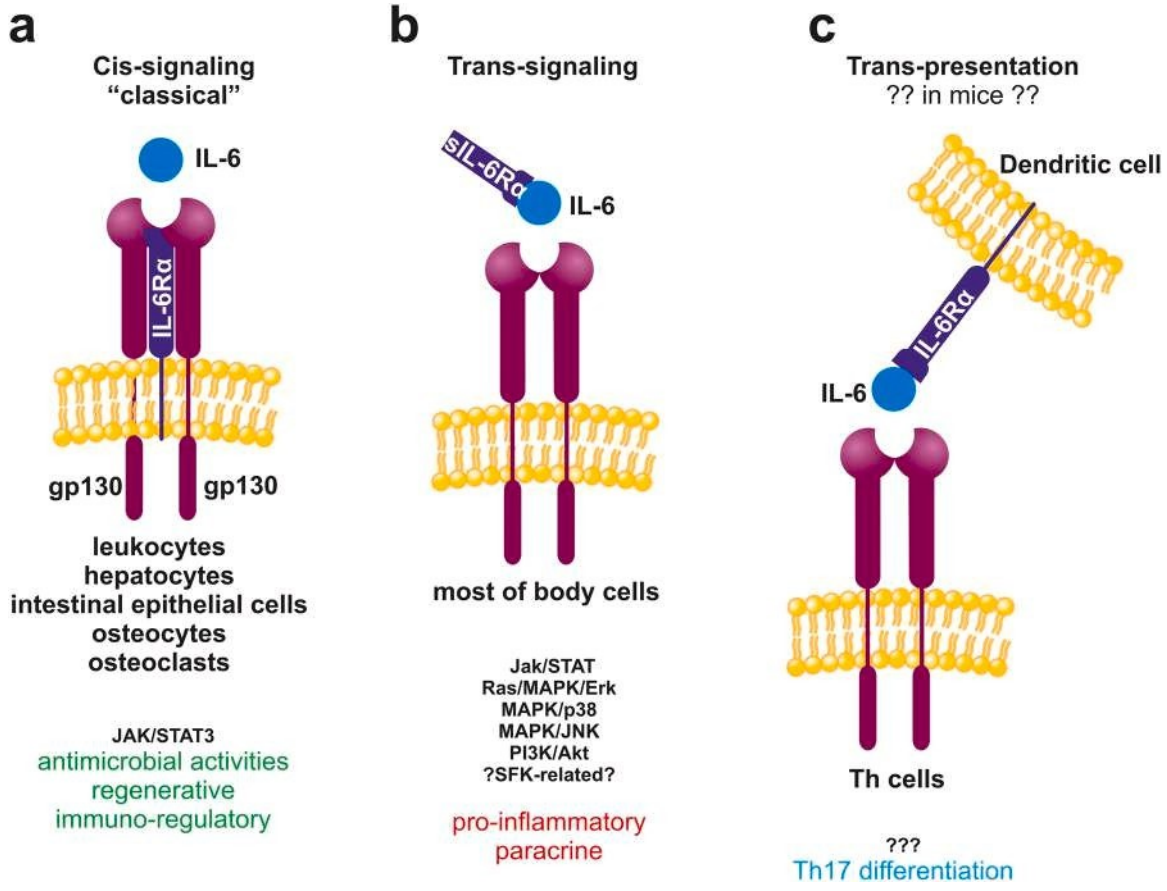

Fig. 2. IL-6 signaling modes. The assembly of the IL-6 signaling complex proceeds in three different ways. **A** Classical signaling takes place when both IL-6Rα and gp130 are membrane-bound. IL-6 initially binds mbIL-6Rα, then IL-6/mbIL-6α complex associates with gp130. Gp130 dimerization activates signaling. Otherwise, IL-6Rα exists in a soluble state. **B** When soluble complex of IL-6/sIL-6Rα assembles; it can activate cells that express gp130 but not mbIL-6Rα. This process is called trans-signaling. **C** Trans-presentation is characterized by direct interaction between cells. IL-6/IL-6Rα complex is assembled within the cell and is expressed on the cell surface, where it interacts with gp130 on the other cell and induces signaling.

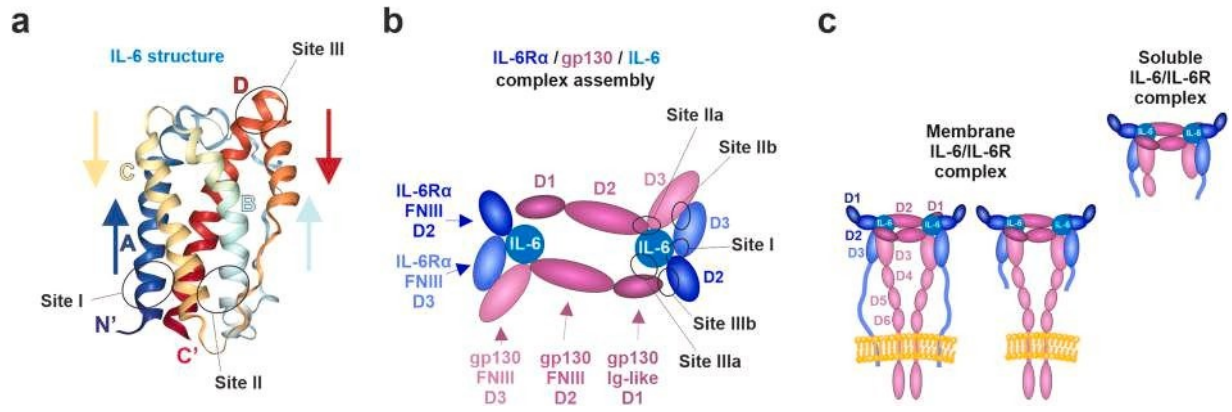

Fig. 3. IL-6 structure and assembly of IL-6/IL-6Rα/gp130 heterohexameric complex. **A**: IL-6 family cytokines have four-α-helix structures with up-up-down-down topology; helices A and B point in one direction, while C and D in the opposite direction, with an additional, short α-helix in the CD loop [141]. **B**: Hexameric receptor complex, consisting of two molecules of IL-6 (turquoise), two IL-6Rα (blue), and two gp130 (pink) molecules. The assembly of heterohexameric complex proceeds in three steps. In the first step, IL-6 forms complex with IL-6Rα chain, which is capable of further interacting with gp130, through binding site I [142,143]. In the second step, IL-6/IL-6Rα complex binds to gp130 by formation of binding site II, which could be further subdivided to subsite IIa and IIb. In the third step IL-6/IL-6Rα/gp130 complex binds to the second gp130 or another already formed complex IL-6/IL-6Rα/gp130 via binding site IIIa and IIIb. **C**: Membrane bound and soluble hexameric complex. Membrane bound hexameric complex contain two molecules either sIL-6Rα or mbIL-6Rα, two gp130, and two molecules IL6. Soluble hexameric complex contain two molecules of sgp130, two molecules of sIL-6Rα and two molecules of IL-6.

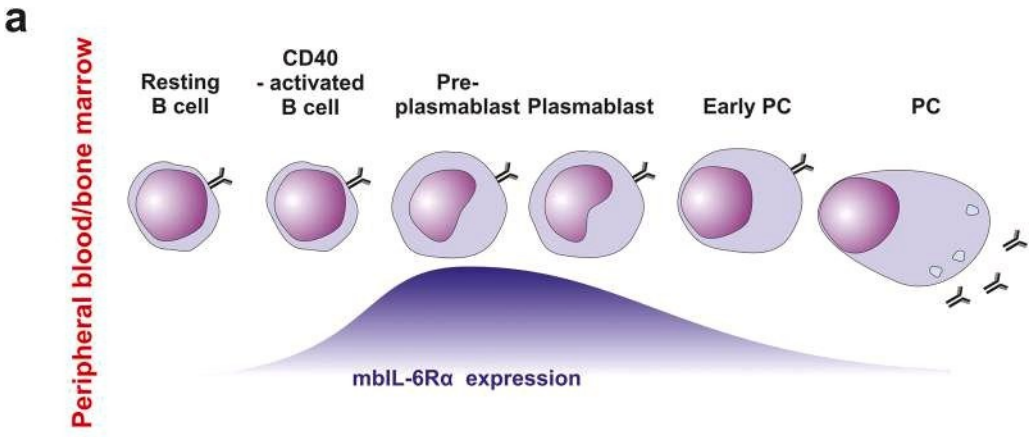

Fig. 4. IL-6Rα expression at various stages of B cells development. **A**: The expression of mbIL-6Rα is initiated upon B cells activation, and is highest in pre-plasmablast. In the later stages of maturation, surface levels of IL-6Rα gradually decrease. **B:** In mucosal tissues, IL-6Rα is expressed on surface of IgA positive, and to a lesser extent also on IgM and IgG positive B cells in the gut-associated lymphoid tissue (GALT). In contrast, tonsillar B cells do not express mbIL-6Rα unless simulated with antigen or Pokeweed mitogen (PWM), after which the response to IL-6 is markedly enhanced as detected by number of cells secreting IgA (preferentially IgA1), IgG, and IgM [30,144].

b

Mucosal tissue

	GALT			Tonsils				
	mbIL-6Rα	Ig secreting cells		mbIL-6Rα	Ig secreting cells			
		NS	+IL-6		NS	+IL-6	+PWM	+PWM +IL-6
IgA1+	++	++	+++	+/-	++	++	+++	++++
IgA2+		+++	++++		+/-	+/-	+	++
IgM+	+	-	-	+/-	+/-	+/-	+	+++
IgG+	+	+	-	+/-	++	++	+	++++

nucleotide exchange factor of Ras (rat sarcoma proto oncogene), which catalyzes the switch of membrane-bound Ras from an inactive, GDP-bound form (Ras/GDP), to a transductionally active, GTP-bound form (Ras/GTP) that initiates Ras/MAPK/Erk pathway activation [52,53]. Activated Erk phosphorylates Gab1 on serine 552 (Grb2-associated binding protein 1), which enables recruitment of Gab1 to the plasma membrane, and its further tyrosin phosphorylation; phosphorylated Y627 and Y659 serve as binding sites for SHP2. Activated Gab1 is essential for MAPK pathway signal amplification [53].

Ras/MAPK activate Erk1/2 and Erk5, which then translocate to the nucleus, where they phosphorylate multiple transcription factors [54]. Known transcription factor substrates for ERK1/2 include c-Myc, Elk-1, nuclear factor for IL-6 expression (NF-IL-6), Tal-1, Ets-2. Erk5 activates expression of Sap1, cFOS, c-Myc, and MEF2. Erk1/2 and Erk5 share 66% sequence identity in their kinase domains, as well as a Thr-Glu-Tyr motif in the activation loop containing sites for dual phosphorylation. Despite this similarity, Erk5 is selectively phosphorylated by MKK5 and is not recognized by the Erk1/2 activator, MKK1/2. IL-6 dependent activation of Ras/MAPK/Erk leads to proliferation and survival of various cell types and is a critical mediator of inflammation driven cancer [55].

MAPK/p38 and MAPK/JNK pathways are also activated by IL-6-mediated signaling [56,57]. The p38 kinase induces the

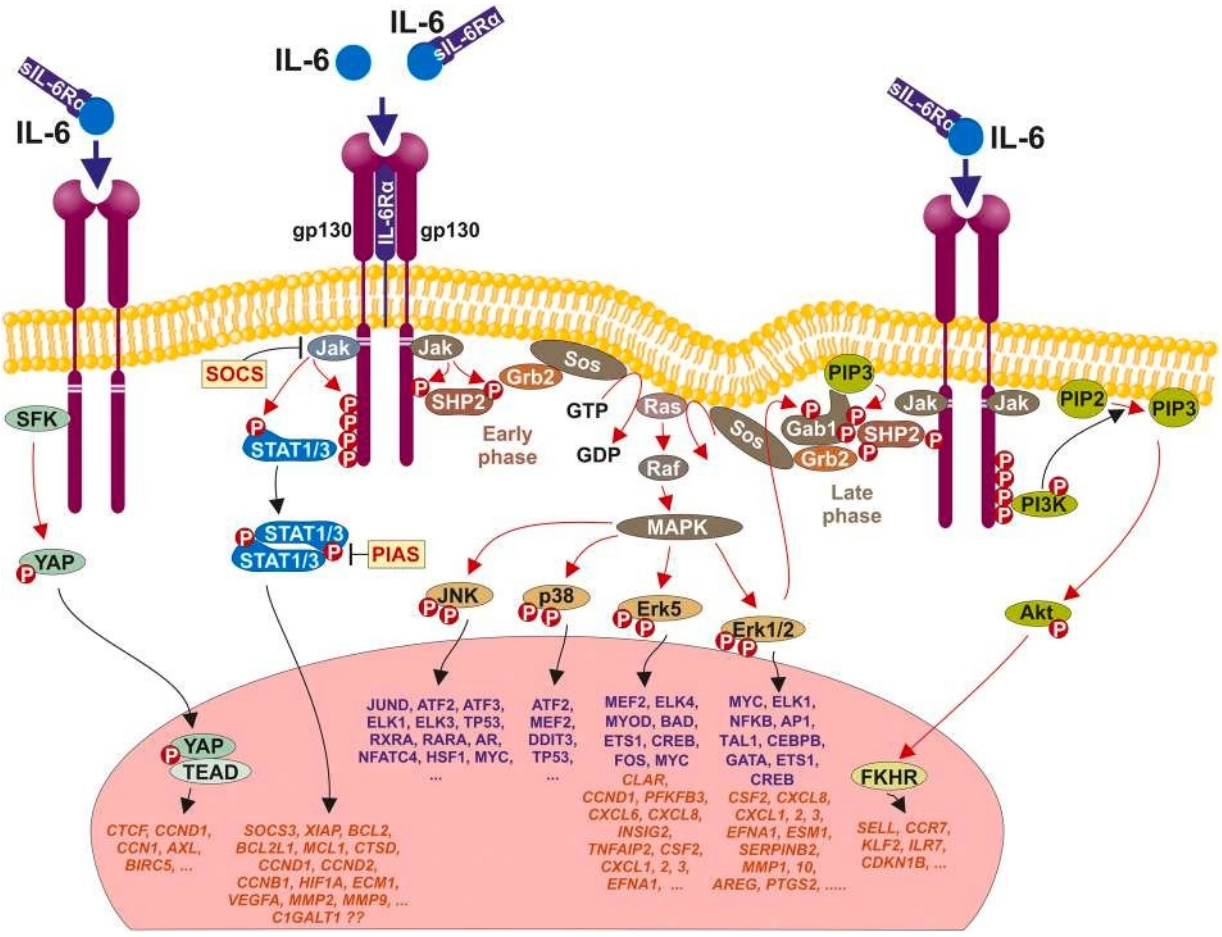

Fig. 5. IL-6 signaling pathways. Jak/STAT is a predominant signaling axis of IL-6. IL-6 receptor assembly initiates recruitment of Jak-kinases to the gp130 intracellular part. Jaks phosphorylate 5 tyrosine residues on gp130, which serve as the docking sites for downstream signaling components containing SHP2 domain. STAT3 and STAT1 are recruited to the phosphorylated tyrosines of Jaks and gp130. Subsequently, STAT itself becomes phosphorylated, dimerizes and relocates to the nucleus, where it activates transcription of the target genes. Alternatively, SHP2 is also being recruited to the gp130 phospho-tyrosine. Jak-dependent phosphorylation of the SHP2 initiates activation of the MAPK pathway. SHP2 recruits Grb2 and SOS. For sustained MAPK pathway Gab1 is required. Complex assembly leads to Ras activation. Ras activates Raf, which in turn phosphorylates and activates MAPK kinase. MAPK phosphorylates JNK, p38, Erk5, and Erk1/2, thereby stimulates their translocation into nucleus. PIP3 is another Jak-SHP2-Gab1 dependent kinase. Finally, SFK member Yes associates with gp130. Yes stabilizes YAP through tyrosine phosphorylation. YAP translocates to the nucleus and functions as a co-activator for transcription factor TEAD2. SOCS and PIAS are proteins involved in down-regulation of IL-6 signaling [145]. Transcription factors in the nucleus are shown in blue. Target genes are shown in brown.

down-regulation of gp130 and thus restricts gp130-mediated signal transduction [58]. The role of MAPK/JNK in IL-6 signaling is not fully elucidated.

1.2.3. PI3K/Akt pathway

The PI3K/Akt (PI3K/Akt/mTORC1) pathway is highly conserved, and its activation is tightly controlled via a multistep process. Activated gp130 directly stimulate PI3K (phosphoinositide 3-kinase) bound via their regulatory subunit or adapter molecules such as the insulin receptor substrate (IRS) proteins. This triggers activation of PI3K and conversion of phosphatidylinositol (3,4)-bisphosphate (PIP_2) lipids to phosphatidylinositol (3,4,5)-trisphosphate (PIP_3) by PI3K catalytic domain. PKB/Akt binds to PIP_3 at the plasma membrane, allowing PDK1 to access and phosphorylate Thr-308 in the "activation loop," leading to partial PKB/Akt activation [59]. Akt phosphorylates forkhead transcription factor (FKHR) and the pro-apoptotic factor Bad (Bcl-2/Bcl-xL-antagonist). Phosphorylated Bad becomes inactive [60]. Also, IL-6 was shown to upregulate muscle protein synthesis and glucose uptake in PI3K/Akt-dependent manner [61].

1.3. Non-canonical IL-6 signaling

IL-6 is a potent activator of the gp130/SFK/YAP pathway (Fig. 5) - non-canonical IL-6 signaling. Gp130 associates with Src family kinases (SFK), which are activated upon receptor engagement to phosphorylate YAP and induce its stabilization and nuclear translocation [62]. In the nucleus YAP binds transcription factors and controls genes that stimulate cell proliferation and tissue growth and inhibit terminal differentiation [63,64].

1.4. IL-6 signaling pathways' inhibitors

The inhibition of IL-6 signaling does not eliminate the cause of the disease, but it decreases the severity of the disorder. IL-6 signaling can be affected by blocking of complex assembly by targeting IL-6 itself, IL-6Rα or gp130 or by blocking of the most dominant IL-6-stimulated pathway Jak/STAT using Jak and STAT inhibitors. Current IL-6 inhibitors are represented by monoclonal antibodies (mAbs), scaffold proteins and small organic molecules [65,66].

Anti-IL-6 monoclonal antibodies used in therapy are chimeric mAb generated in hybridoma cells of mouse origin (siltuximab), humanized mAbs with extension of the chimera strategy in which all regions of the

mouse antibody are replaced with human counterparts (olokizumab, clazakizumab, tocilizumab, etc.), and the newest generation of therapeutic antibodies - fully human-based mAbs (sirukumab, sarilumab, mAb 1339 and PF-04236921) [67]. Monoclonal antibodies tested in IL-6 signaling modification are summarized in Table 1. Administration of IL-6-specific mAb leads to formation of circulating immune complexes of IL-6/anti-IL-6 mAb which protect IL-6 cytokine from kidney clearance. Therefore, the serum IL-6 concentration reaches mg/ml levels clinically expressed by fever, fatigue, recurrence of bone pain and hypercalcaemia [65,66]. An alternative to monoclonal antibodies represents avimers. Avimers are multidomain proteins generated by sequential selection of individual binding domains, each of which recognizes a different epitope, thereby generating a protein that can bind multiple sites on a ligand or ligands. Linking multiple independent binding domains on one molecule or stable molecular complex enhances avidity and specificity. The avimer that inhibits IL-6 contains not only IL-6 recognizing domains, but also IgG domain, which prolongs binder's half-life [68]. Next promising cytokine inhibitors are cytokine traps - fusion proteins of the extracellular parts of receptor subunits. IL-6 cytokine trap is composed of extracellular parts of gp130 and IL-6Rα fused to immunoglobulin Fc region [69]. Unfortunately, no clinical studies using avimers or cytokine traps have been reported.

Blocking of IL-6Rα is considered as an alternative therapeutic strategy with limitations such as the amount of inhibitor, which is much higher with comparison of direct IL-6 inhibitor - IL-6Rα inhibitor must inhibit both cell mbIL-6Rα and sIL-6Rα, and lower specificity, since IL-6Rα can bind not only IL-6, but also all IL-6 family members. Potent inhibitor of IL-6Rα is its super-antagonist SANT-7, which binds IL-6Rα with higher affinity than the natural ligand, and blocks its binding to gp130 and consequently blocks its intracellular signaling [70].

Selective blocking of trans-signaling provides the possibility to specifically modulate inflammatory conditions such as in autoimmune disease without compromising IL-6 signaling via the membrane-bound IL-6Rα. Therefore, olamkicept, the chimeric construct fusing sgp130 with immunoglobulin Fc was designed to make a dimeric form sgp130-Fc with enhanced plasma halftime and stronger interaction than natural monomeric sgp130 [71]. The sgp130Fc protein was shown not to interfere with IL-6 signaling via the membrane-bound IL-6Rα *in vitro* [72].

Intracellularly, Jaks can be blocked by small-molecule kinase inhibitors with different selectivity (ruxolitinib, tofacitinib or filgotinib). Two Jak inhibitors are approved by the FDA: ruxolitinib (Jakafi, selective for Jak1/2) and tofacitinib (selective for Jak1/3). Both are competitive inhibitors that bind ATP-binding pocket of the kinase. Selective Jak1 inhibitors filgotinib, upadacitinib, PF-04965842, and GLPG0634 are currently in clinical trials as well as Jak2 inhibitors fedratinib, AZD1480, and XL019. STAT3 can be targeted by Stattic, CpG–STAT3 decoys or CpG–STAT3 small interfering RNA (siRNA) [71]. STAT3 inhibitor that reached a clinical trial is ochromycinone (STA-21), which is a small chemical compound that inhibits STAT3 dimerization and DNA-binding. The clinical trials of many above mentioned antibodies are ongoing (sirukumab, olokizumab and clazakizumab), and some of them are already approved (tocilizumab, sarilumab, siltuximab).

2. IL-6 in autoimmune diseases

Autoimmune diseases are thought to result from a breakdown in self-tolerance and/or dysregulation of immune responses. It is suggested that the activation of immune response to the target tissue may be a consequence of local immune stimulation targeting inadvertently surrounding tissue in a manner dependent on genetic and/or environmental factors. IL-6 is an important mediator during increased activation of immune system, since it augments production of various cytokines including IL-6 itself, epiregulin, TNF-α, chemokines, and growth factors in non-immune cells. IL-6 is increased in serum and synovial fluid of patients with rheumatoid arthritis (RA) [73], which is characterized by systemic and joint inflammation, contributing to joint destruction.

Serum levels of IL-6 are elevated in human systemic lupus erythematosus (SLE) and IL-6 correlates with disease activity [74,75]. The main features of autoimmunity in SLE are B cell hyperactivity and production of IL-6, spontaneous lymphocyte proliferation, and the production of pathogenic antibodies recognizing self-antigens. In patients with lupus nephritis, the urinary levels of IL-6 also correlate with disease activity and the expression of IL-6 has been reported within the kidney tissue particularly in renal mesangial cells [76,77]. Engagement of the B-cell receptor (BCR) with autoantigen together with B cell overexpressed IL-6 down-regulates the level of B cell activation inhibitor - membrane CD5, promoting the activation and expansion of autoreactive B cells in SLE patients [78]. IL-6 levels are also elevated in sputum [7] and in the tears [79] in Sjo¨gren's syndrome, an autoimmune disease characterized by lymphocytes infiltration of the salivary gland and production of autoantibodies. IL-6 is also implicated in the type 2 diabetes, since it may reduce liver insulin sensitivity by induction of the SOCS3 which associates with Insulin receptor substrate proteins (IRS) and triggers them for proteasomal degradation [80].

3. IL-6 and IgA nephropathy

IgA nephropathy (IgAN) is the most common form of primary glomerulonephritis in many countries. The pathologic features of IgAN include mesangial deposits of IgA1, often with co-deposits of C3 and IgG, mesangial cell proliferation and matrix expansion [81,82].

IgA1 differs from IgA2 in that it contains a longer hinge region between the first and second heavy-chain constant-region domains. Hinge region of IgA1 contains up to six *O*-liked glycans, which consist of *N*-acetylgalactosamine (GalNAc) and usually a β1,3-linked galactose (Gal) [83]. Sialic acid (SA) may be attached to the β1,3-linked Gal through an α2,3 linkage or to the GalNAc by an α2,6 linkage. *O*-linked glycans are synthesized in a step-wise manner, beginning with attachment of GalNAc to Ser or Thr. A member of the UDP-GalNAc transferase (GalNAcT) enzyme family catalyzes this first step. It has been proposed that all members of this enzyme family can glycosylate a wide range of acceptors, but only one, GalNAc-T2, can glycosylate IgA1. It has been shown that GalNAc-T2 initiates synthesis of all *O*-linked glycans in the hinge region of IgA1 [84,85]. The *O*-glycan chain is then extended by sequential attachment of Gal and/or SA residues to the GalNAc [3]. The addition of Gal is mediated by core 1 β1,3-galactosyltransferase (C1β3GalT1) that transfers Gal from UDP-Gal to a GalNAc on Ser/Thr of IgA1. The stability of this enzyme apparently depends on its interaction with the C1β3GalT1-specific molecular chaperone Cosmc, that assists in the folding of the protein. SA may be attached to the GalNAc by an α-2,6 linkage catalyzed by the α-N-acetylgalactosaminide α-2,6-sialyltransferase 2 (ST6GalNAc-II) or to the Gal through an α2,3 linkage catalyzed by one of several α-2,3-sialyltransferases (ST3Gal) [83,86].

In healthy individuals the prevailing *O*-glycans are represented by Gal-GalNAc disaccharide, and its mono and disialylated forms. In IgAN patients the aberrantly glycosylated form of IgA1 with terminal GalNAc or sialylated GalNAc is commonly found in serum [87]. The aberrant glycosylation of IgA1 consisting of Gal-deficiency is one of crucial hits in multistep etiopathogenesis of IgAN [81, 88, 89]. The Gd-IgA1 production is related to decreased expression and activity of C1GalT1, and correspondingly, the expression of Cosmc necessary for stability of the nascent C1GalT1 protein is downregulated [3, 90, 91]. IgAN is further connected with elevated expression and activity of ST6GalNAc-II, which is likely responsible for sialylation of GalNAc of Gal-deficient IgA1 [92]. Attachment of SA to GalNAc represents "premature" sialylation which precludes subsequent attachment of Gal, forming Gal-deficient *O*-linked glycans [3,93].

Gd-IgA1 in mesangial deposits of IgAN patients is enriched in polymeric IgA1 form [94–96] in analogy to serum polymeric Gd-IgA1 [87]. The terminal GalNAc, sialylated GalNAc, or fragment of the hinge region

with Gal-deficient *O*-glycans is recognized by naturally occurring or affinity matured IgG or IgA1 antibodies [81, 88, 91, 97, 98] leading to generation of Gd-IgA1-containing circulating immune complexes (CIC) [87,97] which depose to glomerular mesangium. Over 50% of IgAN patients exhibit increased serum levels of both IgA and CIC. Production of Gd-IgA1 is at least partially a heritable trait [99]. Asymptomatic blood relatives of IgAN patients have often significantly higher levels of Gd-IgA1 than do unrelated healthy controls. There are several reports identifying involvement of IL-6 in both Gd-IgA1 production and kidney mesangium activation in IgAN [100–104].Table.2.

3.1. IL-6 and mesangial cells activation

Mesangial cells participate in the regulation of glomerular hemodynamics and are critical for renal glomerular function. They comprise multiple functions including structural support for capillary loops, modulation of glomerular filtration, mesangial matrix formation, phagocytosis, monitoring of capillary lumen glucose concentration, the secretion of extracellular matrix proteins, growth factors, and cytokines, regulation of immune cells recruitment to kidney mesangium, and the uptake of macromolecules and immune complexes. Change in physiology of mesangial cells seems to be an early event in progressive glomerular injury leading to modified composition of extracellular matrix (ECM) and glomerular sclerotic changes and finally renal failure.

Activation of mesangial cells leads to their proliferation and the release of many pro-inflammatory and pro-fibrotic mediators which includes TNF-α, platelet activating factor (PAF), IL-1β, IL-6, platelet derived growth factor (PDGF), fibroblast growth factor (FGF), TGF-β, and various chemokines [105,106]. High-molecular-mass IgA1--containing CIC (IgA1-CICs) activate mesangial cells' MAPK/ERK and PI3K/Akt signaling pathways [104], of which PI3K/Akt/FKHRL1 pathway is involved in mesangial cells proliferation and MAPK/ERK pathway in stimulation of cytokine production (including IL-6 secretion) and glomerular damage in IgAN [104,107]. IL-6 is strong activator of

Table 2
IL-6/IL-6R inhibitors and their application reported.

Name	*Target*	*Approved/clinical trial/preclinical trial*	*Substance*
Antibodies			
Siltuximab (CNTO 328, Sylvant)	IL-6; Site I	FDA and EMA approved for iMCD Phase 3 for COVID-19	Chimeric mAb
Olokizumab (Artlegia)	IL-6; Site III	Phase 3 for RA Phase 3 for COVID-19	Humanized mAb
Clazakizumab (ALD518, BMS-945429)	IL-6; Site I	Phase 2 for RA Phase 2 for Antibody-mediated rejection Phase 2 for COVID-19	Humanized mAb
PF-04236921	IL-6; Site I	Phase 2 for CD Phase 2 for SLE Phase 1 for RA	Human mAb
Sirukumab (CNTO 136, Plivensia)	IL-6	Phase 2 for MDD Phase 3 for RA Phase 2 for COVID-19 Phase 2 for Lupus ephritis	Human mAb
mAb 1339	IL-6	preclinical trial	Human mAb
EBI-031	IL-6 site II	preclinical trial	Humanized mAb
MEDI5117	IL-6	preclinical trial	Humanized mAb
Tocilizumab (Actemra)	IL-6R	FDA and EMA approved for RA, GCA, JIA, CRS FDA approved for SSc-ILD Phase 4 for RA Phase 4 for Schizophrenia Phase 3 and 4 for COVID-19 Phase 3 for SS, Polymyalgia Rheumatica, Hand Osteoarthritis, Takayasu Arthritis, Thyroid associated Opthalmopathies, Neuromyelitis Optica Phase 2 for HIV, ALS, Diabetes Melitus Type 1, and others	Humanized mAb
Sarilumab (SAR153191, REGN88, Kevzara)	IL-6R	FDA and EMA approved for RA Phase 3 for COVID-19 Phase 2 for Uveitis	Human mAb
Vobarilizumab (ALX-0061)	IL-6R	Phase 2 for RA Phase 2 for SLE	Bivalent nanobody, humanized
Satralizumab (Enpryng)	IL-6R	FDA and EMA approved for Neuromyelitis Optica Spectrum Disorder	Humanized mAb
Recombinant protein			
C326	IL-6	preclinical trial	Avimer scaffold
Cytokine trap	IL-6	preclinical trial	Gp130 and IL-6R fused to Fc protein
NRI	IL-6R	preclinical trial	Tocilizumab ScFv fused to IgG1 Fc
SANT-7	IL-6R	preclinical trial	Mutated IL-6
Olamkicept (FE 999301, FE301, TJ301)	IL-6/sIL-6R complex	Phase 2 for Ulcerative colitis	sgp130-Fc dimer
Small organic molecules			
6a	IL-6	preclinical trial	pyrrolidinesulphonylaryl
ERBF	IL-6R	preclinical trial	20 S,21-epoxyresibufogenin-3-formate)
ERBA	IL-6R	preclinical trial	20 S,21-epoxyresibufogenin-3-acetate

FDA – Food and Drug Administration, EMA - European Medicines Agency.
iMCD - idiopathic multicentric Castleman's disease; RA – rheumatoid arthritis; SLE – systemic lupus erythematosus; MDD – major depressive disorder; GCA - giant cell arteritis; JIA - juvenile idiopathic arthritis; SS - systemic sclerosis, CRS – cytokine release syndrome, SSc-ILD - systemic sclerosis-interstitial lung disease

mesangial cells and could act as an autocrine growth factor for them. Nevertheless, because human mesangial cells express only the gp130 but not the mbIL-6Rα, IL-6 could stimulate human mesangial cells only in the form of complex with sIL-6Rα [106]. Such stimulation activates preferentially trans signaling (proinflammatory response) and induces the release of MCP-1 (monocyte chemoattractant protein type 1, CCL2), an enhancer of monocyte recruitment [106]. IL-6 secretion could be induced also by a factors such as LPS, IL-1β, TNF-α, angiotensin II [107–113]. In a mouse model, overexpression of human IL-6 gene leads to high plasma levels of IL-6 and profound mesangial proliferation [114]. In human nevertheless, IL-6 alone does not activate proliferation of mesangial cells but it is considered as a "competence" factor acting together with a "progression" factors such as FGF [106]. Renal IL-6 mRNA analysis suggests that the kidney could serve as the substantial source of IL-6 in the uremic state and IL-6 leads to increases in FGF expression in acute and chronic kidney disease [115]. Therefore, increased IL-6 levels observed in IgAN patients may be responsible for the pathological mesangial cells proliferation if other factors are presented in the kidney mesangium.

Production of IL-6 by mesangial cells can be also induced by complex of Gd-IgA1 formed with surface-located protein M from group A streptococcus. Thus, streptococcal IgA-bound M protein takes an important part in the initiation and propagation of an inflammatory response in the kidney during IgAN [116]. Secretion of the pro-inflammatory cytokine IL-6 leads to the differentiation of Th17 cells. Correspondingly, Th17-associated cytokines in serum and urine (IL-2, IL-12, TNF-α, IL-6, IL-10, IL-17, MCP-1 and MIP-1β) were elevated and correlated with renal pathological change in IgAN patients [117,118].

3.2. IL-6 signaling in other kidney cells

IL-6 can be secreted by podocytes, endothelial cells, tubular and glomerular epithelial cells [119]. Podocytes produce relatively low levels of IL-6 under basal conditions but stimuli such as LPS, TNF, and IL-1β, or high glucose concentration induce podocytes to increase IL-6 expression [120]. TNF released from the mesangium after IgA deposition induces TNF synthesis by podocytes in an autocrine manner, since TNF upregulates the expression of TNF receptors in podocytes [121]. Autocrine signaling is also involved in IL-6 production, as podocytes are the only population of human resident renal cells that express IL-6Rα [120, 122–124].

Numerous systemic or local insults, including hypoxemia, nephrotoxic substances, oxidized lipid, advanced glycation end products, immune complexes, cytokines, and chemokines could initiate renal tubular epithelial cells (TEC) to synthesize and secrete IL-6 [125]. Glomerular injury is a potent inducer for IL-6 generation in TEC which presents one aspect of glomeruli-tubules cross talk. The combinatory effect of CD40L with IL-1 or IL-17 on TEC exhibited very strong activation potential toward IL-6 production [126]. The effect of CD40L was further potentiated in hypoxic conditions [127].

3.3. IL-6 and clinicopathological features of IgAN patients

Urinary level of IL-6 correlates with the severity of chronic histological changes in renal biopsy specimens [117] and with creatinine clearance and are thought to be a prognostic marker for the progression of renal damage in IgAN [118, 128, 129]. The immunosuppression therapy by corticosteroids and azathioprine does not have an impact on urinary IL-6 levels in IgAN patients [130,131]. The most recent study of the predictive value of urinary IL-6 levels in IgAN patients revealed statistically significant association between IL-6 levels and the extent of focal glomerulosclerosis, interstitial fibrosis lesions area and proteinuria [132]. The greatest power for prediction of the interstitial fibrosis lesions was seen with the model that combines patients' age, glomerular filtration rate, urinary level of MCP-1 and urinary IL-6. This noninvasive test may improve the estimation of the interstitial fibrosis lesions severity [132].

Biopsy is essential tool for IgAN diagnosis. Typical IgAN sample shows the presence of IgA in the glomerular mesangium. Further analysis of biopsy tissue demonstrates IL-6 gene expression and the presence of IL-6 in the glomerular and vascular endothelial sites of IgAN patients at the time of diagnosis [133]. In the contrary to urinary levels of IL-6, which does not respond to corticoids therapy, IL-6 disappeared after steroids mini-pulse therapy and in remission of the disease [134]. Correspondingly to this finding, IL-6 positive patients, who suffer from more severe symptoms then IL-6 negative IgAN patients, benefited from steroids therapy [135]. It remains to be answered why the steroids therapy did not have the impact on the urinary levels of IL-6 [130,131].

3.4. IL-6 and Gd-IgA1 production in IgAN

Several cytokines, IL-6, IL-10, IFN-γ, and TNF-α increase production of IgA1 in EBV-immortalized IgA1-producing cells from peripheral blood of patients with IgA nephropathy. However, only the IL-6 stimulation leads to the elevation of Gd-IgA1 synthesis, whereas analogous stimulation with cytokines such as IL-1, IL-5, IL-10, IFN-γ, TGF-β, or TNF-α does not affect the Gd-IgA1 production substantially [3,101]. As was shown, IL-6 decreases expression and activity of C1GalT1 and Cosmc, and increases expression and activity of ST6GalNAc-II [3,86]. Analogously tested IL-4 decreased expression of C1GalT1 and Cosms, but did not affect expression or activity of ST6GalNAc-II, and only moderately reduced enzymatic activity of C1GalT1. IL-4 also enhanced Gd-IgA1 production, but to a lesser extent compared with IL-6. We therefore assume that during infections of the upper respiratory or gastrointestinal tract, commonly associated in IgAN with episodes of macroscopic hematuria, exposition of IgA1-producing cells to locally produced IL-6 could accentuate Gd-IgA1 production [88]. Furthermore, during bacterial infections, pathogen associated molecular patterns (PAMP) activate the TLR9-MyD88 signaling pathway and probably other PAMP signaling, which leads to significantly increased synthesis of IL-6 [136]. Besides the direct IL-6 stimulation, TLR9 activation in IgA1-secreting cells enhanced synthesis of aberrantly glycosylated IgA1, since TLR9 signaling augmented also synthesis of the APRIL, which independently as well as in synergy with IL-6 increases production of Gd-IgA1 [137] (Fig. 6). Interestingly, the polymorphisms of TLR9 is associated with the clinical severity of IgAN [138].

To elucidate the mechanism responsible for observed IL-6-stimulated Gd-IgA1 production in IgAN patients, Jak/STAT3 pathway activation upon IL-6 stimulation was compared among IgA1-producing cells from IgAN patients and healthy controls. IL-6-induced STAT3 phosphorylation at Y705 was more intensive and persisted longer in cells from IgAN patients compared with those from control subjects [101]. Phosphorylated Y705 is crucial for the formation of active STAT3 dimers [139]. Phosphorylation of STAT3 Y727 was not affected. The effects of IL-6 associated with extended Y705 phosphorylation and Gd-IgA1 production was reversed by STAT3 inhibitor Stattic and Jak2 inhibitor AZD1480, proving evidence that the JA2/STAT3 pathway is involved in the IL-6-enhanced expression of Gd-IgA1 in the cells of IgAN patients. IL-6/STAT3 signaling may be involved in downregulation of C1GalT1 through transcription factor SP1/3 and its binding site at the promoter of *C1GALT1* gene. Enhanced and extended IL-6-induced activation of STAT3 phosphorylation represents a pathogenic process in IgAN that results in the overproduction of Gd-IgA1 [101]. And consequently IL-6 increased Gal deficiency of secreted IgA1 in cells derived from IgAN patients but not from healthy controls [3,101].

LIF, interleukin-6 family member, which acts through the receptors gp130 and LIF-R, increased the production of Gd-IgA1 in the IgA1-producing cell lines derived from IgAN patients but not in the analogously prepared cells from healthy controls. In contrast to IL-6, the production of total IgA1 was not affected [102]. Increased production of Gd-IgA1 relates to induced STAT1 phosphorylation. Abnormal activation of STAT1 in IgAN is Src family protein kinases dependent, but not

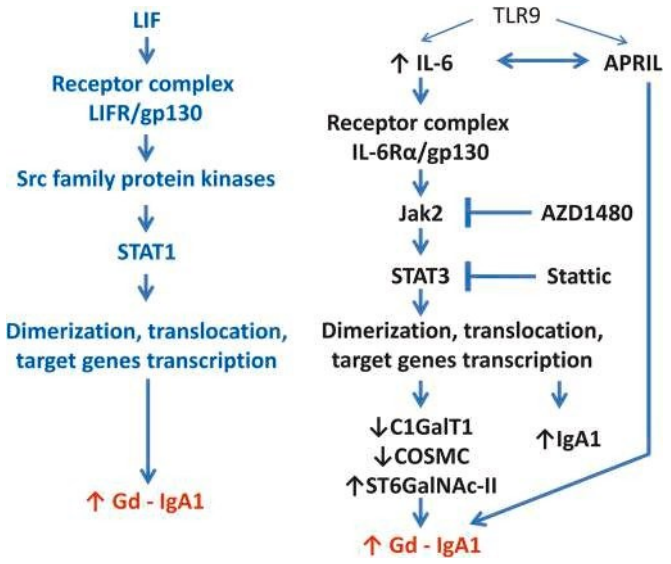

Fig. 6. Effect of IL-6 signaling on the production of Gd-IgA1. Abnormal signaling of IgA producing cells from IgAN patients. Signaling of the IL-6 family cytokines LIF and IL-6 leads to the increase in production of Gd-IgA1 in the cells from IgAN patients. Upon TLR9 receptor activation, the cells elevate the production of IL-6 and APRIL. IL-6 activates IL-6 receptor complex and relay the signal through the Jak2/STAT3 pathway. Prolonged STAT3 phosphorylation is one of the pathogenic processes in IgAN cells. Phosphorylation of Jak2 and STAT3 can be inhibited by AZD1480 and Stattic, the artificial inhibitors, which block this pathway. Phosphorylated STAT3 dimerize, translocate to the nucleus and, as a transcription factor, influences transcription of target genes. This leads to deregulation of glycosyltransferases C1GalT1 levels and ST6GalNAc-II levels which results in increase of the production of Gd-IgA1. On the other hand, LIF signaling in the cells from IgAN patients does not use the Jak/STAT pathway to produce Gd-IgA1. The signal is relayed by Src family protein kinases which phosphorylate STAT1. STAT1 as a transcription factor activates its target genes which causes elevation in Gd-IgA1 production.

Jak2 dependent (Fig. 6) [102]. Genome-wide association study revealed a strong association of the genomic locus that encodes LIF with the risk of IgAN [140].

Funding

The research was supported by Ministry of School, Youth, and Sport, Czech Republic grant CZ.02.1.01/0.0/0.0/16_025/0007397 awarded to M.R. and P.M., grant of the Internal Grant Agency of Palacky University (IGA_LF UP_2022_011) awarded to M.R. and grant of Institutional Research Concept RVO: (86652036) awarded to P.M.

CRediT authorship contribution statement

Yaroslava Groza and Jana Jemelkova have contributed equally to the article. **Yaroslava Groza:** Writing – original draft. **Jana Jemelkova:** Writing – original draft. **Leona Raskova Kafkova:** Writing – original draft, Writing – review & editing. Milan Raska: Writing – review & editing, Visualization, Funding acquisition. **Petr Maly:** Writing – review & editing, Funding acquisition.

Declarations

None.

Declaration of Competing Interest

The authors declare that they have no known competing financial interests or personal relationships that could have appeared to influence the work reported in this paper.

Acknowledgments

The research was supported by Ministry of School, Youth, and Sport, Czech Republic grant CZ.02.1.01/0.0/0.0/16_025/0007397 awarded to M.R. and P.M. and grant of the Internal Grant Agency of Palacky University (IGA_LF UP_2022_011) awarded to M.R.

References

[1] M. Mogi, M. Harada, T. Kondo, P. Riederer, H. Inagaki, M. Minami, T. Nagatsu, Interleukin-1 beta, interleukin-6, epidermal growth factor and transforming growth factor-alpha are elevated in the brain from parkinsonian patients, Neurosci. Lett. 180 (2) (1994) 147–150.
[2] M. Rothaug, C. Becker-Pauly, S. Rose-John, The role of interleukin-6 signaling in nervous tissue, Biochim. Biophys. Acta 1863 (6 Pt A) (2016) 1218–1227.
[3] H. Suzuki, M. Raska, K. Yamada, Z. Moldoveanu, B.A. Julian, R.J. Wyatt, Y. Tomino, A.G. Gharavi, J. Novak, Cytokines alter IgA1 O-glycosylation by dysregulating C1GalT1 and ST6GalNAc-II enzymes, J. Biol. Chem. 289 (8) (2014) 5330–5339.
[4] J. Spranger, A. Kroke, M. Mohlig, K. Hoffmann, M.M. Bergmann, M. Ristow, H. Boeing, A.F. Pfeiffer, Inflammatory cytokines and the risk to develop type 2 diabetes: Results of the prospective population-based European Prospective Investigation into Cancer and Nutrition (EPIC)-potsdam study, Diabetes 52 (3) (2003) 812–817.
[5] L. Lacina, J. Brabek, V. Kral, O. Kodet, K. Smetana Jr., Interleukin-6: a molecule with complex biological impact in cancer, Histol. Histopathol. 34 (2) (2019) 125–136.
[6] G.S. Hotamisligil, E. Erbay, Nutrient sensing and inflammation in metabolic diseases, Nat. Rev. Immunol. 8 (12) (2008) 923–934.
[7] A.M. Nilsson, E. Tufvesson, R. Hesselstrand, P. Olsson, P. Wollmer, T. Mandl, Increased B-cell activating factor, interleukin-6, and interleukin-8 in induced sputum from primary Sjogren's syndrome patients, Scand. J. Rheumatol. 48 (2) (2019) 149–156.
[8] S.A. Apostolidis, L.A. Lieberman, K. Kis-Toth, J.C. Crispin, G.C. Tsokos, The dysregulation of cytokine networks in systemic lupus erythematosus, J. Interf. Cytokine Res.: Off. J. Int. S. Interf. Cytokine Res. 31 (10) (2011) 769–779.
[9] F.A. Houssiau, Cytokines in rheumatoid arthritis, Clin. Rheumatol. 14 (Suppl 2) (1995) 10–13.
[10] H. Han, Q. Ma, C. Li, R. Liu, L. Zhao, W. Wang, P. Zhang, X. Liu, G. Gao, F. Liu, Y. Jiang, X. Cheng, C. Zhu, Y. Xia, Profiling serum cytokines in COVID-19 patients reveals IL-6 and IL-10 are disease severity predictors, Emerg. Microb. Infect. 9 (1) (2020) 1123–1130.
[11] J.V. Castell, M.J. Gomez-Lechon, M. David, T. Hirano, T. Kishimoto, P. C. Heinrich, Recombinant human interleukin-6 (IL-6/BSF-2/HSF) regulates the synthesis of acute phase proteins in human hepatocytes, FEBS Lett. 232 (2) (1988) 347–350.
[12] J.V. Castell, M.J. Gomez-Lechon, M. David, T. Andus, T. Geiger, R. Trullengue, R. Fabra, P.C. Heinrich, Interleukin-6 is the major regulator of acute phase protein synthesis in adult human hepatocytes, FEBS Lett 242 (1989) 237–239.
[13] J.M. Fernandez-Real, M. Vayreda, C. Richart, C. Gutierrez, M. Broch, J. Vendrell, W. Ricart, Circulating interleukin 6 levels blood pressure, and insulin sensitivity in apparently healthy men and women, J. Clin. Endocr. Metab. 86 (3) (2001) 1154–1159.
[14] A. Waage, P. Brandtzaeg, A. Halstensen, P. Kierulf, T. Espevik, The complex pattern of cytokines in serum from patients with meningococcal septic shock - association between Interleukin-6, Interleukin-1, and fatal outcome, J. Exp. Med. 169 (1) (1989) 333–338.
[15] M. Narazaki, T. Kishimoto, The two-faced Cytokine IL-6 in host defense and diseases, Int. J. Mol. Sci. 19 (11) (2018).
[16] A. Pagani, A. Nai, L. Silvestri, C. Camaschella, Hepcidin and anemia: A tight relationship, Front. Physiol. 10 (2019) 1294.
[17] O. Dienz, S.M. Eaton, J.P. Bond, W. Neveu, D. Moquin, R. Noubade, E.M. Briso, C. Charland, W.J. Leonard, G. Ciliberto, C. Teuscher, L. Haynes, M. Rincon, The induction of antibody production by IL-6 is indirectly mediated by IL-21 produced by CD4+ T cells, J. Exp. Med. 206 (1) (2009) 69–78.
[18] D. Eto, C. Lao, D. DiToro, B. Barnett, T.C. Escobar, R. Kageyama, I. Yusuf, S. Crotty, IL-21 and IL-6 are critical for different aspects of B cell immunity and redundantly induce optimal follicular helper CD4 T cell (Tfh) differentiation, PLoS One 6 (3) (2011), e17739.
[19] G. Jego, R. Bataille, C. Pellat-Deceunynck, Interleukin-6 is a growth factor for nonmalignant human plasmablasts, Blood 97 (6) (2001) 1817–1822.
[20] L. Vernino, L.M. McAnally, J. Ramberg, P.E. Lipsky, Generation of nondividing high rate Ig-secreting plasma cells in cultures of human B cells stimulated with anti-CD3-activated T cells, J. Immunol. 148 (2) (1992) 404–410.
[21] Y. Yang, J. Ochando, A. Yopp, J.S. Bromberg, Y. Ding, IL-6 plays a unique role in initiating c-Maf expression during early stage of CD4 T cell activation, J. Immunol. 174 (5) (2005) 2720–2729.
[22] S. Diehl, J. Anguita, A. Hoffmeyer, T. Zapton, J.N. Ihle, E. Fikrig, M. Rincon, Inhibition of Th1 differentiation by IL-6 is mediated by SOCS1, Immunity 13 (6) (2000) 805–815.

[23] E. Bettelli, Y. Carrier, W. Gao, T. Korn, T.B. Strom, M. Oukka, H.L. Weiner, V. K. Kuchroo, Reciprocal developmental pathways for the generation of pathogenic effector TH17 and regulatory T cells, Nature 441 (7090) (2006) 235–238.
[24] R. Yang, A.R. Masters, K.A. Fortner, D.P. Champagne, N. Yanguas-Casas, D. J. Silberger, C.T. Weaver, L. Haynes, M. Rincon, IL-6 promotes the differentiation of a subset of naive CD8+ T cells into IL-21-producing B helper CD8+ T cells, J. Exp. Med. 213 (11) (2016) 2281–2291.
[25] P.C. Heinrich, I. Behrmann, S. Haan, H.M. Hermanns, G. Muller-Newen, F. Schaper, Principles of interleukin (IL)-6-type cytokine signalling and its regulation, Biochem. J. 374 (Pt 1) (2003) 1–20.
[26] J. Scheller, A. Chalaris, D. Schmidt-Arras, S. Rose-John, The pro- and anti-inflammatory properties of the cytokine interleukin-6, Biochim. Biophys. Acta 1813 (5) (2011) 878–888.
[27] Y. Hirata, T. Taga, M. Hibi, N. Nakano, T. Hirano, T. Kishimoto, Characterization of IL-6 receptor expression by monoclonal and polyclonal antibodies, J. Immunol. 143 (9) (1989) 2900–2906.
[28] D. Chauhan, S. Kharbanda, H. Uchiyama, M. Urashima, R. Fragoso, J. Sen, D. W. Kufe, K.C. Anderson, Identification of upstream signals regulating Interleukin-6 gene-expression during in-vitro treatment of human B-Cells with pokeweed mitogen, Blood 84 (7) (1994) 2243–2252.
[29] T. Taga, Y. Kawanishi, R.R. Hardy, T. Hirano, T. Kishimoto, Receptors for B cell stimulatory factor 2. Quantitation, specificity, distribution, and regulation of their expression, J. Exp. Med. 166 (4) (1987) 967–981.
[30] K. Fujihashi, J.R. McGhee, C. Lue, K.W. Beagley, T. Taga, T. Hirano, T. Kishimoto, J. Mestecky, H. Kiyono, Human appendix B cells naturally express receptors for and respond to interleukin 6 with selective IgA1 and IgA2 synthesis, J. Clin. Invest. 88 (1) (1991) 248–252.
[31] M. Peters, S. Jacobs, M. Ehlers, P. Vollmer, J. Mullberg, E. Wolf, G. Brem, K. H. Meyer zum Buschenfelde, S. Rose-John, The function of the soluble interleukin 6 (IL-6) receptor in vivo: Sensitization of human soluble IL-6 receptor transgenic mice towards IL-6 and prolongation of the plasma half-life of IL-6, J. Exp. Med. 183 (4) (1996) 1399–1406.
[32] D. Novick, H. Engelmann, D. Wallach, M. Rubinstein, Soluble cytokine receptors are present in normal human urine, J. Exp. Med. 170 (4) (1989) 1409–1414.
[33] P. Baran, S. Hansen, G.H. Waetzig, M. Akbarzadeh, L. Lamertz, H.J. Huber, M. R. Ahmadian, J.M. Moll, J. Scheller, The balance of interleukin (IL)-6, IL-6.soluble IL-6 receptor (sIL-6R), and IL-6.sIL-6R.sgp130 complexes allows simultaneous classic and trans-signaling, J. Biol. Chem. 293 (18) (2018) 6762–6775.
[34] T. Barkhausen, T. Tschernig, P. Rosenstiel, M. van Griensven, R.P. Vonberg, M. Dorsch, A. Mueller-Heine, A. Chalaris, J. Scheller, S. Rose-John, D. Seegert, C. Krettek, G.H. Waetzig, Selective blockade of interleukin-6 trans-signaling improves survival in a murine polymicrobial sepsis model, Crit. Care Med. 39 (6) (2011) 1407–1413.
[35] P. Chomarat, J. Banchereau, J. Davoust, A.K. Palucka, IL-6 switches the differentiation of monocytes from dendritic cells to macrophages, Nat. Immunol. 1 (6) (2000) 510–514.
[36] M. Peters, M. Odenthal, P. Schirmacher, M. Blessing, E. Fattori, G. Ciliberto, K. H. Meyer zum Buschenfelde, S. Rose-John, Soluble IL-6 receptor leads to a paracrine modulation of the IL-6-induced hepatic acute phase response in double transgenic mice, J. Immunol. 159 (3) (1997) 1474–1481.
[37] S. Heink, N. Yogev, C. Garbers, M. Herwerth, L. Aly, C. Gasperi, V. Husterer, A. L. Croxford, K. Moller-Hackbarth, H.S. Bartsch, K. Sotlar, S. Krebs, T. Regen, H. Blum, B. Hemmer, T. Misgeld, T.F. Wunderlich, J. Hidalgo, M. Oukka, S. Rose-John, M. Schmidt-Supprian, A. Waisman, T. Korn, Trans-presentation of IL-6 by dendritic cells is required for the priming of pathogenic TH17 cells, Nat. Immunol. 18 (1) (2017) 74–85.
[38] D. Guschin, N. Rogers, J. Briscoe, B. Witthuhn, D. Watling, F. Horn, S. Pellegrini, K. Yasukawa, P. Heinrich, G.R. Stark, et al., A major role for the protein tyrosine kinase JAK1 in the JAK/STAT signal transduction pathway in response to interleukin-6, EMBO J. 14 (7) (1995) 1421–1429.
[39] Y. Minegishi, M. Saito, T. Morio, K. Watanabe, K. Agematsu, S. Tsuchiya, H. Takada, T. Hara, N. Kawamura, T. Ariga, H. Kaneko, N. Kondo, I. Tsuge, A. Yachie, Y. Sakiyama, T. Iwata, F. Bessho, T. Ohishi, K. Joh, K. Imai, K. Kogawa, M. Shinohara, M. Fujieda, H. Wakiguchi, S. Pasic, M. Abinun, H.D. Ochs, E. D. Renner, A. Jansson, B.H. Belohradsky, A. Metin, N. Shimizu, S. Mizutani, T. Miyawaki, S. Nonoyama, H. Karasuyama, Human tyrosine kinase 2 deficiency reveals its requisite roles in multiple cytokine signals involved in innate and acquired immunity, Immunity 25 (5) (2006) 745–755.
[40] A.Y. Kreins, M.J. Ciancanelli, S. Okada, X.F. Kong, N. Ramirez-Alejo, S.S. Kilic, J. El Baghdadi, S. Nonoyama, S.A. Mahdaviani, F. Ailal, A. Bousfiha, D. Mansouri, E. Nievas, C.S. Ma, G. Rao, A. Bernasconi, H. Sun Kuehn, J. Niemela, J. Stoddard, P. Deveau, A. Cobat, S. El Azbaoui, A. Sabri, C.K. Lim, M. Sundin, D.T. Avery, R. Halwani, A.V. Grant, B. Boisson, D. Bogunovic, Y. Itan, M. Moncada-Velez, R. Martinez-Barricarte, M. Migaud, C. Deswarte, L. Alsina, D. Kotlarz, C. Klein, I. Muller-Fleckenstein, B. Fleckenstein, V. Cormier-Daire, S. Rose-John, C. Picard, L. Hammarstrom, A. Puel, S. Al-Muhsen, L. Abel, D. Chaussabel, S.D. Rosenzweig, Y. Minegishi, S.G. Tangye, J. Bustamante, J.L. Casanova, S. Boisson-Dupuis, Human TYK2 deficiency: Mycobacterial and viral infections without hyper-IgE syndrome, J. Exp. Med. 212 (10) (2015) 1641–1662.
[41] C. Gerhartz, B. Heesel, J. Sasse, U. Hemmann, C. Landgraf, J. Schneider-Mergener, F. Horn, P.C. Heinrich, L. Graeve, Differential activation of acute phase response factor/STAT3 and STAT1 via the cytoplasmic domain of the interleukin 6 signal transducer gp130. I. Definition of a novel phosphotyrosine motif mediating STAT1 activation, J. Biol. Chem. 271 (22) (1996), 12991-8.
[42] A.K. Kretzschmar, M.C. Dinger, C. Henze, K. Brocke-Heidrich, F. Horn, Analysis of Stat3 (signal transducer and activator of transcription 3) dimerization by fluorescence resonance energy transfer in living cells, Biochem. J. 377 (Pt 2) (2004) 289–297.
[43] A. Dittrich, C. Khouri, S.D. Sackett, C. Ehlting, O. Bohmer, U. Albrecht, J.G. Bode, C. Trautwein, F. Schaper, Glucocorticoids increase interleukin-6-dependent gene induction by interfering with the expression of the suppressor of cytokine signaling 3 feedback inhibitor, Hepatology 55 (1) (2012) 256–266.
[44] M.I. Irandoust, L.H. Aarts, O. Roovers, J. Gits, S.J. Erkeland, I.P. Touw, Suppressor of cytokine signaling 3 controls lysosomal routing of G-CSF receptor, EMBO J. 26 (7) (2007) 1782–1793.
[45] J. Bollrath, T.J. Phesse, V.A. von Burstin, T. Putoczki, M. Bennecke, T. Bateman, T. Nebelsiek, T. Lundgren-May, O. Canli, S. Schwitalla, V. Matthews, R. M. Schmid, T. Kirchner, M.C. Arkan, M. Ernst, F.R. Greten, gp130-mediated Stat3 activation in enterocytes regulates cell survival and cell-cycle progression during colitis-associated tumorigenesis, Cancer Cell 15 (2) (2009) 91–102.
[46] J.E. Jung, H.G. Lee, I.H. Cho, D.H. Chung, S.H. Yoon, Y.M. Yang, J.W. Lee, S. Choi, J.W. Park, S.K. Ye, M.H. Chung, STAT3 is a potential modulator of HIF-1-mediated VEGF expression in human renal carcinoma cells, FASEB J. 19 (10) (2005) 1296–1298.
[47] S.J. Cutler, J.D. Doecke, I. Ghazawi, J. Yang, L.R. Griffiths, K.J. Spring, S.J. Ralph, A.S. Mellick, Novel STAT binding elements mediate IL-6 regulation of MMP-1 and MMP-3, Sci. Rep. 7 (1) (2017) 8526.
[48] T. Shirogane, T. Fukada, J.M. Muller, D.T. Shima, M. Hibi, T. Hirano, Synergistic roles for Pim-1 and c-Myc in STAT3-mediated cell cycle progression and antiapoptosis, Immunity 11 (6) (1999) 709–719.
[49] T. Fukada, T. Ohtani, Y. Yoshida, T. Shirogane, K. Nishida, K. Nakajima, M. Hibi, T. Hirano, STAT3 orchestrates contradictory signals in cytokine-induced G1 to S cell-cycle transition, EMBO J. 17 (22) (1998) 6670–6677.
[50] N. Manel, D. Unutmaz, D.R. Littman, The differentiation of human T(H)-17 cells requires transforming growth factor-beta and induction of the nuclear receptor RORgammat, Nat. Immunol. 9 (6) (2008) 641–649.
[51] Y. Niwa, H. Kanda, Y. Shikauchi, A. Saiura, K. Matsubara, T. Kitagawa, J. Yamamoto, T. Kubo, H. Yoshikawa, Methylation silencing of SOCS-3 promotes cell growth and migration by enhancing JAK/STAT and FAK signalings in human hepatocellular carcinoma, Oncogene 24 (42) (2005) 6406–6417.
[52] W.P. Schiemann, J.L. Bartoe, N.M. Nathanson, Box 3-independent signaling mechanisms are involved in leukemia inhibitory factor receptor alpha- and gp130-mediated stimulation of mitogen-activated protein kinase. Evidence for participation of multiple signaling pathways which converge at Ras, J. Biol. Chem. 272 (26) (1997) 16631–16636.
[53] H. Bongartz, K. Gille, W. Hessenkemper, K. Mandel, M. Lewitzky, S.M. Feller, F. Schaper, The multi-site docking protein Grb2-associated binder 1 (Gab1) enhances interleukin-6-induced MAPK-pathway activation in an SHP2-, Grb2-, and time-dependent manner, Cell Commun. Signal 17 (1) (2019) 135.
[54] R.E. Schweppe, T.H. Cheung, N.G. Ahn, Global gene expression analysis of ERK5 and ERK1/2 signaling reveals a role for HIF-1 in ERK5-mediated responses, J. Biol. Chem. 281 (30) (2006) 20993–21003.
[55] K.G. Finegan, D. Perez-Madrigal, J.R. Hitchin, C.C. Davies, A.M. Jordan, C. Tournier, ERK5 is a critical mediator of inflammation-driven cancer, Cancer Res. 75 (4) (2015) 742–753.
[56] A. Zauberman, D. Zipori, M. Krupsky, R. Ben-Levy, Stress activated protein kinase p38 is involved in IL-6 induced transcriptional activation of STAT3, Oncogene 18 (26) (1999) 3886–3893.
[57] C. Johnson, Y. Han, N. Hughart, J. McCarra, G. Alpini, F. Meng, Interleukin-6 and its receptor, key players in hepatobiliary inflammation and cancer, Transl. Gastrointest Cancer 1 (1) (2012) 58–70.
[58] N. Honke, K. Ohl, A. Wiener, J. Bierwagen, J. Peitz, S. Di Fiore, R. Fischer, N. Wagner, S. Wuller, K. Tenbrock, The p38-mediated rapid down-regulation of cell surface gp130 expression impairs interleukin-6 signaling in the synovial fluid of juvenile idiopathic arthritis patients, Arthritis Rheumatol. 66 (2) (2014) 470–478.
[59] D.R. Alessi, S.R. James, C.P. Downes, A.B. Holmes, P.R. Gaffney, C.B. Reese, P. Cohen, Characterization of a 3-phosphoinositide-dependent protein kinase which phosphorylates and activates protein kinase Balpha, Curr. Biology: CB 7 (4) (1997) 261–269.
[60] S. Negoro, H. Oh, E. Tone, K. Kunisada, Y. Fujio, K. Walsh, T. Kishimoto, K. Yamauchi-Takihara, Glycoprotein 130 regulates cardiac myocyte survival in doxorubicin-induced apoptosis through phosphatidylinositol 3-kinase/Akt phosphorylation and Bcl-xL/caspase-3 interaction, Circulation 103 (4) (2001) 555–561.
[61] S. Gao, J.L. Durstine, H.J. Koh, W.E. Carver, N. Frizzell, J.A. Carson, Acute myotube protein synthesis regulation by IL-6-related cytokines, Am. J. Physiol. Cell Physiol. 313 (5) (2017) C487–C500.
[62] K. Taniguchi, L.W. Wu, S.I. Grivennikov, P.R. de Jong, I. Lian, F.X. Yu, K. Wang, S. B. Ho, B.S. Boland, J.T. Chang, W.J. Sandborn, G. Hardiman, E. Raz, Y. Maehara, A. Yoshimura, J. Zucman-Rossi, K.L. Guan, M. Karin, A gp130-Src-YAP module links inflammation to epithelial regeneration, Nature 519 (7541) (2015) 57–62.
[63] F.X. Yu, K.L. Guan, The Hippo pathway: Regulators and regulations, Genes Dev. 27 (4) (2013) 355–371.
[64] C. Tamm, N. Bower, C. Anneren, Regulation of mouse embryonic stem cell self-renewal by a Yes-YAP-TEAD2 signaling pathway downstream of LIF, J. Cell Sci. 124 (Pt 7) (2011) 1136–1144.
[65] Z.Y. Lu, J. Brochier, J. Wijdenes, H. Brailly, R. Bataille, B. Klein, High amounts of circulating interleukin (IL)-6 in the form of monomeric immune complexes during anti-IL-6 therapy. Towards a new methodology for measuring overall cytokine production in human in vivo, Eur. J. Immunol. 22 (11) (1992) 2819–2824.

[66] B. Klein, J. Wijdenes, X.G. Zhang, M. Jourdan, J.M. Boiron, J. Brochier, J. Liautard, M. Merlin, C. Clement, B. Morel-Fournier, et al., Murine anti-interleukin-6 monoclonal antibody therapy for a patient with plasma cell leukemia, Blood 78 (5) (1991) 1198–1204.
[67] T.H. Heo, J. Wahler, N. Suh, Potential therapeutic implications of IL-6/IL-6R/gp130-targeting agents in breast cancer, Oncotarget 7 (13) (2016) 15460–15473.
[68] J. Silverman, Q. Liu, A. Bakker, W. To, A Duguay, R. Smith, B.M. Alba, A. Rivas, P. Li, H. Le, E. Whitehorn, K.W. Moore, C. Swimmer, V. Perlroth, M. Vogt, J. Kolkman, W.P Stemmer, Multivalent avimer proteins evolved by exon shuffling of a family of human receptor domains, Nat. Biotechnol. 23 (12) (2005) 1556–1561.
[69] A.N. Economides, L.R. Carpenter, J.S. Rudge, V. Wong, E.M. Koehler-Stec, C. Hartnett, E.A. Pyles, X. Xu, T.J. Daly, M.R. Young, J.P. Fandl, F. Lee, S. Carver, J. McNay, K. Bailey, S. Ramakanth, R. Hutabarat, T.T. Huang, C. Radziejewski, G. D. Yancopoulos, N. Stahl, Cytokine traps: Multi-component, high-affinity blockers of cytokine action, Nat. Med. 9 (1) (2003) 47–52.
[70] R. Savino, L. Ciapponi, A. Lahm, A. Demartis, A. Cabibbo, C. Toniatti, P. Delmastro, S. Altamura, G. Ciliberto, Rational design of a receptor super-antagonist of human interleukin-6, EMBO J. 13 (24) (1994) 5863–5870.
[71] C. Garbers, S. Heink, T. Korn, S. Rose-John, Interleukin-6: designing specific therapeutics for a complex cytokine, Nat. Rev. Drug Discov. 17 (6) (2018) 395–412.
[72] C. Garbers, W. Thaiss, G.W. Jones, G.H. Waetzig, I. Lorenzen, F. Guilhot, R. Lissilaa, W.G. Ferlin, J. Grotzinger, S.A. Jones, S. Rose-John, J. Scheller, Inhibition of classic signaling is a novel function of soluble glycoprotein 130 (sgp130), which is controlled by the ratio of interleukin 6 and soluble interleukin 6 receptor, J. Biol. Chem. 286 (50) (2011) 42959–42970.
[73] F.A. Houssiau, J.P. Devogelaer, J. Van Damme, C.N. de Deuxchaisnes, J. Van Snick, Interleukin-6 in synovial fluid and serum of patients with rheumatoid arthritis and other inflammatory arthritides, Arthritis Rheum. 31 (6) (1988) 784–788.
[74] G. Grondal, I. Gunnarsson, J. Ronnelid, S. Rogberg, L. Klareskog, I. Lundberg, Cytokine production, serum levels and disease activity in systemic lupus erythematosus, Clin. Exp. Rheumatol. 18 (5) (2000) 565–570.
[75] E. Peterson, A.D. Robertson, W. Emlen, Serum and urinary interleukin-6 in systemic lupus erythematosus, Lupus 5 (6) (1996) 571–575.
[76] R. Herrera-Esparza, O. Barbosa-Cisneros, R. Villalobos-Hurtado, E. Avalos-Diaz, Renal expression of IL-6 and TNFalpha genes in lupus nephritis, Lupus 7 (3) (1998) 154–158.
[77] D. Malide, P. Russo, M. Bendayan, Presence of tumor necrosis factor alpha and interleukin-6 in renal mesangial cells of lupus nephritis patients, Human Pathol. 26 (5) (1995) 558–564.
[78] S. Garaud, C. Le Dantec, S. Jousse-Joulin, C. Hanrotel-Saliou, A. Saraux, R. A. Mageed, P. Youinou, Y. Renaudineau, IL-6 modulates CD5 expression in B cells from patients with lupus by regulating DNA methylation, J. Immunol. 182 (9) (2009) 5623–5632.
[79] M. Tishler, I. Yaron, O. Geyer, I. Shirazi, E. Naftaliev, M. Yaron, Elevated tear interleukin-6 levels in patients with Sjogren syndrome, Ophthalmology 105 (12) (1998) 2327–2329.
[80] J.J. Senn, P.J. Klover, I.A. Nowak, T.A. Zimmers, L.G. Koniaris, R.W. Furlanetto, R.A. Mooney, Suppressor of cytokine signaling-3 (SOCS-3), a potential mediator of interleukin-6-dependent insulin resistance in hepatocytes, J. Biol. Chem. 278 (16) (2003) 13740–13746.
[81] J. Mestecky, M. Raska, B.A. Julian, A.G. Gharavi, M.B. Renfrow, Z. Moldoveanu, L. Novak, K. Matousovic, J. Novak, IgA nephropathy: Molecular mechanisms of the disease, Annu. Rev. Pathol. 8 (2013) 217–240.
[82] J.C. Rodrigues, M. Haas, H.N. Reich, IgA nephropathy, Clin. J. Am. Soc. Nephrol.: CJASN 12 (4) (2017) 677–686.
[83] M. Stuchlova Horynova, M. Raska, H. Clausen, J. Novak, Aberrant O-glycosylation and anti-glycan antibodies in an autoimmune disease IgA nephropathy and breast adenocarcinoma, Cell Mol. Life Sci. 70 (5) (2013) 829–839.
[84] T.J. Stewart, K. Takahashi, R.H. Whitaker, M. Raska, W.J. Placzek, J. Novak, M. B. Renfrow, IgA1 hinge-region clustered glycan fidelity is established early during semi-ordered glycosylation by GalNAc-T2, Glycobiology 29 (7) (2019) 543–556.
[85] T.J. Stewart, K. Takahashi, N. Xu, A. Prakash, R. Brown, M. Raska, M.B. Renfrow, J. Novak, Quantitative assessment of successive carbohydrate additions to the clustered O-glycosylation sites of IgA1 by glycosyltransferases, Glycobiology 31 (5) (2021) 540–556.
[86] M. Raska, Z. Moldoveanu, H. Suzuki, R. Brown, R. Kulhavy, J. Andrasi, S. Hall, H. L. Vu, F. Carlsson, G. Lindahl, M. Tomana, B.A. Julian, R.J. Wyatt, J. Mestecky, J. Novak, Identification and characterization of CMP-NeuAc:GalNAc-IgA1 alpha2,6-sialyltransferase in IgA1-producing cells, J. Mol. Biol. 369 (1) (2007) 69–78.
[87] Z. Moldoveanu, R.J. Wyatt, J.Y. Lee, M. Tomana, B.A. Julian, J. Mestecky, W. Q. Huang, S.R. Anreddy, S. Hall, M.C. Hastings, K.K. Lau, W.J. Cook, J. Novak, Patients with IgA nephropathy have increased serum galactose-deficient IgA1 levels, Kidney Int. 71 (11) (2007) 1148–1154.
[88] J. Mestecky, J. Novak, Z. Moldoveanu, M. Raska, IgA nephropathy enigma, Clin. Immunol. 172 (2016) 72–77.
[89] H. Suzuki, K. Kiryluk, J. Novak, Z. Moldoveanu, A.B. Herr, M.B. Renfrow, R. J. Wyatt, F. Scolari, J. Mestecky, A.G. Gharavi, B.A. Julian, The pathophysiology of IgA nephropathy, J. Am. Soc. Nephrol.: JASN 22 (10) (2011) 1795–1803.
[90] A.C. Allen, P.S. Topham, S.J. Harper, J. Feehally, Leucocyte beta 1,3 galactosyltransferase activity in IgA nephropathy, nephrology, dialysis, transplantation: official publication of the european dialysis and transplant association, Eur. Ren. Assoc. 12 (4) (1997) 701–706.
[91] H. Suzuki, Z. Moldoveanu, S. Hall, R. Brown, H.L. Vu, L. Novak, B.A. Julian, M. Tomana, R.J. Wyatt, J.C. Edberg, G.S. Alarcon, R.P. Kimberly, Y. Tomino, J. Mestecky, J. Novak, IgA1-secreting cell lines from patients with IgA nephropathy produce aberrantly glycosylated IgA1, J. Clin. Invest. 118 (2) (2008) 629–639.
[92] M. Stuchlova Horynova, A. Vrablikova, T.J. Stewart, K. Takahashi, L. Czernekova, K. Yamada, H. Suzuki, B.A. Julian, M.B. Renfrow, J. Novak, M. Raska, N-acetylgalactosaminide alpha2,6-sialyltransferase II is a candidate enzyme for sialylation of galactose-deficient IgA1, the key autoantigen in IgA nephropathy, Nephrology, dialysis, transplantation: Official publication of the european dialysis and transplant association, Eur. Ren. Assoc. 30 (2) (2015) 234–238.
[93] Y. Komiyama, L.R. Kafkova, A. Barasch, G.R. Shah, J.T. Grbic, Z. Novak, K. Komiyama, J. Novak, J. Mestecky, Z. Moldoveanu, Origin of galactose-deficient immunoglobulin g in gingival crevicular fluid in periodontitis, J. Periodontol. 85 (12) (2014) 1779–1785.
[94] Y. Hiki, T. Kokubo, H. Iwase, Y. Masaki, T. Sano, A. Tanaka, K. Toma, K. Hotta, Y. Kobayashi, Underglycosylation of IgA1 hinge plays a certain role for its glomerular deposition in IgA nephropathy, J. Am. Soc. Nephrol.: JASN 10 (4) (1999) 760–769.
[95] A.C. Allen, E.M. Bailey, P.E. Brenchley, K.S. Buck, J. Barratt, J. Feehally, Mesangial IgA1 in IgA nephropathy exhibits aberrant O-glycosylation: observations in three patients, Kidney Inte. 60 (3) (2001) 969–973.
[96] H. Suzuki, J. Yasutake, Y. Makita, Y. Tanbo, K. Yamasaki, T. Sofue, T. Kano, Y. Suzuki, IgA nephropathy and IgA vasculitis with nephritis have a shared feature involving galactose-deficient IgA1-oriented pathogenesis, Kidney Int. 93 (3) (2018) 700–705.
[97] H. Suzuki, R. Fan, Z. Zhang, R. Brown, S. Hall, B.A. Julian, W.W. Chatham, Y. Suzuki, R.J. Wyatt, Z. Moldoveanu, J.Y. Lee, J. Robinson, M. Tomana, Y. Tomino, J. Mestecky, J. Novak, Aberrantly glycosylated IgA1 in IgA nephropathy patients is recognized by IgG antibodies with restricted heterogeneity, J. Clin. Invest. 119 (6) (2009) 1668–1677.
[98] Z.Q. Huang, M. Raska, T.J. Stewart, C. Reily, R.G. King, D.K. Crossman, M. R. Crowley, A. Hargett, Z. Zhang, H. Suzuki, S. Hall, R.J. Wyatt, B.A. Julian, M. B. Renfrow, A.G. Gharavi, J. Novak, Somatic mutations modulate autoantibodies against galactose-deficient IgA1 in IgA nephropathy, J. Am. Soc. Nephrol.: JASN 27 (11) (2016) 3278–3284.
[99] A.G. Gharavi, Z. Moldoveanu, R.J. Wyatt, C.V. Barker, S.Y. Woodford, R.P. Lifton, J. Mestecky, J. Novak, B.A. Julian, Aberrant IgA1 glycosylation is inherited in familial and sporadic IgA nephropathy, J. Am. Soc. Nephrol.: JASN 19 (5) (2008) 1008–1014.
[100] K. Yamada, M. Raska, Z. Moldoveanu, H. Suzuki, K. Kiryluk, B.A. Julian, R. J. Wyatt, Y. Tomino, J. Mestecky, A.G. Gharavi, J. Novak, Effect of gp130 cytokines on IgA1-producing cells from patients with IgA nephropathy, J. Am. Soc. Nephrol. 22 (2011) 625A.
[101] K. Yamada, Z.Q. Huang, M. Raska, C. Reily, J.C. Anderson, H. Suzuki, H. Ueda, Z. Moldoveanu, K. Kiryluk, Y. Suzuki, R.J. Wyatt, Y. Tomino, A.G. Gharavi, A. Weinmann, B.A. Julian, C.D. Willey, J. Novak, Inhibition of STAT3 signaling reduces IgA1 autoantigen production in IgA nephropathy, Kidney Int. Rep. 2 (6) (2017) 1194–1207.
[102] K. Yamada, Z.Q. Huang, M. Raska, C. Reily, J.C. Anderson, H. Suzuki, K. Kiryluk, A.G. Gharavi, B.A. Julian, C.D. Willey, J. Novak, Leukemia inhibitory factor signaling enhances production of galactose-deficient IgA1 in IgA nephropathy, Kidney Dis. 6 (2020) 168–180.
[103] J. Novak, L. Raskova Kafkova, H. Suzuki, M. Tomana, K. Matousovic, R. Brown, S. Hall, J.T. Sanders, T.M. Eison, Z. Moldoveanu, L. Novak, Z. Novak, R. Mayne, B. A. Julian, J. Mestecky, R.J. Wyatt, IgA1 immune complexes from pediatric patients with IgA nephropathy activate cultured human mesangial cells, Nephrology, dialysis, transplantation: official publication of the European Dialysis and Transplant Association, Eur. Ren. Assoc. 26 (11) (2011) 3451–3457.
[104] H. Tamouza, J.M. Chemouny, L. Raskova Kafkova, L. Berthelot, M. Flamant, M. Demion, L. Mesnard, E. Paubelle, F. Walker, B.A. Julian, E. Tissandie, M. K. Tiwari, N.O. Camara, F. Vrtovsnik, M. Benhamou, J. Novak, R.C. Monteiro, I. C. Moura, The IgA1 immune complex-mediated activation of the MAPK/ERK kinase pathway in mesangial cells is associated with glomerular damage in IgA nephropathy, Kidney Int. 82 (12) (2012) 1284–1296.
[105] S.I.-H. Hsu, J. Feehally, The molecular basis of IgA nephropathy, in: D.B. Mount, M.R. Pollak (Eds.), Molecular and Genetic Basis of Renal Disease, Saunders Elsevier, Philadelphia, 2008, pp. 481–497.
[106] I. Coletta, L. Soldo, N. Polentarutti, F. Mancini, A. Guglielmotti, M. Pinza, A. Mantovani, C. Milanese, Selective induction of MCP-1 in human mesangial cells by the IL-6/sIL-6R complex, Exp. Nephrol. 8 (1) (2000) 37–43.
[107] M.E. van den Dobbelsteen, F.J. van der Woude, W.E. Schroeijers, A.W. van den Wall Bake, L.A. van Es, M.R. Daha, Binding of dimeric and polymeric IgA to rat renal mesangial cells enhances the release of interleukin 6, Kidney Int. 46 (2) (1994) 512–519.
[108] I.C. Moura, M. Arcos-Fajardo, A. Gdoura, V. Leroy, C. Sadaka, N. Mahlaoui, Y. Lepelletier, F. Vrtovsnik, E. Haddad, M. Benhamou, R.C. Monteiro, Engagement of transferrin receptor by polymeric IgA1: Evidence for a positive feedback loop involving increased receptor expression and mesangial cell proliferation in IgA nephropathy, J. Am. Soc. Nephrol.: JASN 16 (9) (2005) 2667–2676.
[109] M. Iwano, K. Dohi, E. Hirata, Y. Horii, H. Shiiki, H. Ishikawa, Induction of interleukin 6 synthesis in mouse glomeruli and cultured mesangial cells, Nephron 62 (1) (1992) 58–65.

[110] C. Zoja, J.M. Wang, S. Bettoni, M. Sironi, D. Renzi, F. Chiaffarino, H.E. Abboud, J. Van Damme, A. Mantovani, G. Remuzzi, et al., Interleukin-1 beta and tumor necrosis factor-alpha induce gene expression and production of leukocyte chemotactic factors, colony-stimulating factors, and interleukin-6 in human mesangial cells, Am. J. Pathol. 138 (4) (1991) 991–1003.
[111] T. Moriyama, M. Fujibayashi, Y. Fujiwara, T. Kaneko, C. Xia, E. Imai, T. Kamada, A. Ando, N. Ueda, Angiotensin II stimulates interleukin-6 release from cultured mouse mesangial cells, J. Am. Soc. Nephrol.: JASN 6 (1) (1995) 95–101.
[112] C.G. Ihm, J.K. Park, H.J. Kim, T.W. Lee, D.R. Cha, Effects of high glucose on interleukin-6 production in human mesangial cells, J. Korean Med. Sci. 17 (2) (2002) 208–212.
[113] C. Gomez-Guerrero, M.J. Lopez-Armada, E. Gonzalez, J. Egido, Soluble IgA and IgG aggregates are catabolized by cultured rat mesangial cells and induce production of TNF-alpha and IL-6, and proliferation, J. Immunol. 153 (11) (1994) 5247–5255.
[114] S. Suematsu, T. Matsuda, K. Aozasa, S. Akira, N. Nakano, S. Ohno, J. Miyazaki, K. Yamamura, T. Hirano, T. Kishimoto, IgG1 plasmacytosis in interleukin 6 transgenic mice, Proc. Natl. Acad. Sci. U.S.A. 86 (19) (1989) 7547–7551.
[115] K. Durlacher-Betzer, A. Hassan, R. Levi, J. Axelrod, J. Silver, T. Naveh-Many, kuwataInterleukin-6 contributes to the increase in fibroblast growth factor 23 expression in acute and chronic kidney disease, Kidney Int. 94 (2) (2018) 315–325.
[116] R. Schmitt, A.L. Stahl, A.I. Olin, A.C. Kristoffersson, J. Rebetz, J. Novak, G. Lindahl, D. Karpman, The combined role of galactose-deficient IgA1 and streptococcal IgA-binding M Protein in inducing IL-6 and C3 secretion from human mesangial cells: implications for IgA nephropathy, J. Immunol. 193 (1) (2014) 317–326.
[117] M. Stangou, E. Alexopoulos, A. Papagianni, A. Pantzaki, C. Bantis, S. Dovas, D. Economidou, M. Leontsini, D. Memmos, Urinary levels of epidermal growth factor, interleukin-6 and monocyte chemoattractant protein-1 may act as predictor markers of renal function outcome in immunoglobulin A nephropathy, Nephrology 14 (6) (2009) 613–620.
[118] M. Stangou, C. Bantis, M. Skoularopoulou, L. Korelidou, D. Kouloukouriotou, M. Scina, I.T. Labropoulou, N.M. Kouri, A. Papagianni, G. Efstratiadis, Th1, Th2 and Treg/T17 cytokines in two types of proliferative glomerulonephritis, Indian J. Nephrol. 26 (3) (2016) 159–166.
[119] H. Su, C.T. Lei, C. Zhang, Interleukin-6 signaling pathway and its role in kidney disease: An update, Front. Immunol. 8 (2017) 405.
[120] S.J. Lee, E. Borsting, A.E. Decleves, P. Singh, R. Cunard, Podocytes express IL-6 and lipocalin 2/ neutrophil gelatinase-associated lipocalin in lipopolysaccharide-induced acute glomerular injury, Nephron. Exp. Nephrol. 121 (3–4) (2012) e86–e96.
[121] K.N. Lai, J.C. Leung, L.Y. Chan, M.A. Saleem, P.W. Mathieson, F.M. Lai, S.C. Tang, Activation of podocytes by mesangial-derived TNF-alpha: glomerulo-podocytic communication in IgA nephropathy, Am. J. Physiol. Ren. Physiol. 294 (4) (2008) F945–F955.
[122] R.D. Wright, M.W. Beresford, Podocytes contribute, and respond, to the inflammatory environment in lupus nephritis, American journal of physiology, Ren. Physiol. 315 (6) (2018) F1683–F1694.
[123] A. Moutabarrik, I. Nakanishi, M. Ishibashi, Interleukin-6 and interleukin-6 receptor are expressed by cultured glomerular epithelial cells, Scand. J. Immunol. 40 (2) (1994) 181–186.
[124] D.I. Kim, S.H. Park, Sequential signaling cascade of IL-6 and PGC-1alpha is involved in high glucose-induced podocyte loss and growth arrest, Biochem. Biophys. Res. Commun. 435 (4) (2013) 702–707.
[125] J. Frank, G. Engler-Blum, H.P. Rodemann, G.A. Muller, Human renal tubular cells as a cytokine source: PDGF-B, GM-CSF and IL-6 mRNA expression in vitro, Exp. Nephrol. 1 (1) (1993) 26–35.
[126] C. van Kooten, M.R. Daha, L.A. van Es, Tubular epithelial cells: A critical cell type in the regulation of renal inflammatory processes, Exp. Nephrol. 7 (5–6) (1999) 429–437.
[127] A. Dewitte, J. Villeneuve, S. Lepreux, M. Bouchecareilh, X. Gauthereau, C. Rigothier, C. Combe, A. Ouattara, J. Ripoche, CD154 Induces Interleukin-6 Secretion by Kidney Tubular Epithelial Cells under Hypoxic Conditions: Inhibition by Chloroquine, Mediat. Inflamm. 2020 (2020) 6357046.
[128] E. Ranieri, L. Gesualdo, F. Petrarulo, F.P. Schena, Urinary IL-6/EGF ratio: a useful prognostic marker for the progression of renal damage in IgA nephropathy, Kidney Int. 50 (6) (1996) 1990–2001.
[129] K. Harada, Y. Akai, N. Kurumatani, M. Iwano, Y. Saito, Prognostic value of urinary interleukin 6 in patients with IgA nephropathy: an 8-year follow-up study, Nephron 92 (4) (2002) 824–826.
[130] P. Kalliakmani, L. Nakopoulou, S. Tsakas, M. Gerolymos, M. Papasotiriou, D. S. Goumenos, Urinary interleukin-6 (IL-6) and transforming growth factor (TGF-beta) levels in corticosteroidtreated patients with IgA nephropathy, Clin. Nephrol. 76 (2) (2011) 144–150.
[131] M. Stangou, A. Papagianni, C. Bantis, D. Moisiadis, S. Kasimatis, M. Spartalis, A. Pantzaki, G. Efstratiadis, D. Memmos, Up-regulation of urinary markers predict outcome in IgA nephropathy but their predictive value is influenced by treatment with steroids and azathioprine, Clin. Nephrol. 80 (3) (2013) 203–210.
[132] A. Segarra-Medrano, C. Carnicer-Caceres, N. Valtierra-Carmeno, I. Agraz-Pamplona, N. Ramos-Terrades, E. Jatem Escalante, E. Ostos-Roldan, Value of urinary levels of interleukin-6, epidermal growth factor, monocyte chemoattractant protein type1 and transforming growth factor beta1 in predicting the extent of fibrosis lesions in kidney biopsies of patients with IgA nephropathy, Nefrologia: Pub. Oficial De la Sociedad Espanola Nefrologia 37 (5) (2017) 531–538.
[133] F.W. Ballardie, M.T. Gordon, P.T. Sharpe, A.M. Darvill, H. Cheng, Intrarenal cytokine mRNA expression and location in normal and IgA nephropathy tissue: TGF alpha, TGF beta, IGF 1, IL-4 and IL-6, Nephrology, dialysis, transplantation: official publication of the European Dialysis and Transplant Association, Eur. Ren. Assoc. 9 (11) (1994) 1545–1552.
[134] Y. Taniguchi, N. Yorioka, H. Oda, S. Okushin, Y. Nishida, M. Yamakido, T. Taguchi, Glomerular localization of interleukin-6 suppressed by steroid mini-pulse therapy in an IgA nephropathy patient, Intern. Med. 34 (12) (1995) 1181–1185.
[135] Y. Taniguchi, N. Yorioka, J. Kumagai, M. Katsutani, M. Kuratsune, D. Amimoto, M. Yamakido, Interleukin-6 localization and the prognosis of IgA nephropathy, Nephron 81 (1) (1999) 94–98.
[136] J. Novak, Z. Moldoveanu, B.A. Julian, M. Raska, R.J. Wyatt, Y. Suzuki, Y. Tomino, A.G. Gharavi, J. Mestecky, H. Suzuki, Aberrant glycosylation of IgA1 and anti-glycan antibodies in IgA nephropathy: role of mucosal immune system, Adv. Otorhinolaryngol. 72 (2011) 60–63.
[137] Y. Makita, H. Suzuki, T. Kano, A. Takahata, B.A. Julian, J. Novak, Y. Suzuki, TLR9 activation induces aberrant IgA glycosylation via APRIL- and IL-6-mediated pathways in IgA nephropathy, Kidney Int. 97 (2) (2020) 340–349.
[138] H. Suzuki, Y. Suzuki, I. Narita, M. Aizawa, M. Kihara, T. Yamanaka, T. Kanou, H. Tsukaguchi, J. Novak, S. Horikoshi, Y. Tomino, Toll-like receptor 9 affects severity of IgA nephropathy, J. Am. Soc. Nephrol.: JASN 19 (12) (2008) 2384–2395.
[139] K. Shuai, C.M. Horvath, L.H. Huang, S.A. Qureshi, D. Cowburn, J.E. Darnell Jr., Interferon activation of the transcription factor Stat91 involves dimerization through SH2-phosphotyrosyl peptide interactions, Cell 76 (5) (1994) 821–828.
[140] A.G. Gharavi, K. Kiryluk, M. Choi, Y. Li, P. Hou, J. Xie, S. Sanna-Cherchi, C. J. Men, B.A. Julian, R.J. Wyatt, J. Novak, J.C. He, H. Wang, J. Lv, L. Zhu, W. Wang, Z. Wang, K. Yasuno, M. Gunel, S. Mane, S. Umlauf, I. Tikhonova, I. Beerman, S. Savoldi, R. Magistroni, G.M. Ghiggeri, M. Bodria, F. Lugani, P. Ravani, C. Ponticelli, L. Allegri, G. Boscutti, G. Frasca, A. Amore, L. Peruzzi, R. Coppo, C. Izzi, B.F. Viola, E. Prati, M. Salvadori, R. Mignani, L. Gesualdo, F. Bertinetto, P. Mesiano, A. Amoroso, F. Scolari, N. Chen, H. Zhang, R.P. Lifton, Genome-wide association study identifies susceptibility loci for IgA nephropathy, Nat. Genet. 43 (4) (2011), 321-7.
[141] W. Somers, M. Stahl, J.S. Seehra, 1.9 A crystal structure of interleukin 6: Implications for a novel mode of receptor dimerization and signaling, EMBO J. 16 (5) (1997) 989–997.
[142] M.J. Boulanger, D.C. Chow, E.E. Brevnova, K.C. Garcia, Hexameric structure and assembly of the interleukin-6/IL-6 alpha-receptor/gp130 complex, Science 300 (5628) (2003) 2101–2104.
[143] A. Schroers, O. Hecht, K.J. Kallen, M. Pachta, S. Rose-John, J. Grotzinger, Dynamics of the gp130 cytokine complex: a model for assembly on the cellular membrane, Protein Sci. 14 (3) (2005) 783–790.
[144] A. Muraguchi, T. Hirano, B. Tang, T. Matsuda, Y. Horii, K. Nakajima, T. Kishimoto, The essential role of B cell stimulatory factor 2 (BSF-2/IL-6) for the terminal differentiation of B cells, J. Exp. Med. 167 (2) (1988) 332–344.
[145] H. Yamaguchi, G.M. Taouk, A potential role of YAP/TAZ in the interplay between metastasis and metabolic alterations, Front. Oncol. 10 (2020) 928.

Yaroslava Groza is a PhD student at the Faculty of Science of the Charles University, Prague, Czech Republic, member of the Laboratory of Ligand Engineering in the Institute of Biotechnology of the Czech Academy of Sciences, Vestec, Czech Republic. She focuses on the development of non-immunoglobulin protein binders with immunomodulatory potential. Particularly, she is interested in the application of the recombinant proteins for interference with cytokine signaling and their therapeutic potential in autoimmune and inflammatory diseases.

Jana Jemelkova is a junior researcher at the Department of Immunology at Palacky University, Olomouc, Czech Republic. She is pursuing her doctorate in Immunology and plans to graduate in 2022. Her primary area of interest is the pathogenesis of IgA nephropathy. The goal for her PhD is to determine the influence of glycosyltransferases levels on production of galactose deficient IgA in IgA nephropathy.

Leona Raskova Kafkova, PhD is Associate professor at Department of Immunology, Palacky University in Olomouc, Czech Republic. She is studying the mechanisms involved in the IgA nephrophaty development, namely she is focused on mechanisms of stimulation of mesangial cell proliferation, and involvement of immune checkpoints. She started her IgA nephropathy work at University of Alabama at Birmingham in collaboration with Jan Novak.

Dr**. Petr Malý, Ph.D.** is the head of Laboratory of Ligand Engineering at the Institute of Biotechnology of the Czech Academy of Sciences in BIOCEV research center in Vestec, Czech Republic. He focuses on the development of small binding proteins derived from protein domain scaffolds as novel diagnostics or theranostics. Recently, he has been interested in generation of anti-inflammatory binders and development of protein mimotopes as potential vaccine antigens

Prof. Milan Raska, Ph.D. is the Head of Immunology Department in Palacky University, Olomouc, Czech Republic. He spent his postdoctoral fellowship at the University of Alabama at Birmingham, Birmingham, AL, USA at the laboratories of prof. Jiri Mestecky and prof. Jan Novak. His major field of interest the etiology of autoimmune disease IgA nephropathy. Further, his research is focused on novel approaches in design of recombinant protein-based and DNA vaccines, and liposome-based delivery systems. He has published more than 90 papers in peer-reviewed journals. His research in IgA nephropathy is focused on the influence of cytokines and other factors on the process of abnormal glycosyalation of IgA molecule, activation and migration of IgA producing cells, and development of approaches for reduction of generation of pathological circulating immune complexes.

3.3. Small protein inhibitors of human IL-22R1 with protective function in murine DSS-induced colitis

Scientific outcomes:

Submitted manuscript: Milan Kuchař, Kristýna Sloupenská, Leona Rašková Kafková, Yaroslava Groza, Jozef Škarda, Petr Kosztyu, Marie Hlavničková, Joanna M. Mierzwicka, Radim Osička, Hana Petroková, Stephen I. Walimbwa, Shiv Bharadwaj, Jiří Černý, Milan Raška, Petr Malý. Human IL-22 receptor-targeted small protein antagonist suppress murine DSS-induced colitis., *Cell Communication and Signaling (under revision).*

Background: During intestinal inflammation in IBD, IL-6 contributes to the disease development via suppressing apoptosis of T lymphocytes, recruitment of lymphocyte and leukocyte, differentiation of Th17 cells. While IL-6 is mostly known for its pro-inflammatory function, IL-22 supports protective and regenerative activities. However, in the context of IBD, IL-22 is recognized as a "dual function" cytokine, exhibiting both protective and pathogenic effects depending on the conditions. IL-22 signals via the receptor complex composed of the high affinity IL-22R1 and low-affinity IL-10R2. IL-22R1 is restricted to cells of non-immune origin, thus determining IL-22 cell specificity. Unique quality of the IL-22 cytokine is that it predominantly influences epithelial cells of barrier surfaces. Typically, IL-22 promotes tissue regeneration, anti-microbial peptides and mucins secretion, and lymphocyte recruitment in case of inflammation. On the other hand, the overexpression of IL-22 is associated with hyper-proliferation and recruitment of pathologic effector cells, leading to tissue damage and chronic inflammation in specific diseases including IBD.

Methods: To generate ABD variants that bind human IL-22R1, we carried out three-round ribosome display selection. ELISA screening of individual variants in the form of bacterial cell lysates was carried out to create a collection of specific binders, named ABR. Inhibitory potential of the engineered ABR variants was tested in the competition ELISA assay. Immunostaining was used for the demonstration of the ability of ABR variants to specifically recognize IL-22R1 on the surface of IL-22R1-pcDNA6-transfected HEK293T cells and cytokine-stimulated HaCaT cells. Additionally, binding of ABR variants to IL-22R1 on a surface of HEK-Blue IL22 reporter cells was confirmed by flow cytometry. Using site-directed mutagenesis, cysteine was substituted for serine in ABR089 and ABR099 variants. Blocking potential of ABR variants demonstrated in ELISA was confirmed using HEK-Blue IL22 reporter assay. Binding affinity and kinetics of the inhibitory ABR variants to the cell surface receptor on transfected HE293T and stimulated HaCaT was characterized using LigandTracer method. *In silico* modelling was carried out to understand the interaction profile between ABR and IL-22R1

proteins. For *in vivo* testing of the detected ABD inhibitor, murine model of colitis induced by 2.5% DSS was used. Histological analysis of the colon epithelial and local expression of selected pro/anti-inflammatory markers (IL-1β, IL-6, IL-10, IL-17A, IL-22, and TNFα) were detected by their mRNA transcript levels using qRT-PCR after selected ABR variant treatment in DSS-induced colitis murine model.

Results: The ABD-derived library was processed through ribosome display selection to generate a library of ABD variants with IL-22R1 inhibitory properties, named ABR. Individual variants were tested in high-throughput ELISA screening using a MaxiSorp immunoplate surface, which provided favorable IL-22R1 orientation. A total of 170 ABR clones were screened, and the DNA sequences of the 39 most promising candidates were verified. Among the 30 selected candidates, 24 unique variants were identified. We tested ABR variants for their ability to bind IL-22R1 on a PolySorp immunoplate surface to eliminate false positives due to high background on the MaxiSorp surface. Accordingly, 16 ABR variants were selected for further investigation in a competitive ELISA to evaluate their inhibitory potential. Corresponding to the ELISA results, 12 variants were identified to interfere with IL-22 binding to IL-22R1 in a concentration-dependent manner. These 12 variants were then tested for binding to transfected HEK293T cells expressing IL-22R1 on the surface using immunostaining. Among these, seven ABR variants (ABR006, ABR023, ABR027, ABR089, ABR099, ABR102, and ABR167) were found to recognize IL-22R1 on the surface of HEK293T cells. Another human keratinocyte cell line, HaCaT, which endogenously expresses IL-22R1 on its surface, was used to verify ABR specific binding. In response to TNFα and IFNγ stimulation, HaCaT cells significantly upregulated IL-22R1 expression in 30-50% of cells, making it detectable via fluorescence microscopy. All seven variants recognized the receptor on stimulated HaCaTs, while none bound to non-stimulated HaCaTs, proving the specificity of the selected binders. Finally, the binding of the seven ABR variants to the reporter cell line HEK-Blue IL22 was detected in a flow cytometry experiment, indicating ABR099 as the strongest binder. The seven ABR proteins (ABR006, ABD023, ABD027, ABR089, ABR099, ABR102, and ABD167) were further tested for their ability to inhibit human IL-22 signaling in the HEK-Blue IL22 reporter assay. ABR089 and ABR167 demonstrated clear inhibitory trends. Cysteine was also substituted with serine in ABR089 and ABR099. Consequently, ABR089S lost its inhibitory potential in the HEK-Blue IL22 reporter assay, while ABR099 gained it. The binding affinity of ABR089, ABR089S, ABR099, ABR099S, and ABR167 for IL-22R1 on the surface of transfected HEK293T and HaCaT cells determined using Ligand Tracer. The results showed that ABR089, ABR099, and ABR167 have Kd values of 3.4 nM, 1.0 nM, and 7.3 nM for HEK293T cells, and 9.7 nM, 3.0 nM, and 5.5 nM for HaCaT cells, respectively. The C/S substitution in ABR089 and ABR099 only slightly reduced binding affinity. Molecular

docking results indicated that the most probable binding poses of the inhibitory ABR variants overlap with the IL-22 binding site on IL-22R1. ABR167 was selected for *in vivo* experiments in a DSS-induced colitis murine model. ABR167-treated DSS-exposed mice showed a significant reduction in gut histology alterations compared to DSS-exposed control mice, based on assessments of epithelial changes, inflammatory infiltrate, and mucosal architecture deterioration. The mRNA expression levels of IL-1β, IL-6, IL-10, and IL-17A in ABR167-treated DSS-exposed mice tended to shift towards normal values compared to DSS-exposed controls.

Contribution: Within the study, I collected information about cells that endogenously express IL-22R1, which was used in the attempt to develop protocol for verification of ABR binding to cell surface IL-22R1. I tested several cell lines for the expression of IL-22R1 and developed protocol for HaCaT cell stimulation with TNFα and IFNγ. I confirmed that seven selected ABR variants are able to recognize endogenously expressed IL-6R1 using fluorescence microscopy. I tested inhibitory potential of ABR variants in HEK Blue IL-22 assay and identified IL-22R1 blockers. I verified inhibitory properties of C/S mutants. During the manuscript preparation I prepared figures, described methods and results for the performed experiments.

Graphical Abstract

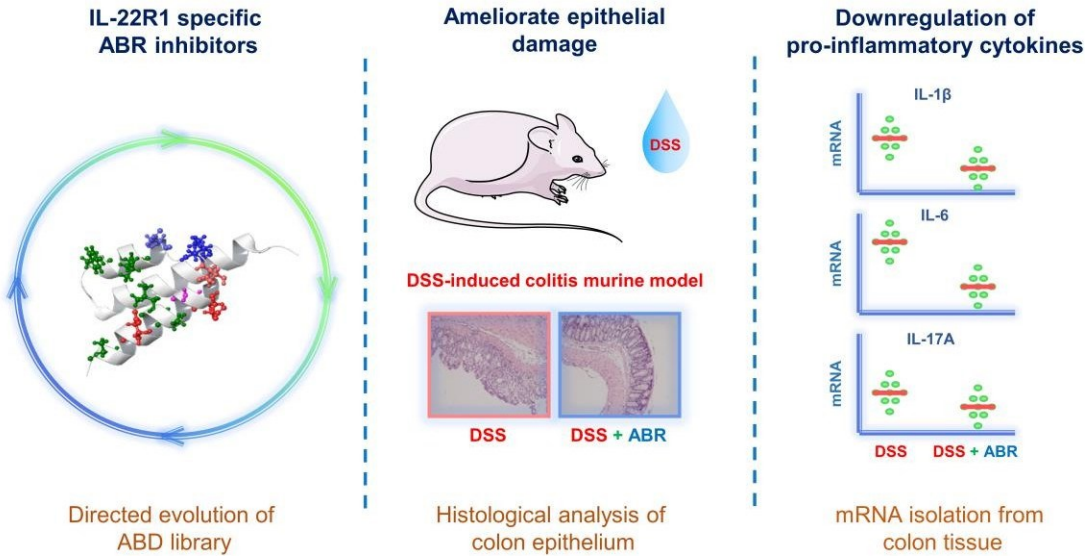

Human IL-22 receptor-targeted small protein antagonist suppress murine DSS-induced colitis

Milan Kuchař[1#], Kristýna Sloupenská[2#], Leona Rašková Kafková[2*], Yaroslava Groza[1], Jozef Škarda[3], Petr Kosztyu[2], Marie Hlavničková[1], Joanna M. Mierzwicka[1], Radim Osička[4], Hana Petroková[1], Stephen I. Walimbwa[2], Shiv Bharadwaj[1], Jiří Černý[5], Milan Raška[2], Petr Malý[1*].

[1]Laboratory of Ligand Engineering, Institute of Biotechnology of the Czech Academy of Sciences, BIOCEV Research Center, Prumyslova 595, 252 50 Vestec, Czech Republic

[2]Department of Immunology, Faculty of Medicine and Dentistry, Palacky University Olomouc, Hnevotinska 3, 779 00, Olomouc, Czech Republic

[3]Department of Pathology, University Hospital Ostrava and Faculty of Medicine, University of Ostrava, Syllabova 19, 708 00 Ostrava, Czech Republic

[4]Laboratory of Molecular Biology of the Bacterial Pathogens, Institute of Microbiology of the Czech Academy of Sciences, Videnska 1083, 14220 Prague, Czech Republic

[5]Laboratory of Structural Bioinformatics of Proteins, Institute of Biotechnology of the Czech Academy of Sciences, BIOCEV Research Center, Prumyslova 595, 252 50 Vestec, Czech Republic

[#] These authors contributed equally to this work

[*]**Authors for correspondence**

Petr Malý, Institute of Biotechnology of the Czech Academy of Sciences, Prumyslova 595, 252 50 Vestec, Czech Republic; Phone: +420 325873763, E-mail: petr.maly@ibt.cas.cz

Leona Rašková Kafková, Faculty of Medicine and Dentistry, Palacky University Olomouc, Hnevotinska 3, 779 00, Olomouc, Czech Republic; E-mail: leona.raskova@upol.cz

Abstract

Background

Human interleukin-22 (IL-22) is known as a "dual function" cytokine that acts as a master regulator to maintain homeostasis, structural integrity of the intestinal epithelial barrier, and shielding against bacterial pathogens. On the other hand, the overexpression of IL-22 is associated with hyper-proliferation and recruitment of pathologic effector cells, leading to tissue damage and chronic inflammation in specific diseases including inflammatory bowel disease (IBD). To study a role of IL-22-mediated signaling axis during intestinal inflammation, we generated a set of small protein blockers of IL-22R1 and verified their inhibitory potential on murine model of colitis.

Methods

We used directed evolution of proteins to identify binders of human IL-22 receptor alpha (IL-22R1), designated as ABR ligands. This approach combines the assembly of a highly complex combinatorial protein library derived from small albumin-binding domain scaffold and selection of promising protein variants using ribosome display followed by large-scale ELISA screening. The binding affinity and specificity of ABR variants were analyzed on transfected HEK293T cells by flow cytometry and Ligand Tracer. Inhibitory function was further verified by competition ELISA, HEK-Blue IL-22 reporter cells, and murine dextran sulfate sodium (DSS)-induced colitis.

Results

We demonstrate that ABR specifically recognizes transgenic IL-22R1 expressed on HEK293T cells and IL-22R1 on TNFα/IFNγ-activated HaCaT cells. Moreover, some ABR binders compete with the IL-22 cytokine and function as IL-22R1 antagonists in HEK-Blue IL22 reporter cells. In a murine model of DSS-induced acute intestinal inflammation, daily intraperitoneal administration of the best IL-22R1 antagonist, ABR167, suppressed the development of clinical and histological markers of colitis including prevention of mucosal inflammation and architecture deterioration. In addition, ABR167 reduces the DSS-induced increase in mRNA transcript levels of inflammatory cytokines such as IL-1β, IL-6, IL-10, and IL-17A.

Conclusions

We developed small anti-human IL-22R1 blockers with antagonistic properties that ascertain a substantial role of IL-22-mediated signaling in the development of intestinal inflammation. The developed ABR blockers can be useful as a molecular clue for further IBD drug development.

Keywords: Interleukin-22; Inflammatory bowel disease; Experimental colitis; Immune suppression; Protein engineering

1. Introduction

Interleukin-22 (IL-22), an innate lymphoid cell type 3 (ILC3) or Th17 signature cytokine, belongs to the interleukin-10 (IL-10) family [1] and it is mainly secreted by γδ T cells, innate lymphoid cells (ILC2 and ILC3), T helper (Th) 17 cells, and NKT cells [2]. IL-22 mediates its biological functions exclusively through a heterodimeric class II cytokine receptor comprising a high-affinity subunit, IL-22 receptor alpha (IL-22Rα or IL-22R1), and a low-affinity subunit, IL-10Rβ or IL-10R2 [3-5]. Notably, IL-22R1 expression is found exclusively on cell lineages originating from non-hematopoietic sources, such as the liver, kidney, pancreas, and barrier surfaces (i.e., lung, intestine, and skin) [6] whereas expression of IL-10R2 has been ubiquitously observed in various organs [2]. Available evidence establishes that IL-22 exhibits no affinity for IL-10R2, while a substantial binding affinity (K_D ranging from 1~20 nM) has been measured with the extracellular moiety of IL-22R1 [7, 8]. Also, attachment of IL-22 to IL-22R1 has been found to induce a conformational shift in IL-22 structure that promotes successive docking of the IL-10R2 subunit to the IL-22/IL-22R1 complex with a considerable recorded affinity (K_D = 7–45 μM) [9]. This structural information conveys that the initial attachment of IL-22 to IL-22R1 is required to initiate the secondary docking of the IL-10R2 subunit, thereby supporting the downstream signaling pathways in the target cells [10]. Importantly, the function of produced IL-22 is regulated by the soluble inhibitor IL-22 binding protein (IL-22BP, or IL-22R2), which is defined as a homolog of IL-22R1 and primarily released by myeloid cells [11, 12]. Likewise, the IL-22R1 expression is also maintained by concanavalin A or lipopolysaccharide (LPS) stimulation of hepatocytes, or IFNγ and TNFα in human skin cells [13], suggesting the IL-22 function may include dynamic variations linked to the expression of IL-22R1. Therefore, the IL-22/IL-22R1 system is involved in major crosstalk functions between epithelia and immune system, especially at the body barriers [1, 14].

In general, IL-22 has been characterized by its dual role − shielding or pathological functions during the initiation and progression of specific autoimmune and inflammatory diseases [6, 15]. Under physiologic conditions, IL-22 can be beneficial by promoting epithelial repair or wound healing regeneration, and tissue integrity against pathogenic invaders [16-18]. Especially, IL-22 acts as a master regulator to maintain the homeostasis and structural integrity of the intestinal epithelial barrier [19, 20]. Also, in synergy with IL-17, IL-22 acts as a proinflammatory cytokine,

which stimulates the upregulation of antimicrobial peptides in the epidermis including β-defensins and psoriasin (S100A7) [16, 21]. Furthermore, IL-22 is also demonstrated for protective functions in several diseases such as asthma, inflammatory bowel disease (IBD), and hepatitis [22-24]. Despite these beneficial functions, several studies suggest that IL-22 exhibits pathogenic functions depending on the discrete microenvironment and phase of the disease advancement [25-27]. In this context, the overexpression of IL-22 has been noted in several pathological conditions, as demonstrated by hyper-proliferation and recruitment of pathologic effector cells [6]. IL-22 overexpression is also reported to cause tissue damage and chronic inflammation in specific diseases including inflammatory bowel disease (IBD)[18].

Based on the published data, the IL-22/IL-22R1 system can be targeted by designed agonists or antagonists for the treatment of specific disorders or diseases. However, there is currently no Food and Drug Administration (FDA)–approved drug that directly targets IL-22, yet several drugs or formulations have been evaluated for selected diseases at different stages of development [14, 28]. Interestingly, most of the trial drugs in the process of being developed consist of modified recombinant IL-22 molecules with improved *in vivo* stability [29, 30]. For instance, Efmarodocokin alfa (UTTR1147A), an IL-22 used with crystallizable fragment (Fc) of human IgG4, showed effective engagement with IL-22R1 and demonstrated dose-dependent pharmacological activity in healthy volunteers under phase 1 trials [31]. In another clinical trial, Efmarodocokin alfa showed a long-term safety and tolerability profile in patients with moderate to severe ulcerative colitis [32]. Likewise, under a multicenter single-arm phase 2 study, designed F-652, a recombinant human interleukin-22, fused with an immunoglobulin constant region (IgG_2-Fc) was noticed for favorable pharmacokinetics (PK) and pharmacodynamic (PD) properties, and was demonstrated as potential treatment for the acute Graft versus host disease (GVHD)-associated dysbiosis in the lower gastrointestinal (GI) tract in combination with systemic corticosteroids [33, 34]. In another clinical trial (phase 2a), fezakinumab (ILV-094) – an IL-22–neutralizing antibody, showed efficacy in patients with moderate to severe atopic dermatitis [35]. Moreover, probiotic *Lactobacillus*-expressing IL-22 has been suggested to deliver bioactive IL-22 directly to the intestinal mucosa to benefit patients with GVHD [36].

To interfere with cytokine-mediated cell signaling controlling the IL-23/IL-17 inflammatory axis, we have previously developed several collections of small binding proteins that function as IL-23 cytokine blockers [37], or IL-23 receptor (IL-23R) [38] and IL-17 receptor A (IL-17RA) antagonists [39, 40]. These small inhibitory ligands of 5 kDa were derived from the structure of the albumin-binding domain (ABD) of streptococcal protein G and identified by ribosome display selection from a highly complex combinatorial ABD library [41]. In this study, we report on the generation and characterization of ABD-derived protein blockers targeting IL-22R1 and discuss the role of IL-22 signaling inhibition during experimental intestinal inflammation induced by Dextran Sulfate Sodium (DSS).

2. Materials and Methods

2.1. Cell lines

Human embryonic kidney cells (HEK293T), human keratinocytes (HaCaT), and HEK-Blue IL22 cells were cultured in high-glucose DMEM medium (Biosera) supplemented by 10% fetal bovine serum (FBS) and streptomycin-penicillin solution (Biosera), and incubated under 5% CO_2 at 37 °C. Streptavidin-phycoerythrin (PE) was purchased from eBioscience, San Diego, CA. Human anti-IL-22R1 APC-conjugated antibody (mouse IgG1 isotype) was procured from R&D Systems, Minneapolis, MN, and mouse IgG1 APC-conjugated isotype control antibody MOPC-21 was obtained from Exbio Praha, a.s., Vestec, Czech Republic.

2.2. Assembly of ABD library

A highly complex combinatorial NNK library (where N means any nucleotide, K is G or T only) derived from a scaffold of albumin-binding domain (ABD) was assembled by multiple PCR steps as previously reported and characterized [41, 42]. Briefly, the ABD library was assembled using two oligonucleotides ABDLIB-setB1c and ABDLIB-setB2c (Table S1) and connected with cDNA coding for the tolA helical linker. Amplified by PCR was purified on 1% agarose (QIAquick Gel Extraction Kit, QIAGEN) and used for *in vitro* transcription and translation using PURExpress® In Vitro Protein Synthesis Kit (New England Biolabs).

2.3. Ribosome display

A modified ribosome display selection procedure was used for the assembled ABD library targeting recombinant human IL-22R1 receptor [43, 44]. For the preselection step, 3% BSA in TBS buffer (50 mM Tris, 150 mM NaCl, DEPC-treated water, pH 7.5), and for the selection steps, IL-22R1 (rhIL-22 Rα1, R&D Systems) diluted in coating buffer (Bicarbonate/carbonate coating buffer, pH 9.6), were coated in wells of NUNC-immune MaxiSorp plates (Thermo Scientific Inc.). Then, all the wells were blocked using Protein-Free (PBS) Blocking Buffer (Thermo Scientific Inc.) and incubated for 3 h at room temperature (RT). Following, the preselection wells were washed thrice and incubated with a mixture of *in vitro* translated ABD library (mRNA-ribosome-protein complex) and ABDwt (25 µg/ml) in WBT buffer (50 mM Tris-base, 150 mM NaCl, 50 mM MgAc, 0.05% Tween-20, DEPC-treated water, acetic acid to pH 7.5) at 8 °C for next 1 h under shaking conditions. Later, the unbound library from preselection wells was transferred into selection wells, washed thrice, and incubated for 1 h at 8 °C under shaking conditions. Finally, the selection wells were washed thrice with WBT buffer while mRNA-ribosome-protein complexes bound to the coated IL-22R1 protein were eluted using 200 µl of EB (50 mM Tris-base, 150 mM NaCl, 50 mM EDTA, DEPC-treated water, pH by acetic acid to pH 7.5). Next, the total mRNA was extracted and purified using mRNA extraction kit. A total of three rounds of preselection/selection were performed with increasing stringency as follows: 1st round – plate coating with 25 µg/ml IL-22R1, washed 5 times by WBT buffer containing 0.05% Tween 20, 2nd round – 25 µg/ml IL-22R1, washed 10 times and 3rd round – 10 µg/ml IL-22R1, washed 10 times by WBT containing 0.1% Tween 20. Also, ABDwt protein was added as a competitor to the library in 1st and 3rd rounds only. Harvested mRNA was reversely transcribed by GoScript™ Reverse Transcriptase (Promega) and resulted a DNA library that was finally inserted into the pET28b vector to form a plasmid library of selected DNA variants.

2.4. Screening of IL-22R1-targeted ABD-derived variants

Escherichia coli BL21 (λDE3) BirA strain cells were transformed by the plasmid cDNA library. Individual bacterial colonies were picked up for overnight culture in 2 ml LB broth at 37 °C with kanamycin (60 µg/ml) and chloramphenicol (30 µg/ml). Next day, 100 times diluted culture was further cultured, and protein production was induced with 1.5 mM IPTG in the presence of 50 µM

d-biotin (5 mM d-biotin solution in 10 mM Bicine buffer, pH 8.3) at 32 °C. After 4 h of incubation, the cells were harvested by centrifugation and obtained bacterial pellets were frozen. For the analysis, pellets were resuspended in PBS buffer and sonicated for 1 minute using ultrasonic disruptor Q700 Sonicator (Qsonica) and centrifuged (18000×g) for 10 minutes at 4 °C. Cell supernatant was diluted 15000 times in PBS/Tween-20/1%BSA (pH 7.4). For the identification of IL-22R1 specific binders, binding ELISA was used. Nunc MaxiSorp and PolySorp ELISA plates were coated with IL-22R1 (2.5 µg/ml). Then, MaxiSorp plates were blocked with Protein-Free (PBS) Blocking Buffer and PolySorp plates were blocked with 1% BSA in PBS-T (PBS, 0.05% Tween-20). Bacterial lysates containing in vivo biotinylated ABD protein variant were tested for binding to immobilized IL-22R1 using streptavidin-HRP (Pierce™ High Sensitivity Streptavidin-HRP, Thermo Scientific Inc.). After 30 minutes incubation, TMB-Complete 2 (3,3',5,5'-Tetramethylbenzidine, H_2O_2, TestLine Clinical Diagnostics s.r.o.) substrate was added and the reaction was stopped by 2 M sulfuric acid. The absorbance was measured at 450 nm using an ELISA microplate reader.

2.5. Competition ELISA

ABD protein variants were purified from bacterial lysates in 50 mM Tris, 300 mM NaCl, and pH 8.0 buffer using affinity chromatography (Ni-NTA agarose, Qiagen). For the competition assay, MaxiSorp plates were coated with human IL-22R1 (1 µg/ml), blocked with Protein-Free (PBS) Blocking Buffer, and purified ABD variants were serially diluted in PBS-T with 1% BSA containing IL-22 cytokine (recombinant human IL-22 protein, Fc Chimera, Abcam) at the concentration 1 nM, and cytokine binding was detected by mouse IgG1 Anti-Human IgG (Fc) HRP (1: 5 000, mouse monoclonal IgG to Fc part of human IgG heavy chain conjugated with horseradish peroxidase, Exbio Praha, a.s.).

2.6. Immunofluorescence staining of transfected HEK293T cells

Full-length IL-22R1 cDNA coding for 574 amino acids protein containing a signal peptide (GenBank: BC029273.1) was cloned in pcDNA™6/myc-His A vector with added Kozak sequence. Before seeding the cells, 24-well plates (TPP Techno Plastic Products AG) were coated with 100 µl of 100 µg/ml poly-D-lysine (Gibco), incubated for 1 h at 37 °C , then washed 3 times with PBS and

left to dry for 20 minutes at RT. Total 1.5 × 10^5 cells were seeded 48h before the transfection or 2.5 × 10^5 cells were seeded 24 h before the transfection. The complete growth medium was exchanged into DMEM without any supplements. Plasmid DNA and PEI mixes were prepared in 50 µl of DMEM medium without supplements, mixed by inversion, incubated for 15 minutes at RT, and then applied dropwise into the wells. HEK293T cells were transiently transfected using cationic polymer polyethylenimine (PEI branched, MW 25,000; Sigma-Aldrich) in concentration 1 mg/ml and in 4.5:1 PEI to plasmid DNA ratio and 1 µg of DNA was used per each well. Transfected cells were incubated in 0.5 ml of DMEM medium without supplements for 18 h and then 0.5 ml of complete culture medium was added to each well. Two days after the transfection, particular protein variants at a concentration of 20 µg/ml were added to DMEM medium, and cells were incubated at 37 °C for 1 h and then 3 times washed with PBS. The primary staining mix contained Streptavidin–Alexa Fluor (AF) 568 conjugate (Thermo Scientific, Inc.) for detection of biotinylated ABD proteins and rabbit polyclonal anti-IL-22R1 antibody for the detection of IL-22R1. After 1 h incubation, cells were washed, and goat anti-rabbit IgG conjugated with AF488 (Abcam) was added for next 1 h staining in the dark. Each well was washed 3 times with PBS and visualized using fluorescence microscopy with further image processing using ImageJ software.

2.7. Binding kinetics measured with LigandTracer method

HEK293T cells were transiently transfected with 1mg/ml PEI (MW 25,000) and the PEI – DNA ratio was 4.5:1. Prior to 24 h before the transfection, 3 ml of cell suspensions (1 × 10^6 cells) was seeded on 100 mm cell dishes (Nunclon TM) in the designated area (marked as target area) and incubated overnight in a tilted position. Before seeding the cells, dishes were coated with 2.3 ml of 100 µg/ml poly-D-lysine, incubated for 1 h at 37 °C, then washed 3 times with PBS and left to dry for 20 minutes. The next day, the medium was exchanged into a medium without supplements and cells were transfected. Plasmid DNA and PEI mixes were prepared in 300 µl of DMEM medium without supplements, mixed by inversion and incubated for 15 minutes at RT. Transfected cells were incubated in 3 ml of DMEM medium without supplements in a tilted position for 18 h and then 6 ml of complete growth medium was added. Cells were incubated at the horizontal position for the next 24 h. For the measurement, the LigandTracer Green Line (Ridgeview Instruments AB,

Uppsala, Sweden) with Red - NIR (632 – 671 nm) detector was used. The fluorescence signal was detected using Streptavidin-APC conjugate (ThermoFisher Scientific). The evaluation of binding kinetics was done using TraceDrawer 1.7.1 software. Kinetic parameters (ka, kd, KD) were calculated using 'One-to-one' or 'One-to-one depletion corrected' evaluation methods.

2.8. Binding of ABR proteins to HaCaT cells

HaCaT were cultured in DMEM with 2 mM L-glutamine, 5.4 g/l glucose, 10% heat-inactivated fetal bovine serum, 100 U/ml Penicillin, 100 µg/ml Streptomycin at 37 °C in 5% CO_2. After overnight incubation, 10 ng/ml TNFα (Abcam) and 10 ng/ml IFNγ (Abcam) were added for 24 h according to the previous study [45] Biotinylated ABR variants were added in DMEM at a concentration 20 µg/ml (≈500 nM) for 1 h at 37 °C. Cells were washed 3 times with PBS. Rabbit anti-IL-22 polyclonal Ab (Abcam) was diluted 100 times in PBS with 1.5% BSA and added to cells and incubated for next 1 h at RT. After 3 times washing with PBS Streptavidin (AF568) (Invitrogen), goat anti-rabbit IgG H&L (AF488) pAb (Abcam,) were added to cells and incubated for 1 h at RT. Both reagents were diluted 200 times in PBS with 1.5 % BSA. Finally, HaCaT cells were washed 5 times with PBS. Then, cell imaging was made with an Olympus CKX41 Inverted Phase Contrast Microscope. For the estimation of binding kinetics by LigandTracer, Streptavidin-APC conjugate was used for ABR protein detection.

2.9. Flow cytometry

Streptavidin-phycoerythrin (PE) was obtained from eBioscience, San Diego, CA. Human anti-IL-22R1 APC-conjugated antibody (mouse IgG1 isotype) was purchased from R&D Systems, Minneapolis, MN, and mouse IgG1 APC-conjugated isotype control antibody MOPC-21 was obtained from Exbio Praha s.r.o., Vestec, Czech Republic. Cultured HEK-Blue IL22 and HEK-293T cells were collected and washed in HEPES-buffered salt solution (HBSS buffer; 10 mM HEPES (pH 7.4), 140 mM NaCl, 5 mM KCl) supplemented with 2 mM $CaCl_2$, 2 mM $MgCl_2$, 1% (w/v) glucose, and 1% (v/v) FCS (cHBSS buffer). 2×10^5 cells/sample in cHBSS buffer were incubated with 1 µg/ml of biotin-labeled ligands (ABRs and ABD) for 30 minutes at 4 °C. After washing with cHBSS buffer, cells were incubated with PE-labeled streptavidin (diluted 1:400) for 30 minutes at 4 °C. Cells were

washed, resuspended in cHBSS buffer, and analyzed by flow cytometry using a FACS LSR II instrument (BD Biosciences, San Jose, CA) in the presence of 1 µg/ml of Hoechst 33258. Data was processed using the FlowJo software (Tree Star, Ashland, OR) and appropriate gating was used to exclude debris, cell aggregates, and dead cells (Hoechst 33258-positive staining). Binding data was deduced from mean fluorescence intensities (MFI) of cell-bound ligands and expressed as relative values, with the highest MFI value of the ligand taken as 100%. For antibody binding, 2×10^5 cells/sample were incubated in cHBSS buffer with anti-IL-22R1 APC-conjugated antibody (diluted 1:100) or IgG1 isotype control (diluted 1:100) for 30 minutes at 4 °C. After washing, cells were resuspended in cHBSS buffer, and analyzed by flow cytometry as described above.

2.10. HEK-Blue IL22 reporter cell inhibition assay

HEK-Blue IL22 Reporter Cell line (InvivoGen) was cultured in DMEM with 2 mM L-glutamine, 5.4 g/l glucose, 10% heat-inactivated fetal bovine serum, 100 U/ml Penicillin, 100 µg/ml Streptomycin, 100 µg/ml Normocin, 10 µg/ml Blasticidin, 10 µg/ml Puromycin, 100 µg/ml Zeocin at 37 °C in 5% CO_2. For the inhibition assay, HEK-Blue IL22 cells were seeded to a NUNC sterile 96-well plate (Thermo Scientific Inc.), 36000 cells per well in a volume of 180 µl. HEK-Blue IL22 cells were grown on a surface treated with Poly-D-Lysine (Gibco™) to ensure uniform attachment without cell clamping which was observed on an untreated surface. Inhibition assay was carried out in DMEM with 2 mM L-glutamine, 5.4 g/l glucose, 100 U/ml Penicillin, 100 µg/ml Streptomycin, 100 µg/ml at 37 °C in 5% CO_2. Cells were incubated with human IL-22 (Abcam) for 22h in the presence of different concentrations of ABR variants. ABR variants were serially diluted in sterile PBS by 5 times per step with the highest concentration being 120 nM and added to cells in 20 µl volume. After 22 h, 20 µl of cell supernatant was mixed with 180 µl of the Quanti-BlueTM Solution (InvivoGen) to detect secreted alkaline phosphatase (SEAP) that was produced by HEK-Blue IL22 cells in response to human IL-22 stimulation. Cell supernatant was incubated with Quanti-BlueTM Solution for 1 h at 37 °C in the dark. Absorbance was measured at 620 nm with Epoch 2 spectrophotometer. HEK-Blue IL22 reporter cells were incubated with 3 ng/ml (≈ 0.2 nM) of human IL-22 and varied concentration of ABR variants. SEAP level for each ABR concentration, as

detected by measuring absorbance at 620 nm, was compared to the SEAP level while human IL-22 was added in the absence of any other protein.

2.11. Molecular modeling

We modeled the structure of the ABD-derived variants ABR089, ABR099, and ABR167 using the MODELLER 9v14 software suite [46] using the structure of the wild type ABD (pdb id 1gjt [47]) as the template. The IL-22R1 structure was obtained from the crystal structure of the IL-22/IL-22R1 complex (pdb id 3dlq [48]). For protein-protein docking with flexible side chains, we utilized a local version of the ClusPro server [49, 50], using chain B from the 3dlq structure (residues missing in the template were modeled using the automodel function of MODELLER taking the best scoring model corresponding to IL-22R1 domains 1 and 2, residues 18 to 228, according to the UniProt [51] record Q8N6P7) as the receptor and the modeled ABR variants as ligands. The docking results were visualized with PyMOL version 2.6.0 (The PyMOL Molecular Graphics System, Schrödinger, LLC).

2.12. Animals and experimental design

8-9 weeks old female C57BL/6 mice (AnLab, Prague, Czech Republic) weighting between 18 and 22 g (weight before treatment) were kept under standardized conditions at temperature between 21–22°C, a 12:12-h light/dark cycle, ad libitum access to food and water. Mice were permitted to acclimatize for 1 week before starting the experiments. Mice were randomly divided into experimental groups and marked with ear tags.

2.13. Induction of acute colitis

Acute colitis was induced by giving drinking water containing 2.5% (w/v) DSS (MW approximately 40 kDa; TdB Labs, Uppsala, Sweden) for 4 days. At the end of the experiment, the animals were anesthetized, bled out, and euthanized by cervical dislocation. The length of the colon was measured between the caecum and proximal rectum. Serum was isolated from blood. Colon was dissected into pieces for quantitative RealTime RT-PCR (qRT-PCR) and histochemistry. All experiment protocols were approved by Ethics Committee of the Faculty of Medicine and

Dentistry (Palacky University Olomouc, Czech Republic), and the Ministry of Education, Youth and Sports, Czech Republic (MSMT-10947/2021-3).

2.14. Preventive treatment of mice by intraperitoneal application (i.p.) of binders

C57BL/6 mice were divided into three groups. Group 1 (naive) – consisting of 10 naive untreated mice. Group 2 (DSS + ABR167) – consisting of 19 mice treated by i.p. administration of 25 µg of ABR167 per mouse every 24 h starting 3 days before DSS-colitis induction and continuing for another 4 days together with DSS administration, and the Group 3 (DSS induction control) – consisting of 13 mice exposed to DSS without the therapy.

2.15. RNA isolation, reverse transcription, and qRT-PCR

Dissected colon tissues were stored in RNA later (Invitrogen, Thermo Scientific Inc.) at -80 °C. Pre-weighed colons were homogenized using Qiashredder (Qiagen, Hilden, Germany) and total RNA was extracted using RNeasy Plus Mini Kit (Qiagen, Hilden, Germany). Column DNase treatment (gDNA Eliminator spin column, Qiagen) was used to eliminate potential DNA contamination. RNA purification was performed via lithium chloride method [52] to remove the traces of DSS. Extracted RNA was reversely transcribed into cDNA using the gb Elite Reverse Transcription Kit (Generi Biotech, Hradec Kralove, Czech Republic). qRT-PCR was performed in triplicates using gb SG PCR Master Mix (Generi Biotech) on LightCycler 480 System (Roche, Basel, Switzerland). All primers (6 µM) used in this study are listed in Table S2. Ct values were normalized to the reference gene, GAPDH, and the relative RNA expression was calculated by $2^{-\Delta\Delta Ct}$ method [53].

2.16. Histochemistry

Formalin-fixed, paraffin embedded tissues were cut, stained with hematoxylin and eosin (H&E) (Merck, Darmstadt, Germany), classified by a professional pathologist, and verified by medical doctor without prior knowledge of clinical parameters using BX43 microscope equipped with CCD camera (Olympus, Tokio, Japan). The representative areas of the most intense mucosal alterations were selected in each section. These areas were scored for given parameters as summarized in the Table S5.

2.17. Statistical analysis

All statistical analyses were performed using GraphPad Prism 8 Software (GraphPad Software Inc., San Diego, CA, USA). All data sets were verified for normal (Gaussian) distribution by Normality test. We performed Kruskal-Wallis one-way ANOVA followed by Dunn´s multiple comparisons test; *P<0.05, **P<0.01, ***P<0.001.

3. Results

3.1. Directed evolution of ABD variants targeting human IL-22R1

To generate ABD variants that inhibit signaling function of human IL-22R1, we used directed evolution and employed MaxiSorp immune-plate for ribosome display selection as ELISA experiment demonstrated the accessibility of IL-22 to the cytokine binding site on IL-22R1 once coated on 96-well plate (Fig. S1). Three-round ribosome display resulted in the generation of ABD library containing cDNA of the selected variants. This library was cloned into pET28b plasmid and used to transform in *E .coli* cells. ELISA screening resulted in the selection of ABD variants with preferential binding to the IL-22R1, which were purified and re-tested in equal concentration using PolySorp plate (Fig. 1A, B, C). Following this approach, a total of 170 ABD variants were assessed for the specific binding to commercial IL-22R1, and 39 variants with considerable binding affinity were further verified by sequence analysis. This identified 24 unique variants expressing full-length protein, and 16 candidate variants were selected for further characterization, especially for the ability to compete with IL-22 cytokine.

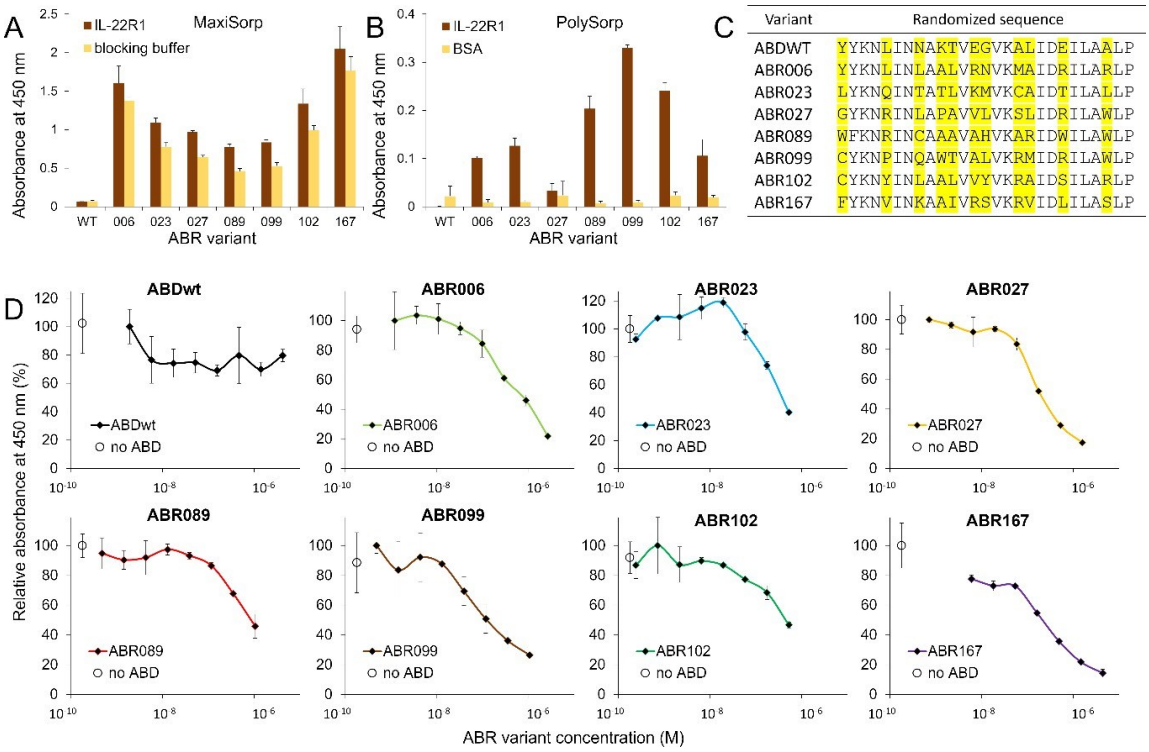

Fig.1. Selection of IL-22R1-binding ABR variants using ELISA. Positive variants and ABDwt as a negative control are shown in **(A)** and **(B)**. For screening, lysates containing *in vivo* biotinylated protein variant diluted in PBS (15 000 times, for protein concentration to be ~10^{-9} M) were tested for binding to immobilized IL-22R1 (2.5 mg/ml) in comparison to only blocked wells, on MaxiSorp plate with blocking by Pierce™ Protein-Free Blocking Buffer **(A)** or on PolySorp plate with blocking by BSA **(B)**. Binding was detected by streptavidin-HRP (1: 10 000) and results represent average values with standard deviation error bars. **(C)** Amino acid sequences of the identified variants as well as ABDwt are shown in a table with marked randomized positions (yellow). **(D)** ELISA based competition assay was carried out with purified protein variants. IL-22R1 (1 mg/ml) was immobilized on MaxiSorp plate, serially diluted ABR variants and negative control ABDwt competed with IL-22 at constant concentration (1 nM) for binding to the receptor and the resulted curves are compared to the average value corresponding to cytokine binding in the absence of the ABR competitor (no ABR). IL-22-Fc binding was detected by mouse Anti-Hu IgG (Fc) HRP (1: 5 000) and average values with standard deviation error bars are presented.

3.2. Engineered ABR variants block IL-22 binding to immobilized and cell-surface expressed IL-22R1

To evaluate the ability of the engineered ABR variants to inhibit binding of IL-22 to IL-22R1, we performed the competition ELISA assay. The blocking effect of selected 16 candidates was monitored on the immobilized IL-22R1 receptor on the MaxiSorp plate (Fig. 1D). The collected results support 12 ABR variants with considerable competition effect using ELISA. Hence, these 12 variants were selected in the second phase for binding to transfected HEK293T cells expressing IL-22R1 on the surface.

Next, we evaluated the ability of ABR variants to recognize IL-22R1 on the surface of HEK293T cells (Fig. 2). Seven ABR variants (ABR006, ABR023, ABR027, ABR089, ABR099, ABR102 and ABR167) recognize IL-22R1 expressed on the surface of HEK293T cells. Other four ABR variants (ABR026, ABR081, ABR087 and ABR156) did not recognize IL-22R1. To confirm the specificity of the ABR proteins to recognize IL-22R1, HaCaT cells expressing endogenously IL-22R1 upon stimulation with TNFα and IFNγ were used for immunofluorescence detection (Fig. S2). This staining was performed for 7 variants positively reacting with HEK293T transfected cells. All selected variants bind to IL-22R1 upon stimulation TNFα and IFNγ (Fig. 3), and show no positivity for unstimulated HaCaT cells.

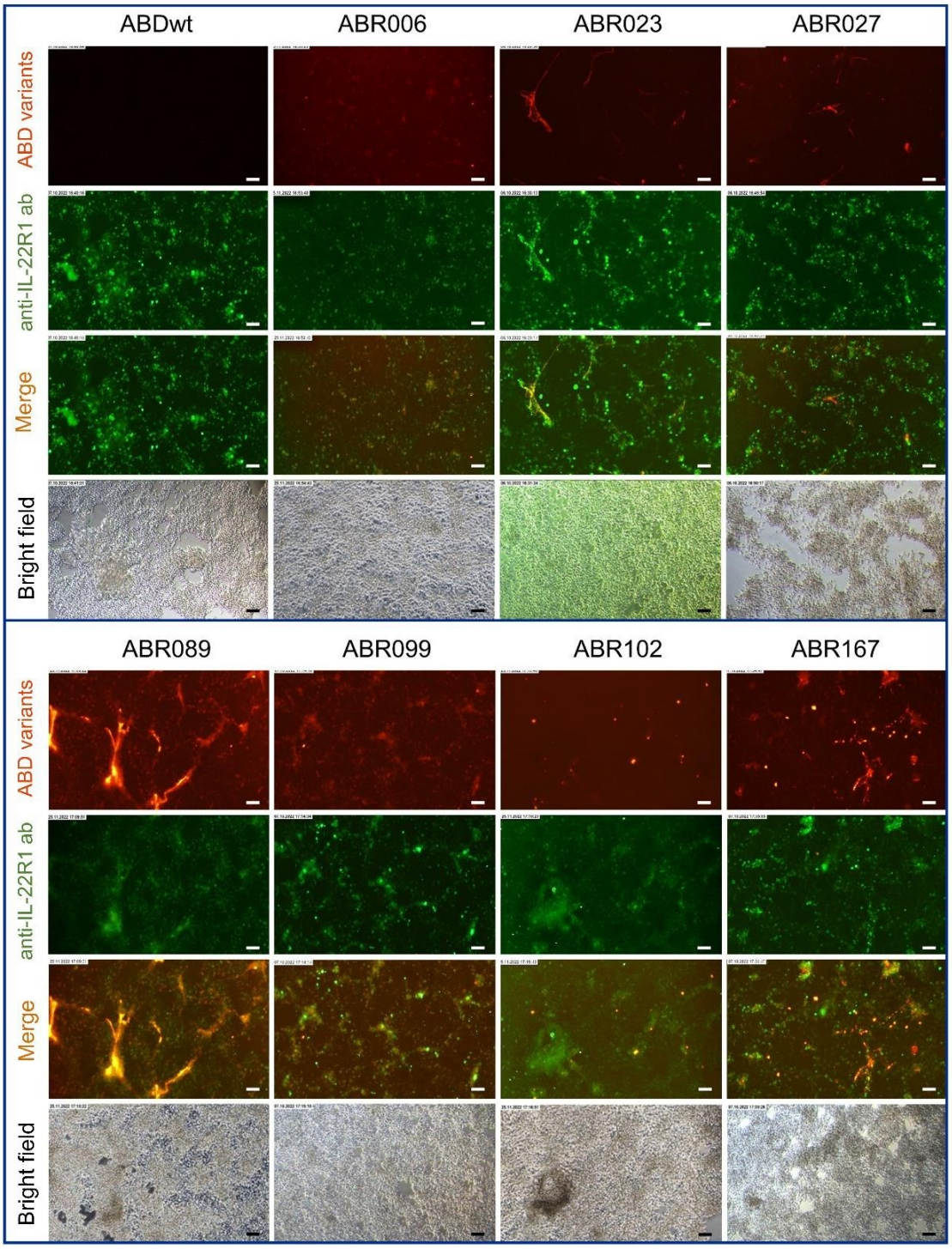

Fig. 2. Detection of IL-22R1 expression on transfected HEK293T cells and binding of ABR variants to IL-22R1. Representative images of HEK293T cells expressing human IL-22R1 on the surface. Cells were incubated with biotinylated ABR variants (ABR006, ABR023, ABR027, ABR089, ABR099, ABR102, and ABR167) and stained with Streptavidin-AF568 (STV-AF568 conjugate) and anti-IL-22R1 antibody (anti-IL-22R1-AF488).

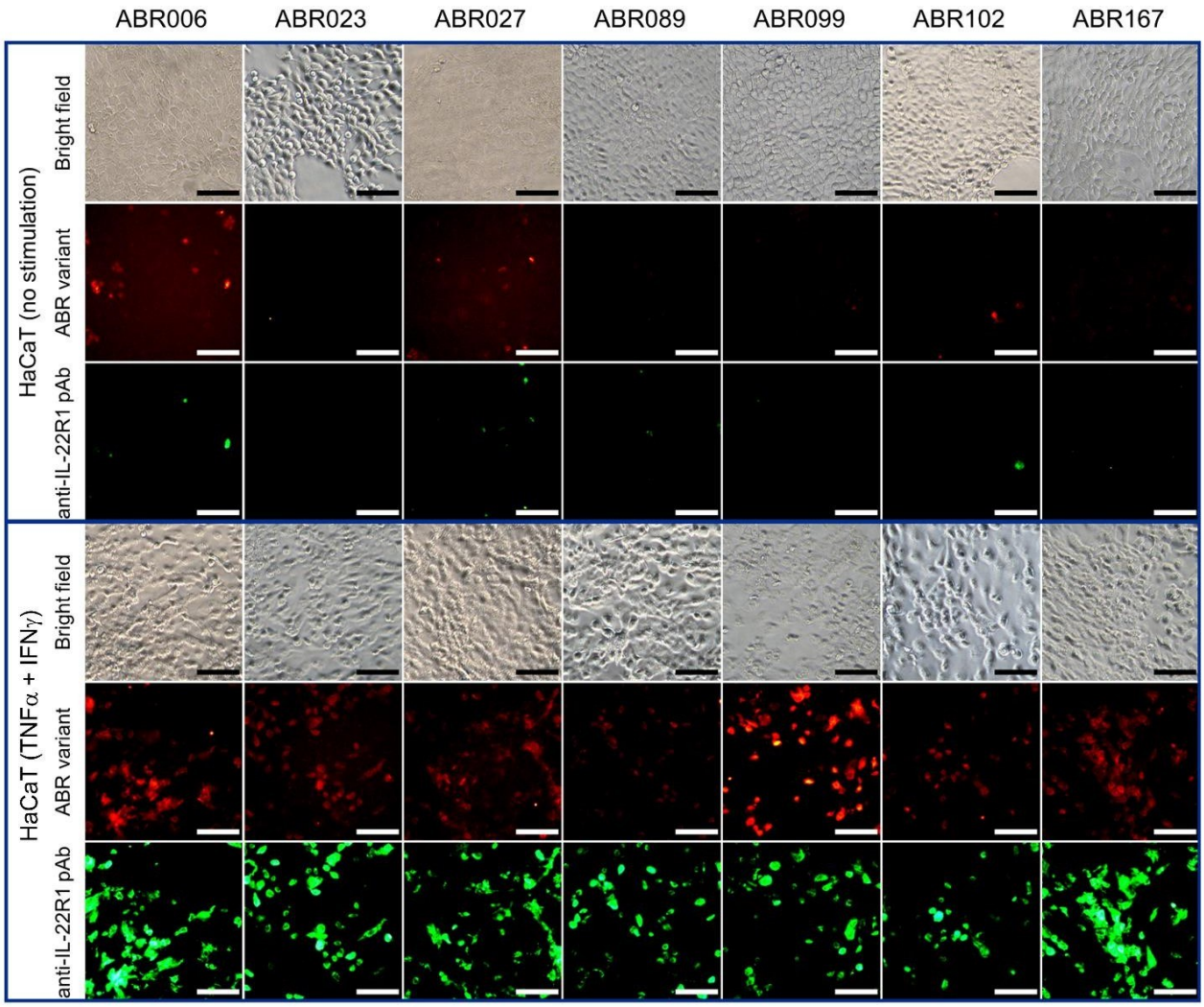

Fig. 3. Fluorescence microscopy images demonstrating ABR variant's binding to the IL-22R1 on stimulated HaCaT cells. HaCaT cells were stimulated with TNFα and IFNγ for 24 h. Double staining of ABR proteins detected by Streptavidine-AF568 conjugate (red) and rabbit anti-IL-22R1 pAb-AF488 (green) was carried out.

3.3. Binding of ABR proteins to HEK-Blue IL22 cell tested by flow cytometry

HEK-Blue IL22 cells, reported as a sensitive cell line to promote IL-22-mediated signaling, were used to verify the specificity of selected ABR protein candidates by flow cytometry. As shown in Figure 4A(i), HEK-Blue IL22 cells substantially express IL-22R1 as documented by the binding of anti-human IL-22R1 antibody in contrast to isotype IgG1 antibody control or non-transfected HEK 293T cells. As further shown in Figure 4A(ii), ABR variants, except for ABR006, bind to HEK-Blue

IL22 cells with the strongest binding of ABR099 protein. The non-randomized ABD parental protein used as a negative control did not bind to these cells, thus documenting the specificity of the tested ABR binders Figure 4A(ii-iii).

3.4. Generation of ABR089 and ABR099 variants with Cysteine-to-Serine substitution

For the selection of proteins variants targeting human IL-22R1, ABD-derived combinatorial library with more restricted degenerate codon (NNK type) was used, thus covering 32 codons. This approach is based on the randomization of single nucleotides (N means any nucleotide, K is G or T only) and results in the generation of codons for all 20 amino acid residues, including Cysteine residues and one of stop codons. As shown in Figure 1C, 4 of 7 identified inhibitory variants (ABR023, ABR089, ABR099, and ABR102) contain a Cysteine residue in the randomized positions. As ABR023 and ABR102 did not demonstrate a substantial binding to HEK293T transfected cells (Fig. 2) and stimulated HaCaT cells (Fig. 3), we used sequences of ABR089 and ABR099 cDNA for the substitution of Cysteine for Serine residue. This was motivated to prevent from an occasional dimer formation that can in some cases block the accessibility to the binding site, thus suppressing the inhibitory function of these proteins. We used site directed mutagenesis to construct ABR089S protein with C27S mutation and ABR99S containing C20S substitution. The analysis of data from ELISA demonstrated that ABR089S as well as ABR099S retained the binding to IL-22R1 receptor in comparison to the non-mutated ABR089 and ABR099 variants (Fig. S3).

3.5. Inhibition of IL-22-mediated signaling by ABR in HEK-Blue IL22 reporter cells

To verify a possible antagonistic effect of ABR ligands, we used HEK-Blue IL22 reporter cells which is available for monitoring of IL-22-mediated signaling. Human IL-22 triggers IL-22R1 assembly with subsequent STAT3 phosphorylation in HEK-Blue IL22 cells, followed by secretion of SEAP into cell supernatant. Seven ABR proteins (ABR006, ABD023, ABD027, ABR089, ABR099, ABR102, and ABD167) were tested for their ability to inhibit human IL-22 signaling in HEK-Blue IL22 reporter cells. Selected ABR variants that were tested in the cell inhibitory assay, outcompeted human IL-22 binding to IL-22R1 in competitive ELISA. ABDwt was used as a negative control. Two ABR

variants, ABR089 and ABR167, showed a persuasive inhibitory trend (Fig. 4B). The decrease in the absorbance up to 70% was observed for the concentration range 0.2 – 129 nM for ABR089 and 0.2-24 nM for ABR167 in comparison to the signal of human IL-22 alone. On the contrary, ABDwt did not demonstrate concentration dependent decrease in absorbance, indicating that inhibitory trends observed for ABR089 and ABR167 were not biased by ABD scaffold properties or cell cytotoxicity. Thus, ABR089 and ABR167 demonstrated the ability to inhibit human IL-22 down-stream signaling in HEK-Blue IL22 reporter cells as noticed in competition ELISA (Fig. 1D).

3.6. Binding kinetics and affinity measurements

Initially, we tested binding of anti-IL-22R1 antibody to HEK-Blue IL22, HEK293T and HaCaT (Fig. S4, Table S4). The obtained results confirmed the presence of the IL-22R1 on the cell surface in all three cell types, and hence, all three cell lines can be used to measure kinetics of ABR ligands. Based on this observation, we selected HEK293T cells transfected with IL-22R1-pcDNA6 and HaCaT cells for the binding kinetics and affinity measurement for the selected ABR variants under similar conditions (Fig. 4C). Kinetic parameters were measured on HEK293T and HaCaT cells for all ABR variants presented in Table S4. The collected results showed that ABR089, ABR099, and ABR167 have Kd = 3.4 nM, Kd = 1.0 nM, and Kd = 7.3 nM as well as Kd = 9.7 nM, Kd = 3.0 nM, and Kd = 5.5 nM for HEK293T and HaCaT cells, respectively. In addition, C/S substitution on the ABR089 and ABR099 did not seem to significantly affect the binding capacity to HEK293T cells (Fig. 4C).

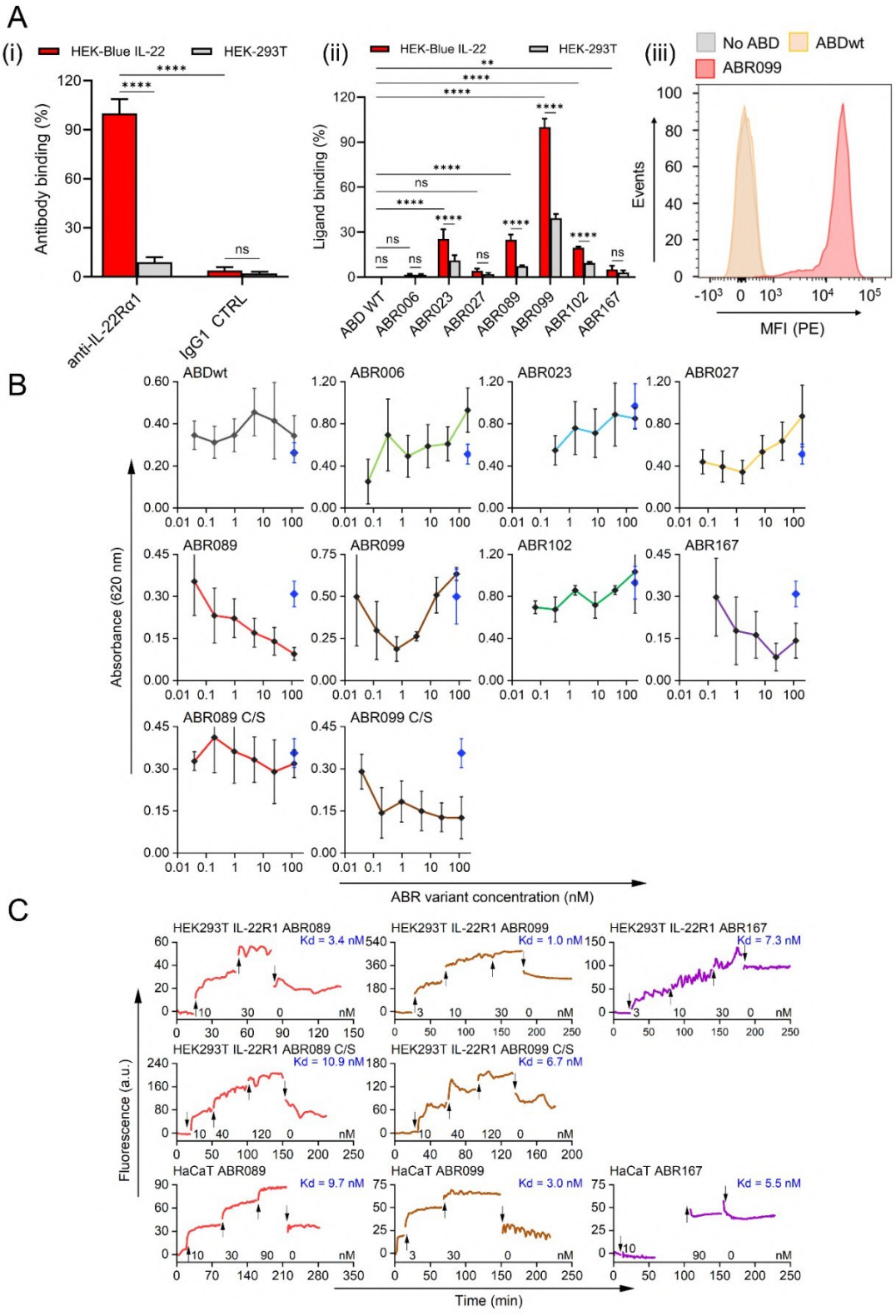

Fig. 4 (A) ABR ligands bind to HEK cells expressing the human IL-22 receptor. (i) HEK-Blue IL22 cells and HEK-293T control cells were incubated with anti-IL-22R1 APC-conjugated antibody or APC-conjugated IgG1 isotype control (IgG1 CTRL). After washing, cells were analyzed by flow cytometry and binding data

were deduced from MFI values. The MFI value for anti-IL-22R1 antibody measured on HEK-Blue IL22 cells was taken as 100%. **(ii)** HEK-Blue IL22 and HEK-293T control cells were incubated with 1 µg/ml of biotinylated ABR variants or with biotinylated ABDwt used as a negative control for 30 minutes at 4 °C. Cell-bound proteins were analyzed by flow cytometry and binding data were deduced from MFI values and expressed as percentage of ABR099 binding to HEK-Blue IL22 cells (taken as 100%). **(i-ii)** Each bar represents the mean value with SD of three independent experiments performed in duplicate (ns, $p > 0.05$; **, $p < 0.01$; ****, $p < 0.0001$; ANOVA). **(iii)** Binding of the ABR099 ligand to HEK-Blue IL22 cells. ABDwt was processed in parallel and used as a negative control. **(B) Inhibitory function of ABR using HEK-Blue IL22 reporter cells.** SEAP reporter secretion was induced by 3 ng/ml hIL-22 and measured at 620 nm. Blue rhombs and black circles joined by a dotted line on the graph represent the absorbance in the absence and presence of varying ABR concentrations, respectively. Background absorbance in the absence of both human IL-22 and ABR variants was subtracted from all values depicted on the graphs. **(C) Binding of ABR proteins to IL-22R1-transfected HEK293T cells and HaCaT cells using Ligand Tracer Green.** Representative binding curves from Ligand Tracer measurements are shown for variants ABR089, ABR099, and ABR167. For ABR089 and ABR099, binding of the proteins to the IL-22R1 expressed on transfected HEK293T cells was also measured for C/S proteins.

3.7. Prediction of binding modes by molecular modeling

To understand the details of interaction between the human IL-22R1 and ABR proteins we prepared *in silico* models of IL-22R1/ABR complexes. Docking results are summarized in Figure 5 showing the three most probable predicted binding modes of ABR proteins to human IL-22R1 in decreasing predicted order of binding in red, orange, and yellow colors. The structure of the IL-22/IL-22R1 complex (pdb id 3dlq) is shown for comparison (Fig. 5A). The docking results for ABR167 (Fig. 5B), ABR089 (Fig. 5D), and ABR099 (Fig. 5F) suggest that their most probable binding modes overlap with the position occupied by the IL-22 cytokine in the experimental structure of the IL-22/IL-22R1 complex. This observation is consistent with the efficient inhibitory action of ABR167 and ABR089 variants as well as a slightly less efficient ABR099 action that could be attributed to its smaller overlap with the IL-22 binding site.

The ABR089 and ABR099 variants contain a Cysteine residue in their sequences, and this can potentially complicate production and stability of these variants. We have thus prepared models with Serine substitutions. The docking results for the ABR089S (Fig. 5C) predict that the

most probable binding site does not overlap with the IL-22 and this variant no longer competes with IL-22 binding also experimentally. On the other hand, the results for the ABR099S variant (Fig. 5E) suggest an improved overlap with the IL-22 binding site. The atomic coordinates of the models are available in a PyMOL session on zenodo (10.5281/zenodo.10418004).

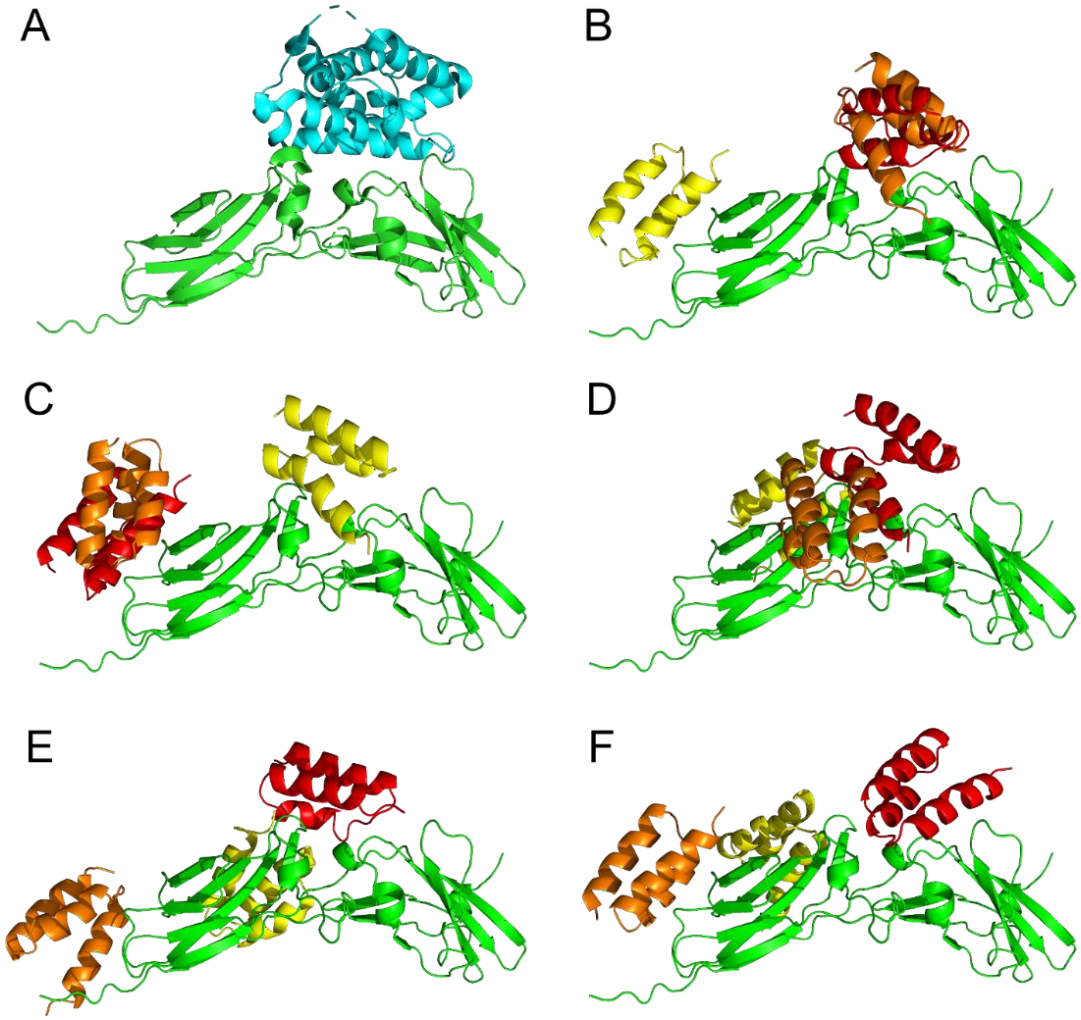

Fig. 5. Prediction of most probable binding modes of ABR proteins to human IL-22R1. (A) The structure of the IL-22/IL-22R1 complex (pdb id 3dlq). The IL-22R1 is shown in green, the IL-22 in cyan. **(B-F)** Summary of ABR variants docking to the structure of the IL-22R1, the IL-22R1 is shown in green and the ABR variants in decreasing predicted order of binding as red, orange, and yellow cartoon; **(B)** shows results for ABR167, **(C)** for ABR089S, **(D)** for ABR089, **(E)** for ABR099S, and **(F)** shows the ABR099/IL-22R1 complex (doi 10.5281/zenodo.10418004).

3.8. Analysis of ABR protein-mediated IL-22R1 blocking function in murine model of experimentally induced colitis

Based on tested signaling inhibitory effect of ABR variants (Fig. 4B), we selected ABR167, as one of most promising, for in vivo testing in murine model of colitis induced by 2.5% DSS provided in drinking water.

Time schedule of the experiment is shown on Figure 6A and is summarized in methods. At time of experiment termination, the length of colon was measured. Compared to DSS-drinking (positive control) mice, administration of ABR167 significantly protected from shortening the length of the colon induced by DSS. In naïve mice the colon length was 8.4 ± 0.8 cm, in DSS drinking mice the length was 6.4 ± 0.9 cm and ABR167 treated mice exhibit mean length 7.9 ± 1.2 cm (Fig. 6B). The histology of terminal part of the colon was assessed on H&E-stained microscopic sections according to classification reported by Erben et al. [54]. The mean score for inflammatory infiltrate (assessed as leukocyte density in the lamina propria and deeper layers), epithelial changes (assessed as an increase in the number of epithelial cells in the longitudinal crypts relative to baseline and a decrease in Goblet cells, cryptitis) and mucosal architecture (assessed as epithelial defects, irregular presence of crypts, loss of crypts and blunting of villi) was calculated for each group (Fig. 6C). Detail classification of individual mice histology is presented in Table S5. Representative H&E pictures are shown in Figure 7. ABR167-treated DSS-exposed mice exhibited significant reduction of gut histology alterations when compared to DSS-exposed control mice based on assessment of epithelial changes, inflammatory infiltrate, and mucosal architecture deterioration (Fig. 6C). Furthermore, the colon tissue samples were analyzed for the changes in the local expression of selected pro/anti-inflammatory markers (IL-1β, IL-6, IL-10, IL-17A, IL-22, and TNFα) by detecting their mRNA transcript levels using qRT-PCR. DSS-exposure induced significantly enhanced level of IL-22 transcript (Fig. 6D), which was not statistically reduced by ABR167 treatment although trend in IL-22 decrease in ABR167 treated mice correspond with less pronounced colon tissue deterioration (Fig. 6C). Among all other tested markers (Fig. 6E), IL-1β, IL-6, IL-10, IL-17A, and TNFα, mRNA transcript levels were increased although, due to inter-individual variability in tissue samples damage, the increase was achieving significance only for IL-1β and TNFα. The mRNAs expression in ABR167-treated DSS-exposed mice tend to shift toward

normal values in comparison to DSS-exposed, otherwise untreated mice (Fig. 6E). Even here the statistical significance was achieved for IL-1β, IL-6, IL-10, and IL-17A mRNA. We also tested systemic (serum) levels of cytokines corresponding to colon mRNA analyses (IL-1β, IL-6, IL-22, and TNFα) and other cytokines associated with systemic response (IL-4, IL-12p40, IL-18, and IL-23). After DSS-induced colitis we detected statistically significant increases in IL-22 and IL-18 concentration and insignificant but clearly visible trend in increase of IL-6 and IL-12p40 (Fig. S5).

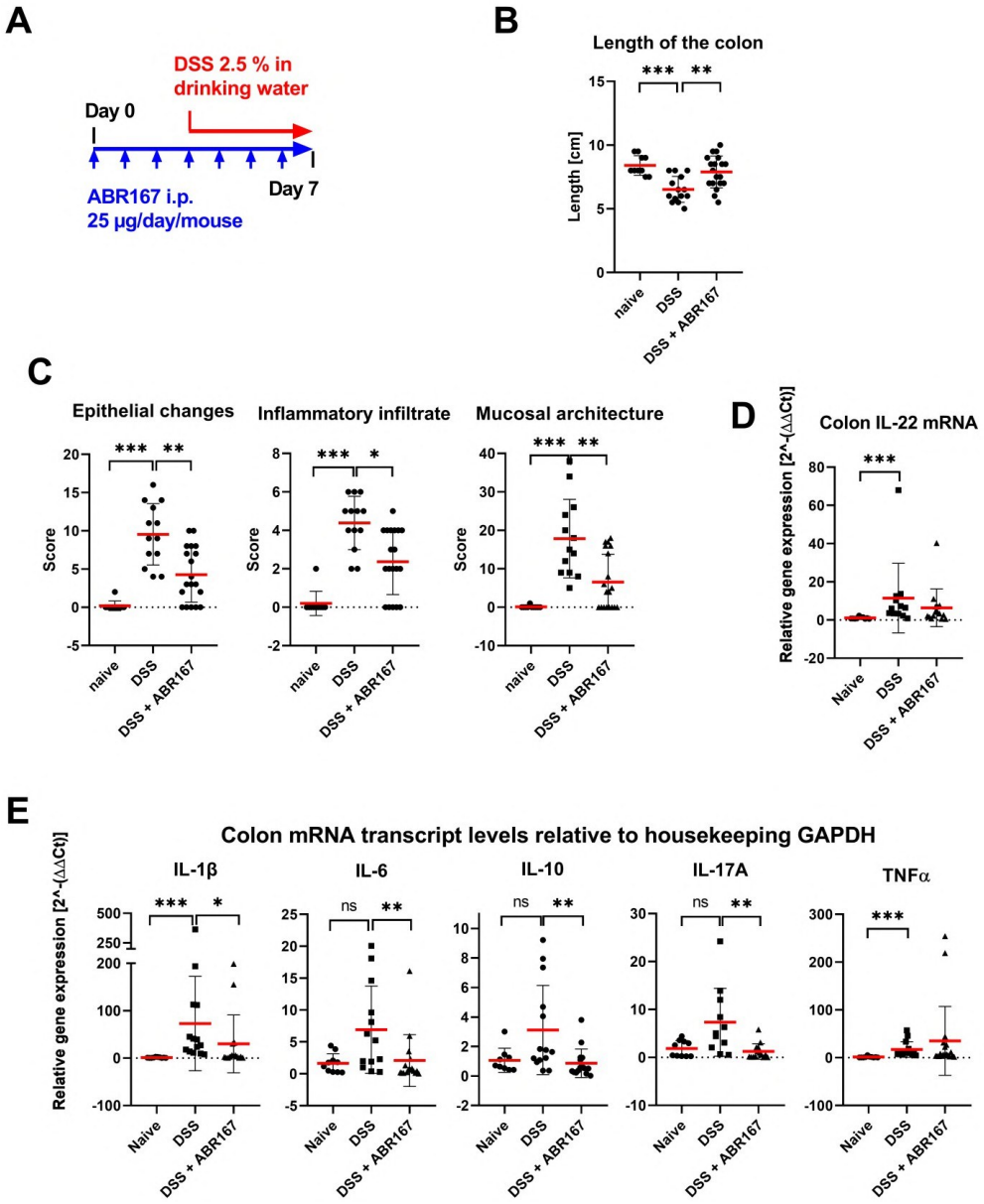

Fig. 6. The effect of ABR167 administration on DSS-induced colitis severity. (A) Scheme of the DSS experiment. **(B)** Comparison of colon length in individually treated groups of mice. ABR167 protects colon against shortening caused by DSS exposure. **(C)** Histological assessment of colon tissues of naïve, DSS-

exposed, and ABR167-treated DSS-exposed mice according to Erben et al. [54]. ABR167 significantly reduces inflammatory infiltrate, epithelial changes, and mucosal architecture according to classification specified in Materials and Methods. **(D)** Gene expression of IL-22 and **(E)** IL-1β, IL-6, IL-10, IL-17A, and TNFα determined by qRT-PCR. Statistical differences were analyzed by Kruskal-Wallis one-way ANOVA followed by Dunn´s multiple comparisons test. Means +/- SD are shown. *P<0.05, **P<0.01, ***P<0.001.

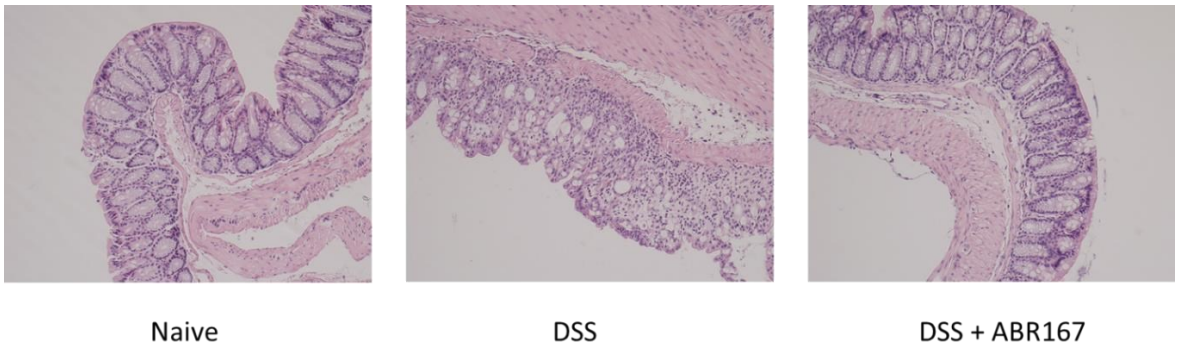

Fig. 7. Representative examples of tissues dissected from colon. Naive – normal colon histology, normal structure of intestinal mucosa with preserved crypts, no active inflammation is present. DSS – erosion of intestinal mucosa with marked crypt loss, crypt hyperplasia and crypt irregularities, nonspecific granulation tissue formation with active inflammation. DSS + ABR167 – colon histology without marks of mucosal damage and without active inflammation.

4. Discussion

Many cytokines exhibit pleiotropic effects, which could be positive or negative, depending on the biological environment [55, 56]. Thus, cytokines are strictly regulated through the host production of a cytokine-binding protein that docks or prevents interaction with cognate cellular receptors, permitting the site-specific regulation of their functions [57]. Although the pleiotropic nature of cytokines is essential for encouraging redundancy and feedback into immune responses, it is also a significant barrier to their use as therapeutic agents [58]. Although the combination of IL-22R1 and IL-10R2 subunits specifically mediates signaling by IL-22, both receptor subunits can be used by other cytokines such as IL-10, IL-26, IL-28 and IL-29 and IL-22R1 subunit also by IL-20 and IL-24 [59-61]. The receptor complex IL-22R1–IL-20R2, therefore, seems to mediate signaling events and effects that are very similar to those mediated by the IL-22R complex [14].

In presented experiments, binding of ABR variants to cell surface IL-22R1 was tested using HEK293 transiently transfected with human IL-22R1 by fluorescent microscopy and HEK-Blue IL22 reporter cell line stably transfected with IL-22R1 in flow cytometry experiments. HaCaT cells endogenously express IL-22R1 upon TNFα and IFNγ stimulation and were here used as induction-control. No IL-22R1 was detected for un-stimulated HaCaT cells, while stimulation with TNFα and IFNγ induced strong expression of IL-22R1 in 30-50% of cells (Fig. S2). Furthermore, HaCaT cells stimulated with TNFα and IFNγ were used to detect ABR variants binding to induced endogenously expressed IL-22R1. Seven ABR variants (ABR006, ABD023, ABD027, ABR089, ABR099, ABR102, and ABD167) exhibited binding to IL-22R1 transfectants (Fig. S2). Double staining carried out with ABR variants and anti-IL-22R1 antibody demonstrated that all ABR variants were able to recognize IL-22R1 on the surface of HaCaT cells with very similar binding patterns to anti-IL-22 antibody. This data indicates that ABR proteins specifically recognize cell surface expressed IL-22R1. Among all tested variants, ABR099 and ABR167 demonstrated the strongest binding and variant ABR167 was selected as a candidate for testing in murine model of ulcerative colitis.

Ulcerative colitis (UC) is a non-specific inflammatory bowel disease (IBD) resulting from a complex interplay between environmental, microbial, and genetic factors, leading to abnormal immunological response with intestinal inflammation. DSS is a water-soluble, negatively charged sulfated polysaccharide of which 40-50 kDa fraction is able to induce colitis in C57BL/6 mice, closely resembling human UC [62]. DSS-colitis represents an acute murine model of colitis in which cytokines of IL-17, IL-23, and IL-22 group are involved [63-65]. IL-17F deficiency resulted in reduced pathology of DSS-induced colitis in mice, whereas IL-17A deficiency was associated with more severe disease [64]. Both cytokines have a redundant but unequal pathogenic role in gut inflammation and balanced inhibition of IL-17A and IL-17F represents promising goal for therapy development in chronic colitis [66]. The IL-23 has emerged as another crucial cytokine and promising therapeutic target in IBD. IL-23 is a heterodimeric cytokine comprised of IL-23p19 and IL-12p40 [67]. In DSS-induced colitis IL-23R signaling by mature lymphocytes reduced pathology but in the absence of lymphocytes IL-23 signaling promotes pathology [63], indicating dichotomy in the function of the IL-23 pathway in adaptive versus innate immune compartments [63, 68]. In

innate (lymphocyte independent) colitis model, IL-23R-related pathology was associated with IL-22 signaling, as neutralization of IL-22 exhibited protectivity [68]. The depletion of innate lymphoid cells nILC2, ILC1, ILC3 eliminated the majority of IL-22 production in the colon lamina propria of DSS-treated $Rag2^{-/-}$ mice indicating that nILC2, ILC1, ILC3 are the major IL-23 responsive innate cells in this model [69, 70], although others have also reported IL-23-dependent IL-22 production by neutrophils [71, 72]. In the present project, we tested the effect of selected IL-22R1 blocker ABR167 as a representative of the most promising candidates, based on their antagonistic activity on IL-22R1-mediated signaling tested on HEK-Blue IL22 reporter cells (Fig. 4B). Here we used oral DSS administration-induced colitis in C57BL/6 mice and showed that intraperitoneal administration of ABR167 (Fig. 6A) could significantly reduce subsequent colitis development as detected by colon length and colon histology (Fig. 6B,C). In tissue samples of colon from DSS-exposed control mice, an increased IL-22 mRNA transcript was confirmed (Fig. 6D) which justifies the usage of ABR167 for IL-22R1 targeting, although we are aware of limitations due to the pleithropy and promiscuity of cytokine to cytokine receptor interaction [14, 59-61]. In treated mice, the increase in IL-22 production was less pronounced which, in accordance with only modest signs of histology inflammation in ABR167-treated mice, indicates a weaker activation of IL-22 producing cells in an affected colon. In accordance, colon production of other pro/anti-inflammatory markers, such as IL-1β, IL-6, and IL-17A or IL-10, was reduced in ABR167-treated mice compared to control DSS-exposed mice (Fig. 6E). Although significantly, TNFα transcript increase was very modest after DSS and the effect of ABR167 treatment on TNFα expression was not significant, which could be linked to used DSS model properties with only moderate level of induced colitis due to experimental protocol setup (only 4 days of 2.5% DSS exposure), which we opted in presented study to detect even moderate improvement in colitis after ABR167 treatment. As we expected, an increase in the systemic (serum) levels of pro-inflammatory cytokines (IL-6, IL-22, IL-12p40, and IL-18) was, therefore, only moderate (Fig. S5). Based on these results, it seems to be reasonable to design further colitis-inducing experiments with an extended duration in combination with other triggering agents such as 2, 4, 6-trinitrobenzenesulfonic acid (TNBS). Such ABR blockers-based strategy can be used as a proof-of-concept for future colitis-modifying drug development.

While ABR167 protein is free of Cysteine residues, ABR089 and ABR099 variants contain Cysteine in the randomized position. This leads to the formation of dimers that could, in particular cases, sterically restrict the accessibility of ABR to the binding site on IL-22R1 and, thus, affect the affinity and blocking potential. Therefore, we used *in silico* modeling to predict, and experimentally verify, function of the Cysteine-substituted ABR variants. Our *in silico* modeling and docking studies provide valuable insights into the binding interactions between human IL-22R1 and ABR proteins. These findings not only shed light on the structural aspects of this interaction but also highlight the potential significance of amino acid substitutions, such as Serine substitutions, in modulating the binding behavior of ABR variants. Analysis of the crystal structure of the IL-22/IL-22R1 complex (PDB ID 3dlq, Fig. 5A) revealed a tight interaction between W208 residue of the IL-22R1 and M172 of the IL-22. A nearly identical interaction is reproduced in the model of the ABR099S variant where the M37 residue interacts with the W208 of the IL-22R1. This interaction was not formed before the C/S substitution and the ABR099S thus successfully combines favorable interactions with removing the unwanted tendency for oligomerization of the initial Cysteine variant ABR099. On the other hand, the Cysteine residue in the ABR089 plays a similar role as the Methionine and is involved in a direct interaction with the W208 of the receptor. This can explain the loss of activity after the C/S substitution and although the ABR089 variant has a potential for oligomerization the initial sequence should be used. Further experimental investigations are warranted to validate and extend these computational findings, ultimately advancing our understanding of the biological implications of these interactions. *In silico* modeling thus opens window for the identification of sequentially improved candidates for future *in vivo* testing.

5. Conclusion

In summary, we report here on the generation of unique small binding proteins that might function as human IL-22R1 antagonists with therapeutic potential. These can be useful as a molecular clue for designing novel IL-22R1-targeted therapies. Our results further ascertain the importance of IL-22 signaling axis in the gut inflammation. As ABD-derived blockers can be effectively produced in genetically engineered *L. lactis* probiotic strains, it offers a promising

avenue for orally administrated IL-22R1-targeted therapy for gut inflammatory conditions such as ulcerative colitis.

DECLARATION STATEMENT

Ethics approval and consent to participate

All animal experiment protocols were approved by Ethics Committee of the Faculty of Medicine and Dentistry (Palacky University Olomouc, Czech Republic), and the Ministry of Education, Youth and Sports, Czech Republic (MSMT-10947/2021-3).

Consent for publication

Not applicable.

Availability of data and materials

All data generated or analyzed during this study are included in this article and its Supplementary Information/Source Data file. Source data are (will be) provided with this paper. The coordinates from ClusPro protein-protein docking and PyMOL session summarizing the results are available from the zenodo repository (doi 10.5281/zenodo.10418004).

Competing interests

The authors declare that they have no competing interests.

Funding

The authors are thankful for the received support by the Czech Science Foundation by the grant LA CEUS No. 21-16423K and for the received support from the Institute of Biotechnology of the Czech Academy of Sciences v.v.i. (Institutional Research Concept, RVO: 86652036).

Authors' contributions

M.K. assembled ABD combinatorial library. M.K. and M.H. performed large scale screening and biochemical analysis of protein variants. Y.G. and J.M.M. performed functional tests and kinetics assessment on cell lines. R.O. performed flow cytometry with ABR binders and analyzed data. J.Č. performed in silico analysis of ABR proteins. P.K., K.S., S.W., J.S., L.R.K. and M.R. performed analysis in murine model of colitis. H.P. and S.B. performed data analysis and wrote the paper. P.M. and M.R. conceptualized the project, designed research, directed research, analyzed data, and wrote the paper.

Acknowledgements

The authors are thankful to Linda Malá and Petra Kadlčáková for excellent experimental assistance. The authors acknowledge CF (CF Biophysic, CF Cryst, CF Diff of CIISB, Instruct-CZ Centre, supported by MEYS CR (LM2023042)) and European Regional Development Fund-Project "UP CIISB" (No. CZ.02.1.01/0.0/0.0/18_046/0015974).

References

1. Dudakov JA, Hanash AM, van den Brink MR: **Interleukin-22: immunobiology and pathology**. *Annu Rev Immunol* 2015, **33**:747-785.
2. Sonnenberg GF, Fouser LA, Artis D: **Border patrol: regulation of immunity, inflammation and tissue homeostasis at barrier surfaces by IL-22**. *Nat Immunol* 2011, **12**(5):383-390.
3. Xie MH, Aggarwal S, Ho WH, Foster J, Zhang ZM, Stinson J, Wood WI, Goddard AD, Gurney AL: **Interleukin (IL)-22, a novel human cytokine that signals through the interferon receptor-related proteins CRF2-4 and IL-22R**. *J Biol Chem* 2000, **275**(40):31335-31339.
4. Keir M, Yi Y, Lu T, Ghilardi N: **The role of IL-22 in intestinal health and disease**. *J Exp Med* 2020, **217**(3):e20192195.
5. Ouyang WJ, O'Garra A: **IL-10 Family Cytokines IL-10 and IL-22: from Basic Science to Clinical Translation**. *Immunity* 2019, **50**(4):871-891.
6. Dudakov JA, Hanash AM, van den Brink MRM: **Interleukin-22: Immunobiology and Pathology**. *Annual Review of Immunology Vol 33* 2015, **33**:747-785.
7. Logsdon NJ, Jones BC, Josephson K, Cook J, Walter MR: **Comparison of interleukin-22 and interleukin-10 soluble receptor complexes**. *J Interf Cytok Res* 2002, **22**(11):1099-1112.
8. Jones BC, Logsdon NJ, Walter MR: **Structure of IL-22 bound to its high-affinity IL-22R1 chain**. *Structure* 2008, **16**(9):1333-1344.
9. Li J, Tomkinson KN, Tan XY, Wu P, Yan G, Spaulding V, Deng BJ, Annis-Freeman B, Heveron K, Zollner R *et al*: **Temporal associations between interleukin 22 and the extracellular domains of IL-22R and IL-10R2**. *Int Immunopharmacol* 2004, **4**(5):693-708.
10. Bleicher L, de Moura PR, Watanabe L, Colau D, Dumoutier L, Renauld JC, Polikarpov I: **Crystal structure of the IL-22/IL-22R1 complex and its implications for the IL-22 signaling mechanism**. *FEBS Lett* 2008, **582**(20):2985-2992.
11. Kempski J, Giannou AD, Riecken K, Zhao L, Steglich B, Lucke J, Garcia-Perez L, Karstens KF, Wostemeier A, Nawrocki M *et al*: **IL22BP Mediates the Antitumor Effects of Lymphotoxin Against Colorectal Tumors in Mice and Humans** . *Gastroenterology* 2020, **159**(4):1417-1430 e1413.
12. Kotenko SV, Izotova LS, Mirochnitchenko OV, Esterova E, Dickensheets H, Donnelly RP, Pestka S: **Identification, cloning, and characterization of a novel soluble receptor that binds IL-22 and neutralizes its activity**. *J Immunol* 2001, **166**(12):7096-7103.
13. Wolk K, Kunz S, Witte E, Friedrich M, Asadullah K, Sabat R: **IL-22 increases the innate immunity of tissues**. *Immunity* 2004, **21**(2):241-254.
14. Sabat R, Ouyang W, Wolk K: **Therapeutic opportunities of the IL-22-IL-22R1 system**. *Nat Rev Drug Discov* 2014, **13**(1):21-38.

15. Zhang N, Pan HF, Ye DQ: **Th22 in inflammatory and autoimmune disease: prospects for therapeutic intervention** . *Mol Cell Biochem* 2011, **353**(1-2):41-46.
16. Sonnenberg GF, Fouser LA, Artis D: **Border patrol: regulation of immunity, inflammation and tissue homeostasis at barrier surfaces by IL-22**. *Nat Immunol* 2011, **12**(5):383-390.
17. Eyerich K, Dimartino V, Cavani A: **IL-17 and IL-22 in immunity: Driving protection and pathology**. *Eur J Immunol* 2017, **47**(4):607-614.
18. Mizoguchi A, Yano A, Himuro H, Ezaki Y, Sadanaga T, Mizoguchi E: **Clinical importance of IL-22 cascade in IBD**. *J Gastroenterol* 2018, **53**(4):465-474.
19. Lindemans CA, Calafiore M, Mertelsmann AM, O'Connor MH, Dudakov JA, Jenq RR, Velardi E, Young LF, Smith OM, Lawrence G *et al*: **Interleukin-22 promotes intestinal-stem-cell-mediated epithelial regeneration** . *Nature* 2015, **528**(7583):560-564.
20. Geng H, Bu HF, Liu FY, Wu LT, Pfeifer K, Chou PM, Wang X, Sun JR, Lu L, Pandey A *et al*: **In Inflamed Intestinal Tissues and Epithelial Cells, Interleukin 22 Signaling Increases Expression of H19 Long Noncoding RNA, Which Promotes Mucosal Regeneration**. *Gastroenterology* 2018, **155**(1):144-155.
21. Pennino D, Eyerich K, Scarponi C, Carbone T, Eyerich S, Nasorri F, Garcovich S, Traidl-Hoffmann C, Albanesi C, Cavani A: **IL-17 amplifies human contact hypersensitivity by licensing hapten nonspecific Th1 cells to kill autologous keratinocytes**. *J Immunol* 2010, **184**(9):4880-4888.
22. Zenewicz LA, Yancopoulos GD, Valenzuela DM, Murphy AJ, Stevens S, Flavell RA: **Innate and adaptive interleukin-22 protects mice from inflammatory bowel disease**. *Immunity* 2008, **29**(6):947-957.
23. Radaeva S, Sun R, Pan HN, Hong F, Gao B: **Interleukin 22 (IL-22) plays a protective role in T cell-mediated murine hepatitis: IL-22 is a survival factor for hepatocytes via STAT3 activation**. *Hepatology* 2004, **39**(5):1332-1342.
24. Ito T, Hirose K, Saku A, Kono K, Takatori H, Tamachi T, Goto Y, Renauld JC, Kiyono H, Nakajima H: **IL-22 induces Reg3gamma and inhibits allergic inflammation in house dust mite-induced asthma models**. *J Exp Med* 2017, **214**(10):3037-3050.
25. Bernshtein B, Curato C, Ioannou M, Thaiss CA, Gross-Vered M, Kolesnikov M, Wang Q, David E, Chappell-Maor L, Harmelin A *et al*: **IL-23-producing IL-10Ralpha-deficient gut macrophages elicit an IL-22-driven proinflammatory epithelial cell response**. *Sci Immunol* 2019, **4**(36).
26. Fujita H: **The role of IL-22 and Th22 cells in human skin diseases** . *J Dermatol Sci* 2013, **72**(1):3-8.
27. Gunasekera DC, Ma JX, Vacharathit V, Shah P, Ramakrishnan A, Uprety P, Shen ZL, Sheh A, Brayton CF, Whary MT *et al*: **The development of colitis in Il10(-/-) mice is dependent on IL-22**. *Mucosal Immunol* 2020, **13**(3):493-506.
28. Hwang S, Hicks A, Hoo CZ, Kwon YS, Cho YE, Moore J, Gao B: **Novel treatment of acute and acute-on-chronic liver failure: Interleukin-22**. *Liver Int* 2023.

29. Stefanich EG, Rae J, Sukumaran S, Lutman J, Lekkerkerker A, Ouyang W, Wang X, Lee D, Danilenko DM, Diehl L *et al*: **Pre-clinical and translational pharmacology of a human interleukin-22 IgG fusion protein for potential treatment of infectious or inflammatory diseases** . *Biochem Pharmacol* 2018, **152**:224-235.
30. Tang KY, Lickliter J, Huang ZH, Xian ZS, Chen HY, Huang C, Xiao C, Wang YP, Tan Y, Xu LF *et al*: **Safety, pharmacokinetics, and biomarkers of F-652, a recombinant human interleukin-22 dimer, in healthy subjects**. *Cell Mol Immunol* 2019, **16**(5):473-482.
31. Lekkerkerker A, Harder B, Kulkarni P, Zhao R, Choi M, Noyes A, Polihrom A, Fillos D, Rae J, Danilenko D *et al*: **Pharmacodynamic biomarkers demonstrate dose-dependent pharmacological activity of the IL-22Fc fusion protein UTR1147A in healthy volunteers in a phase 1a clinical trial** . *J Crohns Colitis* 2017, **11**:S289-S289.
32. Wagner F, Mansfield JC, Lekkerkerker AN, Wang YH, Keir M, Dash A, Butcher B, Harder B, Orozco LD, Mar JS *et al*: **Dose escalation randomised study of efmarodocokin alfa in healthy volunteers and patients with ulcerative colitis**. *Gut* 2023, **72**(8):1451-1461.
33. Tang KY, Lickliter J, Huang ZH, Xian ZS, Chen HY, Huang C, Xiao C, Wang YP, Tan Y, Xu LF *et al*: **Safety, pharmacokinetics, and biomarkers of F-652, a recombinant human interleukin-22 dimer, in healthy subjects**. *Cellular & Molecular Immunology* 2019, **16**(5):473-482.
34. Ponce DM, Alousi AM, Nakamura R, Sandhu KS, Barker JN, Shia J, Yan XQ, Daley WL, Moore G, Fatmi S *et al*: **A Phase 2 Study of F-652, a Novel Tissue-Targeted Recombinant Human Interleukin-22 (IL-22) Dimer, for Treatment of Newly Diagnosed Acute Gvhd of the Lower GI Tract** . *Biol Blood Marrow Tr* 2020, **26**(3):S51-S52.
35. Guttman-Yassky E, Brunner PM, Neumann AU, Khattri S, Pavel AB, Malik K, Singer GK, Baum D, Gilleaudeau P, Sullivan-Whalen M *et al*: **Efficacy and safety of fezakinumab (an IL-22 monoclonal antibody) in adults with moderate-to-severe atopic dermatitis inadequately controlled by conventional treatments: A randomized, double-blind, phase 2a trial**. *J Am Acad Dermatol* 2018, **78**(5):872-881 e876.
36. Lin Y, Krogh-Andersen K, Hammarstrom L, Marcotte H: **Lactobacillus delivery of bioactive interleukin-22**. *Microb Cell Fact* 2017, **16**(1):148.
37. Krízová L, Kuchar M, Petroková H, Osicka R, Hlavnicková M, Pelák O, Cerny J, Kalina T, Maly P: **p19-targeted ABD-derived protein variants inhibit IL-23 binding and exert suppressive control over IL-23-stimulated expansion of primary human IL-17+T-cells**. *Autoimmunity* 2017, **50**(2):102-113.
38. Kuchar M, Vanková L, Petroková H, Cerny J, Osicka R, Pelák O, Sípová H, Schneider B, Homola J, Sebo P *et al*: **Human interleukin-23 receptor antagonists derived from an albumin-binding domain scaffold inhibit IL-23-dependent expansion of IL-17-producing T-cells**. *Proteins* 2014, **82**(6):975-989.

39. Hlavnicková M, Kuchar M, Osicka R, Vanková L, Petroková H, Maly M, Cerny J, Arenberger P, Maly P: **ABD-Derived Protein Blockers of Human IL-17 Receptor A as Non-IgG Alternatives for Modulation of IL-17-Dependent Pro-Inflammatory Axis**. *Int J Mol Sci* 2018, **19**(10).
40. Smejkal J, Maly P, Kuchar M, Panova N, Semerádtová A, Aubrecht P, Stofik M, Maly J: **Cell immunocapture microfluidic chip based on high-affinity recombinant protein binders**. *Biosens Bioelectron* 2021, **172**.
41. Ahmad JN, Li JJ, Biedermannova L, Kuchar M, Sipova H, Semeradtova A, Cerny J, Petrokova H, Mikulecky P, Polinek J *et al*: **Novel high-affinity binders of human interferon gamma derived from albumin-binding domain of protein G**. *Proteins* 2012, **80**(3):774-789.
42. Kuchar M, Vankova L, Petrokova H, Cerny J, Osicka R, Pelak O, Sipova H, Schneider B, Homola J, Sebo P *et al*: **Human interleukin-23 receptor antagonists derived from an albumin-binding domain scaffold inhibit IL-23-dependent ex vivo expansion of IL-17-producing T-cells**. *Proteins* 2014, **82**(6):975-989.
43. Hlavnickova M, Kuchar M, Osicka R, Vankova L, Petrokova H, Maly M, Cerny J, Arenberger P, Maly P: **ABD-Derived Protein Blockers of Human IL-17 Receptor A as Non-IgG Alternatives for Modulation of IL-17-Dependent Pro-Inflammatory Axis**. *Int J Mol Sci* 2018, **19**(10).
44. Krizova L, Kuchar M, Petrokova H, Osicka R, Hlavnickova M, Pelak O, Cerny J, Kalina T, Maly P: **p19-targeted ABD-derived protein variants inhibit IL-23 binding and exert suppressive control over IL-23-stimulated expansion of primary human IL-17+T-cells**. *Autoimmunity* 2017, **50**(2):102-113.
45. Jang M, Kim H, Kim Y, Choi J, Jeon J, Hwang Y, Kang JS, Lee WJ: **The crucial role of IL-22 and its receptor in thymus and activation regulated chemokine production and T-cell migration by house dust mite extract** . *Exp Dermatol* 2016, **25**(8):598-603.
46. Sali A, Blundell TL: **Comparative Protein Modeling by Satisfaction of Spatial Restraints**. *J Mol Biol* 1993, **234**(3):779-815.
47. Johansson MU, Frick IM, Nilsson H, Kraulis PJ, Hober S, Jonasson P, Linhult M, Nygren PA, Uhlen M, Bjorck L *et al*: **Structure, specificity, and mode of interaction for bacterial albumin-binding modules**. *J Biol Chem* 2002, **277**(10):8114-8120.
48. Bleicher L, de Moura PR, Watanabe L, Colau D, Dumoutier L, Renauld JC, Polikarpov I: **Crystal structure of the IL-22/IL-22R1 complex and its implications for the IL-22 signaling mechanism**. *Febs Lett* 2008, **582**(20):2985-2992.
49. Kozakov D, Beglov D, Bohnuud T, Mottarella SE, Xia B, Hall DR, Vajda S: **How good is automated protein docking?** *Proteins* 2013, **81**(12):2159-2166.
50. Kozakov D, Brenke R, Comeau SR, Vajda S: **PIPER: An FFT-based protein docking program with pairwise potentials**. *Proteins* 2006, **65**(2):392-406.
51. UniProt C: **UniProt: a worldwide hub of protein knowledge**. *Nucleic Acids Res* 2019, **47**(D1):D506-D515.

52. Juritsch AF, Moreau R: **Rapid removal of dextran sulfate sodium from tissue RNA preparations for measurement of inflammation biomarkers** . *Anal Biochem* 2019, **579**:18-24.
53. Livak KJ, Schmittgen TD: **Analysis of relative gene expression data using real-time quantitative PCR and the 2(-Delta Delta C(T)) Method**. *Methods* 2001, **25**(4):402-408.
54. Erben U, Loddenkemper C, Doerfel K, Spieckermann S, Haller D , Heimesaat MM, Zeitz M, Siegmund B, Kühl AA: **A guide to histomorphological evaluation of intestinal inflammation in mouse models** . *Int J Clin Exp Patho* 2014, **7**(8):4557-U4527.
55. Lin JX, Leonard WJ: **Fine-Tuning Cytokine Signals**. *Annu Rev Immunol* 2019, **37**:295-324.
56. Wang X, Lupardus P, Laporte SL, Garcia KC: **Structural biology of shared cytokine receptors**. *Annu Rev Immunol* 2009, **27**:29-60.
57. Zenewicz LA: **IL-22 Binding Protein (IL-22BP) in the Regulation of IL-22 Biology**. *Front Immunol* 2021, **12**.
58. Saxton RA, Henneberg LT, Calafiore M, Su L, Jude KM, Hanash AM, Garcia KC: **The tissue protective functions of interleukin-22 can be decoupled from pro-inflammatory actions through structure-based design**. *Immunity* 2021, **54**(4):660-+.
59. Sabat R: **IL-10 family of cytokines**. *Cytokine Growth Factor Rev* 2010, **21**(5):315-324.
60. Dumoutier L, Leemans C, Lejeune D, Kotenko SV, Renauld JC: **Cutting edge: STAT activation by IL-19, IL-20 and mda-7 through IL-20 receptor complexes of two types**. *J Immunol* 2001, **167**(7):3545-3549.
61. Wang M, Tan Z, Zhang R, Kotenko SV, Liang P: **Interleukin 24 (MDA-7/MOB-5) signals through two heterodimeric receptors, IL-22R1/IL-20R2 and IL-20R1/IL-20R2**. *J Biol Chem* 2002, **277**(9):7341-7347.
62. Okayasu I, Hatakeyama S, Yamada M, Ohkusa T, Inagaki Y, Nakaya R: **A novel method in the induction of reliable experimental acute and chronic ulcerative colitis in mice**. *Gastroenterology* 1990, **98**(3):694-702.
63. Cox JH, Kljavin NM, Ota N, Leonard J, Roose-Girma M, Diehl L, Ouyang W, Ghilardi N: **Opposing consequences of IL-23 signaling mediated by innate and adaptive cells in chemically induced colitis in mice** . *Mucosal Immunol* 2012, **5**(1):99-109.
64. Yang XO, Seon HC, Park H, Nurieva R, Shah B, Acero L, Wang YH, Schluns KS, Broaddus RR, Zhu Z *et al*: **Regulation of inflammatory responses by IL-17F**. *Journal of Experimental Medicine* 2008, **205**(5):1063-1075.
65. Yan J, Yu J, Yuan SZ, Tang WQ, Ma W, Yang X, Liu YJ, Liang HP, Zhong XM, Shao J *et al*: **Musculin is highly enriched in Th17 and IL-22-producing ILC3s and restrains pro-inflammatory cytokines in murine colitis** . *European Journal of Immunology* 2021, **51**(4):995-998.
66. Leppkes M, Becker C, Ivanov, II, Hirth S, Wirtz S, Neufert C, Pouly S, Murphy AJ, Valenzuela DM, Yancopoulos GD *et al*: **RORgamma-expressing Th17 cells**

induce murine chronic intestinal inflammation via redundant effects of IL-17A and IL-17F. *Gastroenterology* 2009, **136**(1):257-267.

67. Oppmann B, Lesley R, Blom B, Timans JC, Xu YM, Hunte B, Vega F, Yu N, Wang J, Singh K *et al*: **Novel p19 protein engages IL-12p40 to form a cytokine, IL-23, with biological activities similar as well as distinct from IL-12**. *Immunity* 2000, **13**(5):715-725.
68. Eken A, Singh AK, Treuting PM, Oukka M: **IL-23R+ innate lymphoid cells induce colitis via interleukin-22-dependent mechanism**. *Mucosal Immunol* 2014, **7**(1):143-154.
69. Panda SK, Colonna M: **Innate Lymphoid Cells in Mucosal Immunity** . *Front Immunol* 2019, **10**.
70. Buonocore S, Ahern PP, Uhlig HH, Ivanov II, Littman DR, Maloy KJ, Powrie F: **Innate lymphoid cells drive interleukin-23-dependent innate intestinal pathology**. *Nature* 2010, **464**(7293):1371-1375.
71. Chen FD, Cao A, Yao SX, Evans-Marin HL, Liu H, Wu W, Carlsen ED, Dann SM, Soong L, Sun JR *et al*: **mTOR Mediates IL-23 Induction of Neutrophil IL-17 and IL-22 Production**. *J Immunol* 2016, **196**(10):4390-4399.
72. Zindl CL, Lai JF, Lee YK, Maynard CL, Harbour SN, Ouyang WJ, Chaplin DD, Weaver CT: **IL-22-producing neutrophils contribute to antimicrobial defense and restitution of colonic epithelial integrity during colitis** . *P Natl Acad Sci USA* 2013, **110**(31):12768-12773.

3.4. Small protein binders of PD-1-targeted for diagnostic purposes

Scientific outcomes:

Publication: Mierzwicka JM, Petroková H, Kafková LR, Kosztyu P, Černý J, Kuchař M, Petřík M, Bendová K, Krasulová K, Groza Y, Vaňková L, Bharadwaj S, Panova N, Křupka M, Škarda J, Raška M, Malý P. Engineering PD-1-targeted small protein variants for in vitro diagnostics and in vivo PET imaging. J Transl Med. 2024 May 6;22(1):426. DOI: 10.1186/s12967-024-05210-x. PMID: 38711085; PMCID: PMC11071268.

Background: PD-1 and its ligand PD-L1 are crucial immune checkpoint proteins that modulate immune responses by inhibiting T cell activity. Many cancers have adjusted to suppress immune response by exhaustion of T cell population by overexpression of PD-L1, which is upregulated due to genetic factors and tumor microenvironment. Both, IL-6 and IL-22 may contribute to PD-L1 expression [314, 315]. Elevated PD-1 is observed in exhausted $CD8^+$ tumor-infiltrating cells across various cancer types. Therefore, checkpoint therapy, including inhibitors targeting PD-1/PD-L1, has become a key strategy in cancer treatment. Combination with TCZ, anti-IL-6Rα mAb, even further improves outcomes of the ICB therapy [316]. However, patient responsiveness to the therapy is not universal. Therefore, diagnostic methods, especially those enhancing the detection and profiling of PD-1/PD-L1 expression, are essential for optimizing these therapies. In NSCLC, these checkpoint inhibition therapy has shown promise, though patient responses vary. The sensitivity to anti-PD-1 therapies and their efficacy largely correlates with an increase in $PD\text{-}1^+$ TILs. Due to the heterogeneity of $PD\text{-}1^+$ populations in solid tumors, novel low molecular weight, high-affinity anti-PD-1 diagnostic probes can enhance the reliability of $PD\text{-}1^+$ TILs expression profiling in tumor tissue biopsies and improve in vivo mapping efficiency using immune-PET imaging.

Methods: Highly complex Myomedin combinatorial library was engineered using a set of primers in multiple PCR reactions. To select binders of hPD-1, the library was put under the selection pressure in three-rounds of ribosome display. Plasmids of individual clones from the enriched library were isolated. Length of the cloned Myomedin variant gene was evaluated using analytical colony PCR. *E. coli* BL21 were transformed with the plasmids carrying in frame cloned Myomedin variant genes. Individual variants, named MBA, were tested in high-throughput ELISA screening. Binding and specificity of the most successful hits according to the screening were confirmed by dose-response binding ELISA. Binding of the MBA binders to cell-surface was evaluated by immunostaining of HEK293T cells transiently expressing hPD-1 receptor and human acute lymphoblastic lymphoma cells (SUP-T1) which express a

substantial level of PD-1 on their surface. Human B cells Dakiki, which do not express hPD-1, were used as a negative control. Affinity was measured using LigandTracer and microscale thermophoresis (MST). MBA variants were radiolabeled with ^{68}Galium isotope via DFO linker. The distribution of MBA was monitored using whole-body positron emission tomography combined with computerized tomography (PET/CT) imaging. *Ex vivo* immunohistochemical analysis of mouse organs was performed. Mouse muscle infection model in which lymphocyte homing is stimulated by a local intramuscular application of bacterial suspension was used to further test MBA binding. To prove the binding ability of MBA to PD-1$^+$ TILs in human tissue, human tonsil resected from a child with tonsillar hypertrophy and on a frozen NSCLC tissue section were used.

Results: We constructed Myomedin β-sheet library and evaluated library quality and random codon distribution. The theoretical complexity of the designed library is 2×10^{15} variants. To detect PD-1 binders, we carried out three rounds of ribosome display. A total of 378 individual colonies were screened using colony PCR, and 220 variants with the expected PCR product size were subsequently sequenced. Of them, 75 variants with required mutations solely in the randomized regions were used in ELISA screening. Binding curves for 25 MBA variants were built using binding ELISA. Eight MBA variants, which specifically recognize recombinant hPD-L1 (MBA003, MBA038, MBA052, MBA066, MBA197, MBA315, MBA323, and MBA414), were selected for further testing. All of them, except MBA038, bound to PD-L1 on a surface of transiently transfected HEK293T and SUP-1 cells. At the same time, none of them bound to PD-1$^-$ Dakki cell line, confirming specificity of the MBA variants. Affinity of the three most promising MBA variants (MBA066, MBA197 and MBA414) to human and mouse PD-1 was measured using LigandTracer and MST thermophoresis. All variants had affinity in nano-molar range with little difference between mouse and human version of the receptor. PET/CT imaging and postmortem organ evaluation demonstrated that unlike wild type Myomedin (MyoWT), MBA414 and MBA197 accumulated mostly in liver with a small clearance via excretion system. PD-1 expression on human tonsil and NSCLC tissue sections was detected using MBA414 variant and rabbit polyclonal anti-PD-1 antibody, where MBA414 was able to detect more PD-1$^+$ cells than commercial antibody.

Contribution: I contributed to the design and execution of the experiments, such as DNA cloning and competition ELISA. Also, I helped with DNA sequencing data analysis. During the manuscript preparation, I assisted with figure assembly and proofreading of the manuscript.

Mierzwicka *et al.*
Journal of Translational Medicine (2024) 22:426
https://doi.org/10.1186/s12967-024-05210-x

Journal of
Translational Medicine

RESEARCH Open Access

Engineering PD-1-targeted small protein variants for in vitro diagnostics and in vivo PET imaging

Joanna Maria Mierzwicka[1†], Hana Petroková[1†], Leona Rašková Kafková[2,3], Petr Kosztyu[2,3], Jiří Černý[4], Milan Kuchař[1], Miloš Petřík[5], Kateřina Bendová[5], Kristýna Krasulová[5], Yaroslava Groza[1], Lucie Vaňková[1], Shiv Bharadwaj[1], Natalya Panova[1], Michal Křupka[2,3], Jozef Škarda[2,3,6], Milan Raška[2,3*] and Petr Malý[1*]

Abstract

Background Programmed cell death 1 (PD-1) belongs to immune checkpoint proteins ensuring negative regulation of the immune response. In non-small cell lung cancer (NSCLC), the sensitivity to treatment with anti-PD-1 therapeutics, and its efficacy, mostly correlated with the increase of tumor infiltrating PD-1$^+$ lymphocytes. Due to solid tumor heterogeneity of PD-1$^+$ populations, novel low molecular weight anti-PD-1 high-affinity diagnostic probes can increase the reliability of expression profiling of PD-1$^+$ tumor infiltrating lymphocytes (TILs) in tumor tissue biopsies and in vivo mapping efficiency using immune-PET imaging.

Methods We designed a 13 kDa ß-sheet Myomedin scaffold combinatorial library by randomization of 12 mutable residues, and in combination with ribosome display, we identified anti-PD-1 Myomedin variants (MBA ligands) that specifically bound to human and murine PD-1-transfected HEK293T cells and human SUP-T1 cells spontaneously overexpressing cell surface PD-1.

Results Binding affinity to cell-surface expressed human and murine PD-1 on transfected HEK293T cells was measured by fluorescence with LigandTracer and resulted in the selection of most promising variants MBA066 (hPD-1 KD = 6.9 nM; mPD-1 KD = 40.5 nM), MBA197 (hPD-1 KD = 29.7 nM; mPD-1 KD = 21.4 nM) and MBA414 (hPD-1 KD = 8.6 nM; mPD-1 KD = 2.4 nM). The potential of MBA proteins for imaging of PD-1$^+$ populations in vivo was demonstrated using deferoxamine-conjugated MBA labeled with ^{68}Galium isotope. Radiochemical purity of ^{68}Ga-MBA proteins reached values 94.7-99.3% and in vitro stability in human serum after 120 min was in the range 94.6-98.2%. The distribution of ^{68}Ga-MBA proteins in mice was monitored using whole-body positron emission tomography combined with computerized tomography (PET/CT) imaging up to 90 min post-injection and *post mortem* examined in 12 mouse organs. The specificity of MBA proteins was proven by co-staining frozen sections of human tonsils and NSCLC tissue biopsies with anti-PD-1 antibody, and demonstrated their potential for mapping PD-1$^+$ populations in solid tumors.

†Joanna Maria Mierzwicka and Hana Petroková contributed equally.

*Correspondence:
Milan Raška
milan.raska@upol.cz
Petr Malý
petr.maly@ibt.cas.cz
Full list of author information is available at the end of the article

Conclusions Using directed evolution, we developed a unique set of small binding proteins that can improve PD-1 diagnostics in vitro as well as in vivo using PET/CT imaging.

Keywords Immune checkpoint, Programmed cell death 1, Non-small cell lung cancer, Cancer diagnostic, Combinatorial library, Protein engineering

Graphical Abstract

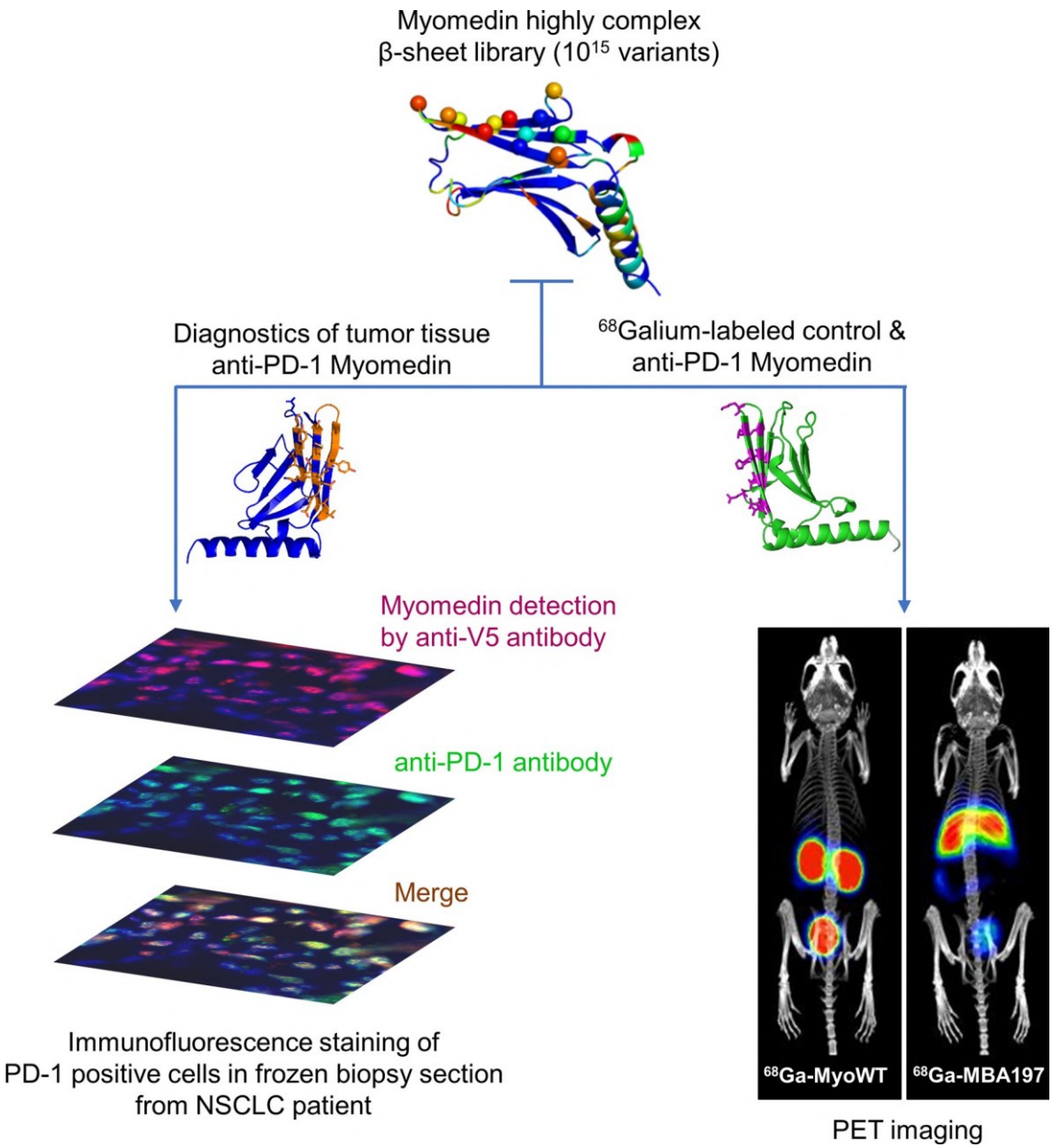

Introduction

Immune checkpoint molecules are cellular receptors that modulate the immunosuppressive signaling pathways. These molecules are essential for maintaining

autoimmune reactions and dampening the excessive activation of immune cells following combating the infection or other threats to minimize the collateral damages [1]. However, overexpression or overactivation of immune checkpoint receptors can cause inhibition or exhaustion of effector immune cells, especially T cells [2]. It is now clear that many cancers enhance immunosuppressive interactions of local immune cells to avoid immune surveillance and clearance, thus promoting cancer growth [1]. Accordingly, growing efforts to target these inhibitory receptors for gaining anticancer immunity have led to the clinical development and licensing of immune checkpoint inhibitors (ICIs) as the therapy for many types of cancer [3, 4].

PD-1 (B7-H1; also CD279) receptor is expressed on the surface of activated B cells, T cells, monocytes, natural killer cells, some myeloid cells and cancer cells [5, 6]. Under normal physiological conditions, upon docking with its ligands (PD-L1 and PD-L2), PD-1 on immune cells promotes a signaling cascade in maintaining the balance between self-tolerance and reactivity to extraneous signals [7]. However, in the context of malignancy, tumor and stromal PD-L1 expression poses a barrier to immune function by promoting the exhaustion of the antitumor T cell population that might otherwise contribute to tumor cells elimination [8]. For instance, high levels of PD-1 expression are detected during some chronic infections, and in exhausted tumor-infiltrating $CD8^+$ cells in many types of cancer [9]. Consequently, the PD-1/PD-L1 pathway has emerged as a critical target for monoclonal antibodies-based inhibitors development targeting PD-1/PD-L1 interaction. Such ICIs have demonstrated impressive activity against many cancers [10–15].

Recent clinical trials exploring the use of ICIs, including monoclonal antibodies, as antagonists of PD-1 or PD-L1 receptors have shown significant improvement in the survival rate of patients with advanced non-small-cell lung cancer (NSCLC) [16, 17]. However, the responses of cancer patients to ICIs vary in success and approximately 60% to 70% of patients' progress within 6 months after ICI therapy initiation [11, 18, 19]. In this context, a recent study illustrated that assessing the immune profile of tumor biopsies in the early course of ICI therapy was a better predictor of response than assessing pretreatment samples [20]. Thereof, unmet needs exist in predicting such responses with accurate biomarkers to maximize the efficacy and minimize the toxicity of ICIs, in particular, to identify patients that are less likely to benefit from ICI therapy [20].

In analogy to molecular biomarkers that have been used for the identification of patients with targetable oncogenes [21], it has been assumed that tumor-infiltrating T lymphocytes (TILs) as predictive biomarker for clinical benefit to PD-1 blockade in patients with advanced NSCLC [22–24]. In this context, pembrolizumab and nivolumab as anti-PD-1 checkpoint inhibitors have been reported to predict the prognostic significance of TILs in a variety of solid tumors, including NSCLC [24, 25]. However, antibodies have some drawbacks due to their large size, including slower clearance from the system [26] and lower penetrance into the solid tumors [27]. For example, PD-1–expressing effector T cells are found infiltrated within solid tissue of PD-L1–expressing tumors [8]. Therefore, antibodies may fail to exhibit penetration and substantial binding to PD-1–expressing T cells within solid tumors, such as NSCLC, which may be leading to suboptimal prognostic score.

For a high efficacy and clinical response to ICI therapy, mapping of PD-1 expression on tumor-infiltrating immune cells and scoring the tumor infiltration but also PD-1 expression on tumor cells is necessary before a treatment strategy decision is made. However, heterogeneity of tumor tissue infiltration and space-and-time changes in PD-1 expression are limiting factors for the easy and reliable detection and scoring of $PD\text{-}1^+$ TILs [28, 29]. In addition, some detection antibodies are susceptible to a variable quality and a loss of specificity or high binding affinity [27, 30, 31]. Therefore, the development of small non-toxic agents with an increased tissue penetration is of general interest.

In this work, we used directed evolution by ribosome display to generate a collection of PD-1-targeted small protein variants of MBA series that were derived from 13 kDa Myomedin scaffold library using randomization of 12 mutable residues located on a flat β-sheet surface. We provide evidence that MBA proteins exhibit high affinity and specificity to human and mouse recombinant or cell surface-exposed PD-1 receptors and can be used as non-immunoglobulin alternatives for monitoring $PD\text{-}1^+$ cell populations in tumor tissue biopsy samples as well as for imaging of organs/tissues containing $PD\text{-}1^+$ cells in vivo. Thus, these engineered MBA proteins can serve as beneficial diagnostic tools for the clinical management of NSCLC patients.

Materials and methods

Myomedin combinatorial library design

The β-sheet Myomedin combinatorial library was derived from structure of human myomesin-1 domain 10. The residues suitable for randomization were identified by in silico mutability screening of all amino acid residues resolved in the crystal structure of human myomesin domains 10 and 11 (PDB ID 3rbs) [32]. All residues were mutated to all 20 amino acids using the

PositionScan routine of FoldX program [33] and a mutability score corresponding to a number of stabilizing substitutions was assigned to each residue. The mutability score was also calculated for the previously characterized stable isolated myomesin-1 domain 10 structure (PDB ID 6t3o) (Fig. 1A–C) [34].

Construction and assembly of Myomedin β-sheet library

A series of PCR steps was used for the construction of Myomedin β-sheet combinatorial library using Q5® High-Fidelity DNA Polymerase (NEB) (Fig. 1D) and a set of primers listed in Additional file 1: Table S1. Individual PCR products were separated in 1–2% agarose and DNA of the desired length was isolated using gel extraction kit (Monarch, NEB). In the 1st PCR of internal non-randomized part of the library was amplified with primers MyoBS_centr _F, MyoBS_centr _R and template from Myomedin wild-type (MyoWT) (64 °C melting temperature, 30 cycles) giving 87 bp product. In the 2nd PCR randomized parts of the library were attached with primers MYOM-BS_1F and MYOM-BS_2R (64 °C melting temperature, 30 cycles) resulting in 210 bp product. By 3rd PCR Myomedin scaffold was completed with primers B-for and B-rev (65 °C melting temperature, 30 cycles) with the product of 333 bp. For use in ribosomal display, RBS, TolA spacer and stem-loops were attached to the library scaffold in two more PCR reactions, as described earlier [34].

Ribosome display

Three rounds of ribosome display selection were performed as described earlier [34] with the following differences. Human PD-1 (hPD-1) protein (R&D Systems) was coated into the wells of MaxiSorp 96-well plate (NUNC) for 1 h at room temperature (RT) with the concentration 2 µg/ml in the 1st and 2nd round and 0.5 µg/ml in the 3rd round. Preselection step was performed in wells just blocked by 3% BSA. Washing of complex of ribosomes RNA and protein attached to the hPD-1 in the well of microtiter plate was done with increasing stringency: 5 times (10 times and 10 times) with TBS-T (50 mM Tris, 150 mM NaCl pH 7.5 with 0.05%, 0.05% and 0.2% of Tween-20, in 1st, 2nd and 3rd round respectively). After 3rd round of selection, resulting cDNA was cloned into the vector pET28b and vector was inserted into the *E. coli* XL1-blue host cells. Randomly selected colonies were sequenced and those with the mutations in randomized positions only were cloned into *E. coli* BL21 (DE3) cells and screened for binding to the hPD-1 in ELISA assay. Construct of MBA variants contains N-terminal His-tag used for purification and C-terminal V5-tag used for specific detection.

In silico modeling by docking

The MBA variants were modeled using the MODELLER 9v14 suite of programs [35] based on the non-mutated myomesin-1 domain 10 structure (PDB ID 3rbs) [32], residues 1246-1358). The model of the extracellular domain of hPD-1 (residues 24 to 170 according to the Q15116 UniProt record) and the hPD-1/hPD-L1 complex were built using local installation of AlphaFold [36]. Flexible side chain protein–protein global docking was performed using a local copy of the ClusPro server [37, 38] docking the MBA variants (as ligands) to the hPD-1 model (as the receptor). The docking results were analyzed using PyMOL version 2.6.0 (The PyMOL Molecular Graphics System, Schrödinger, LLC.)

Bioconjugation of MBA binders

Bioconjugation of MBA proteins was performed using *p*-isothiocyanatobenzyl-deferoxamine (p-NCS-Bz-DFO; CheMatech, France). Briefly, 0.5 mg of particular binder in elution buffer was dialyzed into 0.5 ml of PBS. The pH was adjusted to 9 with 0.1 M Na_2CO_3 and p-NCS-Bz-DFO diluted in DMSO was added in 3 molar excess. Mixture was incubated for 1 h at 37 °C. Unreacted deferoxamine was removed and buffer exchange into water was performed using Zeba spin desalting column (Thermo Fisher Scientific, MA, USA).

^{68}Galium-labeling of MBA proteins

DFO-conjugated binders were radiolabeled with ^{68}Galium (^{68}Ga) 100 µl of MBA binders (0.1–1.4 mg/ml)

(See figure on next page.)

Fig. 1 Concept of Myomedin ß-sheet combinatorial library and selected MBA variants' binding curves measured by ELISA. **A** Side view and **B** top view to the human myomesin-1 domain 10 in cartoon representation, showing positions of residues selected for randomization. Highlighted are the C_α positions of residues N1276, I1278, E1281, T1315, T1317, Q1319, Q1321, K1324, T1326, H1328, T1330, and V1332 numbered according to the UniProt (UniProt, 2019) P52179 record. The residue color scale represents the mutability score, from blue to red for low to high mutability. **C** Surface representation of the Myomedin scaffold with the ß-sheet patch in magenta and the previously defined Myomedin loop library in red [34]. **D** Scheme of Myomedin ß-sheet library assembly using multistep PCR. **E** Binding of selected MBA variants to recombinant hPD-1 receptor assessed by ELISA assay. Detection of the signal was performed using anti-V5 tag-HRP conjugated antibody at 450 nm

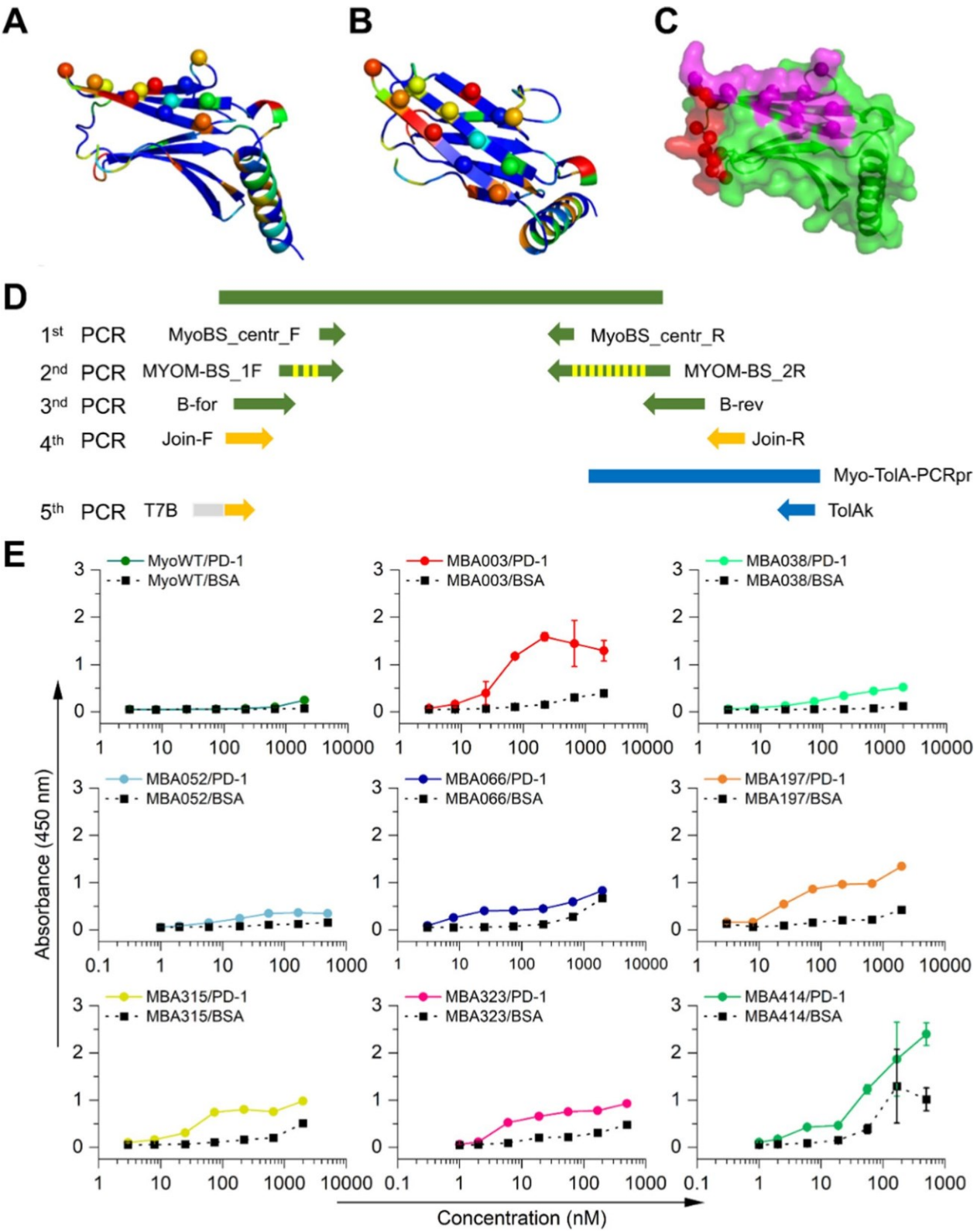

Fig. 1 (See legend on previous page.)

were mixed with 30 µl of sodium acetate (155 mg/ml) and 300 µl (25–50 MBq) of ^{68}Ga-eluate from ^{68}Ge/^{68}Ga-generator (Eckert and Ziegler). The mixture was incubated for 15 min at room temperature. Radiochemical purity was then assessed by iTLC chromatography using two different mobile phases, A) 0.1 M sodium citrate and B) 1 M sodium acetate + methanol (1:1).

In vivo and ex vivo analysis of biodistribution of MBA proteins in mouse tissues

All the animal experiments were conducted in accordance with regulations and guidelines of the Czech Animal Protection Act (No. 246/1992), and with the approval of the Czech Ministry of Education, Youth, and Sports (MSMT-24421/2021-4) and the institutional Animal Welfare Committee of the Faculty of Medicine and Dentistry of Palacky University in Olomouc. 10 weeks old female Balb/c mice were housed under standard laboratory conditions. The number of mice used in biodistribution study was reduced as much as possible to three mice for each binder. The labeled binders for ex vivo biodistribution were retro-orbitally injected into mice at the dose of 100 µl representing 1–2 MBq of ^{68}Ga and 1.5–3 µg of the peptide. The animals were sacrificed 30- and 90-min post-injection by cervical dislocation. The blood, spleen, pancreas, stomach, intestines, kidneys, liver, heart, lungs, muscle, and bone were collected and weighed. The radioactivity of obtained tissue samples was measured in a γ-counter (2480 Wizard^2 automatic gamma counter; PerkinElmer, Waltham, USA). The biodistribution data were calculated as the percentage of injected dose per gram of tissue (% ID/g).

Experimental animals for PET/CT imaging were retro-orbitally injected with ^{68}Ga labelled MBA binders (approximately ~ 4–6 µg of binder) at a dose of 6–8 MBq per animal and placed in the PET/CT scanner (nanoScan PET/CT, Mediso Medical Imaging Systems, Budapest, Hungary) immediately after the injection of the binder for dynamic imaging or 45 min after the injection for static imaging. A 10 min PET scan was performed for static imaging, while dynamic PET imaging was performed for 90 min in the form of 18 consecutive 5 min PET scans allowing monitoring of temporal changes in connective tissue biodistribution, followed by whole-body helical CT scan (50 kVp/980 µA, 720 projections).

Mouse infection model

In vivo distribution of ^{68}Ga-MBA066 and ^{68}Ga-MyoWT was studied in a mouse model of acute myositis. The murine myositis model was established by intramuscular injection of *E. coli* CCM 5172 suspension. Mice were inoculated with 5×10^7 CFUs of live bacteria in the left hind leg and saline in the right hind leg. The microbial infection was allowed to develop for 5 h. The animals were then injected with ^{68}Ga-labeled binders and imaged by PET/CT as described above.

Immunohistochemistry staining

Tissues were collected into OCT medium and immediately frozen on dry ice and transferred into − 80 °C where stored until analysis. Sections were cut on cryotome machine, hydrated with PBS, fixed in 4% formaldehyde, and blocked with PBS + 1% FBS for 1 h. 100 ng of MBA414 or 1 µg of anti-PD-1 antibody-FITC (Novus) were left overnight at 4 °C. Anti-V5 Alexa Fluor 647 antibody (Invitrogen) was used next day for 1 h. Mounting medium with DAPI (Merck) was used for final preparation of specimen for microscopy. Microscope Leica connected with camera was used for observation of tissues, software was used for preparation of images. Co-localization was quantified by ImageJ software (LOCI, University of Wisconsin) supplemented with plugin JACoP (Fabrice P. Cordelières, Bordeaux Imaging Center (France). Fabrice.Cordelieres@gmail.com, Susanne Bolte, IFR 83, Paris (France). Susanne.Bolte@upmc.fr).

Additional part of methodology is provided in Additional file. In this study, selection criteria for experimental analysis of MBA variants is given as Additional file 1: Table S2.

Results

Concept and description of Myomedin β-sheet combinatorial library

In our previous work, we demonstrated that the human myomesin-1 domain 10 structure exhibited sufficient stability to be used as a scaffold for the generation of a highly complex combinatorial library using randomization of 12 mutable amino acid residues located in the three-domain loops, named Myomedin scaffold [34, 39]. Based on the available crystal structure of mouse/human PD-1/PD-L1 complex (PDB ID 3bik), it seems to be evident that critical interaction residues of human PD-L1 required for the recognition of PD-1 receptor are located on β-sheet surface (Additional file 1: Fig. S1a). Due to the substantial structural similarity between human PD-L1 and Myomedin scaffold (see the superposition in Fig. S1b and built human/human PD-1/PD-L1 complex homology model in Additional file 1: Fig. S1c), we first investigated a mutability potential for amino acid residues within the cognate Myomedin β-sheets.

The mutability score was used as a criterion for the final selection of candidate residues to find a continuous patch of accessible surface residues with high mutability (suggesting a lower probability of overall fold destabilization upon randomization). Herein, an in silico procedure identified a patch of suitable residues localized on

the β-sheet surface of human myomesin-1 domain 10 (Fig. 1A–C). The residues N1276, I1278, E1281, T1315, T1317, Q1319, Q1321, K1324, T1326, H1328, T1330, and V1332 numbered according to the UniProt [40] P52179 record were used for randomization. The selected β-sheet residue patch (Fig. 1C magenta) is located in the proximity of loop-randomized surface sharing a single amino acid residue (Fig. 1C red). The theoretical complexity of the designed Myomedin β-sheet library is 2×10^{15} variants.

Myomedin combinatorial library assembly and identification of PD-1 binding proteins

The new type of highly complex Myomedin combinatorial library carrying 12 mutable amino acid residues located in the β-sheet region was engineered using a set of primers (Additional file 1: Table S1) in multiple PCR reactions (Fig. 1D). Randomization of amino acid codons within the primers was introduced by synthetic trinucleotide technology (TRIM) with the elimination of cysteine residue to prevent the formation of disulfide bridges. After assembly of full-length DNA library and its insertion into a plasmid cloning vector, *E. coli* XL1 cells were transformed with the generated cDNA plasmid library and randomly picked bacterial colonies were used to sequence individual DNA samples for the evaluation of the quality of DNA library and verification of a random codon distribution in the predesigned mutable residues.

To select binders specific to hPD-1 from the Myomedin β-sheet library, three rounds of ribosome display were performed with recombinant hPD-1 receptor as a molecular target immobilized in a 96-well microtiter plate. Then, the library of DNA transcripts was inserted into the plasmid vector by molecular cloning and the generated cDNA plasmid library was used to transform *E. coli* XL1-Blue cells. A total of 378 individual colonies were screened by colony PCR and 220 variants with expected PCR product size were further sequenced. Of them, 75 variants with required mutations solely in the randomized regions were used to transform *E. coli* BL21 (DE3) cells and bacterial lysates of these Myomedin-containing clones were tested in ELISA assay for binding to immobilized hPD-1. A total of 25 MBA variants with specific binding to PD-1 were produced and purified on Ni–NTA agarose matrix and particular binding curves to hPD-1 were analyzed by ELISA. Finally, Myomedin variants MBA003, MBA038, MBA052, MBA066, MBA197, MBA315, MBA323, and MBA414 binding to recombinant hPD-1 (Fig. 1E) were selected for further characterization. Variants MBA038 and MBA066 were produced in cytosolic extract while variants MBA003, MBA052, MBA197, MBA315, MBA323, and MBA414 were present in inclusion bodies.

MBA variants exhibit specific binding to cell-surface expressed human PD-1

HEK293T cells transiently expressing hPD-1 receptor were stained with the selected MBA variants and co-stained with anti-PD-1-specific monoclonal antibody (mAb) to visualize binding of the MBA proteins to surface-expressed hPD-1. Results of immunofluorescence microscopy showed that all the selected MBA variants, except MBA038, exhibited a specific binding to hPD-1-expressing HEK293T cells which correlated with anti-PD-1 mAb staining (Fig. 2A). To further verify the sensitivity and specificity of MBA variants for cell surface hPD-1 staining, we used human acute lymphoblastic lymphoma cells (SUP-T1) which have been reported to express a substantial level of PD-1 on their surface [41]. With the exception for MBA038 variant, double immunofluorescence staining of SUP-T1 cells with all other 7 MBA variants proven their binding to the surface of the SUP-T1 cells in correlation with anti-PD-1 mAb staining (Fig. 2B). Furthermore, hPD-1-HEK293T transfectants, SUP-T1, and MOLT-4 cells showed no staining by fluorescence signal with Myomedin wild-type protein in contrast to anti-PD-1 mAb staining (MyoWT, Fig. 2A–C), revealing the specificity of the tested MBA variants against the hPD-1 receptor. To further confirm the hPD-1 specificity of MBA proteins, we verified binding of 6 MBA variants to human B-cells Dakiki, which lack the expression of hPD-1 and is reported by negative anti-PD-1 polyclonal antibody staining (Fig. 2D).

(See figure on next page.)

Fig. 2 Binding of MBA variants to human cells. **A** HEK293T cells transiently transfected with plasmid carrying cDNA of hPD-1 and stained with selected 8 MBA variants or MyoWT as a control. **B** Binding of 7 selected MBA variants or MyoWT as a control to human acute lymphoblastic lymphoma cells (SUP-T1). **C** Binding of 6 most promising MBA variants and MyoWT to paraformaldehyde-fixed T-cell adult acute lymphocytic leukemia cells MOLT-4. **D** Negative control staining on B cell line Dakiki not expressing PD-1 with selected MBA proteins. **E** hPD-1-transfected HEK293T cells: secondary antibody control staining to results in **A**. The staining with selected MBA proteins was performed without anti-PD-1 primary antibody using the secondary antibody donkey anti-goat Alexa Fluor 488. MBA variants used in figure containing C-terminal V5 tag were detected using mouse monoclonal anti-V5-tag-Alexa Fluor 488 conjugated antibody. Expression of hPD-1 on HEK293T transfected cells as well as on SUP-T1 and MOLT-4 cells was monitored with goat anti-human polyclonal anti-PD-1 antibody followed by secondary donkey anti-goat IgG conjugated with Alexa Fluor 568

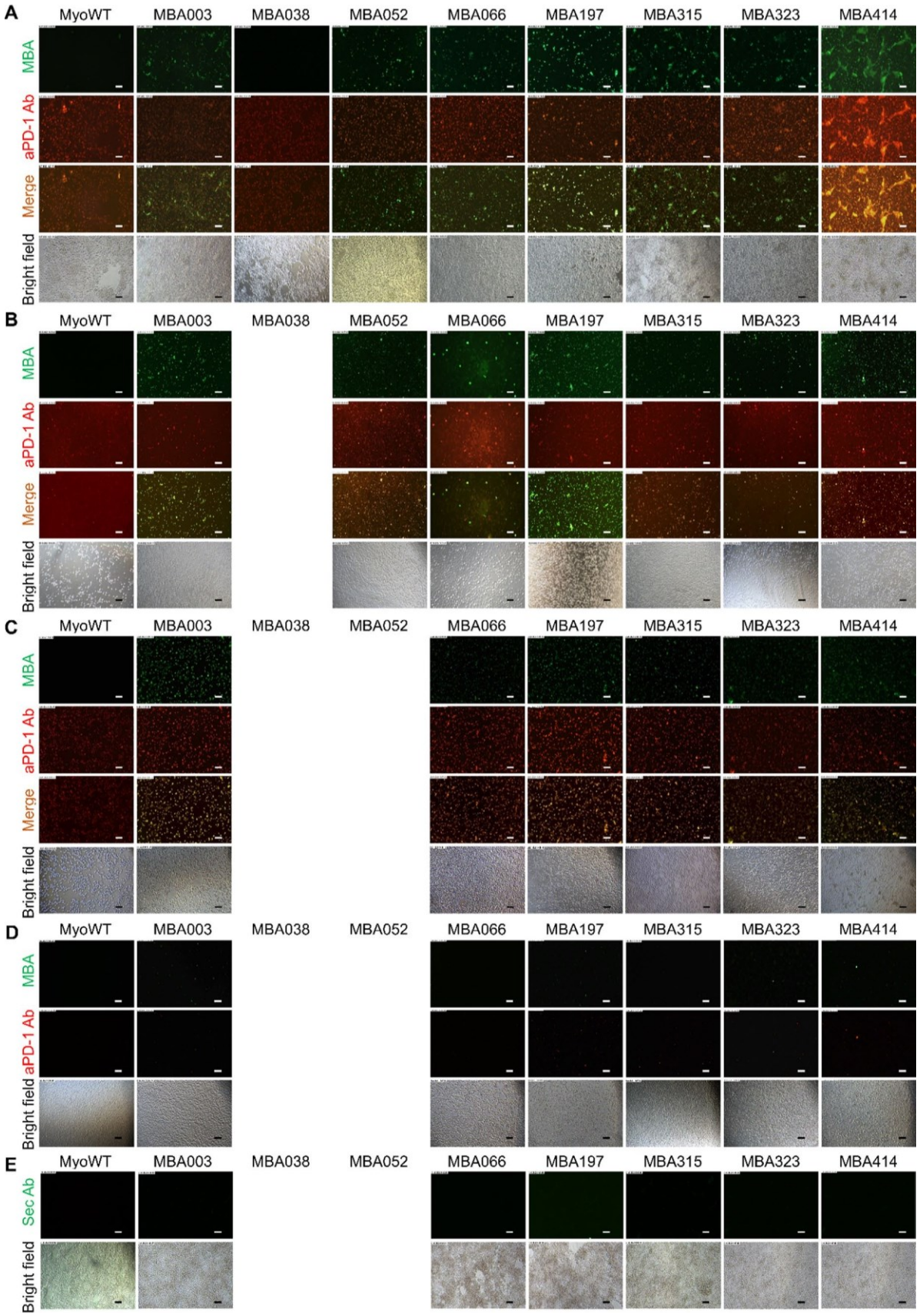

Fig. 2 (See legend on previous page.)

The specificity of secondary antibody conjugate used in Fig. 2A is documented in Fig. 2E.

Prediction of MBA/PD-1 binding modes by docking

The individual MBA variants were modeled using the amino acid sequence (Additional file 1: Fig. S2a) and docked with hPD-1 model. The protein–protein docking results are summarized in Figure S2b-g showing the first three most probable predicted MBA binding modes for each MBA variant (color coded by decreasing probability from red to yellow). The PD-1 geometry resembles a triangular prism with three relatively flat faces available for interaction. The docking results show a clear preference for interaction with one of the sides and all the most probable predicted modes occupy the same side of the PD-1 model. For variants MBA197, MBA315, and MBA323, the docking procedure also predicts interactions with the second side of PD-1. All the predicted binding modes, however, occupy these two PD-1 sides and only marginally approach the third side responsible for the binding of the PD-L1 described by the available structure and predicted hPD-1/hPD-L1 model (see Additional file 1: Fig. S1).

Characterization of binding affinity, kinetics, and specificity of MBA variants

To verify binding affinity and kinetics for 7 MBA variants, HEK293T cells were transfected with pcDNA6 plasmid carrying hPD-1 cDNA. Two days after the transfection, binding kinetics for 7 Myomedin variants was measured using a LigandTracer Green Line instrument. During the measurements, increasing concentrations of the MBA proteins were added to the culture medium, and measurements were collected in real-time until the saturation state was observed. Kinetic on- and off-rates were evaluated for all the measured Myomedin variants. Based on the measurements, the lowest estimated KD was measured for variants MBA323 (6.59 nM), MBA066 (6.92 nM), and MBA414 (8.63 nM). The slowest off-rate was represented by MBA003, MBA066, and MBA197 (kd [1/s] was 1.71×10^{-5}, 4.63×10^{-5}, and 7.30×10^{-5}, respectively (Fig. 3A, Additional file 1: Table S3). In addition to fluorescent microscopy, KD calculation using LigandTracer technique confirmed the binding of all 7 MBA proteins to PD-1–expressing cells. To independently verify the binding affinity, an alternative estimation of Kd values for MBA066, MBA197 and MBA414 variants to recombinant hPD-1 in solution was performed using microscale thermophoresis (MST). Figure 3B indicates considerable Kd values for MBA197 (4.21 ± 1.15 nM) and MBA414 (6.11 ± 0.99 nM), except MBA066 with showed remarkably higher Kd value (2917 ± 223.22).

As we intended to use the most promising MBA variants for in vivo monitoring of PD-1$^+$ cell populations in mice, we aimed to verify whether selected MBA variants retain high-affinity binding to murine PD-1 receptor. To this goal, sequence comparison between human and murine extracellular moiety of the PD-1 (Additional file 1: Table S4) indicated a conserved binding consensus important for interaction with PD-L1. After that, HEK293T cells were transiently transfected with pcDNA6 vector carrying murine PD-1 cDNA, and after two days, cells were stained with MBA066, MBA197, and MBA414 proteins. Results presented in Fig. 3C, D and Additional file 1: Table S5 document that all three MBA proteins bind to murine PD-1 transiently expressed on HEK293T transfectants.

Biodistribution of radiolabeled MBA proteins and in vivo PET/CT imaging

Myomedins variants, named MBA066, MBA197, MBA414, and MyoWT as control, were selected as the most promising candidates for biodistribution analysis in the mouse model. Before radiolabeling of Myomedins, the proteins were conjugated with a chelator Deferoxamine (DFO) using NH_2 group of Myomedin lysine residues, which are naturally presented in this scaffold protein. For conjugation to NH_2 groups, p-SCN-Bz-Deferoxamine was used. For radiolabeling of MBA proteins, ^{68}Galium isotope was chosen and ^{68}Ga-DFO-MBA variants were dialyzed to PBS. The radiochemical purity of the labeled Myomedins was verified by instant thin-layer chromatography (iTLC) and reached values around 95% (Additional file 1: Table S6), which meets the typical criteria

(See figure on next page.)

Fig. 3 Characterization of binding affinity and specificity of the most important MBA variants. **A** Binding affinity and kinetics measurement for the selected MBA variants to hPD-1 expressed on transfected HEK293T cells using LigandTracer Green Line instrument. **B** Determination of binding dissociation constant of the most promising MBA variants to recombinant hPD-1 by micro-scale thermophoresis. **C** MBA variants tested for binding to murine PD-1 expressed on HEK293T cells. Cells were stained with either both antibodies (anti-V5 tag for MBA recognition and anti-PD-1 mAb for staining of the murine PD-1 receptor) or with anti-V5 tag antibody only. **D** Measurement of binding kinetics and affinity of MBA066, MBA197, and MBA414 to murine PD-1 expressed on HEK293T transfected cells using LigandTracer Green. In **A** and **D**, colored lines indicate signals from cells subtracted from the background

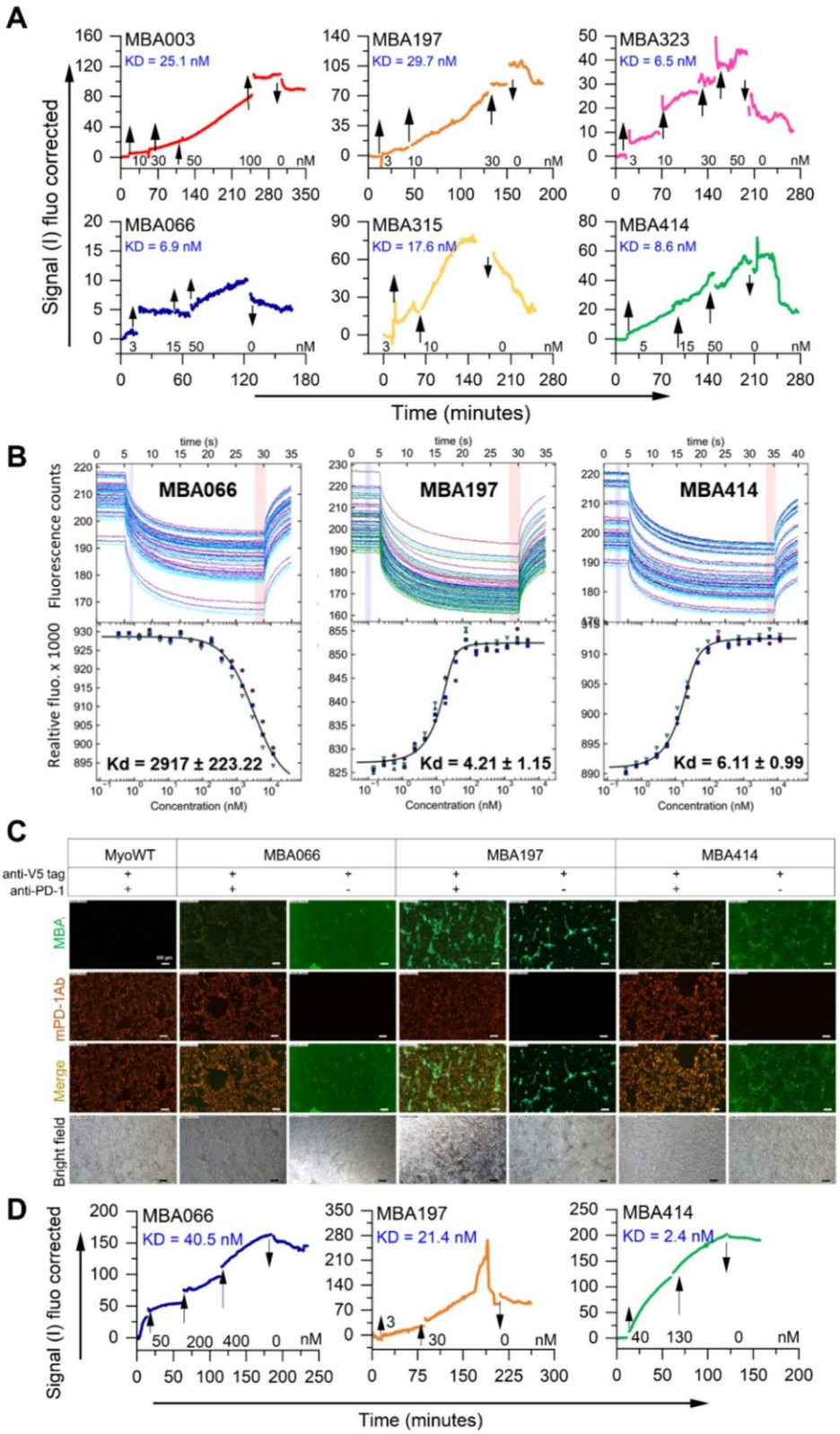

Fig. 3 (See legend on previous page.)

for clinically used diagnostic radiopharmaceuticals. The stability of the radiolabeled Myomedins proteins in human serum was assessed after 30, 60 or 120 min. In vitro, stability of ^{68}Ga-MBA066, ^{68}Ga-MBA197, and ^{68}Ga-MBA414 after 2 h in human serum reaches values between 89.6–98.2% and did not differ from values for ^{68}Ga-labeled parental non-mutated Myomedin wild-type protein (95.9–98.0%), as shown in Additional file 1: Table S6.

In vivo, the biodistribution of radiolabeled MBA066, MBA197 and MBA414 proteins in comparison to MyoWT parental non-mutated protein was tested in BALB/c mice. After retro-orbital injection of ^{68}Ga-Myomedins, the distribution of proteins was monitored using whole-body positron emission tomography combined with computerized tomography (PET/CT) imaging up to 90 min post-injection. Results presented in Fig. 4A demonstrate that ^{68}Ga-MyoWT is quickly accumulated in the kidneys and excreted from the body via the bladder. This indicates that parental MyoWT did not substantially accumulate in any particular organs, except excretory system, and therefore, can be used as a negative control for in vivo PET/CT imaging. In the case of MBA066, a rapid accumulation of radiolabeled protein is visible in the heart, where it is presented during first 25 min monitoring period. The substantial amount of signal is detected in the liver for all monitoring duration (Fig. 4B). In striking contrast to MyoWT, both MBA197 and MBA414 exhibited a substantial accumulation in the liver and remained concentrated there for entire monitoring period, with only a slow clearance via kidneys into the bladder (Fig. 4C, D). This suggests a specific interaction to PD-1$^+$ cell population mostly in the liver, but also in a lower content in other tissues.

Furthermore, to investigate more precisely the biodistribution of PD-1 binding Myomedins, we performed *post mortem* ex vivo analysis of ^{68}Ga-Myomedins content in multiple mouse organs. In this study, quantification of radiolabeled MBA066, MBA197, MBA414, and MyoWT proteins after 30 or 90 min of administration was assessed in peripheral blood and other 10 organs of interest in mice. As shown in Fig. 4E, MyoWT is substantially accumulated in the kidneys and weakly observed in liver, spleen, and blood. In contrast to MyoWT organ distribution, MBA197 and MBA414 were prominently concentrated in liver (6–7 times), spleen (4–7 times), and lung (8–10 times) (Fig. 4G, H). In addition, MBA197 and MBA414 did not exhibit significant accumulation in other organs, such as kidneys, pancreas, stomach, heart, muscle, femur, and blood (Fig. 4G, H). These observations suggested that MBA197 and MBA414 could specifically interact with PD-1-expressing cells and, due to high affinity binding, thus remain concentrated in organs with substantial lymphocyte populations, at least for the monitored 90 min period.

To further support this hypothesis, we used a mouse muscle infection model in which lymphocyte homing is stimulated by a local intramuscular application of bacterial suspension into the mouse leg. Therefore, *E. coli* suspension (5×10^7 CFU) was administrated 5 h before the PET/CT imaging of Myomedin proteins was initiated. As presented by a non-infected dynamic biodistribution study on the ^{68}Ga-MBA066 variant (Fig. 4B), this protein also predominantly binds to liver cell populations, but in comparison to MBA197 and MBA414 variants, it is faster cleared via kidneys, probably due to lower binding affinity. When ^{68}Ga-MBA066 protein was administrated in the mouse infection model, a distinct local signal concentration, in comparison to ^{68}Ga-MyoWT control, was detected in the site of infection 45 min post-injection (Additional file 1: Fig. S3). Thus, ^{68}Ga-MBA066 exhibited a slower pharmacokinetics and increased local concentration in contrast to ^{68}Ga-MyoWT. This further supports the expectation that ^{68}Ga-MBA066 might specifically recognize PD-1$^+$ lymphocytes expectedly homing into the site of infection.

Staining of PD-1 expressing cells with MBA proteins on frozen sections of human tonsils and NSCLC tissues

To prove the binding ability of MBA414 to PD-1 in normal human tissue, we used a human tonsil resected from a child with tonsillar hypertrophy. In tonsils, B cells follicles are surrounded by T cell zones. The PD-1 receptor is expressed here preferentially on activated T cells, B cells, dendritic cells, macrophages, monocytes, and NK cells [42, 43]. IHC staining proved the ability of MBA414 to recognize PD-1$^+$ cells with pattern of staining similar to that pattern obtained with rabbit polyclonal

(See figure on next page.)

Fig. 4 In vivo imaging and ex vivo analysis of ^{68}Ga-labeled MBA distribution in Balb/c mice. **A** ^{68}Ga-MyoWT, **B** ^{68}Ga-MBA066, **C** ^{68}Ga-MBA197, **D** ^{68}Ga-MBA414. Mice were retro-orbitally injected with particular MBA binders and immediately scanned by a PET/CT scanner. PET imaging was performed in the form of eighteen consecutive 5-min PET scans. **E** ^{68}Ga-myoWT, **F** ^{68}Ga-MBA066, **G** ^{68}Ga-MBA197, **H** ^{68}Ga-MBA414. Mice were retro-orbitally injected with ^{68}Ga-binders ($n = 3$ mice per group). Blood, spleen, pancreas, stomach, intestines, kidneys, liver, heart, lungs, muscle, and bone were collected at 30 and 90 min after injection. The tissue samples obtained were weighed, and radioactivity was measured in a γ-counter. The biodistribution data were calculated as the percentage of injected dose per gram of tissue (% ID/g)

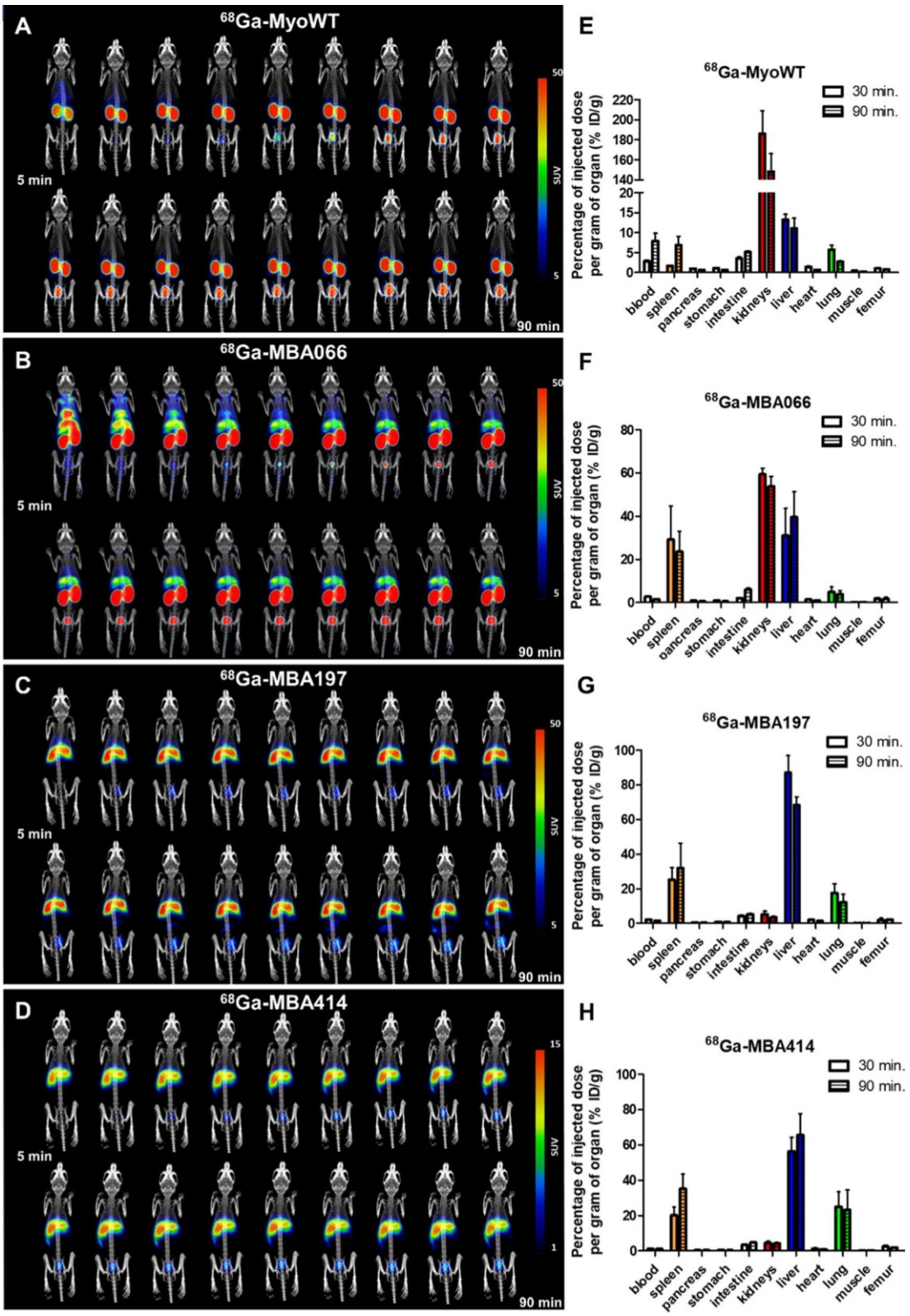

Fig. 4 (See legend on previous page.)

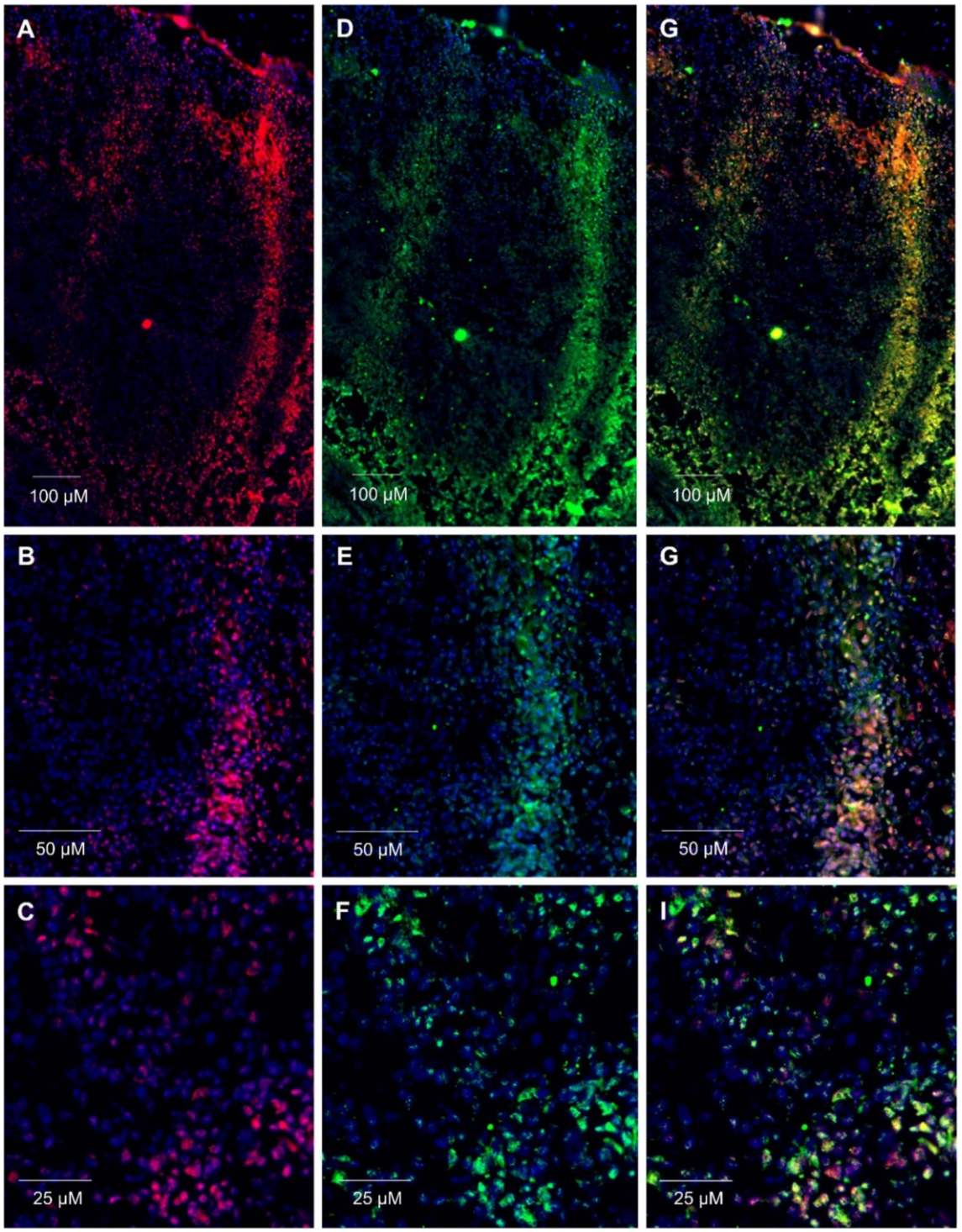

Fig. 5 Immunofluorescence staining of PD-1$^+$ T cells on human tonsil frozen sections. **A**–**C** Tissue was stained with MBA414 variant detected by anti-V5 IgG-Alexa Fluor 647 antibody. **D**–**F** Staining with rabbit anti-PD-1 IgG-FITC antibody. **G**–**I** Merge of **A** and **D**, **B** and **E**, **C** and **F** demonstrate superimposed fluorescence signals. Magnifications of tissues sections are ×200 **A**, **D**, **G**, ×400 **B**, **E**, **H** and ×1000 **C**, **F**, **I**. Significant co-localization of MBA414 variant detected by anti-V5 IgG-Alexa Fluor 647 antibody (**A**) and rabbit anti-PD-1 IgG-FITC (**D**) was analyzed through Pearson´s correlation coefficient (r) calculated by ImageJ software with JACoP co-localization tool, r = 0.779

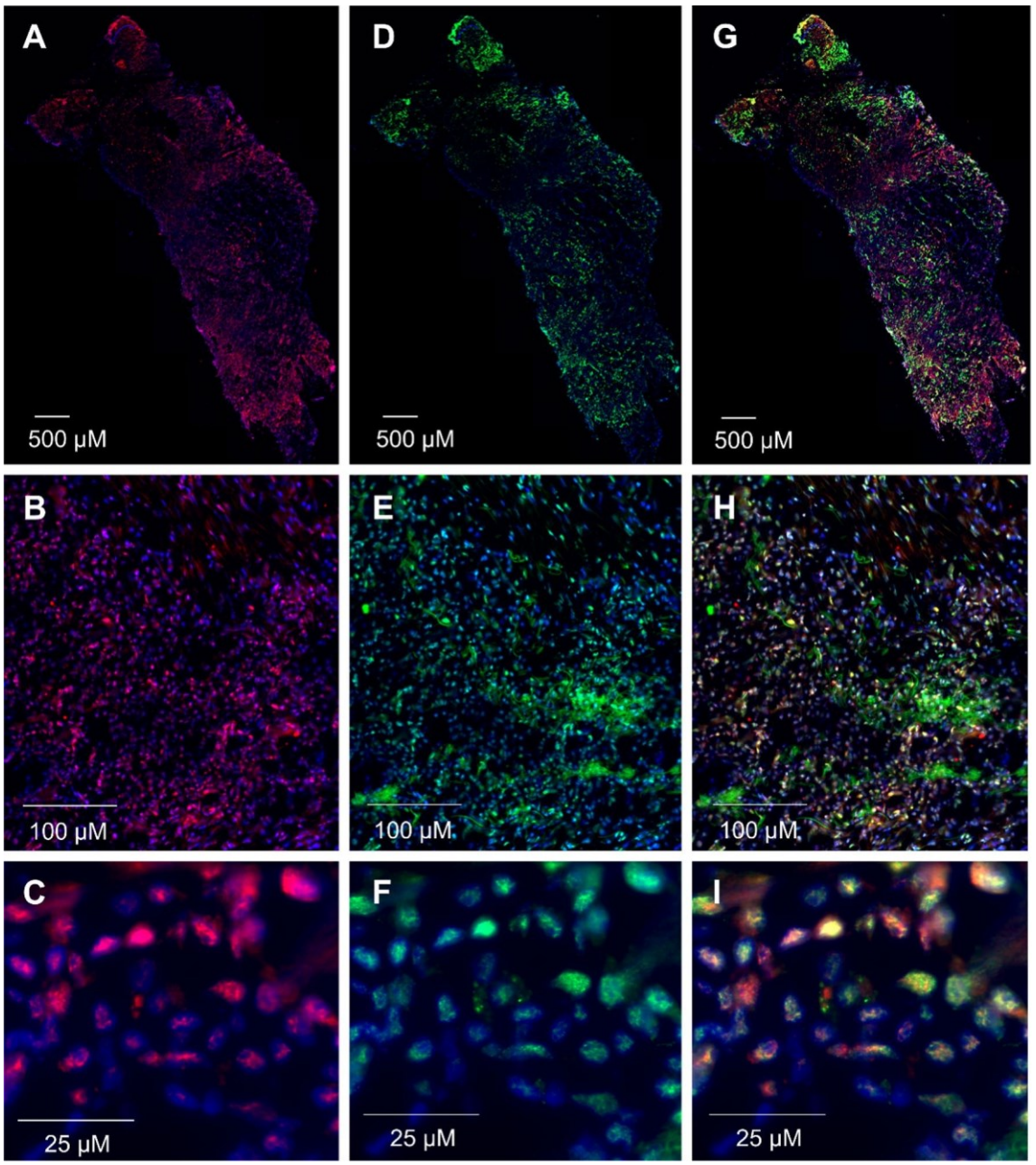

Fig. 6 Immunostaining of PD-1$^+$ cells on NSCLC tissue. **A**–**C** Frozen sections of tumor tissue were stained with MBA414 variant detected by anti-V5 IgG-Alexa Fluor 647 conjugate and **D**–**F** rabbit anti-PD-1 IgG-FITC conjugated antibody. Panel **G**–**I** merge fluorescence signals of MBA414 (Alexa Fluor 647) and anti-PD-1 IgG (FITC). Magnifications of tissue sections are ×200 (**A**, **D**, **G**), ×400 (**B**, **E**, **H**) and ×1000 (**C**, **F**, **I**). Significant co-localization of MBA414 variant detected by anti-V5 IgG-Alexa Fluor 647 antibody (**A**) and rabbit anti-PD-1 IgG-FITC (**D**) was analyzed through Pearson´s correlation coefficient (r) calculated by ImageJ software with JACoP co-localization tool, r = 0.846

anti-PD-1 antibody (Fig. 5). Double-positive cells are clearly identifiable after merging fluorescence signals from MBA414-Alexa Fluor 647 and anti-PD-1 IgG-FITC (Fig. 5G–I). Next, we proofed MBA414 binding on a frozen NSCLC tissue section (Fig. 6). In analogy to tonsillar tissue (Fig. 5), PD-1 expression on NSCLC sections was detected using MBA414 variant and rabbit polyclonal anti-PD-1 antibody. Merged pictures show an overlap of fluorescence signals from MBA414-Alexa Fluor 647 and anti-PD-1 IgG-FITC (Fig. 6G–I). The comparison

indicates that MBA414 detects more cells than the anti-PD-1 antibody, which corresponds to our expectations.

Discussion

Tumor-infiltrating lymphocytes (TILs), also known as the "immunoscore" [44, 45], are characterized as lymphocytes within and around cancer cells in tumor microenvironment (TME) and have been associated with better prognosis, and correlated with the traditional tumor-node-metastasis (TNM) staging and microsatellite instability (MSI) status in cancer patients [46]. Moreover, TILs were also used to envisage the clinical benefit of anti-PD1 immunotherapy, especially at the invasive margin where they were directly correlated with response to anti-PD-1 immunotherapy and an immunohistochemistry-based assessment of $CD8^+$ T cell density in the core of the tumor [47, 48].

Among the dominant challenges for the laboratory diagnosis of PD-1 and its cognate PD-L1 counterpart in tumor tissue samples are the highly variable expression dynamics within different areas of the same tissue, the lack of reliable antibodies and diagnostic kits for some types of solid tumors, the expression heterogeneity of both biomarkers in the context of TILs and tumor cells, and above all, insufficient evidence of a correlation between PD-1 or PD-L1 expression and the treatment response. This makes the assessment of cutoff points rather difficult. A typical case, for example, is colorectal carcinoma, for which, until now, there has been no definite scoring system developed. The above-mentioned factors can be the cause of why patients with low PD-1 and PD-L1 expression as assessed by current histopathological scoring methods can benefit from immunotherapy. This could be a reason why some centers give immunotherapy to all patients based on their current clinical performance status.

Employment of identified MBA binders could offer an alternative to antibody-based diagnostics applicable for in vitro and in vivo testing (Additional file 1: Table S7). In the case of NSCLC in vitro diagnostics, MBA414 variant exhibited similar PD-1 positivity pattern as available anti-PD-1 mAb in fluorescence microscopy (Fig. 6; Pearson's correlation coefficient 0.846). This is promising for testing of MBA binders in large cohort NSCLC biopsies and also other tumors. Nevertheless, more accurate assessment of the in vitro diagnostic potential of MBA requires further testing, particularly in studies evaluating the potential to predict response to anti-PD-1 immunotherapy. Due to a small size of MBA, we could expect an improved penetration into the tumor tissue in comparison to mAb. Thus, it is also possible to hypothesize that radiolabeled MBA could offer an enhanced sensitivity of tumor PD-1 expression analyses for PET/CT body imaging techniques.

Another point to consider is that in routine histopathological practice, at least in most countries, the expression of the above-mentioned factors is examined from primary tumors, and physicians treat the metastatic disease. It is generally known that the expression of these factors differs in primary tumor and metastasis. Also, the area of the examined tissue does not represent the whole tumor. The most important point to consider is that the histopathologic assessment represents a static picture and does not reflect the dynamics of tumor development and consequent reaction of the immune system.

Although unprecedented success has been achieved in the diagnosis and treatment of cancer patients with antibodies, non-antibody biologics have attracted considerable attention [49, 50]. Based on our knowledge, only one small-size protein scaffold library (repebody) [51], one de novo-designed hyperstable miniprotein PD1 agonist [52], and two affinity-optimized soluble human PD-L1 (L3B3-hPD-L1 and L3C7-hPD-L1) [53], have been proven as efficient non-antibody anti-PD-1 biologics. Additionally, several bioactive small-molecules and peptide-based inhibitors as potential alternatives to mAbs targeting PD-1 protein are also reported (reviewed in Refs. [54, 55]). In considering small proteins for mapping $PD1^+$ TILs using immuno-PET imaging, their small size provides an enhanced tumor penetration, together with an increased glomerular filtration and renal losses [14]. Furthermore, PET imaging can be used for a repeated assessment of the tumor growth progression, thereby completing diagnostic information reached by immunohistochemical approaches [14].

The primary goal of our study was to identify high-affinity and high-specificity PD-1 binding proteins for ex vivo diagnostics and in vivo imaging; however, the used library concept with the randomization of 12 amino acid residues on β-sheet surface enabled us to also identify potential PD-1 blocking variants. Indeed, two of the most promising variants, MBA003 and MBA323, competed with a soluble form of the human PD-L1 for binding to hPD-1 (Additional file 1: Figs. S4, S5, S6). Based on competition ELISA data, we can estimate the binding affinity for the PD-L1 interaction binding site. For the MBA003 variant, the estimated binding affinity is 10 μM and for MBA323 is 30 μM. These values are comparable to the modest 8.2 μM binding affinity described for the extracellular moiety of natural human PD-L1 [56]. To independently confirm the inhibitory potential of MBA003 and MBA323 proteins, we treated hPD-1-transfected HEK293T cells with 50 nM human PD-L1, then incubated with 40 μg/ml MBA variants (and MyoWT control) and fluorescently detected the binding in the

presence or absence of the human PD-L1 competitor. Also, we performed the staining with anti-PD-1 antibody to verify a co-localization of the signal. As expected in the correlation to competition ELISA data (Additional file 1: Fig. S4), the binding of MBA003 and MBA323 to hPD-1-HEK293T transfectants was substantially diminished in comparison to non-competing variants MBA066, MBA197, and MBA414 (Additional file 1: Fig. S5).

Furthermore, we performed a competition binding assay using LigandTracer. We compared binding curves for competing variants MBA003 and MBA323 in the presence of hPD-L1 with those for non-competing variants MBA066 and MBA414 using hPD-1-transfected HEK293T cells (Additional file 1: Fig. S6). Results again confirm an overlapping binding site of MBA003 and MBA323 with competing hPD-L1 on the hPD-1 receptor. Thus, we complete data of three different molecular approaches—competition ELISA, competition fluorescent microscopy, and competition real-time imaging by LigandTracer method. These two MBA proteins (MBA003, MBA323), therefore, could be further improved to increase a blocking potential by affinity maturation approaches.

Based on structural data (PDB ID 3bik), the overall shape of the PD-L1 interacting face is partially concave due to the surrounding hairpin/loop regions. It was shown that these outer regions contribute to receptor/ligand recognition and can be considered as an allosteric region of the PD-1 protein [57]. While our model of the hPD-1/hPD-L1 shows clear differences in geometry of the previously described CC' and FG loops, the largest rearrangement was observed for the loop formed by residues E84 to R94. As our selection approach was not set up for a screening of PD-L1 competing variants, we rather identified high-affinity non-competing variants in the KD range 6.59–29.7 nM (Additional file 1: Table S3). This is consistent with the most probable binding modes of all six MBA variants predicted by docking, occupying the PD-1 face not involved in the PD-L1 interaction (Additional file 1: Fig. S2, Table S4).

The crystal structures of murine PD-1 and human PD-L1 complexes (PDB ID 3bik and 3sbw) revealed a contact interface involving 16 residues of mPD-1 and 14 residues of hPD-L1 [58]. There is 64% protein sequence identity between murine and human PD-1 (Additional file 1: Table S4), which can cross interact with PD-L1 of both species with similar affinities [59–61]. Indeed, the estimated KD value for MBA414 variant measured by cell surface interaction with hPD-1 on HEK293T transfectant cells (KD = 8.6 nM, Fig. 3A) correlates with that for murine PD-1 (KD = 2.48 nM, Fig. 3D, Additional file 1: Table S5). MBA197 binds to hPD-1 with similar binding affinity as compared to murine PD-1 (KD = 29.7 nM versus KD = 21.4 nM, respectively, Fig. 3A, D, Additional file 1: Table S5). However, in the case of MBA066, the affinity to hPD-1 (KD = 6.9 nM, Fig. 3A) is substantially decreased for murine PD-1 (KD = 40.5 nM, Fig. 3D, Additional file 1: Table S5). Such a loss of binding affinity for murine PD-1 could explain the observed difference in biodistribution time course in mice (Fig. 4B) with an increased kidney clearance in contrast to MBA197 and MBA414 with a non-exacerbated affinity for murine PD-1.

To assess the penetration of MBA proteins into tissues overexpressing PD-1, we employed a murine model of local acute immune system activation based on intramuscular injection of viable *E. coli* cells. During immune activation, PD-1 is overexpressed on many cell types including macrophages, dendritic cells, $CD4^+$ and $CD8^+$ T cells, NKT cells, and B cells. During bacterial infection, PD-1 expression could be induced by antigen-dependent stimulation such as IgM crosslinking on B cells, TCR-mediated activation of $CD4^+$ T cells, by bacteria pathogen-associated molecular patterns, such as lipopolysaccharide, which in mice activates both B cells and macrophages, or by inflammatory cytokines IL-1β, IL-6, and TNF-α [62, 63]. PD-1 expression could be induced by NFATc1 and/or NF-κB pathways of activation. After the comparison with wild-type non-randomized Myomedin parental protein (MyoWT), a significant increase in the accumulation of ^{68}Ga-MBA066 was detected at the site of injection (Additional file 1: Fig. S3).

Small protein-derived diagnostics and therapeutics are of a hot focus. Those include nanobodies-based PD-1-Nb-B20 as small IgG-derived protein targeting linear PD-1125–136 (AISLAPKAQIKE) peptide [64]. This small protein was developed for the therapeutic purpose with only a limited characterization (the specificity by flow cytometry, binding to PD-1 reduced by 84.8, 93.5, and 93.9% in BxPC-3 cells after treatment with 1, 10, and 100 µg/ml of nanobody, respectively) [64]. Also, Miyazaki et al. demonstrated peptide-barcoded nanobody (PBNb) targeting PD-1 with PBC1, PBC2, and PBC9 candidates with the 1–52 nM affinity estimated by ELISA [65]. Zhang et al. [66] developed anti-PD-1 Nb-Fc nanobody targeting PD-1 with 6.6 nM affinity measured by SPR. Ding et al. [67] reported nanobody-based trispecific T cell engager (Nb-TriTE) generated with KD values measured by SPR for hPD-1 as 782 nM, for human CD3 as 104 nM, and human fibroblast activation protein as 77.7 nM. In summary, all PD-1–specific nanobodies were developed primarily for therapeutic, not diagnostic purpose. Some candidates were characterized only partially using limited biophysical approaches and were not tested for in vivo imaging nor ex vivo diagnostic reliability. In contrast to nanobodies with the randomization of protein

loop residues, our non-immunoglobulin cysteine-free Myomedin scaffold concept provides different geometry by randomization of β-sheet residues that resulted in a portfolio of 6 MBA variants with high-affinity to hPD-1 for diagnosis or blocking effect. Myomedins with 13 kDa molecular weight provide an excellent tissue penetration, sufficient sensitivity for frozen tissue sections staining and cheap prokaryotic production costs compared to the immunoglobulin molecules.

In this manuscript, we analyzed the distribution of ^{68}Ga-labelled MBAs for up to 90 min via ex vivo biodistribution study and dynamic PET/CT imaging. The injected substances were well tolerated for several days after application as the mice used for the imaging study were sacrificed approximately 2 weeks after the imaging without clinical and neurological marks of alterations. In support, we have previously published experiments on Myomedin-derived binders (each containing 10 µg) for immunization (in Freund adjuvant) through intradermal application of experimental BALB/c mice [34, 39]. We did not record any marks of somatic or behavioral alterations, with exception of local irritation due to adjuvant co-administered with individual Myomedins. Also, we tested whether the sera from Myomedin-immunized mice recognize murine cellular antigens to investigate the potential of Myomedins acting as an autoantigens (Additional file 1: Fig. S7). We incubated pooled Myomedin-immunized sera (dilution 1:50) and naive sera with Triton-X100-permeabilized murine fibroblasts NIH 3T3 followed by IgG binding detection with Alexa Fluor 488-labeled anti-IgG antibody. In Additional file 1: Fig. S7, no detectable reaction of Myomedin-immunized mice sera with cell antigens was noticed. As a positive control, we used formerly collected sera from mice immunized with murine heat shock protein 70 kDa (Hsp70). In contrast to no reactivity of Myomedin-immunized mice, the sera from Hsp70-immunized mice recognized moderately the intracellular antigens, according to observed pattern probably inside mitochondrion or endoplasmic reticulum (Additional file 1: Fig. S7).

Collectively, we present here a concept of highly complex β-sheet combinatorial library developed on Myomedin scaffold as a valuable alternative for the generation of small protein binders for biomedical applications. Randomization of amino acid residues on a flat β-sheet surface provides a proof-of-concept for the selection of high-affinity binders and, thus, completes a portfolio of loop-type scaffold libraries [34, 39, 51] and three-helix bundle-based libraries [68–70]. Herein, we provide evidence that β-sheet-derived MBA variants exhibit PD-1 specificity and stability in human serum. The binding affinity of the best MBA-series candidates is sufficient for selective in vitro diagnostics of tumor tissue biopsies and sensitive for in vivo PET/CT imaging. Due to small size of Myomedin binders, which allows an increased tumor tissue penetration, the engineered MBA protein variants should be beneficial for monitoring PD-1$^+$ cell populations in solid tumors, including NSCLC.

Supplementary Information

The online version contains supplementary material available at https://doi.org/10.1186/s12967-024-05210-x.

Additional file1. SI Methodology: Screening of PD-1 specific variants by ELISA; Production and purification of MBA variants; Cell cultures; DNA plasmid preparation and transfections of HEK293T cells; Transfection of HEK293T cells for immunofluorescence staining; Transfection of HEK293T cells for binding affinity measurement using LigandTracer; Detection of MBA binding to cell surface by immunofluorescence staining; Binding kinetics of MBA proteins measured with Ligand Tracer and competition assay; Competition ELISA; Determination of K_d by micro-scale thermophoresis (MST); **SI Results:** Figure S1. Summary of experimental and predicted geometries of PD-1/PD-L1 complexes. Table S1. List of primers used for assembly of myomedin beta sheet combinatorial library where XXX indicates randomized position. Figure S2. List of sequences of selected MBA variants and summary of most probable predicted PD-1 binding modes. Table S2. Criteria for selection of MBA variants for experiments performed on (A) tissue sections and in vivo experiments performed on (B) mice. Table S3. Estimation of kinetic parameters for six MBA variants binding to human PD-1 cDNA-transfected HEK293T cells analyzed by LigandTracer Green. Table S4. Sequence comparison between extracellular part of human and mouse PD-1. Table S5. Estimation of kinetic parameters for three MBA variants binding to murine PD-1 cDNAtransfected HEK293T cells analyzed by LigandTracer Green. Table S6. Radiochemical purity of 68Ga-binders and in vitro stability in human serum. Figure S3. Distribution of 68Galium-labeled MBA066 and MyoWT proteins in *E. coli* infected Balb/c mice. Figure S4. Competition of MBA proteins with human PD-L1 for binding to PD-1 using ELISA. Figure S5. Competition of MBA proteins with human PD-L1 for binding to PD-1-transfected HEK293T cells. Figure S6. Competition of MBA proteins with hPD-L1 for binding to hPD-1 using LigandTracer. Table S7. Comprehensive overview of MBA Myomedin variants used in this study. Figure S7. Myomedins do not elicit autoantibodies after immunization of experimental mice.

Acknowledgements

The authors acknowledge CF CF Biophysic, CF Cryst, CF Diff of CIISB, Instruct-CZ Centre, supported by MEYS CR (LM2023042) and European Regional Development Fund-Project "UP CIISB"(No. CZ.02.1.01/0.0/0.0/18_046/0015974).

Author contributions

J.M.M., H.P and L.V. assembled Myomedin combinatorial library, performed large scale screening and analysis of protein variants and wrote the paper. M.K., Y.G., N.P. designed and performed research and analyzed data. J.Č designed the Myomedin library concept, performed bioinformatics analysis, modeling by docking and wrote the paper. L.R.K., J.Š performed histochemical evaluation on tissue sections, analyzed data and wrote the paper. P.K., M.P., K.B. and K.K. performed in vivo and ex vivo analysis of protein biodistribution, analyzed data and wrote the paper. S.B. performed bioinformatics, analyzed data and wrote the paper. P.M. and M.R. conceptualized the project, directed research, designed research, analyzed data, and wrote the paper.

Funding

The authors are thankful for the received support by Czech Health Research Council, Ministry of Health of the Czech Republic by the Grant No. NU21-03-00372, the project National Institute of Virology and Bacteriology (Programme EXCELES, ID Project No. LX22NPO5103) funded by the European Union – Next Generation EU, the Institute of Biotechnology of the Czech Academy of Sciences v.v.i. (Institutional Research Concept, RVO: 86652036) and University Hospital Olomouc (Conceptual development of research organization grant MHCZ- DRO, FNOL, 00098892.

Data availability
All data generated or analyzed during this study are included in this article and its Supplementary Information/Source Data file. Source data are (will be) provided with this paper. The coordinates from ClusPro protein-protein docking and PyMOL session summarizing the results are available from the zenodo repository (https://doi.org/10.5281/zenodo.8182102).

Declarations

Ethics approval and consent to participate
All of the animal experiments were conducted in accordance with regulations and guidelines of the Czech Animal Protection Act (No. 246/1992), and with the approval of the Czech Ministry of Education, Youth, and Sports (MSMT-24421/2021-4) and the institutional Animal Welfare Committee of the Faculty of Medicine and Dentistry of Palacky University in Olomouc.

Consent for publication
Not applicable.

Competing interests
All authors have read the journal's policy on disclosure of potential conflicts of interest and declared no conflict of interest.

Author details
[1]Laboratory of Ligand Engineering, Institute of Biotechnology of the Czech Academy of Sciences, BIOCEV Research Center, Průmyslová 595, 252 50 Vestec, Czech Republic. [2]Department of Immunology, University Hospital Olomouc, Zdravotníků 248/7, 77900 Olomouc, Czech Republic. [3]Department of Immunology, Faculty of Medicine and Dentistry, Palacky University Olomouc, Hněvotínská 3, 779 00 Olomouc, Czech Republic. [4]Laboratory of Structural Bioinformatics of Proteins, Institute of Biotechnology of the Czech Academy of Sciences, BIOCEV Research Center, Průmyslová 595, 252 50 Vestec, Czech Republic. [5]Institute of Molecular and Translational Medicine, Faculty of Medicine and Dentistry and Czech Advanced Technology and Research Institute, Palacky University Olomouc, Hněvotínská 5, 779 00 Olomouc, Czech Republic. [6]Institute of Clinical and Molecular Pathology, Faculty of Medicine and Dentistry, Palacky University Olomouc, Hněvotínská 3, 779 00 Olomouc, Czech Republic.

Received: 3 October 2023 Accepted: 16 April 2024
Published online: 06 May 2024

References

1. Wykes MN, Lewin SR. Immune checkpoint blockade in infectious diseases. Nat Rev Immunol. 2018;18(2):91–104.
2. Wherry EJ. T cell exhaustion. Nat Immunol. 2011;12(6):492–9.
3. Pardoll DM. The blockade of immune checkpoints in cancer immunotherapy. Nat Rev Cancer. 2012;12(4):252–64.
4. He X, Xu C. Immune checkpoint signaling and cancer immunotherapy. Cell Res. 2020;30(8):660–9.
5. Ishida Y, Agata Y, Shibahara K, Honjo T. Induced expression of Pd-1, a novel member of the immunoglobulin gene superfamily. Upon Programmed Cell-Death Embo J. 1992;11(11):3887–95.
6. Sharpe AH, Pauken KE. The diverse functions of the PD1 inhibitory pathway. Nat Rev Immunol. 2018;18(3):153–67.
7. Chemnitz JM, Parry RV, Nichols KE, June CH, Riley JL. SHP-1 and SHP-2 associate with immunoreceptor tyrosine-based switch motif of programmed death 1 upon primary human T cell stimulation, but only receptor ligation prevents T cell activation. J Immunol. 2004;173(2):945–54.
8. Iwai Y, Ishida M, Tanaka Y, Okazaki T, Honjo T, Minato N. Involvement of PD-L1 on tumor cells in the escape from host immune system and tumor immunotherapy by PD-L1 blockade. Proc Natl Acad Sci U S A. 2002;99(19):12293-7.
9. Barber DL, Wherry EJ, Masopust D, Zhu B, Allison JP, Sharpe AH, Freeman GJ, Ahmed R. Restoring function in exhausted CD8 T cells during chronic viral infection. Nature. 2006;439(7077):682–7.
10. Antonia SJ, Kim SW, Spira AI, Ahn MJ, Ou SHI, Stjepanovic N, Fasolo A, Jagert D, Ottt PA, Wainberg ZA, et al. Safety and clinical activity of durvalumab (MEDI4736), an anti-PD-L1 antibody, in treatment-naive patients with advanced non small-cell lung cancer. J Clin Oncol. 2016;34(15):9029.
11. Borghaei H, Paz-Ares L, Horn L, Spigel DR, Steins M, Ready NE, Chow LQ, Vokes EE, Felip E, Holgado E, et al. Nivolumab versus Docetaxel in Advanced Nonsquamous Non-Small-Cell Lung Cancer. N Engl J Med. 2015;373(17):1627–39.
12. Robert C, Schachter J, Long GV, Arance A, Grob JJ, Mortier L, Daud A, Carlino MS, McNeil C, Lotem M. Pembrolizumab versus ipilimumab in advanced melanoma. N Engl J Med. 2015;372(26):2521–32.
13. Brahmer JR, Tykodi SS, Chow LQM, Hwu WJ, Topalian SL, Hwu P, Drake CG, Camacho LH, Kauh J, Odunsi K, et al. Safety and activity of anti-PD-L1 antibody in patients with advanced cancer. N Engl J Med. 2012;366(26):2455–65.
14. Maute RL, Gordon SR, Mayer AT, McCracken MN, Natarajan A, Ring NG, Kimura R, Tsai JM, Manglik A, Kruse AC, et al. Engineering high-affinity PD-1 variants for optimized immunotherapy and immuno-PET imaging. Proc Natl Acad Sci USA. 2015;112(47):E6506-6514.
15. Nishi W, Wakamatsu E, Machiyama H, Matsushima R, Saito K, Yoshida Y, Nishikawa T, Takehara T, Toyota H, Furuhata M, et al. Evaluation of therapeutic PD-1 antibodies by an advanced single-molecule imaging system detecting human PD-1 microclusters. Nat Commun. 2023;14(1):3157.
16. Ninomiya K, Hotta K. Pembrolizumab for the first-line treatment of non-small cell lung cancer. Expert Opin Biol Th. 2018;18(10):1015–21.
17. Antonia SJ, Villegas A, Daniel D, Vicente D, Murakami S, Hui R, Yokoi T, Chiappori A, Lee KH, de Wit M, et al. Durvalumab after chemoradiotherapy in stage III non-small-cell lung cancer. N Engl J Med. 2017;377(20):1919–29.
18. Rittmeyer A, Barlesi F, Waterkamp D, Park K, Ciardiello F, von Pawel J, Gadgeel SM, Hida T, Kowalski DM, Dols MC, et al. Atezolizumab versus docetaxel in patients with previously treated non-small-cell lung cancer (OAK): a phase 3, open-label, multicentre randomised controlled trial. Lancet. 2017;389(10066):255–65.
19. Brahmer J, Reckamp KL, Baas P, Crino L, Eberhardt WE, Poddubskaya E, Antonia S, Pluzanski A, Vokes EE, Holgado E, et al. Nivolumab versus docetaxel in advanced squamous-cell non-small-cell lung cancer. N Engl J Med. 2015;373(2):123–35.
20. Chen PL, Roh W, Reuben A, Cooper ZA, Spencer CN, Prieto PA, Miller JP, Bassett RL, Gopalakrishnan V, Wani K, et al. Analysis of immune signatures in longitudinal tumor samples yields insight into biomarkers of response and mechanisms of resistance to immune checkpoint blockade. Cancer Discov. 2016;6(8):827–37.
21. Camidge DR, Doebele RC, Kerr KM. Comparing and contrasting predictive biomarkers for immunotherapy and targeted therapy of NSCLC. Nat Rev Clin Oncol. 2019;16(6):341–55.
22. Hummelink K, van der Noort V, Muller M, Schouten RD, Lalezari F, Peters D, Theelen WSME, Koelzer VH, Mertz KD, Zippelius A, et al. PD-1T TILs as a predictive biomarker for clinical benefit to PD-1 blockade in patients with advanced NSCLC. Clin Cancer Res. 2022;28(22):4893–906.
23. Uryvaev A, Passhak M, Hershkovits D, Sabo E, Bar-Sela G. The role of tumor-infiltrating lymphocytes (TILs) as a predictive biomarker of response to anti-PD1 therapy in patients with metastatic non-small cell lung cancer or metastatic melanoma. Med Oncol. 2018;35(3):25.
24. Kaira K, Yamaguchi O, Kawasaki T, Hashimoto K, Miura Y, Shiono A, Mouri A, Imai H, Kobayashi K, Yasuda M, et al. Prognostic significance of tumor infiltrating lymphocytes on first-line pembrolizumab efficacy in advanced non-small cell lung cancer. Discov Oncol. 2023;14(1):6.
25. Niemeijer AN, Leung D, Huisman MC, Bahce I, Hoekstra OS, van Dongen G, Boellaard R, Du S, Hayes W, Smith R, et al. Whole body PD-1 and PD-L1 positron emission tomography in patients with non-small-cell lung cancer. Nat Commun. 2018;9(1):4664.
26. Ryman JT, Meibohm B. Pharmacokinetics of monoclonal antibodies. CPT Pharmacometrics Syst Pharmacol. 2017;6(9):576–88.
27. Lee CM, Tannock IF. The distribution of the therapeutic monoclonal antibodies cetuximab and trastuzumab within solid tumors. BMC Cancer. 2010;10:255.
28. Wu F, Fan J, He Y, Xiong A, Yu J, Li Y, Zhang Y, Zhao W, Zhou F, Li W, et al. Single-cell profiling of tumor heterogeneity and the microenvironment in advanced non-small cell lung cancer. Nat Commun. 2021;12(1):2540.
29. Karamitopoulou-Diamantis E, Andreou A, Perren A, Gloor B. Spatial immunoarchitectural intra-tumor heterogeneity is associated with early tumor recurrence in pancreatic cancer. Lab Invest. 2021;101(Suppl 1):1047–8.

30. Francis DM, Thomas SN. Progress and opportunities for enhancing the delivery and efficacy of checkpoint inhibitors for cancer immunotherapy. Adv Drug Deliv Rev. 2017;114:33–42.
31. Deng R, Bumbaca D, Pastuskovas CV, Boswell CA, West D, Cowan KJ, Chiu H, McBride J, Johnson C, Xin Y, et al. Preclinical pharmacokinetics, pharmacodynamics, tissue distribution, and tumor penetration of anti-PD-L1 monoclonal antibody, an immune checkpoint inhibitor. Mabs-Austin. 2016;8(3):593–603.
32. Pinotsis N, Chatziefthimiou SD, Berkemeier F, Beuron F, Mavridis IM, Konarev PV, Svergun DI, Morris E, Rief M, Wilmanns M. Superhelical architecture of the myosin filament-linking protein myomesin with unusual elastic properties. PLoS Biol. 2012;10(2): e1001261.
33. Schymkowitz J, Borg J, Stricher F, Nys R, Rousseau F, Serrano L. The FoldX web server: an online force field. Nucleic Acids Res. 2005;33(Web Server issue):W382-388.
34. Kuchar M, Kosztyu P, Liskova VD, Cerny J, Petrokova H, Vroblova E, Maly M, Vankova L, Krupka M, Kafkova LR, et al. Myomedin scaffold variants targeted to 10E8 HIV-1 broadly neutralizing antibody mimic gp41 epitope and elicit HIV-1 virus-neutralizing sera in mice. Virulence. 2021;12(1):1271–87.
35. Sali A, Blundell TL. Comparative protein modeling by satisfaction of spatial restraints. J Mol Biol. 1993;234(3):779–815.
36. Jumper J, Evans R, Pritzel A, Green T, Figurnov M, Ronneberger O, Tunyasuvunakool K, Bates R, Zidek A, Potapenko A, et al. Highly accurate protein structure prediction with AlphaFold. Nature. 2021;596(7873):583–9.
37. Kozakov D, Beglov D, Bohnuud T, Mottarella SE, Xia B, Hall DR, Vajda S. How good is automated protein docking? Proteins. 2013;81(12):2159–66.
38. Kozakov D, Brenke R, Comeau SR, Vajda S. PIPER: an FFT-based protein docking program with pairwise potentials. Proteins. 2006;65(2):392–406.
39. Daniel Liskova V, Kosztyu P, Kuchar M, Cerny J, Bharadwaj S, Petrokova H, Vroblova E, Krupka M, Maly M, Zosincukova T, et al. Myomedin replicas of gp120 V3 loop glycan epitopes recognized by PGT121 and PGT126 antibodies as non-cognate antigens for stimulation of HIV-1 broadly neutralizing antibodies. Front Immunol. 2022;13:1066361.
40. UniProt C. UniProt: a worldwide hub of protein knowledge. Nucleic Acids Res. 2019;47(D1):D506–15.
41. Islam S, Vick E, Huber B, Morales C, Spier C, Cooke L, Weterings E, Mahadevan D. Co-targeting aurora kinase with PD-L1 and PI3K abrogates immune checkpoint mediated proliferation in peripheral T-cell lymphoma: a novel therapeutic strategy. Oncotarget. 2017;8(59):100326–38.
42. Ahmadzadeh M, Johnson LA, Heemskerk B, Wunderlich JR, Dudley ME, White DE, Rosenberg SA. Tumor antigen-specific CD8 T cells infiltrating the tumor express high levels of PD-1 and are functionally impaired. Blood. 2009;114(8):1537–44.
43. Han Y, Liu D, Li L. PD-1/PD-L1 pathway: current researches in cancer. Am J Cancer Res. 2020;10(3):727–42.
44. Fridman WH, Pages F, Sautes-Fridman C, Galon J. The immune contexture in human tumours: impact on clinical outcome. Nat Rev Cancer. 2012;12(4):298–306.
45. Bruni D, Angell HK, Galon J. The immune contexture and Immunoscore in cancer prognosis and therapeutic efficacy. Nat Rev Cancer. 2020;20(11):662–80.
46. Pages F, Mlecnik B, Marliot F, Bindea G, Ou FS, Bifulco C, Lugli A, Zlobec I, Rau TT, Berger MD, et al. International validation of the consensus Immunoscore for the classification of colon cancer: a prognostic and accuracy study. Lancet. 2018;391(10135):2128–39.
47. Havel JJ, Chowell D, Chan TA. The evolving landscape of biomarkers for checkpoint inhibitor immunotherapy. Nat Rev Cancer. 2019;19(3):133–50.
48. Tumeh PC, Harview CL, Yearley JH, Shintaku IP, Taylor EJM, Robert L, Chmielowski B, Spasic M, Henry G, Ciobanu V, et al. PD-1 blockade induces responses by inhibiting adaptive immune resistance. Nature. 2014;515(7528):568.
49. Richards DA. Exploring alternative antibody scaffolds: antibody fragments and antibody mimics for targeted drug delivery. Drug Discov Today Technol. 2018;30:35–46.
50. Vazquez-Lombardi R, Phan TG, Zimmermann C, Lowe D, Jermutus L, Christ D. Challenges and opportunities for non-antibody scaffold drugs. Drug Discov Today. 2015;20(10):1271–83.
51. Son S, Park J, Seo H, Lee HT, Heo YS, Kim HS. A small-sized protein binder specific for human PD-1 effectively suppresses the tumour growth in tumour mouse model. J Drug Target. 2020;28(4):419–27.
52. Bryan CM, Rocklin GJ, Bick MJ, Ford A, Majri-Morrison S, Kroll AV, Miller CJ, Carter L, Goreshnik I, Kang A, et al. Computational design of a synthetic PD-1 agonist. Proc Natl Acad Sci U S A. 2021;118(29): e2102164118.
53. Liang Z, Tian Y, Cai W, Weng Z, Li Y, Zhang H, Bao Y, Li Y. High-affinity human PD-L1 variants attenuate the suppression of T cell activation. Oncotarget. 2017;8(51):88360–75.
54. Lin X, Lu X, Luo G, Xiang H. Progress in PD-1/PD-L1 pathway inhibitors: from biomacromolecules to small molecules. Eur J Med Chem. 2020;186: 111876.
55. Wu Q, Jiang L, Li SC, He QJ, Yang B, Cao J. Small molecule inhibitors targeting the PD-1/PD-L1 signaling pathway. Acta Pharmacol Sin. 2021;42(1):1–9.
56. Cheng X, Veverka V, Radhakrishnan A, Waters LC, Muskett FW, Morgan SH, Huo J, Yu C, Evans EJ, Leslie AJ, et al. Structure and interactions of the human programmed cell death 1 receptor. J Biol Chem. 2013;288(17):11771–85.
57. Tang S, Kim PS. A high-affinity human PD-1/PD-L2 complex informs avenues for small-molecule immune checkpoint drug discovery. Proc Natl Acad Sci U S A. 2019;116(49):24500–6.
58. Lin DY, Tanaka Y, Iwasaki M, Gittis AG, Su HP, Mikami B, Okazaki T, Honjo T, Minato N, Garboczi DN. The PD-1/PD-L1 complex resembles the antigen-binding Fv domains of antibodies and T cell receptors. Proc Natl Acad Sci USA. 2008;105(8):3011–6.
59. Latchman Y, Wood C, Chemova T, Iwai Y, Malenkovich N, Long A, Bourque K, Boussiotis V, Nishimura H, Honjo T, et al. PD-L2, a novel B7 homologue, is a second ligand for PD-1 and inhibits T cell activation. Faseb J. 2001;15(4):A345-A345.
60. Freeman GJ, Long AJ, Iwai Y, Bourque K, Chernova T, Nishimura H, Fitz LJ, Malenkovich N, Okazaki T, Byrne MC, et al. Engagement of the PD-1 immunoinhibitory receptor by a novel B7 family member leads to negative regulation of lymphocyte activation. J Exp Med. 2000;192(7):1027–34.
61. Zhang X, Schwartz JC, Guo X, Bhatia S, Cao E, Lorenz M, Cammer M, Chen L, Zhang ZY, Edidin MA, et al. Structural and functional analysis of the costimulatory receptor programmed death-1. Immunity. 2004;20(3):337–47.
62. Said EA, Dupuy FP, Trautmann L, Zhang Y, Shi Y, El-Far M, Hill BJ, Noto A, Ancuta P, Peretz Y, et al. Programmed death-1-induced interleukin-10 production by monocytes impairs CD4+ T cell activation during HIV infection. Nat Med. 2010;16(4):452–9.
63. Bally AP, Lu P, Tang Y, Austin JW, Scharer CD, Ahmed R, Boss JM. NF-κB regulates PD-1 expression in macrophages. J Immunol. 2015;194(9):4545–54.
64. Wen BY, Zhao L, Wang YC, Qiu CN, Xu ZM, Huang KL, Zhu H, Li ZM, Li HJ. Nanobodies targeting the interaction interface of programmed death receptor 1 (PD-1)/PD-1 ligand 1 (PD-1/PD-L1). Prep Biochem Biotech. 2020;50(3):252–9.
65. Miyazaki T, Aoki W, Koike N, Sato T, Ueda M. Application of peptide barcoding to obtain high-affinity anti-PD-1 nanobodies. J Biosci Bioeng. 2023;136(3):173–81.
66. Zhang Y, Yang S, Jiang D, Li Y, Ma S, Wang L, Li G, Wang H, Zhang A, Xu G. Screening and identification of an anti-PD-1 nanobody with antitumor activity. Biosci Rep. 2022;43(1): BSR20221546.
67. Ding ZQ, Sun SY, Wang X, Yang XM, Shi W, Huang XN, Xie SX, Mo FZ, Hou XQ, Liu AQ, et al. Nanobody-based trispecific T cell engager (Nb-TriTE) enhances therapeutic efficacy by overcoming tumor-mediated immunosuppression. J Hematol Oncol. 2023;16(1):115.
68. Kosztyu P, Kuchar M, Cerny J, Barkocziova L, Maly M, Petrokova H, Czernekova L, Liskova V, Raskova Kafkova L, Knotigova P, et al. Proteins mimicking epitope of HIV-1 virus neutralizing antibody induce virus-neutralizing sera in mice. EBioMedicine. 2019;47:247–56.
69. Smejkal J, Maly P, Kuchar M, Panova N, Semeradtova A, Aubrecht P, Stofik M, Maly J. Cell immunocapture microfluidic chip based on high-affinity recombinant protein binders. Biosens Bioelectron. 2021;172: 112784.
70. Frejd FY, Kim KT. Affibody molecules as engineered protein drugs. Exp Mol Med. 2017;49: e306.

Publisher's Note

3.5. TREM-2 physiological and pathological functions.

Scientific outcomes:

Publication: Bharadwaj S, Groza Y, Mierzwicka JM, Malý P. Current understanding on TREM-2 molecular biology and physiopathological functions. Int Immunopharmacol. 2024 Jun 15;134:112042. DOI: 10.1016/j.intimp.2024.112042. Epub 2024 May 3. PMID: 38703564.

Background: TREM-2 is a glycosylated receptor from the immunoglobulin superfamily, predominantly expressed in the myeloid cell lineage. It is recognized for its role in regulating both adaptive and innate immunity. TREM-2 influences NK cell differentiation via the PI3K and PLCγ signaling pathways and can partially activate or directly inhibit T cells. Overexpression of TREM-2 is associated with enhanced phagocytosis, reduced TLR-mediated inflammatory cytokine production, increased transcription of anti-inflammatory cytokines, and altered T cell function. In contrast, TREM-2-deficient cells show reduced phagocytic function and increased production of proinflammatory cytokines, leading to inflammatory injuries and an immunosuppressive environment that promotes disease progression. Despite extensive research linking TREM-2^{+} cells to various diseases, including neurodegenerative disorders and cancer, many aspects of TREM-2 signaling in pathological conditions remain poorly understood. This review summarizes current knowledge on TREM-2 biology and its cell-specific expression, highlighting key TREM-2-dependent functions in pathophysiological conditions. Additionally, we discuss the molecular regulation and broader biological significance of TREM-2, proposing alternative strategies for mitigating TREM-2-associated abnormalities. Finally, we explore TREM-2's role in supporting an immunosuppressive cancer environment and its potential as a drug target for cancer immunotherapy. TREM-2 stimulates suppressive cells like TAMs and MDSCs. This comprehensive overview aims to address the challenges in developing effective clinical therapies for TREM-2-related diseases. Its potential as a therapeutic target, particularly in combination with PD-1/PD-L1 checkpoint inhibitors, offers a promising avenue for enhancing cancer immunotherapy. However, further research is needed to elucidate the precise mechanisms of TREM2's action.

Contribution: I collected information for the publication and contributed to assembling passages about TREM-2 function and role in cancer. Also, I assembled tables about TREM-2 expression on different cancer cell types and TILs.

Graphical abstract

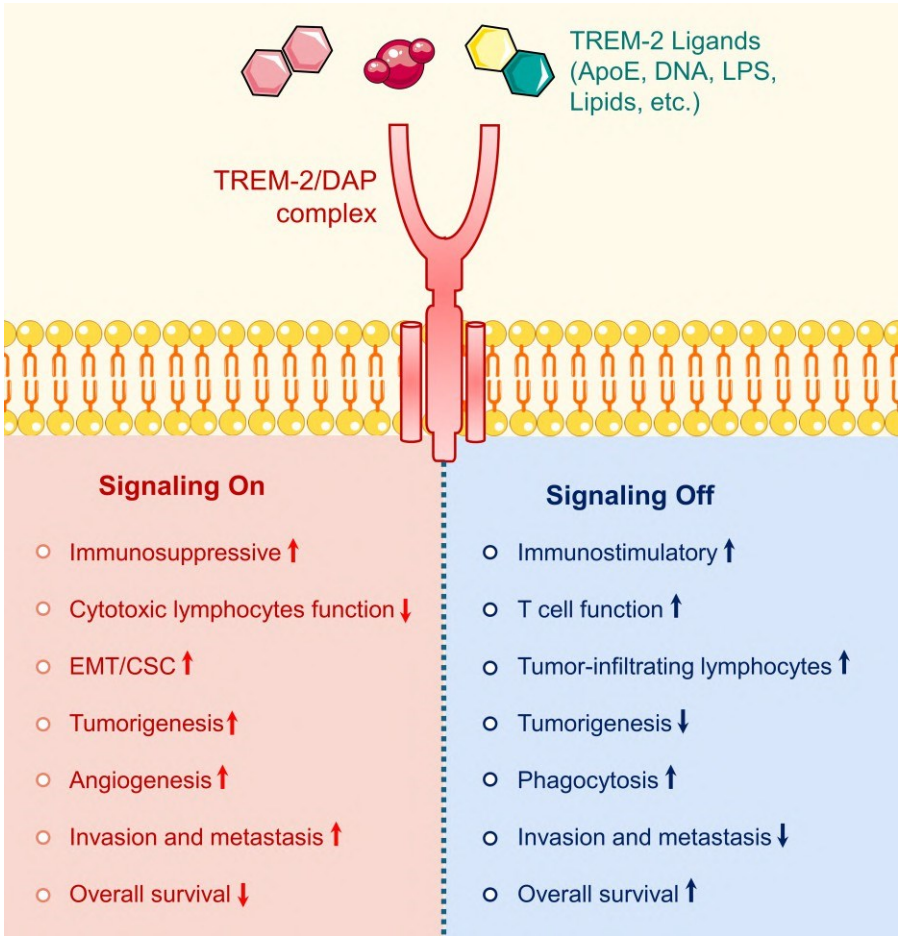

International Immunopharmacology 134 (2024) 112042

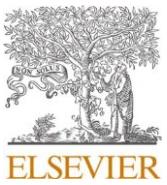

Contents lists available at ScienceDirect

International Immunopharmacology

journal homepage: www.elsevier.com/locate/intimp

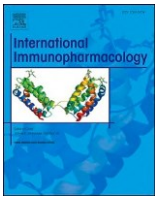

Review

Current understanding on TREM-2 molecular biology and physiopathological functions

Shiv Bharadwaj *, Yaroslava Groza, Joanna M. Mierzwicka, Petr Malý *

Laboratory of Ligand Engineering, Institute of Biotechnology of the Czech Academy of Sciences, BIOCEV Research Center, Průmyslová 595, 252 50 Vestec, Czech Republic

ARTICLE INFO

Editor: Noriyasu Hirasawa

Keywords:
Cancer
Cell signaling
Cytokines
Inflammation
Immunotherapy

ABSTRACT

Triggering receptor expressed on myeloid cells 2 (TREM-2), a glycosylated receptor belonging to the immunoglobin superfamily and especially expressed in the myeloid cell lineage, is frequently explained as a reminiscent receptor for both adaptive and innate immunity regulation. TREM-2 is also acknowledged to influence NK cell differentiation via the PI3K and PLCγ signaling pathways, as well as the partial activation or direct inhibition of T cells. Additionally, TREM-2 overexpression is substantially linked to cell-specific functions, such as enhanced phagocytosis, reduced toll-like receptor (TLR)-mediated inflammatory cytokine production, increased transcription of anti-inflammatory cytokines, and reshaped T cell function. Whereas TREM-2-deficient cells exhibit diminished phagocytic function and enhanced proinflammatory cytokines production, proceeding to inflammatory injuries and an immunosuppressive environment for disease progression. Despite the growing literature supporting TREM-2^{+} cells in various diseases, such as neurodegenerative disorders and cancer, substantial facets of TREM-2-mediated signaling remain inadequately understood relevant to pathophysiology conditions. In this direction, herein, we have summarized the current knowledge on TREM-2 biology and cell-specific TREM-2 expression, particularly in the modulation of pivotal TREM-2-dependent functions under physiopathological conditions. Furthermore, molecular regulation and generic biological relevance of TREM-2 are also discussed, which might provide an alternative approach for preventing or reducing TREM-2-associated deformities. At last, we discussed the TREM-2 function in supporting an immunosuppressive cancer environment and as a potential drug target for cancer immunotherapy. Hence, summarized knowledge of TREM-2 might provide a window to overcome challenges in clinically effective therapies for TREM-2-induced diseases in humans.

1. Introduction

Cell-cell communication and regulation of effector function are pivotal in inflammation and innate immune responses, which are strictly directive by immunoglobin (Ig) superfamily receptors [1,2]. Triggering receptor expressed on myeloid cells (TREMs) group, a set of glycosylated cell-surface specific receptors belongs to the Ig superfamily and typically expressed in the myeloid cell lineage, is involved in the regulation of various cellular crosstalk to inflammation and pathogen-induced stimuli responses [3,4]. Till now, a gene cluster including, *NCR2* (encoding NKp44), *TREM1* (also known as CD354), *TREML4* (TREM-like gene), *TREML2*, *TREM2*, and *TREML1* genes, with low sequence homology has been identified on chromosome 6p21 loci in humans (Fig. 1) [5,6]. Of note, no protein expression is reported for TREM-like genes while TREM-1 and TREM-2 are commonly studied for their modulatory function [4,7]. In particular the *TREM2* gene encoding TREM-2 protein, as the focus of this comprehensive review, is typically expressed on the cell-surfaces while its intracellular expression, in some cases, is also documented [8,9]. This intracellular expression is assumed due to the trafficking of cell-surface expressed receptor into the cytoplasm by cellular phagocytic function. In this perspective, the presenilin 1 (PS1) catalytic subunit of the γ-secretase complex has been linked to the intracellular trafficking of the TREM-2 receptor in microglia [10].

Recent genome-wide association and functional assay studies have deciphered a key role of diseases-associated myeloid cell lineage in diverse pathologies, including neurodegenerative diseases (NDDs) and cancers [11–13]. In turn, high TREM-2 expression in these cells was significantly correlated to cell-specific functions, such as enhanced phagocytosis, reduced toll-like receptor (TLR)-mediated inflammatory cytokine production, increased transcription of anti-inflammatory

* Corresponding authors.
E-mail addresses: shiv.bharadwaj@ibt.cas.cz (S. Bharadwaj), petr.maly@ibt.cas.cz (P. Malý).

https://doi.org/10.1016/j.intimp.2024.112042
Received 8 February 2024; Received in revised form 5 April 2024; Accepted 5 April 2024
Available online 3 May 2024

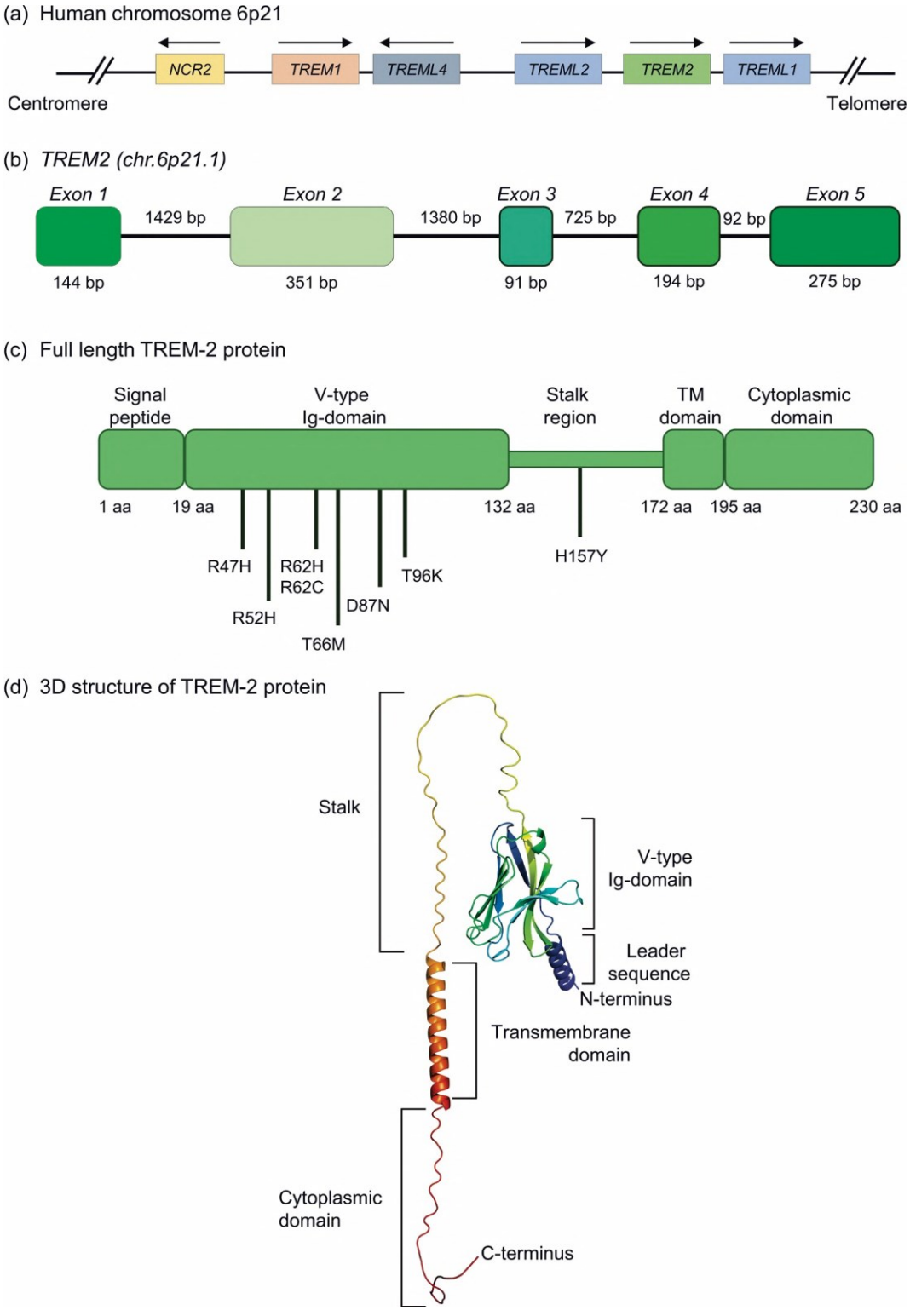

Fig. 1. Genomic location and molecular structure of TREM-2 receptor. (a) Human TREM gene clusters located on human chromosome 6p21 locus, including TREM1, TREM2, TREML1, TREML2, and TREML4 genes. Also, this locus contains the NCR2 gene encoding NKp44, a typical cell-surface receptor of Natural killer (NK) cells and group 3 innate lymphoid cells. (b) Human chromosome 6p21.1 loci for TREM2 sequence representing exons with base pair (bp) number and (c) translated full-length TREM-2 receptor labelled with amino acids (aa), structural domains, and some important mutations. (d) A three-dimensional structure of the full-length TREM-2 protein, which is predicted by AlphaFold [70]. Herein, the extracellular structure of TREM-2 contains a V-like Ig domain linked with a long stock followed by a TM domain. Also, the N-terminus leader sequence and C-terminus along with cytoplasmic domains are depicted in the predicted TREM-2 protein model.

cytokines, and reshaped T cell function [13–17]. On the contrary, deficiency of the TREM-2 receptor in myeloid lineage cells is substantially established with their reduced phagocytic function and enhanced proinflammatory cytokines production [18–21], hence resulting in inflammatory injuries. Besides, several mutations in the *TREM2* gene were identified that significantly influenced the cell-surface TREM-2 expression and distribution [22,23]. Consequently, various produced TREM-2 variants were correlated with elevated risks of NDDs development such as Alzheimer's disease (AD), Parkinson's disease (PD), Nasu-Hakola disease (NHD), Frontotemporal lobar degeneration (FTLD), and FTLD-like syndrome [24–28]. Likewise, aberrant TREM-2 expression was evidently united to tumorigenesis in multiple malignancies including gliomas [29,30], triple-negative breast cancer (TNBC) [31,32], gastric cancer (GC) [33,34], hepatocellular carcinoma (HCC) [35], and renal cell carcinoma (RCC) [36]. In addition, TREM-2 is characterized as an immunosuppressive receptor for modulating the tumor microenvironment (TME) [37], where it can stimulate suppressive cells, such as tumor-associated macrophages (TAMs) and myeloid-derived suppressor cells (MDSCs) [38,39], to prevent the anti-tumor immune responses [32].

Considering the available literature, it is convincible that TREM-2-expressing cells play a major functional role in a plethora of disease-related immune signaling hubs; thereof, the TREM-2 receptor has been projected as an important new therapeutic target [35,40,41]. Of interest, recent attention has been drawn to the fact that the TREM-2 receptor or its variants or isoforms exhibit complex pathways to have or gain specific functional activity, which substantially depends on the type of cells expressing it [35,42–46]. However, cell-specific expression of TREM-2 can be controlled transcriptionally; for instance, by the non-coding elements, transcriptional factors, and epigenetic alterations, but also through post-transcriptional modifications available to the TREM-2 receptor in the tissue or cellular microenvironment. Notably, despite mounting evidence indicating an association between TREM-2 and various cancers, substantial aspects of TREM-2 signaling, including insights on receptor-ligand interactions and modulation of TREM-2-mediated signaling in the TME, remain inadequately understood [11,40]. Therefore, in this review, first we have discussed the recent advances in structural biology of TREM-2 and associated ligands followed by adopted downstream signaling pathways, in particular modulating the pivotal TREM-2-dependent functions under physiological and pathological conditions. Also, we have aimed at pinpointing the cell-specific expression and molecular regulation of TREM-2 expression that can be used to advance our understanding of how to attenuate relevant diseases. Finally, we have confirmed generic TREM-2-associated functions as well as the clinical relevance of TREM-2 dysregulation in a cancer immunosuppressive environment and discussed it as a potential therapeutic target in cancer immunotherapy.

2. Molecular architecture and biology of TREM-2

2.1. TREM-2 structure, isoforms, and variants

The *Triggering receptor expressed on myeloid cells 2* (*TREM2*) gene is located on human chromosome 6 and consists of five exons (~693-bp complementary DNA) translating ~ 230 amino acids (aa) of type I transmembrane (TM) TREM-2 receptor (26 kDa) (Fig. 1) [6,47]. Although no crystal structure for the full-length TREM-2 receptor is available and only partial sequence (126 aa) structures for wild type and some variants are studied [48], the sequence-to-structure analysis revealed that TREM-2 contains three domains: an extracellular domain, a TM domain in the N-terminal, and a short C-terminal intracellular tail (Fig. 1). The TREM-2′s extracellular domain comprises a V-type single Ig-structure tailed by a short stalk region (ectodomain = 1–172 aa), preceding a single TM helix (173–195 aa), and a short intracellular structure lacking a signaling domain or trafficking motifs (196–230 aa) [12,49]. Of note, the TREM-2′s extracellular domain is well characterized for participation in molecular recognition and ligand binding with disulfide bonds, N-linked glycosylation, and phosphorylation sites [23,47,50,51], which are essentially required by the functional canonical TREM-2 receptor. For instance, glycosylated V-type single Ig-structure in the ectodomain was predicted to promote intermolecular interactions, including two disulfide bonds; C36 ↔ C110 and C51 ↔ C60 residues to support a specific ligand-binding pocket [48]. Importantly, there is limited structural data published on the TREM-2 ectodomain motifs participating in ligand binding or modulating TREM-2 functions [52]. Furthermore, the TM domain worked in anchoring the TREM-2 protein to the cellular membrane and comprises intramembranous lysine residue vital for alliance with its intracellular membrane adaptor proteins, named DNAX-activating protein of 10 (DAP10, 10 kDa, also known as haematopoietic cell signal transducer) and DNAX-activation protein 12 (DAP12, 12 kDa, also known as TYRO protein tyrosine kinase-binding protein, or KARAP). Meanwhile, the function of the short cytoplasmic tail in the TREM-2 receptor is yet to be solved [48].

Previously high expression of TREM-2 exons 3 and 4 was reported using microarray-based gene expression analysis in advanced AD cases [53], suggesting an alternative splicing of the TREM-2 receptor in AD [54,55]. In support, a recent RNA-seq (RNA-sequencing) data analysis in AD mice model also predicted that 15–20 % of transcripts are generated by alternative splicing of the TREM-2 receptor [56]. Besides, methylation within the *TREM2* gene was also advocated to impact alternative splicing [57]. For example, DNA methylation was noticed within exon 2 of TREM-2 [58], suggesting that the context-dependent modifications in the methylation pattern can directly influence the splicing of the TREM-2 protein. Based on these observations, thus, at least three TREM-2 isoforms have been identified in the brain tissue of AD patients by alternatively splicing of *TREM2* gene. Precisely, isoform 1 (230 aa), encoded as the canonical or full-length TREM-2 receptor, is substantially produced in humans [58]. Whereas, the transcript translating a 219-residue represents a spliced TREM-2 isoform (isoform II, results from skipping of exon 4 leading to a frameshift on exon 5) was observed for low expression compared to isoform I in the hippocampus region of AD patients [54]. Meanwhile, the transcript encoding a 222-residue spliced TREM-2 isoform (isoform III, which is produced by an alternative splice site causing a frameshift on exon 4) is yet to be resolved [59]. Additionally, spliced TREM-2 isoform IV (designated as TREM2$^{\Delta e2}$ transcript) has recently been demonstrated as a consequence of exon 2 skipping while keeping all other exons in-frame [60]. Importantly, high expression of the full-length and spliced TREM-2 isoforms have been found in AD tissue only, implying synchronized regulation of all TREM-2 isoforms expression [54]. However, it should be noted that no evidence is available demonstrating a direct translation of alternatively spliced mRNAs in humans.

In addition to the membrane-bound full-length TREM-2 isoform, alternative splicing lacking the TM domain (175–195 aa) within exon 4 and sequential proteolytic processing within the TREM-2 protein stalk by disintegrin and metalloproteases (ADAMs) [61–63] are shown to produce a soluble TREM-2 (sTREM-2) receptor [60,63,64]. At the molecular level, mechanistic insights suggested that ADAM10 and ADAM17 digest the human TREM-2 protein at the H157-S158 residual peptide bond to free the ectodomain of TREM-2 receptor [62]. Whereas an outstanding membrane-connected TREM-2 C-terminus endures intramembrane cleave by γ-secretase to release its intracellular structural domain [63]. Thus, γ-secretase-mediated TREM-2 digestion results in high production of TREM-2 C-terminal fragments (CTFs) at the plasma membrane [23,63,65]. In this perspective, a high level of TREM-2 CTFs assemblies was detected within human brain extracts [54] and cell lines [22,23,63], indicating a two-step proteolytic digestion event for sTREM-2 production. Although the exact regulatory mechanism for this process is not yet deciphered, at least in some circumstances, a substantial role of DAP12 is suggested in the sTREM-2 receptor production [66]. Likewise, the functional role of metalloprotease meprin β as a promoter to enhance

TREM-2 shedding from macrophages [67] and interleukin (IL)-13-induced sTREM-2 production in bone-marrow-derived macrophages (BMDMs) is also reported [66]. Moreover, frameshifts [55] or insertions [68] preceding exon 4 terminations at the TM domain in TREM-2 are similarly advocated for the substantial secretion of the sTREM-2 receptor. Consequently, sTREM-2, which is cleaved and released from the plasma membrane through various mechanisms, has been detected in serum and cerebrospinal fluid (CSF) [69]. However, the functional role of sTREM-2 in the extracellular fluids remains to be determined; thus, it would be interesting to further explore the possibility of sTREM-2 in biological fluids as a biomarker for different TREM-2-associated diseases.

Intriguingly, various genetic modifications have been predicted or/and validated in the *TREM2* gene, summarised elsewhere [71–73]. Accordingly, several genetic modifications contributing to disease progression, especially linked to NDDs [24–28], have been discovered in the *TREM2* gene (Table 1), For instance, genetic variations like homozygous mutations, including early-stop codons [74,75], splice site mutations [76,77], the coding stalk mutations (D134G and K186N) [78] and the coding ectodomain mutations (Y38C, T66M, and V126G) [79–81], and heterozygous variants [59,82], have been reported for the *TREM2* gene. In this perspective, most of the disease-associated TREM-2 variants' expression was noted as a result of alternative splicing of the TREM-2 isoforms [76,83–87]. Generally, the disease-associated TREM-2 variants are categorized in exon 2 that modified the ligand-binding structural domains like the ones' needed for association of DAP12, functional protein folding, and stability of the TREM-2 receptor. For instance, the polycystic lipomembranous osteodysplasia with sclerosing leukoencephalopathy (PLOSL)-associated TREM-2 variant c.482 + 2 T > C carrying a single nucleotide switch at a splice-donor consensus position within intron 3 site consequences in the loss of exon 3 in supplement to exon 2 and/or exon 4 [78]. This kind of splicing is typically established for the release of sTREM-2, which either lacks the TM domain or both the TM domain and ectodomain [76]. Also, disease-associated TREM-2 variants were related to a loss of protective activity by the TREM-2 receptor [88,89] while some mutations in TREM-2 appeared to lock immune cells in their homeostatic stage [90,91]. Likewise, an essential role of some mutations, such as Y38C, T66M, and V126G, is mentioned in the folding of the TREM-2 receptor [48]. Accordingly, Y38C and T66M mutations-induced structural modifications were determined in the release of sTREM-2 in cultured cells [22,92]. Similarly, obvious modifications were demonstrated for the T66M variant in homozygous [22,93] and heterozygous individuals for the sTREM-2 secretion [92]. Moreover, consistent with impaired protein folding, the TREM-2^{Y38C} and TREM-2^{T66M} variants also showed a high tendency for proteasomal degradation [94]. In contrast, some NDDs-associated TREM-2 mutations, i.e., R62H, T96K, and D87N, displayed on the protein surface were not anticipated for substantial structural modifications [95] but rather reported to disturb the binding of the ligand with the receptor [48]. However, the role of the NDDs-associated R47H mutation was demonstrated to alter the TREM-2 protein stability [96] and decrease its binding affinity with lipid ligands [97,98]. In this context, Athena et al. [52] reported high-resolution crystal structures of the extracellular domain for apo-TREM-2 wild type (TREM-2^{wt}) and TREM-2^{R47H} variants at 2.2 and 1.8 Å, respectively. Structural analysis of the TREM-2^{wt} variant discovered that Arg^{47} residue from the N-terminal region of complementarity-determining region 1 (CDR1) protruded to form several hydrogen bonds (including the side chain of Ser^{65}, the backbone carbonyls of Thr^{66} and His^{67}, and the side chain of Asn^{68}) with residues in CDR2. This collectively produced structural stability of the CDR2 loop and the putative positive ligand–interacting surface (PLIS, responsible for ligand recognition and binding), which together maintained the receptor conformation for docking with ligands [52]. Conversely, in the TREM-2^{R47H} variant, side chains of the His^{47} residue from CDR1 failed to

Table 1
TREM-2 predicted or/and validated variants and their effects in the expressed receptor and diseases.

TREM-2 variants	Genomics modification, Codon, Region	TREM-2 isoform, Function	CSF sTREM-2 level	Shedding of TREM-2 ectodomain	Ligand-TREM-2 affinity	Related disease	References
E14X	Substitution, Missense, GAG to TAG, Exon 1	Isoform I, Complete loss	—-	—-	—-	NHD	[74,78]
A28V	Substitution, Missense, GCG to GTG, Exon 2	Isoform I	—-	—-	—-	AD, FTD	[101,103]
Q33X	Point, Nonsense CAG to TAG, Exon 2	Isoform I, Complete loss	Reduced	Reduced	Reduced	NHD, FTD	[23]
Y38C	Substitution, Missense, TAT to TGT, Exon 2	Isoform I, Complete loss	Reduced	Reduced	Reduced	NHD, FTD	[48]
D39E	Point, Missense GAC to GAG, Exon 2	Isoform I	—-	—-	—-	AD risk	[104]
R47H	Point, Missense CGC to CAC, Exon 2	Isoform I, Partial loss	Increase	Increase	Reduced	PD, AD	[22,48,105–107]
R62H	Point, Missense CGT to CAT, Exon 2	Isoform I, Partial loss	No effect	No effect	Reduced or no effect	AD risk	[48,102,108]
T66M	Substitution, Missense, ACG to ATG, Exon 2	Isoform I, Partial loss	Reduced	Reduced	Reduced	NHD, FTD	[22]
D87N	Point, Missense GAT to AAT, Exon 2	Isoform I, Partial loss	Reduced	Reduced	Reduced or increase ligand-dependent activation.	AD	[48,102]
T96K	Substitution, Missense, ACG to AAG, Exon 2	Isoform I, Partial loss	Reduced	Reduced	Increase	AD	[48]
R98W	Point, Missense CGG to TGG, Exon 2	Isoform I, Partial loss	—-	Reduced	—-	AD	[25]
R136Q	Substitution, Missense, CGG to CAG, Exon 3	Isoform I, Reduced	Reduced	Reduced	No effect	AD	[101]
H157Y	Point, Missense CAC to TAC, Exon 3	Isoform I	—-	Increase	No effect	AD	[100]
W191X	Substitution, Nonsense, TGG to TAG, Exon 4	Isoform II, Partial loss	Reduced	—-	—-	late-onset Alzheimer's disease (LOAD)	[86]
W198X	Substitution, Missense, TGG to TGA, Exon 4	Isoform I	—-	—-	—-	FTD	[109]
L211P	Substitution, Missense, CTG to CCG, Exon 4	Isoform I, Partial loss	Reduced	—-	—-	AD, FTD	[86,92]

maintain the same set of contacts to CDR2 as noted in TREM-2^{wt} Instead, His^{47} residue formed the direct hydrogen bonds with Lys^{48} in the C-terminus of the CDR1 loop and Thr^{66} in the N-terminus of CDR2 loop as well as exhibited π-π stacking with His^{67} from the CDR2 loop. Whereas His^{67} residue showed a swing (~180°) towards the C-terminal of CDR1 to maintain the interaction with His^{47} residue. As a consequence, the swing of His^{67} to make His^{47}–His^{67} stacking, the TREM-2^{R47H} variant experienced a substantial alternation in the native conformation of the CDR2 as well as its interactions with CDR1. Additionally, His^{67} as a key residue in combination with His^{47} residue was suggested to alter the pH dependence of the TREM-2^{R47H} variant, which is apt to be more sensitive to pH change, resulting in subsequent remodeling of the PLIS [52]. Collectively, such modifications were suggested to induce an increase in structural flexibility of the CDR2 loop and a reduction in the PLIS, as demonstrated by an increase in B-factors; thus, reducing or abolishing the ligand binding to the TREM-2^{R47H} variant [52]. Additionally, these alternations in the TREM-2^{R47H} variant are also assumed to be the considerable factor responsible for reduced thermal stability *in vitro*, and solubility of the TREM-2^{R47H} variant *in vivo* [52]. Similarly, molecular dynamics simulation studies also predicted that AD-associated TREM-2^{R47H} variant induced substantial conformational flexibility in the CDR1-3 loops bordering to the PLIS followed by a loss in the TREM-2 structural integrity and function [96,99]. In addition, analysis of transfectants carrying TREM-2^{R47H} constructs revealed an increase in the half-life of TREM-2 protein and resistance against proteolytic digestion in the endoplasmic reticulum (ER) by comparison to wild-type receptor [50]. Although the TREM-2^{R47H} variant showed a similar function to wild-type *in vitro* assays for sTREM-2 secretion [22], it also induced a low production of the intracellular domain (ICD) in sTREM-2 and TREM-2 [50]. Another study observed a high tendency for 219-residue TREM-2 isoform with the R47H risk allele in cortices of late-stage AD patients compared to a considerable increase in this particular TREM-2 variant expression in non-carrier AD patients [54]. Likewise, another TREM-2^{H157Y} variant was associated with abrogating TREM-2 signaling through rapid shedding of cell surface TREM-2 receptor [61,100]. Also, substantially altered glycosylation has been reported for some of the TREM-2 variants. For instance, altered glycosylation was confirmed in cells transfected with Y38C and T66M types of TREM-2 variants [22], however, not examined in several other variants [101]. Likewise, another study showed reduced glycosylation in the TREM-2^{R47H} variant *in vitro*, but not to the same degree as detected in other TREM-2 variants [22]. Interestingly, no significant variation was reported in the glycosylation level on the TREM-2^{wt} while the TREM-2^{R47H} variant induced considerable difference in the glycosylation pattern in humans [23,50,54]. Thus, further investigations are required to understand the different pathological effects of TREM-2 variants with modified glycosylation on signal transduction [102]. As the wild-type TREM-2 and disease-associated TREM-2 variants' structure continue to be determined,such results may assist in providing a better insight into the specific structural assembly and qualities essential for multifaceted roles in TREM-2 biology.

2.2. TREM-2 singling networks: Ligands and adopted cascades

As an anti-inflammatory receptor [110,111], TREM-2 has received major attention in the scientific community. Thus, using biochemical and *in vitro* assays, various ligands and adopted signaling pathways have been suggested for the TREM-2 receptor [40,112]. According to accessible literature, although the physiologic ligand(s) for the TREM-2 receptor are not yet known, numerous agents that can bind with TREM-2 have been identified, extending from several anionic molecules: phospholipids, free and bound to the plasma membrane, including deoxyribonucleic acid (DNA), lipoproteins (LDL, low-density lipoprotein), lipopolysaccharides (LPS), bacterial products, apolipoprotein E (ApoE),

Table 2
Reported ligands from various sources known for interaction with the TREM-2 receptor on different myeloid lineage cells.

Source	Ligands for TREM-2 receptor	References
Mammalian cells	THP-1 monocytes	[48]
	Heat shock protein 60	[113]
	Bone marrow-derived macrophages	[111]
	Bone marrow derived dendritic cells	[126]
	Astrocytes	[20,113,115]
	Jurkat cells	[116]
	Apoptotic cells (like Neuro2A cells, BWZ and 2B4 reporter cells)	[48,114,116,127]
Mammalian cell products	Heat shock protein 60	[113]
	β-amyloid/oligomeric Aβ	[117,118,128]
	Plexin-A1	[124]
	TREML1 (short transcript)	[129]
	Apolipoproteins (A,B,E,J)	[108,130,131]
	Lipoparticles	[102,108]
	Aminophospholipids (phosphatidylserine and phosphatidylethanolamine), Cardiolipin, Zwitterionic lipids	[116]
	Cyclophilin A	[123]
	Galectin-3	[132]
	Sphingosine-1-phosphate	[133]
	Interleukin-34	[44]
	TREM-2 ligand	[111,134]
	Transgelin-2	[135]
Bacteria/bacterial components	Whole bacteria	[117,127,136]
	LPS, lipoteichoic acid, and peptidoglycan from *E. coli*	[115]
	Campylobacter jejuni lysate	[137]
	Lipooligosaccharides from *N. gonorrhoeae*	[138]
	Anionic bacterial carbohydrates	[115]
	Cholera toxin B	[139]
Virus/viral components	Herpes simplex virus type 1 (HSV1)	[140]
	Porcine reproductive and respiratory syndrome virus (PRRSV), GP2a, GP3, GP4, GP5, Np2, and M proteins	[141]
	Severe acute respiratory syndrome coronavirus 2 (SARS-CoV-2) Main protein	[17]
Anionic molecules	Phospholipids, Glycolipids and sulfolipids	[48,102,116,130,144–146]
	DNA	[127]
	Sulfated proteoglycans	[48]
	Glycosaminoglycans	[48]
Synthetic molecules	Sulfolipid (Sulfavant A)	[145]

and heat shock proteins (HSPs) [108,112–114], and others, as detailed in Table 2. In some cases, physiologic TREM-2 ligands were identified on the cell surfaces, such as in astrocytes [115], neurons and apoptotic cells [114], peritoneal (pMAC) and BMDMs [3]. Moreover, certain tissue microenvironmental conditions, including normal cultured cells [20,114], apoptotic cells [114,116], and oligomeric Aβ [117,118], have been reported to trigger TREM-2-mediated intracellular signalling. In this context, Cyclophilin A (CypA) secretion by various stimulated cells, such as LPS-stimulated smooth muscle cells and LPS-induced macrophages, and secretion upon cell death [119–122], is considered as a typical endogenous ligand of the TREM-2 receptor [123]. In support, an external CypA treatment in myeloid cells was found to enhance the TREM-2-specific signaling transduction and upregulate proinflammatory cytokine production [123]. Furthermore, high-order protein complex formation has been reported for the TREM-2 receptor to stimulate downstream signaling transduction. In this context, Takegahara and team suggested that TREM-2 expressed on the dendritic cells (DCs) partners with another cell surface receptor, named Plexin-A1, to organize a receptor complex encompassing Plexin-A1, TREM-2, and DAP12 [124]. Intriguingly, inhibition of Plexin-A1 receptor activation by its ligand, named semaphorin 6D, was stated by lowering either DAP12 or TREM-2 expression, further supporting the functional relationship between Plexin-A1/semaphorin 6D and TREM-2/DAP12 signaling hubs [124]. Moreover, Phexin-A1 receptor-assisted binding of TREM-2 to anionic ligands on the bacterial surface was discovered to function as a phagocytic receptor to neutralize bacterial infection [115,125]. In short, based on these observations, the investigation to find the ligands for the TREM-2 receptor may incorporate the affinity with other partner-binding proteins; therefore, sophisticated approaches encompassing possible co-receptors are required for TREM-2 ligands identification.

Under classical signaling transduction (Fig. 2), the TREM-2 transmembrane domain associates with the adaptor molecules DAP12 and DAP10 to intervene downstream signaling pathway [112]. It is important to mention that DAP12 contains an immunoreceptor tyrosine-based activation motif (ITAM) in its cytosolic domain, which is absent in DAP10. Notably, TREM-2 is known to form heterodimers after attachment with DAP12 or DAP10 [146]. Thus, following the docking of ligands with TREM-2 at the extracellular domain in the monomer/heterodimer complex, the adaptor proteins endure phosphorylation to stimulate downstream pathways. In the case of TREM-2/DAP12 signaling, DAP12 is activated by Src kinase followed by recruitment of Sos1/2 and GRB2 junction proteins, whereas the RAS/MEK/ERK or mitogen-activated protein kinase (MAPK) pathway is blocked, which reduces or inhibits the release of proinflammatory cytokines [147]. Importantly, the DAP12 signals to stimulate or inhibit the inflammatory response directly correspond to the receptor it binds or the respective tissue microenvironment [3,148]. For example, TREM-2/DAP12

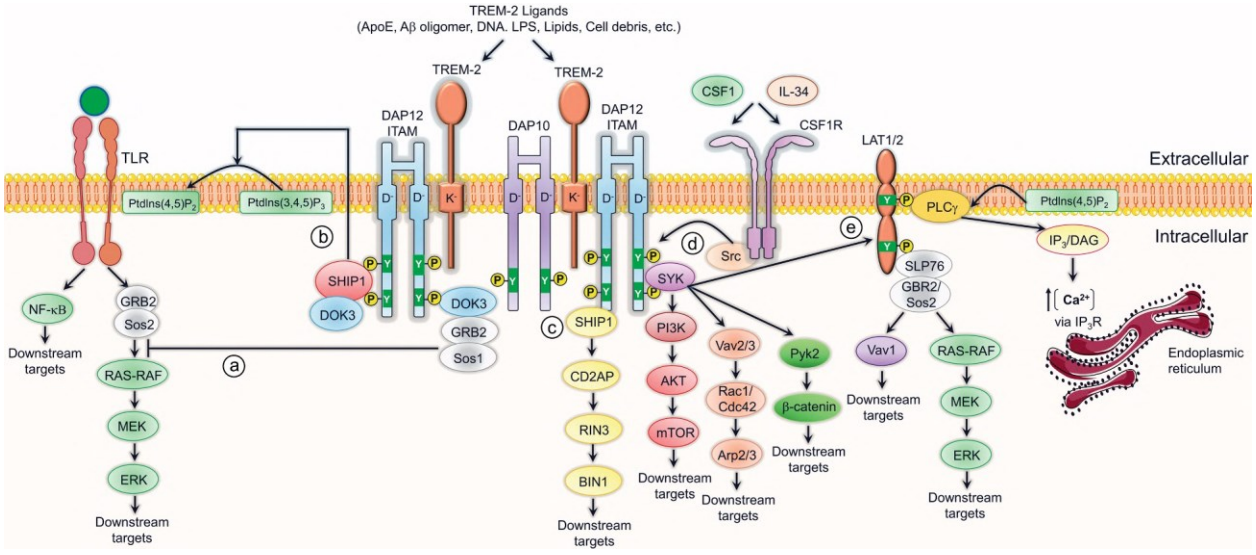

Fig. 2. TREM-2 activating different downstream signaling through DAP12/DAP10, or/and other cell surface expressed receptors after ligand detection in myeloid lineage cells. In a typical TREM-2/DAP12 modulating signaling pathway, DAP12 can transmit inhibitory signals that regulate the TLRs signaling. (a) In particular, DAP12/ITAMs dock with the phosphotyrosine-binding domain downstream of kinase 3 (DOK3), which further recruits the adapters proteins, i.e., growth factor receptor bound protein 2 (GRB2) and son of sevenless 2 (Sos2), to block GRB2/Sos1 in TLRs-mediated pathway and thereby intervening with the TLRs capacity to commence extracellular signal-regulated kinase (ERK) mediated pathways. (b) On the other hand, DAP12 and DOK3 can also recruit the Src homology 2 (SH2) domain-containing inositol phosphatase-1 (SHIP1), which further reduces phosphatidylinositol 3,4,5-trisphosphate (PtdIns(3,4,5)P_3) to phosphatidylinositol 4,5-bisphosphate (PtdIns(4,5)P_2), thus regulating the participation and activation of intracellular signalling proteins/molecules attached to the membrane by PtdIns (3,4,5)P_3. (c) Whereas Src phosphorylation of DAP12 can also regulate interaction with the SHIP1, SHIP1 further contacts the adaptor protein CD2-associated protein (CD2AP), which binds with the RAB5-activating guanine nucleotide exchange factor (RIN3), in turn, docked with Bridging Integrator 1 (BIN1). The resulting pathway, for instance, reported an increase in Aβ uptake and degradation by microglia. (d) Furthermore, TREM-2 can form a heteromeric complex with DAP12 or DAP10 to exhibit crosslinking with other surface receptors, CSF1R is considered as an example for illustration as it can modulate TREM-2/DAP12 signaling through DAP12/ITAM phosphorylation by Src kinase. Typically, in this pathway, spleen tyrosine kinase (SYK), is recruited by the TREM-2 heteromeric complex after phosphorylation by Src kinase and initiates different downstream signaling pathways using signaling molecules, such as several guanine nucleotide exchange factors Vav2/3, the nonreceptor tyrosine kinase-like proline-rich tyrosine kinase 2 (Pyk2), and phosphatidylinositol 3-kinase (PI3K); recruited to the membrane with help from DAP10. In part (e), SYK also activates via phosphorylation of the adaptors: linker for activation of T cells family member 1 (LAT1) and/or LAT2 to form docking sites for the adaptors SLP76, GRB2, and Sos2. In addition, LAT2 phosphotyrosines form docking sites for phospholipase Cγ2 (PLCγ2), which degrades phosphatidylinositol 4,5-bisphosphate (PtdIns(4,5)P_2) into inositol 1,4,5-triphosphate (Ins(1,4,5)P_3) and diacylglycerol (DAG) to elicit calcium (Ca^{2+}) mobilization from the endoplasmic reticulum through inositol trisphosphate (IP_3) receptor — Ca^{2+} channel required to control physiological and cellular processes [169]. Depending on the context, these signaling cascades can be differentially and synergistically engaged, thereby affecting a variety of cellular functions that include receptor-mediated phagocytosis, transcriptional regulation mediated by β-catenin and mTOR complex 1, metabolic homeostasis through $PIP_2/_3$-mediated activation of AKT and mTOR complex 2, RAS/MEK/ERK activation leading to transcriptional regulation of proinflammatory molecules, and Ca^{2+} modulation leading to actin remodeling. The depicted diverse signaling pathways adopted by the TREM-2 receptor were sourced from published literature [7,40,49,146,170].

pathway activation was noted to promote oligodendrocyte and osteoclast differentiation under homeostatic conditions, whereas inflammatory conditions favoured macrophages, DCs, and microglia differentiation [149]. Furthermore, the association between TREM-2/DAP12 complex and respective elicited biological functions may be influenced or altered by the incidence of TREM-2 ligands carrying varied affinity and avidity, as well as by supplementary DAP12-associated receptors. Together, these factors can considerably sponsor the production of either activating or inhibitory stimulatory molecules via the TREM-2/DAP12 pathway [150]. In this context, TREM-2/DAP12 signaling was identified to encourage colony-stimulating factor 1 (CSF1) signaling through crosstalk with the CSF1 receptor (CSF1R) [151,152] (Fig. 2). Moreover, cross-linking of TREM-2 in the presence of DAP12 and DAP10 was reported to induce AKT, ERK1/2, SYK, PLCγ2, and Vav guanine nucleotide exchange factor 3 (Vav3) phosphorylation, resulting in the activation of multiple signaling cascades for the modulation of cell actin cytoskeleton (Vav3 and SYK), differentiation and activation (PLCγ2, SYK, and ERK1/2), and survival (AKT and MCL-1) [146]. Meanwhile, in the TREM-2/DAP10-mediated signaling pathway, the downstream activation of DAP10 typically initiated the recruitment of phosphatidylinositol 3-kinase (PI3K) [146] and activation of GRB2, leading to AKT and ERK-dependent signaling pathways, respectively [146]. Of note, downstream targets for AKT singaling included a mechanistic target of rapamycin (mTOR), glycogen synthase kinase-3 beta, (GSK-3 beta), and transcription factor forkhead box O3 protein (FOXO3a), which are well established in the modulation of protein synthesis, cell cycle, and apoptosis [153]. Thus, activation of TREM-2/DAP12 or DAP10 signaling can stimulate protein and lipid phosphorylation cascades, resulting in calcium (Ca^{2+}) mobilization, integrin activation, cytoskeleton rearrangement, mTOR and MAPK pathway activation, stimulation of energetic metabolism, and other downstream molecules (Fig. 2) [146,154–157].

Importantly, due to interactions with diverse ligands, the strength and direction of TREM-2-mediated signaling can be differentially regulated in dissimilar biological environments. In this perspective, TREM-2-mediated activation of PI3K/AKT signaling showed an increase in reactive oxygen species (ROS) production, which is required to neutralize the engulfed pathogens by macrophages [158]. Also, TREM-2 activation addresses the generated anti-inflammatory responses, which liberally provokes a toll-like-receptor-4 (TLR-4)-mediated inflammatory reaction by controlling the nuclear factor kappa B (NF-κB) and c-Jun N-terminal kinase (JNK) pathways in DCs [159]. In this context, Wu et al. [160] documented that suppression of TREM-2 enhances the NF-κB signaling by accelerating the phosphorylation of NF-κB in focal cerebral ischemia/reperfusion rats. Likewise, LPS treatment was noted to diminish TREM-2 expression by triggering the JNK and NF-κB pathways, causing a synergistic effect to enhance the inflammatory responses [161]. In other studies, the TREM-2/DAP12/SYK-mediated pathway results in the activation of the PI3K and MAPK pathways, which determines the fates of different cells including macrophages and microglia survival [148,157]. For example, in the case of microglia, the TREM-2/DAP12/SYK complex has been identified to induce downstream signaling through the recruitment of an intracellular lipase, phospholipase C gamma 2 (PLCγ2), for regulating essential cellular function, including survival, lipid metabolism, phagocytosis, processing of neuronal debris, and inflammatory signaling via TLRs [162]. Interestingly, PLCγ2 activation downstream of the TREM-2 receptor is also studied to promote proliferation and metabolic pathways in pluripotent stem cell (iPSC)-derived wild-type microglia [41]. Accordingly, a lack of PLCγ2 expression was found to reduce TREM-2-dependent phagocytic activity and survival of human iPSC-derived microglia, emphasizing the critical role of PLCγ2 in TREM-2-mediated key microglia functions [163]. Additionally, in accordance with the Goldilocks principle, optimal activation of TREM-2/PLCγ2 signaling is characterized by a "just enough" level, which supports beneficial immune responses and blocks detrimental effects that could severely influence the functional activity of the immune system, impairing its response-ability effectively to insults [164]. Therefore, TREM-2/PLCγ2 pathway activation has been marked as a potential biomarker to predict a specific responsive cell phase for the microglia [164]. On the other hand, the TREM-2-mediated signaling is widely accepted as a legitimate mediator to balance the apoptosis, inflammatory response, phagocytosis, and survival pathways by microglia [165–167]. In this context, TREM-2 signaling has been elucidated to regulate microglial survival by stimulating proliferation and decreasing apoptosis through stabilization of β-catenin via an AKT/GSK3β dependent mechanism, which further stimulated the expression of responsible genes including Bcl-2, cyclin D1, and c-Myc [168]. Together, these results marked the TREM-2 receptor for modulating various functions in TREM-2^{+} cells, depending on the cellular state and the influence of the local environment [154].

Collectively, the molecular machinery of TREM-2 signaling is expected to adopt several downstream cascades specific to physiological niches and pathological contexts. However, many aspects of TREM-2-mediated interactions and cell communications remain to be fully understood. Additionally, precise TREM-2-mediated pathways under different tissue microenvironments are not yet clear but may be correlated with the difference in terms of cellular expression, critical versus persistent signaling, non-cell autonomous signaling, or phenotypic modifications in myeloid cell lineage that appear once they leave their resident tissue environment.

3. Cellular expression of TREM-2

Expression and function of TREM-2 have been determined in different cell types, supporting both normal physiological functions and promoting disease-induced pathogenesis under specific conditions, including altered expression and dysregulated function (Table 3). Also, a recent study suggested gender-specific TREM-2 expression in that only male animals were observed for TREM-2-dependent changes compared to female animals [171].

Initially, cellular TREM-2 expression was considered only during monocyte differentiation into macrophages [172], while other studies reported the absence or expression of TREM-2 in a tiny subgroup of monocytes in humans [102,173–175] and mice [176]. Also, unactivated monocytes were discovered without TREM-2 expression, whereas immature DCs and pMACs differentiated from monocytes displayed considerable TREM-2 expression [47,177]. However, a high TREM-2 expression was observed in monocytes under certain conditions; for example, in monocytes isolated from the CSF of multiple sclerosis (MS) patients [178]. Therefore, along with other reports, including the detection of TREM-2 in whole blood monocytes in humans [102,174,175], a low TREM-2 expression was established in monocytes. Furthermore, no TREM-2 expression was observed in lymphocytes [179], while an increase in TREM-2 expression was detected in DCs, osteoclasts (OCs), and macrophages derived from peripheral monocytes [172,174], emphasizing the active function of TREM-2 in the cell differentiation process [175]. Similarly, TREM-2 expression on $CD4^{+}$ and $CD8^{+}$ T cells was positively correlated with the representation of TCR-dependent activation-induced markers, such as CD25, CD69, CD134 (OX40), and CD137 (4-1BB) [17], while other studies suggested a direct inhibitory function of the TREM-2 receptor against T cell activation [32,37]. In another study, high TREM-2 expression was reported in $CD4^{+}$ T cells induced by infection and inflammation, where the TREM-2 receptor showed considerable interaction with the TCR-CD3ζ-ZAP70 complex as well as the IFN-γ receptors to produce proinflammatory Th1 responses via activation of the STAT1/STAT4 pathway [134]. These observations marked TREM-2 for mediating the regulatory mechanism in adaptive immunity and host inflammation [134]. Altogether, these observations inferred that basal expression of TREM-2 is highly controlled by the cellular microenvironment, which may be dependent on the cell differentiation state. Accordingly, using genome-wide association and protein interaction analysis, a distinctive TREM-2 expression

Table 3
Cell-specific TREM-2′s expression and its functional impact on various physiopathological processes.

Cells	TREM-2 expression	TREM-2 mediated physiopathological function	References
Dendritic cells	High	Enhanced differentiation of primary myeloid precursors to produce DCs. Partial maturation and survival of DCs. homeostatic motion of DCs to lymph nodes. DCs may promote the Bones destruction in a cholesteatoma mouse model. TREM-2/DAP12-mediated maturation of DCs to promote partial T cell activation. In nephritis DCs, reduced progression of chronic kidney disease (CKD).	[47,172,191–194]
Eosinophils	Moderate	Linked with total leukocyte count and donor body mass index in human. Enhancement in eosinophil and eosinophilic inflammation in Asthma patients.	[195,196]
Monocytes	High or low	Involved in immune responses and inflammation.	[102,173–175,178]
Macrophages	High	Proinflammatory macrophage transition into a restorative macrophage during recovery from liver laceration. Linked with tissue damage and inflammation in tissue environment. Survival and proliferation of M2-type macrophages in a respiratory virus-induced COPD mouse model. Preventing hair growth by sustaining HFSCs in a dormant state. Macrophage-mediated phagocytosis of bacteria. TAMs promote resistant to ICB therapy.	[40,66,136,197–200]
Mesenchymal stem cells	High	Negatively control the expression of TLRs on subpopulations and LPS-induced inflammatory cytokine secretion. Promotes high secretion of anti-inflammatory cytokine IL-10 under LPS-induced inflammation. Modulate tissue regeneration.	[201–204]
Microglia	High	Transition of microglia from a homeostatic to a disease-activated state. Regulation of microglial proliferation and survival by Wnt/β-catenin pathway activation. Induces inflammatory responses and enhances microglial survival. Specific TREM-2 variants prevent the maturation and loss of functional activity in microglia. Associated with an onset and progression of NDD.	[21,22,130,131,157,168,205–208]
Myeloid-derived suppressive cells	High	Causes immunosuppression in TME. Sustained myeloid cell viability under extreme conditions.	[157,202,209]
Natural killer cells	High	Promotes NK cells differentiation from pNK cells. Promote their anti-tumor responses.	[210,211]
Neutrophils	High	Immunosuppressive TREM-2^{+} neutrophils contribution in cancer development.	[212]
T cells	High	Regulatory mechanism in adaptive immunity and host inflammation.	[32,37]
Osteoclasts	High	Contributed in osteoclastogenesis and cognitive maintenance during an early AD mouse model. Mediates OC differentiation as well as bone homeostasis via controlling the rate of osteoclastogenesis.	[172,213,214]

on the cell surface has been elucidated, which is highly specific and varies according to cell type and context [180,181]. Therefore, TREM-2 expression was identified in different types of cells originating from the myeloid lineages, including granulocytes [179], DCs [173,174,179], BMDMs and monocyte-derived macrophages (MDMs) [174,175,182,183], alveolar macrophages [184,185], and OCs [74,186,187]. In contrast, Quan et al. [138] were the first to demonstrate constitutive TREM-2 expression on non-myeloid lineage differentiated cells, i.e., fallopian tube epithelium (FTE) and genitourinary epithelial cells (GECs), in humans. Later, TREM-2 expression was also estimated in mouse oligodendrocytes, as well as a low expression in neurons [8,188], mouse liver endothelial cells [189], and human fibroblasts [190]. Of note, upon LPS treatment, cell-type-specific and context-dependent downregulation (microglia, monocytes) or upregulation (DCs) have been documented for spliced TREM-2 transcript levels [55,68]. For instance, treatment with IL-13 and IL-4 on BMDMs showed an improvement in sTREM-2 secretion [66]. These observations indicated the association of TREM-2 expression with a lineage decision or differentiation phase rather than with the activation state of the cells [68]. Therefore, considering the substantial TREM-2 expression in the cell types differentiated from myeloid lineages and indeed exhibiting varied functional TREM-2 activity, the following sections discuss the widely studied cell-type-specific TREM-2 expression and its biological role in normal or pathological conditions.

3.1. Dendritic cells

The identification and characterization of TREM-2 were originally performed in human DCs, discrete bone marrow–derived leukocytes (BMDLs) required to recruit primary and secondary immune responses [215], derived from blood monocytes treated with gran- ulocyte–macrophage colony-stimulating factor (GM-CSF) and IL-4 *in vitro* [47]. Subsequently, the role of TREM-2 was studied in the enhanced differentiation of primary myeloid precursors to produce DCs in the presence of GM-CSF and IL-4 [172]. Typically, TREM-2/DAP12- mediated signaling promotes CC-chemokine receptor 7 (CCR7) expres- sion to induce partial maturation and survival of DCs through protein tyrosine kinases and extracellular signal-regulated kinase stimulation. Unlike classical activation of DCs triggered by LPS, the TREM-2/DAP12 pathway did not cause an upregulation of intercellular adhesion mole- cule 1 (ICAM-1, also known as CD54) and CD83 or IL-12 secretion, and exclusively exhibited function independent of NF-κB and p38/SAPK signaling hubs [47]. Under such conditions, in the absence of pathogens, the DAP12-associated receptor was reported to control the homeostatic motion of DCs from the periphery to the lymph nodes, aiding in the regeneration of lymph node DCs [47]. Whereas, an enhanced expression of TREM-2 in the lymph nodes suggested a definitive contribution of TREM-2 protein in the adopted migratory mechanism by DC subsets [192]. Therefore, induction of TREM-2^{+} DCs in the lymph nodes and airways is reasonably assumed to impair the defense mechanism, which was originally aimed at diminishing rather than escalating the inflammation [192]. In a similar context, Jiang et al. [193] published research

demonstrating that DCs may promote bone destruction in a mouse model of cholesteatoma through high TREM-2 expression. In contrast, Ito et al. [126] discovered that TREM-2-deficient DCs released higher concentrations of interleukins, such as IL-6, IL-12, TNF-α, and IFN-I, by comparison to wild-type DCs treated with TLR ligands. Moreover, DCs differentiated from the bone marrow of *TREM-2* knockout mice were observed to stimulate T cell proliferation with high efficiency after treatment with TLR ligands compared to the DCs of wild-type mice [126]. In addition, cross-linking of the TREM-2 receptor on immature DCs has been demonstrated to trigger high expression of some T cell co-stimulatory molecules, including MHC class II, CD40, and CD86 [47]. The TREM-2/DAP12-mediated maturation of DCs, therefore, has been suggested to promote partial T cell activation in the absence of exogenous antigens. Such type of activation is presumably essential for the homeostasis and survival of the T cell population [194]. Additionally, TREM-2 expression in nephritis DCs was documented to promote nitric oxide (NO) production to suppress Th17 differentiation and alleviate the progression of chronic kidney disease (CKD) [191]. These observations indicate that expression of TREM-2 on DCs has a multifaceted function in immune regulation, with context-dependent effects on inflammation reduction and immune enhancement.

3.2. Eosinophils

Eosinophils, characterized as granulocytes, initially originated in the bone marrow followed by their distribution in peripheral blood prior to their residency in somatic tissues. Notably, a prominent differential TREM-2 expression was detected in mouse eosinophils extracted from muscle tissue of mdx, mdx.*IL5tg*, and *IL5tg* mice models, but only a small fraction of the eosinophils showed immunoreactive TREM-2 receptor [195]. In support, proteolytic mechanisms were suggested for rapid digestion and liberation of TREM-2 from the surface of eosinophils [195]. Also, immunoreactive TREM-2 expression was noted in peripheral blood eosinophils at amounts that were linked with total leukocyte count and donor body mass index in humans [195]. Another study showed an increase in TREM-2 expression in resident cells of bronchoalveolar lavage fluid (BALF) from patients with asthma and was associated with an enhancement in eosinophil and eosinophilic inflammation [196]. Therefore, the absence of adequate literature on TREM-2 expression in relation to eosinophils draws attention to the potential of TREM-2′s relevance in identifying eosinophil function under inflammatory or disease-associated conditions.

3.3. Macrophages

Macrophages are the first line of innate immune cells, acting as protective shields against invading pathogens and malignant cells. Thus, evident heterogeneity along with strong plasticity has been reported in different macrophage subsets under various physiological and pathological conditions [216]. Accordingly, macrophages are usually grouped as proinflammatory macrophages (M1) and anti-inflammatory macrophages (M2) [216]. Besides, macrophages perform a wide range of physiological functions, including antigen processing and presentation, removal of apoptotic cells or cell debris, and phagocytosis [217], which can initiate both innate and adaptive immune responses. Typically, TREM-2 overexpression during monocyte differentiation into macrophages is suggested to be partially contributed by chromatin modification, i.e., trimethylation of Histone H3 at Lysine 4 (H3K4me3) [174]. Also, TREM-2 expression has been detected in resident macrophages of the adrenal gland, adipose tissue, and placenta [218] while a high TREM-2$^+$ macrophage population in tissue microenvironment was correlated with damage and inflammation [40]. Accordingly, high TREM-2 expression on M2-type macrophages was indicated as a marker to sort this type of cells from the pool of macrophages [219–221]. Meanwhile, in mouse macrophages, TREM-2 suppressed the TLR signaling by the adaptor protein myeloid differentiation primary-response gene 88 (MYD88) which further causes a reduction of the inflammatory response [110,111]. In this perspective, TREM-2-mediated inhibition of the inflammatory response was supported by attenuating macrophage activation through LPS stimulation [110]. Moreover, TREM-2 signaling is reported to stimulate macrophage survival under low growth factor reduction conditions (like low levels of CSF-1) *in vitro* and stressful microenvironments (such as inflammation, tissue damage, and antibody toxicity) *in vivo* [66,116,157]. In support, one study found a correlation between survival and proliferation of alternatively activated M2-type macrophages with TREM-2 expression in a respiratory virus-induced chronic obstructive pulmonary disease (COPD) mouse model [66]. Similarly, sTREM-2 released by TREM-2$^+$ macrophages was observed to inhibit apoptosis during acute viral infection, which triggered a feed-forward increase in lung macrophages and further contributed to the transformation of acute infection into a chronic inflammatory disease [66]. Also, in the skin, dermal TREM-2$^+$ macrophages were discovered to secrete the multifunctional cytokine Oncostatin M (OSM), which played an essential role in preventing hair growth by sustaining hair follicle stem cells (HFSCs) in a dormant state [198]. Besides, as a phagocytic receptor, the functional activity of TREM-2 was presented to stimulate the macrophage-mediated killing of bacteria [136]. Meanwhile, TREM-2$^+$ TAMs were detected in TME of several tumor types and linked to non-responsive patients or resistant to immune checkpoint blockade (ICB) therapy [199,200]. In contrast, TREM-2 expression was demonstrated to promote the proinflammatory macrophage transition into a restorative macrophage state as well as endothelia development during recovery from liver laceration [197]. Based on the available literature, TREM-2 emerges as a pivotal governor of two major functions depicted by macrophages, i.e., (i) TREM-2 can serve as a phagocytic receptor and (ii) as an immune regulatory receptor. Hence, further exploration of TREM-2-mediated functions in macrophages is required to improve the understanding of immune response modulation and as a potential therapeutic target.

3.4. Mesenchymal stem cells

Mesenchymal stem cells (MSCs), a type of multipotent progenitor cells (MPCs), are a heterogeneous population of cells with self-renewal ability that dwell in different organs of the human body. Classically, differentiation of MSCs results in the formation of many specialized cell types like adipocytes, chondrocytes, endothelial cells, osteoblasts, myocytes, and neural cells [222]. Correspondingly, an extensive immunomodulatory effect has been elucidated for versatile MSCs in tissue engineering and immune regulation [223,224]. Of interest, as high TREM-2 expression in MSCs was reported under LPS stimulation, it was suggested to negatively control the expression of TLRs on subpopulations and LPS-induced inflammatory cytokine secretion [201,202]. In support, small interfering RNA (siRNA)-mediated *TREM-2* knockdown in bone marrow-derived human MSCs was reported with upregulation of pro-inflammatory cytokines (MIP-2, IL-6, and IL-1β), downregulation of several TLRs (TLR1, TLR2, TLR3, TLR4, and TLR6), and inhibition of the adipogenic, chondrogenic, and osteogenic differentiation under an explicit stimulated environment [201]. Also, in rat bone marrow transfected TREM-2$^+$ MSCs, LPS-induced inflammatory responses were mainly downregulated by phosphorylation of downstream signaling molecules such as NF-κB, p65, ERK1/2, AKT, and p38MAPK [202]. Mechanistic insights described that TREM-2 overexpression in MSCs substantially reduced the inflammatory cytokines, i.e., TNF-α and IL-1β, production in MSCs while accelerating the high secretion of anti-inflammatory cytokine IL-10, which was further associated with an increase in the phosphorylated level of the AKT serine/threonine kinase signaling protein [202]. Likewise, other studies supported the modulation of human MSCs by TREM-2 through TLR activity [203,204]. These observations indicated that TREM-2 functions to reduce LPS-induced inflammation in MSCs [202–204]. Additionally, knockdown experimental studies on MSCs further proved the TREM-2

functional role in tissue regeneration and modulation of inflammatory responses [201,202]. However, TREM-2-mediated signaling in MSCs is not clearly established [201,202] and clinical applications of human MSCs may not be yet efficient [225]. Thus, profound analysis of TREM-2-mediated signaling in human MSCs or/and TREM-2-mediated regulatory functions in the polarization of human MSCs through downstream TLRs signaling may provide essential insights to understand the equilibrium between human MSCs differentiation and self-renewal abilities for use in current stem cell-based therapies.

3.5. Microglia

Microglia are the resident macrophages in the central nervous system (CNS), where they function in apoptotic cell clearance and synaptic pruning during the development of the nervous system [226,227]. Several studies have reported TREM-2 expression on both the cell surface and intracellular regions of amoeboid microglial cells (AMCs) [228–230]. As TREM-2 can exhibit both functional processes in micro- glia, a high expression of the TREM-2 protein was observed in the phagocytic and migratory phenotypes of AMCs, [167]. Accordingly, TREM-2 expression was suggested as an indicator to determine the transition of microglia from a homeostatic to a disease-activated state [21,206]. Besides, TREM-2 deficiency in microglia was associated with a rapid decline in Wnt/β-catenin signaling, low cell survival, and a high cell death rate, endorsing the TREM-2 essential role in the regulation of microglial proliferation and survival by Wnt/β-catenin pathway activation [168]. In support, augmented stimulation of the Wnt/β-catenin pathway decreases GSK3β, repairs β-catenin signaling, and encourages TREM-2-deficient microglial survival *in vitro* and *in vivo* [168]. Similarly, sTREM2 was reported for AKT/GSK3β/β-catenin pathway activation to terminate the apoptosis in microglia [207]. Additionally, TREM-2 has been reported for crosstalk with CSF1R signaling, which is obligatorily required for microglial survival [151,231]. In this perspective, TREM-2 deficiency in murine microglia was established with a high cell death count, assumed to be achieved by a macrophage colony-stimulating factor (M—CSF)-dependent pathway [168]. Another study reported that primary microglia transfected with *TREM2* showed crosslinking to enhance phosphorylation of ERK1/2 and CCR7 expression but not for upregulation of CD86 or MHC class II levels, directing viable cell-type-specific variations in TREM-2-mediated signaling [167]. Besides, overexpression of TREM-2 was linked to a decrease in TNF-α expression and inducible nitric oxide synthase (iNOS) levels in microglia upon treatment with apoptotic neurons [167], while inhibition of TREM-2 expression during the effector phase was observed for exacerbation, including high diffusion of CNS inflammatory infiltrates and demyelination in experimental autoimmune encephalomyelitis [20]. Furthermore, a high TREM-2 expression was found in murine microglia cells stimulated by the chemokine CX3CL1 release by MSCs [232]. Likewise, Wang et al. [116] demonstrated the functional role of TREM-2 in regulating microglial survival during reactive microgliosis in a *TREM2*$^{-/-}$ AD mice model. In addition, genome-wide association studies (GWAS) further linked the pathological role of TREM-2 in microglia with the onset and progression of NDDs [157,205]. By merging transcriptomic and functional studies on a chimeric AD mouse model, deficiency of TREM-2 was associated with reduced microglial survival, defective phagocytosis of key substrates, like ApoE, and inhibition of SDF-1α/CXCR4-mediated chemotaxis, resulting in a diminished response to β-amyloid plaques *in vivo* [21]. Also, supraphysiological TREM-2 expression (acquired in bacterial artificial chromosome (BAC) transgenic mice with both endogenous TREM-2 and transgenic human TREM-2 expression) was described to diminish neuritic dystrophy in the 5XFAD mice model of AD [157,233]. In support, microglia sorted from *TREM2*$^{-/-}$ mice showed downregulation of homeostatic microglia markers and declined to acquire much of the neurodegeneration-associated signatures [116,206]. For example, in the AD mice model, TREM-2 deficient microglia exhibited a low glycolytic gene expression and defects in mTOR signaling activation, resulting in altered cell energetic and biosynthetic metabolism [157]. Also, TREM-2 deficient microglia were noted for reduced activation and enhancement in ramified morphology *in vitro* [127]. Additionally, TREM-2 deficient microglia showed a decrease in cell size and surface area, and an enhanced process interval in the AD mouse model, resulting in reduced activation of microglia [116]. Such altered or defective TREM-2 activation in microglia was advocated to produce disease-associated microglia (DAMs) [206,234]. Besides, certain mutations in the TREM-2 receptor were also studied to prevent the maturation and loss of functional activity in microglia [22,130,131,208]. In context to cancer, TREM-2 deficient microglial cells were detected to promote immunoactive microglial differentiation to reduce the glioblastoma growth in co-culture and tumour initiation *in vivo* [16,235], indicating the immunosuppressive role of TREM-2 microglia in glioblastoma. Likewise, another study presented TREM-2^{+} microglia as an essential factor in promoting glioma through enhanced angiogenesis [171]. In contrast, TREM-2 deficiency in microglia was demonstrated to be dispensable for gliomagenesis and exclusively detected for regulation of phagocytosis via SYK signaling of tumour cells [236]. Together, considering the underlying molecular mechanisms reported in the TREM-2^{+} microglia and glioblastoma [16,171,235,236], cross-validation of these studies is required using advanced experiments. Also, despite the TREM-2 expression has been detected in the microglia of both mice and humans but there is still a debate about whether TREM-2 expression occurred only in a subset or all of the microglia types [68]. Therefore, based on these observations, the molecular and cellular processes accountable for microglia dysfunction in the absence of TREM-2 are not well defined. Overall, TREM-2 expression plays a critical role in normal microglia function and in controlling NDDs and cancer development. However, further research is needed to unravel the physiological and pathological function of TREM-2^{+} microglia, which may offer insights into the optimal design of microglia-based therapeutic strategies for intervention or modulation of brain diseases in humans.

3.6. Myeloid-derived suppressive cells

Myeloid-derived suppressive cells (MDSCs) are classified as a subset of immature myeloid cells, which primarily infiltrate the TME to inhibit the anti-tumor T cell responses during tumorigenesis. Thus, in the tumor-bearing host, degraded recruitment and improved differentiation of immunosuppressive MDSCs substantially enhance the growth of tumors and metastases [237]. Intriguingly, TREM-2^{+} myeloid populations were detected in the TME to promote immunosuppressive function, suggesting a potential role of TREM-2 in the acquisition of immunosuppression by MDSCs [202]. Accordingly, the surface-TREM-2 expression level on circulating monocytic MDSCs (M—MDSCs) was positively linked to the intracellular-ARG1 level and negatively related to the total circulating CD8^{+} T cell count [238]. Moreover, a higher surface-TREM-2 level in circulating M—MDSCs has been associated with a high International Prognostic Index (IPI)-risk score, as well as low overall survival (OS) and progression-free survival (PFS) [238]. In addition, TREM-2 deficient cells were stated to exert a similar differentiation process as cells carrying functional TREM-2 receptors but shortly endure apoptosis, implying the restricted role of TREM-2-mediated pathways in sustaining myeloid cell viability under extreme conditions [157,209]. Therefore, progressive clinical investigations are required to assess the intricate dynamics of TREM-2 expression and associated signaling pathways in MDSCs, especially in terms of immunosuppressive TME, which could offer a potential avenue for enhancing anti-tumor immunity and improving prognoses in cancer patients.

3.7. Natural killer cells

Natural killer (NK) cells present an important population of anti-tumor immune cells, which could destroy tumor cells directly by

supplying granulation and perforin enzymes. Particularly, TREM-2 expression in NK cells is described to promote their anti-tumor responses. In support, inoculation of bone marrow cells from TREM-2 overexpressed transgenic (*TREM2*-TG) mice, carrying a high tendency of CD3 — $CD122^{+}NK1.1^{+}$ precursor NK (pNK) cells, in a tumor-nearing mice substantially restrain tumor progression, and also conveys TREM-2 receptor role to advance differentiation and function of NK cells [210]. Additionally, TREM-2 has been studied to upregulate the expression of transcription factor nuclear factor interleukin-3-regulated protein (NFIL3, also known as E4BP4), a necessary factor for the NK cells differentiation from pNK cells [211], and was downregulated upon PLCγ inhibitor therapy [210]. This observation, therefore, marked TREM-2 protein to influence NK cell differentiation via the PI3K and PLCγ signaling pathways [210]. Overall, due to the limited investigation of TREM-2 in NK cells, further research initiatives are required to unveil the associated factors and signaling pathways to optimize over-expressing TREM-2 NK cells-based innovative therapies.

3.8. Neutrophils

Neutrophils, also known as heterophils, neutrocytes, or polymorphonuclear or granular leukocytes, are a type of white blood cells (WBCs) which plays an essential role in host-biomaterial integration, innate immunity, and inflammation [239]. Although neutrophils are not widely studied or reported for TREM-2 expression, but their combined contribution has been suggested in cancer or tumor development. For instance, ApoE released by prostate tumor cells was discovered to interact with a subset of immunosuppressive $TREM\text{-}2^{+}$ neutrophils, also known as polymorphonuclear-myeloid derived-suppressor cells (PMN-MDSCs), to promote their senescence [212]. Also, enhanced tumor infiltration of $TREM\text{-}2^{+}$ neutrophils in human tumor samples has been linked to a high Gleason score and poor patient survival [212]. Besides, as the selective decrease in senescent-like neutrophils indicated a reduction in the tumor burden, thereof targeting TREM-2 has been suggested as a new side of immunotherapy for patients with prostate cancer [212]. Therefore, further research is essential to decipher the role of TREM-2 in neutrophils under normal physiological conditions and other types of cancers or neutrophil-associated disorders.

3.9. Osteoclasts

Osteoclasts (OCs) as multinucleated cells are differentiated from monocyte/macrophage lineages and are required in the remodeling of bone by adsorption of mature bone tissue [240,241]. As OCs are also reported with high TREM-2 expression, available evidence indicates an essential role of TREM-2 in the derivation of functional multinucleated OCs from mononuclear myeloid precursor cells [172,186]. Consistent with this study, the TREM-2/DAP12 pathway was proven to perform a key role in osteoclastogenesis and cognitive maintenance during an early AD mouse model [213]. Yeng et al. [242] proposed that the TREM-2/DAP12/SYK-dependent pathway acts as a fundamental intracellular signaling cascade for ROS amplification in osteoclastogenesis using a mouse model of periodontitis [242]. In another study, the TREM-2/β-catenin pathway was interpreted in the regulation of bone mass by controlling the percentage of OCs generation, indicating that TREM-2 mediates bone homeostasis by controlling the rate of osteoclastogenesis [214]. In support, no OCs differentiation was observed in TREM-2 deficient patients, resulting in immature OCs aggregation and altered bone resorptive activity [172]. Another study demonstrated the role of Src homology 2 (SH2) domain-containing inositol polyphosphate 5-phosphatase 1 (SHIP1)-mediated TREM-2 inhibition to prevent the uncontrolled activation and survival of OCs [146]. Meanwhile, immunofluorescence staining analysis indicated that Cystatin A (CSTA, a cysteine protease inhibitor, which is highly upregulated during osteoporosis) and DAP12 were co-expressed in OCs, and the demise of either DAP12 or TREM-2 prevented OCs differentiation and resorption in bone [243]. Similarly, the upregulation of TREM-2 in OCs was linked to bone damage in a murine model of acquired cholesteatoma [193]. Together, TREM-2-mediated pathways emerged as an essential regulator in OC biology, influencing differentiation, function, and bone homeostasis, highlighting TREM-2′s intricate role in bone health. Negative aspects, such as SHIP1-mediated inhibition and the interplay with Cystatin A, emphasize the complexity of TREM-2′s influence on OCs, offering both therapeutic potential and challenges for addressing bone-related disorders.

4. Regulatory choreography of TREM-2

For the ideal functioning of the immune system, an adopted balance between activating and inhibitory pathways is critical for immune homeostasis in the human body. Adaptive and innate immune responses, therefore, are strictly modulated through categorically assorted sets of cell-surface expressed or secreted receptors in association with signaling intermediates for common downstream pathways. As a member of the Ig superfamily, regulation of the *TREM2* gene and TREM-2 receptor expression can substantially influence the extent and balance of mediated signaling pathways involved in normal physiological and pathological conditions. Although available facts established cell-type and context-definite dependent expression of TREM-2, the involved molecular regulatory processes strictly leading to this highly specialized cellular TREM-2-expression are just beginning to be understood. Accordingly, various regulatory factors and mechanisms have been submitted for the regulation of *TREM2* gene expression [40,244]. In addition, TREM-2 levels can be regulated by continuous proteasomal degradation; thus, a high turnover rate for the TREM-2 protein expression has been detected in $TREM\text{-}2^{+}$ cells [189,245]. Moreover, a recent study advocated that *TREM2* is a thyroid hormone-regulated gene and that its expression in macrophages and microglia can be triggered by both thyroid hormone and synthetic thyroid hormone agonists (thyromimetics) [246]. Therefore, this section reviews the different aspects of the regulatory factors, including epigenetics and posttranscriptional-mediated regulation, narrated in the literature for the cellular expression of the TREM-2 receptor.

4.1. Epigenetics regulation

Epigenetics refers to the study of heritable changes in gene function that appear without changing the underlying DNA sequence. Accordingly, DNA methylation and histone modifications are generally studied as the primary mechanisms involved in the epigenetic regulation of genes. Interestingly, the *TREM2* promoter region has been found to have DNA methylation at the CpG islands as an essential determinant for its expression. Consequently, hypomethylation and hypermethylation in the *TREM2* promoter region are correlated with an increase in *TREM2* gene expression and silencing, respectively. For instance, hippocampal enrichment of 5-hydroxymethylcytosine (5hmc) as an active demethylation marker at the *TREM2* transcription site and in exon 2 was positively related to TREM-2 mRNA expression levels in humans [58]. Appropriately, an active methylation in upstream of the *TREM2* transcription initiation site was positively linked to the TREM-2 mRNA level in AD patients [58]. Concurrently, methylation of intron 1 at the CpG sites was negatively related to the TREM-2 mRNA expression levels in human leukocytes while reduced methylation in these regions has been significantly linked to AD patients [247]. Furthermore, histone modifications, such as acetylation and methylation, are similarly documented in the regulation of TREM-2 protein expression [176]. Usually, an acetylation of histones is associated with an open chromatin structure and active gene transcription while histone deacetylases (HDACs) are correlated with the inhibition of TREM-2 expression by condensing the chromatin structure [176]. Another study established the association of enhanced histone modifications, viz., H3Kme2 and H3Kme3, with active gene transcription at the *TREM2* locus in the adipose tissue of db/db

(diabetic) mouse [248], as well as during differentiation of DCs and macrophages *in vitro* [174]. Of note, an association between DNA methylation and *TREM2* gene regulation could be significantly complex, as gene body methylation may result in alternative splicing [249]. In summary, further research to inspect other epigenetic changes and involve procedures along the complete length of the *TREM2* gene must be assumed to conclusively quantify the modifications that could occur at both cellular and disease-state levels. This initiative may further open the possibility of monitoring the functional regulation of the *TREM2* gene in different cells and the aetiology of TREM-2-associated disease.

4.2. Transcription regulatory factors

Regulation of *TREM2* expression in different cells is classically controlled by genetic factors. Thus, various transcription factor binding sites are predicted and investigated in promoters and untranslated regions (UTRs) for the regulation of *TREM2* expression. However, only a few regions are positively correlated with *TREM2* expression. In this context, a recent study established that the conventional *TREM2* expression, which is initiated from the downstream AUG (*dTREM2*), can be significantly downregulated by the 5′-UTR in an upstream start codon (uAUG)-mediated manner under amino acid starvation and polyinosinic-polycytidylic acid or poly(I:C) treatment in humans [250]. Moreover, PU.1, a transcription factor essential for myeloid differentiation, has been demonstrated to bind at the E26 transformation-specific (Ets) site in the *TREM2* promoter region [180,251]. In support, chromatin immunoprecipitation followed by sequencing (ChIP-seq) further highlighted the occupancy of PU.1 at the *TREM2* locus, demonstrating its functional role in the modulation of TREM-2 expression in macrophages and microglia [110]. Besides, in addition to PU.1, the 1131 bp *TREM2* promoter region also contained C/EBPα binding sites, and this region has been well-acknowledged for the regulation of myeloid cell differentiation and function [252]. Therefore, in co-transfection experiments with PU.1 and the C/EBPα study, PU.1 failed to trigger the full-length *TREM2* promoter or binding to the PU.1 consensus region while deletion of the PU.1 binding site showed no changes in the transcriptional activity. These observations essentially convey the direct role of C/EBPα and the indirect participation of PU.1 transcription factor in *TREM2* regulation [252].

Additionally, stimulation of the retinoid X receptor (RXR), nuclear receptors peroxisome proliferator-activated receptor (PPARg and PPARd), and liver X receptor (LXR) have been anticipated to encourage the TREM-2 expression as well as other phagocytosis-related cell-surface receptors in mice [253,254]. For instance, the RXR binding site was noted for regulating and promoting the expression of the whole region carrying *TREM* family genes [253]. Thus, the RXR agonist, bexarotene, has been demonstrated to act as a transcription factor and promote enhanced *TREM2* expression [253,255]. In this context, the regulatory effect of bexarotene on enhanced *TREM2* expression has been established in AD mice only [256] but failed to influence *TREM2* expression in healthy mice [257]. Subsequently, these results envisioned that bexarotene could especially boost cellular *TREM2* expression under certain stress or pathological conditions [258]. Likewise, the nuclear factor of activated T cells (NFAT) [187] and Protein E [259] were determined to regulate *TREM2* expression in assorted cell types, but it has not been specified whether these factors absolutely control *TREM2* expression. Notably, mechanistic insights directed the translocation of NFAT into the nucleus after activation, where it associates with additional transcription factors to modulate immune-related gene expression [116,260,261]. Similarly, Yin Yang 1 (YY1) was recently characterized as a transcriptional protein for the minimal promoter of the *TREM2* gene using *in silico* predictions and later confirmed by electrophoretic mobility shift assay (EMSA) and DNA pull-down assay [262]. In this study, shRNA-mediated silencing of YY1 expression was substantially associated with a reduction in the *TREM2* minimal promoter activity and TREM-2 protein levels in the neuroblastoma Neuro2A and microglial cell line BV2 [262]. Besides, LPS treatment on microglial cell line BV2 and AD model mice further exhibited downregulation of *TREM2* and YY1 levels, demonstrating the crucial function of YY1 in the regulation of *TREM2* expression [262]. Therefore, based on these observations, YY1 protein has been proposed as a therapeutic target to prevent AD progression [262]. Furthermore, variation analysis of high-expressing regulons among TREM-2$^+$-lipid-associated macrophage (LAM)-like cells and other monocyte-macrophage subsets predicted HIF1A, MAF, and NR1H3 as potential transcriptional modulators of TREM-2$^+$ LAM-like cells [263]. Also, trajectory inference analysis of single-cell transcriptomics data decoded that TREM-2$^+$ LAM-like cells differentiated from monocytes, in accordance with the generation of TREM-2$^+$ LAMs and TREM-2$^+$ scar-associated macrophages (SAMs) [263]. Moreover, the interferon regulatory factor (IRF) family of transcription factors has been demonstrated to regulate TREM-2 expression during the differentiation of DCs [151]. Conclusively, though advances have been made in transcription factor identification regulating *TREM2* expression, challenges remain in understanding their intricate complex interactions and context-specific effects. Thus, future investigations are obliged to examine the synergistic or antagonistic functions of new or predicted transcription factors under diverse physiopathological conditions.

4.3. Post-transcriptional regulation

Following transcription, TREM-2 mRNA is subjected to numerous post-transcriptional modifications that can alter its stability, cellular localization, and translation into protein. Additionally, some post-transcriptional factors can be involved to maintain the stability of the TREM-2 mRNA. In this context, microRNAs (miRNAs), a class of single-stranded noncoding ribonucleotide, have been identified as those critical post-transcriptional modulators that can attach to the 3′-untranslated region (3′-UTR) of TREM-2 mRNA, leading to its translation repression or degradation. For example, TREM-2 protein production was post-transcriptionally downregulated by NF-κB-sensitive miR-34a (encoded at chr1p36.22) activation in the deteriorating brains of AD patients and the eyes of age-related macular degeneration (AMD) patients and supported by cell reporter assay [58,244,264]. Also, collected results from *in vitro* and *in vivo* experiments indicate that the miR-3473b directly targets the 3′-UTR of TREM-2 and downregulates its expression in microglia, which further suppressed the ULK1 activity — a component of the Atg1 complex involved in autophagy [265]. Thus, miRNA-3473b expression and activity have been established to promote the proinflammatory mediators secretion and diminish autophagy during PD pathogenesis [265]. In another study, miR-31-5p was identified for directly targeting the 3′-UTR region of TREM-2 mRNA to downregulate its expression in HCC tissues to encourage cancer development using both bioinformatics analysis and luciferase reporter assay [153].

Additionally, cellular TREM-2 expression is also assumed to be modulated by inflammation at the molecular level; however, the consequences of the inflammation on TREM-2 expression assessed through *in vitro* and *in vivo* studies are not stable [266]. For instance, the application of anti-inflammatory molecules, such as vasoactive intestinal peptide [267] and IL-4 [110], *in vitro* studies demonstrated an increase in TREM-2 expression while proinflammatory molecules (TNF-α [47,244], IL1β [47], ROS [244,268], IFNγ [4], TLR agonists, involving LPS [47,110,175,269], CpGs [270] and other TLR ligands [186,271,272,273], mitochondrial lysates [274], and bacteria [275]) caused a reduction in TREM-2 expression. Furthermore, upregulation of TREM-2 expression was found upon receptor activator of nuclear factor kappa-B ligand (RANKL) stimulation, but TREM-2 downregulation was noted upon treatment by LPS and IL-10 in OCs [186,276]. Consistent with these observations, IL-10 was observed to suppress the methylation of histone H3 on lysine 4 (defined as “poised” and transcriptionally active promoters) at the *TREM2* site in OCs, suggesting a regulatory function of IL-10 in TREM-2 expression [276]. In another study, Park-Min et al. [276] established that IL-10 can inhibit osteoclastogenesis

induced by RANK and selectively hamper Ca^{2+} signaling downstream of RANK by blocking *TREM2* transcription. Thereof, downregulation of *TREM2* expression leads to reduced RANKL-induced activation of the calcium/calmodulin-dependent protein kinase (CaMKs)/MEK/ERK pathway and decreased nuclear factor of activated T cells 1 (NFATc1) expression level, a master modulator of osteoclastogenesis [276]. Also, pathological conditions have been regularly demonstrated to enhance the *TREM2* expression in *in vivo*. For example, intensified *TREM2* expression levels were noticed in amyloid and tau pathological mouse models [277], as well as in AD patients [278].

Furthermore, the crucial role of RNA-binding proteins (RBPs) is also determined in the essential stability and translation of TREM-2 mRNA. As an example, RBP HuR was shown to stabilize TREM-2 mRNA, thereby promoting its expression under inflammatory conditions [108]. Also, specific opposing regulatory mechanisms have been suggested between *TREM* genes such as *TREM1* and *TREM2* [279]. For instance, certain AD-associated variants were identified to reduce *TREM1* expression levels but also advanced an increase in *TREM2* expression, whereas non-pathogenic TREM-2 variants were established to reduce both *TREM1* and *TREM2* expression [280]. However, various factors involved in such opposing pathways of TREMs are not yet fully understood while a ratio between *TREM1* and *TREM2* expression levels has been suggested as a required factor for NDDs development rather than an absolute change in TREMs expression [258]. Moreover, most of the protein-coding genes are regulated by alternative splicing events attained by coordination between the spliceosome and RNA-binding proteins (RBPs) in humans [64]. Therefore, the role of RBPs, such as CELF2, has been documented in the regulation of alternative splicing of *TREM2* exon 3 in microglia [64]. Hence, TREM-2 expression can be auxiliary manipulated at the mRNA, protein expression, and secretion stages in different cell-types by processes that are not yet determined.

Collectively, the regulation of TREM-2 expression is a complex process involving an intricate network of epigenetic modifications, transcription factors, post-transcriptional mechanisms, and mRNA stability proteins that are expressed in various cell types. Understanding the precise regulatory pathways of TREM-2 is critical, especially given its role in various pathologies including neurodegenerative diseases, bone disorders, and inflammatory responses. Therefore, continued research in this area not only promises to elucidate fundamental biological processes but also holds the potential for developing therapeutic interventions targeting TREM-2 regulation.

5. Biological pertinence of TREM-2

Under a regular physiological state, TREM-2 exhibits varied biological functions, such as anti-inflammatory activation, homeostasis, lipid metabolism, metabolic metastasis, initiation of phagocytosis, and promotion of cell survival, in context to the microenvironment and cell phenotype [97,157,176,281,282]. In contrast, under pathological conditions, TREM-2 expression has been associated with tissue damage and injury in AD [283,284], respiratory viral infection [66], chronic obstructive pulmonary disease (COPD) [285]. colonic injury [286], hepatosteatosis [287,288], hepatic injury [289], and rheumatoid arthritis [290]. Also, TREM-2 has been marked to mediate multiple signaling cascades, including the TLR [289], p38 [291], and PI3K pathways under different tissue microenvironments [158]. Whereas TREM-2 deficiency is well-defined to attenuate inflammatory responses in macrophages and DCs [245,292]. Consistent with the function of full-length TREM-2, the essential role of sTREM-2 was also studied under various biological conditions. For instance, sTREM-2 was reported to improve macrophage survival after viral infection in the lung, supporting an increased immune-mediated lung pathology [66]. Also, CSF1 deprivation-induced apoptosis in TREM-2-deficient BMDMs was retreated upon treatment with sTREM-2 *in vitro*, which promoted the molecular pathways linked to cell survival like ERK1 and/or ERK2 and MAPK14 phosphorylation [66]. Similarly, sTREM-2 potentially forestalled apoptosis in microglia by triggering the AKT/GSK3β/β-catenin pathway and induced inflammation cytokine production via NF-κB pathway activation [207]. In addition, based on cell biology studies, transition of TREM-2 protein has been reported between the plasma membrane and cytoplasmic vesicles in the secretory pathway [9,63]. Accordingly, TREM-2 also endures a complex maturation through glycosylation during secretory transport and biosynthesis processes [22,23,63], but the biological relevance of such modifications in TREM-2 remains to be determined. However, change in TREM-2 functional activity may occur as per disease stage and location; thus, this section summarizes the broadly exhibited biological functions, such as inflammation, metabolism, and phagocytosis, by the TREM-2-expressing cells in the human body.

5.1. Inflammation

Inflammation, a complex immune response stimulated by innate and adaptive immunity, is essential for protecting the host during the initial stages of infections and diseases. Importantly, strict regulation of such immunity is critical to avoid excessive inflammation and resultant tissue or organ damage. As one of the Ig-superfamily members, TREM-2 is frequently explained as an important reparative [4,111] and anti-inflammatory receptor through the suppression of TLRs or PI3K/NF-κB/JNK signaling [111,146,161,273,293,294]. Thus, TREM-2 is widely advocated for the regulation of both adaptive and innate immunity [47]. Typically, TREM-2 can regulate the triggered immune responses either by amplifying or dampening both TLRs and Fc receptor-induced signals [111]. For instance, TREM-2 was detected to inhibit the inflammatory responses stimulated by TLRs activation in non-parenchymal cells and initiated the multifactorial protective pathways to secure the liver against HCC and injury [295,296]. Accordingly, induction of various anti-inflammatory genes, including *Interleukin 1 receptor antagonist* (*Il1rn*), *Galectin*-1 and —*3* (*Lgals1* and *Lgals3*), and *Progranulin* (*Grn*), were directly correlated with TREM-2 expression in mice microglia and macrophages [218]. Likewise, in Kupffer cells, TREM-2 was studied to reduce inflammation by downregulating MAPK phosphorylation [296]. Also, the functional role of TREM-2 has been suggested in the regulation of both NO expression and iNOS production [294,297]. For instance, in TREM-2 deficient DCs, low NO production was reported to diminish RORγt nitration and improve differentiation of Th17 cells [191]. Consequently, a high number of Th17 cells were found to encourage neutrophil intrusion and inflammatory pathology in *TREM2*$^{-/-}$ unilateral ureteral obstruction (UUO) mice model [191]. In the same manner, the knockdown of *TREM2* in the senescence-accelerated mouse P8 (SAMP8) model exhibited an increase in inflammatory cytokines production [298]. Likewise, evidence from *TREM2*$^{-/-}$ mice fed on a high-fat diet (HFD) revealed a low number of penetrating F4/80^{+}CD11c^{+} macrophages in adipose tissue and advanced augmentation in proinflammatory cytokines (IL-6 and IL-1b), hepatic steatosis, adipocyte hypertrophy, iNOS, and insulin resistance compared to wild-type controls [299]. Also, *TREM2* knockdown microglia was demonstrated with high iNOS protein expression in subsequent oxygen–glucose deprivation culture conditions [297], while reduced iNOS^{+} microglia numbers were noted during cuprizone-induced demyelination in TREM-2 deficient mice model [300]. In another study, overexpression of TREM-2 in microglia cell line BV-2 was noted with a decrease in LPS-mediated NO production [294]. Interestingly, both iNOS expression and NO production were decreased in *TREM2* knockdown DC2.4 and *TREM2*$^{-/-}$ BMDCs cells, suggesting a positive regulatory role of TREM-2 in preserving iNOS levels and NO expression [191]. In support, an increase in iNOS^{+} inflammatory macrophage numbers was observed after TREM-2 inhibition in cancer [37]. Collectively, these observations clearly supported the anti-inflammatory function of TREM-2. On the contrary, several studies have also highlighted the TREM-2-mediated signaling in the amplification of inflammatory responses. For example, in a mice experimental study, upregulation of TREM-2 in the lymph nodes and

lungs, along with enhanced Th17 and Th2 cytokines transcript levels in the lymph nodes upon treatment with ovalbumin, indicated the considerable TREM-2 function in the initiation or succession of allergic airway inflammation [192]. Correspondingly, in asthma patients, BALF analysis revealed a high TREM-2 expression, which was linked to increased eosinophils and eosinophilic inflammation [196]. Similarly, TREM-2 overexpression was monitored in the lungs of an experimentally induced melioidosis whereas *TREM2*$^{-/-}$ mice displayed a significant reduction in the inflammation [301]. Relatedly, *TREM2* overexpression was linked to mucosal inflammation in an acute or chronic colitis-induced mice model, as well as within the inflamed mucosa of inflammatory bowel disease (IBD) patients [292]. In another study, the TREM-2^{+}CD9^{+} subset of macrophages derived from circulating monocytes exhibited expansion during liver cirrhosis and exhibited a significant contribution to liver fibrosis development [263,287,302]. Whereas, TREM-2 deficient DCs were observed with a diminished ability for proinflammatory cytokines (TNF-α, IL-6, and IL-10) secretion upon being treated with bacteria-associated antigens [126]. Thus, in addition to the cell-type and context-dependent, TREM-2-mediated function can also be varied based on the strength and duration of the stimulus [146,303]. In this agreement, expression of TREM-2 on macrophages and microglia was noted for an anti-inflammatory function [110,160], while TREM-2 typically promotes proinflammatory responses in DCs [292,304]. Also, both proinflammatory and anti-inflammatory pathway activation in the context of the external stimulus have been studied in microglia [49], as depicted in Fig. 3. Conclusively, available research data conveys both anti-inflammatory and proinflammatory effects of TREM-2 expression, which corresponds to cell phenotype expressing it and tissue microenvironment including cytokine milieu.

5.2. Metabolism

Obesity, as a result of dysregulated metabolism, also increases the possibility of several metabolic disorders, including cancer, hypertension, osteoarthritis, NAFLD, myocardial infarction, stroke, and type 2 diabetes mellitus [305]. As lipids are anticipated as candidates for TREM-2 receptor ligands, either as free molecules, complexed in myelin, or ApoE particles [116,130,131,142]; thus, TREM-2 activation is widely accepted to encourage cell survival and metabolic programs [116,146,157]. In this context, TREM-2 has been observed for an intimate connection with lipid metabolism in microglia [142,300]. Interestingly, a distinct molecular mechanism, involving activation of a basic mTOR signaling pathway to support cell growth, survival, proliferation, and long-term cell tropism rather than drastic metabolic reprogramming, has been observed for microglia operated by TREM-2 receptor in AD [306]. Such a reminiscent role of TREM-2 is assumed to closely resemble the tonic function exhibited by mature B cell antigen receptors, which produce essential survival molecules by PI3K [306]. Otherwise, TREM-2deficient microglia, or expression of dysfunctional TREM-2 variant (such as TREM-2^{T66M}), in human microglia can cause metabolic faults, including diminished glucose consumption ensuing in a shortage in glycolysis and lower ATP production, which results in low cell survival rate [88,157]. As a consequence of collective metabolic stress, TREM-2 deficient microglia also failed to comply with the obligatory responses proficiently against stressful effects like growth factor starvation *in vitro* or Aβ toxicity *in vivo* [157]. Also, another study demonstrated the TREM-2 receptor as a microglial sensor for lipid mediator molecules, which are secreted from the terminals of damaged sensory nerves or other cells in the dorsal horn (DH) [48,95]. Moreover, based on the obesity mouse model, TREM-2^{+} LAMs were found to assist their sustainability in the adipose tissue as well as accelerate gene expression programs required for lipid metabolism and phagocytosis

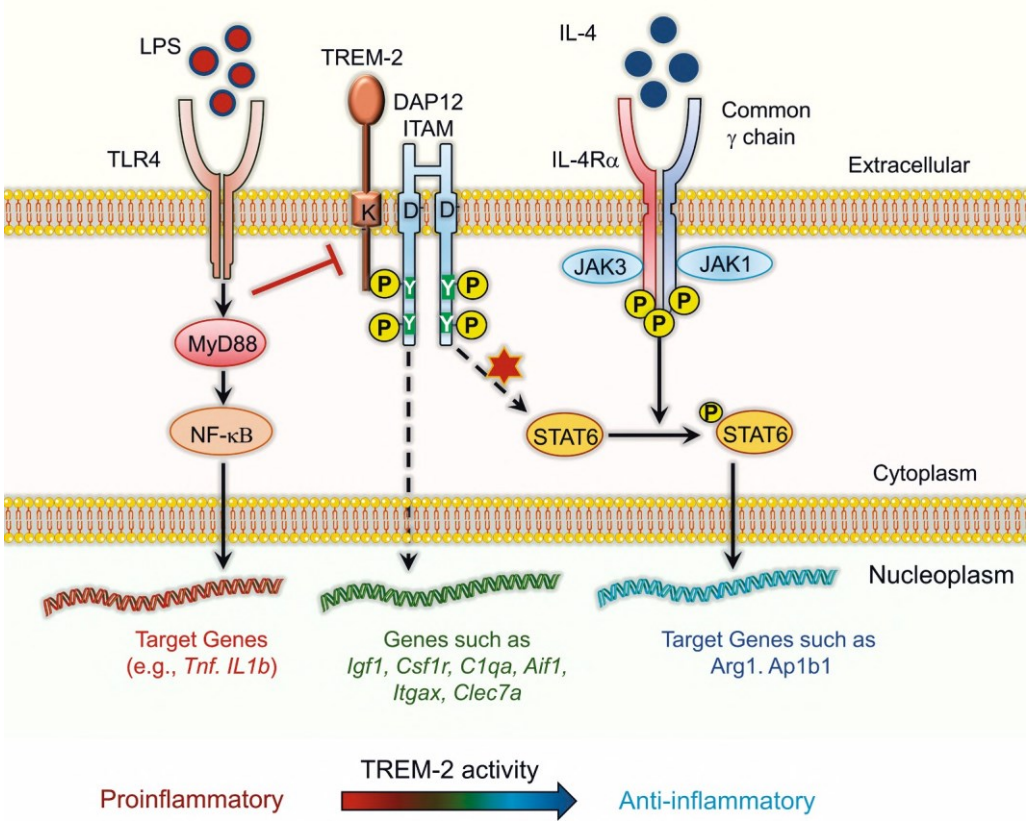

Fig. 3. Proposed functional model for the TREM-2 involvement in the TLR4-triggered proinflammatory and IL-4-induced anti-inflammatory responses in the microglia, adopted and sketched based on the published Ref. [49].

[218]. Accordingly, scRNA sequence analysis further supported the conspicuous incidence of TREM-2$^+$ LAMs in both the adipose tissue and liver during obesity [288,302]. Whereas enriched TREM-2$^+$ macrophages specializing in lipid catabolism were discovered in atherosclerotic lesions [307]. Intriguingly, the deletion of TREM-2 abrogated the recruitment of macrophages in enlarged adipocytes and triggered inflammation, glucose intolerance, massive adipocyte hypertrophy, and systemic hypercholesterolemia, indicating the protective function of TREM-2$^+$ macrophages [218]. Another study deciphered that the superimposition of diabetes mellitus can promote TREM-2/MAPK signaling in cognitive deficits, including neuroinflammation and neuron death [308]. Therefore, in LAMs, knockout of the *TREM2* gene intensified while *TREM2* enrichment silenced the proinflammatory response and MAPK signaling under high glucose and hypoxic conditions [308]. However, metabolic studies in both globally overexpressing *TREM2* mice [94] or with global *TREM2*$^{-/-}$ mice [218,299] reported an enhanced body weight gain and exacerbated insulin resistance, which demands further investigations for the TREM-2 role in diabetes. Hou et al. [309] discovered that hepatic modulation of lipid overload required metabolic coordination of hepatocytes and macrophages, which is partially mediated by TREM-2 expression. Correspondingly, overexpressing TREM-2 macrophages were observed to enhance the hepatic energy supply, indicating TREM-2$^+$ macrophage-mediated hepatocytic energy metabolism in non-alcoholic fatty liver disease (NAFLD) [309]. In this assessment, deficiency of TREM-2$^+$ macrophages has been associated with accelerated NAFLD progression in the NAFLD-associated sepsis mouse model [309], which is consistent with the results that *TREM2*$^{-/-}$ mice fed on a chronic high-fat diet (HFD) showed high severity in hepatic steatosis [299]. In addition, nonalcoholic steatohepatitis (NASH) — the most severe form of NAFLD, HFD showed remodeling of Kupffer cells (KCs, liver-resident macrophages) gene expression drivers which results in the overexpression of CD9$^+$ and TREM-2$^+$ macrophages, especially SAMs phenotype, and cell death [288]. Consequently, dead KCs were restored by monocyte-derived macrophages to acquire the convergent programs, including TREM-2 levels, suggesting TREM-2 expression in liver macrophages with the severity of NASH [288,302]. Overall, these observations support TREM-2 expression in the liver-associated cells and endorse TREM-2 inhibition approaches to restore efferocytosis as an effective strategy in the NASH treatment [310]. In summary, the available studies suggest that TREM-2 is a novel marker and regulator of adipogenesis, therefore, blockade of TREM-2 signaling may offer a potential therapeutic approach in obesity and insulin resistance.

5.3. Phagocytosis

Phagocytosis, a pivotal function to remove the apoptotic debris displayed by innate immune cells, is an essential mechanism to avoid secondary necrosis and the secretion of unwanted endogenous proinflammatory signals. The absence or dysfunction of such a mechanism has been attributed to the development of inflammatory disorders. For example, mice deficient in several factors required for apoptotic debris mechanisms exhibited the onset of chronic inflammation [238]. Notably, the TREM-2 receptor is well deciphered to function in enhancing phagocytosis, and concurrently, in inhibiting immune activation [110,126]. For instance, TREM-2/DAP12 signaling activation by transfection with TREM-2 in microglia has been discovered to stimulate ERK1/2 phosphorylation [311], which is associated with suppressing the inflammatory reactions and phagocytosis of apoptotic debris or cells. In contrast, deletion or dysfunction of TREM-2 showed a significant reduction in phagocytosis of antibodies, apoptotic cells, bacteria, lipoproteins, and cellular debris *in vitro* or *in vivo* [88,167]. In support, upon pathogen detection in the CNS, TREM-2 positively promoted phagocytosis and substantially inhibited the TNF-α and IL-6 cytokines secretion in microglia to sustain the local immunosuppressive tissue microenvironment [167]. Moreover, microglia rich in TREM-2 and PLCγ2 receptors have been suggested to support key activities in the CNS, including phagocytosis and lipid sensing [164]. Consistent with the critical involvement of TREM-2 in myeloid phagocytosis [40], the characterization of phagocytic phenotypes directed by dependency on TREM-2 overexpression has been demonstrated in both microglia and MΦ_Infils in traumatic spinal cord injury (SCI) [312]. Complementarily, an enhanced expression of TREM-2/DAP12 chimera in cells lacking phagocytic machinery, like Chinese hamster ovary (CHO) cells, were observed for significant phagocytosis of cellular debris, lipoproteins, and bacteria [125,167]. Furthermore, *TREM2* knockout in microglia results in low phagocytosis of β-amyloid human synaptosomes but not zymosan A, and such a microglia phenotype arises partially through diminished SYK signaling in *TREM2* knockout cells [21]. Another study suggested that *TREM2* knockdown in microglia causes reduced phagocytosis of apoptotic neurons by approximately 43 %, whereas TREM-2 overexpression ensuing improved phagocytosis of neurons by 1.6-fold compared to respective controls [167]. Likewise, about 30 % of the phagocytosis of *Escherichia coli* by macrophages was marked for the functional role of TREM-2 using knockdown approaches [125]. Additionally, TREM-2-mediated phagocytosis for bacteria and external granules has been suggested for intimate correlation to downstream PI3K/AKT pathway activation rather than via the ERK1/2 pathway [125,313]. Meanwhile, TREM-2 overexpression in macrophages was also implicated in phagocytosis and clearance of apoptotic cells in a NASH mouse model [314]. Notably, HSP60, a mitochondrial chaperone, is also characterized as a TREM-2-binding protein expressed on the surface of astrocytes and neurons [113]. Accordingly, HSP60 treatment was characterized to trigger TREM-2-dependent phagocytosis in the microglia [113]. Likewise, pharmacological inhibition of ADAM proteases to inhibit TREM-2 shedding showed increased phagocytosis of bacteria by a TREM-2$^+$ rat microglial cell line (BV2), indicating TREM-2-dependent phagocytosis mechanisms required a full-length TREM-2 receptor. However, the precise mechanism governing TREM-2-dependent phagocytosis is not yet fully understood [88]. Altogether, the TREM-2 receptor can be concluded for a substantial acceleration of immune cell-mediated phagocytosis and in the negative regulation of autoimmunity.

6. TREM-2 clinical relevance and potential in cancer therapy

Antitumor immunity is diminished by several factors, including dysfunction of immune cells or/and the unique ability of cancer cells to evade immune surveillance and being killed by T cells [315]. Recently, accumulating evidence suggested that TREM-2 has an impact on the occurrence and development of tumors. As the TREM-2 receptor is considerably expressed in TAMs and MDSCs, it is widely reported to affect the prognosis and clinical phenotype of various tumors [316]. In this perspective, high TREM-2 expression on TAMs has been associated with deteriorating outcomes in some solid tumor progression, including glioma, GC, and RCC [29,34,36,316]. However, like cell-specific TREM-2 expression and function, contradicting results on TREM-2 functions are also reported in some cancers. For example, TREM-2 expression was predicted to inhibit colorectal cancer (CRC) progression [317] while high TREM-2 expression in GCs and non–small cell lung (NSCLC) was associated with their poor prognosis [34,318]. Similarly, TREM-2 expression on myeloid cells: microglia and macrophages, has been reported to induced an immunosuppressive environment and angiogenesis to promote glioblastoma [16,171,235] while another study demonstrated TREM-2$^+$ microglia as a regulator of phagocytosis of brain tumor cells [236]. At the molecular level, these contrary observations in some tumors can be explained by considering the condition that cancer stromal cells might express the TREM-2 receptor, which can impose differential effects during tumor progression [40]. Accordingly, high TREM-2 expression has been identified in certain solid tumor cells [34,295,318,319]. In this context, TREM-2 expression analysis in various primary and metastatic tumors compared to corresponding

normal tissues suggested a significantly higher TREM-2 expression in tumor tissues, summarized in Table 4. Besides, the proto-oncogene TREM-2 effect on epithelial-mesenchymal transition (EMT) via PI3K/AKT pathway is also predicted and verified in GC [33]. Interestingly, a recent study identified TREM-2 as a novel receptor for IL-34, which mediates myeloid differentiation by inhibiting RAS/ERK1/2 signaling, thereby influencing the characteristics of acute myeloid leukemia (AML) [44]. Despite the extensive literature supporting the role of TREM-2 cells in cancer, but mechanistic contribution of ligands which might initiate the TREM-2$^+$ TAM phenotype function in tumors has not yet been described in cancer models or patients thus far. As TREM-2 has been established to interact with lipids, such as lipidated ApoE, phospholipids, and lipoproteins [108,116,131], the TREM-2 receptor might potentially be engaged with cell membrane components of dying or engulfed cancer cells to initiate immunosuppressive TME. For example, some germline variants of ApoE were linked with lower anti-tumor responses, high risk of melanoma progression, and poor OS in patients [320], suggesting a novel function of the ApoE/TREM-2 axis in cancer. Additionally, TREM-2$^+$ LAMs have been detected in different tumors and are frequently associated with lipid metabolism as well as established for the accumulation of lipid droplets [321,322]. Since TREM-2 expression is also established to progress foam cell formation, TREM-2$^+$ LAMs in TME might function to initiate an immunosuppressive state to promote cancer development [218]. Altogether, these observations suggest that TREM-2 expression can occur in both immune and non-immune cells, but the significance of TREM-2 expression is poorly understood in cancers and assumed to depend on the tumor type. Hence, this section provides insights into the critical function of TREM-2 expression in immunosuppressive TME development as well as TREM-2 signaling inhibition to achieve a stronger antitumor effect.

Table 4
TREM-2 expression noted in different types of cancers and its functional role or adopted pathway in cancer development.

Cancer	TREM-2 adopted functional pathway/role	References
Bladder urothelial carcinoma	—-	[31]
Breast cancer		[31]
Cervical squamous cell carcinoma/Endocervical adenocarcinoma	—-	[31]
Cholangiocarcinoma	—-	[31]
Colon cancer	Supressed cancer metastasis by Wnt/ERK/GSK-3β pathway	[31,317]
Esophageal carcinoma	—-	[31]
Gastric cancer	Promotes EMT via the PI3K/AKT pathway	[33,34]
Glioblastoma multiforme	—-	[31]
Glioblastomas/Gliomas with a mesenchymal subtype/ Gliomas with wild-type isocitrate dehydrogenase/ Gliomas without 1p/19q deletion	Regulates CXCL10/CXCR3 axis assumes to glioma cells proliferation and invasion.	[29,323]
Head and neck squamous cell carcinoma	—-	[31]
Hepatocytes in hepatocellular carcinoma	Supresses EMT and metastasis via PI3K/AKT/ β-catenin pathway	[31,153,295,324]
Kidney renal clear cell carcinoma/Kidney renal papillary cell carcinoma/ Kidney chromophobe	—-	[31]
Lung squamous cell carcinoma/ Non-small cell lung cancer	—-	[31]
Pancreatic cancer	—-	[153]
Prostate adenocarcinoma	Promote cancer by PI3K/ AKT axis	[31,325]
Renal cell carcinoma	Promotes cancer by cell proliferation, recued cell apoptosis, and regulation of PTEN-PI3K/AKT pathway	[36]
Skin cutaneous melanoma	Predicted as prognostic biomarker and associated with immune infiltrates in patients.	[326]
Thyroid carcinoma	—-	[31]
Uterine corpus endometrial carcinoma	—-	[31]

6.1. Cancer immunosuppressive microenvironment

Both the innate and adaptive immune systems provide protection against tumor development [327]. However, immune surveillance dysfunction, caused by immune cells errors' in the identification of tumors or by immunosuppressive TME generation, apparently directs to tumor development [328]. Usually, immunosuppressive TME formation is triggered by several factors, involving infiltration or collection of immunosuppressive cells (e.g., TAMs), overexpression of immune checkpoint receptors (e.g., PD-1, and CTLA4), and ligands (e.g. PD-L1) [329]. Notably, TAMs have been identified as one of the prominent immune cell populations infiltrated in TME, causing an insignificant prognosis and minimal immunotherapy effect [330]. Accordingly, TAMs have been suggested to promote tumor angiogenesis and pathogenesis through the secretion of immunosuppressive cytokines (TGF-β, IL-10, arginase-1, etc.) and epidermal growth factor (EGF) [331,332]. Also, crosstalk between cancer cells and various immune and non-immune cell types in TME, involving regulatory T cells, cancer-associated fibroblasts (CAFs), regulatory T cells (Tregs), and M2-type macrophages, are studied to dampen the activity of cytotoxic CD8$^+$ T cells to promote immunosuppressive TME [333].

Notably, the TREM-2$^+$ immune cells role has been consistently demonstrated in serval studies for the reduction of anti-tumor immune responses, resulting in immunosuppressive microenvironment development to permit better proliferation and progression of cancers [32,199,200]. In this context, accumulating evidence has suggested that TREM-2$^+$ cells, such as TREM-2$^+$ TAMs, constitute a significant cellular fraction of the human TME in many tumors and have been described to inhibit T cell responses through multiple mechanisms [32,334,335]. In particular, analysis of various primary carcinoma samples in humans, with those of the breast, bladder, colon, skin, liver, lung, pancreas, stomach, and kidney, were identified for carrying TREM-2$^+$ macrophages in 75 % of samples [32]. Additionally, analysis of brain metastases from different cancer types, including melanoma, breast, lung, ovarian, colorectal, and renal cancer, were also estimated for a cluster of TREM-2$^+$ macrophages [336]. In another cohort study analysis on 49 different human cancers, TREM-2 expression analysis by flow cytometry was validated for the enrichment of TREM-2$^+$ TAMs at the protein level [337]. For example, in CRC patient cohorts, TREM-2 was marked as part of the core signature of C1QC$^+$ macrophages being accumulated in the tumor compared to the healthy colon tissue [318,338]. Notably, C1QC$^+$TREM-2$^+$ macrophages promoted the expression of immunosuppression-associated genes but also displayed immunostimulatory functions through the expression of CXCL9 and CXCL10 [339]. In another study, tumor-specific C1Q$^+$TREM-2$^+$ApoE$^+$ macrophages were described in clear CRC type for post-surgical disease recurrence in patients [340], suggesting the TREM-2$^+$ TAMs function in a pro-tumorigenic environment. Moreover, at the molecular level, TREM-2 overexpression in TAMs and peripheral blood monocytes showed a negative immune regulation effect via the SYK pathway depending on IL-10 expression in lung cancer by comparison to healthy controls [39] while others have marked high TREM-2$^+$ TAMs infiltration for the advance tumor progression in NSCLC patients [318]. In this context, expression analysis of a large NSCLC dataset showed association of TREM-2$^+$ macrophages with immunosuppression, concluded based on the higher countenance of CD206, ARG-1, and IL-10 levels [318].

Likewise, TREM-2$^+$ TAMs were correlated to the exhaustion of CD8$^+$ tumor-infiltrating lymphocytes (TILs) in mouse syngeneic tumor models and several other histological types of human solid tumors [337]. In another study, TREM-2$^+$ TAMs were reported to influence the regulatory T cells (Tregs) immunosuppressive activity and potentiated exhaustion of CD8$^+$ T cells in NSCLC [318]. Additionally, TREM-2$^+$ DCs in lung cancer were shown to exercise a substantial inhibitory effect on T cell proliferation [39]. Whereas, scRNA-seq analysis of the TME from lung cancer was predicted for high TREM-2 expression in various subsets of myeloid cells, including subgroups sharing characteristics of MDSCs [38]. In line with this, a correlative analysis in a variety of liver cancer cohorts reported the enrichment of two different macrophage subsets: SPP1$^+$TREM-2$^+$TAMs and FOLR2$^+$CD163$^+$TAMs, where the latter population being the one linked to immunosuppression [341]. However, it is important to mention that the function of TREM-2$^+$ macrophages in HCC development is controversial and require extensive investigation [155,342]. For instance, in one study, TREM-2$^+$ was negatively associated with survival rate in HCC patients [343], indicating an immunosuppressive role of TREM-2$^+$ TAMs in the TME of HCC. This result was further supported by the observation that *TREM2*knockdown in HCC could lead to an increase in proinflammatory cytokine expression and suppression of anti-inflammatory cytokine production, indicating TREM-2$^+$ TAMs can be sustained in immunosuppressive TME and promote HCC [342]. Additionally, TREM-2 expression in hepatic cells was also correlated with pathological properties, including BCLC stage, vascular invasion, tumor encapsulation, tumor size, and tumor differentiation, implying the association of TREM-2 with HCC progression [153]. Likewise, the mechanistic analysis showed that TREM-2 overexpression can inhibit metastasis of HCC via the PI3K/AKT/β-catenin signaling pathway, however, downregulated by miR-31-5p to promote metastasis and recurrence of HCC [153], as depicted in Fig. 4. In contrast, TREM-2 deficient mice exposed to the hepatocarcinogenesis protocol showed an increase in the size and number of tumors in the liver [295]. Therefore, this paradox might be justified by considering the TREM-2 function in restricting liver inflammation by transforming proinflammatory macrophage type into a tissue reparative phenotype [197]; however, further research is also required for validation in human HCC.

Together, these results support TREM-2 expression on immune cells, such as TAMs, which results in immunosuppressive TME; however, these observations do not exclude other immune cells or non-immune cells in the tumors like tumor stromal cells (Table 5), which might produce TREM-2 protein and participate in the development of immunosuppressive TME [40]. For instance, the FOLR2$^+$CD163$^+$TAMs subset was identified and associated with more immunosuppressive activity than SPP1$^+$TREM-2$^+$TAMs [341]. In addition, TREM-2 expression in cancer cells of esophageal adenocarcinoma has been documented to directly influence their growth and survival [344]. In another study, elevated levels of mRNA and protein for the TREM-2 receptor were validated in prostate adenocarcinoma (PRAD) cell lines, and knockdown of TREM-2 resulted in inhibition of both the invasive and migratory properties of PRAD cell lines via the PI3K/AKT axis [325]. Wang and his team reported a significant TREM-2 overexpression in glioma tissues compared to non-tumorous brain tissues while TREM-2 down-regulation was predicted to cause a significant reduction in cell proliferation, migration, and invasion, as well as a substantial increase in S phase arrest and cell apoptosis [29]. Furthermore, significantly high TREM-2 mRNA and protein expression in GC samples by comparison to normal gastric tissues suggested TREM-2 as a prognostic factor for OS in GC patients; however, TREM-2 expression was not ascribed to any particular cell type [34]. In another study depletion of TREM-2 expression resulted in a considerable reduction in chemokine receptor-3 (CXCR3), chemokine ligand-10 (CXCL10), matrix metalloproteinase-2 (MMP-2), and MMP-9 production, all known for critical function in TME [29]. In addition, an absence of TREM-2, initiated accumulation of NK cells and cytotoxic T cells in the TME whereas PD1- and Tim-3-expressing dysfunctional CD8$^+$ T cells were reduced by comparison to wild-type mice [37]. These observations supported that TREM-2 deficiency results in a reduction of

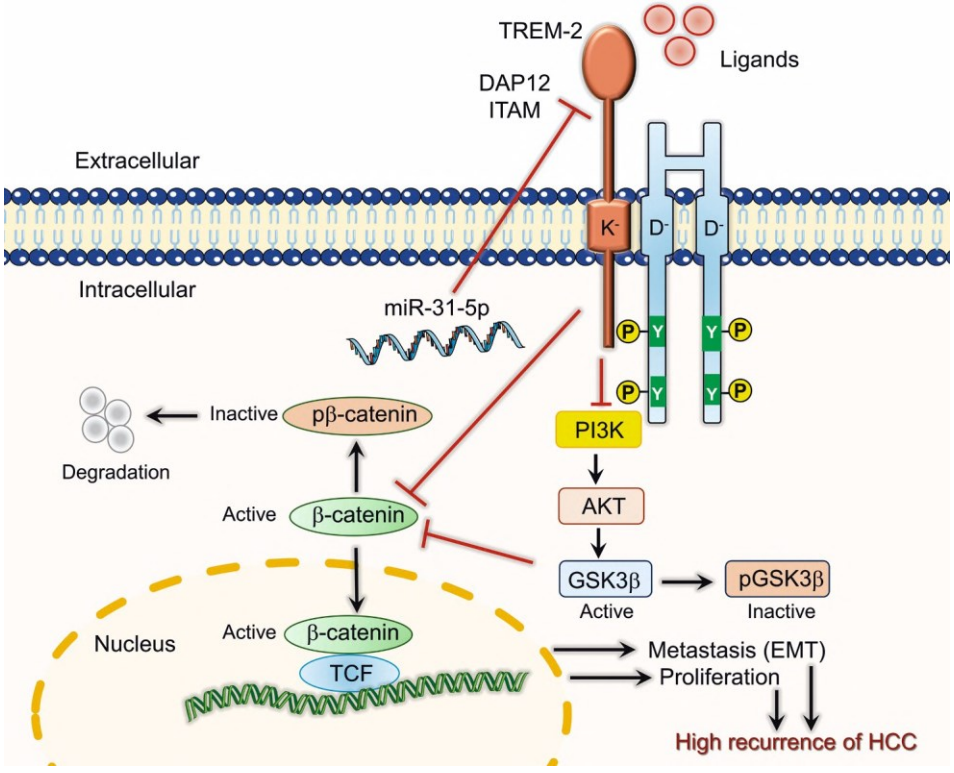

Fig. 4. Schematic diagram for TREM-2-mediated pathways in HCC progression and metastasis. miR-31-5p expressed by cancer cells can cause a loss of TREM-2 expression in tumor tissues, which could activate β-catenin and AKT and GSK3β phosphorylation to attenuate oncogenic and metastatic behaviours of HCC [153].

Table 5
Cancer types with infiltrated TREM-2$^+$ immune cells in TME to promote cancer progression and development.

Cancer	Immune cells/phenotypes	References
Glioblastoma	Macrophages and microglia	[16,171,323,345]
Breast cancer	Tumor-associated macrophages	[346–348]
Triple negative breast cancer	Lipid-associated macrophages, Tumor-associated macrophages	[349,350]
Diffuse large B-cell lymphoma	Monocytic myeloid-derived suppressive cells	[42]
Sarcoma	Tumor-associated macrophages, Tumor-infiltrating macrophages. Myeloid-derived suppressor cells	[32,37]
Melanoma	Tumor-associated macrophages	[199]
Hepatocellular Carcinoma	Tumor-associated macrophages, Lipid-associated macrophages, Scar-associated macrophages, Monocyte-derived macrophages	[295,324,342]
Pancreatic ductal adenocarcinoma	Tumor-associated macrophages	[351]
Prostate cancer	Immunosuppressive neutrophils	[212]
Lung cancer	Monocytes, monocyte-derived macrophages, dendritic cells, macrophages (Mφs),	[43,352]
Lung adenocarcinoma	Tumor-associated macrophages	[38]
Non-small cell lung cancer	Tumor-associated macrophages, Monocyte-derived macrophages	[318,353]
Oral Squamous Cell Carcinoma	Macrophages in peripheral blood mononuclear cells, tumor-associated macrophages	[354]
Colorectal cancer	Tumor-associated macrophages Myeloid-derived suppressor cells	[337,338,355]
Renal Cell Carcinoma	Tumor-infiltrating myeloid cells	[356]
Clear cell renal carcinoma	Tumor-associated macrophages (M2 type) Tissue-resident monocytes	[340,357]
Ovarian cancer	Tumor-associated macrophages	[337]

immunosuppressive TME and promotes anti-tumor activity [32,37]. Based on reported TREM-2 function and expression in immune cells and some solid tumors, TREM-2 substantially contributes to immunosuppressive TME development and imposes differential effects on tumor progression. Thus, any attempt to enhance TREM-2 expression might improve the immune response against malignant cells, which signifies a form of potential cancer immunotherapy.

6.2. Cancer immunotherapy

TREM-2 deficiency and TREM-2 blockade are widely advocated to encourage stronger anti-tumor responses using mice models [32,37]. Accordingly, to achieve TREM-2-based immunotherapy, several approaches can be applied to inhibit the TREM-2 receptor or TREM-2-mediated signaling pathway, such as blockage of the TREM-2 extracellular domain using specific monoclonal antibodies (mAbs), depletion of conditional TREM-2 ligands that occur in the immunosuppressive TME, or direct inhibition of molecules involved in TREM-2 downstream singling. Even though little clinical research has been done or is being conducted now on targeting TREM-2 in cancer, the therapeutic potential of anti-TREM-2 therapy for clinical translation remains vast.

As TAMs have been characterized as promoting cancer progression and development [32,334,335], thus, the deletion of suppressive TAM phenotypes has been suggested as a promising therapeutic strategy for cancer immunotherapy [358]. In this context, TREM-2 depletion and anti-TREM-2 antibodies have been informed to enhance the curative efficacy of anti-PD-1 treatment [338]. Similarly, in other studies, macrophage-specific deletion of TREM-2 was noted to encourage anti-tumor immune functions [37] and TREM-2-targeted antibodies were shown to have mounting anti-PD1 efficacy in syngeneic renal cancer models [32]. However, even within the same cancers, such as HCC, TREM-2 may exhibit differential or even inverse functions [295,342]. Thus, direct targeting of TREM-2 in tumors where TREM-2 displays a tumor suppressor character may result in drug resistance development or boost tumor progression. However, The Cancer Genome Atlas (TCGA) database analysis suggested that anti-TREM-2 treatment may be particularly promising in CRC and TNBC because TREM-2 expression has been inversely correlated with OS and relapse in these cancer patients [32]. Likewise, in NK cells, targeting TREM-2 may block the NK cells' maturation and their competence to destroy tumor cells [210]. For instance, in the TREM-2 knockout mice model of HCC, a significant upregulation of NK cells and CD8$^+$ T cells was noted along with enhanced production of PD-1 and IFN-γ in CD8$^+$ T cells, suggesting that deficiency of TREM-2 promoted the infiltration of NK/CD8$^+$ T cells to endorse CD8$^+$ T cells activation and mediated cytotoxicity [35]. Additionally, a recent study on a murine lung adenocarcinoma model showed that phagocytosis of tumor debris by monocyte-derived macrophages stimulates a TREM-2-mediated pro-tumorigenic cascade. As a result, TREM-2$^+$ monocyte-derived macrophages were noticed to reduce the activity of NK cells through regulation of IL-18/IL-18BP decoy interactions and IL-15 generation [43]. Moreover, genetic deletion of TREM-2 on monocyte-derived macrophages rescued NK cell accumulation and enabled an NK cell-mediated regression of lung tumors [43]. Therefore, TREM-2 inhibition synergized with an NK cell-activating agent to further block tumor growth has been advocated as a new strategy to boost antitumor immunity [43].

In the quest for anti-TREM-2, therefore, Fc domain-enhanced anti-TREM-2 monoclonal antibody (mAb 178, carrying a mutation to neutralize its Fc-binding properties) based elimination and modulation of the TREM-2$^+$ TAM population have been demonstrated to enhance the anti-tumor immunity by improving the infiltration and effector function of CD8$^+$ TILs infiltration in an aggressive orthotopic ovarian cancer model [32]. Similarly, administration of an anti-TREM-2 fully fucosylated humanized monoclonal antibody (PY314 mAb) in an EMT6 mammary cancer model showed strong antibody-dependent cellular cytotoxicity (ADCC) that significantly contributed to the tumor growth inhibition, which was assumed to happen due to the depletion of TREM-2$^+$ immunosuppressive TAMs [337]. Also, the administration of PY314 mAb along with anti-PD in colon carcinoma subcutaneous tumors showed a reduction in anti-PD1 resistance [337]. Moreover, effective anti-TREM-2 antibody-based treatment was suggested in ovarian cancer because of the highly immunosuppressed TME carrying abundant TREM-2$^+$ TAMs, as well as based on the anti-tumor response exhibited by the anti-TREM-2 mAb in a preclinical orthotopic model of ovarian cancer [337]. Overall, molecular insights associated the therapeutic effects of PY314 with a reduction in invasion of pro-tumorigenic M2 type macrophage phenotypes while improving the intrusion of NK cells, CD8$^+$ T cells, and M1 type macrophage phenotypes in the TME [337]. Presently, a Phase I clinical trial (ClinicalTrials.gov identifier: NCT04691375) for the anti-TREM-2 PY314 mAb is underway, where it is directed either as a single agent or in combination with pembrolizumab (αPD-1) in patients with locally advanced and/or metastatic solid tumors, which are relapsed or unmanageable by standard of care treatment (ClinicalTrials.gov identifier: NCT04691375). Accordingly, data published from a phase 1b open-label study to evaluate the performance of PY314 mAb combined with pembrolizumab in checkpoint inhibition (CPI)-refractory advanced RCC patients demonstrated considerable safety but limited anti-tumor effect (ClinicalTrials.gov identifier: NCT04691375) [359]. Moreover, a kind of platinum-based TREM-2 inhibitor is also under evaluation to inhibit tumor growth in an MC38-bearing mouse model [360].

In summary, despite the limited preclinical and clinical studies available on anti-TREM-2, pharmacological targeting of TREM-2 signaling on different immune cells, especially TREM-2$^+$ TAMs, and specific TREM-2$^+$ tumor cells may exhibit or promote anti-tumor immunity. Moreover, as TREM-2 essentially acts in cell survival, metabolism, migration, and chemokine production, anti-TREM-2 agents may potentially intervene with respective TREM-2-mediated pathways in

TREM-2$^+$ cells [32,146,157]. Thus, targeting TREM-2 by anti-TREM-2 agents offers a strong rationale for designing new immunotherapy to achieve a stronger antitumor effect. However, anti-TREM-2 may also over-activate rather than inhibit TREM-2-mediated signaling pathways, resulting in anergy and/or exhaustion [32]. Therefore, advanced experiments would be required to characterize the anti-TREM-2 therapeutic effects on different TREM-2-mediated pathways in immune and/or non-immune cells in TME.

7. Conclusion and future perspective

Available literature advocates the central role of TREM-2 in various cells derived from myeloid lineages for different biological functions, including cell differentiation and survival, metabolism, and immunomodulation. For example, in healthy tissues, TREM-2 expression is exclusively restricted to microglia, alveolar, and placental macrophages, which provides a potent immunosuppressive environment to advance lenience for the semi-allogeneic fetus [32,361]. Even after understanding the complex biology of TREM-2 since its identification in DCs and other immune cells, several questions remain to be addressed. In this perspective, given that the TREM-2 receptor exhibits a specific signaling cascade by interaction with multiple ligands, a complete understanding of the adopted downstream signaling pathways has been hampered by the failure to determine the specific physiologic ligands for the TREM-2 receptor. Also, the TREM-2 receptor is reported to form self-heteromeric and/or multimeric complexes by crosslinking with other cell surface-expressed receptors to exhibit specific biological functions. For instance, TREM-2 docked with the TCR-CD3ζ-ZAP70 complex and the IFN-γR in CD4$^+$ T cells to enhance proinflammatory Th1 responses [134] and Phexin-A receptor for demonstrating phagocytic function to neutralise bacterial infection [115,125], further hinders the process of TREM-2 ligand identification. However, at the same time, it also offers an avenue for research in TREM-2 biology, including in TREM-2-mediated innate and adaptive immunity. Thus, prospective biochemical and molecular studies, including three-dimensional crystal structure elucidation methods can be designed to define the TREM-2 homomeric and heteromeric complexes with relative binding affinities to specific endogenous or exogenous ligands, and their cell-specific-mediated signaling in normal physiological or pathological tissue microenvironment.

Using bioinformatics and experimental methods, several genetic changes in the *TREM2* gene have been established in microglia that affect the neuroimmune system, while most of them have been associated with an elevated risk of NDDs, in addition to their contribution to secreting the sTREM-2 isoform or interfere with TREM-2 ligand binding. In regard to other TREM-2-linked disorders, the role of known TREM-2 variants, sTREM-2, and other isoforms is not studied in other myeloid-derived cells for functional activity. Thus, a rational combination of deep mutational analysis of TREM-2 with full-length and/or cell-type TREM-2 expression may provide a profound understanding of the underlying molecular mechanism associated with TREM-2 and other pathologies, such as autoimmune diseases and cancers, like HCC and brain tumors, in humans. Moreover, a correlation between mutations within TREM-2 and diseases-associated genes or translated proteins can further bid the potential to decipher the relationship between TREM-2 variants or isoforms and TREM-2-assocated disorders like occurred due to altered phagocytic function, enhanced expression of pro-inflammatory signals, and failure to respond after docking with specific ligand to the receptor.

In context to sTREM-2, its high levels in CSF have been found to have beneficial effects in AD reducing tau-induced pathology [135,362,363]. Remarkably, sTREM-2 can increase both inflammation cytokine production by depending on the NF-κB pathway and survival in a PI3K/AKT-dependent manner in cultured microglia [207]. Thus, a trimmed form of sTREM-2 can be used to achieve the beneficial effects only. Correspondingly, Zhang et al. [135] reported a 13-residue peptide mimicking sTREM2 (77–89 aa) as a potential therapeutic intervention for tau-induced pathology in AD. However, the sTREM-2 role is yet to be understood in other TREM-2-associated disorders, and if found beneficial, as in AD, recombinant sTREM-2 or peptides mimicking sTREM-2 beneficial activity-based treatments may be extended as therapeutic in other studies, such as liver-associated metabolic disorders and cancer immunotherapy.

Furthermore, the functional role of surplus TREM-2 signaling is yet to be answered under pathological conditions. Notably, the TREM-2^{T96K} variant was shown to promote the ligand binding or downstream signaling cascade [48,102], but this variant has not been robustly linked to reported disorders in humans. In another study, TREM-2 overexpression showed diminished inflammation and enhanced phagocytosis of microglia *in vitro* [167]. Thereof, it would also be of utmost importance to identify the gain-of-function TREM-2 mutants and establish their functional role in TREM-2-associated other diseases. These results could be helpful in adopting antagonist (such as reducing inflammation) or agonist (like promoting cell survival and differentiation)-based TREM-2 therapeutic strategies. As various TREM-2 variants have been identified and reviewed elsewhere, especially in the context of NDDs [71,72,170], genome-wide association studies on human populations involving or comparing other than Americans and Europeans should be considered to completely understand the impact of TREM-2 heterogeneity on the genetic architecture of TREM-2-mediated disorders.

Besides, the TREM-2 receptor appears to highly exhibit cell-type and content-specific biological function, where it is highlighted for both protective and detrimental effects. For example, TREM-2 promotes clearance of *Pseudomonas aeruginosa* keratitis [364] while aggravate pneumococcal pneumonia and Sendai virus respiratory infection [66,275]. Thus, molecular understanding of TREM-2 regulatory factors and downstream effectors in the cytosol can further provide insights into the underlying singling pathway, which can be studied as alternative drug targets to manipulate TREM-2 expression and mediated cascades under pathological conditions. Meanwhile, the regulatory effect of UTRs, epigenetics, and posttranscriptional modifications is also documented on TREM-2 expression, but it is limited to a few cell types and needs validation in other TREM-2$^+$ cells under different tissue microenvironments. Thus, understanding the TREM-2 expression mechanism, location, and involved regulators in immune cells and non-immune cells can provide insights into TREM-2-linked functions under both normal and pathological conditions. Meanwhile, TREM-2 glycosylation, as a major post-translational modification, has been found in immune cells, but no specific biological role has been associated with this type of modification. Thus, further research is required to determine the glycosylated TREM-2 receptor function in both immune and non-immune cells. In particular, the identification of glycosylated TREM-2 with specific glycan modifications, such as N- or O-glycosylation, can be exploited for the design of anti-glycan antibodies or small protein-based binders for TREM-2-associated disorders such as chronic infections, autoimmune diseases, and NDDs.

In the context of tumorigenesis, TREM-2 seems to exert immunesuppressive activities to promote immune evasion and tumor progression, in part through TAMs-mediated immunosuppression development [32,332,334,335,365] and modulating T cell function [32]; thereof, labeled as a marker of TAMs in numerous tumor types, in both humans and murine models [366]. Accordingly, inactivation of the TREM-2 receptor or depletion of TREM-2$^+$ TAMs in the immunosuppressive TME has been widely advocated as a potential strategy to reactivate the T cell-mediated anti-tumor immune responses. Consequently, anti-TREM-2 antibody-dependent cellular cytotoxicity (ADCC) or monoclonal antibodies acting as TREM-2 antagonists are two leading strategies for reversing the myeloid immune-suppressive environment and are emerging as a promising approach in cancer immunotherapy [32,337]. Also, the potential therapeutic applications of sTREM-2 in cancer immunotherapy may present hopeful prospects, albeit with uncertainties. Therefore, it is predictable that these approaches will further

develop through a new generation of TREM agonists and antagonists which may impact ligand binding or delivery of intracellular signals through DAP12 or DAP10 adapters, as well as associated downstream cascade molecules. Therefore, modified TREM-2 agonists or antagonists can also be developed to increase efficacy and reduce the potential activation of TREM-2^{+} cells in other organs, such as the brain, lungs, and liver.

Intriguingly, most *in vivo* studies to understand the functional role of TREM-2 have been performed in knockout mice models. Although human and mouse TREM-2 proteins are expected to have conserved functions, but TREM-2 receptor appears to exhibit species-specific regulatory mechanisms [250]. In support, a recent report established the divergence of TREM-2 alternative splicing at exon 3 between humans and mice mediated by CELF2 RBPs, presented a novel regulatory factor of TREM-2 expression, and emphasised a species-dependent difference in TREM-2 regulation [64]. Thus, it will be important to establish whether the presence of additional and/or non-homologous TREM-2 receptors in mice might impact disease models. Perhaps generating new mouse models that more closely recapitulate human TREM-2, such as transgenic humanized mice, would be appropriate for further studies on the exploration of TREM-2 biology, including endogenous ligands, signaling properties, crosslinking with other receptors or pathways, and successive impact in various pathophysiological conditions.

Conclusively, despite significant strides in TREM-2 biology, including understanding TREM-2′s diverse role in various myeloid cell lineage and associated disorders, a critical gap still persists, mostly due to multifactorial challenges, including a broad portfolio of ligands, crosslinking of TREM-2 protein with other cell surface receptors, and downstream signalling pathways, some of which are not yet acknowledged. Addressing these gaps through continued research on TREM-2′s regulation, expression, cell- and content-specific functions, as well as species-specific differences, is essential for its implications as a drug target and for developing relevant TREM-2 antagonist or agonist-based therapies. Therefore, further research on integrating large-scale genomic and proteomics data with comprehensive humanized animal models that closely mimic human TREMs may provide a more accurate understanding of TREM-2 in physiological and pathological conditions.

CRediT authorship contribution statement

Shiv Bharadwaj: Writing – review & editing, Writing – original draft, Visualization, Validation, Resources, Data curation, Conceptualization. **Yaroslava Groza:** Writing – review & editing, Writing – original draft, Visualization, Data curation. **Joanna M. Mierzwicka:** Writing – review & editing, Writing – original draft, Data curation. **Petr Malý:** Writing – review & editing, Writing – original draft, Validation, Supervision, Resources, Formal analysis.

Declaration of Competing Interest

The authors declare that they have no known competing financial interests or personal relationships that could have appeared to influence the work reported in this paper.

Acknowledgement

The authors acknowledge the support from the Institute of Biotechnology of the Czech Academy of Sciences v.v.i. (Institutional Research Concept, RVO: 86652036).

References

[1] T. Chavakis, Leucocyte recruitment in inflammation and novel endogenous negative regulators thereof, Eur. J. Clin. Invest. 42 (6) (2012) 686–691.
[2] K.A. Thomas, R.G. King, C.M. Sestero, L.B. Justement, TREM-like transcript 2 is stored in human neutrophil primary granules and is up-regulated in response to inflammatory mediators, J. Leukoc. Biol. 100 (1) (2016) 177–184.
[3] J.W. Ford, D.W. McVicar, TREM and TREM-like receptors in inflammation and disease, Curr. Opin. Immunol. 21 (1) (2009) 38–46.
[4] J. Klesney-Tait, I.R. Turnbull, M. Colonna, The TREM receptor family and signal integration, Nat. Immunol. 7 (12) (2006) 1266–1273.
[5] H. Singh, V. Rai, S.K. Nooti, D.K. Agrawal, Novel ligands and modulators of triggering receptor expressed on myeloid cells receptor family: 2015–2020 updates, Expert Opin. Ther. Pat. 31 (6) (2021) 549–561.
[6] R.J.N. Allcock, A.D. Barrow, S. Forbes, S. Beck, J. Trowsdale, The human TREM gene cluster at 6p21.1 encodes both activating and inhibitory single IgV domain receptors and includes NKp44, Eur. J. Immunol. 33 (2) (2003) 567–577.
[7] M. Colonna, The biology of TREM receptors, Nat. Rev. Immunol. (2023).
[8] G. Sessa, P. Podini, M. Mariani, A. Meroni, R. Spreafico, F. Sinigaglia, M. Colonna, P. Panina, J. Meldolesi, Distribution and signaling of TREM2/DAP12, the receptor system mutated in human polycystic lipomembraneous osteodysplasia with sclerosing leukoencephalopathy dementia, Eur. J. Neurosci. 20 (10) (2004) 2617–2628.
[9] I. Prada, G.N. Ongania, C. Buonsanti, P. Panina-Bordignon, J. Meldolesi, Triggering receptor expressed in myeloid cells 2 (TREM2) trafficking in microglial cells: continuous shuttling to and from the plasma membrane regulated by cell stimulation, Neuroscience 140 (4) (2006) 1139–1148.
[10] Y.J. Zhao, X.G. Li, T. Huang, L.L. Jiang, Z.Q. Tan, M.X. Zhang, I.H.J. Cheng, X. Wang, G.J. Bu, Y.W. Zhang, Q. Wang, H.X. Xu, Intracellular trafficking of TREM2 is regulated by presenilin 1, Exp. Mol. Med. 49 (2017).
[11] Y.H. Wang, Y. Chu, F.H. Cao, Z.H. Chen, H.X. Xu, S.J. Wang, J. Ma, The emerging role of triggering receptor expressed on myeloid cell-2 in malignant tumor, Cent Eur J Immunol 47 (4) (2022) 373–381.
[12] J.L. Yang, Z.H. Fu, X.Y. Zhang, M. Xiong, L.X. Meng, Z.T. Zhang, TREM2 ectodomain and its soluble form in Alzheimer's disease, J Neuroinflamm 17 (1) (2020).
[13] R. Dhandapani, M. Neri, M. Bernhard, I. Brzak, T. Schweizer, S. Rudin, S. Joller, R. Berth, J. Kernen, A. Neuhaus, A. Waldt, R. Cuttat, U. Naumann, C.G. Keller, G. Roma, D. Feuerbach, D.R. Shimshek, U. Neumann, F. Gasparini, I. Galimberti, Sustained Trem2 stabilization accelerates microglia heterogeneity and Af3 pathology in a mouse model of Alzheimer's disease, Cell Rep. 39 (9) (2022).
[14] H. Neumann, K. Takahashi, Essential role of the microglial triggering receptor expressed on myeloid cells-2 (TREM2) for central nervous tissue immune homeostasis, J. Neuroimmunol. 184 (1–2) (2007) 92–99.
[15] A. Paradowska-Gorycka, M. Jurkowska, Structure, expression pattern and biological activity of molecular complex TREM-2/DAP12, Hum. Immunol. 74 (6) (2013) 730–737.
[16] R. Sun, R.W. Han, C. McCornack, S. Khan, G.T. Tabor, Y. Chen, J.C. Hou, H. W. Jiang, K.M. Schoch, D.D. Mao, R. Cleary, A.L.C. Yang, Q. Liu, J.Q. Luo, A. Petti, T.M. Miller, J.D. Ulrich, D.M. Holtzman, A.H. Kim, TREM2 inhibition triggers antitumor cell activity of myeloid cells in glioblastoma, Sci. Adv. 9 (19) (2023).
[17] Y.J. Wu, M.N. Wang, H. Yin, S.Q. Ming, X.Y. Li, G.M. Jiang, Y. Liu, P.H. Wang, G. D. Zhou, L. Liu, S.T. Gong, H.B. Zhou, H. Shan, X. Huang, TREM-2 is a sensor and activator of T cell response in SARS-CoV-2 infection, Sci. Adv. 7 (50) (2021).
[18] M. Hwang, C. Savarin, J. Kim, J. Powers, N. Towne, H. Oh, C.C. Bergmann, Trem2 deficiency impairs recovery and phagocytosis and dysregulates myeloid gene expression during virus-induced demyelination, J Neuroinflamm 19 (1) (2022).
[19] W.C. Zhou, Y.T. Zhou, J.C. He, Y.Q. Rao, P. Fei, J. Li, TREM2 deficiency in microglia accelerates photoreceptor cell death and immune cell infiltration following retinal detachment, Cell Death Dis. 14 (3) (2023).
[20] L. Piccio, C. Buonsanti, M. Mariani, M. Cella, S. Gilfillan, A.H. Cross, M. Colonna, P. Panina-Bordignon, Blockade of TREM-2 exacerbates experimental autoimmune encephalomyelitis, Eur. J. Immunol. 37 (5) (2007) 1290–1301.
[21] A. McQuade, Y.J. Kang, J. Hasselmann, A. Jairaman, A. Sotelo, M. Coburn, S. K. Shabestari, J.P. Chadarevian, G. Fote, C.H. Tu, E. Danhash, J. Silva, E. Martinez, C. Cotman, G.A. Prieto, L.M. Thompson, J.S. Steffan, I. Smith, H. Davtyan, M. Cahalan, H. Cho, M. Blurton-Jones, Gene expression and functional deficits underlie TREM2-knockout microglia responses in human models of Alzheimer's disease (vol 11, 5370, 2020), Nat. Commun. 14 (1) (2023).
[22] G. Kleinberger, Y. Yamanishi, M. Suarez-Calvet, E. Czirr, E. Lohmann, E. Cuyvers, H. Struyfs, N. Pettkus, A. Wenninger-Weinzierl, F. Mazaheri, S. Tahirovic, A. Lleo, D. Alcolea, J. Fortea, M. Willem, S. Lammich, J.L. Molinuevo, R. Sanchez-Valle, A. Antonell, A. Ramirez, M.T. Heneka, K. Sleegers, J. van der Zee, J.J. Martin, S. Engelborghs, A. Demirtas-Tatlidede, H. Zetterberg, C. Van Broeckhoven, H. Gurvit, T. Wyss-Coray, J. Hardy, M. Colonna, C. Haass, TREM2 mutations implicated in neurodegeneration impair cell surface transport and phagocytosis, Sci. Transl. Med. 6 (243) (2014).
[23] J.S. Park, I.J. Ji, H.J. An, M.J. Kang, S.W. Kang, D.H. Kim, S.Y. Yoon, Disease-associated mutations of TREM2 alter THE PROCESSING OF N-LINKED OLIGOSACCHARIDES IN THE GOLGI APparatus, Traffic 16 (5) (2015) 510–518.
[24] B. Borroni, F. Ferrari, D. Galimberti, B. Nacmias, C. Barone, S. Bagnoli, C. Fenoglio, I. Piaceri, S. Archetti, C. Bonvicini, M. Gennarelli, M. Turla, E. Scarpini, S. Sorbi, A. Padovani, Heterozygous mutations in frontotemporal dementia, Neurobiol. Aging 35 (4) (2014).
[25] R. Guerreiro, A. Wojtas, J. Bras, M. Carrasquillo, E. Rogaeva, E. Majounie, C. Cruchaga, C. Sassi, J.S. Kauwe, S. Younkin, L. Hazrati, J. Collinge, J. Pocock, T. Lashley, J. Williams, J.C. Lambert, P. Amouyel, A. Goate, R. Rademakers, K. Morgan, J. Powell, P. St George-Hyslop, A. Singleton, J. Hardy, G. Alzheimer Genetic Analysis, TREM2 variants in Alzheimer's disease, N Engl J Med 368(2) (2013) 117-27.
[26] S. Rayaprolu, B. Mullen, M. Baker, T. Lynch, E. Finger, W.W. Seeley, K. J. Hatanpaa, C. Lomen-Hoerth, A. Kertesz, E.H. Bigio, C. Lippa, K.A. Josephs, D.

S. Knopman, C.L. White 3rd, R. Caselli, I.R. Mackenzie, B.L. Miller, M. Boczarska-Jedynak, G. Opala, A. Krygowska-Wajs, M. Barcikowska, S.G. Younkin, R. C. Petersen, N. Ertekin-Taner, R.J. Uitti, J.F. Meschia, K.B. Boylan, B.F. Boeve, N. R. Graff-Radford, Z.K. Wszolek, D.W. Dickson, R. Rademakers, O.A. Ross, TREM2 in neurodegeneration: evidence for association of the p. R47H variant with frontotemporal dementia and Parkinson's disease, Mol. Neurodegener. 8 (2013) 19.

[27] H. Klünemann, B.H. Ridha, L. Magy, J.R. Wherrett, D.M. Hemelsoet, R.W. Keen, J. L. DeBleecker, M.N. Rossor, J. Marienhagen, H.E. Klein, L. Peltonen, J. Paloneva, The genetic causes of basal ganglia calcification, dementia, and bone cysts: DAP12 and TREM2, Neurology 66 (4) (2006) 615–616.

[28] T.D. Bird, R.M. Koerker, B.J. Leaird, B.W. Vlcek, D.R. Thorning, Lipomembranous polycystic osteodysplasia (brain, bone, and fat disease) - a genetic cause of presenile-dementia, Neurology 33 (1) (1983) 81–86.

[29] X.Q. Wang, B.B. Tao, B. Li, X.H. Wang, W.C. Zhang, L. Wan, X.M. Hua, S.T. Li, Overexpression of TREM2 enhances glioma cell proliferation and invasion: a therapeutic target in human glioma, Oncotarget 7 (3) (2016) 2354–2366.

[30] K. Kluckova, J. Kozak, K. Szaboova, B. Rychly, M. Svajdler, M. Suchankova, E. Tibenska, B. Filova, J. Steno, V. Matejcik, M. Homolova, M. Bucova, TREM-1 and TREM-2 expression on blood monocytes could help predict survival in high-grade glioma patients, Mediat Inflamm 2020 (2020).

[31] X. Cheng, X. Wang, K. Nie, L. Cheng, Z. Zhang, Y. Hu, W. Peng, Systematic pan-cancer analysis identifies TREM2 as an immunological and prognostic biomarker, Front. Immunol. 12 (2021) 646523.

[32] M. Molgora, E. Esaulova, W. Vermi, J.C. Hou, Y. Chen, J.Q. Luo, S. Brioschi, M. Bugatti, A.S. Omodei, B. Ricci, C. Fronick, S.K. Panda, Y. Takeuchi, M. M. Gubin, R. Faccio, M. Cella, S. Gilfillan, E.R. Unanue, M.N. Artyomov, R. D. Schreiber, M. Colonna, TREM2 modulation remodels the tumor myeloid landscape enhancing anti-PD-1 immunotherapy, Cell 182 (4) (2020) 886-+.

[33] C.M. Li, X.M. Hou, S.A. Yuan, Y.G. Zhang, W.Z. Yuan, X.G. Liu, J. Li, Y.P. Wang, Q.L. Guan, Y.N. Zhou, High expression of TREM2 promotes EMT via the PI3K/AKT pathway in gastric cancer: bioinformatics analysis and experimental verification, J. Cancer 12 (11) (2021) 3277–3290.

[34] X. Zhang, W. Wang, P. Li, X. Wang, K. Ni, High TREM2 expression correlates with poor prognosis in gastric cancer, Hum. Pathol. 72 (2018) 91–99.

[35] J.Z. Tan, W.Z. Fan, T. Liu, B.W. Zhu, Y.F. Liu, S.T. Wang, J. Wu, J. Liu, F. Zou, J. L. Wei, L.W. Liu, X.K. Zhang, J.L. Zhuang, Y. Wang, H.B. Lin, X.Z. Huang, S. L. Chen, M. Kuang, J.P. Li, TREM2+macrophages suppress CD8+T-cell infiltration after transarterial chemoembolisation in hepatocellular carcinoma, J. Hepatol. 79 (1) (2023) 126–140.

[36] H.J. Zhang, L. Sheng, J. Tao, R. Chen, Y. Li, Z.Q. Sun, W.Q. Qian, Depletion of the triggering receptor expressed on myeloid cells 2 inhibits progression of renal cell carcinoma via regulating related protein expression and PTEN-PI3K/Akt pathway, Int. J. Oncol. 49 (6) (2016) 2498–2506.

[37] Y. Katzenelenbogen, F. Sheban, A. Yalin, I. Yofe, D. Svetlichnyy, D.A. Jaitin, C. Bornstein, A. Moshe, H. Keren-Shaul, M. Cohen, S.Y. Wang, B.G. Li, E. David, T. M. Salame, A. Weiner, I. Amit, Coupled scRNA-Seq and intracellular protein activity reveal an immunosuppressive role of TREM2 in cancer, Cell 182 (4) (2020) 872-+.

[38] Y. Lavin, S. Kobayashi, A. Leader, E.D. Amir, N. Elefant, C. Bigenwald, R. Remark, R. Sweeney, C.D. Becker, J.H. Levine, K. Meinhof, A. Chow, S. Kim-Shulze, A. Wolf, C. Medaglia, H. Li, J.A. Rytlewski, R.O. Emerson, A. Solovyov, B. D. Greenbaum, C. Sanders, M. Vignali, M.B. Beasley, R. Flores, S. Gnjatic, D. Pe'er, A. Rahman, I. Amit, M. Merad, Innate immune landscape in early lung adenocarcinoma by paired single-cell analyses, Cell 169 (4) (2017) 750–765 e17.

[39] Y.A. Yao, H.Q. Li, J.J. Chen, W.Y. Xu, G.D. Yang, Z. Bao, D.J. Xia, G.H. Lu, S. W. Hu, J.Y. Zhou, TREM-2 serves as a negative immune regulator through Syk pathway in an IL-10 dependent manner in lung cancer, Oncotarget 7 (20) (2016) 29620–29634.

[40] A. Deczkowska, A. Weiner, I. Amit, The physiology, pathology, and potential therapeutic applications of the TREM2 signaling pathway, Cell 181 (6) (2020) 1207–1217.

[41] B. van Lengerich, L.H. Zhan, D. Xia, D. Chan, D. Joy, J.I. Park, D. Tatarakis, M. Calvert, S. Hummel, S. Lianoglou, M.E. Pizzo, R. Prorok, E. Thomsen, L. M. Bartos, P. Beumers, A. Capell, S.S. Davis, L. de Weerd, J.C. Dugas, J. Duque, T. Earr, K. Gadkar, T. Giese, A. Gill, J. Gno¨rich, C. Ha, M. Kannuswamy, D.J. Kim, S.T. Kunte, L.H. Kunze, D. Lac, K. Lechtenberg, A.W.S. Leung, C.C. Liang, I. Lopez, P. McQuade, A. Modi, V.O. Torres, H.N. Nguyen, I. Pes¨amaa, N. Propson, M. Reich, Y. Robles-Colmenares, K. Schlepckow, L. Slemann, H. Solanoy, J. H. Suh, R.G. Thorne, C. Vieira, K. Wind-Mark, K. Xiong, Y.J.Y. Zuchero, D. Diaz, M.S. Dennis, F. Huang, K. Scearce-Levie, R.J. Watts, C. Haass, J.W. Lewcock, G. Di Paolo, M. Brendel, P.E. Sanchez, K.M. Monroe, A TREM2-activating antibody with a blood-brain barrier transport vehicle enhances microglial metabolism in Alzheimer's disease models, Nat. Neurosci. 26 (3) (2023) 416-+.

[42] H.Y. Wang, F.C. Yang, C.F. Yang, Y.C. Liu, P.S. Ko, C.J. Li, C.K. Tsai, Y.L. Chung, N.J. Chen, Surface TREM2 on circulating M-MDSCs as a novel prognostic factor for adults with treatment-naive diffuse large B-cell lymphoma, Exp. Hematol. Oncol. 12 (1) (2023).

[43] M.D. Park, I. Reyes-Torres, J. LeBerichel, P. Hamon, N.M. LaMarche, S. Hegde, M. Belabed, L. Troncoso, J.A. Grout, A. Magen, E. Humblin, A. Nair, M. Molgora, J.C. Hou, J.H. Newman, A.M. Farkas, A.M. Leader, T. Dawson, D. D'Souza, S. Hamel, A.R. Sanchez-Paulete, B. Maier, N. Bhardwaj, J.C. Martin, A. O. Kamphorst, E. Kenigsberg, M. Casanova-Acebes, A. Horowitz, B.D. Brown, L. F. De Andrade, M. Colonna, T.U. Marron, M. Merad, TREM2 macrophages drive NK cell paucity and dysfunction in lung cancer, Nat. Immunol. (2023).

[44] X.L. Xie, W.J. Zhang, M. Xiao, T.T. Wei, Y.Q. Qiu, J.Y. Qiu, H. Wang, Z.Y. Qiu, S. Zhang, Y.T. Pan, L.L. Mao, Y.H. Li, B. Guo, W.W. Yang, Y.X. Hu, S.J. Hu, Y. Gong, J. Yang, G.Z. Xiao, Y. Zhang, X.C. Bai, TREM2 acts as a receptor for IL-34 to suppress acute myeloid leukemia in mice, Blood 141 (26) (2023) 3184–3198.

[45] W.H. Qiao, Y.X. Chen, J. Zhong, B.J. Madden, C.M. Charlesworth, Y.A. Martens, C.C. Liu, J. Knight, T.C. Ikezu, K. Aishe, Y.Y. Zhu, A. Meneses, C.L. Rosenberg, L. A. Kuchenbecker, L.K. Vanmaele, F.Y. Li, K. Chen, F. Shue, M.V. Dacquel, J. Fryer, A. Pandey, N. Zhao, G.J. Bu, H157Y increases soluble TREM2 production and reduces amyloid pathology (vol 18, 8, 2023), Mol. Neurodegener. 18 (1) (2023).

[46] K.M. Tran, S. Kawauchi, E.A. Kram´ar, N. Rezaie, H.Y. Liang, J.S. Sakr, A. Gomez-Arboledas, M.A. Arreola, C. da Cunha, J. Phan, S.L. Wang, S. Collins, A. Walker, K.X. Shi, J. Neumann, G. Filimban, Z.C. Shi, G. Milinkeviciute, D.I. Javonillo, K. Tran, M. Gantuz, S. Forner, V. Swarup, A.J. Tenner, F.M. LaFerla, M.A. Wood, A. Mortazavi, G.R. MacGregor, K.N. Green, A Trem2R47H mouse model without cryptic splicing drives age- and disease-dependent tissue damage and synaptic loss in response to plaques, Mol. Neurodegener. 18 (1) (2023).

[47] A. Bouchon, C. Hernandez-Munain, M. Cella, M. Colonna, A DAP12-mediated pathway regulates expression of CC chemokine receptor 7 and maturation of human dendritic cells, J. Exp. Med. 194 (8) (2001) 1111–1122.

[48] D.L. Kober, J.M. Alexander-Brett, C.M. Karch, C. Cruchaga, M. Colonna, M. J. Holtzman, T.J. Brett, Neurodegenerative disease mutations in TREM2 reveal a functional surface and distinct loss-of-function mechanisms, Elife 5 (2016).

[49] M. Colonna, Y. Wang, TREM2 variants: new keys to decipher Alzheimer disease pathogenesis, Nat. Rev. Neurosci. 17 (4) (2016) 201–207.

[50] J.S. Park, I.J. Ji, D.H. Kim, H.J. An, S.Y. Yoon, The Alzheimer's disease-associated R47HVariant of TREM2 has an altered glycosylation pattern and protein stability, Front Neurosci-Switz 10 (2017).

[51] P. Gervois, I. Lambrichts, The emerging role of triggering receptor expressed on myeloid cells 2 as a target for immunomodulation in ischemic stroke, Front. Immunol. 10 (2019).

[52] A. Sudom, S. Talreja, J. Danao, E. Bragg, R. Kegel, X.S. Min, J. Richardson, Z. Q. Zhang, N. Sharkov, E. Marcora, S. Thibault, J. Bradley, S. Wood, A.C. Lim, H. Chen, S.L. Wang, I.N. Foltz, S. Sambashivan, Z.L. Wang, Molecular basis for the loss-of-function effects of the Alzheimer's disease-associated R47H variant of the immune receptor TREM2, J. Biol. Chem. 293 (32) (2018) 12634–12646.

[53] H. Martiskainen, J. Viswanathan, N.P. Nyka¨nen, M. Kurki, S. Helisalmi, T. Natunen, T. Saraj¨arvi, K.M.A. Kurkinen, J.P. Pursiheimo, T. Rauramaa, I. Alafuzoff, J.E. J¨a¨askel¨ainen, V. Leinonen, H. Soininen, A. Haapasalo, H. J. Huttunen, M. Hiltunen, Transcriptomics and mechanistic elucidation of Alzheimer's disease risk genes in the brain and in vitro models, Neurobiol. Aging 36 (2) (2015).

[54] L. Ma, M. Allen, N. Sakae, N. Ertekin-Taner, N.R. Graff-Radford, D.W. Dickson, S. G. Younkin, D. Sevlever, Expression and processing analyses of wild type and p. R47H TREM2 variant in Alzheimer's disease brains, Mol. Neurodegener. 11 (2016).

[55] N.A. Begum, K. Ishii, M. Kurita-Taniguchi, M. Tanabe, M. Kobayashi, Y. Moriwaki, M. Matsumoto, Y. Fukumori, I. Azuma, K. Toyoshima, T. Seya, BCG cell wall-specific differentially expressed genes identified by differential display and cDNA subtraction in human macrophages, Infect. Immun. 72 (2) (2004) 937–948.

[56] F.L. Yeh, D.V. Hansen, M. Sheng, TREM2, microglia, and neurodegenerative diseases, Trends Mol. Med. 23 (6) (2017) 512–533.

[57] A.R. Smith, R.G. Smith, D. Condliffe, E. Hannon, L. Schalkwyk, J. Mill, K. Lunnon, Increased DNA methylation near TREM2 is consistently seen in the superior temporal gyrus in Alzheimer's disease brain, Neurobiol. Aging 47 (2016) 35–40.

[58] N. Celarain, J. Sanchez-Ruiz de Gordoa, M.V. Zelaya, M. Roldan, R. Larumbe, L. Pulido, C. Echavarri, M. Mendioroz, TREM2 upregulation correlates with 5-hydroxymethycytosine enrichment in Alzheimer's disease hippocampus, Clin. Epigenetics 8 (2016) 37.

[59] S.C. Jin, B.A. Benitez, C.M. Karch, B. Cooper, T. Skorupa, D. Carrell, J.B. Norton, S. Hsu, O. Harari, Y.F. Cai, S. Bertelsen, A.M. Goate, C. Cruchaga, Coding variants in increase risk for Alzheimer's disease, Hum. Mol. Genet. 23 (21) (2014) 5838–5846.

[60] K. Kiianitsa, I. Kurtz, N. Beeman, M. Matsushita, W.M. Chien, W.H. Raskind, O. Korvatska, Novel TREM2 splicing isoform that lacks the V-set immunoglobulin domain is abundant in the human brain, J. Leukoc. Biol. 110 (5) (2021) 829–837.

[61] K. Schlepckow, G. Kleinberger, A. Fukumori, R. Feederle, S.F. Lichtenthaler, H. Steiner, C. Haass, An Alzheimer-associated TREM2 variant occurs at the ADAM cleavage site and affects shedding and phagocytic function, EMBO Mol. Med. 9 (10) (2017) 1356–1365.

[62] D. Feuerbach, P. Schindler, C. Barske, S. Joller, E. Beng-Louka, K.A. Worringer, S. Kommineni, A. Kaykas, D.J. Ho, C.Y. Ye, K. Welzenbach, G. Elain, L. Klein, I. Brzak, A.K. Mir, C.J. Farady, R. Aichholz, S. Popp, N. George, U. Neumann, ADAM17 is the main sheddase for the generation of human triggering receptor expressed in myeloid cells (hTREM2) ectodomain and cleaves TREM2 after Histidine 157, Neurosci. Lett. 660 (2017) 109–114.

[63] P. Wunderlich, K. Glebov, N. Kemmerling, N.T. Tien, H. Neumann, J. Walter, Sequential proteolytic processing of the triggering receptor expressed on myeloid cells-2 (TREM2) protein by ectodomain shedding and γ-secretase-dependent intramembranous cleavage, J. Biol. Chem. 288 (46) (2013) 33027–33036.

[64] M. Yanaizu, C. Washizu, N. Nukina, J.I. Satoh, Y. Kino, CELF2 regulates the species-specific alternative splicing of, Sci Rep-Uk 10 (1) (2020).

[65] K. Glebov, P. Wunderlich, I. Karaca, J. Walter, Functional involvement of γ-secretase in signaling of the triggering receptor expressed on myeloid cells-2 (TREM2), J Neuroinflamm 13 (2016).

[66] K. Wu, D.E. Byers, X.H. Jin, E. Agapov, J. Alexander-Brett, A.C. Patel, M. Cella, S. Gilfilan, M. Colonna, D.L. Kober, T.J. Brett, M.J. Holtzman, TREM-2 promotes macrophage survival and lung disease after respiratory viral infection, J. Exp. Med. 212 (5) (2015) 681–697.
[67] D.K. Berner, L. Wessolowski, F. Armbrust, J. Schneppenheim, K. Schlepckow, T. Koudelka, F. Scharfenberg, R. Lucius, A. Tholey, G. Kleinberger, C. Haass, P. Arnold, C. Becker-Pauly, Meprin β cleaves TREM2 and controls its phagocytic activity on macrophages, FASEB J. 34 (5) (2020) 6675–6687.
[68] C.D. Schmid, L.N. Sautkulis, P.E. Danielson, J. Cooper, K.W. Hasel, B.S. Hilbush, J.G. Sutcliffe, M.J. Carson, Heterogeneous expression of the triggering receptor expressed on myeloid cells-2 on adult murine microglia, J. Neurochem. 83 (6) (2002) 1309–1320.
[69] F. Filipello, C. Goldsbury, S.F. You, A. Locca, C.M. Karch, L. Piccio, Soluble TREM2: Innocent bystander or active player in neurological diseases? Neurobiol. Dis. 165 (2022).
[70] J. Jumper, R. Evans, A. Pritzel, T. Green, M. Figurnov, O. Ronneberger, K. Tunyasuvunakool, R. Bates, A. Zídek, A. Potapenko, A. Bridgland, C. Meyer, S. A.A. Kohl, A.J. Ballard, A. Cowie, B. Romera-Paredes, S. Nikolov, R. Jain, J. Adler, T. Back, S. Petersen, D. Reiman, E. Clancy, M. Zielinski, M. Steinegger, M. Pacholska, T. Berghammer, S. Bodenstein, D. Silver, O. Vinyals, A.W. Senior, K. Kavukcuoglu, P. Kohli, D. Hassabis, Highly accurate protein structure prediction with AlphaFold, Nature 596 (7873) (2021) 583-+.
[71] Q. Qin, Z.Q. Teng, C.M. Liu, Q. Li, Y.S. Yin, Y. Tang, TREM2, microglia, and Alzheimer's disease, Mech. Ageing Dev. 195 (2021).
[72] E.O. Olufunmilayo, R.M.D. Holsinger, Variant TREM2 signaling in Alzheimer's disease, J. Mol. Biol. 434 (7) (2022).
[73] R. Li, X. Wang, P.F. He, The most prevalent rare coding variants of TREM2 conferring risk of Alzheimer's disease: a systematic review and meta-analysis, Exp. Ther. Med. 21 (4) (2021).
[74] J. Paloneva, J. Mandelin, A. Kiialainen, T. Bo¨hling, J. Prudlo, P. Hakola, M. Hatia, Y.T. Konttinen, L. Peltonen, DAP12/TREM2 deficiency results in impaired osteoclast differentiation and osteoporotic features, J. Exp. Med. 198 (4) (2003) 669–675.
[75] D. Soragna, L. Papi, M.T. Ratti, R. Sestini, R. Tupler, L. Montalbetti, An Italian family affected by Nasu-Hakola disease with a novel genetic mutation in the TREM2 gene(vol 74, pg 825, 2003), J Neurol Neurosur Ps 74 (8) (2003) 1165.
[76] Y. Numasawa, C. Yamaura, S. Ishihara, S. Shintani, M. Yamazaki, H. Tabunoki, J. I. Satoh, Nasu-Hakola disease with a splicing mutation of TREM2 in a Japanese family, Eur. J. Neurol. 18 (9) (2011) 1179–1183.
[77] E. Chouery, V. Delague, A. Bergougnoux, S. Koussa, J.L. Serre, A. M´egarban´e, Mutations in lead to pure early-onset dementia without bone cysts, Hum. Mutat. 29 (9) (2008) E194–E204.
[78] Paloneva, Mutations in two genes encoding different subunits of a receptor signaling complex result in an identical disease phenotype (vol 71, pg 656, 2002), Am. J. Hum. Genet. 721 (2003) 225.
[79] R. Guerreiro, B. Bilgic, G. Guven, J. Br´as, J. Rohrer, E. Lohmann, H. Hanagasi, H. Gurvit, M. Emre, A novel compound heterozygous mutation in found in a Turkish frontotemporal dementia-like family, Neurobiol. Aging 34 (12) (2013).
[80] R.J. Guerreiro, E. Lohmann, J.M. Br´as, J.R. Gibbs, J.D. Rohrer, N. Gurunlian, B. Dursun, B. Bilgic, H. Hanagasi, H. Gurvit, M. Emre, A. Singleton, J. Hardy, Using exome sequencing to reveal mutations in presenting as a frontotemporal dementia-like syndrome without bone involvement, JAMA Neurol. 70 (1) (2013) 78–84.
[81] I. Le Ber, A. De Septenville, R. Guerreiro, J. Bras, A. Camuzat, P. Caroppo, S. Lattante, P. Couarch, E. Kabashi, K. Bouya-Ahmed, B. Dubois, A. Brice, Homozygous TREM2 mutation in a family with atypical frontotemporal dementia, Neurobiol. Aging 35 (10) (2014).
[82] P.G. Ridge, K.B. Hoyt, K. Boehme, S. Mukherjee, P.K. Crane, J.L. Haines, R. Mayeux, L.A. Farrer, M.A. Pericak-Vance, G.D. Schellenberg, J.S.K. Kauwe, A.s. D. Genetics, assessment of the genetic variance of late-onset Alzheimer's disease, Neurobiol. Aging 41 (2016).
[83] M. Ghani, C. Sato, E.G. Kakhki, J.R. Gibbs, B. Traynor, P. St George-Hyslop, E. Rogaeva, Mutation analysis of the and gene clusters in a case-control Alzheimer's disease data set, Neurobiol. Aging 42 (2016).
[84] E. Cuyvers, K. Bettens, S. Philtjens, T. Van Langenhove, I. Gijselinck, J. van der Zee, S. Engelborghs, M. Vandenbulcke, J. Van Dongen, N. Geerts, G. Maes, M. Mattheijssens, K. Peeters, P. Cras, R. Vandenberghe, P.P. De Deyn, C. Van Broeckhoven, M. Cruts, K. Sleegers, B. Consortium, Investigating the role of rare heterozygous variants in Alzheimer's disease and frontotemporal dementia, Neurobiol Aging 35(3) (2014).
[85] T. Jiang, L. Tan, Q. Chen, M.S. Tan, J.S. Zhou, X.C. Zhu, H. Lu, H.F. Wang, Y. D. Zhang, J.T. Yu, A rare coding variant in increases risk for Alzheimer's disease in Han Chinese, Neurobiol. Aging 42 (2016).
[86] S.C. Jin, M.M. Carrasquillo, B.A. Benitez, T. Skorupa, D. Carrell, D. Patel, S. Lincoln, S. Krishnan, M. Kachadoorian, C. Reitz, R. Mayeux, T.S. Wingo, J. J. Lah, A.I. Levey, J. Murrell, H. Hendrie, T. Foroud, N.R. Graff-Radford, A. M. Goate, C. Cruchaga, N. Ertekin-Taner, TREM2 is associated with increased risk for Alzheimer's disease in African Americans, Mol. Neurodegener. 10 (2015).
[87] J.I. Satoh, M. Yanaizu, Y. Tosaki, K. Sakai, Y. Kino, Targeted sequencing approach to identify genetic mutations in Nasu-Hakola disease, Intractable Rare Dis. Res. 5 (4) (2016) 269–274.
[88] G. Kleinberger, M. Brendel, E. Mracsko, B. Wefers, L. Groeneweg, X. Xiang, C. Focke, M. Deussing, M. Suarez-Calvet, F. Mazaheri, S. Parhizkar, N. Pettkus, W. Wurst, R. Feederle, P. Bartenstein, T. Mueggler, T. Arzberger, I. Knuesel, A. Rominger, C. Haass, The FTD-like syndrome causing TREM2 T66M mutation impairs microglia function, brain perfusion, and glucose metabolism, EMBO J. 36 (13) (2017) 1837–1853.
[89] W.M. Song, S. Joshita, Y.Y. Zhou, T.K. Ulland, S. Gilfillan, M. Colonna, Humanized TREM2 mice reveal microglia-intrinsic and -extrinsic effects of R47H polymorphism, J. Exp. Med. 215 (3) (2018) 745–760.
[90] S. Krasemann, C. Madore, R. Cialic, C. Baufeld, N. Calcagno, R. El Fatimy, L. Beckers, E. O'Loughlin, Y. Xu, Z. Fanek, D.J. Greco, S.T. Smith, G. Tweet, Z. Humulock, T. Zrzavy, P. Conde-Sanroman, M. Gacias, Z.P. Weng, H. Chen, E. Tjon, F. Mazaheri, K. Hartmann, A. Madi, J.D. Ulrich, M. Glatzel, A. Worthmann, J. Heeren, B. Budnik, C. Lemere, T. Ikezu, F.L. Heppner, V. Litvak, D.M. Holtzman, H. Lassmann, H.L. Weiner, J. Ochando, C. Haass, O. Butovsky, The TREM2-APOE pathway drives the transcriptional phenotype of dysfunctional microglia in Neurodegenerative diseases, Immunity 47 (3) (2017) 566-+.
[91] F. Mazaheri, N. Snaidero, G. Kleinberger, C. Madore, A. Daria, G. Werner, S. Krasemann, A. Capell, D. Trümbach, W. Wurst, B. Brunner, S. Bultmann, S. Tahirovic, M. Kerschensteiner, T. Misgeld, O. Butovsky, C. Haass, TREM2 deficiency impairs chemotaxis and microglial responses to neuronal injury, EMBO Rep. 18 (7) (2017) 1186–1198.
[92] L. Piccio, Y. Deming, J.L. Del-Aguila, L. Ghezzi, D.M. Holtzman, A.M. Fagan, C. Fenoglio, D. Galimberti, B. Borroni, C. Cruchaga, Cerebrospinal fluid soluble TREM2 is higher in Alzheimer disease and associated with mutation status, Acta Neuropathol. 131 (6) (2016) 925–933.
[93] K. Henjum, I.S. Almdahl, V. Årskog, L. Minthon, O. Hansson, T. Fladby, L.N. G. Nilsson, Cerebrospinal fluid soluble TREM2 in aging and Alzheimer's disease, Alzheimers Res. Ther. 8 (2016).
[94] M. Park, J.W. Yi, E.M. Kim, I.J. Yoon, E.H. Lee, H.Y. Lee, K.Y. Ji, K.H. Lee, J. H. Jang, S.S. Oh, C.H. Yun, S.H. Kim, K.M. Lee, M.G. Song, D.H. Kim, H.S. Kang, Triggering receptor expressed on myeloid cells 2 (TREM2) promotes adipogenesis and diet-induced obesity, Diabetes 64 (1) (2015) 117–127.
[95] D.L. Kober, K.M. Wanhainen, B.M. Johnson, D.T. Randolph, M.J. Holtzman, T. J. Brett, Preparation, crystallization, and preliminary crystallographic analysis of wild-type and mutant human TREM-2 ectodomains linked to neurodegenerative and inflammatory diseases, Protein Expres Purif 96 (2014) 32–38.
[96] Z. Abduljaleel, F.A. Al-Allaf, W. Khan, M. Athar, N. Shahzad, M.M. Taher, M. Elrobh, M.S. Alanazi, W. El-Huneidi, Evidence of trem2 variant associated with triple risk of Alzheimer's disease, PLoS One 9 (3) (2014) e92648.
[97] A.A. Nugent, K. Lin, B. van Lengerich, S. Lianoglou, L. Przybyla, S.S. Davis, C. Llapashtica, J. Wang, D.J. Kim, D. Xia, A. Lucas, S. Baskaran, P.C.G. Haddick, M. Lenser, T.K. Earr, J. Shi, J.C. Dugas, B.J. Andreone, T. Logan, H.O. Solanoy, H. Chen, A. Srivastava, S.B. Poda, P.E. Sanchez, R.J. Watts, T. Sandmann, G. Astarita, J.W. Lewcock, K.M. Monroe, G. Di Paolo, TREM2 regulates microglial cholesterol metabolism upon chronic phagocytic challenge, Neuron 105 (5) (2020) 837-+.
[98] B.W. Kunkle, B. Grenier-Boley, R. Sims, J.C. Bis, V. Damotte, A.C. Naj, A. Boland, M. Vronskaya, S.J. van der Lee, A. Amlie-Wolf, C. Bellenguez, A. Frizatti, V. Chouraki, E.R. Martin, K. Sleegers, N. Badarinarayan, J. Jakobsdottir, K.L. Hamilton-Nelson, S. Moreno-Grau, R. Olaso, R. Raybould, Y.N. Chen, A.B. Kuzma, M. Hiltunen, T. Morgan, S. Ahmad, B.N. Vardarajan, J. Epelbaum, P. Hoffmann, M. Boada, G.W. Beecham, J.G. Garnier, D. Harold, A.L. Fitzpatrick, O. Valladares, M.L. Moutet, A. Gerrish, A.V. Smith, L.M. Qu, D. Bacq, N. Denning, X.Q. Jian, Y. Zhao, M. Del Zompo, N.C. Fox, S.H. Choi, I. Mateo, J.T. Hughes, H.H. Adams, J. Malamon, F. Sanchez-Garcia, Y. Patel, J.A. Brody, B.A. Dombroski, M.C.D. Naranjo, M. Daniilidou, G. Eiriksdottir, S. Mukherjee, D. Wallon, J. Uphill, T. Aspelund, L.B. Cantwell, F. Garzia, D. Galimberti, E. Hofer, M. Butkiewicz, B. Fin, E. Scarpini, C. Sarnowski, W.S. Bush, S. Meslage, J. Kornhuber, C.C. White, Y. Song, R.C. Barber, S. Engelborghs, S. Sordon, D. Voijnovic, P.M. Adams, R. Vandenberghe, M. Mayhaus, L.A. Cupples, M.S. Albert, P.P. De Deyn, W. Gu, J.J. Himali, D. Beekly, A. Squassina, A.M. Hartmann, A. Orellana, D. Blacker, E. Rodriguez-Rodriguez, S. Lovestone, M.E. Garcia, R.S. Doody, C. Munoz-Fernadez, R. Sussams, H.H. Lin, T.J. Fairchild, Y.A. Benito, C. Holmes, H. Karamujic-Comic, M.P. Frosch, H. Thonberg, W. Maier, G. Roshchupkin, B. Ghetti, V. Giedraitis, A. Kawalia, S. Li, R.M. Huebinger, L. Kilander, S. Moebus, I. Hern´andez, M.I. Kamboh, R. Brundin, J. Turton, Q. Yang, M.J. Katz, L. Concari, J. Lord, A.S. Beiser, C.D. Keene, S. Helisalmi, I. Kloszewska, W.A. Kukull, A.M. Koivisto, A. Lynch, L. Tarraga, E.B. Larson, A. Haapasalo, B. Lawlor, T.H. Mosley, R.B. Lipton, V. Solfrizzi, M. Gill, W.T. Longstreth, T.J. Montine, V. Frisardi, M. Diez-Fairen, F. Rivadeneira, R.C. Petersen, V. Deramecourt, I. Alvarez, F. Salani, A. Ciaramella, E. Boerwinkle, E.M. Reiman, N. Fievet, J.I. Rotter, J.S. Reisch, O. Hanon, C. Cupidi, A.G.A. Uitterlinden, D.R. Royall, C. Dufouil, R.G. Maletta, I. de Rojas, M. Sano, A. Brice, R. Cecchetti, P. St George-Hyslop, K. Ritchie, M. Tsolaki, D.W. Tsuang, B. Dubois, D. Craig, C.K. Wu, H. Soininen, D. Avramidou, R.L. Albin, L. Fratiglioni, A. Germanou, L.G. Apostolova, L. Keller, M. Koutroumani, S.E. Arnold, F. Panza, O. Gkatzima, S. Asthana, D. Hannequin, P. Whitehead, C.S. Atwood, P. Caffarra, H. Hampel, I. Quintela, A. Carracedo, L. Lannfelt, D.C. Rubinsztein, L.L. Barnes, F. Pasquier, L. Fro¨lich, S. Barral, B. McGuinness, T.G. Beach, J.A. Johnston, J.T. Becker, P. Passmore, E.H. Bigio, J.M. Schott, T.D. Bird, J.D. Warren, B.F. Boeve, M.K. Lupton, J.D. Bowen, P. Proitsi, A. Boxer, J.F. Powell, J.R. Burke, J.S.K. Kauwe, J.M. Burns, M. Mancuso, J.D. Buxbaum, U. Bonuccelli, N.J. Cairns, A. McQuillin, C.H. Cao, G. Livingston, C.S. Carlson, N.J. Bass, C.M. Carlsson, J. Hardy, R.M. Carney, J. Bras, M.M. Carrasquillo, R. Guerreiro, M. Allen, H.C. Chui, E. Fisher, C. Masullo, E.A. Crocco, C. DeCarli, G. Bisceglio, M. Dick, L. Ma, R. Duara, N.R. Graff-Radford, D.A. Evans, A. Hodges, K. M. Faber, M. Scherer, K.B. Fallon, M. Riemenschneider, D.W. Fardo, R. Heun, M. R. Farlow, H. Ko¨lsch, S. Ferris, M. Leber, T.M. Foroud, I. Heuser, D.R. Galasko, I. Giegling, M. Gearing, M. Hüll, D.H. Geschwind, J.R. Gilbert, J. Morris, R.C. Green, K. Mayo, J.H. Growdon, T. Feulner, R.L. Hamilton, L.E. Harrell, D. Drichel,

L.S. Honig, T.D. Cushion, M.J. Huentelman, P. Hollingworth, C.M. Hulette, B.T. Hyman, R. Marshall, G.P. Jarvik, A. Meggy, E. Abner, G.E. Menzies, L.W. Jin, G. Leonenko, L.M. Real, G.R. Jun, C.T. Baldwin, D. Grozeva, A. Karydas, G. Russo, J. A. Kaye, R. Kim, F. Jessen, N.W. Kowall, B. Vellas, J.H. Kramer, E. Vardy, F.M. LaFerla, K.H. Jo¨ckel, J.J. Lah, M. Dichgans, J.B. Leverenz, D. Mann, A.I. Levey, S. Pickering-Brown, A.P. Lieberman, N. Klopp, K.L. Lunetta, H.E. Wichmann, C.G. Lyketsos, K. Morgan, D.C. Marson, K. Brown, F. Martiniuk, C. Medway, D.C. Mash, M.M. No¨then, E. Masliah, N.M. Hooper, W.C. McCormick, A. Daniele, S.M. McCurry, A. Bayer, A.N. McDavid, J. Gallacher, A.C. Mckee, H. van den Bussche, M. Mesulam, C. Brayne, B.L. Miller, S. Riedel-Heller, C.A. Miller, J.W. Miller, A. Al-Chalabi, J.C. Morris, C.E. Shaw, A.J. Myers, J. Wiltfang, S. O'Bryant, J.M. Olichney, V. Alvarez, J.E. Parisi, A.B. Singleton, H.L. Paulson, J. Collinge, W.R. Perry, S. Mead, E. Peskind, D.H. Cribbs, M. Rossor, A. Pierce, N.S. Ryan, W.W. Poon, B. Nacmias, H. Potter, S. Sorbi, J.F. Quinn, E. Sacchinelli, A. Raj, G. Spalletta, M. Raskind, C. Caltagirone, P. Bossù, M.D. Orfei, B. Reisberg, R. Clarke, C. Reitz, A.D. Smith, J.M. Ringman, D. Warden, E.D. Roberson, G. Wilcock, E. Rogaeva, A.C. Bruni, H.J. Rosen, M. Gallo, R.N. Rosenberg, Y. Ben-Shlomo, M.A. Sager, P. Mecocci, A.J. Saykin, P. Pastor, M.L. Cuccaro, J.M. Vance, J.A. Schneider, L.S. Schneider, S. Slifer, W.W. Seeley, A.G. Smith, J.A. Sonnen, S. Spina, R.A. Stern, R.H. Swerdlow, M. Tang, R.E. Tanzi, J.Q. Trojanowski, J.C. Troncoso, V.M. Van Deerlin, L.J. Van Eldik, H.V. Vinters, J.P. Vonsattel, S. Weintraub, K.A. Welsh-Bohmer, K.C. Wilhelmsen, J. Williamson, T.S. Wingo, R.L. Woltjer, C.B. Wright, C.E. Yu, L. Yu, Y. Saba, A. Pilotto, M.J. Bullido, O. Peters, P. K. Crane, D. Bennett, P. Bosco, E. Coto, V. Boccardi, P.L. De Jager, A. Lleo, N. Warner, O.L. Lopez, M. Ingelsson, P. Deloukas, C. Cruchaga, C. Graff, R. Gwilliam, M. Fornage, A.M. Goate, P. Sanchez-Juan, P.G. Kehoe, N. Amin, N. Ertekin-Taner, C. Berr, S. Debette, S. Love, L.J. Launer, S.G. Younkin, J.F. Dartigues, C. Corcoran, M.A. Ikram, D.W. Dickson, G. Nicolas, D. Campion, J. Tschanz, H. Schmidt, H. Hakonarson, J. Clarimon, R. Munger, R. Schmidt, L.A. Farrer, C. Van Broeckhoven, M.C. O'Donovan, A.L. DeStefano, L. Jones, J.L. Haines, J.F. Deleuze, M.J. Owen, V. Gudnason, R. Mayeux, V. Escott-Price, B.M. Psaty, A. Ramirez, L.S. Wang, A. Ruiz, C.M. van Duijn, P.A. Holmans, S. Seshadri, J. Williams, P. Amouyel, G.D. Schellenberg, J.C. Lambert, M.A. Pericak-Vance, ADGC, EADI, C.H.A.R. Genomic, G.E.R.A. Defining, Genetic meta-analysis of diagnosed Alzheimer's disease identifies new risk loci and implicates Aβ, tau, immunity and lipid processing (vol 51, pg 414, 2019), Nat Genet 51(9) (2019) 1423-1424.

[99] H.B. Dean, E.D. Roberson, Y.H. Song, Neurodegenerative disease-associated variants in TREM2 destabilize the apical ligand-binding region of the immunoglobulin domain, Front. Neurol. 10 (2019).

[100] P. Thornton, J. Sevalle, M.J. Deery, G. Fraser, Y. Zhou, S. Ståhl, E.H. Franssen, R. B. Dodd, S. Qamar, B.G. Perez-Nievas, L.S.C. Nicol, S. Eketj¨all, J. Revell, C. Jones, A. Billinton, P.H. St George-Hyslop, I. Chessell, D.C. Crowther, TREM2 shedding by cleavage at the H157–S158 bond is accelerated for the Alzheimer's disease-associated H157Y variant, EMBO Mol. Med. 9 (10) (2017) 1366–1378.

[101] D.W. Sirkis, L.W. Bonham, R.E. Aparicio, E.G. Geier, E.M. Ramos, Q. Wang, A. Karydas, Z.A. Miller, B.L. Miller, G. Coppola, J.S. Yokoyama, Rare TREM2 variants associated with Alzheimer's disease display reduced cell surface expression, Acta Neuropathol Com 4 (2016).

[102] W. Song, B. Hooli, K. Mullin, S.C. Jin, M. Cella, T.K. Ulland, Y.M. Wang, R. E. Tanzi, M. Colonna, Alzheimer's disease-associated TREM2 variants exhibit either decreased or increased ligand-dependent activation, Alzheimers Dement. 13 (4) (2017) 381–387.

[103] M. Thelen, C. Razquin, I. Herna´ndez, A. Gorostidi, R. S´anchez-Valle, S. Ortega-Cubero, S. Wolfsgruber, D. Drichel, K. Fliessbach, T. Duenkel, M. Damian, S. Heilmann, A. Slotosch, M. Lennarz, M. Seijo-Martínez, R. Rene, J. Kornhuber, O. Peters, C. Luckhaus, H. Jahn, M. Hüll, E. Rüther, J. Wiltfang, E. Lorenzo, J. Gascon, A. Lleo´, A. Llado´, J. Campdelacreu, F. Moreno, H. Ahmadzadehfar, J. Fortea, B. Indakoetxea, M.T. Heneka, A. Wetter, M.A. Pastor, M. Riverol, T. Becker, L. Fro¨lich, L. T´arraga, M. Boada, M. Wagner, F. Jessen, W. Maier, J. Clarimon, A.L. de Munain, A. Ruiz, P. Pastor, A. Ramirez, D.G.S. Consorti, Investigation of the role of rare TREM2 variants in frontotemporal dementia subtypes, Neurobiol. Aging 35 (11) (2014).

[104] R. Sims, S.J. van der Lee, A.C. Naj, C. Bellenguez, N. Badarinarayan, J. Jakobsdottir, B.W. Kunkle, A. Boland, R. Raybould, J.C. Bis, E.R. Martin, B. Grenier-Boley, S. Heilmann-Heimbach, V. Chouraki, A.B. Kuzma, K. Sleegers, M. Vronskaya, A. Ruiz, R.R. Graham, R. Olaso, P. Hoffmann, M.L. Grove, B.N. Vardarajan, M. Hiltunen, M.M. No¨then, C.C. White, K.L. Hamilton-Nelson, J. Epelbaum, W. Maier, S.H. Choi, G.W. Beecham, C. Dulary, S. Herms, A.V. Smith, C.C. Funk, C. Derbois, A.J. Forstner, S. Ahmad, H.D. Li, D. Bacq, D. Harold, C.L. Satizabal, O. Valladares, A. Squassina, R. Thomas, J.A. Brody, L.M. Qu, P. Sa´nchez-Juan, T. Morgan, F.J. Wolters, Y. Zhao, F.S. Garcia, N. Denning, M. Fornage, J. Malamon, M.C.D. Naranjo, E. Majounie, T.H. Mosley, B. Dombroski, D. Wallon, M.K. Lupton, J. Dupuis, P. Whitehead, L. Fratiglioni, C. Medway, X.Q. Jian, S. Mukherjee, L. Keller, K. Brown, H.H. Lin, L.B. Cantwell, F. Panza, B. McGuinness, S. Moreno-Grau, J.D. Burgess, V. Solfrizzi, P. Proitsi, H.H. Adams, M. Allen, D. Seripa, P. Pastor, L.A. Cupples, N.D. Price, D. Hannequin, A. Frank-Garcia, D. Levy, P. Chakrabarty, P. Caffarra, I. Giegling, A.S. Beiser, V. Giedraitis, H. Hampel, M.E. Garcia, X. Wang, L. Lannfelt, P. Mecocci, G. Eiriksdottir, P.K. Crane, F. Pasquier, V. Boccardi, I. Hen´andez, R.C. Barber, M. Scherer, L. Tarraga, P.M. Adams, M. Leber, Y. Chen, M.S. Albert, S. Riedel-Heller, V. Emilsson, D. Beekly, A. Braae, R. Schmidt, D. Blacker, C. Masullo, H. Schmidt, R.S. Doody, G. Spalletta, W.T. Longstreth, T.J. Fairchild, P. Bossù, O.L. Lopez, M.P. Frosch, E. Sacchinelli, B. Ghetti, Q. Yang, R.M. Huebinger, F. Jessen, S. Li, M.I. Kamboh, J. Morris, O. Sotolongo-Grau, M.J. Katz, C. Corcoran, M. Dunstan, A. Braddel, C. Thomas, A. Meggy, R. Marshall, A. Gerrish, J. Chapman, M. Aguilar, S. Taylor, M. Hill, M.D. Fair´en, A. Hodges, B. Vellas, H. Soininen, I. Kloszewska, M. Daniilidou, J. Uphill, Y. Patel, J.T. Hughes, J. Lord, J. Turton, A.M. Hartmann, R. Cecchetti, C. Fenoglio, M. Serpente, M. Arcaro, C. Caltagirone, M.D. Orfei, A. Ciaramella, S. Pichler, M. Mayhaus, W. Gu, A. Lleo´, J. Forte, R. Blesa, I.S. Barber, K. Brookes, C. Cupidi, R.G. Maletta, D. Carrell, S. Sorbi, S. Moebus, M. Urbano, A. Pilotto, J. Kornhuber, P. Bosco, S. Todd, D. Craig, J. Johnston, M. Gill, B. Lawlor, A. Lynch, N.C. Fox, J. Hardy, R.L. Albin, L.G. Apostolova, S.E. Arnold, S. Asthana, C.S. Atwood, C.T. Baldwin, L.L. Barnes, S. Barral, T.G. Beach, J.T. Becker, E.H. Bigio, T.D. Bird, B.F. Boeve, J.D. Bowen, A. Boxer, J.R. Burke, J.M. Burns, J.D. Buxbaum, N.J. Cairns, C.H. Cao, C.S. Carlson, C.M. Carlsson, R.M. Carney, M.M. Carrasquillo, S.L. Carroll, C.C. Diaz, H.C. Chui, D.G. Clark, D.H. Cribbs, E.A. Crocco, C. DeCarli, M. Dick, R. Duara, D.A. Evans, K.M. Faber, K.B. Fallon, D.W. Fardo, M.R. Farlow, S. Ferris, T.M. Foroud, D.R. Galasko, M. Gearing, D.H. Geschwind, J.R. Gilbert, N.R. Graff-Radford, R.C. Green, J.H. Growdon, R.L. Hamilton, L.E. Harrell, L.S. Honig, M.J. Huentelman, C.M. Hulette, B.T. Hyman, G.P. Jarvik, E. Abner, L.W. Jin, G. Jun, A. Karydas, J.A. Kaye, R. Kim, N.W. Kowall, J.H. Kramer, F.M. LaFerla, J.J. Lah, J.B. Leverenz, A.I. Levey, G. Li, A.P. Lieberman, K.L. Lunetta, C.G. Lyketsos, D.C. Marson, F. Martiniuk, D.C. Mash, E. Masliah, W.C. McCormick, S.M. McCurry, A.N. McDavid, A.C. Mckee, M. Mesulam, B.L. Miller, C.A. Miller, J.W. Miller, J.C. Morris, J.R. Murrell, A.J. Myers, S. O'Bryant, V.S. Pankratz, V.S. Pankratz, J.E. Parisi, H.L. Paulson, W. Perry, E. Peskind, A. Pierce, W.W. Poon, H. Potter, J.F. Quinn, A. Raj, M. Raskind, B. Reisberg, C. Reitz, J.M. Ringman, E.D. Roberson, E. Rogaeva, H.J. Rosen, R.N. Rosenberg, M.A. Sager, A.J. Saykin, J.A. Schneider, L.S. Schneider, W.W. Seeley, A.G. Smith, J.A. Sonnen, S. Spina, R.A. Stern, R.H. Swerdlow, R.E. Tanzi, T.A. Thornton-Wells, J.Q. Trojanowski, J.C. Troncoso, V.M. Van Deerlin, L.J. Van Eldik, H.V. Vinters, J.P. Vonsattel, S. Weintraub, K.A. Welsh-Bohmer, K.C. Wilhelmsen, J. Williamson, R.L. Woltjer, C.B. Wright, C.E. Yu, L. Yu, F. Garzia, F. Golamaully, G. Septier, S. Engelborghs, R. Vandenberghe, P.P. De Deyn, C.M. Fernadez, Y.A. Benito, H. Thonberg, C. Forsell, L. Lilius, A. Kinhult-St¨ahlbom, L. Kilander, R. Brundin, L. Concari, S. Helisalmi, A.M. Koivisto, A. Haapasalo, V. Dermecourt, N. Fievet, O. Hanon, C. Dufouil, A. Brice, K. Ritchie, B. Dubois, J.J. Himali, C.D. Keene, J. Tschanz, A.L. Fitzpatrick, W.A. Kukull, M. Norton, T. Aspelund, E.B. Larson, R. Munger, J.I. Rotter, R.B. Lipton, M.J. Bullido, A. Hofman, T.J. Montine, E. Coto, E. Boerwinkle, R.C. Petersen, V. Alvarez, F. Rivadeneira, E.M. Reiman, M. Gallo, C.J. O'Donnell, J.S. Reisch, A.C. Bruni, D.R. Royall, M. Dichgans, M. Sano, D. Galimberti, P. St George-Hyslop, E. Scarpini, D. W. Tsuang, M. Mancuso, U. Bonuccelli, A.R. Winslow, A. Daniele, C.K. Wu, O. Peters, B. Nacmias, M. Riemenschneider, R. Heun, C. Brayne, D.C. Rubinsztein, J. Bras, R. Guerreiro, A. Al-Chalabi, C.E. Shaw, J. Collinge, D. Mann, M. Tsolaki, J. Clarimo´n, R. Sussams, S. Lovestone, M.C. O'Donovan, M.J. Owen, T.W. Behrens, S. Mead, A.M. Goate, A.G. Uitterlinden, C. Holmes, C. Cruchaga, M. Ingelsson, D. A. Bennett, J. Powell, T.E. Golde, C. Graff, P.L. De Jager, K. Morgan, N. Ertekin-Taner, O. Combarros, B.M. Psaty, P. Passmore, S.G. Younkin, C. Berr, V. Gudnason, D. Rujescu, D.W. Dickson, J.F. Dartigues, A.L. DeStefano, S. Ortega-Cubero, H. Hakonarson, D. Campion, M. Boada, J.K. Kauwe, L.A. Farrer, C. Van Broeckhoven, M.A. Ikram, L. Jones, J.L. Haines, C. Tzourio, L.J. Launer, V. Escott-Price, R. Mayeux-, J.F. Deleuze, N. Amin, P.A. Holmans, M.A. Pericak-Vance, P. Amouyel, C.M. van Duijn, A. Ramirez, L.S. Wang, J.C. Lambert, S. Seshadri, J. Williams, G.D. Schellenberg, ARUKConsortium, G. PERADES, CHARGE, ADGC, EADI, Rare coding variants in PLCG2, ABI3, and TREM2 implicate microglial-mediated innate immunity in Alzheimer's disease, Nat Genet 49(9) (2017) 1373-+.

[105] E.O. Luis, S. Ortega-Cubero, I. Lamet, C. Razquin, C. Cruchaga, B.A. Benitez, E. Lorenzo, J. Irigoyen, M.A. Pastor, P. Pastor, Adni, Frontobasal Gray Matter Loss Is Associated with the p 35 (2014) 2681–2690. R47H variant,.

[106] Z.M. Li, L. Zhong, L. Gu, W.Q. Huang, X.Z. Shi, X.L. Zhang, X.K. An, Q. Lin, C. M. Tzeng, Association study of TREM2 polymorphism rs75932628 with leucoaraiosis or Parkinson's disease in the Han Chinese population, BMJ Open 6 (1) (2016).

[107] T. Tan, Z. Song, L.M. Yuan, W. Xiong, X. Deng, B. Ni, Y. Chen, H. Deng, Genetic analysis of TREM2 variants in Chinese Han patients with sporadic Parkinson's disease, Neurosci. Lett. 612 (2016) 189–192.

[108] F.L. Yeh, Y.Y. Wang, I. Tom, L.C. Gonzalez, M. Sheng, TREM2 binds to apolipoproteins, including APOE and CLU/APOJ, and thereby facilitates uptake of amyloid-beta by microglia, Neuron 91 (2) (2016) 328–340.

[109] M. Giraldo, F. Lopera, A.L. Siniard, J.J. Corneveaux, I. Schrauwen, J. Carvajal, C. Mun˜oz, M. Ramirez-Restrepo, C. Gaiteri, A.J. Myers, R.J. Caselli, K.S. Kosik, E. M. Reiman, M.J. Huentelman, Variants in triggering receptor expressed on myeloid cells 2 are associated with both behavioral variant frontotemporal lobar degeneration and Alzheimer's disease, Neurobiol. Aging 34 (8) (2013).

[110] I.R. Turnbull, S. Gilfillan, M. Cella, T. Aoshi, M. Miller, L. Piccio, M. Hernandez, M. Colonna, Cutting edge: TREM-2 attenuates macrophage activation, J. Immunol. 177 (6) (2006) 3520–3524.

[111] J.A. Hamerman, J.R. Jarjoura, M.B. Humphrey, M.C. Nakamura, W.E. Seaman, L. L. Lanier, Cutting edge: inhibition of TLR and FcR responses in macrophages by triggering receptor expressed on myeloid cells (TREM)-2 and DAP12, J. Immunol. 177 (4) (2006) 2051–2055.

[112] D.L. Kober, T.J. Brett, TREM2-Ligand Interactions in Health and Disease, J. Mol. Biol. 429 (11) (2017) 1607–1629.

[113] L. Stefano, G. Racchetti, F. Bianco, N. Passini, R.S. Gupta, P.P. Bordignon, J. Meldolesi, The surface-exposed chaperone, Hsp60, is an agonist of the microglial TREM2 receptor, J. Neurochem. 110 (1) (2009) 284–294.

[114] C.L. Hsieh, M. Koike, S.C. Spusta, E.C. Niemi, M. Yenari, M.C. Nakamura, W. E. Seaman, A role for TREM2 ligands in the phagocytosis of apoptotic neuronal cells by microglia, J. Neurochem. 109 (4) (2009) 1144–1156.

[115] M.R. Daws, P.M. Sullam, E.C. Niemi, T.T. Chen, N.K. Tchao, W.E. Seaman, Pattern recognition by TREM-2: binding of anionic ligands, J. Immunol. 171 (2) (2003) 594–599.
[116] Y.M. Wang, M. Cella, K. Mallinson, J.D. Ulrich, K.L. Young, M.L. Robinette, S. Gilfillan, G.M. Krishnan, S. Sudhakar, B.H. Zinselmeyer, D.M. Holtzman, J. R. Cirrito, M. Colonna, TREM2 lipid sensing sustains the microglial response in an Alzheimer's disease model, Cell 160 (6) (2015) 1061–1071.
[117] L. Zhong, Z.Q. Wang, D.X. Wang, Z. Wang, Y.A. Martens, L.B. Wu, Y. Xu, K. Wang, J.G. Li, R.Z. Huang, D. Can, H.X. Xu, G.J. Bu, X.F. Chen, Amyloid-beta modulates microglial responses by binding to the triggering receptor expressed on myeloid cells 2 (TREM2), Mol. Neurodegener. 13 (2018).
[118] C.B. Lessard, S.L. Malnik, Y.Y. Zhou, T.B. Ladd, P.E. Cruz, Y. Ran, T.E. Mahan, P. Chakrabaty, D.M. Holtzman, J.D. Ulrich, M. Colonna, T.E. Golde, High-affinity interactions and signal transduction between Aβ oligomers and TREM2, EMBO Mol. Med. 10 (11) (2018).
[119] V. Yurchenko, S. Constant, E. Eisenmesser, M. Bukrinsky, Cyclophilin-CD147 interactions: a new target for anti-inflammatory therapeutics, Clin. Exp. Immunol. 160 (3) (2010) 305–317.
[120] B. Sherry, N. Yarlett, A. Strupp, A. Cerami, Identification of cyclophilin as a proinflammatory secretory product of lipopolysaccharide-activated macrophages, P Natl Acad Sci USA 89 (8) (1992) 3511–3515.
[121] Z.G. Jin, M.G. Melaragno, D.F. Liao, C. Yan, J. Haendeler, Y.A. Suh, J.D. Lambeth, B.C. Berk, Cyclophilin A is a secreted growth factor induced by oxidative stress, Circ. Res. 87 (9) (2000) 789–796.
[122] J. Suzuki, Z.G. Jin, D.F. Meoli, T. Matoba, B.C. Berk, Cyclophilin A is secreted by a vesicular pathway in vascular smooth muscle cells, Circ. Res. 98 (6) (2006) 811–817.
[123] K.Y. Ji, S.M. Kim, S.M. Yee, M.J. Kim, Y.J. Ban, E.M. Kim, E.H. Lee, H. Choi, H. Yun, C.W. Lee, C.H. Yun, C.J. Lee, H.B. Lee, H.S. Kang, Cyclophilin A is an endogenous ligand for the triggering receptor expressed on myeloid cells-2 (TREM2), FASEB J. 35 (4) (2021).
[124] N. Takegahara, H. Takamatsu, T. Toyofuku, T. Tsujimura, T. Okuno, K. Yukawa, M. Mizui, M. Yamamoto, D.V.R. Prasad, K. Suzuki, M. Ishii, K. Terai, M. Moriya, Y. Nakatsuji, S. Sakoda, S. Sato, S. Akira, K. Takeda, M. Inui, T. Takai, M. Ikawa, M. Okabe, A. Kumanogoh, H. Kikutani, Plexin-A1 and its interaction with DAP12 in immune responses and bone homeostasis, Nat. Cell Biol. 8 (6) (2006) 615–622.
[125] E.N. N'Diaye, C.S. Branda, S.S. Branda, L. Nevarez, M. Colonna, C. Lowell, J. A. Hamerman, W.E. Seaman, TREM-2 (triggering receptor expressed on myeloid cells 2) is a phagocytic receptor for bacteria, J. Cell Biol. 184 (2) (2009) 215–223.
[126] H. Ito, J.A. Hamerman, TREM-2, triggering receptor expressed on myeloid cell-2, negatively regulates TLR responses in dendritic cells, Eur. J. Immunol. 42 (1) (2012) 176–185.
[127] M. Kawabori, R. Kacimi, T. Kauppinen, C. Calosing, J.Y. Kim, C.L. Hsieh, M. C. Nakamura, M.A. Yenari, Triggering receptor expressed on myeloid cells 2 (TREM2) deficiency attenuates phagocytic activities of microglia and exacerbates ischemic damage in experimental stroke, J. Neurosci. 35 (8) (2015) 3384–3396.
[128] Y.J. Zhao, X.L. Wu, X.G. Li, L.L. Jiang, X. Gui, Y. Liu, Y. Sun, B. Zhu, J.C. Pin˜a-Crespo, M.X. Zhang, N.Y. Zhang, X.C. Chen, G.J. Bu, Z.Q. An, T.Y. Huang, H. X. Xu, TREM2 Is a Receptor for β-Amyloid that Mediates Microglial Function, Neuron 97 (5) (2018) 1023-+.
[129] S.H. Yoon, Y.D. Lee, J. Ha, Y. Lee, H.H. Kim, TLT-1s, alternative transcripts of triggering receptor expressed on myeloid cell-like transcript-1 (TLT-1), inhibits the triggering receptor expressed on myeloid cell-2 (TREM-2)-mediated Signaling Pathway during Osteoclastogenesis, J. Biol. Chem. 287 (35) (2012) 29620–29626.
[130] C.C. Bailey, L.B. DeVaux, M. Farzan, The triggering receptor expressed on myeloid cells 2 binds apolipoprotein E, J. Biol. Chem. 290 (43) (2015) 26033–26042.
[131] Y. Atagi, C.C. Liu, M.M. Painter, X.F. Chen, C. Verbeeck, H.H. Zheng, X. Li, R. Rademakers, S.S. Kang, H.X. Xu, S. Younkin, P. Das, J.D. Fryer, G.J. Bu, Apolipoprotein E is a ligand for triggering receptor expressed on myeloid cells 2 (TREM2), J. Biol. Chem. 290 (43) (2015) 26043–26050.
[132] A. Boza-Serrano, R. Ruiz, R. Sanchez-Varo, J. Garcia-Revilla, Y. Yang, I. Jimenez-Ferrer, A. Paulus, M. Wennstroem, A. Vilalta, D. Allendorf, J.C. Davila, J. Stegmayr, S. Jimenez, M.A. Roca-Ceballos, V. Navarro-Garrido, M. Swanberg, C.L. Hsieh, L.M. Real, E. Englund, S. Linse, H. Leffler, U.J. Nilsson, G.C. Brown, A. Gutierrez, J. Vitorica, J.L. Venero, T. Deierborg, Galectin-3, a novel endogenous TREM2 ligand, detrimentally regulates inflammatory response in Alzheimer's disease, Acta Neuropathol. 138 (2) (2019) 251–273.
[133] T.F. Xue, J. Ji, Y.Q. Sun, X.X. Huang, Z.Y. Cai, J. Yang, W. Guo, R.B. Guo, H. Cheng, X.L. Sun, Sphingosine-1-phosphate, a novel TREM2 ligand, promotes microglial phagocytosis to protect against ischemic brain injury, Acta Pharm. Sin. B 12 (4) (2022) 1885–1898.
[134] Y.J. Wu, M.H. Wu, S.Q. Ming, X.X. Zhan, S.F. Hu, X.Y. Li, H. Yin, C. Cao, J. Liu, J. A. Li, Z.L. Wu, J. Zhou, L. Liu, S.T. Gong, D.M. He, X. Huang, TREM-2 promotes Th1 responses by interacting with the CD3ζ-ZAP70 complex following infection, J. Clin. Invest. 131 (17) (2021).
[135] X.Y. Zhang, L. Tang, J.L. Yang, L.X. Meng, J.H. Chen, L.Y. Zhou, J.Y. Wang, M. Xiong, Z.T. Zhang, Soluble TREM2 ameliorates tau phosphorylation and cognitive deficits through activating transgelin-2 in Alzheimer's disease, Nat. Commun. 14 (1) (2023).
[136] J.F. Charles, M.B. Humphrey, X.D. Zhao, E. Quarles, M.C. Nakamura, A. Aderem, W.E. Seaman, K.D. Smith, The innate immune response to Salmonella enterica serovar typhimurium by macrophages is dependent on TREM2-DAP12, Infect. Immun. 76 (6) (2008) 2439–2447.
[137] V. Phongsisay, targets immunoglobulin-like receptor LMIR5, Mol. Immunol. 63 (2) (2015) 574–578.
[138] D.N. Quan, M.D. Cooper, J.L. Potter, M.H. Roberts, H. Cheng, G.A. Jarvis, TREM-2 binds to lipooligosaccharides of neisseria gonorrhoeae and is expressed on reproductive tract epithelial cells, Mucosal Immunol. 1 (3) (2008) 229–238.
[139] V. Phongsisay, E. Iizasa, H. Hara, H. Yoshida, Evidence for TLR4 and FcRγ-CARD9 activation by cholera toxin B subunit and its direct bindings to TREM2 and LMIR5 receptors, Mol. Immunol. 66 (2) (2015) 463–471.
[140] S. Fruhwürth, L.S. Reinert, C. O ̈berg, M. Sakr, M. Henricsson, H. Zetterberg, S. R. Paludan, TREM2 is down-regulated by HSV1 in microglia and involved in antiviral defense in the brain, Sci. Adv. 9 (33) (2023).
[141] Z.B. Zhu, X.X. Zhang, W.J. Dong, X.Y. Wang, S. He, H. Zhang, X. Wang, R.P. Wei, Y.S. Chen, X.H. Liu, C.H. Guo, TREM2 suppresses the proinflammatory response to facilitate PRRSV infection via PI3K/NF-κB signaling, PLoS Pathog. 16 (5) (2020).
[142] P.L. Poliani, Y.M. Wang, E. Fontana, M.L. Robinette, Y. Yamanish, S. Gilfillan, M. Colonna, TREM2 sustains microglial expansion during aging and response to demyelination, J. Clin. Invest. 125 (5) (2015) 2161–2170.
[143] J.P. Cannon, M. O'Driscoll, G.W. Litman, Specific lipid recognition is a general feature of CD300 and TREM molecules, Immunogenetics 64 (1) (2012) 39–47.
[144] V. Phongsisay, E. Iizasa, H. Hara, S. Yamasaki, 3-O-sulfo-β-d-galactose moiety of endogenous sulfoglycolipids is a potential ligand for immunoglobulin-like receptor LMIR5, Mol. Immunol. 63 (2) (2015) 595–599.
[145] C. Gallo, E. Manzo, G. Barra, L. Fioretto, M. Ziaco, G. Nuzzo, G. d'Ippolito, F. Ferrera, P. Contini, D. Castiglia, C. Angelini, R. De Palma, A. Fontana, Sulfavant A as the first synthetic TREM2 ligand discloses a homeostatic response of dendritic cells after receptor engagement, Cell. Mol. Life Sci. 79 (7) (2022).
[146] Q.S. Peng, S. Malhotra, J.A. Torchia, W.G. Kerr, K.M. Coggeshall, M.B. Humphrey, TREM2-and DAP12-dependent activation of PI3K requires DAP10 and is inhibited by SHIP1, Sci. Signal. 3 (122) (2010).
[147] H. Konishi, H. Kiyama, Microglial TREM2/DAP12 Signaling: a double-edged sword in neural diseases, Front. Cell. Neurosci. 12 (2018).
[148] L.L. Lanier, DAP10- and DAP12-associated receptors in innate immunity, Immunol. Rev. 227 (1) (2009) 150–160.
[149] M. Colonna, DAP12 signaling: from immune cells to bone modeling and brain myelination, J. Clin. Invest. 111 (3) (2003) 313–314.
[150] M. Colonna, I. Turnbull, J. Klesney-Tait, The enigmatic function of TREM-2 in osteoclastogenesis, Adv Exp Med Biol 602 (2007) 97-+.
[151] K. Otero, I.R. Turnbull, P.L. Poliani, W. Vermi, E. Cerutti, T. Aoshi, I. Tassi, T. Takai, S.L. Stanley, M. Miller, A.S. Shaw, M. Colonna, Macrophage colony-stimulating factor induces the proliferation and survival of macrophages via a pathway involving DAP12 and β-catenin, Nat. Immunol. 10 (7) (2009) 734–U90.
[152] W. Zou, J.L. Reeve, Y.L. Liu, S.L. Teitelbaum, F.P. Ross, DAP12 couples c-Fms activation to the osteoclast cytoskeleton by recruitment of Syk, Mol. Cell 31 (3) (2008) 422–431.
[153] W.Q. Tang, B. Lv, B.W. Yang, Y.K. Chen, F.F. Yuan, L.J. Ma, S. Chen, S. Zhang, J. L. Xia, TREM2 acts as a tumor suppressor in hepatocellular carcinoma by targeting the PI3K/Akt/β-catenin pathway, Oncogenesis 8 (2019).
[154] J. Xing, A.R. Titus, M. Beth Humphrey, The TREM2-DAP12 signaling pathway in Nasu–Hakola disease: a molecular genetics perspective, Res. Rep. Biochem. (2015) 89–100.
[155] A. Mo ́csai, J. Ruland, V.L.J. Tybulewicz, The SYK tyrosine kinase: a crucial player in diverse biological functions, Nat. Rev. Immunol. 10 (6) (2010) 387–402.
[156] C.A. Lowell, Src-family and Syk kinases in activating and inhibitory pathways in innate immune cells: signaling cross talk, Csh Perspect Biol 3 (3) (2011).
[157] T.K. Ulland, W.M. Song, S.C. Huang, J.D. Ulrich, A. Sergushichev, W.L. Beatty, A. A. Loboda, Y. Zhou, N.J. Cairns, A. Kambal, E. Loginicheva, S. Gilfillan, M. Cella, H.W. Virgin, E.R. Unanue, Y. Wang, M.N. Artyomov, D.M. Holtzman, M. Colonna, TREM2 maintains microglial metabolic fitness in Alzheimer's disease, Cell 170 (4) (2017) 649–663 (e13).
[158] M. Zhu, D. Li, Y. Wu, X. Huang, M. Wu, TREM-2 promotes macrophage-mediated eradication of Pseudomonas aeruginosa via a PI3K/Akt pathway, Scand. J. Immunol. 79 (3) (2014) 187–196.
[159] J.A. Hamerman, Y.L. Yu, K.Y. Shen, C.A. Lowell, L.L. Lanier, C.L. Chu, Increased TLR responses in dendritic cells lacking the ITAM-containing adapters DAP12 and FcRγ, FASEB J. 22 (2008).
[160] R. Wu, X.P. Li, P.F. Xu, L.K. Huang, J.P. Cheng, X.L. Huang, J.R. Jiang, L.J. Wu, Y. M. Tang, TREM2 protects against cerebral ischemia/reperfusion injury, Mol. Brain 10 (2017).
[161] L. Zhong, Z.L. Zhang, X.X. Li, C.Y. Liao, P.F. Mou, T.T. Wang, Z.Q. Wang, Z. Wang, M. Wei, H.X. Xu, G.J. Bu, X.F. Chen, TREM2/DAP12 complex regulates inflammatory responses in microglia via the JNK signaling pathway, Front. Aging Neurosci. 9 (2017).
[162] B.J. Andreone, L. Przybyla, C. Llapashtica, A. Rana, S.S. Davis, B. van Lengerich, K.R. Lin, J. Shi, Y. Mei, G. Astarita, G. Di Paolo, T. Sandmann, K.M. Monroe, J. W. Lewcock, Alzheimer's-associated PLCγ2 is a signaling node required for both TREM2 function and the inflammatory response in human microglia, Nat. Neurosci. 23 (8) (2020) 927-+.
[163] J. Obst, H.L. Hall-Roberts, T.B. Smith, M. Kreuzer, L. Magno, E. Di Daniel, J. B. Davis, E. Mead, PLCγ2 regulates TREM2 signalling and integrin-mediated adhesion and migration of human iPSC-derived macrophages, Sci Rep-Uk 11 (1) (2021).
[164] L. Magno, T.D. Bunney, E. Mead, F. Svensson, M.N. Bictash, TREM2/PLCγ2 signalling in immune cells: function, structural insight, and potential therapeutic modulation, Mol. Neurodegener. 16 (1) (2021).
[165] C. Mecca, I. Giambanco, R. Donato, C. Arcuri, Microglia and aging: the role of the TREM2-DAP12 and CX3CL1-CX3CR1 axes, Int. J. Mol. Sci. 19 (1) (2018).

[166] H.L. Yao, K. Coppola, J.E. Schweig, F. Crawford, M. Mullan, D. Paris, Distinct signaling pathways regulate TREM2 phagocytic and NFκB antagonistic activities, Front. Cell. Neurosci. 13 (2019).
[167] K. Takahashi, C.D.P. Rochford, H. Neumann, Clearance of apoptotic neurons without inflammation by microglial triggering receptor expressed on myeloid cells-2, J. Exp. Med. 201 (4) (2005) 647–657.
[168] H.H. Zheng, L. Jia, C.C. Liu, Z.Y. Rong, L. Zhong, L.Y. Yang, X.F. Chen, J.D. Fryer, X. Wang, Y.W. Zhang, H.X. Xu, G.J. Bu, TREM2 promotes microglial survival by activating Wnt/β-catenin pathway, J. Neurosci. 37 (7) (2017) 1772–1784.
[169] X.J. Song, N. Kirtipal, S.J. Lee, P. Maly, S. Bharadwaj, Current therapeutic targets and multifaceted physiological impacts of caffeine, Phytother. Res. 37 (12) (2023) 5558–5598.
[170] J. Walter, The triggering receptor expressed on myeloid cells 2: a molecular link of neuroinflammation and neurodegenerative diseases, J. Biol. Chem. 291 (9) (2016) 4334–4341.
[171] X.Z. Chen, Y. Zhao, Y.M. Huang, K.C. Zhu, F. Zeng, J.Y. Zhao, H.Q. Zhang, X. Z. Zhu, H. Kettenmann, X.Y. Xiang, TREM2 promotes glioma progression and angiogenesis mediated by microglia/brain macrophages, Glia (2023).
[172] M. Cella, C. Buonsanti, C. Strader, T. Kondo, A. Salmaggi, M. Colonna, Impaired differentiation of osteoclasts in TREM-2-deficient individuals, J. Exp. Med. 198 (4) (2003) 645–651.
[173] P. Forabosco, A. Ramasamy, D. Trabzuni, R. Walker, C. Smith, J. Bras, A. P. Levine, J. Hardy, J.M. Pocock, R. Guerreiro, M.E. Weale, M. Ryten, Insights into TREM2 biology by network analysis of human brain gene expression data, Neurobiol. Aging 34 (12) (2013) 2699–2714.
[174] L. Tserel, R. Kolde, A. Rebane, K. Kisand, T. Org, H. Peterson, J. Vilo, P. Peterson, Genome-wide promoter analysis of histone modifications in human monocyte-derived antigen presenting cells, BMC Genomics 11 (2010).
[175] A. Kiialainen, V. Veckman, J. Saharinen, J. Paloneva, M. Gentile, P. Hakola, D. Hemelsoet, B. Ridha, O. Kopra, I. Julkunen, L. Peltonen, Transcript profiles of dendritic cells of PLOSL patients link demyelinating CNS disorders with abnormalities in pathways of actin bundling and immune response, J. Mol. Med. 85 (9) (2007) 971–983.
[176] Y.M. Wang, T.K. Ulland, J.D. Ulrich, W. Song, J.A. Tzaferis, J.T. Hole, P. Yuan, T. E. Mahan, Y. Shi, S. Gilfillan, M. Cella, J. Grutzendler, R.B. DeMattos, J.R. Cirrito, D.M. Holtzman, M. Colonna, TREM2-mediated early microglial response limits diffusion and toxicity of amyloid plaques, J. Exp. Med. 213 (5) (2016) 667–675.
[177] M.R. Daws, D.H. Chung, L.L. Lanier, W.E. Seaman, J.C. Ryan, Cloning and characterization of a novel mouse myeloid DAP12-associated receptor family, FASEB J. 15 (4) (2001) A713–A.
[178] L. Piccio, C. Buonsanti, M. Cella, I. Tassi, R.E. Schmidt, C. Fenoglio, J. Rinker, R. T. Naismith, P. Panina-Bordignon, N. Passini, D. Galimberti, E. Scarpini, M. Colonna, A.H. Cross, Identification of soluble TREM-2 in the cerebrospinal fluid and its association with multiple sclerosis and CNS inflammation, Brain 131 (2008) 3081–3091.
[179] N. Hu, M.S. Tan, J.T. Yu, L. Sun, L. Tan, Y.L. Wang, T. Jiang, L. Tan, Increased expression of TREM2 in peripheral blood of Alzheimer's disease patients, J. Alzheimers Dis. 38 (3) (2014) 497–501.
[180] J. Satoh, N. Asahina, S. Kitano, Y. Kino, A Comprehensive Profile of ChIP-seq-based PU.1/Spi1 target genes in microglia, Gene Regul Syst Bio 8 (2014) 127–139.
[181] T.R. Jay, V.E. von Saucken, G.E. Landreth, TREM2 in Neurodegenerative diseases, Mol. Neurodegener. 12 (2017).
[182] F. Rae, K. Woods, T. Sasmono, N. Campanale, D. Taylor, D.A. Ovchinnikov, S. M. Grimmond, D.A. Hume, S.D. Ricardo, M.H. Little, Characterisation and trophic functions of murine embryonic macrophages based upon the use of a Csf1r-EGFP transgene reporter, Dev. Biol. 308 (1) (2007) 232–246.
[183] S. Konig, T. Regen, K. Dittmann, M. Engelke, J. Wienands, R. Schwendener, U. K. Hanisch, T. Pukrop, H. Hahn, Empty liposomes induce antitumoral effects associated with macrophage responses distinct from those of the TLR1/2 agonist Pam3CSK 4 (BLP), Cancer Immunol. Immunother. 62 (10) (2013) 1587–1597.
[184] L.L. Koth, C.J. Cambier, A. Ellwanger, M. Solon, L. Hou, L.L. Lanier, C.L. Abram, J. A. Hamerman, P.G. Woodruff, DAP12 is required for macrophage recruitment to the lung in response to cigarette smoke and chemotaxis toward CCL2, J. Immunol. 184 (11) (2010) 6522–6528.
[185] J.H. Oh, M.J. Yang, J.D. Heo, Y.S. Yang, H.J. Park, S.M. Park, M.S. Kwon, C. W. Song, S. Yoon, I.J. Yu, Inflammatory response in rat lungs with recurrent exposure to welding fumes: a transcriptomic approach, Toxicol. Ind. Health 28 (3) (2012) 203–215.
[186] M.B. Humphrey, M.R. Daws, S.C. Spusta, E.C. Niemi, J.A. Torchia, L.L. Lanier, W. E. Seaman, M.C. Nakamura, TREM2, a DAP12-associated receptor, regulates osteoclast differentiation and function, J. Bone Miner. Res. 21 (2) (2006) 237–245.
[187] M.S.F. Zawawi, A.A.S.S.K. Dharmapatni, M.D. Cantley, K.P. McHugh, D. R. Haynes, T.N. Crotti, Regulation of ITAM adaptor molecules and their receptors by inhibition of calcineurin-NFAT signalling during late stage osteoclast differentiation, Biochem Bioph Res Co 427 (2) (2012) 404–409.
[188] A. Kiialainen, K. Hovanes, J. Paloneva, O. Kopra, L. Peltonen, Dap12 and Trem2, molecules involved in innate immunity and neurodegeneration, are co-expressed in the CNS, Neurobiol. Dis. 18 (2) (2005) 314–322.
[189] L.C. Chen, J.D. Laskin, M.K. Gordon, D.L. Laskin, Regulation of TREM expression in hepatic macrophages and endothelial cells during acute endotoxemia, Exp. Mol. Pathol. 84 (2) (2008) 145–155.
[190] T.N. Crotti, A.A.S.S.K. Dharmapatni, E. Alias, A.C.W. Zannettino, M.D. Smith, D. R. Haynes, The immunoreceptor tyrosine-based activation motif (ITAM) -related factors are increased in synovial tissue and vasculature of rheumatoid arthritic joints, Arthritis Res. Ther. 14 (6) (2012).
[191] C.C. Lin, T.Y. Chang, Y.C. Lu, Y.S. Wu, W. Huang, W.C. Lo, G.F. Liu, W.C. Hsu, P. S. Ohashi, T.W. Mak, J.L. Fuh, H.C. Chen, D.C. Tarng, N.J. Chen, TREM-2 mediates dendritic cell-induced NO to suppress Th17 activation and ameliorate chronic kidney diseases, J. Mol. Med. 100 (6) (2022) 917–931.
[192] S.C. Hall, D.K. Agrawal, Increased TREM-2 expression on the subsets of CD11c+ cells in the lungs and lymph nodes during allergic airway inflammation, Sci Rep-Uk 7 (2017).
[193] H.L. Jiang, Y. Si, Z.H. Li, X. Huang, S.J. Chen, Y.Q. Zheng, G. Xu, X.M. Chen, Y. B. Chen, Y. Liu, H. Xiong, Q.H. Huang, M.J. Liang, Z.G. Zhang, TREM-2 promotes acquired cholesteatoma-induced bone destruction by modulating TLR4 signaling pathway and osteoclasts activation, Sci Rep-Uk 6 (2016).
[194] C. Tanchot, F.A. Lemonnier, B. Perarnau, A.A. Freitas, B. Rocha, Differential requirements for survival and proliferation of CD8 naive or memory T cells, Science 276 (5321) (1997) 2057–2062.
[195] A.C. Sek, C.M. Percopo, A.K. Boddapati, M. Ma, W.E. Geslewitz, J.O. Krumholz, J. B. Lack, H.F. Rosenberg, Differential expression of Triggering Receptor Expressed on Myeloid cells 2 (Trem2) in tissue eosinophils, J. Leukoc. Biol. 110 (4) (2021) 679–691.
[196] M. Bucova, M. Suchankova, E. Tibenska, I. Majer, H. Novosadova, S. Urban, Diagnostic value of TREM-1 and TREM-2 expression in bronchoalveolar lavage fluid in sarcoidosis and other lung diseases, Bratisl Med J 116 (12) (2015) 707–713.
[197] I. Coelho, N. Duarte, A. Barros, M.P. Macedo, C. Penha-Gonçalves, Trem-2 promotes emergence of restorative macrophages and endothelial cells during recovery from hepatic tissue damage, Front. Immunol. 11 (2021).
[198] E.C.E. Wang, Z.P. Dai, A.W. Ferrante, C.G. Drake, A.M. Christiano, A Subset of TREM2+ dermal macrophages secretes oncostatin M to maintain hair follicle stem cell quiescence and inhibit hair growth, Cell Stem Cell 24 (4) (2019) 654-+.
[199] D. Xiong, Y. Wang, M. You, A gene expression signature of TREM2(hi) macrophages and gammadelta T cells predicts immunotherapy response, Nat. Commun. 11 (1) (2020) 5084.
[200] L.S. Zhou, M.L. Wang, H.R. Guo, J. Hou, Y.N. Zhang, M. Li, X.W. Wu, X.L. Chen, L. H. Wang, Integrated analysis highlights the immunosuppressive role of TREM2+ macrophages in hepatocellular carcinoma, Front. Immunol. 13 (2022).
[201] W.Q. Zhang, S.H. Huang, X. Huang, J.H. Li, P. Ye, J.H. Xu, P.Z. Zheng, H.Y. Shen, J.R. Huang, Regulation of human mesenchymal stem cell differentiation by TREM-2, Hum. Immunol. 77 (6) (2016) 476–482.
[202] P. Ye, D.W. Xu, J.H. Xu, G.W. Liu, S.H. Huang, W.Q. Zhang, P.Z. Zheng, J.H. Li, J. R. Huang, TREM-2 negatively regulates LPS-mediated inflammatory response in rat bone marrow-derived MSCs, Mol. Med. Rep. 16 (4) (2017) 4777–4783.
[203] M. Pevsner-Fischer, V. Morad, M. Cohen-Sfady, L. Rousso-Noori, A. Zanin-Zhorov, S. Cohen, I.R. Cohen, D. Zipori, Toll-like receptors and their ligands control mesenchymal stem cell functions, Blood 109 (4) (2007) 1422–1432.
[204] H.H. Cho, Y.C. Bae, J.S. Jung, Role of toll-like receptors on human adipose-derived stromal cells, Stem Cells 24 (12) (2006) 2744–2752.
[205] T. Jonsson, H. Stefansson, S. Steinberg, I. Jonsdottir, P.V. Jonsson, J. Snaedal, S. Bjornsson, J. Huttenlocher, A.I. Levey, J.J. Lah, D. Rujescu, H. Hampel, I. Giegling, O.A. Andreassen, K. Engedal, I. Ulstein, S. Djurovic, C. Ibrahim-Verbaas, A. Hofman, M.A. Ikram, C.M. van Duijn, U. Thorsteinsdottir, A. Kong, K. Stefansson, Variant of TREM2 associated with the risk of Alzheimer's disease, N. Engl. J. Med. 368 (2) (2013) 107–116.
[206] H. Keren-Shaul, A. Spinrad, A. Weiner, O. Matcovitch-Natan, R. Dvir-Szternfeld, T.K. Ulland, E. David, K. Baruch, D. Lara-Astaiso, B. Toth, S. Itzkovitz, M. Colonna, M. Schwartz, I. Amit, A unique microglia type associated with restricting development of Alzheimer's disease, Cell 169 (7) (2017) 1276-+.
[207] L. Zhong, X.F. Chen, T.T. Wang, Z. Wang, C.Y. Liao, Z.Q. Wang, R.Z. Huang, D. X. Wang, X.X. Li, L.B. Wu, L. Jia, H.H. Zheng, M. Painter, Y. Atagi, C.C. Liu, Y. W. Zhang, J.D. Fryer, H.X. Xu, G.J. Bu, Soluble TREM2 induces inflammatory responses and enhances microglial survival, J. Exp. Med. 214 (3) (2017) 597–607.
[208] M.W. Sieber, N. Jaenisch, M. Brehm, M. Guenther, B. Linnartz-Gerlach, H. Neumann, O.W. Witte, C. Frahm, Attenuated inflammatory response in triggering receptor expressed on myeloid cells 2 (TREM2) knock-out mice following stroke, PLoS One 8 (1) (2013).
[209] A. Deczkowska, H. Keren-Shaul, A. Weiner, M. Colonna, M. Schwartz, I. Amit, Disease-associated microglia: a universal immune sensor of neurodegeneration, Cell 173 (5) (2018) 1073–1081.
[210] H.Y. Lee, E.H. Lee, J. Yi, K.Y. Ji, S.M. Kim, H. Choi, S.M. Yee, H.S. Kang, E.M. Kim, TREM2 promotes natural killer cell development in CD3—CD122+NK1.1+ pNK cells, BMC Immunol. 22 (1) (2021).
[211] D.M. Gascoyne, E. Long, H. Veiga-Fernandes, J. de Boer, O. Williams, B. Seddon, M. Coles, D. Kioussis, H.J.M. Brady, The basic leucine zipper transcription factor E4BP4 is essential for natural killer cell development (vol 10, pg 1118, 2009), Nat. Immunol. 11 (6) (2010) 543.
[212] N. Bancaro, B. Cali, M. Troiani, A.R. Elia, R.A. Arzola, G. Attanasio, P. Lai, M. Crespo, B. Gurel, R. Pereira, C.S.A. Guo, S. Mosole, D. Brina, M. D'Ambrosio, E. Pasquini, C. Spataro, E. Zagato, A. Rinaldi, M. Pedotti, S. Di Lascio, F. Meani, M. Montopoli, M. Ferrari, A. Gallina, L. Varani, R.P. Mestre, M. Bolis, S. G. Sommer, J. de Bono, A. Calcinotto, A. Alimonti, Apolipoprotein E induces pathogenic senescent-like myeloid cells in prostate cancer, Cancer Cell 41 (3) (2023) 602-+.
[213] J.V. Haure-Mirande, M. Audrain, T. Fanutza, S.H. Kim, W.L. Klein, C. Glabe, B. Readhead, J.T. Dudley, R.D. Blitzer, M.H. Wang, B. Zhang, E.E. Schadt, S. Gandy, M.E. Ehrlich, Deficiency of TYROBP, an adapter protein for TREM2 and

CR3 receptors, is neuroprotective in a mouse model of early Alzheimer's pathology, Acta Neuropathol. 134 (5) (2017) 769–788.
[214] K. Otero, M. Shinohara, H. Zhao, M. Cella, S. Gilfillan, A. Colucci, R. Faccio, F. P. Ross, S.L. Teitelbaum, H. Takayanagi, M. Colonna, TREM2 and β-catenin regulate bone homeostasis by controlling the rate of osteoclastogenesis (vol 188, pg 2612, 2012), J. Immunol. 188 (11) (2012) 5802.
[215] J. Banchereau, R.M. Steinman, Dendritic cells and the control of immunity, Nature 392 (6673) (1998) 245–252.
[216] T.A. Wynn, A. Chawla, J.W. Pollard, Macrophage biology in development, homeostasis and disease, Nature 496 (7446) (2013) 445–455.
[217] G. Kolios, V. Valatas, E. Kouroumalis, Role of Kupffer cells in the pathogenesis of liver disease, World J Gastroentero 12 (46) (2006) 7413–7420.
[218] D.A. Jaitin, L. Adlung, C.A. Thaiss, A. Weiner, B. Li, H. Descamps, P. Lundgren, C. Bleriot, Z. Liu, A. Deczkowska, H. Keren-Shaul, E. David, N. Zmora, S.M. Eldar, N. Lubezky, O. Shibolet, D.A. Hill, M.A. Lazar, M. Colonna, F. Ginhoux, H. Shapiro, E. Elinav, I. Amit, Lipid-associated macrophages control metabolic homeostasis in a trem2-dependent manner, Cell 178 (3) (2019) 686–698 e14.
[219] E. Ydens, A. Cauwels, B. Asselbergh, S. Goethals, L. Peeraer, G. Lornet, L. Almeida-Souza, J.A. Van Ginderachter, V. Timmerman, S. Janssens, Acute injury in the peripheral nervous system triggers an alternative macrophage response, J Neuroinflamm 9 (2012).
[220] Y. Nakanishi, M. Nakatsuji, H. Seno, S. Ishizu, R. Akitake-Kawano, K. Kanda, T. Ueo, H. Komekado, M. Kawada, M. Minami, T. Chiba, COX-2 inhibition alters the phenotype of tumor-associated macrophages from M2 to M1 in ApcMin/+ mouse polyps, Carcinogenesis 32 (9) (2011) 1333–1339.
[221] C. Gustafsson, J. Mjo¨sberg, A. Matussek, R. Geffers, L. Matthiesen, G. Berg, S. Sharma, J. Buer, J. Ernerudh, Gene expression profiling of human decidual macrophages: evidence for immunosuppressive phenotype, PLoS One 3 (4) (2008).
[222] M.F. Pittenger, A.M. Mackay, S.C. Beck, R.K. Jaiswal, R. Douglas, J.D. Mosca, M. A. Moorman, D.W. Simonetti, S. Craig, D.R. Marshak, Multilineage potential of adult human mesenchymal stem cells, Science 284 (5411) (1999) 143–147.
[223] L. Müller, A. Tunger, M. Wobus, M. von Bonin, R. Towers, M. Bornh¨auser, F. Dazzi, R. Wehner, M. Schmitz, Immunomodulatory properties of mesenchymal stromal cells: an update, Front. Cell Dev. Biol. 9 (2021).
[224] D.J. Prockop, D.J. Kota, N. Bazhanov, R.L. Reger, Evolving paradigms for repair of tissues by adult stem/progenitor cells (MSCs), J. Cell Mol. Med. 14 (9) (2010) 2190–2199.
[225] R.S. Waterman, S.L. Tomchuck, S.L. Henkle, A.M. Betancourt, A New mesenchymal stem cell (MSC) paradigm: polarization into a pro-inflammatory MSC1 or an immunosuppressive MSC2 phenotype, PLoS One 5 (4) (2010).
[226] R.C. Paolicelli, G. Bolasco, F. Pagani, L. Maggi, M. Scianni, P. Panzanelli, M. Giustetto, T.A. Ferreira, E. Guiducci, L. Dumas, D. Ragozzino, C.T. Gross, Synaptic pruning by microglia is necessary for normal brain development, Science 333 (6048) (2011) 1456–1458.
[227] S. Hong, V.F. Beja-Glasser, B.M. Nfonoyim, A. Frouin, S.M. Li, S. Ramakrishnan, K.M. Merry, Q.Q. Shi, A. Rosenthal, B.A. Barres, C.A. Lemere, D.J. Selkoe, B. Stevens, Complement and microglia mediate early synapse loss in Alzheimer mouse models, Science 352 (6286) (2016) 712–716.
[228] M. Chertoff, K. Shrivastava, B. Gonzalez, L. Acarin, L. Gim´enez-Llort, Differential modulation of TREM2 protein during postnatal brain development in mice, PLoS One 8 (8) (2013).
[229] N. Daisuke, T. Kazuya, Y. Takashi, Y. Masahito, M. Sachiko, In vitro differentiation of lineage-negative bone marrow cells and monocyte into microglia-like cells, J. Neuroimmunol. 228 (1–2) (2010) 23.
[230] J. Satoh, Y. Kino, N. Motohashi, T. Ishida, S. Yagishita, K. Jinnai, N. Arai, K. Nakamagoe, A. Tamaoka, Y. Saito, K. Arima, Immunohistochemical characterization of CD33 expression on microglia in Nasu-Hakola disease brains, Neuropathology 35 (6) (2015) 529–537.
[231] J. Sosna, S. Philipp, R. Albay, J.M. Reyes-Ruiz, D. Baglietto-Vargas, F.M. LaFerla, C.G. Glabe, Early long-term administration of the CSF1R inhibitor PLX3397 ablates microglia and reduces accumulation of intraneuronal amyloid, neuritic plaque deposition and pre-fibrillar oligomers in 5XFAD mouse model of Alzheimer's disease, Mol. Neurodegener. 13 (2018).
[232] D. Giunti, B. Parodi, C. Usai, L. Vergani, S. Casazza, S. Bruzzone, G. Mancardi, A. Uccelli, Mesenchymal stem cells shape microglia effector functions through the release of CX3CL1, Stem Cells 30 (9) (2012) 2044–2053.
[233] C.Y.D. Lee, A. Daggett, X.F. Gu, L.L. Jiang, P. Langfelder, X.G. Li, N. Wang, Y. J. Zhao, C.S. Park, Y. Cooper, I. Ferando, I. Mody, G. Coppola, H.X. Xu, X. W. Yang, Elevated TREM2 gene dosage reprograms microglia responsivity and ameliorates pathological phenotypes in Alzheimer's disease models, Neuron 97 (5) (2018) 1032-+.
[234] T.K. Ulland, M. Colonna, TREM2-a key player in microglial biology and Alzheimer disease, Nat. Rev. Neurol. 14 (11) (2018) 667–675.
[235] R. Sun, R. Han, C. McCornack, G.T. Tabor, J. Hou, R. Cleary, D. Mao, Q. Liu, K. Schoch, J. Luo, A. Petti, T. Miller, J. Ulrich, D. Holtzman, A. Kim, IMMU-28. Trem2 inhibition reprograms myeloid cells to stimulate anti-tumor immunity through both direct and indirect mechanisms, Neuro-Oncology 25 (Supplement_5) (2023) v148.
[236] M.M. Peshoff, P. Gupta, S. Oberai, R. Trivedi, H. Katayama, P. Chakrapani, M. H. Dang, S. Migliozzi, J. Gumin, D.B. Kadri, J.K. Lin, N.K. Milam, M.E. Maynard, B.D. Vaillant, B. Parker-Kerrigan, F.F. Lang, J.T. Huse, A. Iavarone, L.H. Wang, K. Clise-Dwyer, K.P. Bhat, Triggering receptor expressed on myeloid cells 2 (TREM2) regulates phagocytosis in glioblastoma, Neuro Oncol. (2024).
[237] Z. Lu, J. Zou, S. Li, M.J. Topper, Y. Tao, H. Zhang, X. Jiao, W. Xie, X. Kong, M. Vaz, H. Li, Y. Cai, L. Xia, P. Huang, K. Rodgers, B. Lee, J.B. Riemer, C.P. Day, R. C. Yen, Y. Cui, Y. Wang, Y. Wang, W. Zhang, H. Easwaran, A. Hulbert, K. Kim, R. A. Juergens, S.C. Yang, R.J. Battafarano, E.L. Bush, S.R. Broderick, S.M. Cattaneo, J.R. Brahmer, C.M. Rudin, J. Wrangle, Y. Mei, Y.J. Kim, B. Zhang, K.K. Wang, P. M. Forde, J.B. Margolick, B.D. Nelkin, C.A. Zahnow, D.M. Pardoll, F. Housseau, S. B. Baylin, L. Shen, M.V. Brock, Epigenetic therapy inhibits metastases by disrupting premetastatic niches, Nature 579 (7798) (2020) 284–290.
[238] N. A-Gonzalez, S.J. Bensinger, C. Hong, S. Beceiro, M.N. Bradley, N. Zelcer, J. Deniz, C. Ramirez, M. Diaz, G. Gallardo, C.R. de Galarreta, J. Salazar, F. Lopez, P. Edwards, J. Parks, M. Andujar, P. Tontonoz, A. Castrillo, Apoptotic Cells Promote Their Own Clearance and Immune Tolerance through Activation of the Nuclear Receptor LXR, Immunity 31(2) (2009) 245-258.
[239] G.S. Selders, A.E. Fetz, M.Z. Radic, G.L. Bowlin, An overview of the role of neutrophils in innate immunity, inflammation and host-biomaterial integration, Regen Biomater 4 (1) (2017) 55–68.
[240] P. Katsimbri, The biology of normal bone remodelling, Eur. J. Cancer Care 26 (6) (2017).
[241] K.F. Kubatzky, F. Uhle, T. Eigenbrod, From macrophage to osteoclast - how metabolism determines function and activity, Cytokine 112 (2018) 102–115.
[242] Y.T. Weng, H.C. Wang, L. Li, Y.H.Z. Feng, S.Y. Xu, Z.L. Wang, Trem2 mediated Syk-dependent ROS amplification is essential for osteoclastogenesis in periodontitis microenvironment, Redox Biol. 40 (2021).
[243] R. Wei, L. Zhang, W. Hu, J. Wu, W. Zhang, CSTA plays a role in osteoclast formation and bone resorption by mediating the DAP12/TREM2 pathway, Biochem Bioph Res Co 627 (2022) 12–20.
[244] S. Bhattacharjee, Y. Zhao, P. Dua, E.I. Rogaev, W.J. Lukiw, microRNA-34a-mediated down-regulation of the microglial-enriched triggering receptor and phagocytosis-sensor TREM2 in age-related macular degeneration (vol 11, e0150211, 2016), PLoS One 11 (4) (2016).
[245] R. Gawish, R. Martins, B. Bohm, T. Wimberger, O. Sharif, K. Lakovits, M. Schmidt, S. Knapp, Triggering receptor expressed on myeloid cells-2 fine-tunes inflammatory responses in murine Gram-negative sepsis, FASEB J. 29 (4) (2015) 1247–1257.
[246] S.J. Ferrara, P. Chaudhary, M.J. DeBell, G. Marracci, H. Miller, E. Calkins, E. Pocius, B.A. Napier, B. Emery, D. Bourdette, T.S. Scanlan, TREM2 is thyroid hormone regulated making the TREM2 pathway druggable with ligands for thyroid hormone receptor, Cell Chem. Biol. 29 (2) (2022) 239-+.
[247] Y. Ozaki, Y. Yoshino, K. Yamazaki, T. Sao, Y. Mori, S. Ochi, T. Yoshida, T. Mori, J. Iga, S. Ueno, DNA methylation changes at TREM2 intron 1 and TREM2 mRNA expression in patients with Alzheimer's disease, J. Psychiatr. Res. 92 (2017) 74–80.
[248] S. Fujimoto, T. Goda, K. Mochizuki, In vivo evidence of enhanced di-methylation of histone H3 K4 on upregulated genes in adipose tissue of diabetic db/db mice, Biochem Bioph Res Co 404 (1) (2011) 223–227.
[249] A.R. Smith, J. Mill, R.G. Smith, K. Lunnon, Elucidating novel dysfunctional pathways in Alzheimer's disease by integrating loci identified in genetic and epigenetic studies, Neuroepigenetics 6 (2016) 32–50.
[250] M. Yanaizu, H. Adachi, M. Araki, K. Kontani, Y. Kino, Translational regulation and protein-coding capacity of the 5′ untranslated region of human TREM2, Commun Biol 6 (1) (2023).
[251] A. Bouchon, J. Dietrich, M. Colonna, Cutting edge: Inflammatory responses can be triggered by TREM-1, a novel receptor expressed on neutrophils and monocytes, J. Immunol. 164 (10) (2000) 4991–4995.
[252] M.M. Mancarelli, L.C. Frusciante, G.F. Cauvi, C. De Rossi, B.E. Torbett, C/EBPalpha Is a key transcriptional regulator of the triggering receptor on myeloid cells-2 gene, Blood 112 (11) (2008) 4762.
[253] B. Daniel, G. Nagy, N. Hah, A. Horvath, Z. Czimmerer, S. Poliska, T. Gyuris, J. Keirsse, C. Gysemans, J.A. Van Ginderachter, B.L. Balint, R.M. Evans, E. Barta, L. Nagy, The active enhancer network operated by liganded RXR supports angiogenic activity in macrophages, Gene Dev 28 (14) (2014) 1562–1577.
[254] J.C. Savage, T. Jay, E. Goduni, C. Quigley, M.M. Mariani, T. Malm, R. M. Ransohoff, B.T. Lamb, G.E. Landreth, Nuclear receptors license phagocytosis by trem2+ myeloid cells in mouse models of Alzheimer's disease, J. Neurosci. 35 (16) (2015) 6532–6543.
[255] J.-I. Satoh, N. Asahina, S. Kitano, Y. Kino, A comprehensive profile of ChIP-Seq-based PU. 1/Spi1 target genes in microglia. Gene Regulation and Systems Biology 8, 2014.
[256] P.N. Alexandrov, Y.H. Zhao, B.M. Jones, S. Bhattacharjee, W.J. Lukiw, Expression of the phagocytosis-essential protein TREM2 is down-regulated by an aluminum-induced miRNA-34a in a murine microglial cell line, J. Inorg. Biochem. 128 (2013) 267–269.
[257] I. Lefterov, J. Schug, A. Mounier, K.N. Nam, N.F. Fitz, R. Koldamova, RNA-sequencing reveals transcriptional up-regulation of Trem2 in response to bexarotene treatment, Neurobiol. Dis. 82 (2015) 132–140.
[258] C. Reitz, R. Mayeux, TREM2 and neurodegenerative disease, N. Engl. J. Med. 369 (16) (2013) 1564.
[259] C.L. Long, W.L. Berry, Y. Zhao, X.H. Sun, M.B. Humphrey, E proteins regulate osteoclast maturation and survival, J. Bone Miner. Res. 27 (12) (2012) 2476–2489.
[260] G.D. Manocha, A. Ghatak, K.L. Puig, S.D. Kraner, C.M. Norris, C.K. Combs, NFATc2 modulates microglial activation in the a beta PP/PS1 mouse model of Alzheimer's disease, J. Alzheimers Dis. 58 (3) (2017) 775–787.
[261] L. Rojanathammanee, A.M. Floden, G.D. Manocha, C.K. Combs, Attenuation of microglial activation in a mouse model of Alzheimer's disease via NFAT inhibition, J. Neuroinflammation 12 (2015) 42.

[262] Y.H. Lu, X.F. Huang, W.P. Liang, Y. Li, M.E. Xing, W.H. Pan, Y. Zhang, Z. Wang, W.H. Song, Regulation of TREM2 expression by transcription factor YY1 and its protective effect against Alzheimer's disease, J. Biol. Chem. 299 (5) (2023).
[263] P. Ramachandran, R. Dobie, J.R. Wilson-Kanamori, E.F. Dora, B.E.P. Henderson, N.T. Luu, J.R. Portman, K.P. Matchett, M. Brice, J.A. Marwick, R.S. Taylor, M. Efremova, R. Vento-Tormo, N.O. Carragher, T.J. Kendall, J.A. Fallowfield, E. M. Harrison, D.J. Mole, S.J. Wigmore, P.N. Newsome, C.J. Weston, J.P. Iredale, F. Tacke, J.W. Pollard, C.P. Ponting, J.C. Marioni, S.A. Teichmann, N. C. Henderson, Resolving the fibrotic niche of human liver cirrhosis at single-cell level, Nature 575 (7783) (2019) 512-+.
[264] Y. Zhao, S. Bhattacharjee, B.M. Jones, P. Dua, P.N. Alexandrov, J.M. Hill, W. J. Lukiw, Regulation of TREM2 expression by an NF-small ka, CyrillicB-sensitive miRNA-34a, Neuroreport 24 (6) (2013) 318–323.
[265] Q.K. Lv, Z. Zhong, B.B. Hu, S. Yan, Y.F. Yan, J.J. Zhang, T. Shi, L.J. Jiang, W. Li, W. Huang, MicroRNA-3473b regulates the expression of TREM2/ULK1 and inhibits autophagy in inflammatory pathogenesis of Parkinson disease, J. Neurochem. 157 (3) (2021) 599–610.
[266] H. Zheng, C.C. Liu, Y. Atagi, X.F. Chen, L. Jia, L. Yang, W. He, X. Zhang, S.S. Kang, T.L. Rosenberry, J.D. Fryer, Y.W. Zhang, H. Xu, G. Bu, Opposing roles of the triggering receptor expressed on myeloid cells 2 and triggering receptor expressed on myeloid cells-like transcript 2 in microglia activation, Neurobiol. Aging 42 (2016) 132–141.
[267] G.Y. Sun, C.X. Guan, Y. Zhou, Y.P. Liu, S.F. Li, H.F. Zhou, C.Y. Tang, X.A. Fang, Vasoactive intestinal peptide re-balances TREM-1/TREM-2 ratio in acute lung injury, Regul Peptides 167 (1) (2011) 56–64.
[268] D. Trudler, O. Weinreb, S.A. Mandel, M.B.H. Youdim, D. Frenkel, DJ-1 deficiency triggers microglia sensitivity dopamine toward a pro-inflammatory phenotype that is attenuated by rasagiline, J. Neurochem. 129 (3) (2014) 434–447.
[269] X.L. Gao, Y.T. Dong, Z.L. Liu, B. Niu, Silencing of triggering receptor expressed on myeloid cells-2 enhances the inflammatory responses of alveolar macrophages to lipopolysaccharide, Mol. Med. Rep. 7 (3) (2013) 921–926.
[270] J.H. Chang, E.J. Chang, H.H. Kim, S.K. Kim, Enhanced inhibitory effects of a novel CpG motif on osteoclast differentiation via TREM-2 down-regulation, Biochem Bioph Res Co 389 (1) (2009) 28–33.
[271] J.D. Ji, K.H. Park-Min, Z.X. Shen, R.J. Fajardo, S.R. Goldring, K.P. McHugh, L. B. Ivashkiv, Inhibition of RANK Expression and Osteoclastogenesis by TLRs and IFN-γ in Human Osteoclast Precursors, J. Immunol. 183 (11) (2009) 7223–7233.
[272] X. Li, K.S. Montine, C.D. Keene, T.J. Montine, Different mechanisms of apolipoprotein E isoform–dependent modulation of prostaglandin E2 production and triggering receptor expressed on myeloid cells 2 (TREM2) expression after innate immune activation of microglia, FASEB J. 29 (5) (2015) 1754.
[273] R. Owens, K. Grabert, C.L. Davies, A. Alfieri, J.P. Antel, L.M. Healy, B.W. McColl, Divergent neuroinflammatory regulation of microglial TREM expression and involvement of NF-κB (vol 11, 56, 2017), Front. Cell. Neurosci. 11 (2017).
[274] H.M. Wilkins, S.M. Carl, S.G. Weber, S.A. Ramanujan, B.W. Festoff, D. A. Linseman, R.H. Swerdlow, Mitochondrial lysates induce inflammation and Alzheimer's disease-relevant changes in microglial and neuronal cells, J. Alzheimers Dis. 45 (1) (2015) 305–318.
[275] O. Sharif, R. Gawish, J.M. Warszawska, R. Martins, K. Lakovits, A. Hladik, B. Doninger, J. Brunner, A. Korosec, R.E. Schwarzenbacher, T. Berg, R. Kralovics, J. Colinge, I. Mesteri, S. Gilfillan, A. Salmaggi, A. Verschoor, M. Colonna, S. Knapp, The triggering receptor expressed on myeloid cells 2 inhibits complement component 1q effector mechanisms and exerts detrimental effects during pneumococcal pneumonia, PLoS Pathog. 10 (6) (2014).
[276] K.H. Park-Min, J.D. Ji, T. Antoniv, A.C. Reid, R.B. Silver, M.B. Humphrey, M. Nakamura, L.B. Ivashkiv, IL-10 suppresses calcium-mediated costimulation of receptor activator NF-kappa B signaling during human osteoclast differentiation by inhibiting TREM-2 expression, J. Immunol. 183 (4) (2009) 2444–2455.
[277] S.E. Perez, M. Nadeem, B. He, J.C. Miguel, M.H. Malek-Ahmadi, K.W. Chen, E. J. Mufson, Neocortical and hippocampal TREM2 protein levels during the progression of Alzheimer's disease, Neurobiol. Aging 54 (2017) 133–143.
[278] L.F. Lue, C.T. Schmitz, G. Serrano, L.I. Sue, T.G. Beach, D.G. Walker, TREM2 protein expression changes correlate with Alzheimer's disease neurodegenerative pathologies in post-mortem temporal cortices, Brain Pathol. 25 (4) (2015) 469–480.
[279] Y.P. Chen, X.P. Chen, X.Y. Guo, W. Song, B. Cao, Q.Q. Wei, R.W. Ou, B. Zhao, H. F. Shang, Assessment of TREM2 rs75932628 association with Parkinson's disease and multiple system atrophy in a Chinese population, Neurol. Sci. 36 (10) (2015) 1903–1906.
[280] G. Liu, No association of TREM1 rs6910730 and TREM2 rs7759295 with Alzheimer disease, Ann. Neurol. 78 (4) (2015) 659.
[281] P.J. Amos, S. Fung, A. Case, J. Kifelew, L. Osnis, C.L. Smith, K. Green, A. Naydenov, M. Aloi, J.J. Hubbard, A. Ramakrishnan, G.A. Garden, S. Jayadev, Modulation of hematopoietic lineage specification impacts TREM2 expression in microglia-like cells derived from human stem cells, ASN Neuro 9 (4) (2017).
[282] P. Yuan, C. Condello, C.D. Keene, Y.M. Wang, T.D. Bird, S.M. Paul, W.J. Luo, M. Colonna, D. Baddeley, J. Grutzendler, TREM2 haplodeficiency in mice and humans impairs the microglia barrier function leading to decreased amyloid compaction and severe axonal dystrophy (vol 90, pg 724, 2016), Neuron 92 (1) (2016) 252–264.
[283] L. Zhong, X.F. Chen, The emerging roles and therapeutic potential of soluble TREM2 in Alzheimer's disease, Front. Aging Neurosci. 11 (2019).
[284] T.R. Hammond, S.E. Marsh, B. Stevens, Immune signaling in neurodegeneration, Immunity 50 (4) (2019) 955–974.
[285] D.E. Byers, K.Y. Wu, G. Dang-Vu, X.H. Jin, E. Agapov, X.F. Zhang, J.T. Battaile, K. Schechtman, R. Yusen, R.A. Pierce, M.J. Holtzman, Triggering receptor expressed on myeloid cells-2 expression tracks with M2-like macrophage activity and disease severity in COPD, Chest 153 (1) (2018) 77–86.
[286] H. Seno, H. Miyoshi, S.L. Brown, M.J. Geske, M. Colonna, T.S. Stappenbeck, Efficient colonic mucosal wound repair requires Trem2 signaling, P Natl Acad Sci USA 106 (1) (2009) 256–261.
[287] X.L. Xiong, H. Kuang, S. Ansari, T.Y. Liu, J.K. Gong, S. Wang, X.Y. Zhao, Y.W. Ji, C. Li, L. Guo, L.K. Zhou, Z.M. Chen, P. Leon-Mimila, M.T. Chung, K. Kurabayashi, J. Opp, F. Campos-P´erez, H. Villamil-Ramírez, S. Canizales-Quinteros, R. Lyons, C.N. Lumeng, B.Y. Zhou, L. Qi, A. Huertas-Vazquez, A.J. Lusis, X.Z.S. Xu, S.M. Li, Y.H. Yu, J.Z. Li, J.D. Lin, Landscape of intercellular crosstalk in healthy and nash liver revealed by single-cell secretome gene analysis, Mol. Cell 75 (3) (2019) 644-+.
[288] J.S. Seidman, T.D. Troutman, M. Sakai, A. Gola, N.J. Spann, H. Bennett, C. M. Bruni, Z.Y. Ouyang, R.Z. Li, X.L. Sun, B.T. Vu, M.P. Pasillas, K.M. Ego, D. Gosselin, V.M. Link, L.W. Chong, R.M. Evans, B.M. Thompson, J.G. McDonald, M. Hosseini, J.L. Witztum, R.N. Germain, C.K. Glass, Niche-specific reprogramming of epigenetic landscapes drives myeloid cell diversity in nonalcoholic steatohepatitis, Immunity 52 (6) (2020) 1057-+.
[289] M.J. Perugorria, A. Esparza-Baquer, F. Oakley, I. Labiano, A. Korosec, A. Jais, J. Mann, D. Tiniakos, A. Santos-Laso, A. Arbelaiz, R. Gawish, A. Sampedro, A. Fontanellas, E. Hijona, R. Jimenez-Agüero, H. Esterbauer, D. Stoiber, L. Bujanda, J.M. Banales, S. Knapp, O. Sharif, D.A. Mann, Non-parenchymal TREM-2 protects the liver from immune-mediated hepatocellular damage, Gut 68 (3) (2019) 533–546.
[290] S. Alivernini, L. MacDonald, A. Elmesmari, S. Finlay, B. Tolusso, M.R. Gigante, L. Petricca, C. Di Mario, L. Bui, S. Perniola, M. Attar, M. Gessi, A.L. Fedele, S. Chilaka, D. Somma, S.N. Sansom, A. Filer, C. McSharry, N.L. Millar, K. Kirschner, A. Nerviani, M.J. Lewis, C. Pitzalis, A.R. Clark, G. Ferraccioli, I. Udalova, C.D. Buckley, E. Gremese, I.B. McInnes, T.D. Otto, M. Kurowska-Stolarska, Distinct synovial tissue macrophage subsets regulate inflammation and remission in rheumatoid arthritis, Nat. Med. 26 (8) (2020) 1295-+.
[291] S.H. Huang, G.W. Liu, J.H. Li, J.H. Xu, D.W. Xu, W.Q. Zhang, J.R. Huang, Expression of TREM-2 and its inhibitory effects on TNF-alpha induced inflammation in fibroblast-like synoviocytes via inhibiting p38 pathway activation, Clin. Exp. Rheumatol. 36 (2) (2018) 185–194.
[292] C. Correale, M. Genua, S. Vetrano, E. Mazzini, C. Martinoli, A. Spinelli, V. Arena, L. Peyrin-Biroulet, F. Caprioli, N. Passini, P. Panina-Bordignon, A. Repici, A. Malesci, S. Rutella, M. Rescigno, S. Danese, Bacterial sensor triggering receptor expressed on myeloid cells-2 regulates the mucosal inflammatory response, Gastroenterology 144 (2) (2013) 346–356 (e3).
[293] G. Rosciszewski, V. Cadena, V. Murta, J. Lukin, A. Villarreal, T. Roger, A. J. Ramos, Toll-like receptor 4 (TLR4) and triggering receptor expressed on myeloid cells-2 (TREM-2) activation balance astrocyte polarization into a proinflammatory phenotype, Mol. Neurobiol. 55 (5) (2018) 3875–3888.
[294] C.X. Li, B. Zhao, C.Z. Lin, Z.P. Gong, X.X. An, TREM2 inhibits inflammatory responses in mouse microglia by suppressing the PI3K/NF-κB signaling, Cell Biol. Int. 43 (4) (2019) 360–372.
[295] A. Esparza-Baquer, I. Labiano, O. Sharif, A. Agirre-Lizaso, F. Oakley, P. M. Rodrigues, E. Zhuravleva, C.J. O'Rourke, E. Hijona, R. Jimenez-Agüero, I. Rian˜o, A. Landa, A. La Casta, M.Y.W. Zaki, P. Munoz-Garrido, M. Azkargorta, F. Elortza, A. Vogel, G. Schabbauer, P. Aspichueta, J.B. Andersen, S. Knapp, D. A. Mann, L. Bujanda, J.M. Banales, M.J. Perugorria, TREM-2 defends the liver against hepatocellular carcinoma through multifactorial protective mechanisms, Gut 70 (7) (2021) 1345–1361.
[296] T. Nakao, Y. Ono, H.L. Dai, R. Nakano, A. Perez-Gutierrez, G. Camirand, H. Huang, D.A. Geller, A.W. Thomson, DNAX activating protein of 12 kDa/ triggering receptor expressed on myeloid cells 2 expression by mouse and human liver dendritic cells: functional implications and regulation of liver ischemia-reperfusion injury, Hepatology 70 (2) (2019) 696–710.
[297] Q. Zhai, F. Li, X.Y. Chen, J. Jia, S.S. Sun, D.D. Zhou, L. Ma, T. Jiang, F.H. Bai, L. Z. Xiong, Q. Wang, Triggering receptor expressed on myeloid cells 2, a novel regulator of immunocyte phenotypes, Confers Neuroprotection by Relieving Neuroinflammation, Anesthesiology 127 (1) (2017) 98–110.
[298] T. Jiang, L. Tan, X.C. Zhu, J.S. Zhou, L. Cao, M.S. Tan, H.F. Wang, Q. Chen, Y. D. Zhang, J.T. Yu, Silencing of TREM2 exacerbates tau pathology, neurodegenerative changes, and spatial learning deficits in P301S tau transgenic mice, Neurobiol. Aging 36 (12) (2015) 3176–3186.
[299] C. Liu, P. Li, H. Li, S. Wang, L. Ding, H. Wang, H. Ye, Y. Jin, J. Hou, X. Fang, Q. Shu, TREM2 regulates obesity-induced insulin resistance via adipose tissue remodeling in mice of high-fat feeding, J. Transl. Med. 17 (1) (2019) 300.
[300] C. Cantoni, B. Bollman, D. Licastro, M.Q. Xie, R. Mikesell, R. Schmidt, C. M. Yuede, D. Galimberti, G. Olivecrona, R.S. Klein, A.H. Cross, K. Otero, L. Piccio, TREM2 regulates microglial cell activation in response to demyelination in vivo, Acta Neuropathol. 129 (3) (2015) 429–447.
[301] T.A.F. Weehuizen, T.J. Hommes, J.M. Lankelma, H.K. de Jong, J.J.T.H. Roelofs, A.F. de Vos, M. Colonna, T. van der Poll, W.J. Wiersinga, Triggering receptor expressed on myeloid cells (TREM)-2 impairs host defense in experimental melioidosis, Plos Neglect Trop D 10 (6) (2016).
[302] S. Daemen, A. Gainullina, G. Kalugotla, L. He, M.M. Chan, J.W. Beals, K.H. Liss, S. Klein, A.E. Feldstein, B.N. Finck, M.N. Artyomov, J.D. Schilling, Dynamic shifts in the composition of resident and recruited macrophages influence tissue remodeling in NASH, Cell Rep. 34 (2) (2021) 108626.
[303] P.D. Wes, F.A. Sayed, F. Bard, L. Gan, Targeting microglia for the treatment of Alzheimer's disease, Glia 64 (10) (2016) 1710–1732.

[304] S.C. Hall, D.K. Agrawal, Increased TREM-2 expression on the subsets of CD11c(+) cells in the lungs and lymph nodes during allergic airway inflammation, Sci. Rep. 7 (1) (2017) 11853.
[305] M. Bluher, Obesity: global epidemiology and pathogenesis, Nat. Rev. Endocrinol. 15 (5) (2019) 288–298.
[306] M. Werner, E. Hobeika, H. Jumaa, Role of PI3K in the generation and survival of B cells, Immunol. Rev. 237 (2010) 55–71.
[307] C. Cochain, E. Vafadarnejad, P. Arampatzi, J. Pelisek, H. Winkels, K. Ley, D. Wolf, A.E. Saliba, A. Zernecke, Single-cell RNA-seq reveals the transcriptional landscape and heterogeneity of aortic macrophages in murine atherosclerosis, Circ. Res. 122 (12) (2018) 1661–1674.
[308] J. Zhang, Y. Liu, Y. Zheng, Y. Luo, Y. Du, Y. Zhao, J. Guan, X. Zhang, J. Fu, TREM-2-p38 MAPK signaling regulates neuroinflammation during chronic cerebral hypoperfusion combined with diabetes mellitus, J. Neuroinflammation 17 (1) (2020) 2.
[309] J.C. Hou, J. Zhang, P. Cui, Y.Y. Zhou, C. Liu, X.L. Wu, Y. Ji, S.C. Wang, B.L. Cheng, H. Ye, L.Q. Shu, K. Zhang, D. Wang, J.L. Xu, Q. Shu, M. Colonna, X.M. Fang, TREM2 sustains macrophage-hepatocyte metabolic coordination in nonalcoholic fatty liver disease and sepsis, J. Clin. Invest. 131 (4) (2021).
[310] X.C. Wang, Q.F. He, C.L. Zhou, Y.Y. Xu, D.H. Liu, N. Fujiwara, N. Kubota, A. Click, P. Henderson, J. Vancil, C.A. Marquez, G. Gunasekaran, M.E. Schwartz, P. Tabrizian, U. Sarpel, M.I. Fiel, Y.R. Diao, B.C. Sun, Y. Hoshida, S. Liang, Z. Y. Zhong, Prolonged hypernutrition impairs TREM2-dependent efferocytosis to license chronic liver inflammation and NASH development, Immunity 56 (1) (2023) 58-+.
[311] K. Takahashi, M. Prinz, M. Stagi, O. Chechneva, H. Neumann, TREM2-transduced myeloid precursors mediate nervous tissue debris clearance and facilitate recovery in an animal model of multiple sclerosis, PLoS Med. 4 (4) (2007) 675–689.
[312] H. Gao, J.W. Di, B.H. Clausen, N.X. Wang, X.Z. Zhu, T.L. Zhao, Y.Y. Chang, M. Pang, Y. Yang, R.H. He, Y.G. Wang, L.M. Zhang, B. Liu, W. Qiu, K. L. Lambertsen, R. Brambilla, L.M. Rong, Distinct myeloid population phenotypes dependent on TREM2 expression levels shape the pathology of traumatic versus demyelinating CNS disorders (vol 42, 112629, 2023), Cell Rep. 42 (7) (2023).
[313] Q.X. Chen, K. Zhang, Y. Jin, T. Zhu, B.L. Cheng, Q. Shu, X.M. Fang, Triggering receptor expressed on myeloid cells-2 protects against polymicrobial sepsis by enhancing bacterial clearance, Am J Resp Crit Care 188 (2) (2013) 201–212.
[314] A. Saviano, N.C. Henderson, T.F. Baumert, Single-cell genomics and spatial transcriptomics: Discovery of novel cell states and cellular interactions in liver physiology and disease biology, J. Hepatol. 73 (5) (2020) 1219–1230.
[315] G.P. Dunn, A.T. Bruce, H. Ikeda, L.J. Old, R.D. Schreiber, Cancer immunoediting: from immunosurveillance to tumor escape, Nat. Immunol. 3 (11) (2002) 991–998.
[316] K. Nakamura, M.J. Smyth, TREM2 marks tumor-associated macrophages, Signal Transduct Tar 5 (1) (2020).
[317] S.M. Kim, E.M. Kim, K.Y. Ji, H.Y. Lee, S.M. Yee, S.M. Woo, J.W. Yi, C.H. Yun, H. Choi, H.S. Kang, TREM2 Acts as a tumor suppressor in colorectal carcinoma through Wnt1/beta-catenin and Erk Signaling, Cancers 11 (9) (2019).
[318] H.Y. Zhang, Z.L. Liu, H.Y. Wen, Y.F. Guo, F.K. Xu, Q.L. Zhu, W. Yuan, R.K. Luo, C. L. Lu, R.H. Liu, J. Gu, D. Ge, Immunosuppressive TREM2(+) macrophages are associated with undesirable prognosis and responses to anti-PD-1 immunotherapy in non-small cell lung cancer, Cancer Immunol Immun 71 (10) (2022) 2511–2522.
[319] S.M. Kim, E.M. Kim, K.Y. Ji, H.Y. Lee, S.M. Yee, S.M. Woo, J.W. Yi, C.H. Yun, H. Choi, H.S. Kang, TREM2 acts as a tumor suppressor in colorectal carcinoma through Wnt1/β-catenin and Erk Signaling, Cancers 11 (9) (2019).
[320] B.N. Ostendorf, J. Bilanovic, N. Adaku, K.N. Tafreshian, B. Tavora, R.D. Vaughan, S.F. Tavazoie, Common germline variants of the human gene modulate melanoma progression and survival, Nat. Med. 26 (7) (2020) 1048-+.
[321] K. Mehla, P.K. Singh, Metabolic regulation of macrophage polarization in cancer, Trends Cancer 5 (12) (2019) 822–834.
[322] H. Wu, Y.J. Han, Y.R. Sillke, H.Z. Deng, S. Siddiqu, C. Treese, F. Schmidt, M. Friedrich, J. Keye, J.J. Wan, Y. Qin, A.A. Kuehl, Z.H. Qin, B. Siegmund, R. Glauben, Lipid droplet-dependent fatty acid metabolism controls the immune suppressive phenotype of tumor-associated macrophages, EMBO Mol. Med. 11 (11) (2019).
[323] M.C. Yu, Y.H. Chang, Y. Zhai, B. Pang, P. Wang, G.Z. Li, T. Jiang, F. Zeng, TREM2 is associated with tumor immunity and implies poor prognosis in glioma, Front. Immunol. 13 (2023).
[324] L.S. Zhou, M.L. Wang, H.R. Guo, J. Hou, Y.N. Zhang, M. Li, X.W. Wu, X.L. Chen, L. H. Wang, Integrated analysis highlights the immunosuppressive role of TREM2 macrophages in hepatocellular carcinoma, Front. Immunol. 13 (2022).
[325] H.T. Gao, Z. Yang, H. Sun, Y. Zhang, Z. Wang, W.Y. Liu, H.Z. Wen, C.B. Qu, X. L. Wang, TREM2 as an independent predictor of poor prognosis promotes the migration via the PI3K/AKT axis in prostate cancer, Am. J. Transl. Res. 15 (2) (2023) 779-+.
[326] X. Zhu, Z. Zeng, M. Chen, X. Chen, D. Hu, W. Jiang, M. Du, T. Chen, T. Chen, W. Liao, C. Zhang, Y. Qu, W. Pan, TREM2 as a potential immune-related biomarker of prognosis in patients with skin cutaneous melanoma microenvironment, Dis. Markers 2023 (2023) 8101837.
[327] R.D. Schreiber, L.J. Old, M.J. Smyth, Cancer immunoediting: integrating immunity's roles in cancer suppression and promotion, Science 331 (6024) (2011) 1565–1570.
[328] G.A. Rabinovich, D. Gabrilovich, E.M. Sotomayor, Immunosuppressive strategies that are mediated by tumor cells, Annu. Rev. Immunol. 25 (2007) 267–296.
[329] V. Velcheti, K. Schalper, Basic overview of current immunotherapy approaches in cancer, Am. Soc. Clin. Oncol. Educ. Book 35 (2016) 298–308.
[330] X.N. Xiang, J.G. Wang, D. Lu, X. Xu, Targeting tumor-associated macrophages to synergize tumor immunotherapy, Signal Transduct Tar 6 (1) (2021).
[331] D.Y. Wu, X.W. Liu, J.T. Mu, J. Yang, F.L. Wu, H.M. Zhou, Therapeutic approaches targeting proteins in tumor-associated macrophages and their applications in cancers, Biomolecules 12 (3) (2022).
[332] L. Cassetta, J.W. Pollard, Targeting macrophages: therapeutic approaches in cancer, Nat. Rev. Drug Discov. 17 (12) (2018) 887–904.
[333] B. Farhood, M. Najafi, K. Mortezaee, CD8+ cytotoxic T lymphocytes in cancer immunotherapy: a review, J. Cell. Physiol. 234 (6) (2019) 8509–8521.
[334] A.M. Georgoudaki, K.E. Prokopec, V.F. Boura, E. Hellqvist, S. Sohn, J. Ostling, R. Dahan, R.A. Harris, M. Rantalainen, D. Klevebring, M. Sund, S.E. Brage, J. Fuxe, C. Rolny, F. Li, J.V. Ravetch, M.C. Karlsson, Reprogramming tumor-associated macrophages by antibody targeting inhibits cancer progression and metastasis, Cell Rep. 15 (9) (2016) 2000–2011.
[335] A. Mantovani, F. Marchesi, A. Malesci, L. Laghi, P. Allavena, Tumour-associated macrophages as treatment targets in oncology, Nat. Rev. Clin. Oncol. 14 (7) (2017) 399–416.
[336] H. Gonzalez, W.B. Mei, I. Robles, C. Hagerling, B.M. Allen, T.L.H. Okholm, A. Nanjaraj, T. Verbeek, S. Kalavacherla, M. van Gogh, S. Georgiou, M. Daras, J. J. Phillips, M.H. Spitzer, J.P. Roose, Z. Werb, Cellular architecture of human brain metastases, Cell 185 (4) (2022) 729-+.
[337] M. Binnewies, J.L. Pollack, J. Rudolph, S. Dash, M. Abushawish, T. Lee, N. S. Jahchan, P. Canaday, E. Lu, M. Norng, S. Mankikar, V.M. Liu, X.Y. Du, A. Chen, R. Mehta, R. Palmer, V. Juric, L.D. Liang, K.P. Baker, L. Reyno, M.F. Krummel, M. Streuli, V. Sriram, Targeting TREM2 on tumor-associated macrophages enhances immunotherapy, Cell Rep. 37 (3) (2021).
[338] L. Zhang, Z.Y. Li, K.M. Skrzypczynska, Q. Fang, W. Zhang, S.A. O'Brien, Y. He, L. Wang, Q.M. Zhang, A. Kim, R.R. Gao, J. Orf, T. Wang, D. Sawant, J.J.L. Kang, D. Bhatt, D. Lu, C.M. Li, A.S. Rapaport, K. Perez, Y.J. Ye, S. Wang, X.D. Hu, X. W. Ren, W.J. Ouyang, Z.L. Shen, J.G. Egen, Z.M. Zhang, X. Yu, Single-cell analyses inform mechanisms of myeloid-targeted therapies in colon cancer, Cell 181 (2) (2020) 442-+.
[339] Y.D. Liu, Q.M. Zhang, B.C. Xing, N. Luo, R.R. Gao, K.Z. Yu, X.D. Hu, Z.D. Bu, J. R. Peng, X.W. Ren, Z.M. Zhang, Immune phenotypic linkage between colorectal cancer and liver metastasis, Cancer Cell 40 (4) (2022) 424-+.
[340] A. Obradovic, N. Chowdhury, S.M. Haake, C. Ager, V. Wang, L. Vlahos, X.Z. V. Guo, D.H. Aggen, W.K. Rathmell, E. Jonasch, J.E. Johnson, M. Roth, K. E. Beckermann, B.I. Rini, J. McKiernan, A. Califano, C.G. Drake, Single-cell protein activity analysis identifies recurrence-associated renal tumor macrophages, Cell 184 (11) (2021) 2988-+.
[341] A. Sharma, J.J.W. Seow, C.A. Dutertre, R. Pai, C. Bl´eriot, A. Mishra, R.M. M. Wong, G.S.N. Singh, S. Sudhagar, S. Khalilnezhad, S. Erdal, H.M. Teo, A. Khalilnezhad, S. Chakarov, T.K.H. Lim, A.C.Y. Fui, A.K.W. Chieh, C.P. Chung, G.K. Bonney, B.K.P. Goh, J.K.Y. Chan, P.K.H. Chow, F. Ginhoux, R. DasGupta, Onco-fetal Reprogramming of endothelial cells drives immunosuppressive macrophages in hepatocellular carcinoma, Cell 183 (2) (2020) 377-+.
[342] Q. Wang, K. Zheng, D. Tan, G. Liang, TREM2 knockdown improves the therapeutic effect of PD-1 blockade in hepatocellular carcinoma, Biochem. Biophys. Res. Commun. 636 (Pt 1) (2022) 140–146.
[343] L.S. Zhou, M.L. Wang, H.R. Guo, J. Hou, Y.N. Zhang, M. Li, X.W. Wu, X.L. Chen, L. H. Wang, Integrated analysis highlights the immunosuppressive role of TREM2(+) macrophages in hepatocellular carcinoma, Front. Immunol. 13 (2022).
[344] S.P. Duggan, C. Garry, F.M. Behan, S. Phipps, H. Kudo, M. Kirca, A. Zaheer, S. McGarrigle, J.V. Reynolds, R. Goldin, S.E. Kalloger, D.F. Schaeffer, A. Long, J. Strid, D. Kelleher, siRNA library screening identifies a druggable immune-signature driving esophageal adenocarcinoma cell growth, Cell. Mol. Gastroenterol. Hepatol. 5 (4) (2018) 569–590.
[345] I. Noorani, K. Sidlauskas, S. Pellow, R. Savage, J.L. Norman, D.S. Chatelet, M. Fabian, P. Grundy, J. Ching, J.A.R. Nicoll, D. Boche, Clinical impact of anti-inflammatory microglia and macrophage phenotypes at glioblastoma margins, Brain Commun 5 (3) (2023).
[346] E. Azizi, A.J. Carr, G. Plitas, A.E. Cornish, C. Konopacki, S. Prabhakaran, J. Nainys, K.M. Wu, V. Kiseliovas, M. Setty, K. Choi, R.M. Fromme, P. Dao, P. T. McKenney, R.C. Wasti, K. Kadaveru, L. Mazutis, A.Y. Rudensky, D. Pe'er, Single-cell map of diverse immune phenotypes in the breast tumor microenvironment, Cell 174 (5) (2018) 1293-+.
[347] R.N. Ramos, Y. Missolo-Koussou, Y. Gerber-Ferder, C.P. Bromley, M. Bugatti, N. G. Nún˜ez, J.T. Boari, W. Richer, L. Menger, J. Denizeau, C. Sedlik, P. Caudana, F. Kotsias, L.L. Niborski, S. Viel, M. Bohec, S. Lameiras, S. Baulande, L. Lesage, A. Nicolas, D. Meseure, A. Vincent-Salomon, F. Reyal, C.A. Dutertre, F. Ginhoux, L. Vimeux, E. Donnadieu, B. Buttard, J. Galon, S. Zelenay, W. Vermi, P. Guermonprez, E. Piaggio, J. Helft, Tissue-resident FOLR2(+) macrophages associate with CD8(+) T cell infiltration in human breast cancer, Cell 185 (7) (2022) 1189-+.
[348] S.Z. Wu, G. Al-Eryani, D.L. Roden, S. Junankar, K. Harvey, A. Andersson, A. Thennavan, C.F. Wang, J.R. Torpy, N. Bartonicek, T.P. Wang, L. Larsson, D. Kaczorowski, N.I. Weisenfeld, C.R. Uytingco, J.G. Chew, Z.W. Bent, C.L. Chan, V. Gnanasambandapillai, C.A. Dutertre, L. Gluch, M.N. Hui, J. Beith, A. Parker, E. Robbins, D. Segara, C. Cooper, C. Mak, B. Chan, S. Warrier, F. Ginhoux, E. Millar, J.E. Powell, S.R. Williams, X.S. Liu, S. O'Toole, E. Lim, J. Lundeberg, C. M. Perou, A. Swarbrick, A single-cell and spatially resolved atlas of human breast cancers, Nat. Genet. 53 (9) (2021) 1334-+.
[349] E. Timperi, P. Gueguen, M. Molgora, I. Magagna, Y. Kieffer, S. Lopez-Lastra, P. Sirven, L.G. Baudrin, S. Baulande, A. Nicolas, G. Champenois, D. Meseure,

A. Vincent-Salomon, A. Tardivon, E. Laas, V. Soumelis, M. Colonna, F. Mechta-Grigoriou, S. Amigorena, E. Romano, Lipid-associated macrophages are induced by cancer-associated fibroblasts and mediate immune suppression in breast cancer, Cancer Res. 82 (18) (2022) 3291–3306.

[350] Y.Y. Zhang, H.Y. Chen, H.N. Mo, X.D. Hu, R.R. Gao, Y.H. Zhao, B.L. Liu, L.J. Niu, X.Y. Sun, X. Yu, Y. Wang, Q. Chang, T.Y. Gong, X.W. Guan, T. Hu, T.Y. Qian, B. H. Xu, F. Ma, Z.M. Zhang, Z.H. Liu, Single-cell analyses reveal key immune cell subsets associated with response to PD-L1 blockade in triple-negative breast cancer, Cancer Cell 39 (12) (2021) 1578-+.

[351] S.B. Kemp, N.G. Steele, E.S. Carpenter, K.L. Donahue, G.G. Bushnell, A.H. Morris, S. The, S.M. Orbach, V.R. Sirihorachai, Z.C. Nwosu, C. Espinoza, F. Lima, K. Brown, A.A. Girgis, V. Gunchick, Y.Q. Zhang, C.A. Lyssiotis, T.L. Frankel, F. Bednar, A. Rao, V. Sahai, L.D. Shea, H.C. Crawford, M.P. di Magliano, Pancreatic cancer is marked by complement-high blood monocytes and tumor-associated macrophages, Life Sci Alliance 4 (6) (2021).

[352] Y.A. Yao, H.Q. Li, Y.H. Wang, J.Y. Zhou, Triggering receptor expressed on myeloid cells-2 (TREM-2) elicited by lung cancer cells to facilitate tumor immune evasion, J. Clin. Oncol. 31 (15) (2013).

[353] A.M. Leader, J.A. Grout, B.B. Maier, B.Y. Nabet, M.D. Park, A. Tabachnikova, C. Chang, L. Walker, A. Lansky, J. Le Berichel, L. Troncoso, N. Malissen, M. Davila, J.C. Martin, G. Magri, K. Tuballes, Z. Zhao, F. Petralia, R. Samstein, N. R. D'Amore, G. Thurston, A.O. Kamphorst, A. Wolf, R. Flores, P. Wang, S. Müller, I. Mellman, M.B. Beasley, H. Salmon, A.H. Rahman, T.U. Marron, E. Kenigsberg, M. Merad, Single-cell analysis of human non-small cell lung cancer lesions refines tumor classification and patient stratification, Cancer Cell 39 (12) (2021) 1594-+.

[354] A.K. Struckmeier, A. Radermacher, M. Fehrenz, D. Alansary, P. Wartenberg, M. Wagner, A. Scheller, J. Hess, J. Moratin, C. Freudlsperger, J. Hoffmann, L. Thurner, K. Roemer, K. Freier, D. Horn, TREM2 is associated with advanced stages and inferior prognosis in oral squamous cell carcinoma, Cancers 14 (19) (2022).

[355] J. Chen, T.C. Zhu, G.M. Jiang, Q. Zeng, Z.J. Li, X. Huang, Target delivery of a PD-1-TREM2 scFv by CAR-T cells enhances anti-tumor efficacy in colorectal cancer, Mol. Cancer 22 (1) (2023).

[356] J.W. Ford, M. Gonzalez-Cotto, A.W. MacFarlane, S. Peri, O.M.Z. Howard, J. J. Subleski, K.J. Ruth, M. Haseebuddin, T. Al-Saleem, Y.F. Yang, P. Rayman, B. Rini, W.M. Linehan, J. Finke, J.M. Weiss, K.S. Campbell, D.W. McVicar, Tumor-infiltrating myeloid cells co-express TREM1 and TREM2 and elevated TREM-1 associates with disease progression in renal cell carcinoma, Front. Oncol. 11 (2022).

[357] A.M. Raghubar, N.A. Matigian, J. Crawford, L. Francis, R. Ellis, H.G. Healy, A. J. Kassianos, M.S.Y. Ng, M.J. Roberts, S. Wood, A.J. Mallett, High risk clear cell renal cell carcinoma microenvironments contain protumour immunophenotypes lacking specific immune checkpoints, Npj Precis. Oncol. 7 (1) (2023).

[358] E. Elinav, R. Nowarski, C.A. Thaiss, B. Hu, C. Jin, R.A. Flavell, Inflammation-induced cancer: crosstalk between tumours, immune cells and microorganisms, Nat. Rev. Cancer 13 (11) (2013) 759–771.

[359] K.E. Beckermann, A. Patnaik, I. Winer, W.S. Tan, B. Bashir, C.E. Kyriakopoulos, R. F. Sweis, M. Chamberlain, B.I. Rini, A phase 1b open-label study to evaluate the safety, tolerability, pharmacokinetics, and pharmacodynamics of py314 in combination with pembrolizumab in patients with advanced renal cell carcinoma, Invest New Drug (2024).

[360] T. Yang, S. Zhang, H. Yuan, Y. Wang, L. Cai, H. Chen, X. Wang, D. Song, X. Wang, Z. Guo, X. Wang, Platinum-based TREM2 inhibitor suppresses tumors by remodeling the immunosuppressive microenvironment, Angew. Chem. Int. Ed. Engl. 62 (2) (2023) e202213337.

[361] M.L. Costa, M.L. Robinette, M. Bugatti, M.S. Longtine, B.N. Colvin, E. Lantelme, W. Vermi, M. Colonna, D.M. Nelson, M. Cella, Two distinct myeloid subsets at the term human fetal-maternal-interface, Front. Immunol. 8 (2017).

[362] E. Morenas-Rodríguez, Y. Li, B. Nuscher, Soluble TREM2 in CSF and its association with other biomarkers and cognition in autosomal-dominant Alzheimer's disease: a longitudinal observational study (vol 21, pg 329, 2022), Lancet Neurol. 21 (5) (2022) E5–E.

[363] M. Su´arez-Calvet, G. Kleinberger, M.A.A. Caballero, M. Brendel, A. Rominger, D. Alcolea, J. Fortea, A. Lleo´, R. Blesa, J.D. Gispert, R. S´anchez-Valle, A. Antonell, L. Rami, J.L. Molinuevo, F. Brosseron, A. Traschütz, M.T. Heneka, H. Struyfs, S. Engelborghs, K. Sleegers, C. Van Broeckhoven, H. Zetterberg, B. Nellgård, K. Blennow, A. Crispin, M. Ewers, C. Haass, sTREM2 cerebrospinal fluid levels are a potential biomarker for microglia activity in early-stage Alzheimer's disease and associate with neuronal injury markers, EMBO Mol. Med. 8 (5) (2016) 466–476.

[364] M.X. Sun, M. Zhu, K. Chen, X.X. Nie, Q.C. Deng, L.D. Hazlett, Y.J. Wu, M.Y. Li, M. H. Wu, X. Huang, TREM-2 promotes host resistance against pseudomonas aeruginosa infection by suppressing corneal inflammation via a PI3K/Akt signaling pathway, Invest Ophth vis Sci 54 (5) (2013) 3451–3462.

[365] M.L. Broz, M.F. Krummel, The emerging understanding of myeloid cells as partners and targets in tumor rejection, Cancer Immunol. Res. 3 (4) (2015) 313–319.

[366] E.M. Wolf, B. Fingleton, A.H. Hasty, The therapeutic potential of TREM2 in cancer, Front. Oncol. 12 (2022).

4. Discussion

4.1. Small protein blockers of human IL-6 receptor alpha inhibit proliferation and migration of cancer cells

In this research project, we developed IL-6Rα-targeted NEF binders from the highly complex ABD scaffold combinatorial library with theoretical complexity of 10^{14}. Ribosome display selection and screening of individual variants resulted in a collection of IL-6Rα binding candidates, whose binding properties we characterized. Binding and specificity of the best hits were confirmed using dose-response binding ELISA with IL-6Rα and irrelevant protein (BSA). Initially, NEF variants were selected based on their ability to recognize recombinant eukaryotically produced IL-6Rα in ELISA. We also confirmed that NEF variants can recognize IL-6Rα on a cell surface of HEK293T transfected with *IL-6Rα* gene, as well as PaTu cells endogenously expressing IL-6Rα and differentiated plasma cells/plasmablasts from human PBMCs. Affinities of the three main NEF variants to the IL-6Rα on a cell surface of transfected HEK293T are in low nano-molar range as measured using LigandTracer method. NEF108, NEF163, and NEF172, have affinities of 5.3 nM, 3.5 nM, and 10.9 nM, respectively. The NEF variants exhibited slightly lower thermal stability than ABDwt with melting temperatures ranging from 54.0°C to 60.5°C compared to 66.5°C of the ABDwt. Yet they maintain sufficient stability for therapeutic applications. Additionally, NEFs secondary structure content is comparable to ABDwt, predominantly preserving α-helical structures.

We proved that NEF proteins exhibit antagonistic activity through a series of experiments investigating IL-6 binding and signaling inhibition at various stages. Initially, we showed that NEF binders effectively prevent IL-6 from binding to its receptor, IL-6Rα, by blocking the binding interface. Subsequently, we illustrated that this blockage prevents the phosphorylation of STAT3 at Y705 in U87MG glioblastoma cells, thereby inhibiting the IL-6 downstream signaling cascade. Effect of NEF on STAT3 phosphorylation was also confirmed in PaTu cells. Additionally, we revealed that gene translation regulated by the pSTAT3 promoter is inhibited, as demonstrated by the reduced reporter gene expression in HEK-Blue IL-6 cell line. Furthermore, we established that this inhibition translates into significant changes in cell physiology. NEF variants (NEF108, NEF163, and NEF172) suppressed cell proliferation in malignant melanoma (G361 and A2058), pancreatic cancer (PaTu) and glioblastoma (GAMG) cell lines and migration in malignant melanoma (A2058), pancreatic cancer (PaTu) and glioblastoma (GAMG). Moreover, $CD19^+$ B cells from human PBMCs differentiation into $CD19^+CD38^+$ plasmablasts/plasma cells in the presence of IL-6 were significantly reduced by NEF variants. The impact on cellular functions was further corroborated by our *in vivo* experiments, where NEF108 reduced IL-1β level, lymphocyte infiltration, and mitigated alterations in epithelial architecture due to inflammation in a DSS-induced

colitis murine model. These findings collectively underscore the potential of NEF binders as powerful inhibitors of IL-6 signaling, offering promising therapeutic implications.

Given that IL-6 can promote cancer growth [317], we decided to test the effect of NEF variants on cancer cell proliferation. We observed real-time proliferation of melanoma cell lines (G361 and A2058) and pancreatic cell lines (PaTu and MiaPaCa) in the presence of IL-6 and NEF variants using iCELLigence method. All three NEF variants have pronounced effect on melanoma cell lines proliferation. Notably, in case of G361, NEF163 almost completely suppressed cell growth. Effect NEF variants on pancreatic cell proliferation was negligible, except for NEF108 in PaTu cells. Suppression of A2058 and PaTu proliferation by NEF variants was independently confirmed using Incucyte as an alternative method. At the same time growth of fibroblasts that do not express IL-6Rα was not affected by the presence of NEF variants. Therefore, NEF variants can slow down cancer cell proliferation and this effect can be specifically attributed to IL-6 signaling inhibition by NEF variants.

In the iCELLigence experiment, cells were cultured on specialized plates equipped with microelectrodes. Cell proliferation impedes electric current, reflecting cell number. In the iCELLigence experiment with the PaTu cell line, the conductivity dramatically dropped in the presence of NEF108. However, as demonstrated by microscopic analysis and the MTT test, this effect was due to the impact of NEF108 on cell migration rather than proliferation. Therefore, we focused on investigating the effects of NEF variants on cell migration using the Incucyte Scratch Wound assay in A2058 and PaTu cells. It was confirmed that all three NEF variants suppressed cell migration, with NEF108 displaying the most pronounced effect on PaTu cells. In a different experiment, NEF163 and NEF172 were able to suppress GAMG cell migration in the scratch assay, while NEF108 had no effect on GAMG cell migration. Consequently, NEF variants have potential to serve as migrastatic agents in cancer therapy.

We used different cancer cell lines to investigate the efficiency of IL-6 signaling, namely melanoma, pancreatic and glioblastoma cells. For both melanoma cell lines used in the research (G361 and A2058), we observed significant growth suppression in response to IL-6Rα blocking by NEF variants. At the same time cell medium supplementation with IL-6 did not affect cell growth significantly indicating endogenous origin of IL-6. This is in line with the observation that at more advanced stages metastatically competent melanoma cells begin to produce endogenous IL-6 that stimulates cell growth in an autocrine fashion [318]. Blocking of both IL-6 and IL-8 was shown to be sufficient to reduce melanoma cell invasiveness in spheroid invasion assay [123]. We observed considerable inhibition of A2058 migration in the presence

of NEF variants in Incutyte Scratch wound healing assay. Human pancreatic adenocarcinoma cells also express IL-6. In case of CAPAN-1 pancreatic adenocarcinoma cells, VEGF production is upregulated by IL-6 signaling which may further facilitate cancer cell metastasis [117]. Alternative study on CAPAN-1 and SW1990 cell lines confirmed that IL-6 signaling promoted cell line growth as well as transcription of mRNA encoding VEGF and MMP-2. Accordingly, IL-6 positively affected cell invasiveness [319]. We observed significant suppression of PaTu cells migration in the presence of NEF variants as confirmed by two independent methods. Another study used broader panel of pancreatic cancer cell lines demonstrated that IL-6 positively regulates survival and proliferation of pancreatic cell lines in autocrine manner. Treatment with anti-IL-6Rα antibody significantly reduced cancer cell survival [320]. In our experiments, NEF variants had less pronounced effect on pancreatic cell lines comparing to melanoma cell lines. Although NEF variants were able to reduce growth rate of PaTu cell line, a moderate effect of NEF binders on MiaPaCa cell line may be explained by low IL-6Rα expression level. In case of glioblastoma, a highly aggressive type of glioma, IL-6 accumulation has been correlated with shorter patient survival [321]. Similarly to pancreatic cancer cell line, VEGF expression up-regulation by IL-6 signaling was demonstrated for glioblastoma cells [322]. Humanized anti-IL-6R mAb TCZ was capable to inhibit glioma cell proliferation in dose-dependent manner [323]. NEF172 and to the lesser extent NEF163 significantly reduced migration of GAMG cell line used in the experiment. Only NEF172 was able to suppress GAMG cell growth at the highest concentration (1.6 μM) used in the experiment. As cell growth was monitored using CKK-8 cell assay for 24h, it is feasible that NEF172 effect on GAMG cell proliferation would be more pronounced at longer monitoring time, as in case with melanoma and pancreatic cell lines.

We compared the effects of NEF variants to the "gold standard" IL-6 signaling inhibitor, TCZ mAb. In experiments with IL-6-induced STAT3 signaling, TCZ inhibited STAT3 phosphorylation more efficiently than NEF binders, as demonstrated by Western blot and HEK-Blue IL-6 reporter cell assay. However, NEF binders significantly inhibited PaTu and A2058 cell migration while TCZ showed no effect. Similarly, while NEF108 significantly affected PaTu cell proliferation, TCZ had no influence. Therefore, NEF variants have more pronounced effect than TCZ in inhibiting IL-6Rα in certain cancer cell types or contexts. There was a significant difference in the efficiencies of investigated NEF variants across different cell lines. NEF108 was the most effective in inhibiting PaTu cell migration and proliferation but showed no effect on pSTAT activation in GAMG cells, as well as GAMG cell migration. Conversely, NEF172 efficiently suppressed GAMG cell migration and was the only variant that influenced GAMG cell growth in the CKK-8 proliferation assay. NEF163 completely suppressed G361

proliferation. Therefore, the effect of IL-6Rα inhibitors can be cancer cell line-specific due to differences in IL-6Rα expression or associated cellular contexts. In some applications, our NEF binders show more prominent effect than TCZ, while their efficiency can also vary depending on the cell line.

We evaluated NEF108 in a DSS-induced colitis mouse model, which is widely used to mimic IBD in humans. The results demonstrated that NEF108 significantly prevented the reduction in colon length typically induced by DSS, indicating a protective effect on the structural integrity of the colon. Additionally, NEF108 provided significant protection against DSS-induced mucosal architecture alterations. Also, level of IL-1β significantly reduced in the presence of NEF108. These findings were statistically significant, highlighting the potent protective effects of NEF108 against the pathological changes associated with DSS-induced colitis. The ability of NEF108 to protect against colonic damage and inflammation in the DSS-induced colitis mouse model suggests that NEF108 potentially could be effective therapeutic agents for reducing intestinal inflammation and preserving mucosal integrity in IBD.

To assess the specificity of NEF binding to IL-6Rα on primary blood cells, PBMCs were stimulated with pokeweed mitogen (PWM) for four days to generate activated plasmablasts/plasma cells ($CD19^+CD38^+$). Flow cytometry analysis showed that NEF proteins (NEF108, NEF163, and NEF172) recognize IL-6Rα with equal or better affinity compared to an anti-IL-6Rα antibody. Furthermore, the NEF variants were able to inhibit IL-6-induced activation and differentiation of B cells within the PBMC population. Under IL-6 stimulation, $CD19^+$ B cells differentiated into plasmablasts/plasma cells expressing the $CD38^+$ marker, reaching 60% of the total $CD19^+$ cells. However, in the presence of NEF binders, the amount of $CD38^+$ plasma cells was significantly reduced to levels comparable with non-stimulated controls. Additionally, within the $CD38^+$ population, $IgA1^+$ B cell differentiation was significantly suppressed by the NEF variants. IL-6 signaling plays a critical role in the differentiation of B cells and the production of immunoglobulins, including IgA. By inhibiting IL-6Rα, NEF binders can modulate the immune response, addressing one of the root causes of IgAN. IgAN patients exhibit significantly higher percentages of $CD38^+$ cells compared to healthy controls [324]. By blocking the maturation of B cells into IgA-producing cells, NEF binders could potentially reduce levels of aberrantly glycosylated IgA1, thereby decreasing the formation of pathogenic immune complexes and reducing glomerular deposition and inflammation. Consequently, we demonstrated an *ex vivo* efficiency of NEF binders in human cells, and preliminary data indicate their potential application in IgAN therapy.

4.2. IL-6 and its role in IgA nephropathy development

IL-6 is a crucial immune system regulator. Many reviews have focused on various aspects of its biology and role in different diseases. However, there was a significant gap concerning IL-6 role in IgAN, which our review addressed. Since its first description by Berger and Hinglais in 1968, many aspects of IgAN have been studied, yet much remains unclear. No specific treatment for IgAN exists. Current therapies aim to reduce proteinuria, control blood pressure, and suppress inflammation using glucocorticoids like prednisone, and immunosuppressive drugs such as azathioprine, mycophenolate mofetil, and cyclophosphamide. Lifestyle modifications, including a low-protein, low-sodium diet, are also recommended. Emerging evidence, summarized in the review, suggests that IL-6 plays a crucial role in IgAN progression. Elevated IL-6 levels in IgAN patients significantly contribute to disease pathogenesis by stimulating mesangial cell proliferation and kidney inflammation. IL-6 also affects glycosyltransferases expression, leading to increased Gd-IgA1 production and CIC formation. Inhibition of IL-6 signaling in IgAN could reduce Gd-IgA1 production and limit mesangial cell proliferation, potentially slowing disease progression and mitigating kidney damage. Understanding IL-6 complex role in IgAN is essential for developing targeted therapies. In our recent study we developed IL-6Rα small protein blockers derived from the ABD protein scaffold. Furthermore, we demonstrated that IL-6Rα blockers suppress IL-6-induced $CD19^+$ $CD38^+$ IgA^+ plasma cell differentiation within PBMCs. This finding lays the foundation for further investigation of novel IL-6 inhibitors in IgAN disease models, potentially advancing IL-6 inhibition therapy for IgAN treatment.

Our review offers a comprehensive summary of IL-6 biology, detailing multiple facets including signaling, target genes, functions, and inhibitors. Unlike most reviews that focus on a single aspect, we have compiled a wide range of information into one thorough resource. This makes our review relevant not only for those interested in IgAN but also for anyone seeking a broader understanding of IL-6 biology.

4.3. Human IL-22 receptor-targeted small protein antagonist suppress murine DSS-induced colitis.

We developed IL-22R1 binders named ABR from the ABD-derived small protein scaffold library using the directed evolution approach. These ABR variants were further tested for their ability to bind cell surface IL-22R1. We identified seven ABR variants that recognize IL-22R1 on the surface of transfected HEK293T cells and endogenously expressed IL-22R1 on cytokine-stimulated HaCaT cells. The specificity of binding was confirmed by the absence of binding to mock-transfected HEK293T cells and unstimulated HaCaT cells. Additionally, binding of the ABR variants to HEK-Blue IL22 reporter cells was detected using flow cytometry. We characterized the binding affinity

and kinetics of the most promising binders (ABR089, ABR099, and ABR167) using LigandTracer experiments with both cell lines. All binders demonstrated affinities in the low nanomolar range, with similar measurements for both cell lines. ABR099 variant exhibited the highest affinity, as measured by LigandTracer, and gave the strongest signal in immunostaining and flow cytometry experiments. Consequently, we generated a collection of high-affinity IL-22R1 binders that specifically recognize IL-22R1 on the cell surface.

In the competition ELISA experiment, 12 ABR variants demonstrated the ability to prevent IL-22 from binding to IL-22R1 in a concentration-dependent manner. Out of these, only seven variants were able to recognize IL-22R1 on the cell surface. These seven variants were then tested using the cell assay to evaluate their potential as IL-22 signaling inhibitors. Two variants, ABR089 and ABR167, showed a clear dose-response inhibitory trend. Consequently, we successfully developed small proteins with IL-22R1 inhibitory properties, which can be valuable research tools for studying IL-22 signaling and may guide the development of new anti-IL-22R1 therapies.

The NNK library was used to develop ABR binders, resulting in some variants containing cysteine at the randomized positions. In some cases, this randomized cysteine may be crucial for protein function, while in others, it might be a "passenger" mutation that can be removed without affecting the binder's function. Substituting cysteine can be desirable to prevent dimer formation via disulphide bond between cysteine containing ABR monomers. ABR089, which demonstrated inhibitory potential in the cell assay, and ABR099, which binds the receptor with the highest affinity, both contain cysteine. We designed mutants of these two variants, replacing cysteine with serine. ABR089S and ABR099S exhibited similar binding to IL-22R1 in ELISA experiment as non-mutated binders. We further measured the binding affinity of the mutants to IL-22R1 on the surface of transfected HEK293T cells. Although the measured values were slightly lower, the difference was not significant. Consequently, the C/S substitution is well-tolerated and does not diminish ABR binding function. However, the mutation affected the inhibitory function of the binders: ABR099S demonstrated an inhibitory trend, unlike the original ABR099, while ABR089S lost an ability to block IL-22 signaling. In silico modeling of ABR binding to IL-22R1 produced models consistent with the experimental observations. Docking results indicate that ABR167, ABR089, and ABR099 likely bind to the same site on IL-22R1 as IL-22, aligning with the strong inhibitory effects of ABR167 and ABR089 and the moderate effect of ABR099, due to its lesser overlap with the IL-22 binding site. For ABR089S, the predicted binding site does not overlap with IL-22, correlating with its lack of competitive binding observed experimentally. Conversely, ABR099S shows improved overlap with the IL-22 binding site.

In this study, ABR167 was evaluated for its effects on DSS-induced colitis, a well-established model for mimicking UC. The DSS-induced colitis model was created by administering 2.5% DSS in drinking water to C57BL/6 mice, which induces acute colitis characterized by epithelial damage and inflammation. ABR167, an IL-22 receptor antagonist, was administered intraperitoneally. ABR167 effect colon length was measured, histological analysis and quantitative real-time PCR (qRT-PCR) for inflammatory markers were performed. The administration of ABR167 significantly protected against DSS-induced colitis, as evidenced by the reduction in colon shortening and improvement in histological markers, such as reduced mucosal inflammation and preservation of intestinal architecture. Additionally, ABR167 treatment led to a decrease in the mRNA levels of pro-inflammatory cytokines IL-1β, IL-6, and IL-17A, which are typically elevated in this model. IL-10 expression level was also reduced. The relevance of these findings to IBD treatment is significant, as the data suggest that targeting IL-22 signaling with small protein antagonists like ABR167 can mitigate intestinal inflammation and tissue damage. This pointed to a potential therapeutic application of ABR167 for managing IBD, thus highlighting the importance of developing IL-22R1 antagonists for clinical use.

As revealed in multiple studies, role of the IL-22 in the IBD development is controversial. In different animal experimental models cytokine demonstrated both pathologic and protective effects in colon inflammation. In DSS-induced and $CD45RB^{high}$ $CD4^{+}$ naive T cell transfer colitis model IL-22 demonstrated protective functions [214, 221, 325], whereas in T_{reg}-depleted $CD45RB^{low}$ $CD4^{+}$ mature T cell transfer and anti-CD40 colitis murine models IL-22 contributed to the disease pathogenesis [220, 221]. IBD pathology is a complex disease characterized by chronic relapsing intestinal inflammation. However, molecular mechanisms of the pathology development may be different as demonstrated in multiple disease animal models. Therefore, it is plausible that IL-22 role in IBD is highly dependent on a local context. For instance, Richard A. Flavell's group published study where they transferred IL-22 knock out ($IL\text{-}22^{-/-}$) and wild type ($IL\text{-}22^{+}$) $CD45RB^{high}$ $CD4^{+}$ naive T cells into immunocompromised $IL\text{-}22^{-/-}$ $Rag^{-/-}$ mice. As a results, $IL\text{-}22^{-/-}$ $CD45RB^{high}$ $CD4^{+}$ caused considerably more severe intestinal damage characterized by weight loss and histopathological changes compared to $IL\text{-}22^{+}$ $CD45RB^{high}$ $CD4^{+}$, which compensated IL-22 expression. At the same time, $Rag1^{-/-}$ mice that were injected with both $IL\text{-}22^{-/-}$ or $IL\text{-}22^{+}$ $CD45RB^{high}$ T cells contained similar level of IL-22 mRNA expression in the colon and had less pronounced intestinal pathology. Consequently, IL-22 presence correlated with milder disease progression, so it was concluded that cytokine has protective role in adaptive colitis model. However, in the research published by the same group several years later it was revealed that transfer of the $IL\text{-}22^{-/-}$ T_{reg}-depleted

$CD45RB^{low}$ $CD4^{+}$ mature T cells to the $Rag1^{-/-}$ mice resulted in milder disease progression than in case of IL-22^{+} $CD45RB^{low}$ T cells transfer. This result indicated that $CD45RB^{low}$ $CD4^{+}$ mature T cells cause IL-22-mediated intestinal pathology. In the same study, it was also demonstrated that IL-22^{+} $CD45RB^{low}$ T cells induced considerably higher IL-22 mRNA expression in the colon of $Rag1^{-/-}$ mice compared to IL-22^{+} $CD45RB^{high}$ T cells. Also, in case of IL-$22^{-/-}$ $CD45RB^{low}$ T cell transfer to $Rag1^{-/-}$ mice, IL-22 mRNA expression was not diminished completely. Based on these observations it is possible to assume that both, IL-22 silencing and IL-22 overexpression, may contribute to IBD development depending on the IL-22 expression level and immunological context. Consistently, in the IL-23-dependent anti-CD40 infusion murine model colon pathology was driven by IL-22, which is a downstream target of IL-23. Neutralizing anti-IL-22 mAb reduced weight loss, colon damage and colitis scores in mice [221]. In our study, DSS administration increased the level of IL-22 mRNA, which is a prerequisite for IL-22R1 inhibitor application. ABR167 administration had protective effect. As a result of IL-22R1 inhibition, we observed reduction of colon shortening and improvement in histological architecture comparable to the observed after DSS application in IL-$23R^{-/-}$ murine model, where IL-23R silencing had protective effect and correlated with decrease IL-22 mRNA expression [325]. In the study of the impact of IL-22 in DSS-induced colitis murine model, disease progression was more severe in IL-$22^{-/-}$ mice compared to IL-22^{+} mice, which led to the conclusion that IL-22 is protective in the DSS-induced colitis [214]. However, although we used the same animal model, our experimental design differed significantly. In our research inflammatory markers were observed immediately after DSS application, whereas in the previous study, mice were monitored for 30 days post-DSS cessation. Also, we inhibited IL-22 signaling with small protein blocker instead of complete silencing of the cytokine. Finally, we focused on IL-22R1, instead of IL-22, blocking. IL-22R1 is used by IL-20 and IL-24 in addition to IL-22, therefore targeting of IL-22R1 can result in different outcome comparing to IL-22 targeting. Our data suggest that inhibiting IL-22 signaling with small protein antagonists like ABR167 can mitigate intestinal inflammation and tissue damage. This points to a potential therapeutic application of ABR167 for managing IBD.

4.4. Engineering PD-1-targeted small protein variants for in vitro diagnostics and in vivo PET imaging

We developed a collection of PD-1 receptor targeting binders from the highly complex Myomedin scaffold library using ribosome display technology. Seven binders named MBA (MBA003, MBA038, MBA052, MBA066, MBA197, MBA315, MBA323, and MBA414) specifically recognized recombinant human PD-1 protein, as well as cell surface PD-1

receptor on transiently transfected HEK293T and SUP-1 cell lines. Absence of binding to PD-1$^-$ cell line Dakki proved specificity of the MBA binders. Further, binding affinity of the six most promising MBA binders was measured using LigandTracer method. Based on the measurements, the variants MBA323, MBA066, and MBA414 had the lowest estimated KD values, 6.59 nM, 6.92 nM, and 8.63 nM, respectively. The slowest off-rates were observed for MBA003, MBA066, and MBA197. An alternative estimation of KD values for MBA066, MBA197, and MBA414 to recombinant hPD-1 protein in solution was performed using MST. Significant similarity of KD values was found for MBA197 (4.21±1.15 nM) and MBA414 (6.11±0.99 nM), whereas MBA066 exhibited a notably higher KD value (2917±223.22 nM). Collectively, we demonstrated that developed MBA binders specifically recognize PD-1 receptor with the high affinity and have a potential to be used as diagnostic tools.

We further tested three most promising candidates (MBA066, MBA197, and MBA414) for the binding to mPD-1 receptor, which shares 64% homology with the human ortholog. The estimated KD value for the MBA414 variant to hPD-1 on HEK293T cells (8.6 nM) is similar to its binding to murine PD-1 (2.48 nM). MBA197 also shows comparable binding affinities to hPD-1 and mPD-1 (29.7 nM vs. 21.4 nM). However, MBA066 has a significantly higher affinity for hPD-1 (6.9 nM) compared to murine PD-1 (40.5 nM). Therefore, we proved that all tested MBA variants retain binding affinity for the mPD-1, thus can be used in mouse studies.

We demonstrated diagnostic potential of the MBA414 by immunohistochemistry on human tonsil resected from a child with tonsillar hypertrophy. This binder showed sensitive competence to recognize PD-1 in frozen tissue section with significant overlap in signal compared to commercial polyclonal anti-PD-1 antibody. Similarly, MBA414 recognized PD-1 receptor in frozen NSCLC tissue section. MBA414 binding showed significant correlation with anti-PD-1 antibody binding (Pearson's correlation coefficient = 0.846). More PD-1$^+$ cells were detected with MBA414 compared to the antibody, demonstrating diagnostic potential of the protein. Further research on the larger cohort of tissue samples of NSCLC cancer patients would be required for better evaluation. However, diagnosis using tumor tissue samples remains challenging due to high heterogeneity of PD-1 expression within the same sample. Furthermore, while biopsies of primary tumors are used for diagnosis, physicians consider treating the metastatic disease. Therefore *in vivo* diagnostics using PET may be more informative about the current status of the disease. Small size of the MBA binders offers significant benefit in this domain due to potentially improved tissue penetration and fast clearance from the body. We labelled MBA with ^{68}Galium isotope and traced tissue penetration of the three most promising MBA ligands (MBA066, MBA197, and MBA414) in BALB/c mice using PET/CT body imaging

technique. MBA197 and MBA414 demonstrated preferential accumulation in liver and slow clearance from the body, which contrasted with MyoWT distribution. The same result was observed in the mouse muscle infection model. MBA066 also had preferential binding in liver, however to the lesser extent than MBA197 and MBA414. This observation can be explained with considerably lower affinity of the MBA066 to murine version of PD-1 compared to human receptor. Imaging with Myomedin binders is well tolerated. Consequently, MBA variants showed potential as diagnostic tools for immunohistochemistry on frozen tissue sections and for real-time *in vivo* imaging.

In the current research, novel Myomedin scaffold was tested with β-sheet binding surface. Based on the crystal structure of the mouse/human PD-1/PD-L1 complex (PDB ID 3bik), the critical interaction residues of hPD-L1 required for recognizing the PD-1 receptor are located on the β-sheet surface. Furthermore, Myomedin scaffold has significant structural similarity with PD-L1. Therefore, MBA binders offer a new binding geometry contrasting to the formerly developed PD-1 small protein binders with loop binding surface, such as nanobodies.

Some MBA binders from the collection demonstrate inhibitory potential. MBA003 and MBA323 competed with a soluble form of the hPD-L1 for binding to hPD-1 in competition ELISA and LigandTracer inhibitory assay. Furthermore, reduced binding of MBA variants to hPD-1-transfected HEK293T was observed in the presence of hPD-L1 by fluorescence microscopy. Estimated binding affinity of MBA003 and MBA323 is 10 μM and 30 μM respectively, which is rather low comparing to PD-L1 affinity of 8.2 μM. Therefore, we were able to develop MBA variants with inhibitory potential. However, further affinity maturation is required for efficient competition for PD-1 binding.

4.5. Current understanding on TREM-2 molecular biology and physiopathological functions.

Triggering receptor expressed on myeloid cells (TREMs) group, a set of glycosylated cell-surface specific receptors belongs to the Ig superfamily and typically expressed in the myeloid cell lineage, is involved in the regulation of various cellular crosstalk to both adaptive and innate immunity regulation [326, 327]. Recent genome-wide association and functional assay studies discovered a key role of diseases-associated myeloid cell lineage in diverse pathologies, including neurodegenerative diseases (NDDs) and cancers [264, 328]. Recently, several genetic modifications contributing to disease progression, especially linked to NDDs [274, 329], have been discovered in the *TREM2* gene. It is important mention that despite mounting evidence indicating an association between TREM-2 and various cancers, substantial aspects of TREM-2 signaling, including insights on receptor-ligand interactions and modulation of TREM-

2-mediated signaling in the TME, remain inadequately understood [328, 330]. Therefore, in this review, first we have discussed the recent advances in structural biology of TREM-2 and associated ligands followed by adopted downstream signaling pathways, in particular modulating the pivotal TREM-2-dependent functions under physiological and pathological conditions. Also, we have aimed at pinpointing the cell-specific expression and molecular regulation of TREM-2 expression that can be used to advance our understanding of how to attenuate relevant diseases. Finally, we have confirmed generic TREM-2-associated functions as well as the clinical relevance of TREM-2 dysregulation in a cancer immunosuppressive environment and discussed it as a potential therapeutic target in cancer immunotherapy. Overall, we observed TREM-2's diverse role in various myeloid cell lineage and associated disorders, yet a critical gap still persists, mostly due to multifactorial challenges, including a broad portfolio of ligands, crosslinking of TREM-2 protein with other cell surface receptors, and downstream signalling pathways, some of which are not yet acknowledged. We suggest that addressing such critical gaps through continued research on TREM-2's regulation, expression, cell- and content-specific functions, as well as species-specific differences, is crucial for its implications as a drug target and for developing relevant TREM-2 antagonist or agonist-based therapies. In this context, further research by integrating large-scale genomic and proteomics data with comprehensive humanized animal models that closely mimic human TREMs might be able to give accurate predictions on the functional role of TREM-2 under physiological and pathological conditions.

5. Conclusions

5.1. Small protein blockers of human IL-6 receptor alpha inhibit proliferation and migration of cancer cells

1. In this study, we successfully generated a collection of NEF protein variants using a combinatorial library derived from an ABD scaffold, specifically targeting IL-6Rα.
2. NEF108, NEF163, and NEF172 demonstrated the ability to inhibit IL-6-mediated signaling in cells assays.
3. The NEF variants inhibited the proliferation of malignant melanoma (G361 and A2058) and pancreatic cancer (PaTu and MiaPaCa) cells. Additionally, they suppressed the migration of melanoma (A2058), pancreatic carcinoma (PaTu), and glioblastoma (GAMG) cells, as demonstrated through real-time cell proliferation experiment and wound healing assay. Therefore, selected NEF variants have a potential for cancer therapy.
4. NEF variants recognized IL-6Rα on mature B cells and effectively inhibited the IL-6-induced differentiation of these B cells into $CD38^+$ cells that express IgA, highlighting their potential to modulate immune cell functions. This finding paves the way for investigation of NEF variants efficiency in IgAN therapy.
5. NEF108 demonstrated functional competence *in vivo*, validating the observations from *in vitro* experiments. In a DSS-induced colitis murine model, NEF108 treatment significantly prevented colon length reduction and protected against mucosal and epithelial damage, demonstrating its protective effects on intestinal tissues during inflammatory conditions. This suggests potential applications of NEF binders in treating IBD like Crohn's disease and ulcerative colitis.

5.2. IL-6 and its role in IgA nephropathy development

1. In the review, we explored the specific role of IL-6 in the development and progression of IgAN, examining the molecular mechanisms involved and the potential for IL-6-targeted therapies in managing this disease.
2. We provided a comprehensive overview of recent advances in understanding IL-6 biology.
3. We reviewed current strategies for inhibiting IL-6 signaling, focusing on the therapeutic applications and limitations of these approaches.

5.3. Human IL-22 receptor-targeted small protein antagonist suppress murine DSS-induced colitis.

1. We developed IL-22R1-targeting ABR binders from the ABD-derived small protein scaffold library using directed evolution, and specific IL-22R1 binding properties of ABR variants were confirmed.

2. ABR089, ABR099, and ABR167 were identified as the most promising binders with low nano-molar affinity and selectivity for IL-22R1.
3. Cysteine-to-Serine substitutions in ABR variants (ABR089S and ABR099S) demonstrated that the mutation was well tolerated and did not significantly impact binding affinity, though it altered the inhibitory function. ABR099S showed improved inhibition while ABR089S lost its blocking capability.
4. Three variants (ABR089, ABR099S, and ABR167) demonstrated dose-dependent inhibition of IL-22 signaling in cell assay, highlighting their potential as research tools and therapeutic candidates for IL-22-driven diseases.
5. In a DSS-induced colitis model, ABR167 significantly reduced colon shortening and inflammation, indicating its potential for treating inflammatory bowel disease by targeting IL-22 signaling.

5.4. Engineering PD-1-targeted small protein variants for in vitro diagnostics and in vivo PET imaging

1. We developed a collection of Myomedin scaffold MBA binders that specifically bind to human and mouse PD-1 receptor with high affinity. Using Myomedin β-sheet concept, we expanded repertoire of binding geometries of the existing PD-1 targeting small protein binders.
2. We demonstrated diagnostic potential of the most promising MBA binders for immunohistochemistry in cancer tissue sections and *in vivo* imaging using PET/CT technique.
3. We developed MBA variants with inhibitory potential that can be further refined by affinity maturation.

5.5. Current understanding on TREM-2 molecular biology and physiopathological functions.

1. This review addressed recent advances in the structural biology of TREM-2 and its associated ligands, highlighting their roles in physiological and pathological conditions to close existing knowledge gaps.
2. By discussing the cell-specific expression and molecular regulation of TREM-2, this review aimed to enhance our understanding of TREM-2's role in disease attenuation.
3. The review confirmed the clinical relevance of TREM-2 dysregulation in cancer immunosuppression and proposed TREM-2 as a potential therapeutic target, emphasizing the need for continued research in this area.

List of Abbreviations

ABD	Albumin-Binding Domain
ADCC	Antibody-Dependent Cellular Cytotoxicity
AICD	Activation-Induced Cell Death
Akt	Protein Kinase B
APCs	Antigen Presenting Cells
APR	Acute Hase Response
BMDMs	Bone Marrow-Derived Macrophages
BSA	Bovine Serum Albumin
CAFs	Cancer-Associated Fibroblasts
CCK-8	Cell Counting Kit-8
CDS	Circular Dichroism Spectroscopy
CD	Crohn's Disease
Chp	Chloramphenicol
CICs	Circulating Immune Complexes
CNTF	Ciliary Neurotrophic Factor
CRP	C-Reactive Protein
CSF1	Colony Stimulating Factor 1
CT-1	Cardiotrophin -1
CTLA-4	Cytotoxic T-Lymphocyte-Associated Protein 4
CTLs	Cytotoxic T Lymphocytes
CYP450	Cytochrome P450
DAMPs	Damage-Associated Molecular Patterns
DAP10	DNAX-Activating Protein Of 10 Kda
DAP12	DNAX-Activating Protein Of 12 Kda
DCs	Dendritic Cells
DMEM	Dulbecco's Modified Eagle's Medium
DMSO	Dimethyl Sulfoxide
DNA	Deoxyribonucleic Acid
DSF	Differential Scanning Fluorimetry
DSS	Dextran Sulfate Sodium
E. coli	Escherichia Coli
ECM	Extracellular Matrix
EDTA	Ethylenediaminetetraacetic Acid
EGFR	Epidermal Growth Factor Receptor
ELISA	Enzyme-Linked Immunosorbent Assay
EMA	European Medicines Agency

EMT	Epithelial-Mesenchymal Transition
ERK	Extracellular Signal-Regulated Kinase
F(ab')2	Fragment Antigen-Binding
FACS	Fluorescence-Activated Cell Sorting
FBS	Fetal Bovine Serum
FCS	Fetal Calf Serum
FDA	Food And Drug Administration
FITC	Fluorescein Isothiocyanate
FMT	Fibroblast-To-Mesenchymal Transition
FOXM1	Forkhead Box Protein M1
FOXP3	Forkhead Box P3
GC	Gastric Cancer
GCA	Giant Cell Arteritis
G-CSF	Granulocyte Colony-Stimulating Factor
Gd-IgA1	Galactose-Deficient Iga1
GI	Gastrointestinal
GM-CSF	Granulocyte-Macrophage Colony-Stimulating Factor
gp130	Glycoprotein 130
HBSS	Hank's Balanced Salt Solution
HCC	Hepatocellular Carcinoma
HEPES	4-(2-Hydroxyethyl)Piperazine-1-Ethanesulfonic Acid
HGF	Hepatocyte Growth Factor
HIF-1α	Hypoxia-Inducible Factor 1-Alpha
HRP	Horseradish Peroxidase
HSPs	Heat Shock Proteins
IBD	Inflammatory Bowel Disease
ICAM-1	Intercellular Adhesion Molecule 1
ICB	Immune Checkpoint Blockage
IFNs	Interferons
IFN-γ	Interferon Gamma
IgAN	Immunoglobulin A Nephropathy
IgG1	Immunoglobulin G1
ILs	Interleukins
IL-1	Interleukin-1
IL-10	Interleukin-10
IL-22	Interleukin-22
IL-22BP	Interleukin-22 Binding Protein
IL-6	Interleukin-6

IL-6R	Interleukin-6 Receptor Complex
IL-6Rα	Interleukin-6 Receptor Alpha
ILCs	Innate Lymphoid Cells
IMAC	Immobilized Metal Affinity Chromatography
iMCD	Idiopathic Multicentric Castleman's Disease
IPTG	Isopropyl B-D-1-Thiogalactopyranoside
ITAM	Immunoreceptor Tyrosine-Based Activation Motif
iTreg	Induced In Cell Culture Regulatory T Cell
JAK	Janus Kinase
JAK/STAT	Janus Kinase/Signal Transducer and Activator Of Transcription
JIA	Juvenile Idiopathic Arthritis
JNK	Jun N-Terminal Kinase
kDa	Kilodaltons
Km	Kanamycin
LB	Lysogeny Broth
LDL	Low-Density Lipoproteins
LIF	Leukaemia Inhibitory Factor,
LPS	Lipopolysaccharide
mAb	Monoclonal Antibody
MAPK	Mitogen-Activated Protein Kinase
MCP1	Monocyte Chemoattractant Protein 1
M-CSF	Macrophage Colony Stimulating Factor
MDD	Major Depressive Disorder
MDSCs	Myeloid-Derived Suppressor Cells
MFI	Mean Fluorescence Intensities
MHC	Major Histocompatibility Complex
MMPs	Matrix Metalloproteinases
MSCs	Mesenchymal Stem Cells
NIR	Near-Infrared
NK cells	Natural Killer Cells
NKT cells	Natural Killer T Cells
NNK	Nucleotide Mixture (Coding For All Amino Acids)
NSCLC	Non-Small Cell Lung Cancer
OD	Optical Density
OSM	Oncostatin-M
pAb	Polyclonal Antibody
PAMPs	Pathogen-Associated Molecular Patterns
PBMCs	Peripheral Blood Mononuclear Cells

PBS	Phosphate-Buffered Saline
PBST	Phosphate-Buffered Saline with Tween
PC	Pancreatic Cancer
PCR	Polymerase Chain Reaction
PD-1	Programmed Cell Death-1
PD-L1	Programmed Cell Death Ligand -1
PE	Phycoerythrin
PFA	Paraformaldehyde
PI3K	Phosphoinositide 3-Kinase
pMACs	Peritoneal Macrophages
RA	Rheumatoid Arthritis
RANKL	Receptor Activator Of Nuclear Factor Kappa Beta
RBS	Ribosome Binding Site
RCC	Renal Cell Carcinoma
Regs	Regenerating Islet-Derived Proteins
ROS	Reactive Oxygen Species
RT	Room Temperature
SAA	Serum Amyloid A
Ser727	Serine 727
SFK	Src Family Kinases
SFK/YAP	Src Family Kinase/Yes-Associated Protein
SLE	Systemic Lupus Erythematosus
SS	Systemic Sclerosis
STAT	Signal Transducer And Activator Of Transcription
STAT1	Signal Transducer And Activator Of Transcription 1
STAT3	Signal Transducer And Activator Of Transcription 3
T7p	Bacteriophage T7 Rna Polymerase Promoter
TAMs	Tumor-Associated Macrophages
TBS	Tris-Buffered Saline
TBSB	Tris-Buffered Saline With Bovine Serum Albumin
TCR	T-Cell Receptor
TCZ	Tocilizumab
Tfh	T Follicular Helpers
TGF-β	Transforming Growth Factor Beta
TILs	Tumor-Infiltrating Lymphocytes
TLRs	Toll-Like Receptors
TMB	3,3',5,5'-Tetramethylbenzidine
TME	Tumor Microenvironment

TNBC	Triple-Negative Breast Cancer
TNFs	Tumor Necrosis Factors
TNFα	Tumor Necrosis Factor-Alpha
TPO	Thyroid Peroxidase
Tregs	Regulatory T Cells
TREM-2	Triggering Receptor Expressed on Myeloid Cells 2
TWIST	Twist-Related Protein
Tyr705	Tyrosine 705
UC	Ulcerative Colitis
VCAM-1	Vascular Cell Adhesion Protein 1
VEGF	Vascular Endothelial Growth Factor
WBT	Washing Buffer Tris
WT	Wild Type
YAP	Yes-Associated Protein

Bibliography

1. Altan-Bonnet G, Mukherjee R: **Cytokine-mediated communication: a quantitative appraisal of immune complexity**. *Nat Rev Immunol* 2019, **19**(4):205-217.
2. Leonard WJ, Lin JX: **Strategies to therapeutically modulate cytokine action**. *Nat Rev Drug Discov* 2023, **22**(10):827-854.
3. Liu C, Chu DW, Kalantar-Zadeh K, George J, Young HA, Liu GZ: **Cytokines: From Clinical Significance to Quantification**. *Adv Sci* 2021, **8**(15).
4. Saenz SA, Taylor BC, Artis D: **Welcome to the neighborhood: epithelial cell-derived cytokines license innate and adaptive immune responses at mucosal sites**. *Immunol Rev* 2008, **226**:172-190.
5. McFarlane A, Pohler E, Moraga I: **Molecular and cellular factors determining the functional pleiotropy of cytokines**. *FEBS J* 2023, **290**(10):2525-2552.
6. Moraga I, Spangler J, Mendoza JL, Garcia KC: **Multifarious determinants of cytokine receptor signaling specificity**. *Adv Immunol* 2014, **121**:1-39.
7. Jiang P, Zhang Y, Ru BB, Yang Y, Vu T, Paul R, Mirza A, Altan-Bonnet G, Liu LR, Ruppin E *et al*: **Systematic investigation of cytokine signaling activity at the tissue and single-cell levels**. *Nat Methods* 2021, **18**(10):1181.
8. Saxton RA, Glassman CR, Garcia KC: **Emerging principles of cytokine pharmacology and therapeutics**. *Nat Rev Drug Discov* 2023, **22**(1):21-37.
9. Hafler DA: **Cytokines and interventional immunology - Foreword**. *Nat Rev Immunol* 2007, **7**(6):423-423.
10. Lipsky PE, van der Heijde DM, St Clair EW, Furst DE, Breedveld FC, Kalden JR, Smolen JS, Weisman M, Emery P, Feldmann M *et al*: **Infliximab and methotrexate in the treatment of rheumatoid arthritis. Anti-Tumor Necrosis Factor Trial in Rheumatoid Arthritis with Concomitant Therapy Study Group**. *N Engl J Med* 2000, **343**(22):1594-1602.
11. Hanauer SB, Sandborn WJ, Rutgeerts P, Fedorak RN, Lukas M, MacIntosh D, Panaccione R, Wolf D, Pollack P: **Human anti-tumor necrosis factor monoclonal antibody (adalimumab) in Crohn's disease: the CLASSIC-I trial**. *Gastroenterology* 2006, **130**(2):323-333; quiz 591.
12. Neurath MF: **Strategies for targeting cytokines in inflammatory bowel disease**. *Nat Rev Immunol* 2024.
13. Tomala J, Cao SD, Spangler JB: **Engineering Anticytokine Antibodies for Immune Modulation**. *J Immunol* 2024, **212**(2):225-234.
14. Deckers J, Anbergen T, Hokke AM, de Dreu A, Schrijver DP, de Bruin K, Toner YC, Beldman TJ, Spangler JB, de Greef TFA *et al*: **Engineering cytokine therapeutics**. *Nat Rev Bioeng* 2023, **1**(4):286-303.
15. Rider P, Carmi Y, Cohen I: **Biologics for Targeting Inflammatory Cytokines, Clinical Uses, and Limitations**. *Int J Cell Biol* 2016, **2016**:9259646.
16. Xue D, Hsu E, Fu YX, Peng H: **Next-generation cytokines for cancer immunotherapy**. *Antib Ther* 2021, **4**(2):123-133.
17. Dinarello CA, van der Meer JW: **Treating inflammation by blocking interleukin-1 in humans**. *Semin Immunol* 2013, **25**(6):469-484.
18. Groza Y, Jemelkova J, Kafkova LR, Maly P, Raska M: **IL-6 and its role in IgA nephropathy development**. *Cytokine Growth Factor Rev* 2022, **66**:1-14.
19. Evangelatos G, Bamias G, Kitas GD, Kollias G, Sfikakis PP: **The second decade of anti-TNF-a therapy in clinical practice: new lessons and future directions in the COVID-19 era**. *Rheumatol Int* 2022, **42**(9):1493-1511.
20. Kimura A, Kishimoto T: **IL-6: Regulator of Treg/Th17 balance**. *Eur J Immunol* 2010, **40**(7):1830-1835.

21. Garbers C, Heink S, Korn T, Rose-John S: **Interleukin-6: designing specific therapeutics for a complex cytokine**. *Nature Reviews Drug Discovery* 2018, **17**(6):395-412.
22. Fielding CA, McLoughlin RM, McLeod L, Colmont CS, Najdovska M, Grail D, Ernst M, Jones SA, Topley N, Jenkins BJ: **IL-6 regulates neutrophil trafficking during acute inflammation via STAT3**. *J Immunol* 2008, **181**(3):2189-2195.
23. Fernandez-Real JM, Vayreda M, Richart C, Gutierrez C, Broch M, Vendrell J, Ricart W: **Circulating interleukin 6 levels, blood pressure, and insulin sensitivity in apparently healthy men and women**. *J Clin Endocrinol Metab* 2001, **86**(3):1154-1159.
24. Waage A, Brandtzaeg P, Halstensen A, Kierulf P, Espevik T: **The Complex Pattern of Cytokines in Serum from Patients with Meningococcal Septic Shock - Association between Interleukin-6, Interleukin-1, and Fatal Outcome**. *J Exp Med* 1989, **169**(1):333-338.
25. Murakami M, Kamimura D, Hirano T: **Pleiotropy and Specificity: Insights from the Interleukin 6 Family of Cytokines**. *Immunity* 2019, **50**(4):812-831.
26. Garbers C, Hermanns HM, Schaper F, Muller-Newen G, Grotzinger J, Rose-John S, Scheller J: **Plasticity and cross-talk of interleukin 6-type cytokines**. *Cytokine Growth Factor Rev* 2012, **23**(3):85-97.
27. Mihara M, Hashizume M, Yoshida H, Suzuki M, Shiina M: **IL-6/IL-6 receptor system and its role in physiological and pathological conditions**. *Clin Sci* 2012, **122**(3-4):143-159.
28. Boulanger MJ, Chow DC, Brevnova EE, Garcia KC: **Hexameric structure and assembly of the interleukin-6/IL-6 alpha-receptor/gp130 complex**. *Science* 2003, **300**(5628):2101-2104.
29. Schroers A, Hecht O, Kallen KJ, Pachta M, Rose-John S, Grötzinger J: **Dynamics of the gp130 cytokine complex:: A model for assembly on the cellular membrane**. *Protein Sci* 2005, **14**(3):783-790.
30. Heinrich PC, Behrmann I, Haan S, Hermanns HM, Muller-Newen G, Schaper F: **Principles of interleukin (IL)-6-type cytokine signalling and its regulation**. *Biochem J* 2003, **374**(Pt 1):1-20.
31. Scheller J, Chalaris A, Schmidt-Arras D, Rose-John S: **The pro- and anti-inflammatory properties of the cytokine interleukin-6**. *Bba-Mol Cell Res* 2011, **1813**(5):878-888.
32. Rose-John S: **Interleukin-6 biology is coordinated by membrane bound and soluble receptors**. *Acta Biochim Pol* 2003, **50**(3):603-611.
33. Baran P, Hansen S, Waetzig GH, Akbarzadeh M, Lamertz L, Huber HJ, Ahmadian MR, Moll JM, Scheller J: **The balance of interleukin (IL)-6, IL-6.soluble IL-6 receptor (sIL-6R), and IL-6.sIL-6R.sgp130 complexes allows simultaneous classic and trans-signaling**. *J Biol Chem* 2018, **293**(18):6762-6775.
34. McElvaney OJ, Curley GF, Rose-John S, McElvaney NG: **Interleukin-6: obstacles to targeting a complex cytokine in critical illness**. *Lancet Respir Med* 2021, **9**(6):643-654.
35. Heink S, Yogev N, Garbers C, Herwerth M, Aly L, Gasperi C, Husterer V, Croxford AL, Möller-Hackbarth K, Bartsch HS *et al*: **Trans-presentation of IL-6 by dendritic cells is required for the priming of pathogenic TH17 cells**. *Nat Immunol* 2017, **18**(1):74-85.
36. Flynn CM, Kespohl B, Daunke T, Garbers Y, Dusterhoft S, Rose-John S, Haybaeck J, Lokau J, Aparicio-Siegmund S, Garbers C: **Interleukin-6 controls recycling and degradation, but not internalization of its receptors**. *J Biol Chem* 2021, **296**:100434.
37. Guschin D, Rogers N, Briscoe J, Witthuhn B, Watling D, Horn F, Pellegrini S, Yasukawa K, Heinrich P, Stark GR *et al*: **A major role for the protein tyrosine kinase JAK1 in the JAK/STAT signal transduction pathway in response to interleukin-6**. *EMBO J* 1995, **14**(7):1421-1429.

38. Decker T, Kovarik P: **Serine phosphorylation of STATs**. *Oncogene* 2000, **19**(21):2628-2637.
39. Wen ZL, Zhong Z, Darnell JE: **Maximal Activation of Transcription by Stat1 and Stat3 Requires Both Tyrosine and Serine Phosphorylation**. *Cell* 1995, **82**(2):241-250.
40. Kim HK, Baumann H: **The carboxyl-terminal region of STAT3 controls gene induction by the mouse haptoglobin promoter**. *J Biol Chem* 1997, **272**(23):14571-14579.
41. Bollrath J, Phesse TJ, von Burstin VA, Putoczki T, Bennecke M, Bateman T, Nebelsiek T, Lundgren-May T, Canli O, Schwitalla S *et al*: **gp130-mediated Stat3 activation in enterocytes regulates cell survival and cell-cycle progression during colitis-associated tumorigenesis**. *Cancer Cell* 2009, **15**(2):91-102.
42. Jung JE, Lee HG, Cho IH, Chung DH, Yoon SH, Yang YM, Lee JW, Choi S, Park JW, Ye SK *et al*: **STAT3 is a potential modulator of HIF-1-mediated VEGF expression in human renal carcinoma cells**. *Faseb J* 2005, **19**(7):1296-+.
43. Cutler SJ, Doecke JD, Ghazawi I, Yang J, Griffiths LR, Spring KJ, Ralph SJ, Mellick AS: **Novel STAT binding elements mediate IL-6 regulation of MMP-1 and MMP-3**. *Sci Rep* 2017, **7**(1):8526.
44. Shirogane T, Fukada T, Muller JM, Shima DT, Hibi M, Hirano T: **Synergistic roles for Pim-1 and c-Myc in STAT3-mediated cell cycle progression and antiapoptosis**. *Immunity* 1999, **11**(6):709-719.
45. Fukada T, Ohtani T, Yoshida Y, Shirogane T, Nishida K, Nakajima K, Hibi M, Hirano T: **STAT3 orchestrates contradictory signals in cytokine-induced G1 to S cell-cycle transition**. *EMBO J* 1998, **17**(22):6670-6677.
46. Bongartz H, Gille K, Hessenkemper W, Mandel K, Lewitzky M, Feller SM, Schaper F: **The multi-site docking protein Grb2-associated binder 1 (Gab1) enhances interleukin-6-induced MAPK-pathway activation in an SHP2-, Grb2-, and time-dependent manner**. *Cell Commun Signal* 2019, **17**(1):135.
47. Negoro S, Oh H, Tone E, Kunisada K, Fujio Y, Walsh K, Kishimoto T, Yamauchi-Takihara K: **Glycoprotein 130 regulates cardiac myocyte survival in doxorubicin-induced apoptosis through phosphatidylinositol 3-kinase/Akt phosphorylation and Bcl-xL/caspase-3 interaction**. *Circulation* 2001, **103**(4):555-561.
48. Taniguchi K, Wu LW, Grivennikov SI, de Jong PR, Lian I, Yu FX, Wang KP, Ho SB, Boland BS, Chang JT *et al*: **A gp130-Src-YAP module links inflammation to epithelial regeneration**. *Nature* 2015, **519**(7541):57-U107.
49. Srivastava A, Sharma H, Khanna S, Balasundaram TS, Chowdhury S, Chowdhury R, Mukherjee S: **Interleukin-6 Induced Proliferation Is Attenuated by Transforming Growth Factor-β-Induced Signaling in Human Hepatocellular Carcinoma Cells**. *Front Oncol* 2022, **11**.
50. Gabay C: **Interleukin-6 and chronic inflammation**. *Arthritis Res Ther* 2006, **8 Suppl 2**(Suppl 2):S3.
51. Narazaki M, Kishimoto T: **The Two-Faced Cytokine IL-6 in Host Defense and Diseases**. *Int J Mol Sci* 2018, **19**(11).
52. Didion SP: **Cellular and Oxidative Mechanisms Associated with Interleukin-6 Signaling in the Vasculature**. *Int J Mol Sci* 2017, **18**(12).
53. Chalaris A, Rabe B, Paliga K, Lange H, Laskay T, Fielding CA, Jones SA, Rose-John S, Scheller J: **Apoptosis is a natural stimulus of IL6R shedding and contributes to the proinflammatory trans-signaling function of neutrophils**. *Blood* 2007, **110**(6):1748-1755.
54. Rose-John S, Winthrop K, Calabrese L: **The role of IL-6 in host defence against infections: immunobiology and clinical implications**. *Nat Rev Rheumatol* 2017, **13**(7):399-409.

55. Jones SA, Jenkins BJ: **Recent insights into targeting the IL-6 cytokine family in inflammatory diseases and cancer**. *Nat Rev Immunol* 2018, **18**(12):773-789.
56. Fazel Modares N, Polz R, Haghighi F, Lamertz L, Behnke K, Zhuang Y, Kordes C, Haussinger D, Sorg UR, Pfeffer K *et al*: **IL-6 Trans-signaling Controls Liver Regeneration After Partial Hepatectomy**. *Hepatology* 2019, **70**(6):2075-2091.
57. Hurst SM, Wilkinson TS, McLoughlin RM, Jones S, Horiuchi S, Yamamoto N, Rose-John S, Fuller GM, Topley N, Jones SA: **IL-6 and its soluble receptor orchestrate a temporal switch in the pattern of leukocyte recruitment seen during acute inflammation**. *Immunity* 2001, **14**(6):705-714.
58. McLoughlin RM, Hurst SM, Nowell MA, Harris DA, Horiuchi S, Morgan LW, Wilkinson TS, Yamamoto N, Topley N, Jones SA: **Differential regulation of neutrophil-activating chemokines by IL-6 and its soluble receptor isoforms**. *The Journal of Immunology* 2004, **172**(9):5676-5683.
59. Kaplanski G, Marin V, Montero-Julian F, Mantovani A, Farnarier C: **IL-6: a regulator of the transition from neutrophil to monocyte recruitment during inflammation**. *Trends Immunol* 2003, **24**(1):25-29.
60. Akdis M, Burgler S, Crameri R, Eiwegger T, Fujita H, Gomez E, Klunker S, Meyer N, O'Mahony L, Palomares O *et al*: **Interleukins, from 1 to 37, and interferon-gamma: receptors, functions, and roles in diseases**. *J Allergy Clin Immunol* 2011, **127**(3):701-721 e701-770.
61. Huang X, Li Y, Fu M, Xin HB: **Polarizing Macrophages In Vitro**. *Methods Mol Biol* 2018, **1784**:119-126.
62. Alegria GC, Devauchelle-Pensec V, Renaudineau Y, Saraux A, Pers JO, Cornec D: **Correction of abnormal B-cell subset distribution by interleukin-6 receptor blockade in polymyalgia rheumatica**. *Rheumatology* 2017, **56**(8):1401-1406.
63. Rosser EC, Oleinika K, Tonon S, Doyle R, Bosma A, Carter NA, Harris KA, Jones SA, Klein N, Mauri C: **Regulatory B cells are induced by gut microbiota-driven interleukin-1beta and interleukin-6 production**. *Nat Med* 2014, **20**(11):1334-1339.
64. Schett G: **Physiological effects of modulating the interleukin-6 axis**. *Rheumatology (Oxford)* 2018, **57**(suppl_2):ii43-ii50.
65. Su H, Lei CT, Zhang C: **Interleukin-6 Signaling Pathway and Its Role in Kidney Disease: An Update**. *Front Immunol* 2017, **8**:405.
66. Ryu JH, Kim SJ: **Interleukin-6-634 C/G and-174 G/C Polymorphisms in Korean Patients Undergoing Hemodialysis**. *Korean J Intern Med* 2012, **27**(3):327-337.
67. Dienz O, Eaton SM, Bond JP, Neveu W, Moquin D, Noubade R, Briso EM, Charland C, Leonard WJ, Ciliberto G *et al*: **The induction of antibody production by IL-6 is indirectly mediated by IL-21 produced by CD4+ T cells**. *J Exp Med* 2009, **206**(1):69-78.
68. Harbour SN, DiToro DF, Witte SJ, Zindl CL, Gao M, Schoeb TR, Jones GW, Jones SA, Hatton RD, Weaver CT: **TH17 cells require ongoing classic IL-6 receptor signaling to retain transcriptional and functional identity**. *Sci Immunol* 2020, **5**(49).
69. Bettelli E, Carrier Y, Gao W, Korn T, Strom TB, Oukka M, Weiner HL, Kuchroo VK: **Reciprocal developmental pathways for the generation of pathogenic effector TH17 and regulatory T cells**. *Nature* 2006, **441**(7090):235-238.
70. Eto D, Lao C, DiToro D, Barnett B, Escobar TC, Kageyama R, Yusuf I, Crotty S: **IL-21 and IL-6 are critical for different aspects of B cell immunity and redundantly induce optimal follicular helper CD4 T cell (Tfh) differentiation**. *PLoS One* 2011, **6**(3):e17739.
71. Jego G, Palucka AK, Blanck JP, Chalouni C, Pascual V, Banchereau J: **Plasmacytoid dendritic cells induce plasma cell differentiation through type I interferon and interleukin 6**. *Immunity* 2003, **19**(2):225-234.

72. Vinuesa CG, Linterman MA, Yu D, MacLennan ICM: **Follicular helper T cells**. *Annual review of immunology* 2016, **34**:335-368.
73. Tsukamoto H, Fujieda K, Hirayama M, Ikeda T, Yuno A, Matsumura K, Fukuma D, Araki K, Mizuta H, Nakayama H *et al*: **Soluble IL6R Expressed by Myeloid Cells Reduces Tumor-Specific Th1 Differentiation and Drives Tumor Progression**. *Cancer Res* 2017, **77**(9):2279-2291.
74. Tsukamoto H, Fujieda K, Senju S, Ikeda T, Oshiumi H, Nishimura Y: **Immune-suppressive effects of interleukin-6 on T-cell-mediated anti-tumor immunity**. *Cancer Sci* 2018, **109**(3):523-530.
75. Johnson BZ, Stevenson AW, Prele CM, Fear MW, Wood FM: **The Role of IL-6 in Skin Fibrosis and Cutaneous Wound Healing**. *Biomedicines* 2020, **8**(5).
76. Luckett-Chastain L, Calhoun K, Schartz T, Gallucci RM: **IL-6 influences the balance between M1 and M2 macrophages in a mouse model of irritant contact dermatitis**. *Journal of Immunology* 2016, **196**.
77. Kaplanski G, Marin V, Montero-Julian F, Mantovani A, Farnarier C: **IL-6: a regulator of the transition from neutrophil to monocyte recruitment during inflammation**. *Trends in Immunology* 2003, **24**(1):25-29.
78. Dienz O, Rincon M: **The effects of IL-6 on CD4 T cell responses**. *Clin Immunol* 2009, **130**(1):27-33.
79. Yang R, Masters AR, Fortner KA, Champagne DP, Yanguas-Casas N, Silberger DJ, Weaver CT, Haynes L, Rincon M: **IL-6 promotes the differentiation of a subset of naive CD8+ T cells into IL-21-producing B helper CD8+ T cells**. *J Exp Med* 2016, **213**(11):2281-2291.
80. Izumi T, Imai J, Yamamoto J, Kawana Y, Endo A, Sugawara H, Kohata M, Asai Y, Takahashi K, Kodama S *et al*: **Vagus-macrophage-hepatocyte link promotes post-injury liver regeneration and whole-body survival through hepatic FoxM1 activation**. *Nat Commun* 2018, **9**.
81. Taub R: **Hepatoprotection via the IL-6/Stat3 pathway**. *J Clin Invest* 2003, **112**(7):978-980.
82. Ji T, Li G, Chen J, Zhao J, Li X, Lin H, Cai X, Cang Y: **Distinct role of interleukin-6 and tumor necrosis factor receptor-1 in oval cell- mediated liver regeneration and inflammation-associated hepatocarcinogenesis**. *Oncotarget* 2016, **7**(41):66635-66646.
83. Lin ZQ, Kondo T, Ishida Y, Takayasu T, Mukaida N: **Essential involvement of IL-6 in the skin wound-healing process as evidenced by delayed wound healing in IL-6-deficient mice**. *J Leukocyte Biol* 2003, **73**(6):713-721.
84. Erta M, Quintana A, Hidalgo J: **Interleukin-6, a major cytokine in the central nervous system**. *Int J Biol Sci* 2012, **8**(9):1254-1266.
85. Gallo J, Raska M, Konttinen YT, Nich C, Goodman SB: **Innate immunity sensors participating in pathophysiology of joint diseases: a brief overview**. *J Long Term Eff Med Implants* 2014, **24**(4):297-317.
86. McGregor NE, Murat M, Elango J, Poulton IJ, Walker EC, Crimeen-Irwin B, Ho PWM, Gooi JH, Martin TJ, Sims NA: **IL-6 exhibits both cis- and trans-signaling in osteocytes and osteoblasts, but only trans-signaling promotes bone formation and osteoclastogenesis**. *J Biol Chem* 2019, **294**(19):7850-7863.
87. Lehrskov LL, Christensen RH: **The role of interleukin-6 in glucose homeostasis and lipid metabolism**. *Semin Immunopathol* 2019, **41**(4):491-499.
88. Taniguchi K, Karin M: **IL-6 and related cytokines as the critical lynchpins between inflammation and cancer**. *Seminars in Immunology* 2014, **26**(1):54-74.
89. Malik M, Britten J, DeAngelis A, Catherino WH: **Cross-talk between Janus kinase-signal transducer and activator of transcription pathway and transforming**

growth factor beta pathways and increased collagen1A1 production in uterine leiomyoma cells. *F S Sci* 2020, **1**(2):206-220.
90. Hagihara K, Nishikawa T, Isobe T, Song J, Sugamata Y, Yoshizaki K: **IL-6 plays a critical role in the synergistic induction of human serum amyloid A (SAA) gene when stimulated with proinflammatory cytokines as analyzed with an SAA isoform real-time quantitative RT-PCR assay system**. *Biochem Bioph Res Co* 2004, **314**(2):363-369.
91. Coletta I, Soldo L, Polentarutti N, Mancini F, Guglielmotti A, Pinza M, Mantovani A, Milanese C: **Selective induction of MCP-1 in human mesangial cells by the IL-6/sIL-6R complex**. *Exp Nephrol* 2000, **8**(1):37-43.
92. Iwano M, Dohi K, Hirata E, Horii Y, Shiiki H, Ishikawa H: **Induction of Interleukin-6 Synthesis in Mouse Glomeruli and Cultured Mesangial Cells**. *Nephron* 1992, **62**(1):58-65.
93. Wang TT, He CQ: **TNF-α and IL-6: The Link between Immune and Bone System**. *Curr Drug Targets* 2020, **21**(3):213-227.
94. Dijkgraaf EM, Welters MJP, Nortier JWR, van der Burg SH, Kroep JR: **Interleukin-6/interleukin-6 Receptor Pathway as a New Therapy Target in Epithelial Ovarian Cancer**. *Curr Pharm Design* 2012, **18**(25):3816-3827.
95. Kang SJ, Tanaka T, Kishimoto T: **Therapeutic uses of anti-interleukin-6 receptor antibody**. *Int Immunol* 2015, **27**(1):21-29.
96. van Rhee F, Wong RS, Munshi N, Rossi JF, Ke XY, Fossa A, Simpson D, Capra M, Liu T, Hsieh RK *et al*: **Siltuximab for multicentric Castleman's disease: a randomised, double-blind, placebo-controlled trial**. *Lancet Oncol* 2014, **15**(9):966-974.
97. Deisseroth A, Ko CW, Nie L, Zirkelbach JF, Zhao L, Bullock J, Mehrotra N, Del Valle P, Saber H, Sheth C *et al*: **FDA approval: siltuximab for the treatment of patients with multicentric Castleman disease**. *Clin Cancer Res* 2015, **21**(5):950-954.
98. Singh JA, Beg S, Lopez-Olivo MA: **Tocilizumab for Rheumatoid Arthritis: A Cochrane Systematic Review**. *J Rheumatol* 2011, **38**(1):10-20.
99. Tanaka T, Narazaki M, Kishimoto T: **Therapeutic targeting of the interleukin-6 receptor**. *Annu Rev Pharmacol Toxicol* 2012, **52**:199-219.
100. Lu ZY, Brochier J, Wijdenes J, Brailly H, Bataille R, Klein B: **High amounts of circulating interleukin (IL)-6 in the form of monomeric immune complexes during anti-IL-6 therapy. Towards a new methodology for measuring overall cytokine production in human in vivo**. *Eur J Immunol* 1992, **22**(11):2819-2824.
101. Klein B, Wijdenes J, Zhang XG, Jourdan M, Boiron JM, Brochier J, Liautard J, Merlin M, Clement C, Morel-Fournier B *et al*: **Murine anti-interleukin-6 monoclonal antibody therapy for a patient with plasma cell leukemia**. *Blood* 1991, **78**(5):1198-1204.
102. Davis CC, Shah KS, Lechowicz MJ: **Clinical development of siltuximab**. *Curr Oncol Rep* 2015, **17**(7):29.
103. Shaw S, Bourne T, Meier C, Carrington B, Gelinas R, Henry A, Popplewell A, Adams R, Baker T, Rapecki S *et al*: **Discovery and characterization of olokizumab: a humanized antibody targeting interleukin-6 and neutralizing gp130-signaling**. *MAbs* 2014, **6**(3):774-782.
104. Heo TH, Wahler J, Suh N: **Potential therapeutic implications of IL-6/IL-6R/gp130-targeting agents in breast cancer**. *Oncotarget* 2016, **7**(13):15460-15473.
105. Kim GW, Lee NR, Pi RH, Lim YS, Lee YM, Lee JM, Jeong HS, Chung SH: **IL-6 inhibitors for treatment of rheumatoid arthritis: past, present, and future**. *Arch Pharm Res* 2015, **38**(5):575-584.
106. Silverman J, Liu Q, Bakker A, To W, Duguay A, Alba BM, Smith R, Rivas A, Li P, Le H *et al*: **Multivalent avimer proteins evolved by exon shuffling of a family of human receptor domains**. *Nat Biotechnol* 2005, **23**(12):1556-1561.

107. Economides AN, Carpenter LR, Rudge JS, Wong V, Koehler-Stec EM, Hartnett C, Pyles EA, Xu X, Daly TJ, Young MR *et al*: **Cytokine traps: multi-component, high-affinity blockers of cytokine action**. *Nat Med* 2003, **9**(1):47-52.
108. Yoshio-Hoshino N, Adachi Y, Aoki C, Pereboev A, Curiel DT, Nishimoto N: **Establishment of a new interleukin-6 (IL-6) receptor inhibitor applicable to the gene therapy for IL-6-dependent tumor**. *Cancer Res* 2007, **67**(3):871-875.
109. Savino R, Ciapponi L, Lahm A, Demartis A, Cabibbo A, Toniatti C, Delmastro P, Altamura S, Ciliberto G: **Rational design of a receptor super-antagonist of human interleukin-6**. *EMBO J* 1994, **13**(24):5863-5870.
110. Dvorak HF: **Tumors: wounds that do not heal—redux**. *Cancer immunology research* 2015, **3**(1):1-11.
111. Lacina L, Brabek J, Kral V, Kodet O, Smetana K, Jr.: **Interleukin-6: a molecule with complex biological impact in cancer**. *Histol Histopathol* 2019, **34**(2):125-136.
112. Rupert JE, Narasimhan A, Jengelley DHA, Jiang YL, Liu JG, Au EN, Silverman LM, Sandusky G, Bonetto A, Cao S *et al*: **Tumor-derived IL-6 and trans-signaling among tumor, fat, and muscle mediate pancreatic cancer cachexia**. *J Exp Med* 2021, **218**(6).
113. Johnson DE, O'Keefe RA, Grandis JR: **Targeting the IL-6/JAK/STAT3 signalling axis in cancer**. *Nat Rev Clin Oncol* 2018, **15**(4):234-248.
114. Kim NH, Kim SK, Kim DS, Zhang D, Park JA, Yi H, Kim JS, Shin HC: **Anti-proliferative action of IL-6R-targeted antibody tocilizumab for non-small cell lung cancer cells**. *Oncol Lett* 2015, **9**(5):2283-2288.
115. Mihara M, Kasutani K, Okazaki M, Nakamura A, Kawai S, Sugimoto M, Matsumoto Y, Ohsugi Y: **Tocilizumab inhibits signal transduction mediated by both mIL-6R and sIL-6R, but not by the receptors of other members of IL-6 cytokine family**. *Int Immunopharmacol* 2005, **5**(12):1731-1740.
116. Chen KG, Sale S, Tan T, Ermoian RP, Sikic BI: **CCAAT/enhancer-binding protein beta (nuclear factor for interleukin 6) transactivates the human MDR1 gene by interaction with an inverted CCAAT box in human cancer cells**. *Mol Pharmacol* 2004, **65**(4):906-916.
117. Tang RF, Wang SX, Zhang FR, Peng L, Wang SX, Xiao Y, Zhang M: **Interleukin-1alpha, 6 regulate the secretion of vascular endothelial growth factor A, C in pancreatic cancer**. *Hepatobiliary Pancreat Dis Int* 2005, **4**(3):460-463.
118. Polyak K, Weinberg RA: **Transitions between epithelial and mesenchymal states: acquisition of malignant and stem cell traits**. *Nat Rev Cancer* 2009, **9**(4):265-273.
119. Seo J, Ha J, Kang E, Cho S: **The role of epithelial-mesenchymal transition-regulating transcription factors in anti-cancer drug resistance**. *Arch Pharm Res* 2021, **44**(3):281-292.
120. Rhim AD, Mirek ET, Aiello NM, Maitra A, Bailey JM, McAllister F, Reichert M, Beatty GL, Rustgi AK, Vonderheide RH *et al*: **EMT and dissemination precede pancreatic tumor formation**. *Cell* 2012, **148**(1-2):349-361.
121. Xiao Y, Yu DH: **Tumor microenvironment as a therapeutic target in cancer**. *Pharmacol Therapeut* 2021, **221**.
122. Urban L, Novak S, Coma M, Dvorankova B, Lacina L, Sachova J, Hradilova M, Svatonova P, Kolar M, Strnad H *et al*: **Unravelling heterogeneous effects of cancer-associated fibroblasts on poor prognosis markers in breast cancer EM-G3 cell line: In vitro-targeted treatment (anti-IL-6, anti-VEGF-A, anti-MFGE8) based on transcriptomic profiling**. *Oncol Rep* 2024, **51**(1).
123. Jobe NP, Rösel D, Dvoránková B, Kodet O, Lacina L, Mateu R, Smetana K, Brábek J: **Simultaneous blocking of IL-6 and IL-8 is sufficient to fully inhibit CAF-induced human melanoma cell invasiveness**. *Histochem Cell Biol* 2016, **146**(2):205-217.

124. Roca H, Varsos ZS, Sud S, Craig MJ, Ying C, Pienta KJ: **CCL2 and interleukin-6 promote survival of human CD11b+ peripheral blood mononuclear cells and induce M2-type macrophage polarization**. *J Biol Chem* 2009, **284**(49):34342-34354.
125. Dehai C, Bo P, Qiang T, Lihua S, Fang L, Shi J, Jingyan C, Yan Y, Guangbin W, Zhenjun Y: **Enhanced invasion of lung adenocarcinoma cells after co-culture with THP-1-derived macrophages via the induction of EMT by IL-6**. *Immunol Lett* 2014, **160**(1):1-10.
126. Li X, Zhong J, Deng X, Guo X, Lu Y, Lin J, Huang X, Wang C: **Targeting Myeloid-Derived Suppressor Cells to Enhance the Antitumor Efficacy of Immune Checkpoint Blockade Therapy**. *Front Immunol* 2021, **12**:754196.
127. Peng DJ, Tanikawa T, Li W, Zhao LL, Vatan L, Szeliga W, Wan SS, Wei S, Wang Y, Liu Y *et al*: **Myeloid-Derived Suppressor Cells Endow Stem-like Qualities to Breast Cancer Cells through IL6/STAT3 and NO/NOTCH Cross-talk Signaling**. *Cancer Research* 2016, **76**(11):3156-3165.
128. Julian BA, Waldo FB, Rifai A, Mestecky J: **IgA nephropathy, the most common glomerulonephritis worldwide. A neglected disease in the United States?** *Am J Med* 1988, **84**(1):129-132.
129. Berthoux FC, Whey H, Aflani A: **Natural history of primary IgA nephropathy**. *Semin Nephrol* 2008, **28**(1):4-9.
130. Wyatt RJ, Julian BA: **IgA nephropathy**. *N Engl J Med* 2013, **368**(25):2402-2414.
131. Gharavi AG, Moldoveanu Z, Wyatt RJ, Barker CV, Woodford SY, Lifton RP, Mestecky J, Novak J, Julian BA: **Aberrant IgA1 glycosylation is inherited in familial and sporadic IgA nephropathy**. *J Am Soc Nephrol* 2008, **19**(5):1008-1014.
132. Mestecky J, Raska M, Julian BA, Gharavi AG, Renfrow MB, Moldoveanu Z, Novak L, Matousovic K, Novak J: **IgA nephropathy: molecular mechanisms of the disease**. *Annu Rev Pathol* 2013, **8**:217-240.
133. Baenziger J, Kornfeld S: **Structure of the carbohydrate units of IgA1 immunoglobulin. II. Structure of the O-glycosidically linked oligosaccharide units**. *J Biol Chem* 1974, **249**(22):7270-7281.
134. Suzuki H, Fan R, Zhang ZX, Brown R, Hall S, Julian BA, Chatham WW, Suzuki Y, Wyatt RJ, Moldoveanu Z *et al*: **Aberrantly glycosylated IgA1 in IgA nephropathy patients is recognized by IgG antibodies with restricted heterogeneity**. *J Clin Invest* 2009, **119**(6):1668-1677.
135. Tomana M, Novak J, Julian BA, Matousovic K, Konecny K, Mestecky J: **Circulating immune complexes in IgA nephropathy consist of IgA1 with galactose-deficient hinge region and antiglycan antibodies**. *J Clin Invest* 1999, **104**(1):73-81.
136. Suzuki H, Kiryluk K, Novak J, Moldoveanu Z, Herr AB, Renfrow MB, Wyatt RJ, Scolari F, Mestecky J, Gharavi AG *et al*: **The pathophysiology of IgA nephropathy**. *J Am Soc Nephrol* 2011, **22**(10):1795-1803.
137. Stangou M, Alexopoulos E, Papagianni A, Pantzaki A, Bantis C, Dovas S, Economidou D, Leontsini M, Memmos D: **Urinary levels of epidermal growth factor, interleukin-6 and monocyte chemoattractant protein-1 may act as predictor markers of renal function outcome in immunoglobulin A nephropathy**. *Nephrology* 2009, **14**(6):613-620.
138. Segarra-Medrano A, Carnicer-Caceres C, Valtierra-Carmeno N, Agraz-Pamplona I, Ramos-Terrades N, Jatem Escalante E, Ostos-Roldan E: **Value of urinary levels of interleukin-6, epidermal growth factor, monocyte chemoattractant protein type1 and transforming growth factor beta1 in predicting the extent of fibrosis lesions in kidney biopsies of patients with IgA nephropathy**. *Nefrologia* 2017, **37**(5):531-538.
139. Cochrane CG, Unanue ER, Dixon FJ: **A Role of Polymorphonuclear Leukocytes and Complement in Nephrotoxic Nephritis**. *J Exp Med* 1965, **122**(1):99-116.

140. Sterzel RB, Pabst R: **The Temporal Relationship between Glomerular Cell-Proliferation and Monocyte Infiltration in Experimental Glomerulonephritis**. *Virchows Arch B* 1982, **38**(3):337-350.
141. Tipping PG, Neale TJ, Holdsworth SR: **T lymphocyte participation in antibody-induced experimental glomerulonephritis**. *Kidney Int* 1985, **27**(3):530-537.
142. Bolton WK, Innes DJ, Jr., Sturgill BC, Kaiser DL: **T-cells and macrophages in rapidly progressive glomerulonephritis: clinicopathologic correlations**. *Kidney Int* 1987, **32**(6):869-876.
143. Nolasco FE, Cameron JS, Hartley B, Coelho A, Hildreth G, Reuben R: **Intraglomerular T cells and monocytes in nephritis: study with monoclonal antibodies**. *Kidney Int* 1987, **31**(5):1160-1166.
144. Tamouza H, Chemouny JM, Kafkova LR, Berthelot L, Flamant M, Demion M, Mesnard L, Paubelle E, Walker F, Julian BA *et al*: **The IgA1 immune complex-mediated activation of the MAPK/ERK kinase pathway in mesangial cells is associated with glomerular damage in IgA nephropathy**. *Kidney International* 2012, **82**(12):1284-1296.
145. van den Dobbelsteen ME, van der Woude FJ, Schroeijers WE, van den Wall Bake AW, van Es LA, Daha MR: **Binding of dimeric and polymeric IgA to rat renal mesangial cells enhances the release of interleukin 6**. *Kidney Int* 1994, **46**(2):512-519.
146. Durlacher-Betzer K, Hassan A, Levi R, Axelrod J, Silver J, Naveh-Many T: **Interleukin-6 contributes to the increase in fibroblast growth factor 23 expression in acute and chronic kidney disease**. *Kidney Int* 2018, **94**(2):315-325.
147. Yang YC, Fu H, Zhang B, Wu YB: **Interleukin-6 Downregulates the Expression of Vascular Endothelial-Cadherin and Increases Permeability in Renal Glomerular Endothelial Cells via the Trans-Signaling Pathway**. *Inflammation* 2022, **45**(6):2544-2558.
148. Rops ALWMM, Jansen E, van der Schaaf A, Pieterse E, Rother N, Hofstra J, Dijkman HBPM, van de Logt AE, Wetzels J, van der Vlag J *et al*: **Interleukin-6 is essential for glomerular immunoglobulin A deposition and the development of renal pathology in Cd37-defcient mice**. *Kidney International* 2018, **93**(6):1356-1366.
149. Bake AWLV, Crowleynowick PA, Kulhavy R, Hermans J, Jackson S, Julian BA, Mestecky J: **Cytokine-Induced Immunoglobulin Production in Primary Iga Nephropathy**. *Am J Kidney Dis* 1992, **20**(6):611-617.
150. Suzuki H, Raska M, Yamada K, Moldoveanu Z, Julian BA, Wyatt RJ, Tomino Y, Gharavi AG, Novak J: **Cytokines Alter IgA1 O- Glycosylation by Dysregulating C1GalT1 and ST6GalNAc-II Enzymes***. *J Biol Chem* 2014, **289**(8):5330-5339.
151. Yamada K, Huang ZQ, Raska M, Reily C, Anderson JC, Suzuki H, Ueda H, Moldoveanu Z, Kiryluk K, Suzuki Y *et al*: **Inhibition of STAT3 Signaling Reduces IgA1 Autoantigen Production in IgA Nephropathy**. *Kidney Int Rep* 2017, **2**(6):1194-1207.
152. Wang YY, Zhang L, Zhao PW, Ma L, Li C, Zou HB, Jiang YF: **Functional implications of regulatory B cells in human IgA nephropathy**. *Scand J Immunol* 2014, **79**(1):51-60.
153. Mestecky J, Novak J, Moldoveanu Z, Raska M: **IgA nephropathy enigma**. *Clin Immunol* 2016, **172**:72-77.
154. Makita Y, Suzuki H, Kano T, Takahata A, Julian BA, Novak J, Suzuki Y: **TLR9 activation induces aberrant IgA glycosylation via APRIL- and IL-6-mediated pathways in IgA nephropathy**. *Kidney International* 2020, **97**(2):340-349.
155. Ahluwalia B, Moraes L, Magnusson MK, Öhman L: **Immunopathogenesis of inflammatory bowel disease and mechanisms of biological therapies**. *Scand J Gastroentero* 2018, **53**(4):379-389.
156. Xu XR, Liu CQ, Feng BS, Liu ZJ: **Dysregulation of mucosal immune response in pathogenesis of inflammatory bowel disease**. *World J Gastroenterol* 2014, **20**(12):3255-3264.

157. Mudter J, Neurath MF: **Il-6 signaling in inflammatory bowel disease: pathophysiological role and clinical relevance**. *Inflamm Bowel Dis* 2007, **13**(8):1016-1023.
158. Yadav V, Varum F, Bravo R, Furrer E, Bojic D, Basit AW: **Inflammatory bowel disease: exploring gut pathophysiology for novel therapeutic targets**. *Transl Res* 2016, **176**:38-68.
159. Rimoldi M, Chieppa M, Salucci V, Avogadri F, Sonzogni A, Sampietro GM, Nespoli A, Viale G, Allavena P, Rescigno M: **Intestinal immune homeostasis is regulated by the crosstalk between epithelial cells and dendritic cells (vol 6, pg 507, 2005)**. *Nat Immunol* 2015, **16**(3):326-326.
160. Hart AL, Al-Hassi HO, Rigby RJ, Bell SJ, Emmanuel AV, Knight SC, Kamm MA, Stagg AJ: **Characteristics of intestinal dendritic cells in inflammatory bowel diseases**. *Gastroenterology* 2005, **129**(1):50-65.
161. Middel P, Raddatz D, Gunawan B, Haller F, Radzun HJ: **Increased number of mature dendritic cells in Crohn's disease: evidence for a chemokine mediated retention mechanism**. *Gut* 2006, **55**(2):220-227.
162. Moldoveanu AC, Diculescu M, Braticevici CF: **Cytokines in inflammatory bowel disease**. *Rom J Intern Med* 2015, **53**(2):118-127.
163. Hanauer SB: **Inflammatory bowel disease: epidemiology, pathogenesis, and therapeutic opportunities**. *Inflamm Bowel Dis* 2006, **12 Suppl 1**:S3-9.
164. Atreya R, Neurath MF: **Involvement of IL-6 in the pathogenesis of inflammatory bowel disease and colon cancer**. *Clin Rev Allergy Immunol* 2005, **28**(3):187-196.
165. Shahini A, Shahini A: **Role of interleukin-6-mediated inflammation in the pathogenesis of inflammatory bowel disease: focus on the available therapeutic approaches and gut microbiome**. *J Cell Commun Signal* 2023, **17**(1):55-74.
166. Bouma G, Strober W: **The immunological and genetic basis of inflammatory bowel disease**. *Nat Rev Immunol* 2003, **3**(7):521-533.
167. Podolsky DK: **Inflammatory bowel disease**. *N Engl J Med* 2002, **347**(6):417-429.
168. Rutgeerts P, Van Deventer S, Schreiber S: **Review article: the expanding role of biological agents in the treatment of inflammatory bowel disease - focus on selective adhesion molecule inhibition**. *Aliment Pharmacol Ther* 2003, **17**(12):1435-1450.
169. Ina K, Binion DG, West GA, Dobrea GM, Fiocchi C: **CROHNS-DISEASE (CD) MUCOSAL T-CELLS ARE RESISTANT TO APOPTOSIS**. In*: 1995*: WB SAUNDERS CO INDEPENDENCE SQUARE WEST CURTIS CENTER, STE 300, PHILADELPHIA ...: A841-A841.
170. Shanahan F: **Inflammatory bowel disease: immunodiagnostics, immunotherapeutics, and ecotherapeutics**. *Gastroenterology* 2001, **120**(3):622-635.
171. Clarke WT, Feuerstein JD: **Colorectal cancer surveillance in inflammatory bowel disease: Practice guidelines and recent developments**. *World J Gastroenterol* 2019, **25**(30):4148-4157.
172. Suzuki Y, Saito H, Kasanuki J, Kishimoto T, Tamura Y, Yoshida S: **Significant Increase of Interleukin-6 Production in Blood Mononuclear Leukocytes Obtained from Patients with Active Inflammatory Bowel-Disease**. *Life Sci* 1990, **47**(24):2193-2197.
173. Reimund JM, Wittersheim C, Dumont S, Muller CD, Kenney JS, Baumann R, Poindron P, Duclos B: **Increased production of tumour necrosis factor-alpha, interleukin-1 beta, and interleukin-6 by morphologically normal intestinal biopsies from patients with Crohn's disease**. *Gut* 1996, **39**(5):684-689.
174. Gross V, Andus T, Caesar I, Roth M, Scholmerich J: **Evidence for Continuous Stimulation of Interleukin-6 Production in Crohns-Disease**. *Gastroenterology* 1992, **102**(2):514-519.

175. Chassaing B, Aitken JD, Malleshappa M, Vijay-Kumar M: **Dextran sulfate sodium (DSS)-induced colitis in mice**. *Curr Protoc Immunol* 2014, **104**:15 25 11-15 25 14.
176. Naito Y, Takagi T, Uchiyama K, Kuroda M, Kokura S, Ichikawa H, Yanagisawa R, Inoue K, Takano H, Satoh M *et al*: **Reduced intestinal inflammation induced by dextran sodium sulfate in interleukin-6-deficient mice**. *Int J Mol Med* 2004, **14**(2):191-196.
177. Hosokawa T, Kusugami K, Ina K, Ando T, Shinoda M, Imada A, Ohsuga M, Sakai T, Matsuura T, Ito K *et al*: **Interleukin-6 and soluble interleukin-6 receptor in the colonic mucosa of inflammatory bowel disease**. *J Gastroenterol Hepatol* 1999, **14**(10):987-996.
178. Atreya R, Mudter J, Finotto S, Mullberg J, Jostock T, Wirtz S, Schutz M, Bartsch B, Holtmann M, Becker C *et al*: **Blockade of interleukin 6 trans signaling suppresses T-cell resistance against apoptosis in chronic intestinal inflammation: evidence in crohn disease and experimental colitis in vivo**. *Nat Med* 2000, **6**(5):583-588.
179. Salmi M, Jalkanen S: **Human leukocyte subpopulations from inflamed gut bind to joint vasculature using distinct sets of adhesion molecules**. *J Immunol* 2001, **166**(7):4650-4657.
180. McLoughlin RM, Jenkins BJ, Grail D, Williams AS, Fielding CA, Parker CR, Ernst M, Topley N, Jones SA: **IL-6 trans-signaling via STAT3 directs T cell infiltration in acute inflammation**. *Proc Natl Acad Sci U S A* 2005, **102**(27):9589-9594.
181. Yang XO, Panopoulos AD, Nurieva R, Chang SH, Wang D, Watowich SS, Dong C: **STAT3 regulates cytokine-mediated generation of inflammatory helper T cells**. *J Biol Chem* 2007, **282**(13):9358-9363.
182. Ogura H, Murakami M, Okuyama Y, Tsuruoka M, Kitabayashi C, Kanamoto M, Nishihara M, Iwakura Y, Hirano T: **Interleukin-17 promotes autoimmunity by triggering a positive-feedback loop via interleukin-6 induction**. *Immunity* 2008, **29**(4):628-636.
183. Yamamoto M, Yoshizaki K, Kishimoto T, Ito H: **IL-6 is required for the development of Th1 cell-mediated murine colitis**. *Journal of Immunology* 2000, **164**(9):4878-4882.
184. Grivennikov S, Karin E, Terzic J, Mucida D, Yu GY, Vallabhapurapu S, Scheller J, Rose-John S, Cheroutre H, Eckmann L *et al*: **IL-6 and Stat3 are required for survival of intestinal epithelial cells and development of colitis-associated cancer**. *Cancer Cell* 2009, **15**(2):103-113.
185. Zhou L, Sonnenberg GF: **Essential immunologic orchestrators of intestinal homeostasis**. *Sci Immunol* 2018, **3**(20).
186. Choi JS, Kim KH, Lau LF: **The matricellular protein CCN1 promotes mucosal healing in murine colitis through IL-6**. *Mucosal Immunol* 2015, **8**(6):1285-1296.
187. Dumoutier L, Louahed J, Renauld JC: **Cloning and characterization of IL-10-related T cell-derived inducible factor (IL-TIF), a novel cytokine structurally related to IL-10 and inducible by IL-9**. *J Immunol* 2000, **164**(4):1814-1819.
188. Xie MH, Aggarwal S, Ho WH, Foster J, Zhang ZM, Stinson J, Wood WI, Goddard AD, Gurney AL: **Interleukin (IL)-22, a novel human cytokine that signals through the interferon receptor-related proteins CRF2-4 and IL-22R**. *J Biol Chem* 2000, **275**(40):31335-31339.
189. Nagem RA, Colau D, Dumoutier L, Renauld JC, Ogata C, Polikarpov I: **Crystal structure of recombinant human interleukin-22**. *Structure* 2002, **10**(8):1051-1062.
190. Liang SC, Tan XY, Luxenberg DP, Karim R, Dunussi-Joannopoulos K, Collins M, Fouser LA: **Interleukin (IL)-22 and IL-17 are coexpressed by Th17 cells and cooperatively enhance expression of antimicrobial peptides**. *J Exp Med* 2006, **203**(10):2271-2279.
191. Witte E, Witte K, Warszawska K, Sabat R, Wolk K: **Interleukin-22: a cytokine produced by T, NK and NKT cell subsets, with importance in the innate immune defense and tissue protection**. *Cytokine Growth Factor Rev* 2010, **21**(5):365-379.

192. Duhen T, Geiger R, Jarrossay D, Lanzavecchia A, Sallusto F: **Production of interleukin 22 but not interleukin 17 by a subset of human skin-homing memory T cells**. *Nat Immunol* 2009, **10**(8):857-863.
193. Kotenko SV, Izotova LS, Mirochnitchenko OV, Esterova E, Dickensheets H, Donnelly RP, Pestka S: **Identification of the functional interleukin-22 (IL-22) receptor complex -: The IL-10R2 chain (IL-10Rβ) is a common chain of both the IL-10 and IL-22 (IL-10-related T cell-derived inducible factor, IL-TIF) receptor complexes**. *J Biol Chem* 2001, **276**(4):2725-2732.
194. Jang M, Kim H, Kim Y, Choi J, Jeon J, Hwang Y, Kang JS, Lee WJ: **The crucial role of IL-22 and its receptor in thymus and activation regulated chemokine production and T-cell migration by house dust mite extract**. *Exp Dermatol* 2016, **25**(8):598-603.
195. Jones BC, Logsdon NJ, Walter MR: **Structure of IL-22 bound to its high-affinity IL-22R1 chain**. *Structure* 2008, **16**(9):1333-1344.
196. Yoon SI, Jones BC, Logsdon NJ, Harris BD, Deshpande A, Radaeva S, Halloran BA, Gao B, Walter MR: **Structure and Mechanism of Receptor Sharing by the IL-10R2 Common Chain**. *Structure* 2010, **18**(5):638-648.
197. Logsdon NJ, Jones BC, Josephson K, Cook J, Walter MR: **Comparison of interleukin-22 and interleukin-10 soluble receptor complexes**. *J Interferon Cytokine Res* 2002, **22**(11):1099-1112.
198. Sabat R, Ouyang W, Wolk K: **Therapeutic opportunities of the IL-22-IL-22R1 system**. *Nat Rev Drug Discov* 2014, **13**(1):21-38.
199. Wolk K, Kunz S, Witte E, Friedrich M, Asadullah K, Sabat R: **IL-22 increases the innate immunity of tissues**. *Immunity* 2004, **21**(2):241-254.
200. Lejeune D, Dumoutier L, Constantinescu S, Kruijer W, Schuringa JJ, Renauld JC: **Interleukin-22 (IL-22) activates the JAK/STAT, ERK, JNK, and p38 MAP kinase pathways in a rat hepatoma cell line - Pathways that are shared with and distinct from IL-10**. *J Biol Chem* 2002, **277**(37):33676-33682.
201. Zenewicz LA: **IL-22 Binding Protein (IL-22BP) in the Regulation of IL-22 Biology**. *Frontiers in Immunology* 2021, **12**.
202. Zheng Y, Valdez PA, Danilenko DM, Hu Y, Sa SM, Gong Q, Abbas AR, Modrusan Z, Ghilardi N, de Sauvage FJ *et al*: **Interleukin-22 mediates early host defense against attaching and effacing bacterial pathogens**. *Nat Med* 2008, **14**(3):282-289.
203. Brand S, Beigel F, Olszak T, Zitzmann K, Eichhorst ST, Otte JM, Diepolder H, Marquardt A, Jagla W, Popp A *et al*: **IL-22 is increased in active Crohn's disease and promotes proinflammatory gene expression and intestinal epithelial cell migration**. *Am J Physiol-Gastr L* 2006, **290**(4):G827-G838.
204. Aujla SJ, Chan YR, Zheng M, Fei M, Askew DJ, Pociask DA, Reinhart TA, McAllister F, Edeal J, Gaus K *et al*: **IL-22 mediates mucosal host defense against Gram-negative bacterial pneumonia**. *Nat Med* 2008, **14**(3):275-281.
205. Wolk K, Witte E, Wallace E, Docke WD, Kunz S, Asadullah K, Volk HD, Sterry W, Sabat R: **IL-22 regulates the expression of genes responsible for antimicrobial defense, cellular differentiation, and mobility in keratinocytes: a potential role in psoriasis**. *Eur J Immunol* 2006, **36**(5):1309-1323.
206. Feng D, Park O, Radaeva S, Wang H, Yin S, Kong X, Zheng M, Zakhari S, Kolls JK, Gao B: **Interleukin-22 ameliorates cerulein-induced pancreatitis in mice by inhibiting the autophagic pathway**. *Int J Biol Sci* 2012, **8**(2):249-257.
207. Sonnenberg GF, Fouser LA, Artis D: **Border patrol: regulation of immunity, inflammation and tissue homeostasis at barrier surfaces by IL-22**. *Nat Immunol* 2011, **12**(5):383-390.
208. Hirose K, Takahashi K, Nakajima H: **Roles of IL-22 in Allergic Airway Inflammation**. *J Allergy (Cairo)* 2013, **2013**:260518.

209. Fu X, Xiu Z, Xu Q, Yue R, Xu H: **Interleukin-22 Alleviates Caerulein-Induced Acute Pancreatitis by Activating AKT/mTOR Pathway**. *Dig Dis Sci* 2024, **69**(5):1691-1700.
210. Wolk K, Haugen HS, Xu W, Witte E, Waggie K, Anderson M, Vom Baur E, Witte K, Warszawska K, Philipp S *et al*: **IL-22 and IL-20 are key mediators of the epidermal alterations in psoriasis while IL-17 and IFN-gamma are not**. *J Mol Med (Berl)* 2009, **87**(5):523-536.
211. Croft M, Benedict CA, Ware CF: **Clinical targeting of the TNF and TNFR superfamilies**. *Nat Rev Drug Discov* 2013, **12**(2):147-168.
212. Dudakov JA, Hanash AM, van den Brink MRM: **Interleukin-22: Immunobiology and Pathology**. *Annu Rev Immunol* 2015, **33**:747-785.
213. Mizoguchi A, Yano A, Himuro H, Ezaki Y, Sadanaga T, Mizoguchi E: **Clinical importance of IL-22 cascade in IBD**. *J Gastroenterol* 2018, **53**(4):465-474.
214. Zenewicz LA, Yancopoulos GD, Valenzuela DM, Murphy AJ, Stevens S, Flavell RA: **Innate and adaptive interleukin-22 protects mice from inflammatory bowel disease**. *Immunity* 2008, **29**(6):947-957.
215. Sugimoto K, Ogawa A, Mizoguchi E, Shimomura Y, Andoh A, Bhan AK, Blumberg RS, Xavier RJ, Mizoguchi A: **IL-22 ameliorates intestinal inflammation in a mouse model of ulcerative colitis**. *J Clin Invest* 2008, **118**(2):534-544.
216. Sekikawa A, Fukui H, Suzuki K, Karibe T, Fujii S, Ichikawa K, Tomita S, Imura J, Shiratori K, Chiba T *et al*: **Involvement of the IL-22/REG Ialpha axis in ulcerative colitis**. *Lab Invest* 2010, **90**(3):496-505.
217. Neufert C, Pickert G, Zheng Y, Wittkopf N, Warntjen M, Nikolaev A, Ouyang W, Neurath MF, Becker C: **Activation of epithelial STAT3 regulates intestinal homeostasis**. *Cell Cycle* 2010, **9**(4):652-655.
218. Lindemans CA, Calafiore M, Mertelsmann AM, O'Connor MH, Dudakov JA, Jenq RR, Velardi E, Young LF, Smith OM, Lawrence G *et al*: **Interleukin-22 promotes intestinal-stem-cell-mediated epithelial regeneration**. *Nature* 2015, **528**(7583):560-564.
219. Aparicio-Domingo P, Romera-Hernandez M, Karrich JJ, Cornelissen F, Papazian N, Lindenbergh-Kortleve DJ, Butler JA, Boon L, Coles MC, Samsom JN *et al*: **Type 3 innate lymphoid cells maintain intestinal epithelial stem cells after tissue damage**. *J Exp Med* 2015, **212**(11):1783-1791.
220. Kamanaka M, Huber S, Zenewicz LA, Gagliani N, Rathinam C, O'Connor W, Jr., Wan YY, Nakae S, Iwakura Y, Hao L *et al*: **Memory/effector (CD45RB(lo)) CD4 T cells are controlled directly by IL-10 and cause IL-22-dependent intestinal pathology**. *J Exp Med* 2011, **208**(5):1027-1040.
221. Eken A, Singh AK, Treuting PM, Oukka M: **IL-23R+ innate lymphoid cells induce colitis via interleukin-22-dependent mechanism**. *Mucosal Immunol* 2014, **7**(1):143-154.
222. Yan J, Yu J, Yuan SZ, Tang WQ, Ma W, Yang X, Liu YJ, Liang HP, Zhong XM, Shao J *et al*: **Musculin is highly enriched in Th17 and IL-22-producing ILC3s and restrains pro-inflammatory cytokines in murine colitis**. *Eur J Immunol* 2021, **51**(4):995-998.
223. Bernshtein B, Curato C, Ioannou M, Thaiss CA, Gross-Vered M, Kolesnikov M, Wang Q, David E, Chappell-Maor L, Harmelin A *et al*: **IL-23-producing IL-10Ralpha-deficient gut macrophages elicit an IL-22-driven proinflammatory epithelial cell response**. *Sci Immunol* 2019, **4**(36).
224. Gunasekera DC, Ma JX, Vacharathit V, Shah P, Ramakrishnan A, Uprety P, Shen ZL, Sheh A, Brayton CF, Whary MT *et al*: **The development of colitis in Il10−/− mice is dependent on IL-22**. *Mucosal Immunol* 2020, **13**(3):493-506.
225. Morrison PJ, Ballantyne SJ, Macdonald SJ, Moore JWJ, Jenkins D, Wright JF, Fouser LA, Kullberg MC: **Differential Requirements for IL-17A and IL-22 in Cecal versus Colonic Inflammation Induced by**. *Am J Pathol* 2015, **185**(12):3290-3303.

226. Cash HL, Whitham CV, Behrendt CL, Hooper LV: **Symbiotic bacteria direct expression of an intestinal bactericidal lectin**. *Science* 2006, **313**(5790):1126-1130.
227. Sharpe AH, Pauken KE: **The diverse functions of the PD1 inhibitory pathway**. *Nat Rev Immunol* 2018, **18**(3):153-167.
228. Nishimura H, Honjo T, Minato N: **Facilitation of beta selection and modification of positive selection in the thymus of PD-1-deficient mice**. *J Exp Med* 2000, **191**(5):891-898.
229. Ghebeh H, Tulbah A, Mohammed S, Eikum N, Bin Amer SM, Al-Tweigeri T, Dermime S: **Expression of B7-H1 in breast cancer patients is strongly associated with high proliferative Ki-67-expressing tumor cells**. *Int J Cancer* 2007, **121**(4):751-758.
230. Nishimura H, Nose M, Hiai H, Minato N, Honjo T: **Development of lupus-like autoimmune diseases by disruption of the PD-1 gene encoding an ITIM motif-carrying immunoreceptor**. *Immunity* 1999, **11**(2):141-151.
231. Barber DL, Wherry EJ, Masopust D, Zhu B, Allison JP, Sharpe AH, Freeman GJ, Ahmed R: **Restoring function in exhausted CD8 T cells during chronic viral infection**. *Nature* 2006, **439**(7077):682-687.
232. Patsoukis N, Wang Q, Strauss L, Boussiotis VA: **Revisiting the PD-1 pathway**. *Sci Adv* 2020, **6**(38).
233. Finger LR, Pu J, Wasserman R, Vibhakar R, Louie E, Hardy RR, Burrows PD, Billips LG: **The human PD-1 gene: complete cDNA, genomic organization, and developmentally regulated expression in B cell progenitors**. *Gene* 1997, **197**(1-2):177-187.
234. Lazar-Molnar E, Scandiuzzi L, Basu I, Quinn T, Sylvestre E, Palmieri E, Ramagopal UA, Nathenson SG, Guha C, Almo SC: **Structure-guided development of a high-affinity human Programmed Cell Death-1: Implications for tumor immunotherapy**. *EBioMedicine* 2017, **17**:30-44.
235. Arasanz H, Gato-Canas M, Zuazo M, Ibanez-Vea M, Breckpot K, Kochan G, Escors D: **PD1 signal transduction pathways in T cells**. *Oncotarget* 2017, **8**(31):51936-51945.
236. Bally AP, Austin JW, Boss JM: **Genetic and Epigenetic Regulation of PD-1 Expression**. *J Immunol* 2016, **196**(6):2431-2437.
237. Iwai Y, Hamanishi J, Chamoto K, Honjo T: **Cancer immunotherapies targeting the PD-1 signaling pathway**. *J Biomed Sci* 2017, **24**(1):26.
238. Jorgensen JT: **An update on companion and complementary diagnostic assays for PD-1/PD-L1 checkpoint inhibitors in NSCLC**. *Expert Rev Mol Diagn* 2021, **21**(5):445-454.
239. Wu X, Gu Z, Chen Y, Chen B, Chen W, Weng L, Liu X: **Application of PD-1 Blockade in Cancer Immunotherapy**. *Comput Struct Biotechnol J* 2019, **17**:661-674.
240. Liu C, Seeram NP, Ma H: **Small molecule inhibitors against PD-1/PD-L1 immune checkpoints and current methodologies for their development: a review**. *Cancer Cell Int* 2021, **21**(1).
241. Chames P, Van Regenmortel M, Weiss E, Baty D: **Therapeutic antibodies: successes, limitations and hopes for the future**. *Br J Pharmacol* 2009, **157**(2):220-233.
242. Roach C, Zhang N, Corigliano E, Jansson M, Toland G, Ponto G, Dolled-Filhart M, Emancipator K, Stanforth D, Kulangara K: **Development of a Companion Diagnostic PD-L1 Immunohistochemistry Assay for Pembrolizumab Therapy in Non-Small-cell Lung Cancer**. *Appl Immunohistochem Mol Morphol* 2016, **24**(6):392-397.
243. Kazandjian D, Suzman DL, Blumenthal G, Mushti S, He K, Libeg M, Keegan P, Pazdur R: **FDA Approval Summary: Nivolumab for the Treatment of Metastatic Non-Small Cell Lung Cancer With Progression On or After Platinum-Based Chemotherapy**. *Oncologist* 2016, **21**(5):634-642.
244. Chen PL, Roh W, Reuben A, Cooper ZA, Spencer CN, Prieto PA, Miller JP, Bassett RL, Gopalakrishnan V, Wani K *et al*: **Analysis of Immune Signatures in Longitudinal**

Tumor Samples Yields Insight into Biomarkers of Response and Mechanisms of Resistance to Immune Checkpoint Blockade. *Cancer Discov* 2016, **6**(8):827-837.
245. Golinski AW, Holec PV, Mischler KM, Hackel BJ: **Biophysical Characterization Platform Informs Protein Scaffold Evolvability**. *ACS Comb Sci* 2019, **21**(4):323-335.
246. Weidle UH, Auer J, Brinkmann U, Georges G, Tiefenthaler G: **The emerging role of new protein scaffold-based agents for treatment of cancer**. *Cancer Genomics Proteomics* 2013, **10**(4):155-168.
247. Packer MS, Liu DR: **Methods for the directed evolution of proteins**. *Nat Rev Genet* 2015, **16**(7):379-394.
248. Virnekas B, Ge L, Pluckthun A, Schneider KC, Wellnhofer G, Moroney SE: **Trinucleotide phosphoramidites: ideal reagents for the synthesis of mixed oligonucleotides for random mutagenesis**. *Nucleic Acids Res* 1994, **22**(25):5600-5607.
249. Kraulis PJ, Jonasson P, Nygren PA, Uhlen M, Jendeberg L, Nilsson B, Kordel J: **The serum albumin-binding domain of streptococcal protein G is a three-helical bundle: A heteronuclear NMR study**. *Febs Lett* 1996, **378**(2):190-194.
250. Nygren PA, Ljungquist C, Tromborg H, Nustad K, Uhlen M: **Species-dependent binding of serum albumins to the streptococcal receptor protein G**. *Eur J Biochem* 1990, **193**(1):143-148.
251. Ahmad JN, Li J, Biedermannova L, Kuchar M, Sipova H, Semeradtova A, Cerny J, Petrokova H, Mikulecky P, Polinek J *et al*: **Novel high-affinity binders of human interferon gamma derived from albumin-binding domain of protein G**. *Proteins* 2012, **80**(3):774-789.
252. Kuchar M, Vankova L, Petrokova H, Cerny J, Osicka R, Pelak O, Sipova H, Schneider B, Homola J, Sebo P *et al*: **Human interleukin-23 receptor antagonists derived from an albumin-binding domain scaffold inhibit IL-23-dependent ex vivo expansion of IL-17-producing T-cells**. *Proteins* 2014, **82**(6):975-989.
253. Hlavnicková M, Kuchar M, Osicka R, Vanková L, Petroková H, Maly M, Cerny J, Arenberger P, Maly P: **ABD-Derived Protein Blockers of Human IL-17 Receptor A as Non-IgG Alternatives for Modulation of IL-17-Dependent Pro-Inflammatory Axis**. *International Journal of Molecular Sciences* 2018, **19**(10).
254. Kuchar M, Kosztyu P, Daniel Liskova V, Cerny J, Petrokova H, Vroblova E, Maly M, Vankova L, Krupka M, Raskova Kafkova L *et al*: **Myomedin scaffold variants targeted to 10E8 HIV-1 broadly neutralizing antibody mimic gp41 epitope and elicit HIV-1 virus-neutralizing sera in mice**. *Virulence* 2021, **12**(1):1271-1287.
255. Chen K, Arnold FH: **Tuning the activity of an enzyme for unusual environments: sequential random mutagenesis of subtilisin E for catalysis in dimethylformamide**. *Proc Natl Acad Sci U S A* 1993, **90**(12):5618-5622.
256. Clackson T, Hoogenboom HR, Griffiths AD, Winter G: **Making antibody fragments using phage display libraries**. *Nature* 1991, **352**(6336):624-628.
257. Boder ET, Wittrup KD: **Yeast surface display for screening combinatorial polypeptide libraries**. *Nature Biotechnology* 1997, **15**(6):553-557.
258. Daugherty PS, Olsen MJ, Iverson BL, Georgiou G: **Development of an optimized expression system for the screening of antibody libraries displayed on the Escherichia coli surface**. *Protein Eng* 1999, **12**(7):613-621.
259. Becker DM, Guarente L: **High-Efficiency Transformation of Yeast by Electroporation**. *Method Enzymol* 1991, **194**:182-187.
260. Dower WJ, Miller JF, Ragsdale CW: **High efficiency transformation of E. coli by high voltage electroporation**. *Nucleic Acids Res* 1988, **16**(13):6127-6145.
261. Wilson DS, Keefe AD, Szostak JW: **The use of mRNA display to select high-affinity protein-binding peptides**. *Proc Natl Acad Sci U S A* 2001, **98**(7):3750-3755.
262. Hanes J, Pluckthun A: **In vitro selection and evolution of functional proteins by using ribosome display**. *Proc Natl Acad Sci U S A* 1997, **94**(10):4937-4942.

263. Sessa G, Podini P, Mariani M, Meroni A, Spreafico R, Sinigaglia F, Colonna M, Panina P, Meldolesi J: **Distribution and signaling of TREM2/DAP12, the receptor system mutated in human polycystic lipomembraneous osteodysplasia with sclerosing leukoencephalopathy dementia**. *Eur J Neurosci* 2004, **20**(10):2617-2628.
264. Dhandapani R, Neri M, Bernhard M, Brzak I, Schweizer T, Rudin S, Joller S, Berth R, Kernen J, Neuhaus A *et al*: **Sustained Trem2 stabilization accelerates microglia heterogeneity and Af3 pathology in a mouse model of Alzheimer's disease**. *Cell Rep* 2022, **39**(9).
265. Neumann H, Takahashi K: **Essential role of the microglial triggering receptor expressed on myeloid cells-2 (TREM2) for central nervous tissue immune homeostasis**. *J Neuroimmunol* 2007, **184**(1-2):92-99.
266. Paradowska-Gorycka A, Jurkowska M: **Structure, expression pattern and biological activity of molecular complex TREM-2/DAP12**. *Hum Immunol* 2013, **74**(6):730-737.
267. Sun R, Han R, McCornack C, Khan S, Tabor GT, Chen Y, Hou J, Jiang H, Schoch KM, Mao DD *et al*: **TREM2 inhibition triggers antitumor cell activity of myeloid cells in glioblastoma**. *Sci Adv* 2023, **9**(19):eade3559.
268. Wu YJ, Wang MN, Yin H, Ming SQ, Li XY, Jiang GM, Liu Y, Wang PH, Zhou GD, Liu L *et al*: **TREM-2 is a sensor and activator of T cell response in SARS-CoV-2 infection**. *Science Advances* 2021, **7**(50).
269. Hwang M, Savarin C, Kim J, Powers J, Towne N, Oh H, Bergmann CC: **Trem2 deficiency impairs recovery and phagocytosis and dysregulates myeloid gene expression during virus-induced demyelination**. *J Neuroinflammation* 2022, **19**(1):267.
270. Zhou W, Zhou Y, He J, Rao Y, Fei P, Li J: **TREM2 deficiency in microglia accelerates photoreceptor cell death and immune cell infiltration following retinal detachment**. *Cell Death Dis* 2023, **14**(3):219.
271. Piccio L, Buonsanti C, Mariani M, Cella M, Gilfillan S, Cross AH, Colonna M, Panina-Bordignon P: **Blockade of TREM-2 exacerbates experimental autoimmune encephalomyelitis**. *Eur J Immunol* 2007, **37**(5):1290-1301.
272. McQuade A, Kang YJ, Hasselmann J, Jairaman A, Sotelo A, Coburn M, Shabestari SK, Chadarevian JP, Fote G, Tu CH *et al*: **Gene expression and functional deficits underlie TREM2-knockout microglia responses in human models of Alzheimer's disease (vol 11, 5370, 2020)**. *Nat Commun* 2023, **14**(1).
273. Borroni B, Ferrari F, Galimberti D, Nacmias B, Barone C, Bagnoli S, Fenoglio C, Piaceri I, Archetti S, Bonvicini C *et al*: **Heterozygous TREM2 mutations in frontotemporal dementia**. *Neurobiol Aging* 2014, **35**(4):934 e937-910.
274. Guerreiro R, Wojtas A, Bras J, Carrasquillo M, Rogaeva E, Majounie E, Cruchaga C, Sassi C, Kauwe JS, Younkin S *et al*: **TREM2 variants in Alzheimer's disease**. *N Engl J Med* 2013, **368**(2):117-127.
275. Rayaprolu S, Mullen B, Baker M, Lynch T, Finger E, Seeley WW, Hatanpaa KJ, Lomen-Hoerth C, Kertesz A, Bigio EH *et al*: **TREM2 in neurodegeneration: evidence for association of the p.R47H variant with frontotemporal dementia and Parkinson's disease**. *Mol Neurodegener* 2013, **8**.
276. Wang XQ, Tao BB, Li B, Wang XH, Zhang WC, Wan L, Hua XM, Li ST: **Overexpression of TREM2 enhances glioma cell proliferation and invasion: a therapeutic target in human glioma**. *Oncotarget* 2016, **7**(3):2354-2366.
277. Kluckova K, Kozak J, Szaboova K, Rychly B, Svajdler M, Suchankova M, Tibenska E, Filova B, Steno J, Matejcik V *et al*: **TREM-1 and TREM-2 Expression on Blood Monocytes Could Help Predict Survival in High-Grade Glioma Patients**. *Mediat Inflamm* 2020, **2020**.
278. Cheng X, Wang XW, Nie KC, Cheng L, Zhang ZY, Hu Y, Peng WJ: **Systematic Pan-Cancer Analysis Identifies TREM2 as an Immunological and Prognostic Biomarker**. *Frontiers in Immunology* 2021, **12**.

279. Molgora M, Esaulova E, Vermi W, Hou J, Chen Y, Luo J, Brioschi S, Bugatti M, Omodei AS, Ricci B *et al*: **TREM2 Modulation Remodels the Tumor Myeloid Landscape Enhancing Anti-PD-1 Immunotherapy**. *Cell* 2020, **182**(4):886-900 e817.
280. Li CM, Hou XM, Yuan SA, Zhang YG, Yuan WZ, Liu XG, Li J, Wang YP, Guan QL, Zhou YN: **High expression of TREM2 promotes EMT via the PI3K/AKT pathway in gastric cancer: bioinformatics analysis and experimental verification**. *J Cancer* 2021, **12**(11):3277-3290.
281. Zhang X, Wang W, Li P, Wang X, Ni K: **High TREM2 expression correlates with poor prognosis in gastric cancer**. *Hum Pathol* 2018, **72**:91-99.
282. Tan J, Fan W, Liu T, Zhu B, Liu Y, Wang S, Wu J, Liu J, Zou F, Wei J *et al*: **TREM2(+) macrophages suppress CD8(+) T-cell infiltration after transarterial chemoembolisation in hepatocellular carcinoma**. *J Hepatol* 2023, **79**(1):126-140.
283. Zhang H, Sheng L, Tao J, Chen R, Li Y, Sun Z, Qian W: **Depletion of the triggering receptor expressed on myeloid cells 2 inhibits progression of renal cell carcinoma via regulating related protein expression and PTEN-PI3K/Akt pathway**. *Int J Oncol* 2016, **49**(6):2498-2506.
284. Allcock RJN, Barrow AD, Forbes S, Beck S, Trowsdale J: **The human TREM gene cluster at 6p21.1 encodes both activating and inhibitory single IgV domain receptors and includes NKp44**. *Eur J Immunol* 2003, **33**(2):567-577.
285. Bekris LM, Khrestian M, Dyne E, Shao Y, Pillai JA, Rao SM, Bemiller SM, Lamb B, Fernandez HH, Leverenz JB: **Soluble TREM2 and biomarkers of central and peripheral inflammation in neurodegenerative disease**. *J Neuroimmunol* 2018, **319**:19-27.
286. Bouchon A, Hernandez-Munain C, Cella M, Colonna M: **A DAP12-mediated pathway regulates expression of CC chemokine receptor 7 and maturation of human dendritic cells**. *J Exp Med* 2001, **194**(8):1111-1122.
287. Peng QS, Malhotra S, Torchia JA, Kerr WG, Coggeshall KM, Humphrey MB: **TREM2-and DAP12-Dependent Activation of PI3K Requires DAP10 and Is Inhibited by SHIP1**. *Sci Signal* 2010, **3**(122).
288. Kober DL, Brett TJ: **TREM2-Ligand Interactions in Health and Disease**. *J Mol Biol* 2017, **429**(11):1607-1629.
289. Konishi H, Kiyama H: **Microglial TREM2/DAP12 Signaling: A Double-Edged Sword in Neural Diseases**. *Front Cell Neurosci* 2018, **12**:206.
290. Tang WQ, Lv B, Yang BW, Chen YK, Yuan FF, Ma LJ, Chen S, Zhang S, Xia JL: **TREM2 acts as a tumor suppressor in hepatocellular carcinoma by targeting the PI3K/Akt/β-catenin pathway**. *Oncogenesis* 2019, **8**.
291. Yeh FL, Wang YY, Tom I, Gonzalez LC, Sheng M: **TREM2 Binds to Apolipoproteins, Including APOE and CLU/APOJ, and Thereby Facilitates Uptake of Amyloid-Beta by Microglia**. *Neuron* 2016, **91**(2):328-340.
292. Stefano L, Racchetti G, Bianco F, Passini N, Gupta RS, Bordignon PP, Meldolesi J: **The surface-exposed chaperone, Hsp60, is an agonist of the microglial TREM2 receptor**. *J Neurochem* 2009, **110**(1):284-294.
293. Hsieh CL, Koike M, Spusta SC, Niemi EC, Yenari M, Nakamura MC, Seaman WE: **A role for TREM2 ligands in the phagocytosis of apoptotic neuronal cells by microglia**. *J Neurochem* 2009, **109**(4):1144-1156.
294. Lee HY, Lee EH, Yi J, Ji KY, Kim SM, Choi H, Yee SM, Kang HS, Kim EM: **TREM2 promotes natural killer cell development in CD3−CD122+NK1.1+ pNK cells**. *Bmc Immunol* 2021, **22**(1).
295. Takahashi K, Rochford CDP, Neumann H: **Clearance of apoptotic neurons without inflammation by microglial triggering receptor expressed on myeloid cells-2**. *J Exp Med* 2005, **201**(4):647-657.

296. Chu CL, Yu YL, Shen KY, Lowell CA, Lanier LL, Hamerman JA: **Increased TLR responses in dendritic cells lacking the ITAM-containing adapters DAP12 and FcRγ**. *Eur J Immunol* 2008, **38**(1):166-173.
297. Zhang WQ, Huang SH, Huang X, Li JH, Ye P, Xu J, Zheng PZ, Shen HY, Huang JR: **Regulation of human mesenchymal stem cell differentiation by TREM-2**. *Hum Immunol* 2016, **77**(6):476-482.
298. Gratuze M, Leyns CEG, Holtzman DM: **New insights into the role of TREM2 in Alzheimer's disease**. *Mol Neurodegener* 2018, **13**.
299. Charles JF, Humphrey MB, Zhao XD, Quarles E, Nakamura MC, Aderem A, Seaman WE, Smith KD: **The innate immune response to Salmonella enterica serovar Typhimurium by macrophages is dependent on TREM2-DAP12**. *Infect Immun* 2008, **76**(6):2439-2447.
300. Ulland TK, Song WM, Huang SC, Ulrich JD, Sergushichev A, Beatty WL, Loboda AA, Zhou Y, Cairns NJ, Kambal A *et al*: **TREM2 Maintains Microglial Metabolic Fitness in Alzheimer's Disease**. *Cell* 2017, **170**(4):649-663 e613.
301. Zhang WQ, Huang SH, Huang X, Li JH, Ye P, Xu JH, Zheng PZ, Shen HY, Huang JR: **Regulation of human mesenchymal stem cell differentiation by TREM-2**. *Human Immunology* 2016, **77**(6):476-482.
302. Wu K, Byers DE, Jin X, Agapov E, Alexander-Brett J, Patel AC, Cella M, Gilfilan S, Colonna M, Kober DL *et al*: **TREM-2 promotes macrophage survival and lung disease after respiratory viral infection**. *J Exp Med* 2015, **212**(5):681-697.
303. Coelho I, Duarte N, Barros A, Macedo MP, Penha-Goncalves C: **Trem-2 Promotes Emergence of Restorative Macrophages and Endothelial Cells During Recovery From Hepatic Tissue Damage**. *Front Immunol* 2020, **11**:616044.
304. Cantoni C, Bollman B, Licastro D, Xie MQ, Mikesell R, Schmidt R, Yuede CM, Galimberti D, Olivecrona G, Klein RS *et al*: **TREM2 regulates microglial cell activation in response to demyelination in vivo**. *Acta Neuropathol* 2015, **129**(3):429-447.
305. Ulland TK, Song WM, Huang SCC, Ulrich JD, Sergushichev A, Beatty WL, Loboda AA, Zhou YY, Caims NJ, Kambal A *et al*: **TREM2 Maintains Microglial Metabolic Fitness in Alzheimer's Disease**. *Cell* 2017, **170**(4):649-+.
306. Kolios G, Valatas V, Kouroumalis E: **Role of Kupffer cells in the pathogenesis of liver disease**. *World J Gastroenterol* 2006, **12**(46):7413-7420.
307. Sudom A, Talreja S, Danao J, Bragg E, Kegel R, Min X, Richardson J, Zhang Z, Sharkov N, Marcora E *et al*: **Molecular basis for the loss-of-function effects of the Alzheimer's disease-associated R47H variant of the immune receptor TREM2**. *J Biol Chem* 2018, **293**(32):12634-12646.
308. Celarain N, Sanchez-Ruiz de Gordoa J, Zelaya MV, Roldan M, Larumbe R, Pulido L, Echavarri C, Mendioroz M: **TREM2 upregulation correlates with 5-hydroxymethycytosine enrichment in Alzheimer's disease hippocampus**. *Clin Epigenetics* 2016, **8**:37.
309. Lavin Y, Kobayashi S, Leader A, Amir ED, Elefant N, Bigenwald C, Remark R, Sweeney R, Becker CD, Levine JH *et al*: **Innate Immune Landscape in Early Lung Adenocarcinoma by Paired Single-Cell Analyses**. *Cell* 2017, **169**(4):750-765 e717.
310. Dunn GP, Bruce AT, Ikeda H, Old LJ, Schreiber RD: **Cancer immunoediting: from immunosurveillance to tumor escape**. *Nat Immunol* 2002, **3**(11):991-998.
311. Nakamura K, Smyth MJ: **TREM2 marks tumor-associated macrophages**. *Signal Transduct Target Ther* 2020, **5**(1):233.
312. Molgora M, Liu YA, Colonna M, Cella M: **TREM2: A new player in the tumor microenvironment**. *Semin Immunol* 2023, **67**:101739.
313. Wolf EM, Fingleton B, Hasty AH: **The therapeutic potential of TREM2 in cancer**. *Front Oncol* 2022, **12**:984193.

314. Chan LC, Li CW, Xia W, Hsu JM, Lee HH, Cha JH, Wang HL, Yang WH, Yen EY, Chang WC *et al*: **IL-6/JAK1 pathway drives PD-L1 Y112 phosphorylation to promote cancer immune evasion**. *J Clin Invest* 2019, **129**(8):3324-3338.
315. Xi X, Hu R, Wang Q, Xu K, Yang H, Cui Z, Zhang Y, Teng M, Xia L, Chen J *et al*: **Interleukin-22 promotes PD-L1 expression via STAT3 in colon cancer cells**. *Oncol Lett* 2021, **22**(4):716.
316. Li J, Xu J, Yan X, Jin K, Li W, Zhang R: **Targeting Interleukin-6 (IL-6) Sensitizes Anti-PD-L1 Treatment in a Colorectal Cancer Preclinical Model**. *Med Sci Monit* 2018, **24**:5501-5508.
317. Hong DS, Angelo LS, Kurzrock R: **Interleukin-6 and its receptor in cancer - Implications for translational therapeutics**. *Cancer-Am Cancer Soc* 2007, **110**(9):1911-1928.
318. Lu C, Kerbel RS: **Interleukin-6 undergoes transition from paracrine growth inhibitor to autocrine stimulator during human melanoma progression**. *J Cell Biol* 1993, **120**(5):1281-1288.
319. Huang C, Yang GA, Jiang T, Huang KJ, Cao J, Qiu ZJ: **Effects of IL-6 and AG490 on regulation of Stat3 signaling pathway and invasion of human pancreatic cancer cells in vitro**. *J Exp Clin Canc Res* 2010, **29**.
320. Bharadwaj U, Marin-Muller C, Li M, Chen C, Yao Q: **Mesothelin overexpression promotes autocrine IL-6/sIL-6R trans-signaling to stimulate pancreatic cancer cell proliferation**. *Carcinogenesis* 2011, **32**(7):1013-1024.
321. Tchirkov A, Khalil T, Chautard E, Mokhtari K, Veronese L, Irthum B, Vago P, Kemeny JL, Verrelle P: **Interleukin-6 gene amplification and shortened survival in glioblastoma patients**. *Br J Cancer* 2007, **96**(3):474-476.
322. Loeffler S, Fayard B, Weis J, Weissenberger J: **Interleukin-6 induces transcriptional activation of vascular endothelial growth factor (VEGF) in astrocytes in vivo and regulates VEGF promoter activity in glioblastoma cells via direct interaction between STAT3 and Sp1**. *Int J Cancer* 2005, **115**(2):202-213.
323. Kudo M, Jono H, Shinriki S, Yano S, Nakamura H, Makino K, Hide T, Muta D, Ueda M, Ota K *et al*: **Antitumor effect of humanized anti-interleukin-6 receptor antibody (tocilizumab) on glioma cell proliferation Laboratory investigation**. *J Neurosurg* 2009, **111**(2):219-225.
324. Wang YY, Zhang L, Zhao PW, Ma L, Li C, Zou HB, Jiang YF: **Functional Implications of Regulatory B Cells in Human IgA Nephropathy**. *Scandinavian Journal of Immunology* 2014, **79**(1):51-60.
325. Cox JH, Kljavin NM, Ota N, Leonard J, Roose-Girma M, Diehl L, Ouyang W, Ghilardi N: **Opposing consequences of IL-23 signaling mediated by innate and adaptive cells in chemically induced colitis in mice**. *Mucosal Immunol* 2012, **5**(1):99-109.
326. Ford JW, McVicar DW: **TREM and TREM-like receptors in inflammation and disease**. *Curr Opin Immunol* 2009, **21**(1):38-46.
327. Klesney-Tait J, Turnbull IR, Colonna M: **The TREM receptor family and signal integration**. *Nat Immunol* 2006, **7**(12):1266-1273.
328. Wang YH, Chu Y, Cao FH, Chen ZH, Xu HX, Wang SJ, Ma J: **The emerging role of triggering receptor expressed on myeloid cell-2 in malignant tumor**. *Cent Eur J Immunol* 2022, **47**(4):373-381.
329. Borroni B, Ferrari F, Galimberti D, Nacmias B, Barone C, Bagnoli S, Fenoglio C, Piaceri I, Archetti S, Bonvicini C *et al*: **Heterozygous mutations in frontotemporal dementia**. *Neurobiology of Aging* 2014, **35**(4).
330. Deczkowska A, Weiner A, Amit I: **The Physiology, Pathology, and Potential Therapeutic Applications of the TREM2 Signaling Pathway**. *Cell* 2020, **181**(6):1207-1217.